

Table of Contents

Executive Summary	ES-1
Introduction	ES-1
The Submerged Aquatic Vegetation /Limerock Concept.....	ES-1
Project Goal	ES-1
Key Project Findings	ES-2
Water Column Phosphorus Removal	ES-2
Sediment Characteristics and Stability	ES-4
Hydraulic Performance.....	ES-5
Ecology of SAV Communities.....	ES-5
Recommendations.....	ES-6
Section 1: Introduction and Project Background	1-1
1.1 Review of Submerged Aquatic Vegetation/ Limerock Technology and Optimization Needs.....	1-3
1.1.1 Vegetation Community Effects on Phosphorus Removal.....	1-3
1.2 Coprecipitation of Phosphorus in Hard Waters	1-5
1.3 STA-1W (ENR) Cell 4	1-6
1.4 Compartmentalization to Enhance Hydraulic Performance	1-8
1.5 DB Environmental’s Experience with the SAV/LR Process.....	1-10
1.5.1 SAV/LR Assessments at DBE’s Facilities	1-10
1.5.2 “Phase I” SAV/LR Assessments at the ENR Supplemental Technology Sites	1-12
1.6 Phosphorus Speciation	1-14
1.7 Project Goals and Assessment Challenges	1-15
1.7.1 Project Goal	1-15
1.7.2 Assessment Challenges	1-15
1.7.3 Mesocosm, Microcosm and Laboratory Assessments	1-17
1.7.4 STA-1W Test Cell Assessments.....	1-20
1.7.5 STA-1W Cell 4 Assessments	1-21
1.7.6 STA-1W Cell 5 Assessments	1-22
Section 2: Mesocosm, Microcosm, and Laboratory Assessments.....	2-1
2.1 Long-Term Phosphorus Removal in Mesocosms	2-1
2.1.1 TP Removal Performance.....	2-2
2.1.2 Vegetation and Sediment P Storage	2-6
2.2 Effects of Water Depth on SAV P Removal Performance	2-9
2.2.1 Background Conditions	2-9
2.2.2 Spatial-Temporal Water Column Investigations Over a Diel Cycle.....	2-10
2.2.3 Vegetation and Sediment Characteristics	2-16
2.2.4 Phosphorus Mass Balances	2-17

2.2.5	Effects of Variable Water Depth on P Removal Performance.....	2-19
2.3	The Effects of Harvesting on the P Removal Efficiency by the SAV Community ...	2-25
2.3.1	Long-Term Phosphorus Monitoring Before and After Harvesting	2-25
2.3.2	Spatial-Temporal Profile	2-27
2.3.3	SAV Recolonization After Biomass Harvest	2-29
2.3.4	Effectiveness of Biomass Harvest on P Mass Removal.....	2-33
2.4	Effects of Pulsed Loading on Phosphorus Retention.....	2-33
2.4.1	Background Conditions	2-34
2.4.2	Pulse Schedule Development	2-34
2.4.3	Effects of Pulsed Loadings on Phosphorus Retention	2-37
2.4.4	Phosphorus Export from Limerock Beds after Resumption of Flows.....	2-43
2.5	Effects of Dryout and Reflooding on Phosphorus Retention.....	2-44
2.5.1	Baseline Monitoring Prior to Drawdown	2-45
2.5.2	Dryout and SAV Sampling	2-46
2.5.3	Characteristics of Harvested SAV.....	2-46
2.5.4	Sediment Consolidation	2-49
2.5.5	Sediment Phosphorus Concentration and Release upon Reflooding: Laboratory Incubations	2-50
2.5.6	Sediment Phosphorus Release upon Reflooding: In-Situ Assessment.....	2-53
2.5.7	SAV Recolonization	2-54
2.5.8	Summary	2-56
2.6	Sequential SAV/LR and Cattail Mesocosms.....	2-56
2.6.1	Long-Term Phosphorus Removal.....	2-56
2.6.2	Vegetation History	2-60
2.6.3	Calcium Effects on P removal	2-60
2.6.4	Spatial-Temporal Water Column Investigation in the Sequential SAV/LR System.....	2-61
2.6.5	Conclusions.....	2-67
2.7	Comparison of Phosphorus Removal Performance by Cattail- and SAV- Dominated Systems	2-67
2.7.1	Phosphorus Removal Comparisons	2-68
2.7.2	Vegetation and Sediment Phosphorus Storage.....	2-72
2.8	Shallow Low Velocity SAV/Periphyton/Limerock Systems.....	2-75
2.9	Growth of SAV in Post-STA Waters on Muck, Limerock, and Sand Substrates.....	2-80
2.10	Effect of Filter Media and Operating Conditions on P Removal Performance	2-86
2.10.1	Media Type and Sizes.....	2-86
2.10.2	Water Depth and Treatment Unit Configuration.....	2-95
2.11	Effects of Calcium/Alkalinity and Soluble Reactive Phosphorus Concentrations on Phosphorus Coprecipitation	2-99
2.11.1	Assessment 1: Batch Incubations	2-99
2.11.2	Assessment 2: Flow-Through Microcosms.....	2-105
2.11.3	Summary	2-122

2.12	Particulate Phosphorus and Dissolved Organic Phosphorus Characterization and Stability	2-122
2.12.1	Particle Concentration Methodology	2-123
2.12.2	Particulate Phosphorus Characterization in the Inflows and Outflows of Test Cells and Cell 4.....	2-124
2.12.3	Alterations in pH/Redox Potential and Phosphatase Enzyme Concentrations on the Mobilization of Phosphorus in Different Size Classes of Particles of Cell 4 Surface Waters	2-137
2.12.4	Alkaline Phosphatase Activity in Ecosystem Compartments (Waters, Plants, and Sediments) of STA-1W.....	2-147
Section 3:	Test Cell Evaluations	3-1
3.1	Plant Management	3-1
3.2	Hydrologic Assessments.....	3-2
3.2.1	Test Cell Stage.....	3-3
3.2.2	Test Cell Inflow	3-4
3.2.3	Test Cell Outflow	3-5
3.2.4	Summary of Hydrologic Parameters for Tracer Assessment	3-7
3.3	Tracer Studies	3-7
3.3.1	Laboratory Analysis of Dye Tracer.....	3-8
3.3.2	Computations for Determining Hydraulic Parameters.....	3-8
3.3.3	Methodology of the First Tracer Assessment.....	3-11
3.3.4	Methodology of Second Tracer Assessment	3-12
3.3.5	Results of the Two Dye Studies.....	3-13
3.4	Limerock Berm Installation and Permeability	3-21
3.4.1	Installation of Limerock Berms	3-21
3.4.2	Limerock Berm Head Loss Assessment.....	3-21
3.5	Sediment Characteristics and Accretion.....	3-22
3.6	Nitrogen and Suspended Solids Removal.....	3-26
3.6.1	Phosphorus Removal Performance	3-27
Section 4:	STA-1W Cell 4 Studies and Model Development.....	4-1
4.1	1998 – 1999 Cell 4 Outflow TP Removal Performance.....	4-1
4.2	Operational and Water Quality Regression Relationships	4-5
4.3	Relationship Between SAV Performance and Flow Velocity	4-7
4.4	Post-1999 Cell 4 Modifications and Operations.....	4-8
4.4.1	Effects of Limerock “Plugs” on Internal Phosphorus Profiles.....	4-8
4.4.2	Temporal and Spatial Phosphorus Profiles.....	4-12
4.4.3	Cell 4 Performance in Response to Fluctuations in Flow, Depth and TP Loadings.....	4-20
4.4.4	Constraints on Cell 4 Outflow Phosphorus Concentrations.....	4-22
4.5	Spatial Characterization of Sediments and SAV	4-23
4.6	Sediment P Stability and Characterization.....	4-25

4.6.1	Methodology.....	4-25
4.6.2	Results and Discussion.....	4-27
4.6.3	Conclusions.....	4-41
4.7	Sediment Diffusion Fluxes at the Inflow and Outflow Regions of Cell 4.....	4-41
4.7.1	Methods.....	4-41
4.7.2	Results and Discussion.....	4-43
4.8	Stable Isotope Sampling and Preparation	4-54
4.8.1	Introduction	4-54
4.8.2	Methods Development.....	4-54
4.8.3	Standard Preparation Procedure for the Dissolved Residue (Filtrate).....	4-56
4.8.4	Results.....	4-57
4.9	Cell 4 Hydraulic Tracer Assessment	4-59
4.9.1	Introduction	4-59
4.9.2	Cell 4 Hydrologic and Hydraulic Conditions	4-60
4.9.3	Flow Measurement Instrumentation.....	4-61
4.9.4	Water Balance During Tracer Assessment Period.....	4-61
4.9.5	Cell 4 Inflows	4-61
4.9.6	Cell 4 Outflows.....	4-63
4.9.7	Cell 4 Stage.....	4-63
4.9.8	Tracer Assessment Methodology.....	4-65
4.9.9	Results.....	4-70
4.10	Literature Review: Modeling Phosphorus Removal in Wetlands.....	4-76
4.10.1	Background	4-76
4.10.2	Empirical Models for P Removal in Wetlands.....	4-77
4.10.3	Mechanistic Models for P Removal in Wetlands.....	4-80
4.11	Description of the Process Model for SAV (PMSAV)	4-84
4.11.1	Model Description and Equations	4-84

Section 5: STA-1W Cell 5 Investigation.....	5-1
5.1 Lime-Addition Assessments.....	5-1
5.1.1 Methods.....	5-1
5.1.2 Results.....	5-2
5.2 SAV Inoculation Assessments in Cell 5	5-5
5.2.1 Methods.....	5-6
5.2.2 Results.....	5-6
5.3 Internal Cell 5 SAV Survey	5-6
5.3.1 Methods.....	5-6
5.3.2 Results.....	5-7
Section 6: References	6-1

Appendices (Located in the Appendices Volume)

- Appendix A: Project Work Plan
- Appendix B: Quality Assurance Information
- Appendix C: Microcosm and Mesocosm – Raw Data
- Appendix D: Test Cell – Raw Data
- Appendix E: STA-1W Cell 4 Tracer Studies - Raw Data
- Appendix F: STA-1W Cell 4 Studies and Model Development - Raw Data
- Appendix G: STA-1W Cell 5 Investigation - Raw Data
- Appendix H: Reviewer Comments

List of Figures

Figure 1.1.	Map of STA-1W assessment sites.....	1-4
Figure 1.2.	Schematic depicting changes in concentration of P species as water passes through an STA treatment wetland.....	1-16
Figure 2.1.	Total phosphorus loading rate over the monitoring period June 1998 – May 2001 as the product of variable inflow total P concentration and fixed hydraulic loading rates of 11, 22, and 53 cm/day.	2-2
Figure 2.2.	Total P concentrations in the inflow and outflows from mesocosms operated at constant hydraulic loading rates of 11, 22, and 53 cm/day from June 1998 – May 2001.....	2-3
Figure 2.3.	Mean soluble reactive, particulate, and dissolved organic phosphorus concentrations in the inflow and outflow from SAV mesocosms and outflow from subsequent limerock filters.....	2-4
Figure 2.4.	Mass phosphorus removal from the water column and sediment P accrual in mesocosms operated at hydraulic retention times of 1.5, 3.5 and 7.0 days for three years.	2-9
Figure 2.5.	Mean total phosphorus concentration profiles during the Spatial-Temporal Diel evaluation on September 23-24, 1999 in the Static Depth treatments at the North Supplemental Technology Site.	2-11
Figure 2.6.	Mean soluble reactive phosphorus concentration profiles during the Spatial-Temporal Diel evaluation on September 23-24, 1999 in the Static Depth treatments.	2-12
Figure 2.7.	Mean dissolved oxygen concentration profiles during the Spatial-Temporal Diel evaluation on September 23-24, 1999 in the Static Depth treatments.....	2-13
Figure 2.8.	Mean values for daytime E_h on November 10, 1999 from three replicates of shallow, moderate and deep mesocosms of the Static Depth assessment.	2-13
Figure 2.9.	Mean dissolved calcium concentration profiles during the Spatial-Temporal Diel evaluation on September 23-24, 1999 in the Static Depth treatments	2-14
Figure 2.10.	Mean total alkalinity concentration profiles during the Spatial-Temporal Diel evaluation on September 23-24, 1999 in the Static Depth treatments.....	2-15
Figure 2.11.	Mean pH value profiles during the Spatial-Temporal Diel evaluation on September 23-24, 1999 in the Static Depth treatments	2-15
Figure 2.12.	Mean temperature profiles during the Spatial-Temporal Diel evaluation on September 23-24, 1999 in the Static Depth treatments	2-16
Figure 2.13.	Depth fluctuation schedule for deep, moderate (control), and shallow depth mesocosms from March to November 2000 (a) and mean total P concentrations in the inflows (n = 3) and outflows (n = 2) of deep, moderate (control), and shallow depth mesocosms from March to November 2000 (b).....	2-21

Figure 2.14. Mass removal rates in mesocosms operated at static water depths of 0.4, 0.8 and 1.2 m from July 23, 1998 through August 20, 1999 (a), and at variable or static depths (see text for details) from March 23 through November 6, 2000 (b).....	2-24
Figure 2.15. Total P concentrations in the inflow (a) and outflows (b) of triplicate harvested and control (unharvested) mesocosms operated from July 1998 to March 15, 2000.	2-26
Figure 2.16. Soluble reactive phosphorus concentrations and pH values during the Spatial-Temporal evaluation, February 7-8, 2000, in harvested and unharvested mesocosms at the NATTS.	2-28
Figure 2.17. Dissolved oxygen concentrations and redox and temperature values during the Spatial-Temporal evaluation, February 7-8, 2000, in harvested and unharvested mesocosms at the NATTS..	2-30
Figure 2.18. Mean relative distribution (% of total dry weight biomass) of SAV genera for three replicate mesocosms on three harvest dates, as compared to the initial stocking distribution.....	2-31
Figure 2.19. Outflow total P concentrations from undisturbed and disturbed mesocosms operated at hydraulic retention times (HRT) of 1.5, 3.5 and 7.0 days	2-35
Figure 2.20. Mean outflow soluble reactive P concentrations from mesocosms that received high, moderate and low pulse loading regimes.	2-38
Figure 2.21. Mean outflow total P concentrations from mesocosms that received high, moderate and low pulse loading regimes.	2-40
Figure 2.22. Outflow total P concentrations from mesocosms that received high, moderate and low flows of Post-BMP waters under pulsed and constant-flow regimes.....	2-42
Figure 2.23. Calcium concentration in the tissues of dominant plant taxa in the inflow and outflow regions of mesocosms that were operated at high and low hydraulic loading rates of 53 and 11 cm/day, respectively.....	2-47
Figure 2.24. Standing crop biomass of dominant plant taxa in the inflow and outflow regions of mesocosms that were operated at high and low hydraulic loading rates of 53 and 11 cm/day, respectively.....	2-47
Figure 2.25. Phosphorus concentration in the tissues of dominant plant taxa in the inflow and outflow regions of mesocosms that were operated at high and low hydraulic loading rates of 53 and 11 cm/day, respectively.	2-48
Figure 2.26. Phosphorus storage in the standing crop biomass of dominant plant taxa in the inflow and outflow regions of mesocosms that were operated at high and low hydraulic loading rates of 53 and 11 cm/day, respectively.	2-48
Figure 2.27. Consolidation during drydown of desiccating sediments originally formed under high and low mean hydraulic loading rates of 53 and 11 cm/day, respectively.	2-49

Figure 2.28. Phosphorus concentration of desiccating sediments as a function of time since onset of desiccation.	2-51
Figure 2.29. The change in SRP concentration in 250-mL of overlying water during 24-hour incubations of sediment cores retrieved from mesocosms that were operated under high and low hydraulic loading rates of 53 and 11 cm/day, respectively, prior to the onset of desiccation (elapsed time of 0 days).	2-52
Figure 2.30. Total P concentrations in the inflow and outflow of two SAV mesocosms before (November 28, 2000 to January 10, 2001) and after (May 1 to July 31, 2001) a 110-day dryout period.	2-55
Figure 2.31. Mean total phosphorus concentrations in the inflow, the deep and shallow SAV mesocosms outflows, and the limerock bed outflow of sequential SAV/LR treatment trains at the North Supplemental Technology Site.	2-59
Figure 2.32. Total phosphorus concentration profiles during the Spatial-Temporal evaluation on September 23-24, 1999 in the Sequential SAV mesocosms at the North Supplemental Technology Site.	2-62
Figure 2.33. Soluble reactive phosphorus concentration profiles during the Spatial-Temporal evaluation on September 23-24, 1999 in the Sequential SAV mesocosms at the North Supplemental Technology Site.	2-63
Figure 2.34. Dissolved oxygen profiles during the Spatial-Temporal evaluation on September 23-24, 1999 in the Sequential SAV mesocosms.	2-64
Figure 2.35. Mean values for daytime Eh profiles on November 10, 1999 in the Sequential SAV mesocosms.	2-64
Figure 2.36. Spatial-Temporal evaluation pH profiles during the on September 23-24, 1999 in the Sequential SAV mesocosms.	2-65
Figure 2.37. Dissolved calcium concentration profiles during the Spatial-Temporal evaluation on September 23-24, 1999 in the Sequential SAV mesocosms.	2-66
Figure 2.38. Alkalinity concentration profiles during the Spatial-Temporal evaluation on September 23-24, 1999 in the Sequential SAV mesocosms.	2-66
Figure 2.39. Total phosphorus concentrations in the inflow (a) and outflow (b) waters from mesocosms dominated by cattail and submerged aquatic vegetation (SAV).	2-71
Figure 2.40. Relative partitioning (a) and total recovered biomass (b) of stored P within the <i>Najas</i> and cattail tissues from the inflow and outflow regions of two cattail-dominated mesocosms operated from December 1998 through August 2001.	2-74
Figure 2.41. Total P concentrations in the inflow and outflows of triplicate shallow, low velocity, SAV/periphyton raceways and in the outflow of the subsequent limerock beds.	2-76
Figure 2.42. Modified flow path and sampling locations for the high velocity SAV/periphyton raceway evaluation.	2-78

Figure 2.43. Total phosphorus concentrations in the inflow (Post-STA) waters and raceway and limerock outflow waters during the “high velocity” (0.27-0.36 cm/sec) operational period.	2-79
Figure 2.44. Photo of three substrate treatments (sand, muck and limerock), each consisting of three mesocosms in series.....	2-81
Figure 2.45. Inflow TP concentrations and P loadings to the substrate mesocosm evaluation.....	2-82
Figure 2.46. Mean TP concentrations in the inflow and outflow waters of the muck, limerock, and sand substrate mesocosms from July 1999 through November 2001.....	2-84
Figure 2.47. Total P concentrations in the inflow and outflow waters of the muck, limerock, and sand substrate mesocosms from July 1999 through November 2001.....	2-85
Figure 2.48. Schematic of the column outflow structure used in the Filter Media evaluation.....	2-88
Figure 2.49. Mean total phosphorus concentrations in the inflow and outflow of duplicate filter columns with each pair containing one of three size fractions of quartz filter matrix.....	2-89
Figure 2.50. Mean total phosphorus concentration in the inflow and outflows of duplicate filter columns with each pair containing one of two size fractions of limerock.....	2-90
Figure 2.51. Mean total phosphorus concentration in the inflow and outflows of duplicate filter columns with each pair containing one of two size fractions of Pro-Sil™ (Ca-Mg silicate).	2-91
Figure 2.52. Mean total phosphorus concentrations in the inflow and outflows of duplicate filter columns with each pair containing a coarse grade of one of three substrate types.....	2-92
Figure 2.53. Mean total phosphorus concentrations in the inflow and outflows of duplicate filter columns with each pair containing a medium grade of one of three substrate types.....	2-93
Figure 2.54. Mean (\pm s.d.) soluble reactive phosphorus concentrations in the inflow and outflow of duplicate iron-coated sand filter columns.....	2-94
Figure 2.55. Schematic of second filter media evaluation at the SATT site after replacing the Pro-Sil™ with limerock on June 22, 2001.	2-96
Figure 2.56. Mean total P concentrations in the inflow and outflows of duplicate limerock filter beds maintained at different water depths.....	2-98
Figure 2.57. Mean soluble reactive phosphorus concentrations in the inflow and outflows of duplicate limerock filter beds maintained at different water depths.....	2-99

Figure 2.58. Time course (29.5 hr) for SRP inoculated at 120 µg P/L initial concentration into high and low calcium/alkalinity water containing <i>Najas</i> previously cultured under P-enriched and P-deficient conditions for 35 days.	2-103
Figure 2.59. Time course (29.5 hr) for pH after SRP (120 µg P/L) was inoculated into high and low calcium/alkalinity water containing <i>Najas</i> previously cultured under P-enriched and P-deficient conditions for 35 days.	2-104
Figure 2.60. Flow chart detailing the evaluation design for the flow-through Coprecipitation Assessment 2.	2-107
Figure 2.61. Mean inflow and outflow pH levels from microcosms which received tap water that was either unamended or amended with concentrations of SRP and Ca/alkalinity for 160 days.	2-110
Figure 2.62. Mean inflow and outflow (A) dissolved calcium and (B) total alkalinity concentrations from microcosms which received tap water amended with Ca/alkalinity and either unamended or amended with SRP for 160 days.	2-112
Figure 2.63. Mean inflow and outflow (A) dissolved calcium and (B) total alkalinity concentrations from microcosms which received tap water without Ca/alkalinity amendments, and either unamended or amended with SRP for 160 days.	2-113
Figure 2.64. Calcium and alkalinity removals from amended Ca/alk treatment waters with and without SRP amendments during the 160-day assessment.	2-115
Figure 2.65. Mean total soluble P concentrations in the inflow and outflow waters from microcosms which received tap water unamended and amended with SRP and Ca/alkalinity for 160 days.	2-117
Figure 2.66. Phosphorus (by mass) stored in <i>Najas</i> and periphyton tissues and the sediments recovered from microcosms which received tap water unamended and amended with SRP and Ca/alkalinity for 160 days.	2-120
Figure 2.67. Distribution of phosphorus (% of P recovered) stored in <i>Najas</i> and periphyton tissues and the sediments recovered from microcosms which received tap water unamended and amended with SRP and Ca/alkalinity for 160 days.	2-121
Figure 2.68. Sequential tangential-flow filtration procedure used in particle concentration of Cell 4 inflow water according to size ranges of 0.05 µm to 0.40 µm.	2-124
Figure 2.69. X-ray diffraction (XRD) patterns of TFF-concentrated particulates from Cell 4 and test cells.	2-131
Figure 2.70. Thermal gravimetric weight loss curves for particulates collected from Cell 4 outflow and inflow region, shown as examples.	2-132
Figure 2.71. Algal abundance illustrated in four-image composite of SEM micrographs (clockwise from upper left) a) centric diatoms present in suspended solids from Cell 2 outflow in the September sample magnified 500x; b) diatoms	

from “a)” magnified 2700x; c) C-based algal ‘cells’ from Cell 2 outflow in the August sample; d) C- based cells and both centric and pinnate diatoms present in Cell 4 inflow region during September.	2-133
Figure 2.72. Two six-image composites of SEM micrographs. a) Left composite: At upper left is the same secondary electron image shown in Figure 24b. Other images are elemental dot maps of Fe, Si, P, S, and Ca, showing an association of Si and P with diatoms. b) Right composite: At upper left is a higher magnification image of the largest diatom shown in the right composite.....	2-134
Figure 2.73. Scatter plots of particulate P with particulate organic matter and suspended solids for Cell 4 inflow and outflow waters.	2-135
Figure 2.74. Scatter plots of particulate P with particulate CaCO ₃ and particulate organic matter for Cell 4 inflow and outflow waters.	2-136
Figure 2.75. Enzymatic hydrolysis of organic P in waters of Cell 4 of STA-1W. The numbers in parentheses indicate the pH of the enzyme incubations. retn. = retentate, and perm. = permeate.	2-142
Figure 2.76. Cumulative P mineralization in waters of Cell 4 of STA-1 West under different redox and pH conditions during 30 days of incubation.....	2-145
Figure 3.1. Photo of NTC-1 distribution manifold, shown during injection of Rhodamine WT dye for the hydraulic tracer assessment.....	3-3
Figure 3.2. Stage histories of north test cells prior to and during the dye tracer assessment.	3-4
Figure 3.3. Tracer response curves for the fluorescent dye Rhodamine-WT applied to the shallow test cells during the first tracer assessment. Graph (a) reflects the South Test Cell (STC-4) and graph (b) reflects the North Test Cell (NTC-15).	3-14
Figure 3.4. Tracer response curves for the fluorescent dye Rhodamine-WT applied to the deeper test cells during the first tracer assessment. Graph (a) reflects the South Test Cell (STC-9) and graph (b) reflects the North Test Cell (NTC-1).	3-15
Figure 3.5. Tracer response curve for the fluorescent dye Rhodamine-WT applied to a deep test cell (NTC-15) during the second tracer assessment.	3-16
Figure 3.6. Tracer response curve for the fluorescent dye Rhodamine-WT applied to NTC-1 during the second tracer assessment.	3-16
Figure 3.7. Dimensionless residence time distribution (RTD) functions for five test cells during the first and second tracer investigations.	3-18
Figure 3.8. Dimensionless residence time distribution (RTD) functions for test cell NTC-15 at depths of 0.49 m (NTC-15 #1, τ =3.6 days) and 0.84 m (NTC-15 #2, τ =6.4 days) during the first and second tracer studies.	3-20
Figure 3.9. Total phosphorus concentrations in the inflows and outflows of two north test cells (NTC-1 and NTC-15) dominated by SAV before (September 1,	

1999 to April 4, 2000) and after (June 23, 2000 to September 14, 2001) the installation of the NTC-15 limerock berm.	3-30
Figure 3.10. Total P removal provided by limerock berms (and downstream “polishing” wetlands) in NTC-15 and STC-9.	3-32
Figure 3.11. Total phosphorus concentrations in the inflows and outflows of two south test cells (STC-4 and STC-9) dominated by SAV before (September 1, 1999 to March 13, 2000) and after (August 4, 2000 to September 14, 2001) the installation of a limerock berm at STC-9.....	3-34
Figure 4.1. Inflow and outflow TP concentrations for STA-1W Cell 4.....	4-2
Figure 4.2. Influent and effluent TP concentrations for 1998 – 1999.....	4-2
Figure 4.3. Frequency distribution of outflow TP concentrations for 1999, based on 51 weekly composites.	4-3
Figure 4.4. Cell 4 hydraulic loading rate (HLR) for 1998 – 1999.	4-4
Figure 4.5. Cell 4 annualized TP mass loading rate for 1998 – 1999.....	4-4
Figure 4.6. Regression analysis of weekly average (composite) outflow TP concentration with weekly average TP mass loading from 1998 – 1999 data.	4-6
Figure 4.7. Regression analysis of weekly average TP settling rate (k) with weekly average TP mass loading from 1998 – 1999 data..	4-6
Figure 4.8. Historical flow record for the Cell 4 inflow levee culverts (G254) and the southernmost outflow culverts (G256).....	4-9
Figure 4.9. Internal sampling locations (44 total) in Cell 4 at which water quality (TP, SRP, pH, temperature) was evaluated on August 9, 2000.....	4-10
Figure 4.10. Total and soluble reactive phosphorus concentration gradients interpolated from 44 stations internal to Cell 4 on August 9, 2000.....	4-11
Figure 4.11. Spatial gradients in total P concentrations within Cell 4 before (sampled December 17, 1999) and after (sampled August 9, 2000) the addition of limerock “plugs”.	4-12
Figure 4.12. Soluble reactive and total P concentration isopleths from internal sampling of Cell 4 on August 9, 2000.	4-13
Figure 4.13. Soluble reactive and total P concentration isopleths from internal sampling of Cell 4 on December 19, 2000.....	4-14
Figure 4.14. Soluble reactive and total P concentration isopleths from internal sampling of Cell 4 on February 8, 2001.....	4-15
Figure 4.15. Soluble reactive and total P concentration isopleths from internal sampling of Cell 4 on April 12, 2001.	4-16
Figure 4.16. Soluble reactive and total P concentration isopleths from internal sampling of Cell 4 on July 26, 2001.....	4-17
Figure 4.17. Soluble reactive and total P concentration isopleths from internal sampling of Cell 4 on October 1, 2001.....	4-18

Figure 4.18. Soluble reactive and total P concentration isopleths from internal sampling of Cell 4 on November 9, 2001.....	4-19
Figure 4.19. Cell 4 flow, water depths and inflow/outflow TP concentrations during fall 2001.....	4-21
Figure 4.20. Inflow and outflow TP concentrations for Cells 2 and 4 during the Cell 4 STSOC 'verification' period.	4-22
Figure 4.21. Time course for SRP release from Cell 4 inflow region sediments exposed to varying pH values.....	4-29
Figure 4.22. Inorganic P fractionation of Cell 4 inflow region sediments before (Initial) and after incubations at varying levels of pH for 12.6 days.....	4-29
Figure 4.23. Time course for SRP release from Cell 4 outflow region sediments exposed to varying pH values..	4-30
Figure 4.24. The effect of pH on the release of SRP from sediments composited from three locations in the inflow region of Cell 4. The incubation period was 302 hours (12.6 days).	4-31
Figure 4.25. Time course for SRP release from Cell 4 inflow region sediments exposed to oxic and anoxic conditions.....	4-32
Figure 4.26. Inorganic phosphorus concentrations of Cell 4 inflow region sediments composited before (Initial) and after incubations under anoxic and oxic conditions for 12.6 days.....	4-32
Figure 4.27. Time course for SRP release from Cell 4 outflow region sediments exposed to oxic and anoxic conditions.	4-33
Figure 4.28. The release of soluble reactive P (SRP) from the desiccation of Cell 4 inflow (a) and outflow (b) sediments over 99 and 72 hours, respectively, upon reflooding with Cell 4 outflow water.....	4-35
Figure 4.29. The release of soluble reactive P (SRP) from Cell 4 inflow (a) and outflow (b) sediments with Ca- and alkalinity-amended (70 – 71 mg Ca/L and 248 – 260 mg CaCO ₃ /L) Cell 4 outflow water.....	4-37
Figure 4.30. Soluble reactive P (SRP) concentrations for the SRP-amended and unamended overlying Cell 4 outflow water in contact with Cell 4 inflow (a) and outflow (b) sediments.	4-39
Figure 4.31. Inorganic P fractionation of composited Cell 4 inflow and outflow region sediments. Error bars indicate +1 standard deviation.	4-40
Figure 4.32. Average porewater soluble reactive P concentrations in the inflow region of Cell 4 on November, 13, 2001.	4-45
Figure 4.33. Average porewater total soluble P concentrations in the inflow region of Cell 4 on November, 13, 2001.	4-45
Figure 4.34. Average porewater dissolved organic P concentrations in the inflow region of Cell 4 on November 13, 2001.....	4-46

Figure 4.35. Average porewater dissolved calcium concentrations in the inflow region of Cell 4 on November 13, 2001.....	4-46
Figure 4.36. Average porewater alkalinity concentrations in the inflow region of Cell 4 on November 13, 2001..	4-47
Figure 4.37. Average porewater pH values in the inflow region of Cell 4 on November, 13, 2001.	4-47
Figure 4.38. Average porewater soluble reactive P concentrations in the outflow region of Cell 4 on December 14, 2001.....	4-48
Figure 4.39. Average porewater total soluble P concentrations in the outflow region of Cell 4 on December 14, 2001..	4-48
Figure 4.40. Average porewater dissolved organic P concentrations in the outflow region of Cell 4 on December 14, 2001.	4-49
Figure 4.41. Average porewater E_h measurements in the outflow region of Cell 4 on December 14, 2001.....	4-49
Figure 4.42. Average porewater dissolved calcium concentrations in the outflow region of Cell 4 on December 14, 2001.....	4-50
Figure 4.43. Average porewater alkalinity concentrations in the outflow region of Cell 4 on December 14, 2001..	4-50
Figure 4.44. Average porewater E_h measurements in the inflow region of Cell 4 on November 13, 2001.....	4-51
Figure 4.45. Average porewater pH values in the outflow region of Cell 4 on December 14, 2001.....	4-52
Figure 4.46. Cell 4 modifications (shown in red) which included construction of G-309, deepening the cell adjacent to the northern berm and canal 7, and the addition of limerock plugs.....	4-60
Figure 4.47. Volumetric flow rate through the nine inlet culverts to Cell 4 for a one week period prior to tracer injection.	4-62
Figure 4.48. Net volumetric flow rate through the nine inlet culverts prior to and during the tracer monitoring period (November 27 to December 23, 2001).....	4-63
Figure 4.49. Net volumetric rate through the G-256 outflow structure prior to and during the tracer monitoring period (November 27 to December 23, 2001).....	4-64
Figure 4.50. Stage fluctuations in Cell 4 during the tracer assessment period.	4-64
Figure 4.51. Locations of the internal tracer and phosphorus sampling stations within Cell 4.....	4-65
Figure 4.52. Tracer response curve of Rhodamine-WT dye applied to Cell 4 on November 27, 2001. Responses to ideal well-mixed (CSTR) and plug flow (PFR) conditions are represented by the exponential decay and vertical (coinciding with the nominal HRT, τ) lines.....	4-70

Figure 4.53. Time series showing the progression of the Rhodamine-WT dye through Cell 4.....	4-72
Figure 4.54. Dimensionless residence time distribution (RTD) functions for Cell 4 during the first (December 16, 1999 – January 15, 2000) and second (November 27 – December 23, 2001) tracer studies.....	4-73
Figure 4.55. Spatial distribution of total phosphorus concentrations within Cell 4 at 25 and 48 hours following tracer injection.....	4-75
Figure 4.56. Literature review of nine different approaches to modeling P removal in aquatic systems.....	4-77
Figure 4.57. General model structure for DMSTA (Kadlec and Walker 2000) and biomachine models (Kadlec 1997).	4-80
Figure 4.58. The wetland water balance.....	4-85
Figure 4.59. In addition to the standard TIS formulation, PMSAV has a hydraulics model specifically aimed at modeling Cell 4 hydraulic processes. The Cell 4 hydraulics model accounts for parallel treatment and short-circuiting pathways, with intermittent mixing between the two.....	4-87
Figure 4.60. Process diagram for P-removal as modeled in PMSAV's treatment zone.	4-91
Figure 5.1. Concentrations of SRP, total P, true and apparent color, alkalinity and calcium for Cell 5 water outside (Ambient Control) and inside (Column Control) <i>in situ</i> columns during November 9 – December 7, 1999.	5-3
Figure 5.2. Concentrations of SRP, total P, true and apparent color, alkalinity and calcium for Cell 5 water contained within <i>in situ</i> columns receiving Low Dose and High Dose lime additions (as $\text{Ca}(\text{OH})_2$). The Column Control was not dosed.	5-4
Figure 5.3. Cell 5 SAV colonization: Presence and distribution of <i>Ceratophyllum</i> during six 120 station qualitative surveys.	5-8
Figure 5.4. Cell 5 SAV colonization: Presence and distribution of <i>Najas</i> during six 120 station qualitative surveys.	5-9
Figure 5.5. Cell 5 SAV colonization: Presence and distribution of <i>Hydrilla</i> during six 120 station qualitative surveys.	5-10
Figure 5.6. Standing crop biomass of SAV species colonizing STA-1W Cell 5 over a nine month period.....	5-11

List of Tables

Table 2.1.	Total phosphorus concentrations in the inflows, and SAV and limerock (LR) bed outflows from mesocosms operated at hydraulic retention times (HRT) of 1.5, 3.5 and 7.0 days since June 1998.	2-5
Table 2.2.	Sediment and SAV phosphorus storages in the inflow and outflow halves of three mesocosms operated at different hydraulic loadings rates (HLR) and retention times (HRT) for a three-year period.	2-7
Table 2.3.	Phosphorus storages recovered in the biomass (vegetation and fauna) and sediments, as compared to the difference in inflow and outflow water column concentrations, from three mesocosms operated at different hydraulic loading rates (HLR) and retention times (HRT) over three years.....	2-8
Table 2.4.	Vegetation P storage, P storage in newly deposited sediments, and overall P mass balance for the shallow, medium, and deep mesocosms.	2-18
Table 2.5.	Water quality characteristics in the inflow and outflows from mesocosms operated at constant and variable water depths ranging from 0.15 - 1.2 m, from March 20 - November 10, 2000.....	2-22
Table 2.6.	Mass removal rates and removal efficiencies in mesocosms operated at static and variable depths.	2-25
Table 2.7.	Mean inflow and outflow total P concentrations of triplicate harvested SAV mesocosms before harvest, and during and after a "recovery" period. Harvesting was performed on August 19, 1999.....	2-27
Table 2.8.	Comparison of STA-2 and DBE loading schedules.....	2-36
Table 2.9.	Forty-week (Feb. 20 - Nov. 24, 2000) pulse loading schedule for low, medium, and high loaded mesocosms in Subtask 5v.....	2-37
Table 2.10.	Average total phosphorus concentrations in the water column (outflow region) of NATTS pulse loaded mesocosms, during quiescent (7 two-week periods) and flowing (13 two-week periods) conditions.....	2-41
Table 2.11.	Water quality characteristics of limerock (LR) outflow during the first 21.5 hours of flow on March 6, 2000, following a two-week period of no flow. The pulsed loading data are compared to the limerock outflows from the constant hydraulic loaded (non-pulsed) mesocosm evaluation during the February-April 2000 quarter.....	2-44
Table 2.12.	Chemical characteristics of the inflows and outflows of mesocosms receiving high and low hydraulic loading rates (HLRs), and of outflows from downstream limerock barrels, during a six-week baseline monitoring period prior to drawdown.....	2-45
Table 2.13.	Characteristics of sediment core incubation water collected from the Cell 4 inflow region on January 10, 2001.....	2-50
Table 2.14.	Recolonization of mesocosms receiving hydraulic loading rates of 53 cm/day and 11 cm/day after a 110-day dryout period.	2-54

Table 2.15.	Comparison between one SAV- and two cattail-dominated mesocosms at the NATTS. Average values and range in the inflow and outflow concentrations of SRP, DOP, PP, TP, dissolved calcium, alkalinity, specific conductance, pH and temperature during the period of record from December 29, 1998 to August 8, 2001.	2-70
Table 2.16.	Phosphorus removed from the water column over the 2.7-year assessment period, and P recovered in the <i>Najas</i> and cattail vegetation and sediments upon termination of the project on August 20, 2001.	2-73
Table 2.17.	Phosphorus concentrations in the live and dead cattail shoots, below-ground cattail (roots and rhizomes), and SAV tissues retrieved from within the cattail-dominated mesocosms on August 20, 2001.	2-73
Table 2.18.	Soluble reactive phosphorus concentrations at four stations along the shallow, low velocity raceway gradient during the February–April 2000 quarter.	2-77
Table 2.19.	Total P concentrations in the inflows and outflows from shallow SAV/periphyton raceways and outflows from subsequent limerock beds during periods of high and low flow velocity.	2-80
Table 2.20.	Mean total phosphorus concentrations in the inflow and outflows from SATT mesocosms established on muck, limerock and sand substrates during the entire period of record (July 1999 – November 2001) and during reduced hydraulic loading (April 17, 2000 – January 9, 2001).	2-83
Table 2.21.	Mean phosphorus concentrations in the inflow and outflows of duplicate substrate mesocosms during an eight-week period (August - September 2000) of low hydraulic loading (3.75 cm/ day).	2-85
Table 2.22.	Media types and sizes used in the Filter Media Evaluation.	2-86
Table 2.23.	Mean TP, SRP, PP, DOP, calcium and alkalinity concentrations in the inflow and outflows of filter media columns during the August 18–November 17, 2000 period of record.	2-88
Table 2.24.	Final concentration of nutrients and micronutrients amended to W. Palm Beach tap water during the P-deficient and P-enriched conditioning period (35 days) and the final incubation (29.5 hr).	2-101
Table 2.25.	Chemical characteristics of water column and plant tissues before and after a 29.5 hr incubation of <i>Najas</i> tissues in low- and high-calcium/alkalinity waters.	2-105
Table 2.26.	Mean (\pm 1 s.d.) total P, TSP, SRP, dissolved Ca and alkalinity concentrations in the inflows and outflows from duplicate aquaria operated under four treatments during the five month evaluation (November 6, 2000 – April 15, 2001).	2-109
Table 2.27.	CaCO ₃ saturation indexes (SI) and pH values in the inflow and outflow waters from microcosms which received tap water unamended and amended with SRP and Ca/ alkalinity for 160 days.	2-111

Table 2.28.	Concentration ranges for inflows and outflows from duplicate microcosms operated under conditions of unamended and amended calcium, alkalinity, and SRP.	2-118
Table 2.29.	Total deposited dry mass and total phosphorus, inorganic carbon, organic carbon and calcium concentrations of sediments collected from microcosms which received tap water unamended and amended with SRP and Ca/alkalinity for 160 days.	2-122
Table 2.30.	Phosphorus concentrations and pH of unfiltered and particle size-fractionated inflow and outflow waters of Cell 4.	2-138
Table 2.31.	The pH and Eh values of Cell 4 unfiltered and size- fractionated inflow and outflow waters incubated under different environmental conditions.	2-140
Table 2.32.	Phosphorus mineralization rates in inflow and outflow waters of the SAV-dominated Cell 4 in STA-1 West under different incubation times and conditions.	2-147
Table 2.33.	Sampling locations of the surface waters, sediments, periphyton, <i>Chara</i> , and cattail used for assaying alkaline phosphatase activity.	2-149
Table 2.34.	SRP, TP, TSP and color concentrations, and pH of the surface waters in NTC-15 and Cell 4 sampled on October 25.	2-151
Table 2.35.	Total phosphorus, nitrogen, carbon, organic and inorganic carbon concentrations, and ash-free dry wt, from inflow and outflow locations where SAV, cattail, periphyton, and sediment were sampled for APA.	2-153
Table 2.36.	Fluorescent background checks for sample water autofluorescence and MUF contamination of the MUF assay enzyme.	2-153
Table 2.37.	Alkaline phosphatase activity for waters collected from NTC-15 and Cell 4 on October 25, 2001.	2-154
Table 2.38.	Alkaline phosphatase activity of the periphyton (<i>Scytonema</i> spp.) collected from the outflow of the shallow raceways on November 4, 2001.	2-154
Table 2.39.	Alkaline phosphatase activity of the <i>Chara</i> collected from the shallow raceways on November 4, and <i>Typha</i> and <i>Chara</i> collected from STC-1 and STC-4 on November 15, 2001.	2-155
Table 2.40.	Alkaline phosphatase activity of SAV- and cattail-dominated sediments.	2-156
Table 3.1.	Summary of calibration measurements for test cell inflows.	3-5
Table 3.2.	Errors in test cell outflow calculations due to head estimation uncertainty.	3-7
Table 3.3.	Summary of hydrologic parameters during the first test cell tracer assessment.	3-7
Table 3.4.	Comparison of recovered dye mass with the dye amounts injected to test cells operated at two different water depths during two separate dye investigations.	3-17

Table 3.5.	Comparison of nominal (τ) and measured (τ_a) hydraulic retention times for four test cells during two separate dye tracer investigations.	3-17
Table 3.6.	Comparison of key hydraulic parameters among four test cells during the first and second dye studies.	3-19
Table 3.7.	Bulk density, total P and total Ca concentrations, P storage, and accrual rate for sediments along a longitudinal gradient in each SAV-dominated test cell.....	3-23
Table 3.8.	Accrual rates (cm/yr) of sediments according to feldspar horizon markers in four SAV-dominated test cells from August 23, 2000 to September 20-21, 2001.....	3-26
Table 3.9.	Mean monthly total Kjeldahl nitrogen (TKN), nitrite + nitrate nitrogen ($\text{NO}_x\text{-N}$), and ammonium nitrogen ($\text{NH}_4\text{-N}$) concentrations in the inflow and outflow of four test cells (NTC-1, NTC-15, STC-4, STC-9) dominated by submersed aquatic vegetation from October 14, 2000 to April 16, 2001 and on July 18, 2001.	3-27
Table 3.10.	The history of water depths, hydraulic loading rates (HLR), and hydraulic retention times (HRT) in the test cells from August 4, 2000 until termination of the assessment (September, 2001)..	3-28
Table 3.11.	Soluble reactive P (SRP), dissolved organic P (DOP), particulate P (PP), and total P (TP) removals in the north test cells before (September 1, 1999 to April 4, 2000) and after (June 23, 2000 to September 14, 2001) the installation of the LR berm at NTC-15.....	3-29
Table 3.12.	Hydraulic loading rate (HLR) and phosphorus mass loading and removal rates for the north and south test cells after installation of limerock berms in NTC-15 and STC-9. Data from the north test cells are divided into the entire period of record after limerock berm installation (6/23/00 to 9/14/01) and a shorter period (6/02/01 to 9/14/01) for when hydraulic loading rates were high (22.4 and 20.5 cm/day).	3-30
Table 3.13.	Soluble reactive P (SRP), dissolved organic P (DOP), particulate P (PP), and total P (TP) removals in the south test cells before (September 1, 1999 to March 13, 2000) and after (August 4, 2000 to September 14, 2001) the installation of the LR berm at STC-9.....	3-33
Table 3.14.	Dissolved calcium and total alkalinity concentrations, specific conductance, and pH in the north and south test cells after the installation of the LR berms at NTC-15 (June 23, 2000 to September 14, 2001) and at STC-9 (August 4, 2000 to September 14, 2001).....	3-35
Table 4.1.	Summary of Cell 4 regression analyses based on 1998 – 1999 Data. Note that K vs. HLR and K vs. mass loading regressions should be interpreted with caution, as there is a degree of auto-correlation in these calculations.....	4-7
Table 4.2.	Summary of Cell 4 and Mesocosm 'Velocity Effect' Comparison.....	4-7
Table 4.3.	Standing stock of SAV and tissue P, N, and Ca contents in the dominant submerged species at 11 locations in Cell 4 on April 25, 2001.	4-24

Table 4.4.	Accrual depth, bulk density and P, N, and Ca concentrations in the native muck and accrued wetland sediments from Cell 4.	4-24
Table 4.5.	The P, N, and Ca sediment and SAV wetland storages in the inflow and outflow halves of Cell 4.	4-25
Table 4.6.	Duration of desiccation, and before (initial) and after (final) dry:wet weight ratios and moisture loss, for the inflow and outflow sediments of Cell 4.	4-34
Table 4.7.	Dissolved calcium and alkalinity concentrations and specific conductance values in Cell 4 inflow and outflow waters before and after Ca/alkalinity amendments.	4-36
Table 4.8.	SRP and dissolved Ca diffusion flux rates (mg/m ² /day) for the inflow region of Cell 4.	4-53
Table 4.9.	SRP and dissolved Ca diffusion flux rates (mg/m ² /day) for the outflow region of Cell 4.	4-53
Table 4.10.	Effects of different evaporation temperatures on the recoveries of N, C, $\delta^{15}\text{N}$, $\delta^{13}\text{C}$ in peptone and dissolved organic matter from surface waters collected in the inflow and outflow of NTC-1 on January 26, 2001.	4-55
Table 4.11.	Stable isotopes ($\delta^{15}\text{N}$ and $\delta^{13}\text{C}$) in particulate organic matter filtered from surface waters collected in the inflow and outflow of NTC-1 on January 26, 2001.	4-56
Table 4.12.	Mean \pm s.d. (n=2) $\delta^{13}\text{C}$ (‰) for dissolved and particulate fractions of surface water samples collected from NTC-15 inflow and outflow, and NTC-5 outflow, from July 26, 2001 to January 27, 2002.	4-57
Table 4.13.	Mean \pm s.d. (n=2) $\delta^{15}\text{N}$ (‰) for dissolved and particulate fractions of surface water samples collected from NTC-15 inflow and outflow, and NTC-5 outflow, from July 26, 2001 to January 27, 2002.	4-58
Table 4.14.	Mean \pm s.d. (n=2) $\delta^{13}\text{C}$ (‰) for dissolved and particulate fractions of surface water samples collected from the inflow and outflow of Cell 2 and Cell 4 from August 10, 2001 to March 8, 2002.	4-58
Table 4.15.	Mean \pm s.d. (n=2) $\delta^{15}\text{N}$ (‰) for dissolved and particulate fractions of surface water samples collected from the inflow and outflow of Cell 2 and Cell 4 from August 10, 2001 to March 8, 2002.	4-59
Table 4.16.	Number of samples collected at the Cell 4 outfall each day after injecting Rhodamine-WT into the wetland.	4-66
Table 4.17.	Key hydrologic variables present during the two Cell 4 tracer studies.	4-73
Table 4.18.	Comparison of key hydraulic parameters for the two tracer studies in Cell 4.	4-74
Table 4.19.	Total P concentrations in the inflows and outflows of Cell 4 during the second dye tracer assessment. Rhodamine-WT was injected on November 27, 2001.	4-76

Table 4.20	Summary of equations in the PMSAV water balance.....	4-86
Table 4.21	Summary of constants in the PMSAV water balance.....	4-86
Table 4.22.	Summary of coefficients and parameters for Cell 4 hydraulic model.....	4-90
Table 4.23.	Summary of equations in the PMSAV P-removal model.....	4-93
Table 4.24.	Summary of calibration constants for PMSAV.....	4-94

List of Abbreviations

APA	alkaline phosphatase activity
ATT	Advanced Treatment Technology
BMP	Best Management Practices
DBE	DB Environmental, Inc.
District	South Florida Water Management District
DOP	Dissolved Organic Phosphorus
EAA	Everglades Agricultural Area
ECP	Everglades Construction Project
EFA	Everglades Forever Act
ENR	Everglades Nutrient Removal Project
EPA	Everglades Protection Area
EPD	Environmental Protection District
ETAC	Everglades Technical Advisory Committee
FDEP	Florida Department of Environmental Protection
HLR	Hydraulic Loading Rate
HRT	Hydraulic Retention Time
MDL	Method Detection Limit
NATTS	North Advanced Treatment Technology Site
NTC	North Test Cells
PP	Particulate Phosphorus
ppb	parts per billion
SATTS	South Advanced Treatment Technology Site
SAV	Submerged Aquatic Vegetation
SAV/LR	Submerged Aquatic Vegetation/Limerock
SRP	Soluble Reactive Phosphorus
STA	Stormwater Treatment Area
STC	South Test Cells
STSOC	Supplemental Technology Standard of Comparison
TP	Total Phosphorus
TRP	Technical Review Panel
TSP	Total Soluble Phosphorus
WCA	Water Conservation Area

Executive Summary

Introduction

The South Florida Water Management District (District) is sponsoring an assessment of Supplemental, or Advanced Treatment Technologies (ATT) that could work in concert with Stormwater Treatment Areas (STAs) to reduce phosphorus (P) loadings from Everglades Agricultural Area (EAA) runoff. This document summarizes results from a “Follow-On” assessment and demonstration project with the submerged aquatic vegetation/limerock (SAV/LR) technology. In addition to District support, the U.S. Environmental Protection Agency (US EPA), through a contract with the Stormwater/Nonpoint Source Management Section of the Florida Department of Environmental Protection (FDEP), provided 30% of the funding for this project through a Section 319 Nonpoint Source Management Program grant. For this effort we addressed key biogeochemical and hydraulic wetland processes, as well as design and management protocols pertaining to the scale-up of SAV/LR technology.

The Submerged Aquatic Vegetation /Limerock Concept

In the submerged aquatic vegetation/limerock (SAV/LR) concept, P-enriched water first flows through a submerged macrophyte dominated wetland, where P is removed by plant uptake as well as by coprecipitation with CaCO_3 under high pH conditions in the water column. Phosphorus removed from the water column in SAV communities is deposited as a component of a relatively stable, high calcium, marl sediment. Limerock, the second component of the SAV/LR system, is deployed as a berm near the outflow region of the SAV wetland. This limerock “filter” can capture particulate P (PP), lower the water pH, and at times, add calcium (Ca) and alkalinity to the water column.

Project Goal

Our project goal was to develop, and evaluate, design criteria and management protocols that result in a technically feasible, cost-effective SAV wetland system that reduces P in Post-BMP waters to lowest possible outflow concentrations. The basis of our assessment and demonstration effort therefore was to gain a greater understanding of the following key processes of SAV wetlands and limerock filters.

- *Biogeochemical Processes:* What are the mechanisms by which SAV systems remove water column P to low levels? Additionally, what can be done to encourage these processes?
- *Hydraulic Processes:* STA cells are prone to hydraulic inefficiencies. We therefore initiated efforts to define the significance of these inefficiencies on treatment performance, and to suggest techniques for improving system hydraulics.
- *Ecological Processes:* Can SAV communities develop on a large scale along the 120 – 10 µg/L total P gradient, and can they be maintained along this nutrient gradient under conditions of varying flows, depths and drought?

For this effort, we performed a suite of evaluations using laboratory, microcosm, mesocosm, pilot-scale and full-scale platforms. A synopsis of key findings follows.

Key Project Findings

Water Column Phosphorus Removal

Phosphorus Removal Mechanisms

For Post-BMP waters that contain a large percentage of labile P (i.e., soluble reactive P [SRP]) and high levels of calcium and alkalinity, both plant assimilation and coprecipitation with CaCO_3 are prominent P removal mechanisms in SAV communities. A portion of the more recalcitrant P forms, such as dissolved organic P (DOP) and particulate P (PP), can also be removed from the water in SAV communities, but this occurs at a much slower rate than for SRP. Particulate matter exported from SAV wetlands consists of macrophyte detritus, plankton and calcite crystals. We found that larger particles ($>0.4\ \mu\text{m}$) are more amenable to bacterial mineralization than to enzymatic hydrolysis, while smaller particles ($<0.4\ \mu\text{m}$) are susceptible to enzyme hydrolysis.

A portion of the water column DOP also is likely removed in SAV communities by enzymatic hydrolysis. In the laboratory we hydrolyzed the bulk of the water column DOP with a diesterase enzyme, and in a full-scale SAV wetland, we found an increase in activity of a monoesterase enzyme from inflow to outflow regions of the wetland. Despite this activity, however, some residual DOP and PP consistently is exported from SAV wetlands.

Phosphorus Removal as a Function of Platform Size and Water Type

We used both mesocosms (~4 m²) and test cells (~2,000 m²) to evaluate P removal from Post-BMP waters. Performance between the two platforms was comparable. At high hydraulic loading rates (11 cm/day), a SAV test cell wetland equipped with a limerock berm reduced inflow TP levels of 73 to 23 µg/L, removing P at a rate of 2.1 g/m²-yr (64% removal). For Post-STA waters that contain mostly PP and DOP, P removal on a mass per unit area basis is reduced compared to Post-BMP waters. The full-scale wetland STA-1W Cell 4 (147 ha) outperformed the 0.2 ha test cells in treating Post-STA waters, providing mean TP inflow and outflow concentrations of 52 and 22 µg/L from February 1, 1995 – September 30, 2001. Mass P removal by Cell 4 during this period averaged 1.6 gP/m²-yr, with a mean TP removal rate of 62%. Small mesocosms provided P removal performance intermediate between Cell 4 and the test cells. With respect to minimum achievable outflow concentrations, both Cell 4 and the mesocosms provided a mean flow-weighted outflow TP concentration of 14 µg/L for a two-year period (1998 – 1999).

Effects of Hydraulic Loading Rate

Findings from all platforms demonstrate that mass P removal rate by the SAV community increases with increasing HLR (which typically equates to increasing P loads). Effluent concentrations, however, can increase with increasing HLRs. In a mesocosm evaluation, SAV wetlands operated for 3 years at HLRs of 11, 22 and 53 cm/day reduced mean TP inflows of 97 µg/L to 25, 31 and 51 µg/L, respectively. For perspective, the mean HLR of the STAs will be 2.6 cm/day.

Effects of Pulsed Hydraulic Loading

Pulsed hydraulic loadings, where long periods of stagnation are interspersed with high flows, reduced overall P removal effectiveness of the SAV mesocosms relative to constant HLR conditions. Detrimental effects of pulsing were most pronounced with mesocosms that received a high average HLR (i.e, 53 cm/day, representing the hydraulic load to the immediate inflow region of an STA), and were minimal in SAV wetlands that received a lower HLR (11 cm/day, representing approximately the first 25% of the STA footprint).

Effects of Water Depth (Fluctuating and Static)

Under static depth conditions, P removal performance by SAV was comparable over a water depth range of 0.4 – 1.2m. SAV mesocosms subjected to a fluctuating depth regime exhibited a slight reduction in P removal performance.

Effects of Vegetation Harvest Regime

Partial harvesting of SAV from mesocosms resulted in short-term (~ 7 weeks) impairment of treatment performance. Because of performance impairment and high costs, SAV harvest is unlikely to be a management practice implemented in full-scale STAs.

Effect of Substrate Type

Over two years, the standing crop of SAV in mesocosms cultured on muck was more robust than SAV cultured on more inert (limerock or sand) substrates. SAV cultured on muck provided comparable P removal performance to SAV cultured on limerock.

Performance of Limerock Berms and Filters

Limerock berms are effective at trapping particulate matter and converting the associated P to SRP. In the 0.2 ha test cells, limerock berms were effective in enhancing P removal from both Post-BMP and Post-STA waters.

Sediment Characteristics and Stability

SAV Wetland Sediment Characteristics

Phosphorus removed from the water column in SAV communities becomes a component of a calcium (Ca) – enriched sediment (~15 - 22% Ca). The sediment accrual rate and P content is related to the P loading history for the particular SAV community. Sediment accrual rates in the inflow and outflow regions of Cell 4 have averaged 1.7 and 0.5 cm/yr, respectively, since the onset of flooding in August 1993. Cell 4 inflow region sediments contain an average of 1,301 mgP/kg and outflow region sediments contain 631 mgP/kg.

Sediment Accrual and Phosphorus Mass balances

SAV mesocosms have proven useful for defining the fate of P sequestered within SAV communities. In mesocosms operated for three years, between 70 – 99% of P removed from the

water column was recovered in sediment and biota compartments, with sediments comprising the primary P sink (78 – 85% of the recovered P).

Stability of SAV Sediments

Phosphorus fractionations revealed that much of the P sequestered in SAV communities is associated with a fairly stable, Ca-bound sediment fraction. Relative to inflow region sediments, Cell 4 outflow region sediments are extremely stable, and exhibit little P release in response to anoxia, desiccation and low pH conditions.

Sediment-Water Column P Fluxes

Porewater equilibrators deployed in Cell 4 further demonstrated the stable nature of the Cell 4 outflow region sediments. Porewater SRP concentrations in Cell 4 inflow region and outflow region sediments averaged 535 and 25 µg/L, respectively. The flux of SRP from sediment to water column was calculated to be 0.10 mg/m²-day for inflow region sediments, and 0.007 mg/m²-day for outflow region sediments.

Hydraulic Performance

Despite providing exemplary P removal performance, Cell 4 exhibits poor hydraulic characteristics. Two tracer studies demonstrated that Cell 4 behaves more like a continuously stirred tank reactor than a plug flow system, exhibiting an extremely low “tanks-in-series” (TIS) value of between 1.1 and 1.4. Levee canals and relic farm canals that lie parallel to flow are responsible for the poor hydraulic performance of the wetland.

Ecology of SAV Communities

SAV Colonization

We assessed the colonization of SAV in STA-1W Cell 5, a 930 ha wetland that was initially flooded in March 1999. Two SAV species, *Ceratophyllum demersum* and *Najas guadalupensis*, were found throughout the wetland within 16 months after flooding. Relic farm canal soils appeared to provide the principal inoculation source for these species. *Hydrilla verticillata* did not appear in Cell 5 until a year after flooding, but since that time it has spread throughout the wetland.

SAV Sustainability

A diverse SAV community, consisting principally of *Ceratophyllum*, *Najas* and *Potamogeton illinoensis*, has thrived in STA-1W Cell 4 for eight years. This, coupled with performance data, confirms that SAV can persist and provide effective water column P removal in the “back half” of an STA at an operational scale.

Impacts of Dessication and Reflooding

We subjected SAV in mesocosms to a 110 day desiccation period, and then reflooded the systems to assess P export and vegetation recovery. Despite the absence of any living biomass at the end of the desiccation period, the SAV community recovered within six weeks of rehydration. Phosphorus was exported briefly upon reflooding, and overall P removal effectiveness was reduced for about two weeks following rehydration.

Recommendations

The existing sustainability and performance data on SAV/LR systems demonstrate that this technology is quite promising. However, information needs related to the successful deployment of SAV wetlands in the STAs are numerous. In our view, the most important are as follows:

- the sustainability and P removal effectiveness of SAV wetlands used for treating Post-BMP waters (waters with higher inflow TP levels than Cell 4) should be verified at an operational scale.
- the performance benefits that can be achieved through hydraulic improvements (farm canal plugging and limerock level spreaders) should be verified at an operational scale.
- the possible detrimental effects of pulsed hydraulic loadings, with respect to stagnation and high peak loadings, should be assessed at an operational scale.
- because water availability will strongly influence the ability to deploy SAV at an operational scale (and also influence the resulting SAV footprints), factors that influence water budgets (e.g., seepage, potential water availability during droughts) should be quantified for each STA.
- large-scale evaluations of drydown and reflooding on SAV sustainability and performance should be performed.

- hydrilla is proving to be an effective competitor in full-scale SAV communities. Its P removal performance therefore should be quantified.
- our findings on SAV performance (all performed at STA-1W) may not be transferable to the other STAs, due to basin-specific differences in soils and inflow water chemistry (e.g., P speciation, calcium content). Key biogeochemical and ecological factors that can influence SAV sustainability and performance should be addressed for each STA.

Section 1: Introduction and Project Background

The Everglades is an internationally recognized ecosystem that covers approximately two million acres in South Florida and represents the largest subtropical wetland in the United States. However, the biotic integrity of the Everglades ecosystem has been endangered by the alterations of hydrological and nutrient regimes due to urban and agricultural development. Reduction of total phosphorus (total P) from the Everglades Agriculture Area (EAA) runoff is a prerequisite to restoring and protecting the remaining Everglades natural resources. The 1994 Everglades Forever Act (EFA, Section 373.4592, Florida Statutes) requires that water released from the EAA into the Everglades Protection Area (EPA) meet a threshold discharge limit for total P. In the first phase of Everglades restoration, the primary focus is placed on evaluating, designing and constructing 41,500 acres of macrophyte-based stormwater treatment areas (STAs). These wetlands are designed to reduce concentrations of total P in waters released to the Water Conservation Areas (WCAs) for compliance with an interim standard of 50 parts per billion (ppb).

The EFA recognized that this interim total P standard may not be low enough to prevent alteration to the aquatic and wetland ecosystems in the remaining Everglades; ongoing assessments and an anticipated formal rule making process shall seek to define what the ultimate total P standard shall be. Some preliminary evaluations within the Everglades has suggested that the ultimate protective threshold total P could be as low as 10 ppb. To achieve a reduction of total P from approximately 50 ppb to levels as low as 10 ppb, the EFA mandates the District to evaluate a series of supplemental treatment technologies to achieve this final reduction goal.

The South Florida Water Management District (District) had previously contracted with Brown and Caldwell Consultants to identify alternative treatment technologies (ATTs) that might be applied to reducing P levels in EAA runoff (Brown and Caldwell 1992, 1993a, 1993b, 1993c). As a follow-up assessment, the District contracted with PEER Consultants/Brown and Caldwell to re-evaluate the existing nutrient treatment technologies, to investigate new and/or unproven

technologies, and to consider using combinations of technologies in the design of an advanced treatment system (PEER Consultants/Brown and Caldwell 1996).

One of the promising ATTs reviewed by Peer Consultants/Brown and Caldwell is the submerged aquatic vegetation/limerock (SAV/LR) concept. The SAV/LR technology was developed by DBE in the early 1990s. In the original SAV/LR concept envisioned by DBE scientists, P-enriched water first flows through a submerged macrophyte dominated wetland, where P is removed by plant uptake as well as by coprecipitation with CaCO_3 under high pH conditions in the water column. Effluent from the SAV system is fed through a limerock bed, where the limerock surfaces act as a nucleating site for further P coprecipitation with CaCO_3 . The limerock also serves to reduce the pH of the wetland outflow water.

In Phase I mesocosm assessments (1998 – 1999) sponsored by the District and the Florida Department of Environmental Protection (FDEP), we demonstrated that SAV wetlands indeed are very effective for water column P removal. Additionally, in our Phase I efforts we observed that the SAV community appears to form a relatively stable, high calcium (Ca) sediment. In contrast to our original hypothesis, however, the back-end limerock filter appears to capture particulate P (PP), rather than serve as a nucleation site for coprecipitation of soluble reactive P (SRP). Under high hydraulic loadings, some of the PP sequestered by the limerock is converted to SRP, which is then exported from the filter. SRP export from limerock filters under low TP loadings appears minimal.

In the late 1990s, the District contracted with DB Environmental, Inc. (DBE) to conduct a thirteen-month (February 1998 - March 1999) mesocosm evaluation. Results from this assessment indicated that the current SAV/LR system was capable of reducing the outflow P level of EAA waters to as low as 10 ppb. However, these results were obtained under ideal hydraulic conditions (i.e., constant water depths and constant hydraulic loading rates). The District and FDEP determined that further assessments were needed to investigate the P removal capacity of SAV/LR system at larger scales under realistic environmental conditions and to allow a meaningful economic analysis to be performed on the feasibility of scaling up this technology to treat EAA runoff at either the basin or sub-basin scale. Furthermore, several

key environmental variables (e.g., fluctuating water depth, pulsed flow, velocity, filter types and marsh dryout) that may have significant influence on total P removal performance by the SAV/LR treatment technology had not yet been examined.

The District has been operating the Everglades Nutrient Removal (ENR) Project since 1994. This is a large treatment wetland system (3,819 acres) located 25 km west of the city of West Palm Beach in Palm Beach County and borders the northwest corner of WCA-1 (Figure 1.1). The ENR Project served as a prototype STA, and now comprises the bulk of STA-1W. The ENR Project consists of four large treatment cells dominated by either emergent or submerged aquatic plants. Preliminary data analysis indicated that the treatment wetland can effectively remove total P from EAA waters (Chimney and Moustafa 1999), with the best performance coming from Cell 4 (Walker 1999a), an SAV system largely dominated by two submerged plants (*Najas guadalupensis* and *Ceratophyllum demersum*) and associated periphyton. However, Cell 4 contains levee canals and relic irrigation ditches that may cause flow short-circuiting, hence impairing hydraulic performance and possibly compromising P removal efficiency. Further efforts are needed to understand the mechanisms that control the fate of total P entering this system and to optimize the performance of this SAV treatment cell.

1.1 Review of Submerged Aquatic Vegetation/ Limerock Technology and Optimization Needs

1.1.1 Vegetation Community Effects on Phosphorus Removal

The effectiveness of different vegetation types or wetland communities for P removal has been a topic of investigation for more than two decades. Short-term P assimilation by vegetation is related to plant productivity and tissue P content, and investigations of emergent and floating macrophytes at a small scale have demonstrated that there are strong interspecific differences in P uptake rates among macrophytes (Reddy and DeBusk 1985; Tanner 1996).

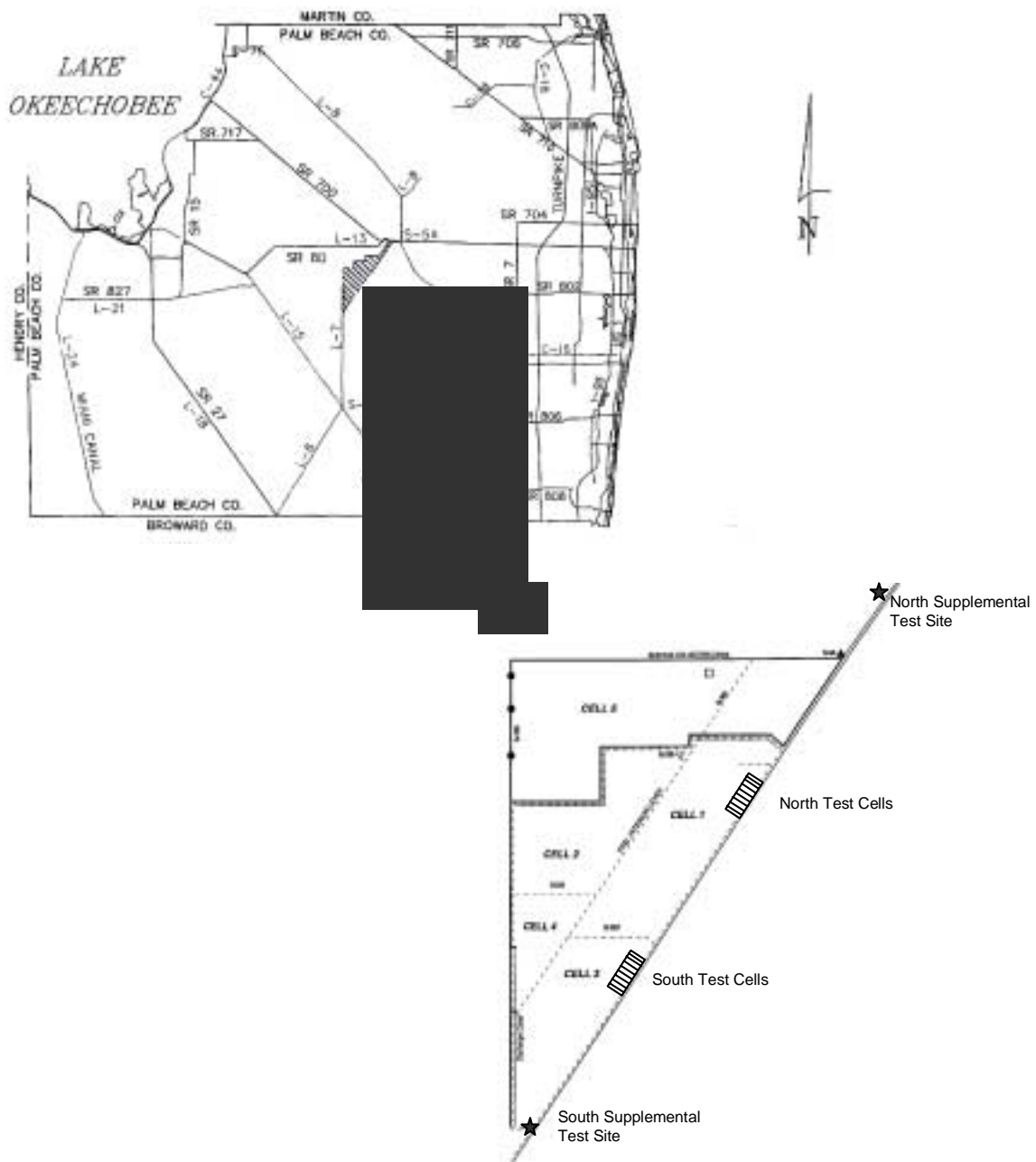


Figure 1.1. Map of STA-1W assessment sites

Interestingly, differences in productivity and nutrient uptake rates observed among macrophyte species do not seem to result in differences in P removal performance of wetlands dominated by these species. During wetland startup, P dynamics in the vegetation compartment are usually masked by the sorption capacity of surficial soils (DeBusk and Dierberg 1999). On a long-term basis, net P accumulation is related to soil and sediment-water interface properties and processes, such as decomposition of plant detritus and microbial scavenging/release of P. Burial of P in sediments is the ultimate P sink in wetlands, and this appears related to the nutrient status of the wetland. Soil P accumulation rates in the northern, nutrient-enriched regions of WCA-2A were found to be as high as 1.2 gP/m²-year, while rates in the southern, nutrient-poor regions were below 0.3 gP/m²-year (Walker 1995).

While nutrient-enriched wetlands generally exhibit high rates of plant productivity and detritus (and P) deposition, much of this deposited P can be released back into the water column under certain environmental conditions (e.g., drought, anaerobic conditions, low pH). The chemical characteristics of the deposited P, as well as the environmental conditions of the sediments and sediment-water interface therefore are master factors in controlling P burial rates. In southern, periphyton-rich regions of WCA-2A, for example, high levels of calcium carbonate are found in the sediments, which is thought to contribute to the stability of sediment P to dryout (Koch and Reddy 1992). In Everglades periphyton communities, the high water column calcium concentrations coupled with high pH levels are also thought to contribute to the effective removal of P from the water column as a calcium carbonate coprecipitation (Reddy et al. 1993; Browder et al 1994).

1.2 Coprecipitation of Phosphorus in Hard Waters

Coprecipitation of phosphates with calcium compounds under alkaline conditions is well documented in the scientific literature. Otsuki and Wetzel (1972) demonstrated 70% removal of phosphate ion in marl waters that contained a calcium content of approximately 70 mg/L. These investigators reported that P removal was only achieved once the water column pH was elevated above 9. They also reported that the reaction time for phosphate removal was only a

matter of minutes once the pH was elevated. This was one of the first studies to directly link phosphate removal under these conditions with formation of particulate carbonates.

Relationships between phosphorus removal, calcium content, and pH elevation have been studied extensively in high-rate algal pond systems (Picot et al. 1991; Moutin et al. 1992; Nurdogan and Oswald 1995). High-rate ponds (HRPs) are frequently employed for treatment of organic wastewaters and share several notable system characteristics (e.g., elevated pH; high Ca concentrations) with SAV wetland systems. Most significantly, both systems are dominated by a water-column biotic community in which daytime photosynthesis produces a substantial pH elevation.

Picot et al. (1991) demonstrated a considerable decrease in ortho-P in HRPs at calcium concentrations between 50-150 mg/L and pH levels between 8-10. Analysis of newly-deposited sediments in the HRP indicated a P concentration of about 60 mg-P/g dry weight, of which 92% was recovered as a calcium bound fraction (Moutin et al. 1992). This effort suggested that assimilation by algae was a secondary removal phenomenon compared to precipitation of calcium phosphate compounds. In laboratory bench evaluations, the coprecipitation reaction was observed to take place immediately at Ca concentration = 108 mg/l when initial pH >8 (Moutin et al. 1992); additionally, phosphate removal efficiency demonstrated a strong correlation with increasing pH ($r^2=0.69$). In similar evaluations, Nurdogan and Oswald (1995) demonstrated that ortho-P removal efficiency increased from 40% to over 90% when the initial calcium concentration was increased from 27 mg/l to 70 mg/l.

1.3 STA-1W (ENR) Cell 4

Insight into the importance of calcium carbonate precipitation to water column P removal in hard water systems led to an important operational recommendation for the startup and management of the ENR project. A scientific Technical Review Panel established by the District recommended that emergent macrophytes in Cell 4 be controlled with water levels and herbicides so that a “periphyton-dominated” community could develop (Kadlec et al. 1991). The report stated: “The final element in the full-scale ENR project (Cell 4) should be focused on lowering P concentrations to values below those normally found in dense macrophyte stands.

Thus the downstream polishing area should be designed and operated to promote algae, including pristine Everglades periphyton species, and associated (sparse) macrophyte communities. The mechanisms of P removal in this cell are anticipated to involve algae-mediated calcium and carbon chemistry. Establishment of such an ecosystem will require initial deep flooding, and maintenance may be necessary to avoid unwanted species. It should also be noted that while the polishing area would contain algae and possibly floating-leaved plants, it may not be possible to duplicate the pristine Everglades ecosystem in the polishing cell".

The District technical staff implemented this recommendation, and has monitored the performance of Cell 4 along with the other three ENR Cells since 1993. Several findings from Cell 4 have proven important to the future performance enhancement of the STAs. First, SAV colonization in Cell 4 demonstrated that large-scale treatment wetlands created from farm fields do not necessarily have to be dominated by cattail. Prior to this experience, it was widely held that at the enormous spatial scale of an STA, little could be done to discourage dense cattail stands. Second, a stable (apparently), diverse submerged plant community has developed and persisted in Cell 4 for eight years. While SAV dominance was not predicted, this community has performed well, exhibiting a P settling rate substantially higher than that of the other Cells (Walker 1999a). The District has compiled a substantial data base on Cell 4, which has allowed a calculation of P mass balance budget (Chimney and Moustafa 1999).

Based on photographic overflight data collected by the District in November 1998, Cell 4 was almost entirely populated by SAV (> 93%). Our more recent observations of the SAV within Cell 4 indicate that *Najas* is the most abundant plant, with major areas colonized by *Ceratophyllum* in the northern (inflow) portion of the cell and *Potamogeton illinoensis* in the southern (outflow) area.

In a December 1998 survey of Cell 4, we found between species, as well as spatial differences in the tissue P concentrations of the major SAV (DBE 1999). Plants sampled from the inflow region contained higher concentrations of P than plants growing near the outflow region. *Najas*, which dominated in both the inflow and outflow regions, exhibited nearly twice the P concentrations at the inflow site than at the outflow region: 1500 vs. 800 mg P/kg. *Ceratophyllum*, which occurs

primarily in the more nutrient enriched inflow zone in the north of the cell, contained an average of 2000 mg P/kg.

Sediment TP data collected by the District in 1998 from the 0-5 cm layer in Cell 4 averaged approximately 600 mg P/kg (Chimney and Moustafa 1999). This compares favorably with the P concentrations (574 mg/kg) we measured for the 0-4 cm sediment depth near the outflow of Cell 4 in December 1998 (DBE 1999). However, the sediments that we retrieved from the inflow region were twice as high in P (1353 mg P/kg) as the sediments collected near the outflow region, indicating an inflow-outflow nutrient gradient exists within the wetland.

1.4 Compartmentalization to Enhance Hydraulic Performance

Presently, each of the Stormwater Treatment Area (STA) wetlands are configured with several large cells (in some cases exceeding 2,000 acres in size) with no other internal compartmentalization. The provision of greater hydraulic control may be needed to improve effluent quality of SAV wetlands. The following discussion addresses potential benefits of additional compartmentalization and flow control.

Performance forecast modeling of treatment wetlands is based on the concept that these systems behave as plug-flow reactors, with flow moving in “lock-step” through the treatment wetland (Kadlec and Knight 1996; Walker 1995). However, tracer studies conducted with emergent, floating and submerged macrophyte-dominated treatment wetlands (DeBusk et al, 1990; DBE 1999; Kadlec and Knight, 1996) reveal that flow patterns may depart widely from ideal plug-flow characteristics. Temperature-related water column density gradients, the heterogeneous and “clumped” nature of vegetation, and uneven microtopographical features can result in the development of rapid flow paths and internal dispersion and mixing (Kadlec, 1990). The net outcome is that some of the influent water reaches the effluent end of the system long before the calculated hydraulic retention time (HRT), and a considerable amount is held longer than the calculated HRT. From a performance forecasting standpoint, these deviations from plug-flow have been addressed by using different hydraulic reactor models, for example, several continuously stirred tank reactors (CSTRs) in series, or a plug-flow reactor followed by multiple CSTRs (Kadlec and Knight, 1996).

Recognition of “non-ideal” flow characteristics, as documented by full-scale tracer studies, has led to most treatment wetlands being designed with a means of evenly distributing the influent across the entire width of the wetland. Once water enters the wetland, however, flows coalesce into small rills, which then combine to create large short-circuiting channels. These flow channels typically remain intact until the water is redistributed by structural means. Both deep channels and earthen berms perpendicular to flow have been used to redistribute water in wetlands (Kadlec and Knight 1996). However, neither rational design parameters nor performance benefits for these structural modifications have been rigorously characterized.

Visual observations in the Everglades Nutrient Removal (ENR) project demonstrated that short-circuiting at the “STA-scale” can also occur along relict farm canals and berms, airboat paths, and/or borrow canals adjacent to external berms. These rapid flow paths conveying only “partially-treated” waters clearly may be limiting the ability of the ENR to achieve lower effluent TP concentrations. Moreover, among treatment wetlands, the STAs exhibit several unique attributes, including pulsed inflows, extremely long flow paths (several km. long) and high current velocities (e.g., 2.7 cm/sec), that may exacerbate the adverse effects of short-circuiting.

Recent performance data has shown that STA cells dominated by submerged aquatic vegetation (SAV) can provide a higher settling rate and lower effluent P concentration than emergent macrophyte-dominated cells (DBEL 1999). While SAV systems appear promising, this plant community is thought to exhibit two characteristics that necessitate greater hydraulic control than emergent macrophyte systems. SAV systems likely have a long recovery time following drydown, so it may be desirable to devise management strategies to keep SAV cells hydrated during extended dry periods. Moreover, rapid inflow pulses may “stack” water on top of SAV beds, resulting in dramatic “vertical” short-circuiting until the submerged vegetation adjusts to the new water elevation. Separation of emergent and submerged vegetation compartments, as well as between-cell hydraulic controls, will likely facilitate survival and P removal performance of SAV communities in an STA.

Further, incorporation of SAV communities in large STA cells also may require internal compartmentalization to maintain integrity of the berms. Submerged species are thought to provide less of an impediment to wind-generated waves than emergent macrophytes, so internal berms may be needed to reduce the degree of wave setup and subsequent erosion.

In summary, incorporation of SAV communities into STAs likely will require additional compartmentalization and hydraulic control, for both ecological and engineering reasons. The flow redistribution provided by internal berms, in addition to benefiting the establishment and performance of SAV communities, should provide overall effluent quality benefits to the STAs.

1.5 DB Environmental's Experience with the SAV/LR Process

Just prior to the time of the startup of the ENR project, DBE scientists began investigating a sequential treatment system based on a SAV wetland followed by a limerock (LR) bed. Based on data from greenhouse-scale performance trials, the SAV/LR concept was selected as one of six candidate "Supplemental Technologies" for further evaluation (PEER Consultants/Brown and Caldwell 1996). The District and FDEP subsequently funded DBE to perform a "Phase I" mesocosm-scale demonstration project from February 1998 through March 1999 at the ENR Northern and Southern Advanced Technology sites. Due to the success of the initial efforts, the District and the Everglades Protection District (EPD) provided additional funding to continue this work through August 1999. This demonstration work, along with in-house evaluations performed by DBE scientists in 1997 and 1998, comprises the only existing technical data on the SAV/LR concept for low-level P removal from EAA waters. A synopsis of both studies follows.

1.5.1 SAV/LR Assessments at DBE's Facilities

From 1997 – 1998, DBE scientists performed a long-term microcosm assessment of the SAV/LR concept. For this 21 month effort, we stocked a small outdoor microcosm with SAV collected from the ENR, and fed Post-BMP water (transported weekly by truck) on a continuous basis through the treatment train, which consisted of a SAV microcosm followed by a downstream limerock bed. Respective hydraulic retention times (HRT) in the SAV and LR unit processes were 1.6 days and 3.8 hours. The SAV microcosm initially was stocked with the macrophyte

Ceratophyllum. During the 21 month effort, the SAV tank gradually became dominated by the macrophyte *Najas*.

For the Post-BMP fed SAV microcosms, total P inflow and outflow over the 21 month evaluation averaged 84 and 30 $\mu\text{g/L}$, respectively. The LR bed further reduced TP to an average of 25 $\mu\text{g/L}$. On a mass basis, the *Najas*-dominated SAV unit process removed approximately 65% of the total inflow P at the extremely short HRT.

Upon completion of this unpublished evaluation, the vegetation and sediments were harvested in order to construct a P mass balance. At this time, the *Najas* biomass exhibited a tissue sediment content of 0.23%, with a P standing stock of 2.3 g P/m². Sediment depths revealed a P accretion rate of 1.1 cm/year, with a P deposition rate of 3.3 g/m²-yr. We found good agreement (85%) between two independent measures of mass P removal rates: aqueous mass P balances [inflow - outflow] and sum of the plant + sediment P storage. At the end of the 21 month period, the sediment in the SAV culture tank contained 72% of the removed P mass (leaving 28% as SAV biomass).

Chemical analysis of the accrued sediment (28% of dry wt as Ca) as well as computed saturation indices strongly suggest that calcium carbonate precipitation was prominent in the SAV microcosm. Despite the occurrence of calcium carbonate precipitation (and likely coprecipitation of P), biological uptake of SRP in the SAV microcosm also appeared to be a significant process. We base this on the poor correlations among the water column concentrations of P and calcium, alkalinity, and pH; the absence of vertical water column SRP concentration gradients during the day; and, consistent SRP effluent concentrations during the diel cycle.

In contrast to our initial hypothesis of SRP precipitation (e.g., as metastable Ca-P precipitates) being the dominant P removal process in the limerock beds, we found particulate P removal to be a more prominent P removal mechanism. Despite the fact that the limerock bed seems to only remove a small fraction of the outflow P from a SAV wetland, inclusion of a LR component in the treatment train may still be useful for the following reasons:

- the LR bed neutralizes the high pH SAV effluent, which can exceed 10.0. This will bring the pH of the final effluent into compliance with receiving water standards.
- LR berms integrated with SAV wetlands can be designed so that they provide multiple benefits, namely enhanced P removal (via particle filtration) and internal flow redistribution.
- for an STA application, the P retention “lifetime” of the LR may be substantial due to the low P loading from the “upstream” SAV unit process.

1.5.2 “Phase I” SAV/LR Assessments at the ENR Supplemental Technology Sites

During the period February 1998 through March 1999, DBE also performed evaluations on the SAV/LR process at three locations in the ENR: the North Supplemental Technology Site, the South Supplemental Technology Site, and within ENR Cells 1 and 4. A synopsis of key findings from this FDEP and District-supported “Phase I” assessments are as follows (DBE 1999).

Pertinent technical findings on Post-BMP waters (North Alternative Technology Site and internal ENR Project measurements)

- The SAV mesocosms operated at HRTs ranging from 7.0 to 1.5 days (HLRs of 11-53 cm/day) removed P at 3.3 to 11.8 g P/m²-yr, mass removal rates that were much higher than those documented for emergent macrophyte wetlands at these nutrient levels.
- Phosphorus removal performance was related to HRT. At a fixed water depth (0.8 m), SAV unit processes operating at 1.5 day (53 cm/day HLR), 3.5 day (23 cm/day) and 7.0 day (11 cm/day) HRTs produced average effluent TP levels of 39, 23 and 18 µg/L, respectively.
- The SAV unit process provided effective TP removal over the range of water depths tested (a range of 0.4 to 1.2 m) at a constant HLR of 10 cm/day.
- The SAV unit process was very effective at removing the SRP (typically 61% of TP) of the influent Post-BMP water. At a 7.0 day HRT (HLR = 11 cm/day), essentially 100% of the SRP was removed by the SAV mesocosms.
- Characteristics and performance of full-scale SAV systems in the ENR Project substantiate our mesocosm findings. Sampling in ENR Cell 1 demonstrated that SRP and dissolved organic P levels in the water column of SAV beds were lower by 10 and 2-fold, respectively, than concentrations of these constituents in emergent macrophyte (*Typha*) stands.

- Despite large day - night fluctuations in pH and dissolved oxygen in the SAV water column, the TP removal performance of the SAV/LR system was consistent on a diel basis.
- Phosphorus removed from the mesocosm influent waters was stored in plant tissues and sediments. Because of the short duration of our studies, SAV tissues were the dominant storage compartment, containing 1.5 times greater mass of P than newly-deposited sediments.
- The newly- deposited sediments in the SAV systems contained high levels of Ca (16%) and moderate P concentrations (503 mg/kg). Sequential extractions of the sediments revealed that the bulk of the P (74-92%) was in non-labile forms (Ca-mineral and residual P). The stability of the remaining “labile” P fractions (e.g., $\text{CaCO}_3\text{-P}$, Fe & Al-P, biogenic P) to environmental perturbations (e.g., low pH, anoxia, desiccation) is unknown.
- Phosphorus stored in the vegetation and newly deposited sediments only accounted for an average of 37% of the P removed from the water column. We attribute our inability to account for the all the P that entered the system to the difficulty in obtaining an accurate sediment accumulation depth due to the short duration of this assessment.
- Because SAV communities are so effective at SRP removal, the challenge to achieving low effluent total P levels (ca. 10 $\mu\text{g/L}$) is to reduce export of particulate P (PP) and dissolved organic P (DOP). These constituents occur in the Post-BMP waters, and can be generated internally within STAs and SAV/LR systems.
- The limerock unit process served principally as a physical filter, removing particulate P. Neither the chemical composition of the rock, nor the physical size of the rock (in a nominal size range of 1.3-5.0 cm in diameter) affected P removal efficiency. Under low P loadings, such as the effluent of a SAV system, a LR bed may be effective for removing PP prior to effluent discharge. Under high loadings, for example near the system influent or mid-point, LR may serve as an efficient transformer of water column PP to SRP, or as a contributor of calcium and alkalinity.
- Fish (bannerfin shiner), zooplankton (water flea), and a unicellular green alga (*Selenastrum capricornutum*) exposed to SAV influent, SAV effluent, and LR effluent waters showed variable chronic toxicity effects. Although the SAV effluent sample slightly reduced fish survival in a statistically significant manner, it was not "biologically" significant. A 50% mortality for the water flea (*Ceriodaphnia dubia*) exposed to the LR effluent was deemed "biologically" significant, but no obvious toxic constituents were found in the water.

- The algal growth potential was reduced 5x-12x in the effluent waters compared to the influent, indicating the effectiveness of the SAV/LR system at reducing nutrient levels.

Pertinent technical findings on Post-STA waters (at the South Alternative Technology Site)

- From July 1998 - February 1999, a shallow (9 cm deep), low velocity periphyton/LR raceway with an HRT of 0.8 days provided a mean effluent TP concentration of 10 µg/L, the tentative “target” concentration for the Alternative Technology program. Influent TP concentrations during this period were low, however, averaging 17 µg/L. A limerock bed with a 1 hr HRT situated at the effluent of the periphyton raceway removed additional P, providing a mean effluent TP concentration of 8 µg/L.
- A deeper (0.65 m) mesocosm system dominated by SAV species and having an HRT of 3.3 days provided a mean effluent TP concentration of only 14 µg/L. Mass P removal for this system was 0.15 g P/m²-yr. A limerock bed with a 1 hr HRT situated at the effluent of the deep SAV system removed additional PP and DOP, reducing TP effluent levels to 11 µg/L.
- Mass balance calculations revealed that nearly all (93 - 102%) of the P removed from the influent water to the low velocity raceway was in the periphyton standing crop. A mass balance could not be performed for the deep SAV system because we could not quantitatively sample the sparse sediments.
- A shallow, high velocity periphyton raceway system (HRT = 6.5-13 minutes) reduced influent TP levels from 17 to 14 µg/L. Mass P removal, based on biomass accumulation of P, averaged 1.4 g P/m²-yr. Productivity and P removal in this routinely harvested system appeared to be limited by low SRP concentrations in the influent waters.
- Neither SAV influent, SAV effluent, nor LR effluent waters caused chronic toxicity effects to fish (bannerfin shiner), zooplankton (water flea), or a unicellular green alga (*Selenastrum*).
- Algal growth potential was reduced in the effluent waters compared to the influent.

1.6 Phosphorus Speciation

An important finding from our “Phase I” effort relates to the role of P speciation in wetland treatment performance. The SAV/LR systems were quite effective at removing SRP, but removal rates of PP and DOP were low. Key issues related to P speciation are the transformations among P species, the transportability of P species, and bioavailability of P

species. These issues are critically important to defining the most appropriate treatment technology (or treatment train), as well as the impacts of these P constituents on downstream receiving waters. At present, however, dynamics and impacts of PP and DOP in South Florida wetlands are largely unknown.

1.7 Project Goals and Assessment Challenges

1.7.1 Project Goal

Develop and test design criteria and management protocols that result in a technically-feasible, cost-effective SAV wetland system that reduces P in Post-BMP waters to lowest possible outflow concentrations.

1.7.2 Assessment Challenges

The ability of the Stormwater Treatment Area (STA) wetlands, along with associated wetland-based “Alternative Technologies”, to meet the Post-BMP water treatment goal of 10 µg/L is complicated by the fact that the Post-BMP waters contain a mix of P species, namely soluble reactive P (SRP), dissolved organic P (DOP) and particulate P (PP). Our analyses of the Post-BMP runoff influent to the STA-1W from June 1998 – May 2001 revealed an average TP concentration of 104 µg/L, with SRP the dominant fraction (49%), followed by PP (36%) and DOP (15%). Our “Phase I” effort demonstrated that the SRP fraction is readily removed by SAV communities, while the DOP and PP fractions are more recalcitrant. Even though the wetland sediments are the ultimate P sink, they, in addition to the standing crop of vegetation, can return each of these P fractions back to the water column (Cooper et al. 1999). Moreover, transformations among the P fractions (between “labile” and “recalcitrant” forms) can occur along the P concentration gradient that is established in the treatment wetland (Figure 1.2).

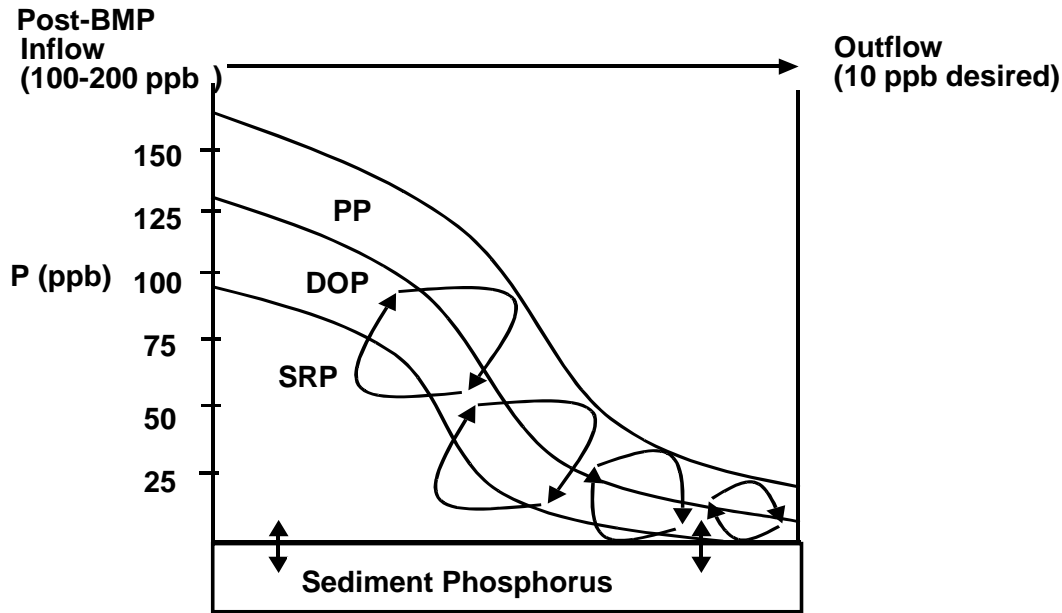


Figure 1.2. Schematic depicting changes in concentration of P species (PP = particulate P; DOP = dissolved organic P; SRP = soluble reactive P) as water passes through an STA treatment wetland. Sediments may act as a P source or sink, and cycling of P forms may occur throughout the wetland.

The task of harnessing large-scale stormwater treatment wetlands to produce extremely low outflow P concentrations is unprecedented, and it is our project team's belief that a sustainable, optimized wetland treatment system can only be achieved through an understanding of key wetland processes. The basis of our Phase II demonstration effort therefore was to gain a greater understanding of the following key processes of SAV wetlands and limerock filters.

- **Biogeochemical Processes:** What are the mechanisms by which SAV systems remove water column P to low levels? Additionally, what can be done to encourage these processes?
- **Hydraulic Processes:** We observed in our Phase I effort that large-scale STA cells are prone to hydraulic inefficiencies. In Phase II we initiated efforts to define the significance of these inefficiencies on treatment performance, and to suggest techniques for improving system hydraulics.

- **Ecological Processes:** Can SAV wetlands be built on a large scale along the 120 – 10 µg/L total P gradient, and can they be maintained along this nutrient gradient under conditions of varying flows, depths and drought?

For our Phase II effort, we performed a suite of evaluations using laboratory, microcosm, mesocosm, pilot-scale and full-scale platforms. A brief synopsis of each Phase II evaluation is provided below, and detailed findings are provided in the following sections of this report. Additional results, focusing on process model simulations, and test cell and Cell 4 performance, are contained in DBE's Supplemental Technology Standard of Comparison (STSOC) final report (DBE 2002).

1.7.3 Mesocosm, Microcosm and Laboratory Assessments

Long-Term Monitoring of SAV Performance

During Phase I, we initiated an assessment (on June 1998) in which sequential SAV wetlands and limerock reactors received Post-BMP waters under three separate hydraulic loading regimes (11, 22 and 53 cm/day HLRs) (DBE 1999). For this effort, we continued operation of these mesocosms to assess long-term performance, and to assess the ultimate fate of sequestered P among the ecosystem compartments (sediments and vegetation).

Impact of Fluctuating Water Depths on SAV Phosphorus Removal Performance

During full-scale operation, the STAs will be subjected to a variable depth regime, with projected depths ranging from 0 to 1.3 meters. During our Phase I studies, we found little difference in P removal performance by SAV mesocosms that received Post-BMP runoff at a 10 cm/day HLR, and operated at steady state water depths of 0.4, 0.8 and 1.2 m. For the current evaluation, we subjected SAV in these mesocosms to a fluctuating depth regime to assess impacts on P removal.

Impact of Vegetation Harvest on SAV Performance

During Phase I, we subjected SAV in mesocosms to a regime of periodic (annual) harvest. For this effort, we continued operations of the mesocosms on Post-BMP waters for several more

months, and performed an additional harvest to assess the impacts of harvesting on P removal performance.

Hydraulic Pulse-Loading Impacts

Hydraulic loadings to the STAs will average about 2.6 cm/day. However, the range of flows will vary widely, with extended periods of no flow interspersed with peak flows in excess of 20 cm/day. We used mesocosms to predict the impact of a pulsed flow regime on SAV performance. Mesocosms that previously were operated with Post-BMP waters under steady-state hydraulic loading conditions were supplied with a “pulsed” HLR regime that mimicked the dynamic STA-2 inflow data set. This 40+ week pulsed regime included periods of stagnant (no flow) conditions, as well as periods of extremely high flows. Performance of the pulsed systems was compared to that of SAV systems operated under steady-flow conditions.

Drawdown – Reflooding Impacts on SAV Wetlands

Our review of the estimated long-term STA-2 flow data set suggests that during extremely dry years, at least a portion of most STAs will totally dry down. Because impacts of drydown are unknown, we performed a mesocosm evaluation to assess drydown impacts on the SAV community and associated sediments. We utilized mesocosms that had received Post-BMP waters under two separate HLRs (11 and 55 cm/day). These mesocosms were dried-down for 105 days. Sediment compaction was assessed over time during drydown, and P-removal/export was evaluated upon re-flooding.

Sequential SAV/LR Systems

During Phase I (October 1998), we established a series of sequential systems (deep SAV followed by shallow SAV followed by LR filters) that were operated under steady HLR conditions, receiving Post-BMP waters. We continued operation of these systems for several months into the Phase II period.

Performance of Cattail vs. SAV

During Phase I (October 1998), we established a pair of cattail mesocosms to provide a performance comparison with adjacent SAV mesocosms. All mesocosms were operated at a 10

cm/day HLR (Post-BMP waters) and at a water depth of 0.4 m. Those operating conditions were continued in Phase II.

Shallow, Low Velocity SAV/Periphyton/Limerock Systems

During Phase I, we established three very shallow (9 cm deep) SAV/periphyton/LR raceways. These systems, receiving Post-STA waters, achieved a relatively consistent 10 µg/L outflow concentration since October 1998. For this effort, we continued operation of these raceways under varying HLR conditions.

Effect of Flow Velocity on P Removal by Shallow, SAV/ Periphyton Communities

We utilized the shallow SAV/periphyton raceways to evaluate effects of flow velocity on P removal performance.

Growth of SAV in Post-STA Waters on Muck, Limerock, and Sand Substrates

Due to concern over the need for an initial, stable substrate in “back-end” SAV communities, we established SAV communities on three substrates (muck, limerock, sand) during Phase I. These mesocosms received varying hydraulic loadings of Post-STA waters.

Effect of Filter Media Type on P Removal Performance

We established outdoor small-scale filter columns and beds to evaluate the P removal effectiveness of different sizes of limerock, as well as other filter media. These systems were tested using Post-STA waters.

Effects of Calcium/Alkalinity and Soluble Reactive P Concentrations on P Coprecipitation in SAV Wetlands

We performed two outdoor microcosm assessments to assess the effects of calcium and alkalinity levels on SAV phosphorus removal performance. Artificial nutrient media, rather than site waters, were used for this effort, due to the difficulty in achieving the desired Ca/alkalinity ranges with STA-1W waters. In the first assessment, “P-enriched” and “P-deficient” *Najas* plants were subjected to high SRP concentrations but varying levels of Ca and alkalinity in a short-term batch evaluation to define the relative importance of SAV uptake vs. coprecipitation in reducing P concentrations in the water column. In our second assessment,

Najas was inoculated into microcosms containing combinations of high and low SRP and Ca/alk concentrations. This flow-through evaluation was performed over a 3-month period, and was designed to facilitate our understanding of the chemical conditions (e.g., pH, alkalinity, Ca and SRP concentrations) that promote P coprecipitation. In this effort we also assessed the quantity and composition of the deposited sediments.

Particulate Phosphorus and Dissolved Organic Phosphorus Characterization and Stability

For this effort, we performed laboratory characterizations of particulate phosphorus (PP) and dissolved organic phosphorus (DOP) collected from ENRP Cell 4, test cells, and mesocosm waters. In one assessment, DOP and PP size fractions isolated from Cell 4 locations were analyzed for enzymatic SRP release, and SRP release under low pH and redox conditions. In a second assessment, alkaline phosphatase activity in ecosystem compartments (sediment, detritus, surface water, and biomass) was analyzed using bench-scale incubations. Finally, PP isolated from SAV and cattail communities inhabiting the inlets and outlets in the test cells and Cell 4 was characterized and compared to assess PP transport and degradation characteristics.

1.7.4 STA-1W Test Cell Assessments

Test Cell Hydraulic Characteristics

Prior to the onset of long-term performance monitoring, we evaluated the hydraulic characteristics of north and south test cells under varying depth and flow regimes.

Test Cell Modification and Long-term Monitoring

At the north bank of test cells, a limerock berm was designed and installed perpendicular to flow 90% down the length of NTC-15. NTC-1 was operated as a control. At the south test cells, a limerock berm was installed perpendicular to flow 90% down the length of STC-9. STC-4 was operated as a control. We monitored P removal performance of the test cells for slightly more than one year, to generate a data set for the District's Standard of Comparison Analysis. Sediment accrual and characterization measurements were performed on each test cell during late 2001.

1.7.5 STA-1W Cell 4 Assessments

Cell 4 Dye Tracer Studies and Hydraulic Optimization Analysis

We performed two hydraulic tracer studies in Cell 4. During both studies, we performed measurements along internal transects as well as at inflow/outflow locations. Time-sequenced maps of spatial dye and total P concentrations, as well as conventional calculations of mean residence time and residence time distribution plots, were used to assess opportunities to improve Cell 4 hydraulics.

Cell 4 Performance Monitoring

We performed internal sampling in Cell 4 to spatially characterize accrued sediment and live SAV biomass. Intensive water quality monitoring at inlet/outlet stations, as well as along internal transects, was also performed to enable us to interpret performance under varying HLR and depth conditions.

Cell 4 Sediment P Stability and Characterization

We performed three types of assessments and analyses to characterize Cell 4 inflow and outflow region sediments. First, we exposed sediments to low and high pH, low redox, low SRP and Ca concentrations, as well as desiccation followed by reflooding. In a second evaluation, we performed inorganic and organic P fractionations to assess P allocation among the various chemical pools and labile/nonlabile forms. Third, we deployed porewater equilibrators to define porewater P concentrations and to quantify diffusion gradients across the sediment-water interface.

Modeling Review and Development

In addition to the above efforts, we developed a predictive model for SAV wetlands, designated Process Model for Submerged Aquatic Vegetation (PMSAV). We used hydraulic and P removal performance data for Cell 4 to guide PMSAV development and calibration efforts.

1.7.6 STA-1W Cell 5 Assessments

Cell 5 SAV Recruitment and Inoculation Studies

As a result of our Phase I efforts, we recommended to the District that STA-1W Cell 5 be flooded quickly, in order to establish SAV communities. To evaluate the rate of SAV colonization in this wetland, we established a vegetation monitoring grid of 120 stations. A semi-quantitative assessment of SAV species was performed quarterly at each station. For this task we also evaluated several SAV inoculation techniques, and performed an *in situ* assessment to evaluate the effect of liming on initial soil P release.

Section 2: Mesocosm, Microcosm, and Laboratory Assessments

The small-scale assessments described in this chapter represent the suite of subtasks described under Task 5 of DBE's Experimental Design Plan (DBE, 2000c). Additional details can be found in that document. The statistical procedures that we employed consisted of first performing a Shapiro-Wilk W test for normality on each treatment and control data set. We also screened the data sets for equal variances. In most cases, the data sets were either non-normally distributed and/or the variances were not equal. We therefore relied on the nonparametric Wilcoxon/Kruskal-Wallis Rank Sums test to examine the significant differences in means between treatments or between a treatment and a control. All statistical tests were performed using version 4 of JMP Statistical Discovery Software (SAS Institute, Cary, NC, USA).

2.1 Long-Term Phosphorus Removal in Mesocosms

In 1998, we established SAV/LR mesocosms at the North Advanced Treatment Technology (NATT) site that were fed Post-BMP waters over a range of hydraulic loading rates. We continued operation of these mesocosms into this Follow-On assessment, primarily to observe P removal performance over a longer duration, and to provide a well-controlled platform for assessing the fate of the sequestered P. The SAV mesocosms were continuously operated at 11, 22 and 53 cm/day HLRs from June 1998 through May 2001. From June 1998 to February 10, 1999, three replicate mesocosms per HLR treatment were sampled, and then again from September 29, 1999 to February 23, 2000. Only one replicate per treatment was sampled between February 10, 1999 and September 29, 1999, and after February 23, 2000 to the end of May 2001.

Prior to November 1999 (during Phase I and the interim 8-month period), we collected weekly grabs for SRP and TP and biweekly grabs for TSP, Ca, and alkalinity from the "long-term monitoring" mesocosms. During fall 1999, we established a new sampling schedule for these mesocosms. Biweekly compositing of weekly grab samples for the SAV mesocosm and LR column (both the 1 and 5 hr retention times) inflows and outflows was initiated on Nov. 17, 1999.

Dissolved organic P (DOP) was calculated as the difference between TSP and SRP; particulate P (PP) was obtained as the difference between TP and TSP. The only P species to measure less than the method detection limit (MDL) in the surface and porewaters was SRP. When this occurred, one-half the MDL (MDL = 2 µg/L) was used for purposes of calculating central tendency and variance.

2.1.1 TP Removal Performance

For this assessment, we controlled the hydraulic loading to the treatment mesocosms at 11, 22 and 53 cm/day, providing hydraulic retention times (HRTs) of 1.5, 3 and 7.0 days. Therefore, the fluctuations in P loading rate that occurred over the 36-month monitoring period (Figure 2.1) were due to variations in inflow TP concentrations (Figure 2.2).

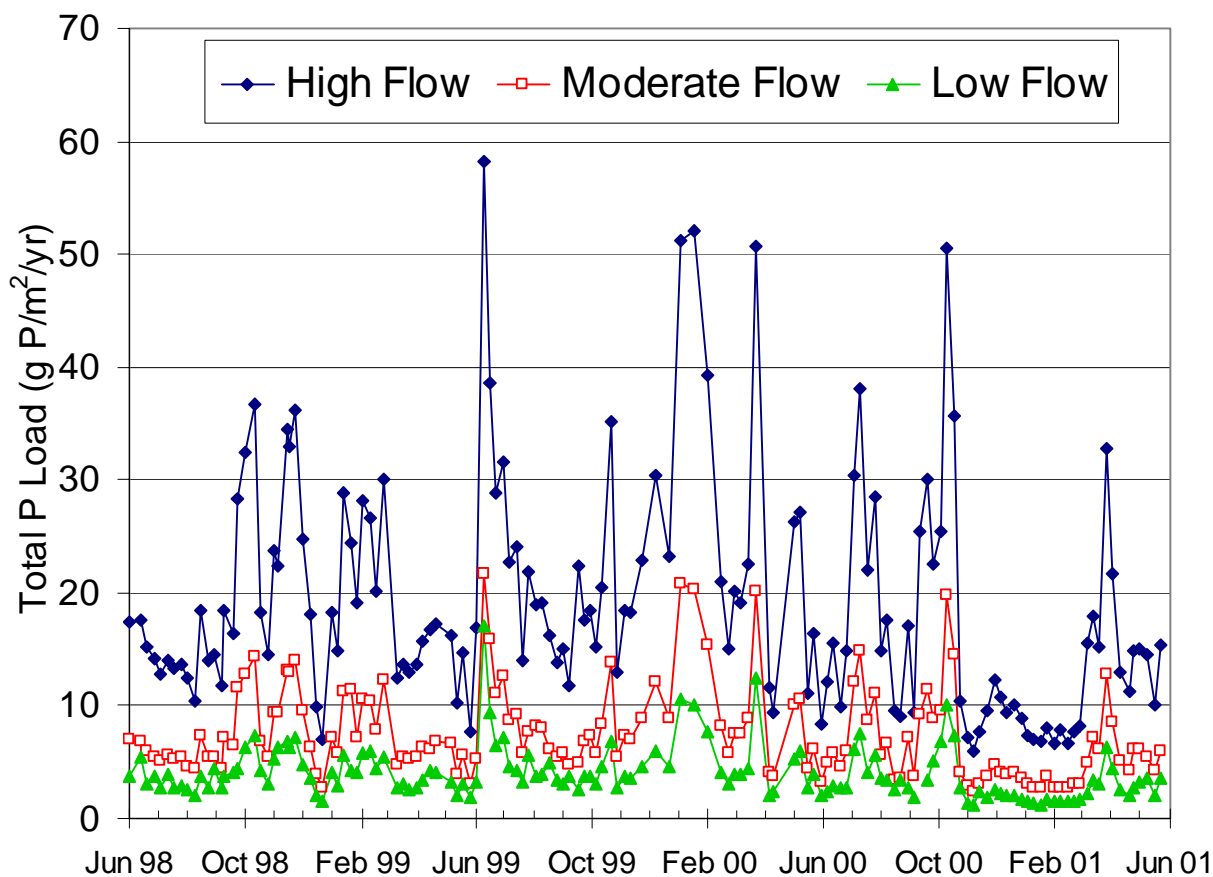


Figure 2.1. Total phosphorus loading rate over the monitoring period June 1998 – May 2001 as the product of variable inflow total P concentration and fixed hydraulic loading rates of 11, 22, and 53 cm/day.

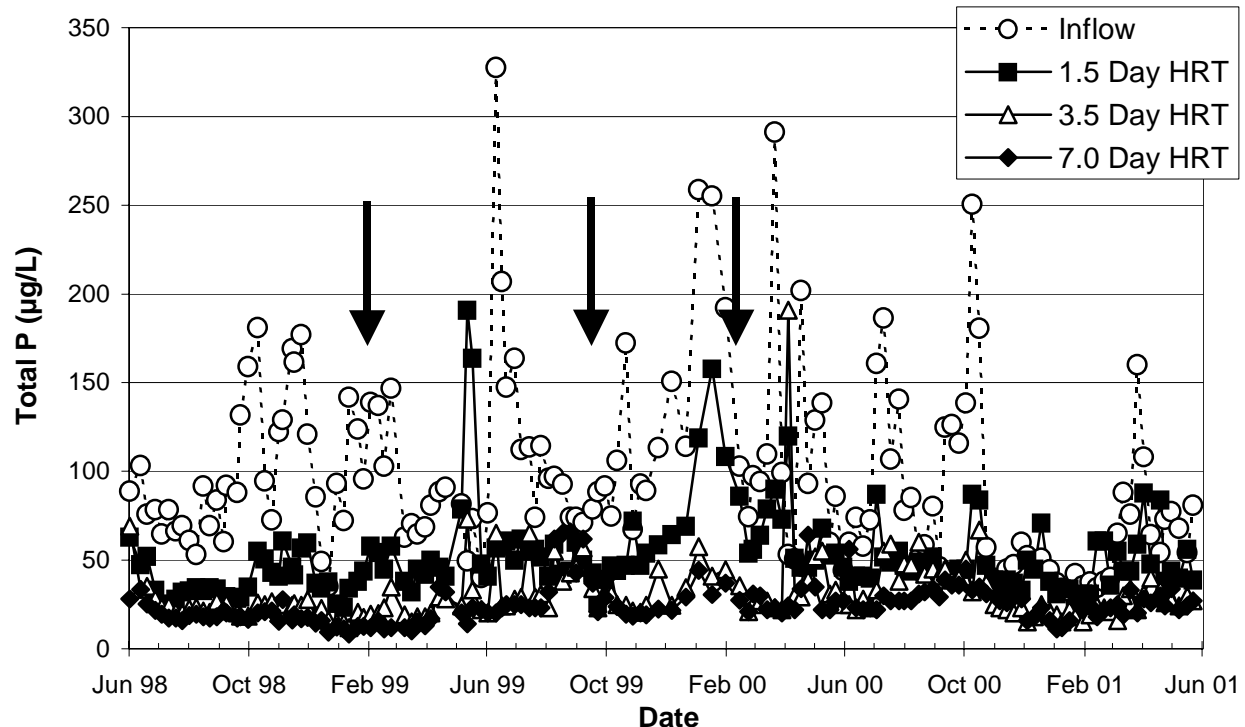


Figure 2.2. Total P concentrations in the inflow and outflows from mesocosms operated at constant hydraulic loading rates of 11, 22, and 53 cm/day from June 1998 – May 2001. Data from one mesocosm of each HRT is presented for the period between February 10 and September 29, 1999 (arrows), and after February 23, 2000, while other values represent means of triplicate mesocosms.

Each of the three mesocosms (HRT = 1.5, 3.5, and 7.0 days) followed the same trend during the long-term POR (June 1998 – May 2001) to what had been established during Phase I (June 1998 to March 1999) (Figure 2.2). That is, effluent SRP and TP concentrations were substantially higher from the 1.5-day HRT mesocosm (12 µg SRP/L and 63 µg TP/L) than from the 3.5- and 7.0-day HRT mesocosms (2 µg SRP/L and 34 µg TP/L for 3.5-day HRT; 2 µg SRP/L and 32 µg TP/L for 7.0-day HRT). Statistical analyses of the TP outflow concentrations from the single mesocosm in each of the three hydraulic treatment groups that had been maintained at a constant HLR indicated that the hydraulic and P loading rates produced significantly different ($P < 0.05$) TP outflow concentrations. The LR columns significantly ($P < 0.05$) reduced TP concentrations further in all three respective HRT treatments to 45, 23, and 18 µg/L, partially by converting PP to SRP (Figure 2.3).

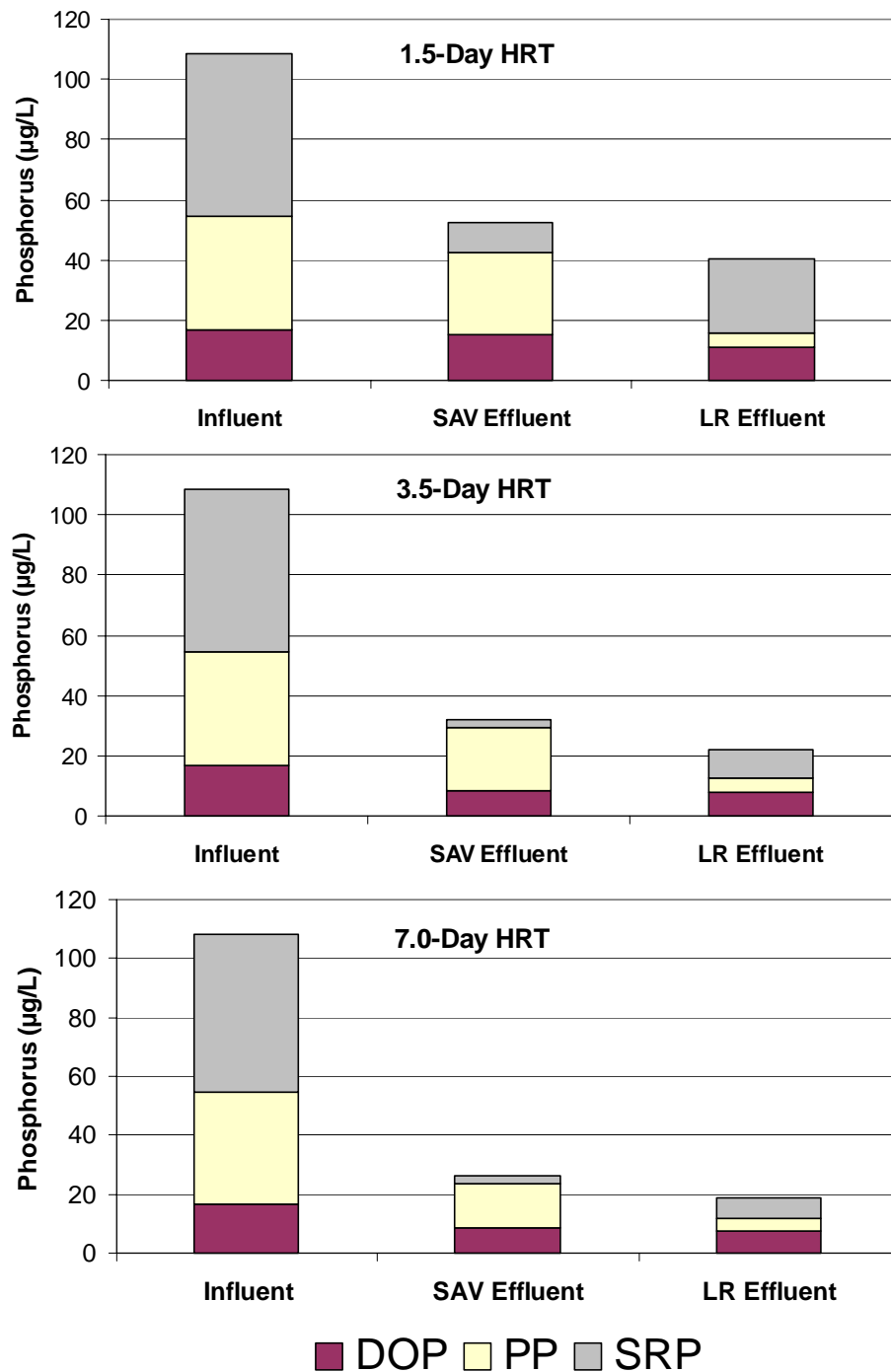


Figure 2.3. Mean soluble reactive, particulate, and dissolved organic phosphorus concentrations in the inflow and outflow from SAV mesocosms and outflow from subsequent limerock filters. SAV systems were operated at HRTs of 1.5, 3.5 and 7.0 days, while each LR filter had an HRT of 5 hours.

Total P loading affected the removal efficiencies within the high HLR treatment (53 cm/day). From November 1999 to January 2000, total P inflow levels (post-BMP waters) were high (~250 µg/L) before returning to levels below 100 µg/L by the end of February 2000 (Figure 2.2). Because of its high HLR (55 cm/day), the outflow from the short retention time mesocosms (1.5 days) tracked the fluctuating inflow concentrations (Table 2.1). Outflow total P concentrations from the 3.5- and 7.0-day HRT mesocosms (37 and 28 µg/L, respectively) were less affected by the high P loading, but still elevated compared to the POR average. They were, however, substantially lower than that of the 1.5-day HRT treatment. From the total P concentration data, it appears that a 1.5-day HRT is too short to successfully dampen the occasional spikes in total P concentrations of the post-BMP drainage waters.

Table 2.1. Total phosphorus concentrations (µg/L) in the inflows, and SAV and limerock (LR) bed outflows from mesocosms operated at hydraulic retention times (HRT) of 1.5, 3.5 and 7.0 days since June 1998.

Period of Record (POR)	Inflow	1.5-Day HRT Outflow		3.5-Day HRT Outflow		7.0-Day HRT Outflow	
		SAV	LR	SAV	LR	SAV	LR
<i>Entire POR</i>							
June 1998 – May 2001	97	51	40	31	21	25	18
<i>Low Inflow TP</i>							
November 2000 – February 2001	42	40	28	20	17	22	18
<i>High Inflow TP</i>							
November 1999 – January 2000	158	80	49	37	21	28	16

The benefit of the LR filter beds at the back-end of the treatment train becomes obvious when comparing the outflows of the mesocosm and LR bed within a given hydraulic treatment during high inflow TP concentrations (November 1999 – January 2000). Within each hydraulic treatment, the LR filter bed provided significant attenuation of the above-average TP concentration in the waters leaving the SAV mesocosms. In fact, the attenuation within the 3.5- and 7.0-day HRT treatments was of such an extent that the outflow TP concentrations from the

LR beds was equal to, or lower than, the respective LR outflow concentrations during the entire POR (Table 2.1). Thus, significant TP reduction of the LR bed is achieved under all TP loading rates, but even more so during high TP loadings.

For the low inflow TP period (November 2000 – February 2001) when the TP concentrations were less than 50% of the average for the entire POR, TP concentrations in the SAV mesocosms outflows were lower than the long-term average for all three hydraulic treatments (Table 2.1). This further illustrates the importance of TP loading on mesocosm outflow TP concentrations, at least over certain P loading ranges.

Soluble reactive P, and to a lesser extent PP, were the P species most susceptible to removal within the SAV mesocosms, regardless of hydraulic treatment. Decreases in dissolved organic P (DOP) were minor (a few $\mu\text{g/L}$) for all hydraulic treatments, but DOP reduction seemed to be more prominent within the longer HRT mesocosms (Figure 2.3). We suspect that longer HRTs provide more time for photolytic, enzymatic and sorption processes to hydrolyze the DOP molecules.

2.1.2 Vegetation and Sediment P Storage

On May 22, 2001, following three years of monitoring, operation of the three long-term mesocosms was terminated. The phosphorus stored within each mesocosm was quantified through vegetation harvest and sediment coring using the following methodology. Flows to each mesocosm were curtailed and the water level was reduced to a depth of 10 cm prior to plant or sediment sampling, which was performed in the “inflow” and the “outflow” half of each mesocosm. All SAV was removed from each region, separated according to species, and wet biomass weights were measured in the field immediately after harvesting. A subsample of each SAV species was returned to the lab for elemental analyses (TP, TN, TCa, TOC, TIC).

Five cores were retrieved from the inflow and outflow regions of each mesocosm. After measuring sediment accretion, the accrued sediments were separated from the underlying muck (former agricultural soils) in the field, composited and returned to the lab for bulk density and elemental analyses. To increase the accuracy of our mass balance, we also collected the fish

and snail populations from within each mesocosm, and quantified P storage by the same methods as the vegetation. Fish and snail biomass were only quantified on a whole tank basis.

Due to the high average TP loading (18.8 g P/m²-yr) in the short (1.5-day) HRT mesocosm, sediment P storage was nearly equal throughout the length of the mesocosm (Table 2.2). However, a noticeable difference was recorded between the inflow and outflow sediments in the 3.5-day HRT (HLR = 22 cm/day), where the outflow sediment contained 14% less P than the inflow sediment. For the highest HRT mesocosm (7.0 days), the inflow sediment contained over three times more P than the outflow sediment. These data clearly indicate that P loading rates affect both the sediment P content and spatial P distribution. The P sequestered in the SAV, on the other hand, was not differentially distributed along the horizontal flow path of any of the three treatments mesocosms (Table 2.2).

Table 2.2. Sediment and SAV phosphorus storages in the inflow and outflow halves of three mesocosms operated at different hydraulic loadings rates (HLR) and retention times (HRT) for a three-year period.

Mesocosm	HLR (cm/day)	HRT (days)	Accrued Sediment (g P/m²)	Δ SAV Biomass (g P/m²)
S-2 Inflow	53	1.5	15.9	1.0
Outflow			15.5	1.0
M-2 Inflow	22	3.5	11.0	0.6
Outflow			9.4	0.6
L-2 Inflow	11	7.0	10.7	0.7
Outflow			3.1	0.7

We used the difference between inflow and outflow water TP concentrations over the course of the POR to calculate the total mass of P removed from the system (Table 2.3). These values were then compared to the observed P stored in accrued sediments and biomass. Mass recovery was greater in the longer retention time mesocosm (7.0 days) and lowest in the shortest retention time mesocosm (1.5 days). The unaccounted P mass in the high flow, short HRT mesocosm could have been due to particle export during short-term events not captured in our biweekly sampling regime. The high flow mesocosm of this evaluation, as well as those in the Pulse-Loading evaluation, were subject to occasional algal blooms, possibly caused by periods of high

inflow SRP concentrations. The storage of P in the sediments relative to measured mass removal from the water column was also greater in the lower flow treatments (Figure 2.4).

Sediment accrual rates ranged from 1.3 cm/yr in the outflow of the mesocosm receiving an HLR of 11 cm/day to 3.1 cm/yr in the 53 cm/day HLR mesocosm. Biomass P increased with increased hydraulic and P loading, but the standing SAV biomass at the end of the 3-year assessment was less than that observed at the end of Phase I efforts (8 month duration). As an SAV system ages, a greater fraction of the P sequestered from the water column would be found in the sediments, as biomass storage is variable but finite, while sediment P accumulation occurs throughout the lifetime of the wetland.

Table 2.3. Phosphorus storages recovered in the biomass (vegetation and fauna) and sediments, as compared to the difference in inflow and outflow water column concentrations, from three mesocosms operated at different hydraulic loading rates (HLR) and retention times (HRT) over three years.

Mesocosm	HLR (cm/day)	HRT (days)	Mass P Loading Rate (g P/m ² -yr)	Storages			Mass P Removed* (g P/m ²)	Mass Recovery (%)
				Accrued Sediment (g P/m ²)	Δ SAV Biomass (g P/m ²)	Fish/Snail Biomass (g P/m ²)		
S-2	53	1.5	18.8	15.7	1.0	1.7	26.2	70
M-2	22	3.5	8.1	10.2	0.6	2.3	16.6	79
L-2	11	7.0	3.9	6.9	0.7	1.0	8.7	99

* calculated from inflow – outflow TP data.

These data, in conjunction with the Harvest assessment data, suggest that management of accrued sediments (e.g. periodic consolidation by drawdown), more so than biomass harvesting, may be necessary to ensure treatment system longevity. We examine the potential for sediment consolidation as part of the Drydown-Reflooding assessment, discussed below.

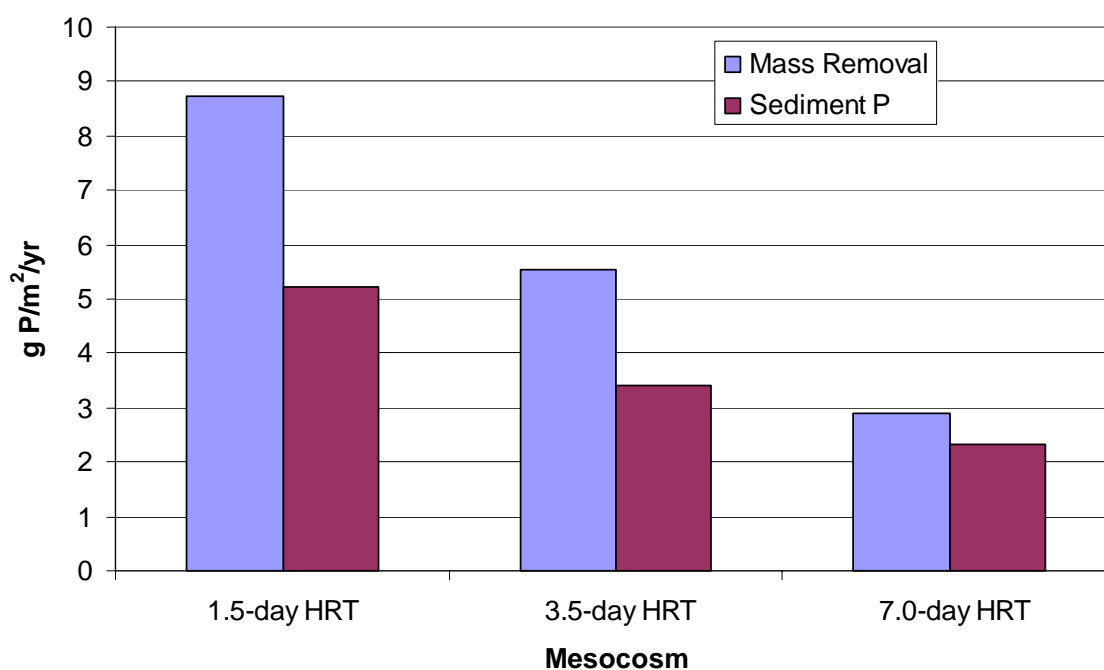


Figure 2.4. Mass phosphorus removal from the water column and sediment P accrual in mesocosms operated at hydraulic retention times of 1.5, 3.5 and 7.0 days (corresponding to 53, 22 and 11 cm/day) for three years.

2.2 Effects of Water Depth on SAV P Removal Performance

2.2.1 Background Conditions

Operational STAs will be subject to wide depth fluctuations, from <0.5 m to 1.2 m. In 1998, we established a 'static depth' evaluation in mesocosms at the NATTS. We continued operation of these mesocosms during the Follow-On assessment, in order to assess effects of fluctuating water depths on P removal performance. The nine mesocosms at the NATTS used in the Variable Depth evaluation had previously been used for the Phase I Static Depth evaluation (DBE 1999), which was operated from July 23, 1998 – March 1999. Following this latter evaluation, the tanks were operated at constant water depths of 0.4, 0.8 and 1.2 m at a hydraulic loading rate of 10 cm/day until May 1, 2000, at which time depth fluctuations were initiated. Phase II efforts under steady and fluctuating water depths are described below.

2.2.2 Spatial-Temporal Water Column Investigations Over a Diel Cycle

The results of our first spatial-temporal diel assessment in February 1999 for each of the three depth treatments were reported in the Final Report of our Phase I Demonstration Project (DBE 1999). Mean outflow TP concentrations from July 1998 to August 1999 (Static Depth monitoring period) were 16 µg/L for the shallow treatment, and 20 and 18 µg/L for the moderate and deep mesocosms, respectively. The inflow TP during this period averaged 108 µg/L. That assessment was performed under cool temperature conditions, with only a partially mature plant community. We performed a second spatial-temporal assessment on September 24-25, 1999, to document the chemical and physical spatial and temporal variations within the water column with a more mature SAV community under warmer temperatures.

Water samples were collected and field measurements (pH, D.O., redox potential, and temperature) performed at several depths (3 and 30 cm for shallow mesocosms; 3, 30, and 60 cm for moderate depth mesocosms; and 3, 30, 60, and 90 cm for deep mesocosms) at both the inflow (near the splash zone behind the baffle) and outflow regions of the mesocosms. These measurements were performed during both afternoon (1215-1800) and early morning (0200-0645). Water samples were returned to the laboratory and analyzed for the following parameters: calcium (Ca), alkalinity, soluble reactive P (SRP), total soluble P (TSP) and total phosphorus (TP). Total P was measured only on surface samples (3 cm) due to the difficulty of collecting undisturbed samples at subsurface depths. Alkalinity and Ca analyses were performed on only the shallowest and deepest stations.

Mean characteristics of the afternoon and early morning (pre-dawn) inflow Post-BMP waters during this sampling event were: 84 and 82 µg TP/L; 49 and 42 µg SRP/L; 18 and 19 µg DOP/L; 17 and 17 µg PP/L; 112 and 111 mg Ca/L; and 351 and 293 mg alkalinity (as CaCO₃)/L.

Total P concentrations within the inflow region of the mesocosms were markedly lower than the TP levels in the inflow waters (Figure 2.5). Surface TP concentrations decreased further towards the outflow region of each mesocosm, with minimal concentration differences observed between the afternoon and early morning sampling times within a given depth treatment. There were also minimal outflow TP concentration differences among the three depth treatments (Figure 2.5).

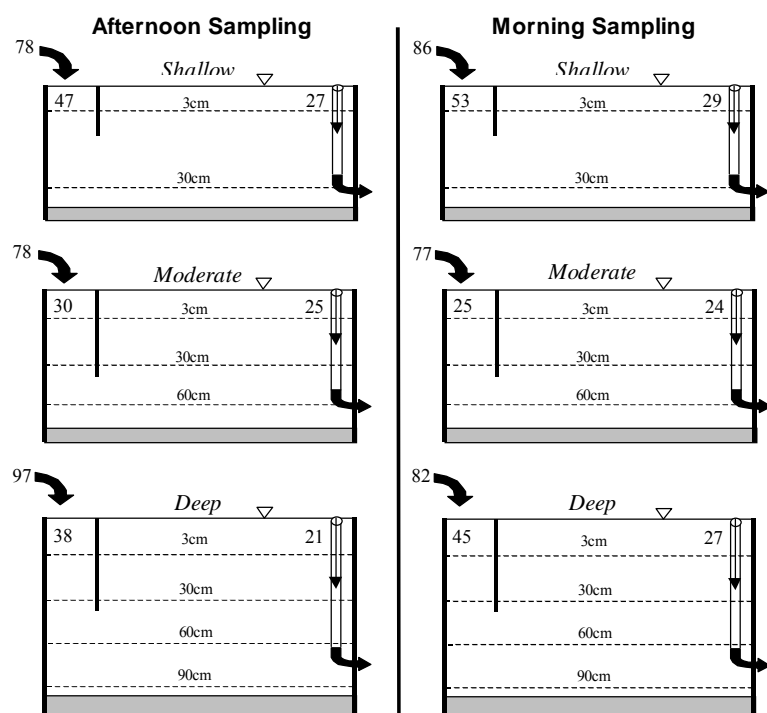


Figure 2.5. Mean total phosphorus concentration ($\mu\text{g/L}$) profiles during the Spatial-Temporal Diel evaluation on September 23-24, 1999 in the Static Depth treatments (shallow = 0.4 m, moderate = 0.8 m, deep = 1.2 m) at the North Supplemental Technology Site. Each P concentration within a treatment is a mean of duplicate mesocosms, except for the inflow concentrations.

The labile nature of SRP within SAV systems is readily seen by the large decreases from the inflow SRP concentrations (Figure 2.6). Even at the inflow ends of each mesocosm, SRP concentrations were considerably lower than inflow levels. Soluble reactive P exhibited more of a dramatic concentration decrease along the horizontal gradient than did total P (cf. Figures 2.5 and 2.6). The SRP concentrations at the outflow ends of the mesocosms were near the method detection limit ($2 \mu\text{g/L}$) in all depth treatments, regardless of the sampling time.

Sediment-water column P fluxes in wetlands are often controlled by iron (Fe). In our mesocosms, the SRP profiles are not what would be expected if the equilibrium P concentrations were dominated by iron chemistry. Dissolved oxygen concentrations were usually below the detection limit of 0.3 mg/L in the 30-90 cm depth zones of all treatments (Figure 2.7), indicating that the bottom waters and sediments were anoxic. Redox measurements taken 46 days later (November 10, 1999) showed reducing conditions existed at or below the potentials associated with the reduction of Fe^{3+} to Fe^{2+} (E_h of approximately +100 to +150 mV), especially in the bottom waters (Figure 2.8). Thus if P was bound to oxyhydrides of Fe, an increase in SRP should have been

recorded within the mesocosms during the spatial-temporal investigation, particularly during the early morning hours.

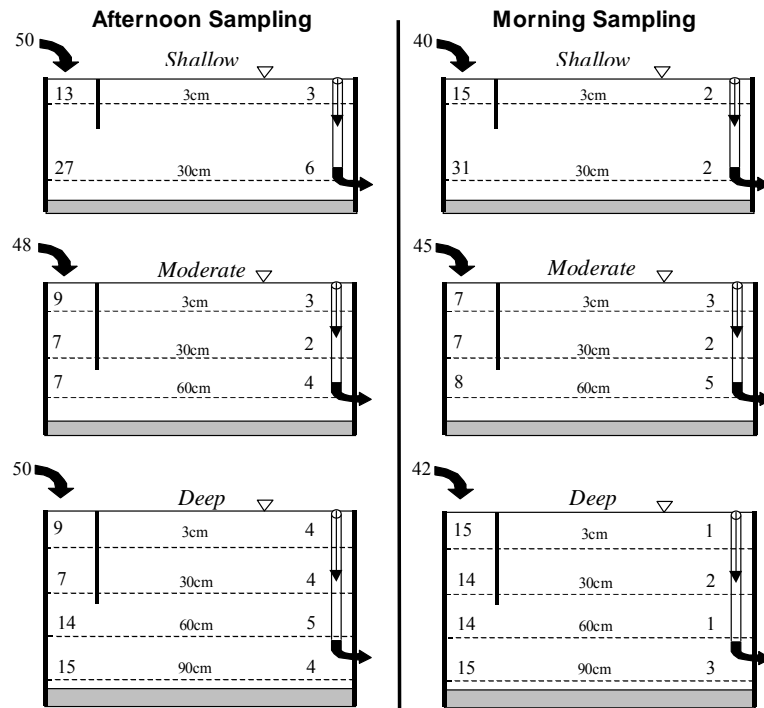


Figure 2.6. Mean soluble reactive phosphorus concentration ($\mu\text{g/L}$) profiles during the Spatial-Temporal Diel evaluation on September 23-24, 1999 in the Static Depth treatments (shallow = 0.4 m, moderate = 0.8 m, deep = 1.2 m). Each SRP concentration within a treatment is a mean of duplicate mesocosms, except for the inflow concentrations.

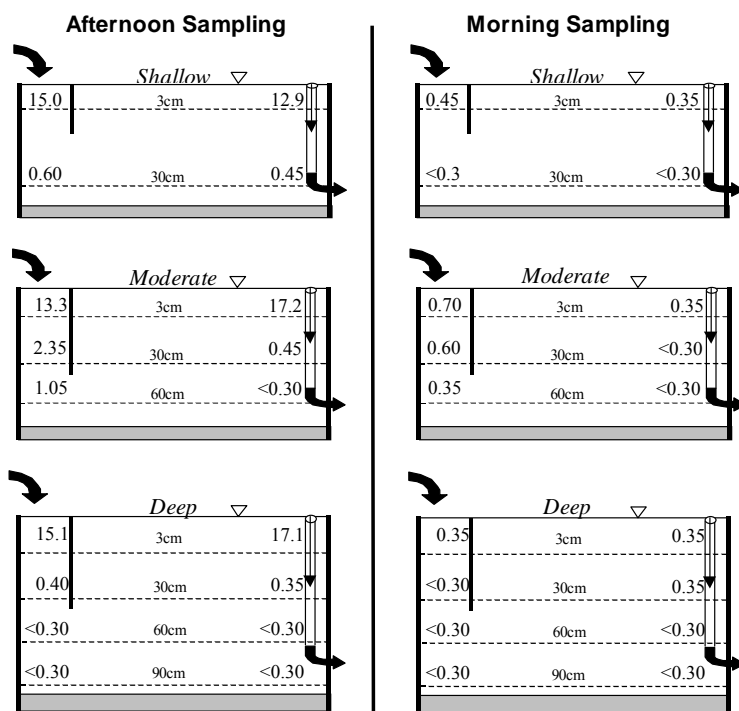
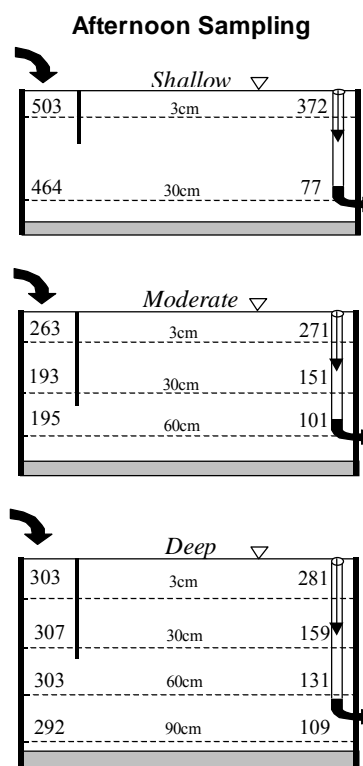


Figure 2.7. Mean dissolved oxygen concentration (mg/L) profiles during the Spatial-Temporal Diel evaluation on September 23-24, 1999 in the Static Depth treatments (shallow = 0.4 m, moderate = 0.8 m, deep = 1.2 m). Each D.O. concentration within a treatment is a mean of duplicate mesocosms.

Figure 2.8. Mean values for daytime E_h (mV) on November 10, 1999 from three replicates of shallow (0.4 m), moderate (0.8 m) and deep (1.2 m) mesocosms of the Static Depth assessment.



Calcium and alkalinity concentrations within the influent region of the mesocosms were also lower than those of the inflow waters (Figures 2.9 and 2.10). However, there was a more marked diel pattern in the spatial Ca and alkalinity concentration changes than was observed for phosphorus. For example, there were pronounced vertical and horizontal gradients for both parameters in the afternoon, but by early morning the gradients had mostly eroded. Slight horizontal gradients for Ca and alkalinity remained at this time in the shallow and moderate depth mesocosms.

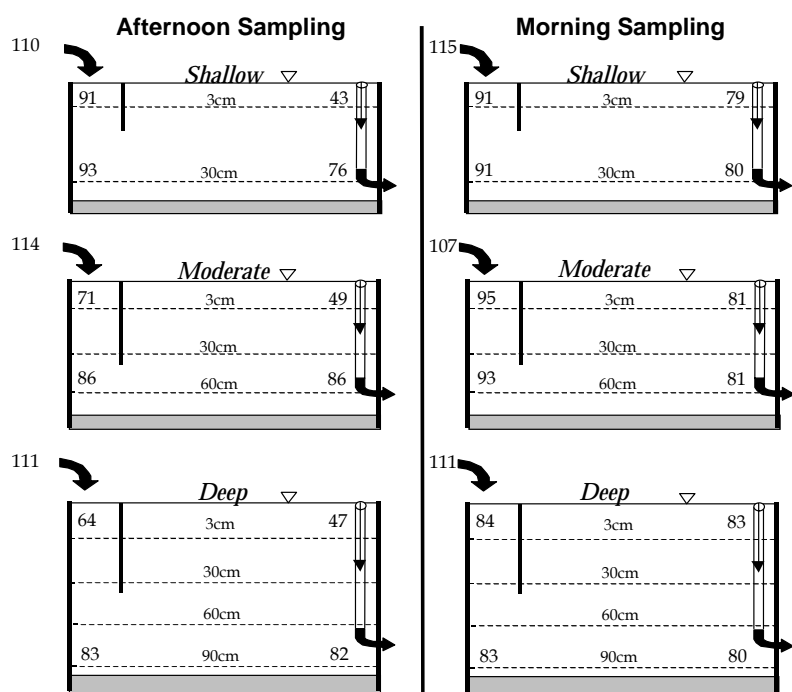


Figure 2.9. Mean dissolved calcium concentration (mg/L) profiles during the Spatial-Temporal Diel evaluation on September 23-24, 1999 in the Static Depth treatments (shallow = 0.4 m, moderate = 0.8 m, deep = 1.2 m). Each dissolved Ca concentration within a treatment is a mean of duplicate mesocosms, except for the inflow concentrations.

The Ca and alkalinity data support the existence of a diel precipitation cycle for calcium carbonate, where pH values increase to above 9.0 in the surface waters during the day (Figure 2.11), resulting in a supersaturation with respect to calcium carbonate, and ensuing precipitation. In addition to the supersaturation of dissolved carbonate and calcium, the 25-30 °C water temperatures (Figure 2.12) would also favor the precipitation of calcium carbonate. Note that the pH values fall to 7.5 - 7.6 during the night, which reduces the saturation index for calcium carbonate precipitation to below 1.0. Under these conditions precipitation is not thermodynamically possible, and this results in the weak horizontal gradient and disappearance of the vertical Ca and alkalinity gradients (Figures 2.9 and 2.10).

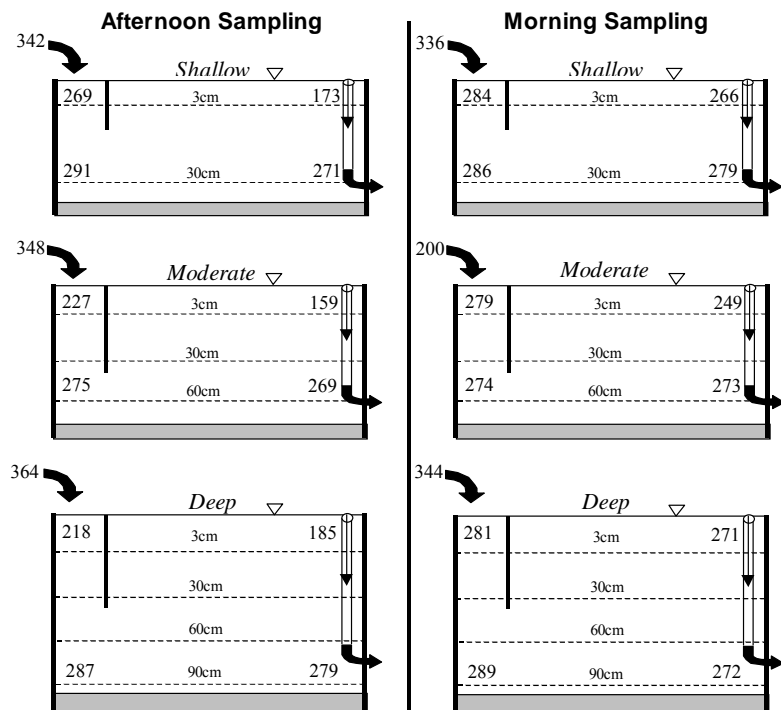


Figure 2.10. Mean total alkalinity concentration (mg CaCO_3/L) profiles during the Spatial-Temporal Diel evaluation on September 23-24, 1999 in the Static Depth treatments (shallow = 0.4 m, moderate = 0.8 m, deep = 1.2 m). Each alkalinity concentration within a treatment is a mean of duplicate mesocosms, except for the inflow concentrations.

Figure 2.11. Mean pH value profiles during the Spatial-Temporal Diel evaluation on September 23-24, 1999 in the Static Depth treatments (shallow = 0.4 m, moderate = 0.8 m, deep = 1.2 m). Each pH value within a treatment is a mean of duplicate mesocosms except for the inflow levels.

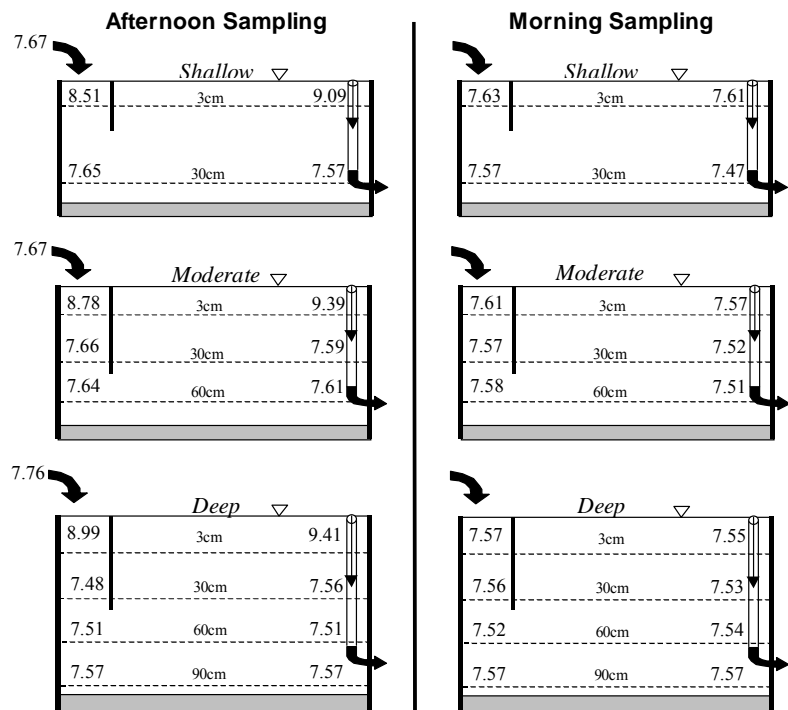
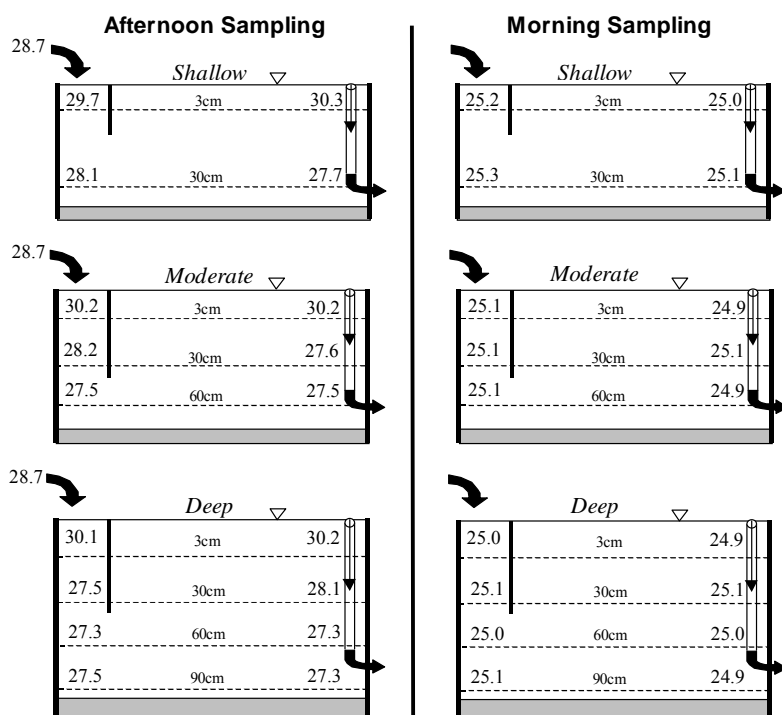


Figure 2.12. Mean temperature (°C) profiles during the Spatial-Temporal Diel evaluation on September 23-24, 1999 in the Static Depth treatments (shallow = 0.4 m, moderate = 0.8 m, deep = 1.2 m). Each temperature within a treatment is a mean of duplicate mesocosms, except for the inflow values.



If P coprecipitation with calcium carbonate is a primary removal mechanism for P in SAV mesocosms, then a relationship between pH, calcium and P would be expected, especially in the surface waters (3 cm depth) during daylight hours. We observed a strong relationship between daytime pH and SRP ($r^2 = 0.78$) and between Ca and SRP ($r^2 = 0.93$) for the surface stations, suggesting that P coprecipitation may occur within the euphotic zones of the mesocosms.

2.2.3 Vegetation and Sediment Characteristics

Upon termination or "close-out" of the Static Depth evaluation in Phase I, we sampled the P in vegetation and sediments in order to calculate a P mass balance. We minimized physical disturbance to the SAV community by harvesting plants from only 0.76 m² (0.38 m² quadrats from each of the inflow and outflow regions), and retrieving only 10 sediment cores (5 cores [77.5 cm²] from each of the inflow and outflow regions) from each mesocosm. The harvested SAV biomass was weighed (wet wt), subsampled, and then returned immediately to the appropriate mesocosms. SAV harvesting was performed on Nov. 10 and 15, 1999; sediments were cored on Nov. 16, 17, and 22. Water quality monitoring was then temporarily discontinued to allow re-establishment of the SAV community.

SAV samples were separated by species in the field, then taken to the lab where it was dried and homogenized. Dominant species were analyzed for wet and dry weight biomass, wet:dry ratios, and elemental constituents (TP, total nitrogen (TN) and total calcium (TCa)).

Najas, *Ceratophyllum*, and *Chara* spp. were present in large amounts with no apparent relationship between species dominance and depth. *Potamogeton*, *Utricularia* sp. and periphyton were also present in smaller amounts in some mesocosms. Tissue contents of *Ceratophyllum* were P enriched (average concentration: 2142 ± 815 mg P/kg) compared to *Najas* and *Chara* tissues (1661 ± 525 and 1289 ± 710 mg P/kg). Calcium was elevated in *Chara* tissues (25 ± 2 %Ca by wt.), and lower in *Najas* ($14.6 \pm 6.8\%$, $n = 13$) and *Ceratophyllum* ($10.2 \pm 3.8\%$, $n = 9$) tissues. Calcium enrichment of *Chara* tissues through CaCO_3 precipitation onto thallus surfaces appears to have diluted the relative P content of this plant species, and also contributed to the high dry:wet weight ratio (0.157 ± 0.031 , $n = 13$) as compared to *Najas* (0.097 ± 0.011 , $n = 13$) or *Ceratophyllum* (0.076 ± 0.012 , $n = 9$).

Within plant species and individual mesocosms, tissue P (and, to a lesser extent, Ca) contents decreased from the inflow region to the outflow. This may be due to luxury uptake of available P in the inflow region, and/or P deficiency in the outflow region. Interestingly, this relationship did not hold for tissue N content, probably because of the non-limiting nature of nitrogen to the plants.

2.2.4 Phosphorus Mass Balances

Because of the short duration of the Static Depth assessment period (15.5 months), the accrued sediments were typically only a couple of centimeters thick. The shallow sediment depth, coupled with the dense SAV canopy and roots, made it extremely difficult to accurately sample and measure the accrued sediments within the mesocosms. Although these factors undoubtedly contributed to variability among replicate measurements, we still successfully accounted for most of the P loaded to each mesocosm (Table 2.4). A higher recovery of P within the mesocosms would likely have been achieved had we harvested the entire plant community and retrieved all the sediments. As noted above, we instead subsampled those storage compartments because it was

necessary to preserve the integrity of the biological community and sediments for the subsequent Fluctuating Water Depth evaluation.

Table 2.4. Vegetation P storage, P storage in newly deposited sediments, and overall P mass balance for the shallow (SD = 0.4 m), medium (MD = 0.8 m), and deep (DD = 1.2 m) mesocosms. Each depth treatment was replicated three times.

Treatment/ Replicate	Phosphorus Mass Removal Rate (g/m ² · yr)				Sediment P to SAV P Ratio	% Recovered
	Input- Output (water)	Storages				
		SAV	Sediment	Total		
SD-1	2.77	0.99	1.71	2.70	1.7	98
SD-2	2.81	0.41	1.32	1.72	3.3	61
SD-3	2.83	0.50	1.46	1.97	3.0	69
<i>SD-Avg.</i>	<i>2.80</i>	<i>0.63</i>	<i>1.50</i>	<i>2.13</i>	<i>2.7</i>	<i>76</i>
MD-1	2.89	0.98	0.87	1.85	0.9	64
MD-2	2.94	0.78	0.83	1.62	1.1	55
MD-3	3.04	0.69	0.83	1.52	1.2	50
<i>MD-Avg.</i>	<i>2.96</i>	<i>0.82</i>	<i>0.84</i>	<i>1.66</i>	<i>1.1</i>	<i>58</i>
DD-1	3.71	0.93	0.99	1.92	1.0	52
DD-2	3.73	1.00	3.34	4.34	3.4	116
DD-3	3.62	1.56	1.76	3.29	1.1	91
<i>DD-Avg.</i>	<i>3.69</i>	<i>1.16</i>	<i>2.02</i>	<i>3.18</i>	<i>1.8</i>	<i>86</i>

For the Static Depth evaluation, we observed differences between treatments with respect to the mass of P stored in the SAV biomass and the accrued sediments (Table 2.4). The P stored in the plant community increased with the depth of the water column. Up to a point, deeper water likely is capable of supporting more SAV biomass than shallower water. The accrued sediment P did not follow the same relationship with water column depth; a greater mass of sediment P was recovered in the shallow depth (0.4 m) mesocosms than in the moderate depth (0.8 m) mesocosms (Table 2.4).

The relative proportions of the stored P within the SAV and sediment compartments also differed among the water depth treatments (Table 2.4). The amount of P stored in the sediments of the shallow depth mesocosms was nearly three times higher than the P mass associated with the SAV.

In contrast, 10% and 80% more P was found in the sediments of the moderate and deep mesocosms, respectively, than in their SAV compartments. This means that a higher percentage of the TP was stored in the SAV of the moderate and deep than shallow treatments. The differences in the P allocation between the two major storage compartments according to water depth indicates that at least during a “start-up” phase, the shallowest SAV systems are more rapidly storing the removed P in the sediment compartment. Over a longer time period, the sediment is expected to represent the dominant P storage compartment in all SAV systems.

2.2.5 Effects of Variable Water Depth on P Removal Performance

Water quality was monitored in the outflow of each mesocosm for TP, SRP, pH and temperature on a weekly grab-sample basis. Inflow samples were collected from one mesocosm of each depth treatment. The mean concentration of the three replicate inflow samples is presented as the inflow concentration to all nine mesocosms. Differences between the replicate inflow TP concentrations over the monitoring period were not significant.

The nine mesocosms were sampled throughout April 2000 for TP and SRP to provide a background performance level prior to water depth fluctuations. Inflow TP concentration ranged from 49 – 147 µg/L (mean = 104 µg/L). Outflow concentrations were similar among the three depths (27 – 36 µg TP/L). The 21 – 177 µg/L inflow SRP range (mean = 54 µg/L) decreased to an average outflow value of 3 µg/L with no discernible differences among depth treatments.

During the period of water level fluctuations, one of each of the shallow and deep mesocosms, and all of the three moderate depth (0.8 m) mesocosms from previous Static Depth assessments, were held at a constant depth to serve as “controls” (i.e., non-fluctuating depth). Water depth fluctuations were initiated May 1, 2000 with a reduction of the water depth to 0.8 m in duplicate deep (1.2 m) mesocosms (referred to as “deep” mesocosms). Additionally, the water depth in two shallow (0.4 m) mesocosms (referred to as “shallow” mesocosms) was increased to 0.8 m. These depths were maintained for 5 weeks, after which time the shallow and deep mesocosms were returned to their original depths of 0.4 m and 1.2 m, respectively. During the subsequent months, the depth fluctuations were imposed every five weeks, providing varying water depths

between 0.4 and 0.8 m for the shallow mesocosms, and between 0.8 and 1.2 for the deep mesocosms (Figure 2.13). The process of raising and lowering water depths was performed gradually over a four-day period.

Beginning at the end of September, we lowered the water level in the shallow and deep depth mesocosms to 0.15 and 0.40 m deep, respectively. After five weeks at these lower than normal depths, the water level in each of the four mesocosms was returned to its previous stage of either 0.4 or 1.2 m for three final weeks (Figure 2.13).

Total P concentrations in the inflow waters ranged from 28-287 $\mu\text{g/L}$, with a mean concentration of 102 $\mu\text{g TP/L}$ over the 32-week assessment period (March 20 – November 10, 2000). Mean concentrations of other parameters for the outflow from both control and variable depth mesocosms are presented in Table 2.5.

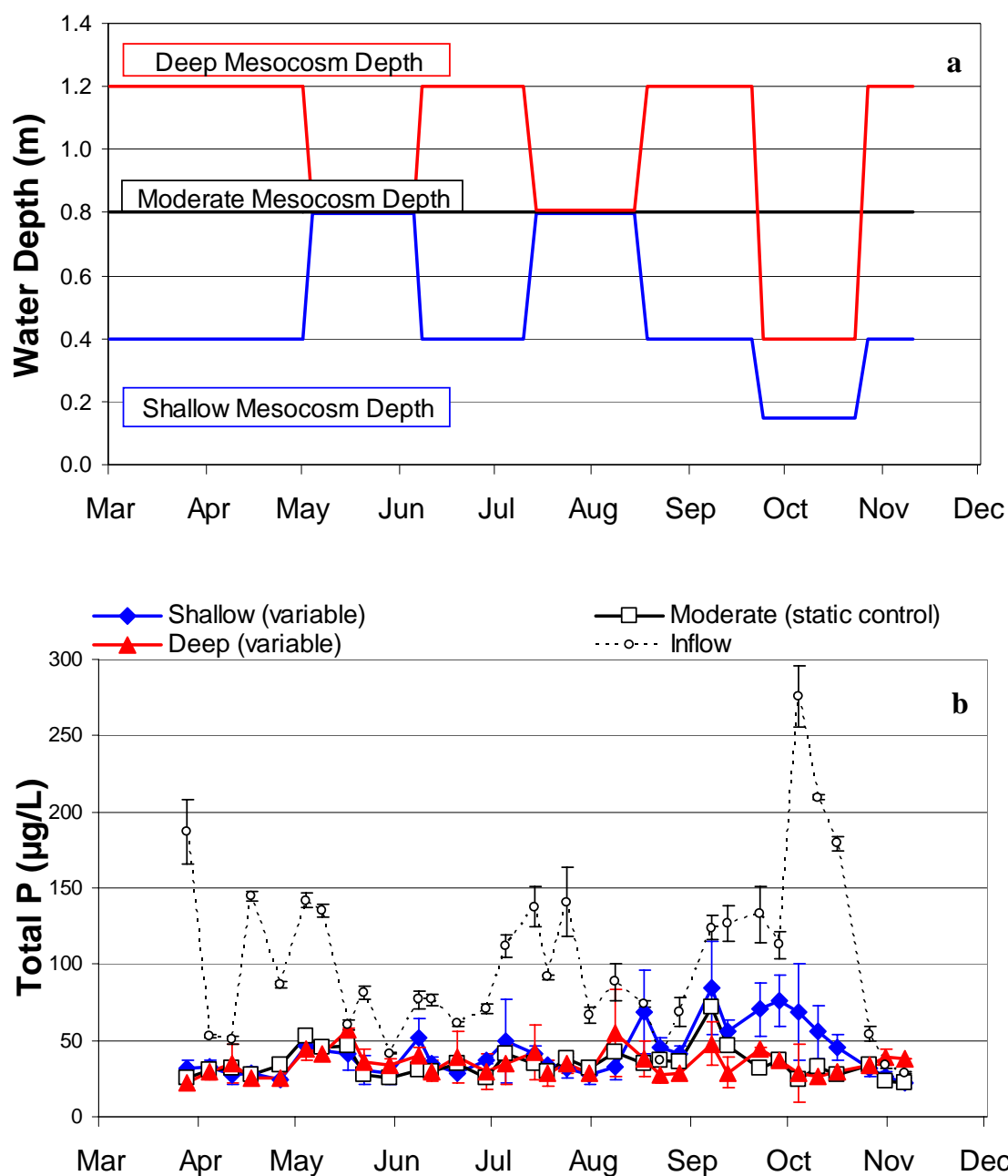


Figure 2.13. Depth fluctuation schedule for deep, moderate (control), and shallow depth mesocosms from March to November 2000 (a) and mean total P concentrations in the inflows (n = 3) and outflows (n = 2) of deep, moderate (control), and shallow depth mesocosms from March to November 2000 (b). Error bars depict \pm one standard deviation from the mean concentration.

Table 2.5. Water quality characteristics in the inflow and outflows from mesocosms operated at constant and variable water depths ranging from 0.15 – 1.2 m, from March 20 – November 10, 2000. Values represent mean \pm s.d. of measurements from duplicate (variable outflow) or triplicate (inflow and moderate outflow) mesocosms (static shallow and deep control outflows were unreplicated). Means for total P followed by the same letter or number are not significantly different ($p>0.05$).

Parameter	Units	Inflow	Outflow				
			Variable		Static		
			Shallow	Deep	Shallow	Moderate	Deep
TP	$\mu\text{g/L}$	102 \pm 7	42 \pm 12 ^a	36 \pm 8 ^a	35 ^{a,1}	33 \pm 11 ^a	30 ^{b,1}
SRP	$\mu\text{g/L}$	52 \pm 4	4 \pm 2	3 \pm 1	4	3 \pm 1	3
pH	SU	7.92 \pm 0.09	8.99 \pm 0.31	8.99 \pm 0.29	9.26	9.19 \pm 0.31	9.29
Temperature	$^{\circ}\text{C}$	29.7 \pm 0.1	30.2 \pm 0.3	30.1 \pm 0.3	30.1	30.4 \pm 0.3	30.1

No substantial differences in the outflow TP concentrations were observed between either variable depth treatments, or between static and variable depth mesocosms, during the first 16 weeks of operation (Figure 2.13). However, in August 2000, the variable shallow depth mesocosms began providing higher outflow TP levels than other treatments. The outflow quality from the shallow variable depth mesocosms did not appear to be impaired by a further depth reduction to 0.15 m (Figure 2.13) for a 5-week interval between the end of September and the end of October, even though we observed some desiccation of the top portion of the SAV (*Chara*) standing crop. Total P outflow concentrations, which were high ($>70 \mu\text{g/L}$) at the end of September, declined during each succeeding week during the remaining 6 weeks of the evaluation.

The deep mesocosms, when lowered to a depth of 0.4 m, did not exhibit elevated outflow TP concentrations when compared to previous varying water depth cycles, or to the 1.2 m static “control” mesocosm (Figure 2.13). However, an increase in the outflow TP concentrations relative to the static “control” mesocosms was observed for the subsequent 3-week period when water depth was returned to 1.2 m at the end of the evaluation. A possible explanation for the poorer P removal efficiency of the variable deep mesocosms after the increase in water depth

from 0.4 to 1.2 m water depths is that inflow water was routed over the top of the collapsed SAV canopy.

Mass removal rates among the treatments and controls were similar throughout the Variable Depth assessment periods, except during periods of elevated inflow P concentration (e.g. June 1999 and October 2000) when the mass removals were the highest (Figure 2.14). This indicates that fluctuating water depths between 0.4 and 1.2 m (deep fluctuating mesocosms), and between 0.15 and 0.8 m (shallow fluctuating mesocosms), appear not to substantially affect the P mass removal rate under low to moderate P loadings (Table 2.6). The lack of a pronounced depth effect on P removal is particularly surprising, since the shallow depths provided a markedly shorter HRT than the deep systems.

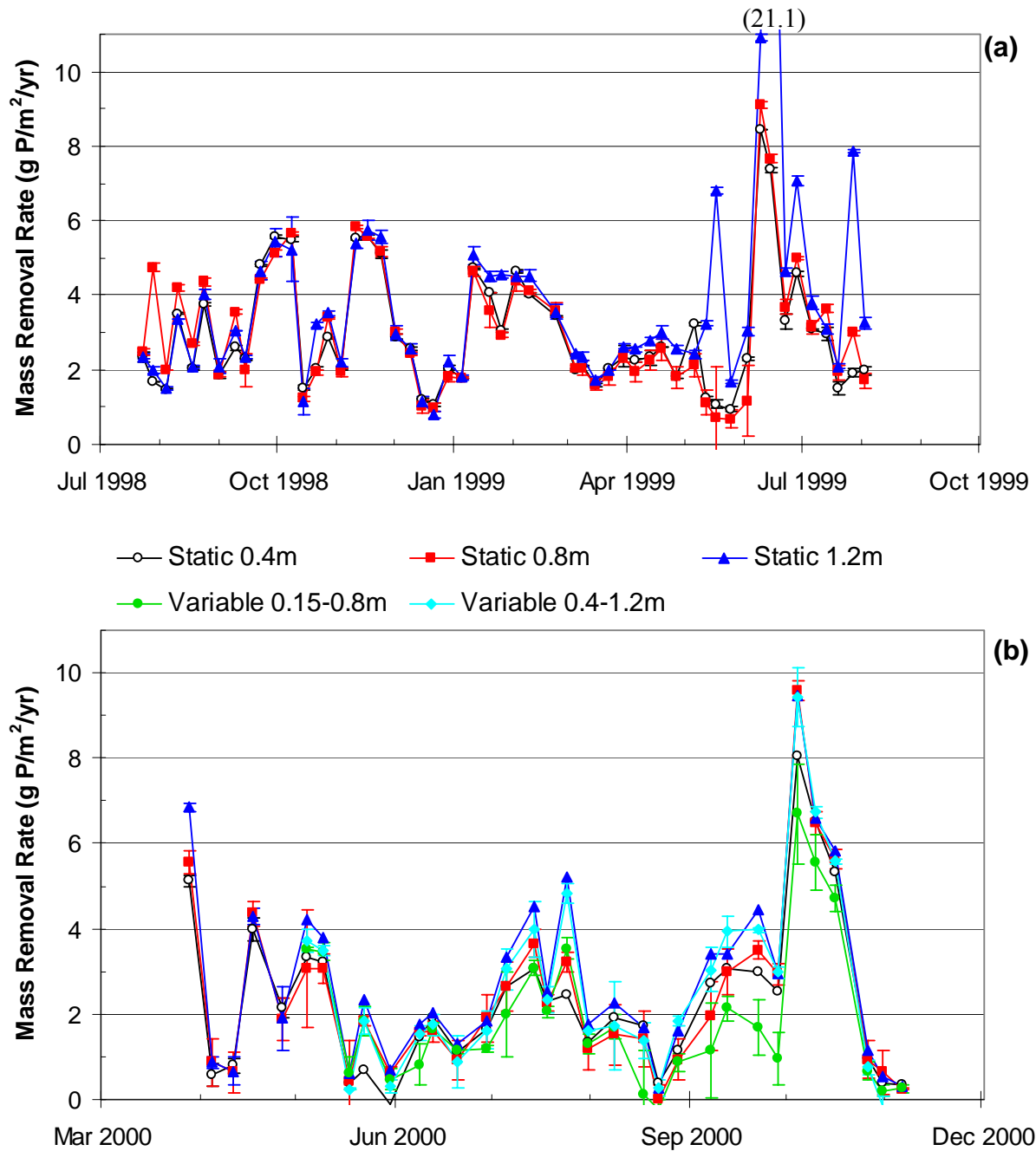


Figure 2.14. Mass removal rates in mesocosms operated at static water depths of 0.4, 0.8 and 1.2 m from July 23, 1998 through August 20, 1999 (a), and at variable or static depths (see text for details) from March 23 through November 6, 2000 (b).

Table 2.6. Mass removal rates and removal efficiencies in mesocosms operated at static and variable depths.

	Static			Variable	
	Shallow	Moderate	Deep	Shallow	Deep
Water Depth (m)	0.4	0.8	1.2	0.15-0.8	0.4-1.2
<i>Static Period(7/23/98-8/2/99)</i>					
Mass Removal					
(gP/m ² /yr)	3.4 ± 0.1	3.2 ± 0.2	3.3 ± 0.1		
% removal	83 ± 2	78 ± 5	80 ± 4		
replication	3	3	3		
<i>Variable Period (3/20/00-11/6/00)</i>					
Mass Removal					
(gP/m ² /yr)	2.4	2.5 ± 0.4	2.6	2.2 ± 0.3	2.4 ± 0.3
% removal	57	58 ± 15	62	50 ± 10	54 ± 9
replication	1	3	1	2	2

2.3 The Effects of Harvesting on the P Removal Efficiency by the SAV Community

For this subtask, we examined the effects that SAV harvesting had on both the plant community and water quality treatment by SAV. The latter was evaluated by long-term monitoring of harvested and non-harvested mesocosms, as well as by conducting a short-term (diel) assessment on a post-harvest, but “fully recovered” SAV system. We documented changes in the SAV community composition prior to the termination of the evaluation by a final biomass harvest.

2.3.1 Long-Term Phosphorus Monitoring Before and After Harvesting

Three mesocosms from our Phase I investigation of the Effects of Harvesting on P Removal were monitored through March 2000. Inflow and outflow TP concentrations of these mesocosms, which initially had been harvested in September 1998, were monitored weekly prior to our second harvest at the end of August 1999. After the second harvest, mesocosm

performance continued to be monitored weekly by comparing performance of the three harvested and three unharvested “control” mesocosms. Each of the six mesocosms was operated at a HLR of 10 cm/day, a constant water depth of 0.8m, and a nominal HRT of 8 days.

We performed a plant harvest on August 19, 1999, by clipping and discarding the top half of the SAV, to simulate the mowing action of an aquatic plant harvester. The P removal efficiency of the mesocosms dropped markedly following harvest. Following a 7-week "recovery" period P removal performance returned to near pre-harvest levels (Table 2.7, Figure 2.15).

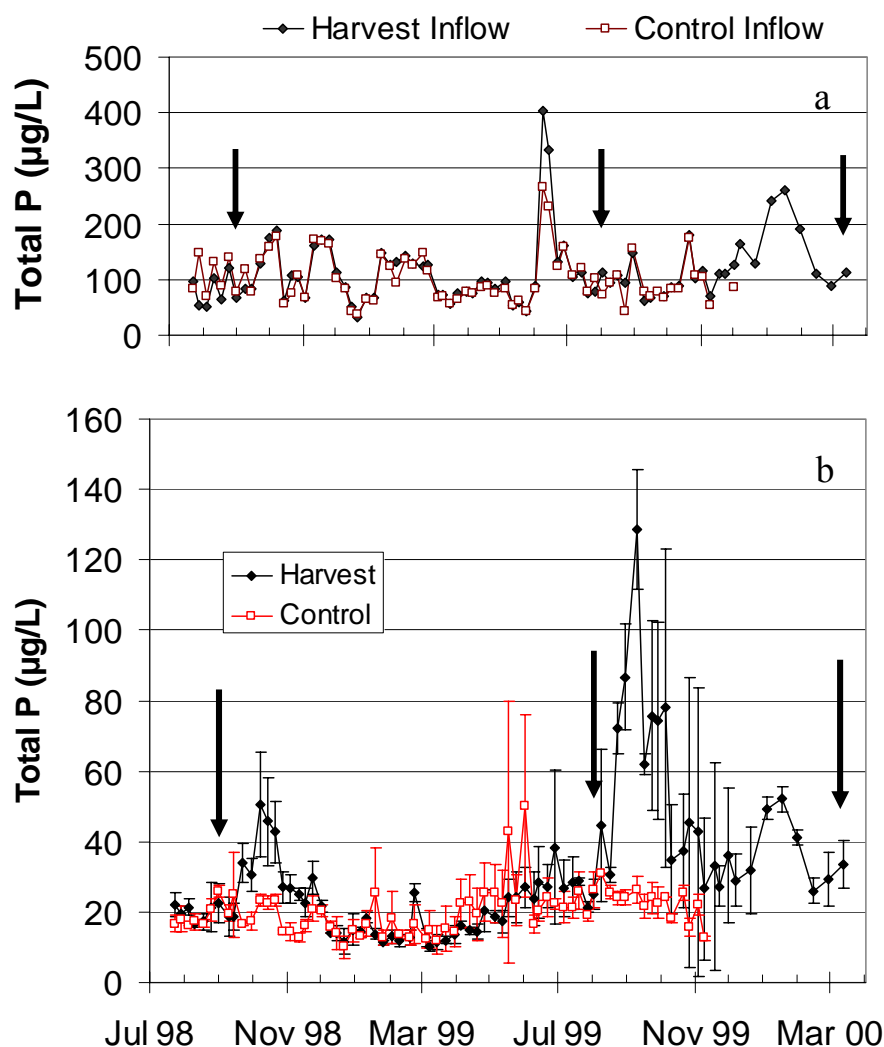


Figure 2.15. Total P concentrations in the inflow (a) and outflows (b) of triplicate harvested and control (unharvested) mesocosms operated from July 1998 to March 15, 2000. Arrows correspond to harvest dates of September 14, 1998, August 19, 1999 and March 15, 2000.

Table 2.7. Mean inflow and outflow total P concentrations ($\mu\text{g/L}$) of triplicate harvested SAV mesocosms before harvest, and during and after a “recovery” period. Harvesting was performed on August 19, 1999.

	Sampling Events	Inflow TP ($\mu\text{g/L}$)	Outflow TP ($\mu\text{g/L}$)	P Removal (%)
Pre-Harvest Period (July 1 – Aug 18, 1999)	7	98	29	70
Recovery Period (Aug 19 – Oct 5, 1999)	7	83	84	-1
Post-Recovery Period (Oct 6 – Jan 31, 2000)	13	144	37	74

2.3.2 Spatial-Temporal Profile

We performed a Spatial-Temporal assessment on February 7 and 8, 2000, 172 days following the “clipped” harvest, with the intent of examining at a finer spatial and temporal resolution the effects that harvesting may have had on the chemical processes in a post-harvest, but "fully recovered" SAV system. For an unharvested "control", we sampled duplicate, long hydraulic retention time (HRT) mesocosms (7-days) scheduled to be used later in the Pulse Loading and Long-Term Monitoring tasks. These tanks shared similar water depths (80 cm), hydraulic loading rates (HLR: 10-11 cm/day) and hydraulic retention times (HRT: 7-8 days) with the harvested tanks.

Water samples were collected and field measurements (pH, D.O., redox potential, and temperature) were recorded from three depths (3, 30, and 60 cm) at both inflow and outflow regions of duplicate mesocosms from the harvested and non-harvested treatments. These measurements were performed during the afternoon (1435-1700) and early morning (0500-0700) on February 7-8, 2000. Water samples were returned to the laboratory and analyzed for soluble reactive P (SRP).

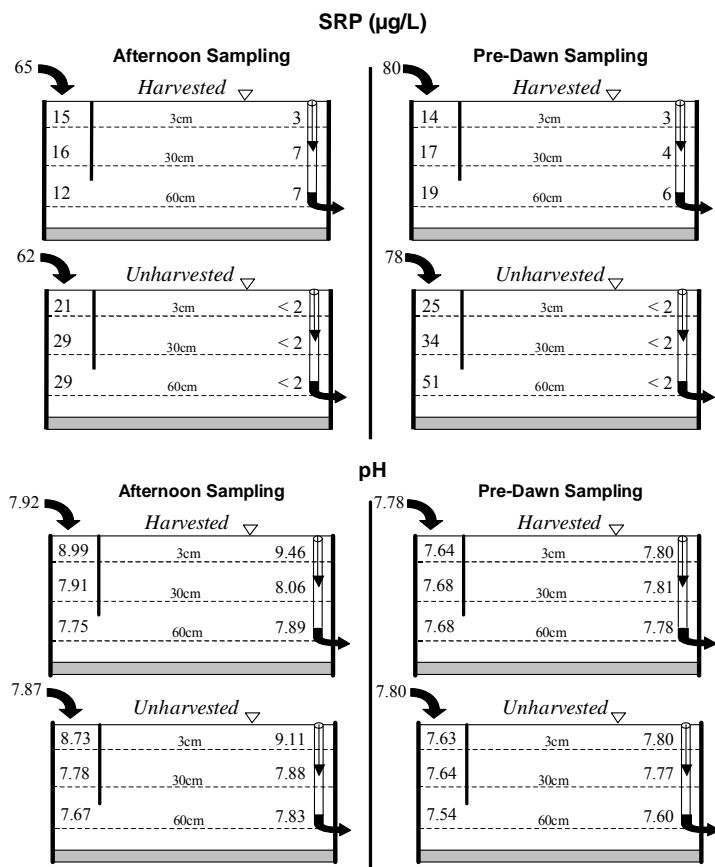
Mean SRP concentrations of the afternoon and early morning (pre-dawn) inflow Post-BMP water during this sampling event were 63 and 79 $\mu\text{g/L}$, respectively. The labile nature of SRP in SAV systems is readily seen by the large decreases from the inflow SRP concentrations within the mesocosms (Figure 2.16). Outflow region SRP concentrations in the unharvested

mesocosms were less than the method detection limit ($2 \mu\text{g/L}$) at all depths, regardless of sampling time. SRP concentrations in the outflow regions of the harvested mesocosms also were low, but above the detection limit.

Within-treatment differences in the SRP concentrations between afternoon and pre-dawn were minimal at all stations, with the only exception being the 60 cm depth at the inflow end of the unharvested mesocosms (Figure 2.16). There were, however, noticeable differences in SRP concentrations as a function of previous harvest history. Compared to the harvested mesocosms, the unharvested mesocosms had higher SRP concentrations at the inflow region, but lower concentrations at the outflow region. The reason for these between-treatment differences in SRP levels is unknown.

Harvesting also appeared to have promoted higher pH values in the water column. Afternoon surface water (3 cm) pH values in the harvested mesocosms were 0.25 to 0.35 units higher than the unharvested controls; there were no pre-dawn differences between the two treatments (Figure 2.16).

Figure 2.16. Soluble reactive phosphorus concentrations and pH values during the Spatial-Temporal evaluation, February 7-8, 2000, in harvested and unharvested mesocosms at the NATTS. Each value within a treatment is a mean of duplicate mesocosms, except for the inflow stations.



As expected, water column dissolved oxygen concentrations varied widely over the diel cycle. Supersaturated conditions, where concentrations exceeded 9.0 mg/L at 21 °C, were detected during the afternoon at the surface of both harvested and unharvested treatments (Figure 2.17). These high daytime concentrations diminished with depth and at night. At no time or location were the mesocosms anoxic, although the lowest concentration recorded (1.0 mg/L) indicates that hypoxic conditions did prevail at the 60 cm depth of the unharvested mesocosms in the early morning. The dissolved oxygen concentrations in the unharvested mesocosms were always slightly lower than in the harvested mesocosms at all times and depths (Figure 2.17), probably due to the higher biomass density (and increased respiration) in the former systems. Reduction-oxidation (redox) potentials corroborated the dissolved oxygen concentrations in that the redox potential in the water column (+394 to +626 mV, Figure 2.17) was always above the range associated with reducing conditions (< +300 mV). Although still within the oxidized range, the redox potentials from unharvested mesocosms were slightly depressed compared to those from the harvested mesocosms.

Temperatures in harvested and unharvested mesocosms for a given depth and sampling time usually differed by less than 1°C (Figure 2.17). There were, however, vertical temperature gradients during the day in both sets of mesocosms, which then dissipated during the night.

In summary, the harvested mesocosms had slightly higher pH, dissolved oxygen concentrations, and redox potentials than the unharvested mesocosms, even though it had been nearly 6 months since the harvesting had been performed. Clipping the plants probably increased primary productivity, which resulted in the higher levels of these constituents. We also observed between-treatment differences in SRP concentrations, but these generally were slight.

2.3.3 SAV Recolonization After Biomass Harvest

On March 15, 2000 we conducted a final biomass harvest in “closing out” the triplicate Harvest Assessment mesocosms. We measured wet weight biomass for each SAV species and dried subsamples at 70–80°C for dry: wet weight ratios. In contrast to the previous harvest (August 19, 1999) where SAV was collected by clipping the SAV occupying the top half of the water

column, the harvest methodology for this final harvest was similar to the original harvest performed on September 14, 1998, in which the entire plant (i.e., including roots) was removed and weighed.

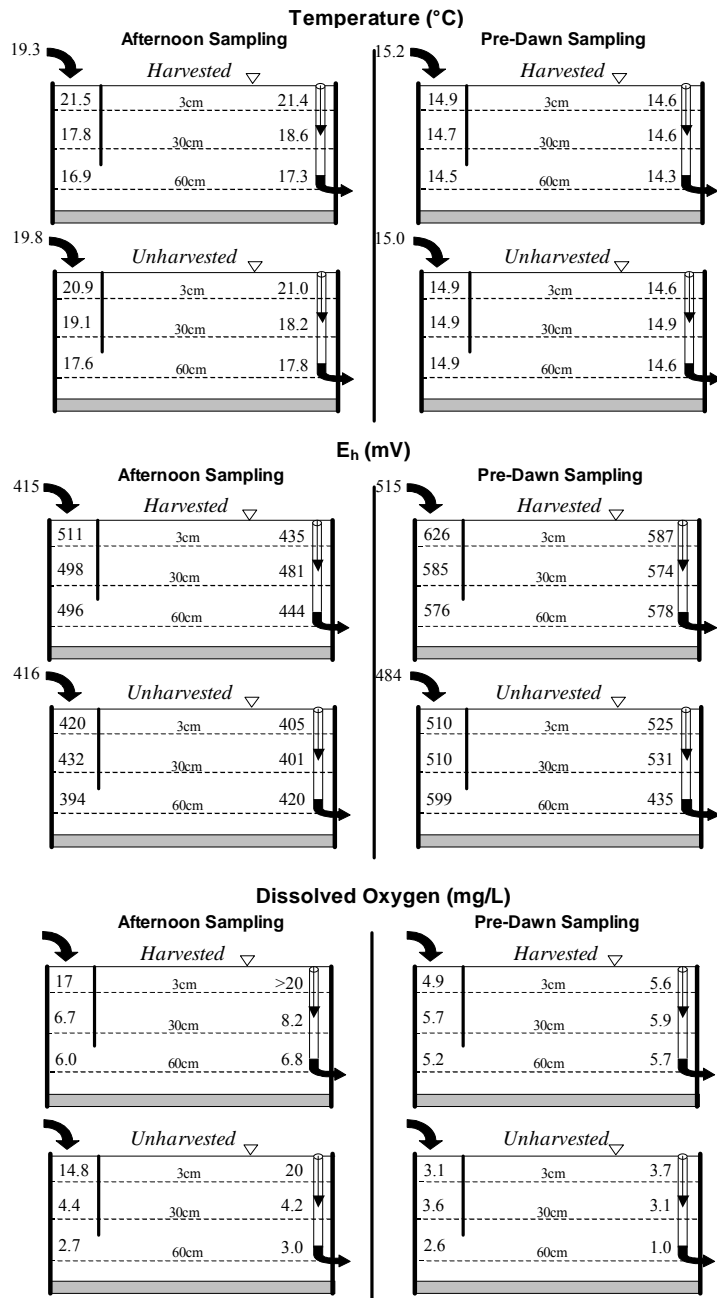


Figure 2.17. Dissolved oxygen concentrations and redox and temperature values during the Spatial-Temporal evaluation, February 7-8, 2000, in harvested and unharvested mesocosms at the NATTS. Each value within a treatment is a mean of duplicate mesocosms, except for the inflow stations.

Noticeable species shifts within the SAV community occurred during the 18-month investigation (Figure 2.18). *Najas* dominated the SAV community in September 1998, comprising $77 \pm 6\%$ of the entire dry weight biomass. However, by August of 1999, *Najas* biomass in the three mesocosms decreased to between 23 and 32% (mean = $28 \pm 5\%$) of the total plant community. The relative distribution of *Najas* among the replicates appeared to stabilize by the March 2000 harvest at $24 \pm 1\%$. *Potamogeton* became more dominant, as it increased from only 3% of the total SAV biomass in September 1998, to 20% and 28% in August 1999 and March 2000, respectively. *Chara* biomass also increased from the initial harvest in September 1998 (Figure 2.18). The distribution of *Ceratophyllum* remained between 12 and 19% during the 18 months following the first harvest. A filamentous alga (periphyton) occurred sporadically in the first two harvests, but increased to nearly 30% of the overall biomass by March 2000.

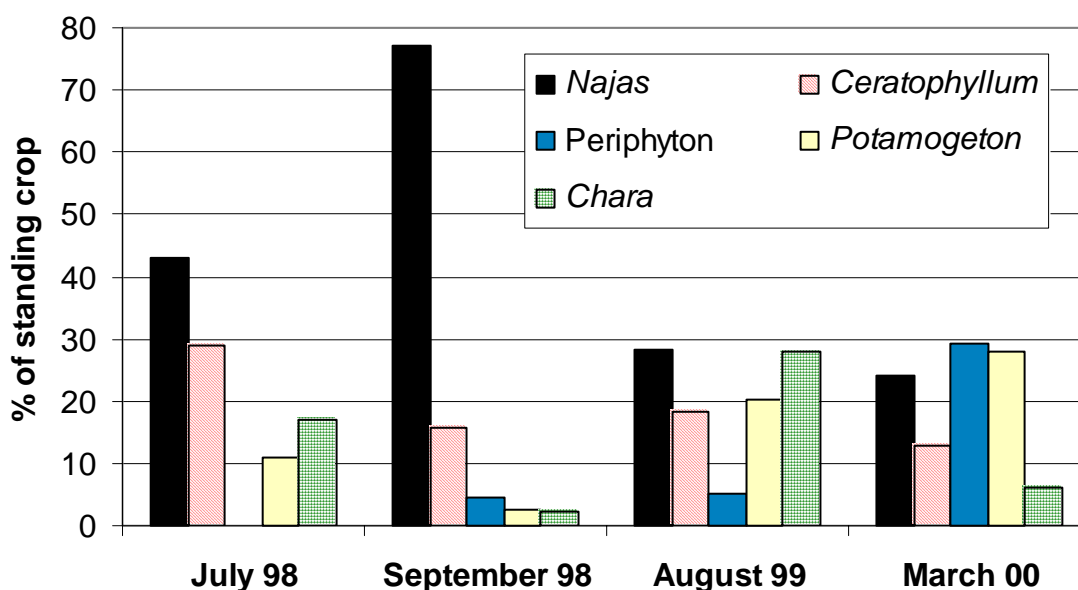


Figure 2.18. Mean relative distribution (% of total dry weight biomass) of SAV genera for three replicate mesocosms on three harvest dates, as compared to the initial stocking distribution. The first harvest, September 14, 1998, was 59 days after initial stocking (July 17, 1998). Whole plants were harvested, weighed and returned to respective mesocosms. During the second harvest (August 19, 1999), 339 days after the first harvest, all plants occupying the top half of the water column were clipped, weighed and discarded. The final harvest occurred March 15, 2000, 208 days after the second harvest, when whole plants were harvested, weighed and returned to respective mesocosms. Following the third harvest, the evaluation was terminated.

Besides harvesting, other factors such as nutritional requirements, seasonal effects and grazing can affect species dominance within the SAV community. We cannot, therefore, state with certainty the ecological effects of harvesting since control (unharvested) mesocosm vegetation was not sampled at the same times as the harvested mesocosms. The control tanks needed to remain undisturbed since they were serving as the 0.8 m depth "control" treatments of the "Fluctuating Depth evaluation".

It appears that harvesting may favor growth of *Potamogeton* and *Chara* (for the September 1998 harvest only) to the detriment of *Najas*. Initial harvests undertaken in other mesocosms at the NATTS during the past two years have yielded only minor amounts (< 5%) of *Potamogeton*. *Chara*, on the other hand, has tended to become a dominant member in those same mesocosms, suggesting that other factors may be more important than harvest history for this genus. *Ceratophyllum* appears to be unaffected by harvesting. Periphyton biomass increased during the period after the second harvest (August 1999 to March 2000), although this may have been unrelated to harvesting since periphyton abundance also fluctuated considerably in the unharvested mesocosms.

Even though harvesting may not be as dominant a factor as nutritional or seasonal effects in determining the composition of the SAV community, the method of harvesting may have played an influential role. For example, we uprooted entire plants and weighed them (wet weight) before returning them to the mesocosms in the first harvest (September 14, 1998), which may have been detrimental to *Najas* with its rooted habit. The clipping performed in the second harvest on August 19, 1999, which left the roots and lower stems intact, may have been more advantageous to *Potamogeton* than *Najas*, perhaps by stimulating *Potamogeton* growth via hormone (i.e., auxin) production, such as is commonly reported for terrestrial plants (Salisbury and Ross 1978).

Besides the possibility of differential production of growth hormones, enhanced light penetration following harvests may also have played an important role in the dominance of *Chara* (after the September 14, 1998 harvest only) and *Potamogeton* (after both the September 14, 1998 and August 19, 1999 harvests). Steinman et al. (1997) reported that light appeared to be a

strong regulator in influencing *Chara* phenology and abundance in Lake Okeechobee. Their data showed that charophyte biomass was inversely related to water depth and positively related to Secchi disk transparency, suggesting that irradiance strongly influences charophyte distribution in the lake. The hypothesis was further supported by laboratory assessments of photosynthetic measurements and photosynthesis irradiance curves: the irradiance at which photosynthesis is initially saturated was an order of magnitude greater than the ambient light reaching the charophyte populations.

Potamogeton also responds to increased light availability by increasing shoot density, and shoot and root biomass (Barko et al. 1982). *Potamogeton* may out-compete *Najas* subsequent to harvesting by quickly forming a canopy with broad leaves, thereby limiting light penetration to the submersed *Najas* plant. Additionally, *Potamogeton* may have an advantage over *Chara* after harvest because of its storage capacity in root structures, which were disturbed during the first harvest (September 14, 1998), but remained intact after the second harvest (August 19, 1999).

2.3.4 Effectiveness of Biomass Harvest on P Mass Removal

In the second biomass harvest on August 19, 1999, we removed 355 ± 155 mg P from the harvest mesocosm systems via clipping of the SAV from the upper half (40 cm) of the water column. As a result of the harvesting, the TP removal performance previously provided by the SAV community was impaired (Figure 2.15). Over the 82 days between August 19 and November 9, 1999, the difference in phosphorus mass removal between control and harvested mesocosms averaged 470 mg P. Though harvesting of SAV may have benefits in terms of managing species composition of the beds as discussed above, or in increasing hydraulic conveyance through the system to avoid stagnant zones of “no treatment”, broad-scale harvesting as a means for increasing P removal from the water column does not appear practical.

2.4 Effects of Pulsed Loading on Phosphorus Retention

Operational STAs will be subject to wide variations in flow, ranging from ‘no flow’, stagnant conditions, to hydraulic loadings that are 20x the average HLR of approximately 2.6 cm/day. For this effort, we utilized nine mesocosms that originally were used for the Phase I hydraulic loading rate (HLR) evaluations (triplicate mesocosms receiving HLRs of 11, 22, and 53 cm/day).

Vegetation in six of the nine mesocosms from that evaluation was harvested and re-stocked in February 1999 (as part of Phase I close-out efforts). We used these six mesocosms to evaluate pulsed loading effects, following a 9-month grow-out period. The remaining three mesocosms from Phase I were maintained at constant HLRs of 11, 22, and 53 cm/day as controls (in conjunction with Long-Term Monitoring).

2.4.1 Background Conditions

On November 17, 1999, we began analyzing two-week composites of weekly grabs to evaluate background conditions of SRP, TP, TSP, Ca and alkalinity prior to start-up of pulse loading efforts. We had analyzed weekly SRP and TP grabs and bi-weekly TSP, Ca, and alkalinity grab samples prior to this time.

The monitoring data at this time suggested that the six SAV mesocosms had fully recovered from the “sampling disturbance” (SAV harvesting and sediment coring) that was performed in February 1999 (Figure 2.19).

2.4.2 Pulse Schedule Development

We based our pulse-loading schedule for mesocosm evaluations on an analysis of Dr. William Walker’s STA-2 data set, which is a 9.75-year projected loading scenario that has been adapted by the District for STA design purposes. We analyzed the STA-2 data set on a seasonal basis by dividing each year’s data into four 13-week ‘seasons’. Each season of each year was analyzed for three parameters: mean seasonal flow, standard deviation of seasonal flow, and percentage of zero-flow weeks. Table 2.8 shows a comparison of key parameters for our seasonal analysis (on a weekly basis) of the STA-2 data set and our biweekly loading schedule (shown for a 2.4 cm/day HLR).

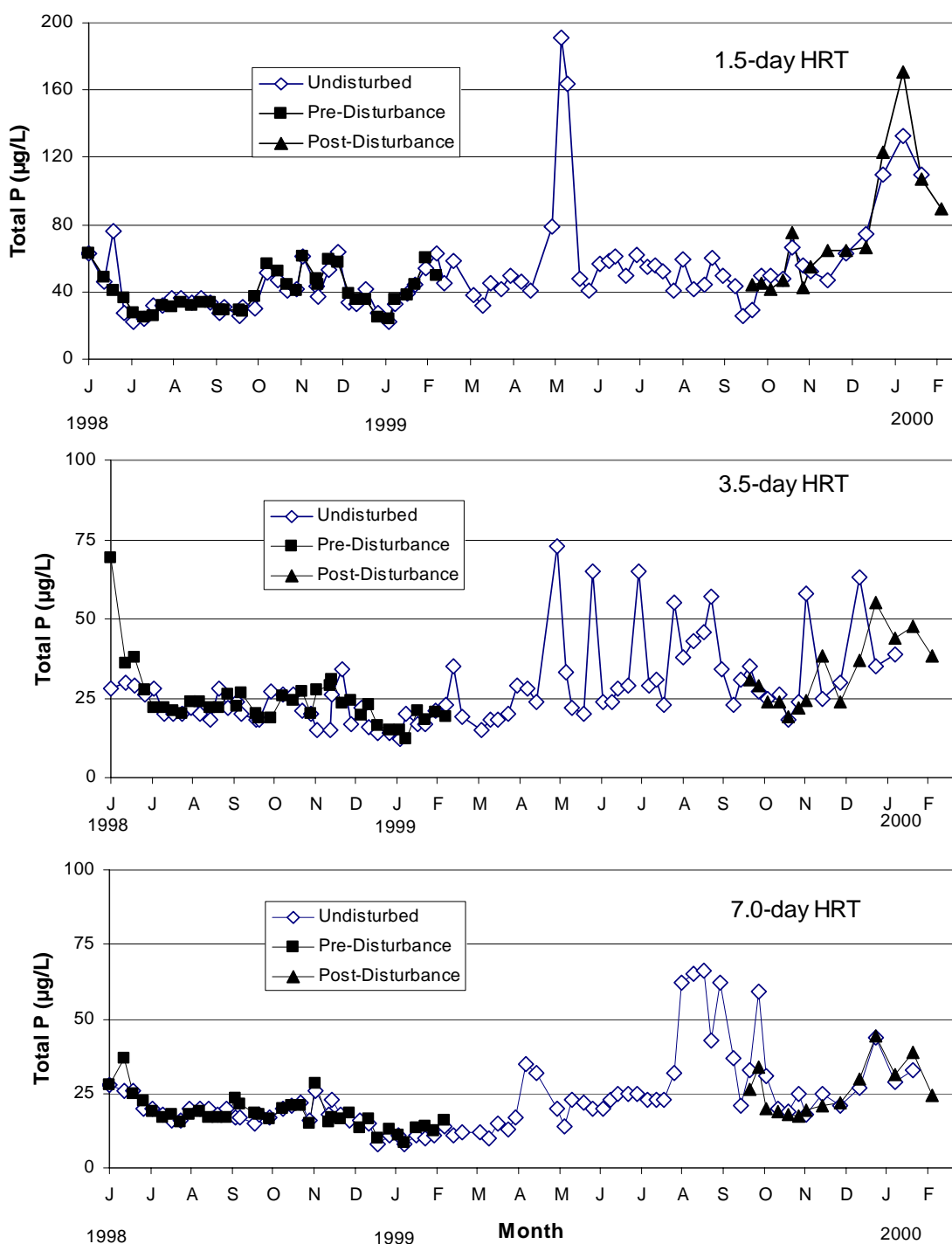


Figure 2.19. Outflow total P concentrations from undisturbed (no SAV harvesting or sediment coring) and disturbed (SAV harvesting and sediment coring on February 10-11, 1999) mesocosms operated at hydraulic retention times (HRT) of 1.5, 3.5 and 7.0 days (HLRs of 53, 22 and 11 cm/day). Data from the disturbed mesocosms represent the mean of two replicates and the data from the undisturbed mesocosms are from only one mesocosm per HRT treatment.

Table 2.8. Comparison of STA-2 and DBE loading schedules.

		STA-2 (analyzed on a weekly basis)	DBE's Biweekly Schedule
% of No-Flow Days	Winter	31%	15%
	Spring	52%	62%
	Summer	13%	15%
	Fall	44%	31%
Average Flow (cm/day)	Winter	1.7	1.8
	Spring	1.7	1.4
	Summer	4.2	4.3
	Fall	1.8	2.1
Standard Deviation (cm/day)	Winter	2.9	1.7
	Spring	3.9	2.2
	Summer	4.7	3.2
	Fall	3.2	2.4

Our pulse-loading schedule for mesocosm evaluations is provided in Table 2.9 and is based on the following premises:

- Each pulse period will last two weeks. This was chosen as a compromise between data collection needs (the longer the time between pulses, the more measurable a flow effect would be) and staying close to the short pulse durations that typify the STA-2 data set.
- DBE's loading schedule has approximately the same average seasonal flow patterns as represented in the STA-2 data set (Table 2.8).
- DBE's loading schedule has approximately the same percentage of "no flow" weeks as the STA-2 data set on a seasonal basis (Table 2.8).
- The standard deviation of flows in DBE's loading schedule is as close as possible to those in the STA-2 data set on a seasonal basis (Table 2.8).

We decided to operate the six mesocosms with paired treatments at mean loadings of 11, 22, and 55 cm/day. These HLR's are scaled by factors of approximately 5, 10, and 25, respectively, over the mean 2.4 cm/day HLR inherent in Dr. Walker's STA-2 data set (Table 2.9). The pulse-loading schedule for the three treatments is identical, except that each treatment applies a different flow scale factor. We initiated the 40-week pulse-loading evaluation in six mesocosms at the NATTS on February 20, 2000.

Table 2.9. Forty-week (Feb. 20 - Nov. 24, 2000) pulse loading schedule for low, medium, and high loaded mesocosms in Subtask 5v.

Loading schedule (cm/day)				Loading schedule (cm/day)			
Week	Low	Medium	High	Week	Low	Medium	High
1*	0	0	0	21	13.2	26.4	66
2	0	0	0	22	13.2	26.4	66
3	22	44	110	23	44	88	220
4	22	44	110	24	44	88	220
5	4.4	8.8	22	25	0	0	0
6	4.4	8.8	22	26	0	0	0
7	0	0	0	27	26.4	52.8	132
8	0	0	0	28	26.4	52.8	132
9	13.2	26.4	66	29	8.8	17.6	44
10	13.2	26.4	66	30	8.8	17.6	44
11	0	0	0	31	35.2	70.4	176
12	0	0	0	32	35.2	70.4	176
13	0	0	0	33	6.6	13.2	33
14	0	0	0	34	6.6	13.2	33
15	26.4	52.8	132	35	11	22	55
16	26.4	52.8	132	36	11	22	55
17	0	0	0	37	22	44	110
18	0	0	0	38	22	44	110
19	17.6	35.2	88	39	0	0	0
20	17.6	35.2	88	40**	0	0	0

* Beginning week for Pulse Loading evaluation: Feb. 20, 2000

** Termination of evaluation: Nov. 24, 2000

2.4.3 Effects of Pulsed Loadings on Phosphorus Retention

Outflow SRP concentrations continuously remained near the detection limit (2 µg/L) in the low and moderate pulse-loaded mesocosms. By contrast, the outflow of the highest loaded mesocosms, which received a HLR from 0 to 220 cm/day, did have measurable SRP levels (5-43 µg/L; mean ± s.d.= 14 ± 10) over the entire POR (February 20 – November 24, 2000). The highest outflow SRP concentrations coincided with the highest hydraulic loading rates (Figure 2.20). These high outflow SRP concentrations were comparable to the outflow SRP levels for the control (non-pulsed) mesocosm receiving a constant HLR of 53 cm/day. This indicates that wide HLR variation inherent in pulse loading did not, in itself, reduce the SRP removal efficiency of the SAV mesocosms. For the highly loaded mesocosms, the inflow SRP concentration was more important in determining outflow SRP concentration than whether the operational mode was pulsed (under the hydraulic loading conditions imposed during the assessment period) or constant.

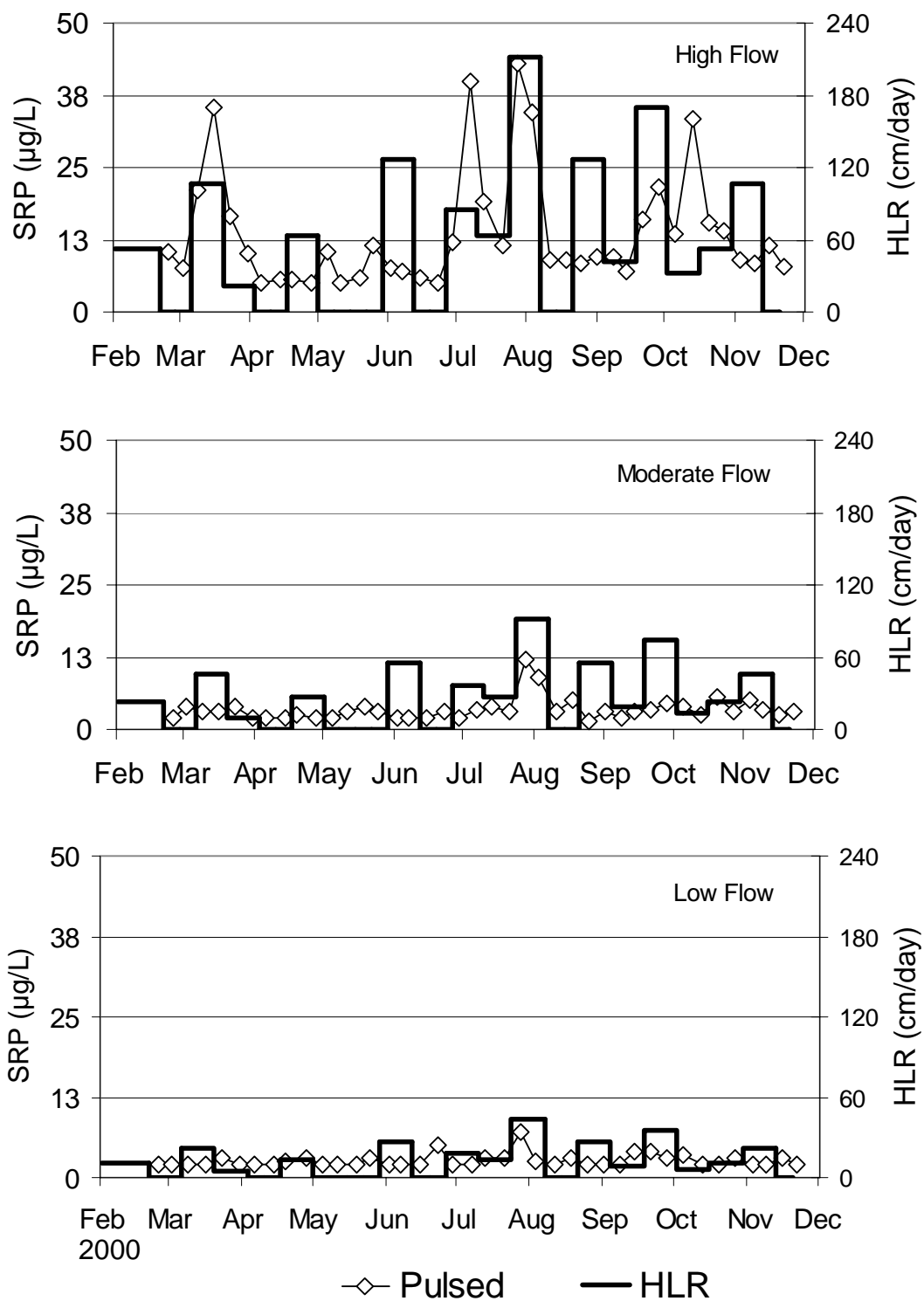


Figure 2.20. Mean outflow soluble reactive P concentrations from mesocosms that received high, moderate and low pulse loading regimes.

Removal of total P by the pulsed mesocosms was less complete than for SRP, and was strongly influenced by HLR. For example, average outflow total P concentrations for the pulsed low HLR mesocosms ranged from 16 to 75 µg/L (mean ± s.d. = 31 ± 10) over the POR. The outflow concentrations for the pulsed medium HLR mesocosms were higher (19–116 µg TP/L, mean ± s.d. = 45 ± 19). We observed sharply elevated total P concentrations (20–462 µg TP/L; mean ± s.d. = 76 ± 42) in the high HLR mesocosms during periods of high loading (>110 cm/day), as well as during periods of no flow, compared to the rest of the period of record (Figure 2.21). The pulsed hydraulic loading rate had a significant effect ($p < 0.05$) on the mean outflow concentrations for all three treatments.

During August–October 2000, the hydraulic loading rates (HLRs) ranged from 0–400% of annual mean flow. These broad fluctuations reflect variable flows associated with “typical” wet season pumping events and periods of “no flow” during the dry season. Low-, moderate- and high-load pulsed mesocosms were operated at HLRs of 44, 88, and 220 cm/day, respectively, during the two-week period of July 24 – August 7, 2000. These HLRs were the highest scheduled during the 40-week mesocosm assessment. They were followed by two weeks of zero flow, during which time we observed relatively high outflow TP concentrations during August in the high and moderate flow treatments (Figure 2.21).

The pulsed-flow investigation, concluded on November 24, 2000, culminated with two weeks of zero flow, the seventh such “no-flow” period during the assessment (Table 2.9). Outflow region water quality was monitored throughout these quiescent periods and was typified by TP equivalent to flow-through conditions in the low and moderate load mesocosms, and higher-than-average TP concentrations in the high load mesocosms. Total P concentrations in the medium and high HLR mesocosm outflow during the weeks with flow were slightly higher than in the mesocosms receiving constant hydraulic loadings (Long-Term Monitoring) for those flow periods (Table 2.10). However, the low HLR mesocosms outflow TP concentrations were comparable under pulse and constant flow conditions.

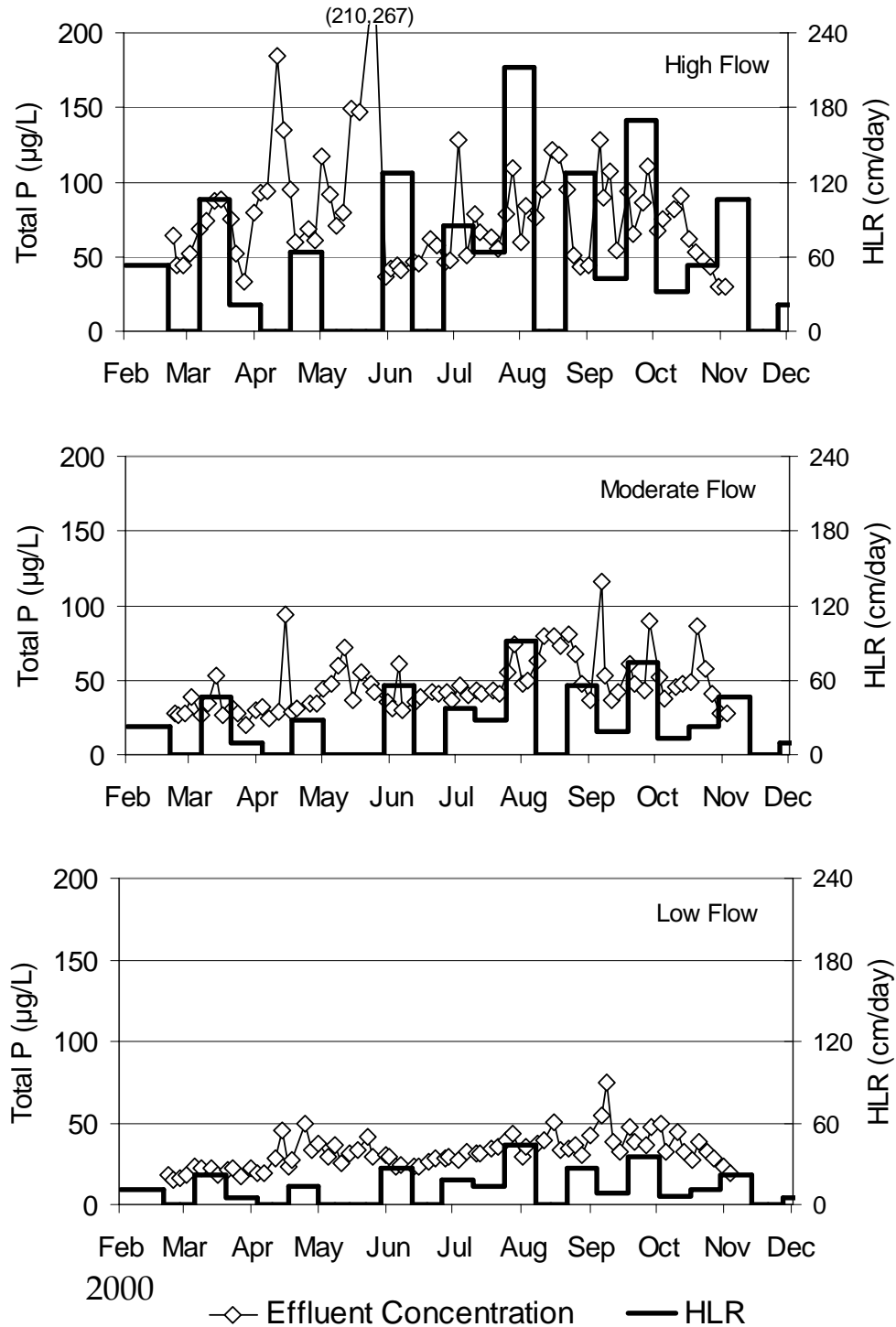


Figure 2.21. Mean outflow total P concentrations from mesocosms that received high, moderate and low pulse loading regimes.

Water column P “spikes” observed during the quiescent periods in the high loading mesocosms frequently resulted in water column phytoplankton blooms. For example, we observed the green alga *Coelastrum* sp. in one of the high loading mesocosms during the “no flow” period on May 23, 2000. These higher loaded mesocosms (i.e., 1.5-day avg. HRT; HLR= 55 cm/day) probably supported greater numbers of phytoplankton because they had received higher historical P loadings, and thus a greater labile P pool would have accrued in the sediments. Higher P release rates therefore would be expected from the more heavily loaded high HLR mesocosms than from the two lower HLR treatments. Results of our Cell 4 sediment evaluation provide additional evidence of the importance of previous P loading history as well as the ambient environmental conditions on sediment P release. Alternatively, the high P loadings introduced in the two weeks prior to the quiescent periods may have produced water column P concentrations that promoted phytoplankton productivity.

Conditions promoting phytoplankton growth within the high HLR mesocosms dissipated, however, when the flow was resumed. This may be related to a phytoplankton “wash-out” phenomenon, the return to more favorable environmental conditions that sequesters labile sediment P, and/or the absence of diffusion-gradient limitations on P uptake by SAV.

Table 2.10. Average total phosphorus concentrations (µg/L) in the water column (outflow region) of NATTS pulse loaded mesocosms, during quiescent (7 two-week periods) and flowing (13 two-week periods) conditions. Pulsed loading mesocosms (two replicates per treatment) were sampled twice weekly; constant loading mesocosms (one mesocosm per treatment) were sampled weekly.

	Low HLR Mean (±1 s.d.)	Medium HLR Mean (±1 s.d.)	High HLR Mean (±1 s.d.)
Quiescent Average TP	28 ±9	45 ±20	93 ±58
Pulse Flow Average TP	32 ±11	45 ±19	67 ±25
Constant Flow Average TP	33 ±10	37 ±12	54 ±17

Differences between the pulsed and constant flow mesocosm outflow TP concentrations were greatest in the high flow systems, which were statistically significant ($P = 0.008$) and statistically lower ($P < 0.05$) in the moderate and low flow systems (Figure 2.22). However, it should be

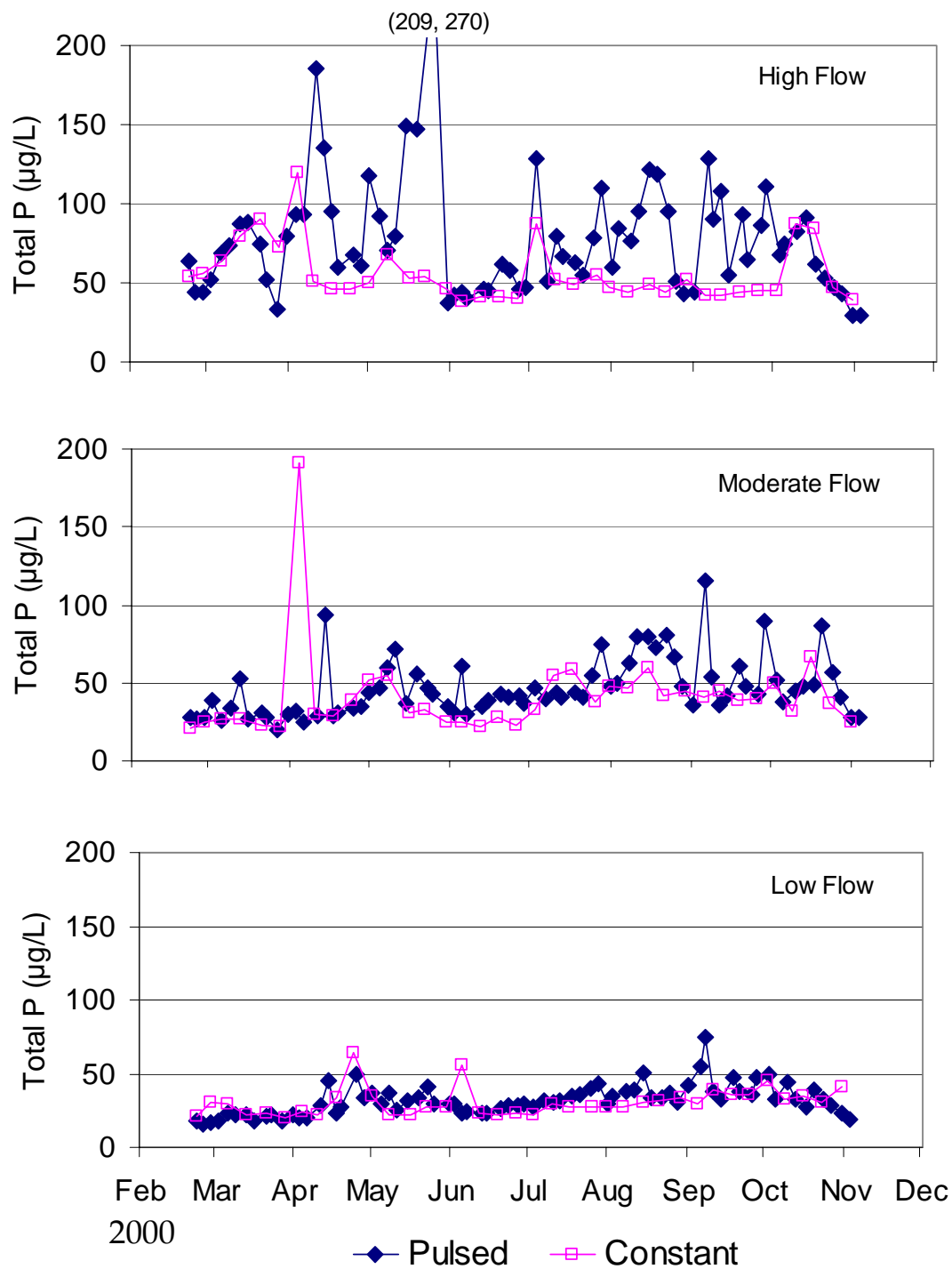


Figure 2.22. Outflow total P concentrations from mesocosms that received high, moderate and low flows of Post-BMP waters under pulsed and constant-flow regimes.

noted that our maximum evaluated HLR (220 cm/day) was two orders of magnitude above the mean design flows for an STA [mean (max.) HLR = 2.6 (53) cm/day]. The data suggest that the reduced performance observed under “high” pulsed loads is not likely to be observed in a full scale SAV-based STA. Pulsed loading may affect performance in the immediate inflow region of a full-scale treatment cell, but little or no effect would probably be detected at the outflow region under current design HLRs of 2.6 cm/day.

2.4.4 Phosphorus Export from Limerock Beds after Resumption of Flows

As an additional component of the pulse-loading evaluation, we investigated the potential for P export from the LR beds immediately following resumption of inflows following a “no flow” period. During a “no flow” period of two weeks or more, the residual interstitial water within the limerock may stagnate, and even evaporate if the dry-out period is long enough. We therefore designed our sampling scheme to capture any “first flush” effects by sampling the LR bed effluent at frequent intervals ($\Delta T = 1, 3, 21.5$ hours) immediately upon resumption of flow. Only short (1.5 days) and moderate (3.5 days) HRT process trains were sampled in this evaluation.

On March 6, flows were resumed to the sequential SAV/LR systems after two weeks of no flow. Prior to the two-week no flow period, the mesocosms had been operated at constant HLRs of 53 (HRT of 1.5 days) and 22 cm/day (HRT of 3.5 days) for 13 months since being harvested and reinoculated in February 1999. Specific conductance values indicated a slight build up of salts within the LR columns during the no flow period, followed by a rapid decrease within the first 24 hours after the resumption of flow (Table 2.11). Total P and DOP concentrations in the LR bed effluents were variable but peaked in the $\Delta T=3$ -hour samples (Table 2.11). SRP concentrations decreased after the first hour following flow resumption. Particulate P (PP) levels increased during the initial 24 hours following resumption of flows (Table 2.11).

In this evaluation we observed substantial between-treatment differences with respect to the export of P species. Limerock bed effluent from the high HLR mesocosms consistently yielded higher concentrations of P species than the LR beds downstream of the moderate HLR

mesocosms. Differences between alkalinity and specific conductance for the systems, however, were negligible (Table 2.11).

Generally, TP and SRP concentrations exiting the LR beds within the first 21.5 hours of flow were elevated compared to the concentrations measured in the non-pulsed (i.e., constant flow rates) Long-Term Monitoring LR beds (Table 2.11). Since the duration of the “first flush” after a period of no flow appears to be brief, the overall, long-term impact on the total mass of P exported would likely be minor. However, P concentrations within the “first flush” may be sufficiently high to warrant preventative measures, such as recycling the LR outflow to the SAV cell(s) for further treatment prior to final discharge.

Table 2.11. Water quality characteristics of limerock (LR) outflow during the first 21.5 hours of flow on March 6, 2000, following a two-week period of no flow. The pulsed loading data are compared to the limerock outflows from the constant hydraulic loaded (non-pulsed) mesocosm evaluation during the February-April 2000 quarter. Each value from the pulsed loading is an average of duplicate LR bed outflows while the constant loading values represent an outflow from a single LR bed.

Loading	Δ Time (hrs)	SRP ($\mu\text{g/L}$)	TP ($\mu\text{g/L}$)	TSP ($\mu\text{g/L}$)	DOP ($\mu\text{g/L}$)	PP ($\mu\text{g/L}$)	Alkalinity (mg CaCO_3/L)	Sp. Cond. ($\mu\text{S/cm}$)
Pulsed High Loading	1.0	37	53	52	15	1	213	943
	3.0	36	75	53	17	22	158	842
	21.5	20	62	31	11	31	133	669
Constant High Loading		31	46	42	11	4	209	898
Pulsed Moderate Loading	1.0	26	40	35	9	5	210	940
	3.0	19	47	36	16	11	143	831
	21.5	7	33	15	8	18	133	631
Constant Moderate Loading		11	21	19	9	2	188	884

2.5 Effects of Dryout and Reflooding on Phosphorus Retention

Upon completion of the Pulse Loading assessment (November 24, 2000), we began a Dryout-Reflooding investigation in two of the six pulsed mesocosms (one each of the high and low flow treatments) in order to assess the impact of sediment desiccation on P removal/export, to gauge

the influence of previous P loading regimes on sediment stability, and to evaluate the ability of the SAV communities to recover after a dryout event.

2.5.1 Baseline Monitoring Prior to Drawdown

Prior to drawing down the water level in selected mesocosms, we began with “baseline” water sampling at the inflow and outflows of the SAV and LR unit processes. During six weeks of baseline sampling the two mesocosms received Post-BMP waters at constant HLRs of 11 and 53 cm/day. Inflow and outflow TP, pH and temperature measurements were performed weekly. Total soluble P (TSP), soluble reactive P (SRP), dissolved calcium and total alkalinity were measured on biweekly composites of weekly grabs.

As expected, TP concentrations were reduced more within the lower loaded mesocosms (L-3) than in the higher loaded mesocosms (S-3) (Table 2.12). For both treatments, slight increases in SRP concentrations occurred within the LR beds. The LR bed was particularly effective in removing the PP leaving the high HLR (53 cm/day) mesocosm. DOP concentrations remained unchanged through the “high-flow” SAV mesocosm, whereas we observed a 50% reduction in DOP in the lower loaded mesocosm (Table 2.12).

Table 2.12. Chemical characteristics of the inflows and outflows of mesocosms receiving high (S-3: 53 cm/day) and low (L-3: 11 cm/day) hydraulic loading rates (HLRs), and of outflows from downstream limerock barrels, during a six-week baseline monitoring period prior to drawdown. Values represent means of six weekly grabs (TP, SRP, pH) or three two-week composites (DOP, PP, alkalinity, dissolved calcium).

	Inflow		SAV Outflow		LR Outflow	
	High HLR (S-3)	Low HLR (L-3)	High HLR (S-3)	Low HLR (L-3)	High HLR (S-3)	Low HLR (L-3)
TP (µg/L)	50	51	44	15	31	17
SRP (µg/L)	28	28	17	2	19	4
DOP (µg/L)	11	11	10	5	9	5
PP (µg/L)	10	12	17	8	2	8
Alk (mg CaCO ₃ /L)	197	196	193	135	193	161
Diss. Ca (mg/L)	63	64	64	41	65	49
pH	7.68	7.83	8.05	8.98	7.80	8.01

2.5.2 Dryout and SAV Sampling

After the six-week baseline monitoring, the water level in both mesocosms was lowered from 0.8 to 0.3 m. Small (0.30 m²) quadrats were sampled in the inflow and outflow regions of each mesocosm to characterize the vegetation standing crop (wet and dry) and to quantify the tissue N, P and Ca contents. A section of above-ground vegetation also was removed from the center region of each tank to facilitate sediment core retrieval. Following these sample collection efforts, the water level was further reduced to 1 cm to initiate the dryout period.

2.5.3 Characteristics of Harvested SAV

Plant decomposition, which releases biomass-P, can be a potential source for P release upon reflooding. For example, one month into the drydown period, all vegetation had decomposed in the mesocosm that had received a HLR of 53 cm/day (S-3), while in the mesocosm hydraulically loaded at 11 cm/day (L-3) much of the dried *Chara* remained intact. Therefore, the high Ca content of *Chara* tissues (Figure 2.23), compared to *Ceratophyllum* tissues in S-3, may attenuate P release from L-3 upon reflooding by retaining more P in the decomposed *Chara* biomass and by providing P sorption sites.

Analysis of the initial vegetation harvested from the two mesocosms revealed differences with respect to SAV species and P content (Figures 2.24 and 2.25). The S-3 mesocosm that historically received an average hydraulic loading rate (HLR) of 53 cm/day was colonized exclusively by *Ceratophyllum*, whereas the lower loaded (L-3) mesocosm (HLR = 11 cm/day) supported a more diverse SAV community consisting of *Chara*, *Najas* and *Potamogeton*, as well as filamentous green periphyton (Figure 2.24). Higher tissue-P content was observed for the vegetation collected from the inflow than outflow regions within each mesocosm (Figure 2.25). This trend reflects the decreasing water column P concentrations from inflow to outflow. Despite higher P concentrations in *Ceratophyllum* tissues from S-3 (Figure 2.25), a similar quantity of P (by mass) had accumulated in the L-3 SAV community due to a larger standing crop biomass at the time of harvest (Figure 2.26).

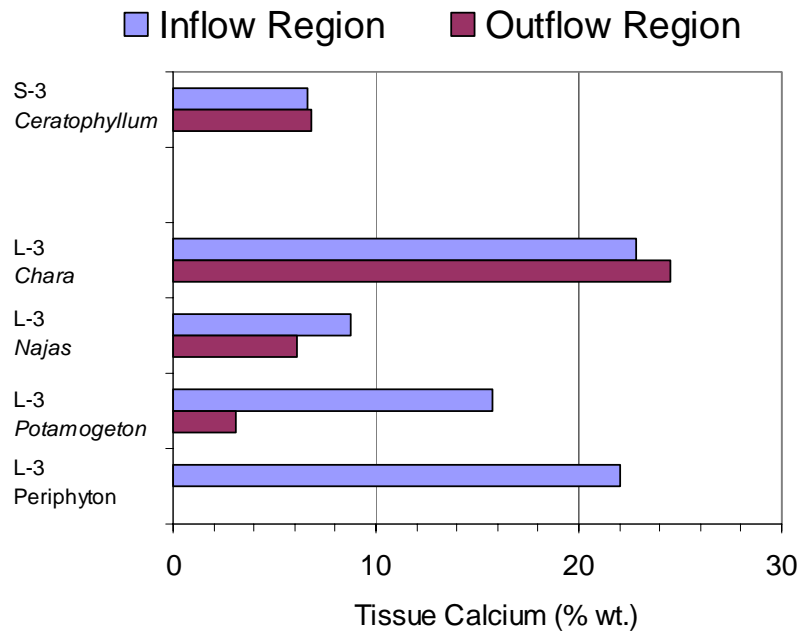


Figure 2.23. Calcium concentration in the tissues of dominant plant taxa in the inflow and outflow regions of mesocosms that were operated at high (S-3) and low (L-3) hydraulic loading rates of 53 and 11 cm/day, respectively.

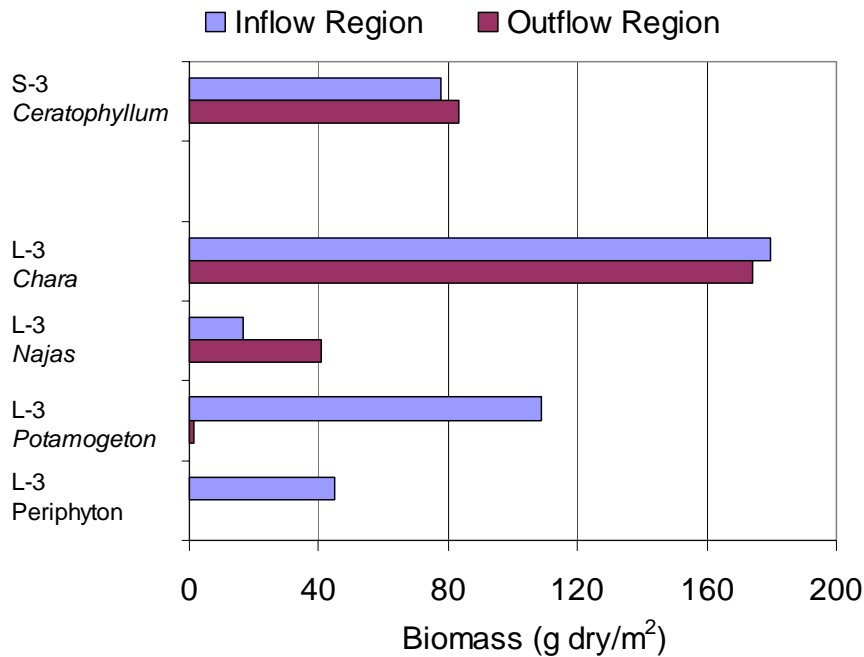


Figure 2.24. Standing crop biomass of dominant plant taxa in the inflow and outflow regions of mesocosms that were operated at high (S-3) and low (L-3) hydraulic loading rates of 53 and 11 cm/day, respectively.

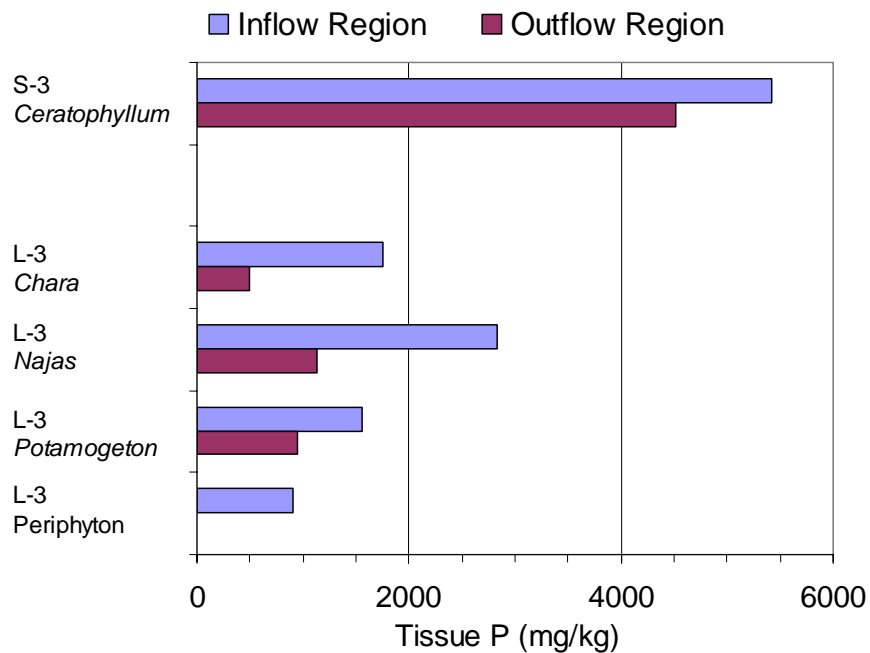


Figure 2.25. Phosphorus concentration in the tissues of dominant plant taxa in the inflow and outflow regions of mesocosms that were operated at high (S-3) and low (L-3) hydraulic loading rates of 53 and 11 cm/day, respectively.

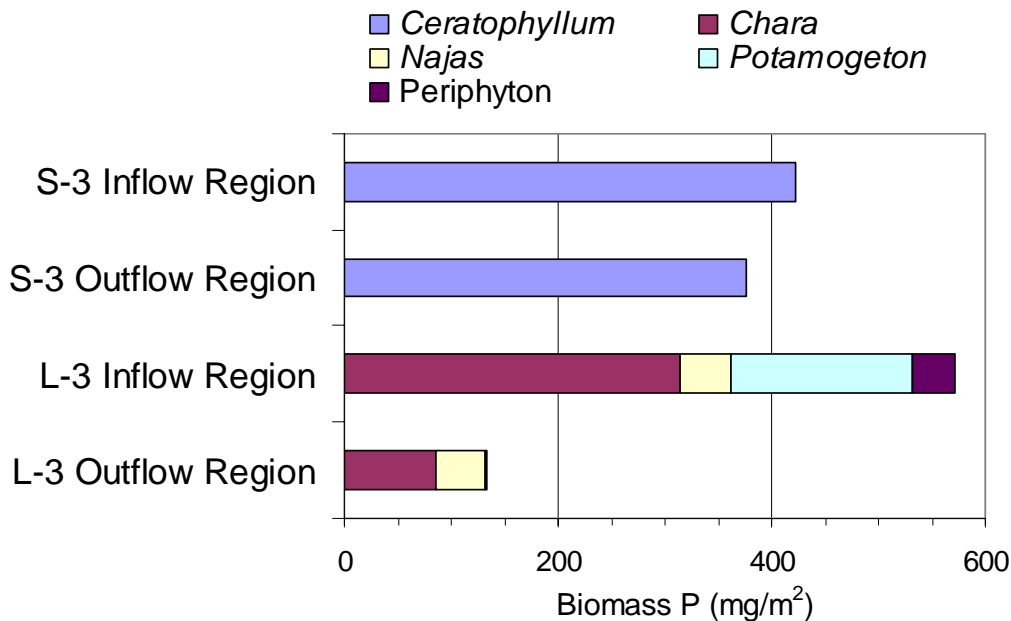


Figure 2.26. Phosphorus storage in the standing crop biomass of dominant plant taxa in the inflow and outflow regions of mesocosms that were operated at high (S-3) and low (L-3) hydraulic loading rates of 53 and 11 cm/day, respectively.

2.5.4 Sediment Consolidation

During the desiccation period, the thickness of the newly-accrued sediment layer in each mesocosm was measured several times per week on either side of the denuded central region to record consolidation of the drying sediments. Figure 2.27 shows greater consolidation of sediments in the S-3 mesocosm, mostly due to the oxidation and shrinkage (dehydration) of the higher organic matter sediment in that mesocosm. After 105 days of desiccation the accrued sediment in both mesocosms had consolidated to 35-40% of the original sediment depth.

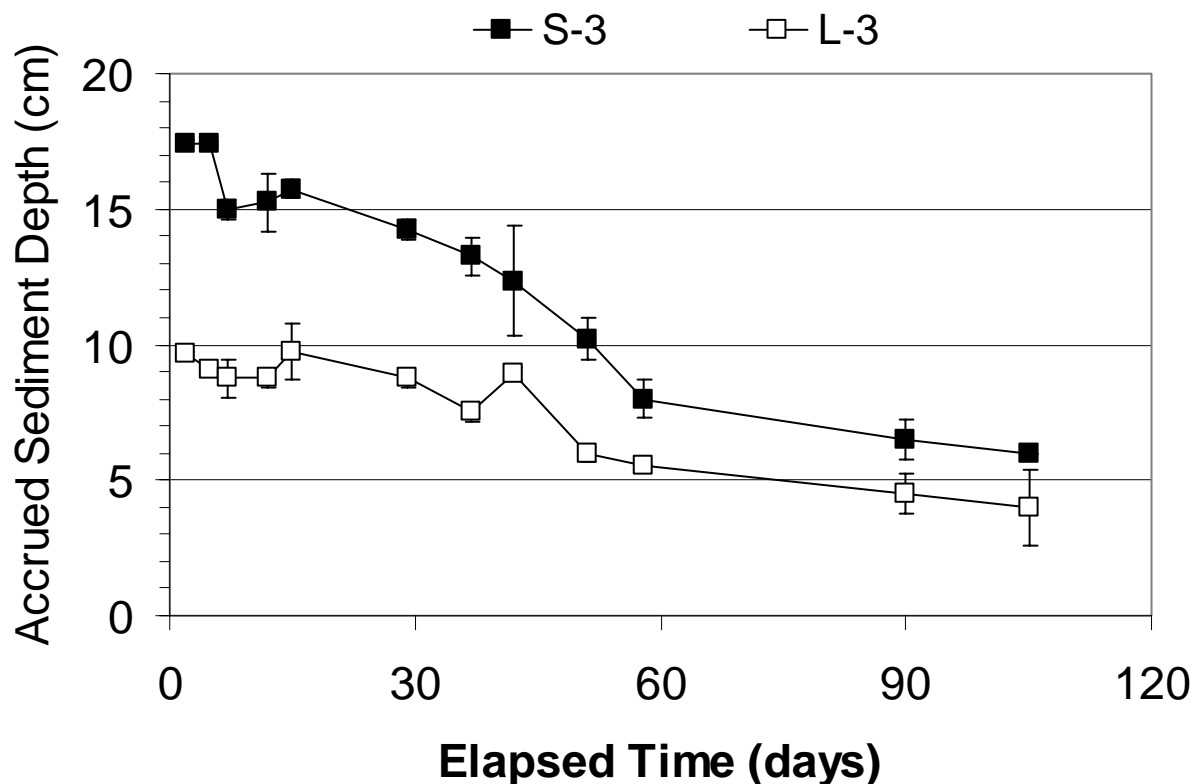


Figure 2.27. Consolidation during drydown of desiccating sediments originally formed under high (S-3) and low (L-3) mean hydraulic loading rates of 53 and 11 cm/day, respectively. Error bars = \pm 1s.d. of duplicate measurements.

2.5.5 Sediment Phosphorus Concentration and Release upon Reflooding: Laboratory Incubations

Triplicate sediment cores (15.9 cm² each) were collected from the exposed central region after 0, 7, 14, 29, 58 and 105 days had elapsed since exposing the sediments to air. The stoppered cores were initially placed on ice during transport to the lab, and then refrigerated at 4 °C until rehydration and incubation, which usually occurred within 48 hours of core retrieval.

The accrued sediment layer, which was easily distinguished from the underlying muck, was extruded from one of the three cores and immediately dried for moisture content and P analysis. The other two intact cores retrieved from each mesocosm were rehydrated with 250 mL Cell 4 inflow water (collected on January 10, 2001 and stored in the dark at 4 °C between trials). The rehydrated cores were then laboratory-incubated in a dark water bath (26 ±1 °C) under light air bubbling for 24 hours.

We chose Cell 4 inflow water as the source water for rehydrating the cores because we believed it would represent an “average” reflood water with respect to Ca, alkalinity and P levels. Cell 4 inflow water also was selected because it is the water that would reflood SAV-dominated Cell 4 should it ever dry out. Initial characteristics of the overlying water are provided in Table 2.13. A control (identical acrylic core with 250 mL overlying water and without sediment) was also incubated with the four sediment cores during each trial.

Table 2.13. Characteristics of sediment core incubation water collected from the Cell 4 inflow region on January 10, 2001.

	pH	TP	SRP	DOP	PP	Alkalinity	Ca
Cell 4 Inflow	7.81	36 µg/L	14 µg/L	13 µg/L	9 µg/L	302 mg CaCO ₃ /L	82 mg/L

Total P concentrations for the two sediment types (S-3 and L-3) remained similar over the five sampling events to those measured prior to drydown, with an average of 1330 ±108 mg P/kg in S-3 sediments and 686 ±107 mg P/kg in L-3 sediments (Figure 2.28).

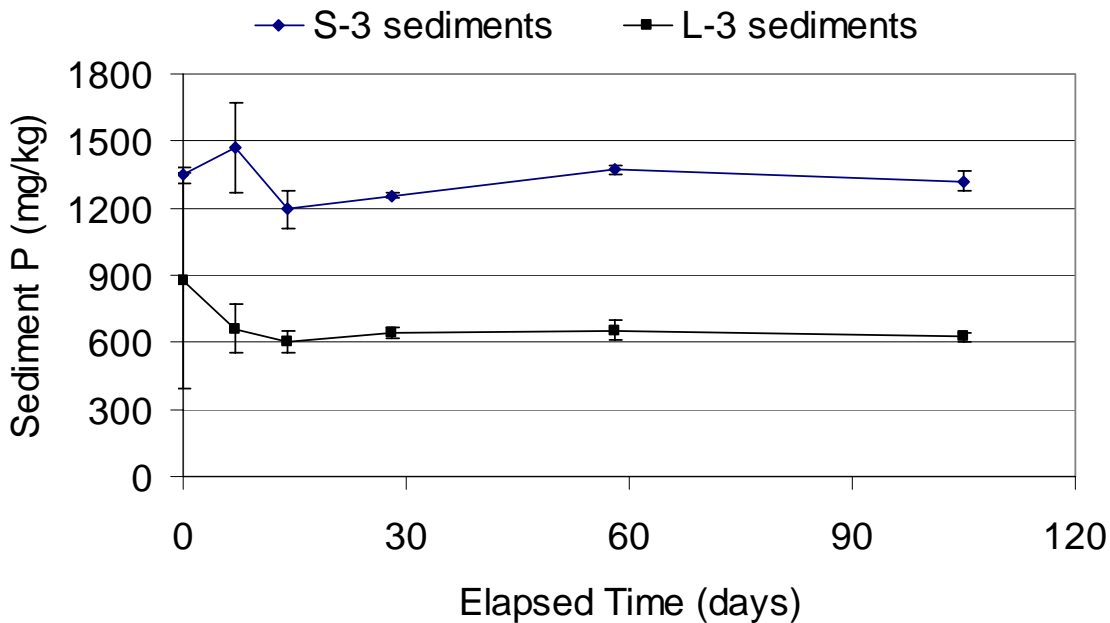


Figure 2.28. Phosphorus concentration of desiccating sediments as a function of time since onset of desiccation. Mesocosms that were operated under high (S-3) and low (L-3) hydraulic loading rates of 53 and 11 cm/day, respectively, prior to the desiccation evaluation. Error bars = ± 1 s.d. of triplicate cores.

Sediment moisture content remained unchanged during the first month of the desiccation period, with $88 \pm 2\%$ water found in cores across all treatments (S-3 and L-3) and trials ($\Delta T = 0, 7, 14$ and 29 days). Sediment moisture content decreased in both treatments to $81 \pm 1\%$ at $\Delta T = 58$ days, and after 105 days, S-3 sediments declined to as low as 53%. Sediments within both mesocosms had thoroughly dried and cracked after 105 days, causing separation from the walls of the mesocosm tanks.

During incubation of cores collected immediately after drawdown ($\Delta T = 0$ days), overlying water SRP concentrations were reduced from 14 $\mu\text{g/L}$ to below the method detection limit (MDL) of 2 $\mu\text{g/L}$ in cores retrieved from the low loading mesocosm (L-3) (Figure 2.29). In contrast, SRP concentrations were relatively unchanged in the high loading mesocosm (S-3) cores (11 ± 4 $\mu\text{g/L}$). Control overlying water (no sediment) was reduced from 14 to 6 $\mu\text{g SRP/L}$ during the 24-hour incubation.

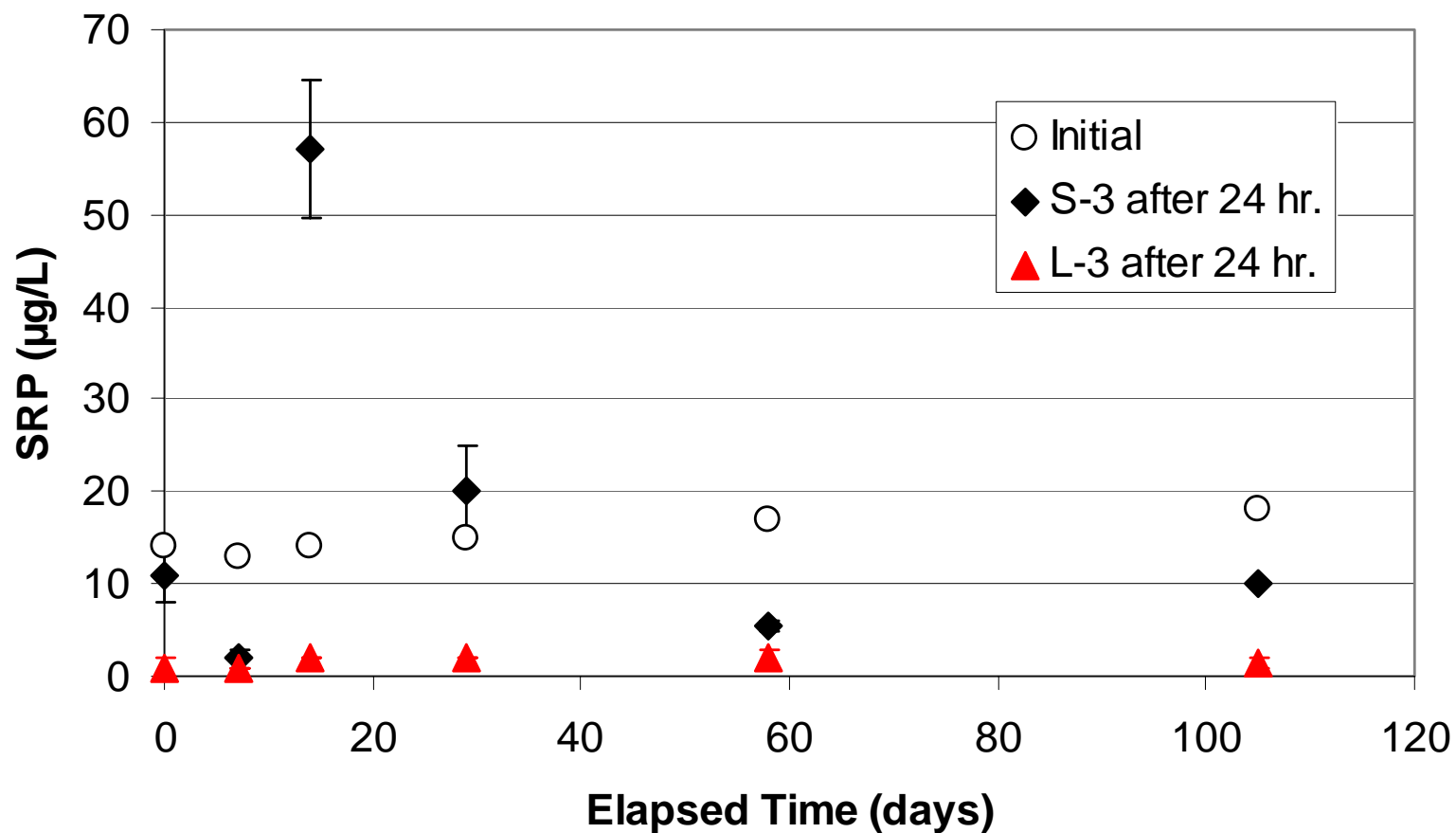


Figure 2.29. The change in SRP concentration in 250-mL of overlying water during 24-hour incubations of sediment cores retrieved from mesocosms that were operated under high (S-3) and low (L-3) hydraulic loading rates of 53 and 11 cm/day, respectively, prior to the onset of desiccation (elapsed time of 0 days). The initial SRP is the concentration in the overlying water prior to exposure to sediment; the S-3 and L-3 data points are the post-incubation SRP concentrations in the overlying water. The S-3 and L-3 data points represent the mean of two replicate cores (bars = ranges) after a 24 hour incubation in contact with the sediments.

For the $\Delta T = 7$ day post-desiccation 24-hr core incubations, SRP concentrations were reduced from 13 to ≤ 3 $\mu\text{g/L}$ in S-3, L-3 and control (no sediment) cores (Figure 2.29). At $\Delta T = 14$ days, however, differences were again observed between treatments. SRP concentrations increased from 14 to 57 $\mu\text{g/L}$ in the overlying water of the S-3 sediment, while waters above L-3 sediments and in the control core were reduced to 2 $\mu\text{g SRP/L}$. SRP release from the incubating S-3 sediments was less at $\Delta T = 29$ days, and by $\Delta T = 58$ days, the overlying water SRP concentration was reduced over the 24 hour incubation period in all treatments. The final incubation of S-3 and L-3 sediments took place after 105 days of desiccation. Sediments from both treatments were noticeably drier than during previous iterations, yet no SRP release was observed during the 24-hour rehydration period. Incubation water pH values increased equally across all treatments during each trial. Initial pH values of 7.81 – 8.27 increased to 8.33 – 8.85 after 24 hrs.

Phosphorus release from drying sediments was expected *a priori* to be greater from S-3 sediments than from L-3 sediments, due to higher TP in the former (DBE 1999). Sediments formed under higher nutrient loadings (such as S-3 and Cell 4 Inflow) typically exhibit higher TP and organic matter concentrations and lower Ca concentrations. Consequently, they release more P upon reflooding when compared to sediments formed under lower nutrient loadings (e.g., L-3 and Cell 4 Outflow locations). However the total SRP release from the S-3 sediments in this dryout evaluation was unexpectedly low, and indicates that sediment compaction/oxidation may be an inexpensive way to prolong wetland treatment without adverse P mobilization upon reflooding.

2.5.6 Sediment Phosphorus Release upon Reflooding: In-Situ Assessment

After the last core retrieval on April 25, 2001 ($\Delta T = 105$ days of desiccation), the mesocosms were reflooded at the original hydraulic loading rates of 11 and 53 cm/day. The sediment moisture content had been reduced from 87-88% to 53% and 70% in the high and low HLR mesocosms, respectively, and the sediment surfaces had developed deep fissures throughout. All of the original SAV contained in both mesocosms had been dried and decomposed to the point of being unrecognizable (except for some *Chara*), and terrestrial vegetation had invaded

the mesocosms. Following reflooding, outflow TP concentrations were monitored for 13 weeks until July 20, 2001. Although there was an initial P flush upon reflooding, it was short-lived in both mesocosms, with the SAV systems attaining their pre-dryout levels after 5 weeks (Figure 2.30).

2.5.7 SAV Recolonization

Although the SAV completely disappeared during the dryout period, being replaced by terrestrial vegetation, SAV propagules in the exposed sediment, and possibly carried into the tanks with the resumption of flow, resulted in the eventual recolonization of SAV in both tanks. Table 2.14 is a qualitative description of the recolonization of SAV after reflooding of dried sediments. Small amounts of SAV biomass were seen after 3 weeks of flow resumption, and full biomass recovery was observed before 101 days had elapsed.

Table 2.14. Recolonization of mesocosms receiving hydraulic loading rates of 53 cm/day (S-3) and 11 cm/day (L-3) after a 110-day dryout period.

Elapsed time since resumption of flows:	
21 days	<p>S-3: Duckweed (<i>Lemna</i> sp.) cover with sparse <i>Ceratophyllum</i> and periphyton</p> <p>L-3: Small <i>Chara</i> inhabiting about 50% of the bottom, along with sparse <i>Potamogeton</i></p>
30 days	<p>S-3: <i>Lemna</i> sparse with a mixture <i>Chara</i>, <i>Najas</i>, and periphyton, and a lesser amount of <i>Ceratophyllum</i></p> <p>L-3: <i>Chara</i> biomass more abundant plus sparse <i>Potamogeton</i></p>
56 days	<p>S-3: Periphyton abundant with sparse <i>Chara</i> and <i>Najas</i></p> <p>L-3: <i>Chara</i> topped-out plus a periphyton mat; <i>Potamogeton</i> sparse</p>
101 days	<p>S-3: Mostly <i>Najas</i> with some <i>Chara</i></p> <p>L-3: Mostly <i>Chara</i> with small amounts of <i>Najas</i> and <i>Potamogeton</i></p>

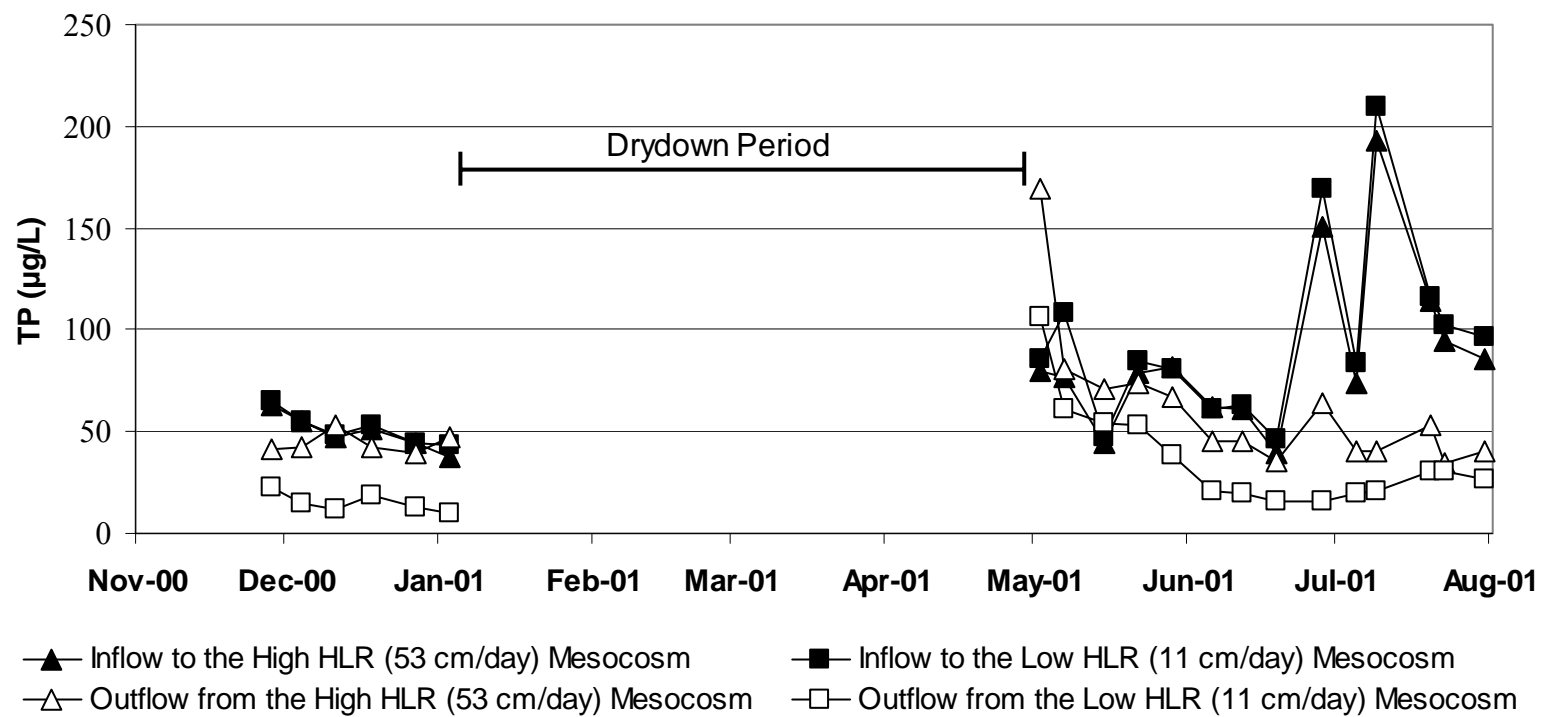


Figure 2.30. Total P concentrations in the inflow and outflow of two SAV mesocosms before (November 28, 2000 to January 10, 2001) and after (May 1 to July 31, 2001) a 110-day dryout period.

2.5.8 Summary

Based on these mesocosm studies, the effects of a prolonged drawdown on the SAV community appear to be temporary. We observed 100% mortality of the SAV during the 110-day drawdown, but SAV recolonization and P removal capabilities were fairly rapid. We anticipate that in a full-scale SAV wetland, selective herbiciding of emergent vegetation may be required prior to or immediately following reflooding. Prior to the regrowth of SAV, some P export also can be expected on a short-term basis (3 or 4 weeks), especially for high P loaded wetlands.

2.6 Sequential SAV/LR and Cattail Mesocosms

During our initial evaluations at the NATTS, we established mesocosms in a sequential fashion (deep SAV followed by shallow SAV followed by LR) in an attempt to optimize treatment performance. We continued operation of these systems into the Follow-On assessment period. Each of the duplicate sequential SAV/LR systems consisted of a 0.8 m deep SAV mesocosm (2.2m L x 0.79m W x 1.0m D) that received Post-BMP feedwater, followed by a shallower, 0.4 m deep SAV mesocosm of equal dimensions. Outflow waters from the shallow system discharged through a LR bed with a 1 hr hydraulic retention time. The overall HRT of this system was 5 days.

2.6.1 Long-Term Phosphorus Removal

From November 18, 1998 through April 19, 1999, the two-tank-in-series SAV component of the system removed 90% of the total inflow P load, providing a mass P removal rate of 4.4 g P/m²-yr, and an average outflow total P concentration of 11 µg/L. However, the P removal efficiency of the 0.8 m deep SAV mesocosm declined in May 1999 (Figure 2.31). The downstream shallow (0.4 m) mesocosm attenuated the elevated outflow concentrations of the deeper mesocosm, with further removal achieved in the LR beds (Figure 2.31). As a consequence of the increased P loadings to the shallow mesocosm, the outflow concentrations of the shallow mesocosms and LR beds did increase (Figure 2.31). Overall, for the period of record (November 18, 1998 to December 21, 2000), the average inflow TP of 111 µg/L was reduced to 65 µg/L after treatment within the 0.8 m deep tank, which was further reduced to 27 µg/L after passage through the 0.4 m deep SAV mesocosm. The LR bed further reduced TP levels to 21 µg/L.

Because of wide variations in post-BMP inflow total P concentrations during January-March 2000 (86-265 µg/L) and a visibly unhealthy plant community, the deeper (0.8 m) SAV mesocosms provided outflow total P concentrations ranging from 58-137 µg/L for that period (Figure 2.31). Significant P removal occurred in both of the shallower (0.4 m) mesocosms, where outflow total P concentrations averaged 31 ± 13 µg/L. Total P removal was not as high in the second replicate treatment train, which may have been due to the more pronounced senescence of *Chara* in that system. Total P concentration changes within the LR beds ranged from export (-11 µg/L) to removal (35 µg/L) during the three-month period.

We believe that one cause of the increased P export from the deeper mesocosm was a response to the development of a thick canopy of *Chara*, which comprised the entire SAV standing crop during this period. The thick canopy reduced the light penetration into the water column, which in turn reduced photosynthetic production and increased respiratory processes. The senescence of the underlying biomass of the macroalga initiated the growth of filamentous algae, which further solidified the *Chara* canopy and rendered the water column anoxic. As CO₂ production increased with respiration and CO₂ uptake decreased due to a restricted photosynthetic zone, the pH of bottom waters decreased. Thus, the calcium carbonate equilibrium shifted from conditions of precipitation to dissolution. A combination of anoxic conditions, dissolution of calcium carbonate, and decomposing *Chara* resulted in P being internally loaded to the mesocosms. This combination of internally loaded P and compromised treatment of the externally loaded P resulted in a mediocre P removal.

We reconfigured the sequential treatment train on July 17, 2000, adding a limerock barrel between the initial, deeper mesocosm, and the subsequent shallower mesocosm. Additionally, we removed ~ 0.3 m of muck substrate from the shallow mesocosm to normalize the substrate thickness to ~ 0.2 m for both mesocosms in each sequential system. We also increased the water depth in the shallow mesocosms from 0.4 m to 0.6 m.

The proliferation of *Chara* in our mesocosms may have been a “start-up” phenomenon: at larger scales, we find *Chara* only in newly-flooded systems. There is little *Chara* in Cells 1 and 4 of STA-1W. We therefore inoculated *Najas* into the shallower (now 0.6 m deep) mesocosms in July,

and we interrupted our bi-weekly TP monitoring of the shallow mesocosm and LR outflows to allow the *Najas* inoculum to acclimate. Beginning on October 31, 2000, we resumed biweekly sampling for TP in both intermediate and final LR outflows, and in the shallow mesocosm outflows.

For the six weeks that monitoring occurred after the reconfiguration, the TP concentration of the LR outflow reduced to levels not seen since the beginning of the evaluation (November 1998 to May 1999) (Figure 2.31). However, this may have been a short-term response to the very low inflow TP concentrations which coincided with the reduced TP concentrations in the LR outflow (Figure 2.31).

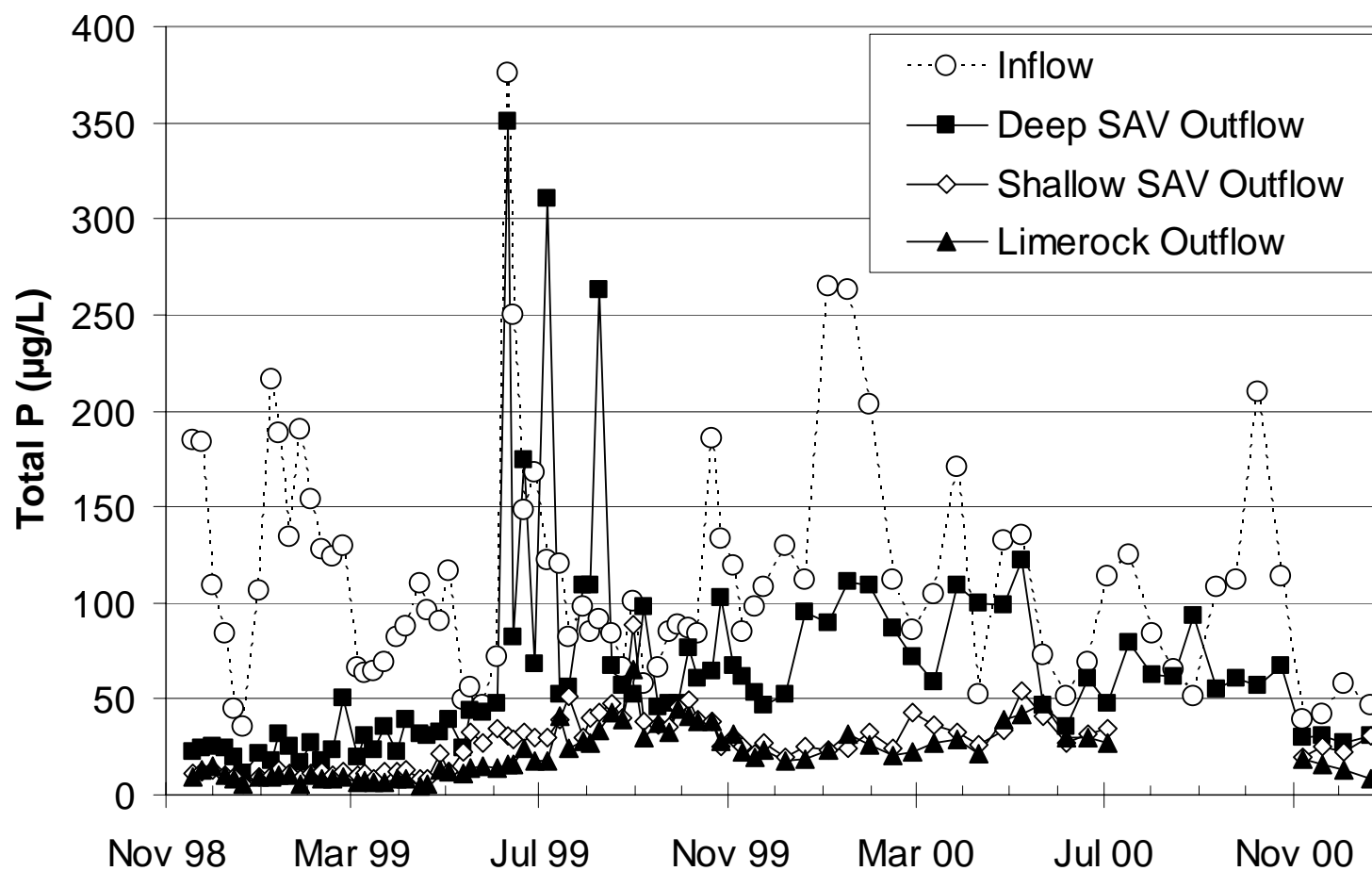


Figure 2.31. Mean total phosphorus concentrations in the inflow, the deep and shallow SAV mesocosms outflows, and the limerock bed outflow of sequential SAV/LR treatment trains at the North Supplemental Technology Site. Each data point represents the mean of duplicate tanks.

2.6.2 Vegetation History

The following is a brief history, based on field notes and algal taxonomic efforts, of the decline of *Chara* populations in these mesocosms. Our first recorded observation was on December 1, 1999, where *Chara* had been displaced by a filamentous green alga in some areas of one of the 0.8 m deep mesocosms. The majority of the area of the mesocosm at this time was open water. Since the *Chara* population had already declined considerably by then it is likely that the population was on the decline several months prior, which coincided with the reduced P removal effectiveness beginning in June 1999 (Figure 2.31). Indeed, phytoplankton surface scums (*Cystodinium bataviense* and *Cosmarium* sp.) were observed in both the deeper (0.8 m) and shallower (0.4 m) mesocosms of one of the replicate treatment trains as far back as June 16, 1999. In the deeper (0.8 m) mesocosm of the other replicate treatment train, thick surface mats of cyanobacteria (*Lyngbya* sp. and *Oscillatoria* sp.) were prevalent on July 7, 1999, persisting at a less dense biomass through August 12 and lasting until at least September 21, 1999. A "*Glenodinium*-type" dinoflagellate was present as light surface scum in the shallower mesocosm of the same replicate treatment train on August 12, 1999.

Both the phytoplankton scum and filamentous algae continued to inhabit some of the mesocosms in February 2000, which also coincided with the observed *Chara* mortality. *Lemna* also invaded some of the mesocosms during this time (February – March 2000). Sulfide odors from the decomposing *Chara* were noted in some of the mesocosms in May 2000, along with floating filamentous and non-filamentous algae. An attempt on May 23, 2000 to restock the mesocosms with *Najas* was unsuccessful, but a later inoculation in July was successful.

2.6.3 Calcium Effects on P removal

During our Phase I demonstration work, we observed dramatic fluctuations in Ca levels of Post-BMP waters, from approximately 40 to 115 mg/L. Since the completion of the first phase in February 1999, however, we have only measured inflow Ca levels intermittently. Those measurements showed low inflow (Post-BMP) Ca concentrations (34 mg/L) June 2, 1999. On June 10, eight days later, the Ca concentration increased to 84 mg/L. Ca levels reached a "typical" value of 101 mg/L on June 21. This cycle of low Ca levels in post-BMP waters occurred again in the following year when 50 – 59 mg/L was measured from April 20 to May

21, 2000. By June 9, the Ca concentration for the Post-BMP influent waters was 79 mg/L, and reached typical levels on July 10 when 93 mg/L was recorded. The low Ca levels likely lead to the appearance of populations of “soft-water” phytoplankton (desmids) in some of the SAV mesocosms.

We suspect that a decline in inflow calcium (Ca) levels may also have impaired the P removal performance of the SAV mesocosms. During a 21-month assessment project on SAV treatment of Post-BMP waters in our laboratory, we only observed declines in effluent quality during periods of low inflow Ca levels. Moreover, this “adverse” response to low Ca levels only occurred late during the second year of operation, a period during which the plant standing crop likely was no longer in a rapid growth phase. A decline in inflow Ca levels could result in the water column being “undersaturated” with respect to CaCO_3 , which could curtail the precipitation of CaCO_3 and/or stimulate the dissolution of sediment CaCO_3 . Either process could result in elevated outflow TP concentrations. *Chara* tissues are also high in Ca content (see Subtask 5iv), which may reflect a preference for high calcium/alkalinity waters. Thus the period of lower inflow Ca concentrations may have adversely affected the *Chara* biomass.

2.6.4 Spatial-Temporal Water Column Investigation in the Sequential SAV/LR System

We also performed temporal and spatial sampling in the Sequential SAV/LR mesocosms at the same time (September 23-24, 1999) we conducted one in the Static Water Depth mesocosms. The sampling procedures for this effort are described in the “Effects of Water Depth on SAV P Removal Performance” section. On November 10, 1999, we measured the daytime redox conditions at various depths and horizontal locations within the mesocosm tanks of the Sequential SAV/LR system in conjunction with the Cattail (this task) and Static Depth assessment mesocosms. Because of the substantial plant community differences between the duplicate sequential treatment mesocosms, the water quality data in Figures 2.32 – 2.38 are not averaged values, but instead are reported for each individual mesocosm.

In the initial, deeper mesocosm of the sequential treatment train, replicate 1 was much more efficient in total P removal in both the afternoon and early morning than replicate 2, where no surface horizontal gradient for P was observed. However, the P removal efficiencies were reversed

for the two replicate shallower depth "back end" mesocosms: higher P removals were observed in replicate 2 than replicate 1 (Figure 2.32). For the combined afternoon and morning periods, the final mean outflow total P concentrations leaving the sequential mesocosms was only slightly higher (by 7 $\mu\text{g TP/L}$) in replicate 2 than replicate 1. Even though inflow P concentrations were similar, the sequential mesocosms were less effective at P removal during this time than the Static Depth mesocosms (cf. Fluctuating Water Depth evaluation and Figure 2.32).

In both the deeper and shallower sequenced tanks, weak vertical SRP concentration profiles existed during both the afternoon and early morning (Figure 2.33). The horizontal SRP concentration gradients were more pronounced than the vertical concentration gradients, with only a slight diel effect. When compared to the Static Depth mesocosms sampled at the same times and locations, SRP concentrations within the sequential SAV mesocosms were higher (cf. Figure 2.6 and Figure 2.33).

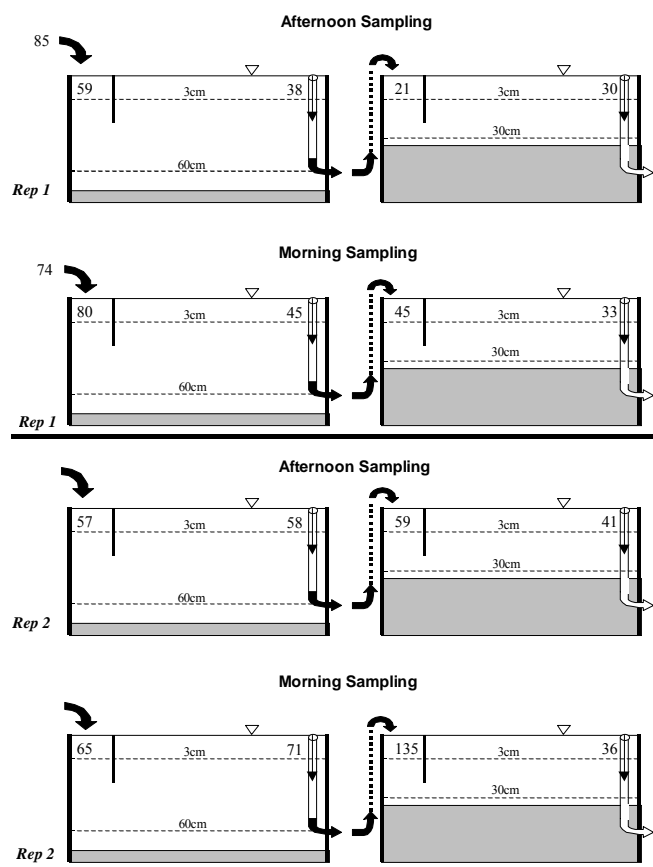


Figure 2.32. Total phosphorus concentration ($\mu\text{g/L}$) profiles during the Spatial-Temporal evaluation on September 23-24, 1999 in the Sequential SAV mesocosms at the North Supplemental Technology Site.

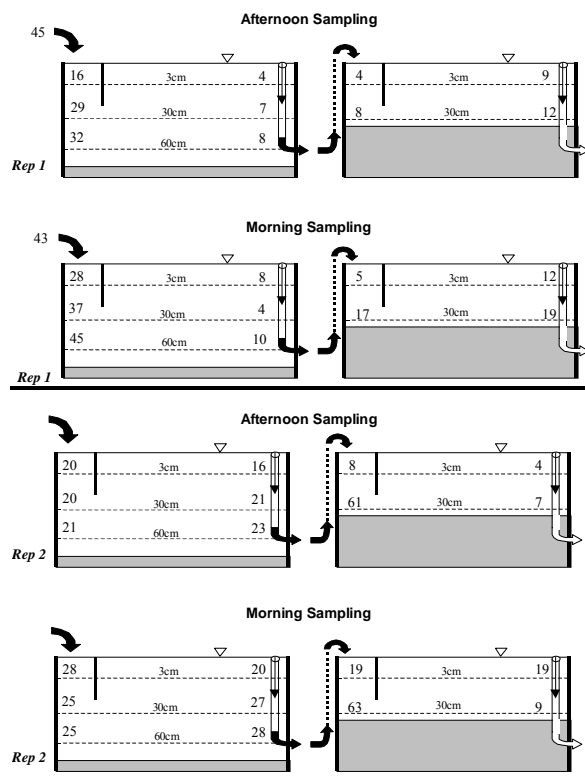


Figure 2.33. Soluble reactive phosphorus concentration ($\mu\text{g/L}$) profiles during the Spatial-Temporal evaluation on September 23-24, 1999 in the Sequential SAV mesocosms at the North Supplemental Technology Site.

The dissolved oxygen (D.O.) concentration profiles followed a pattern that was similar to the Static Depth mesocosms, except that there were frequent instances of depressed surface D.O. concentrations during the daytime in the Sequential mesocosms (Figure 2.34). Supersaturation was typical at these stations in the Static Depth mesocosms (cf. Fluctuating Water Depth assessment). Redox potentials, which were measured 46 days later for both evaluations (Static Depth and Sequential), demonstrated more highly reducing conditions in the Sequential mesocosms than in the Static Depth mesocosms, especially in the bottom waters (cf. Figure 2.8 and Figure 2.35).

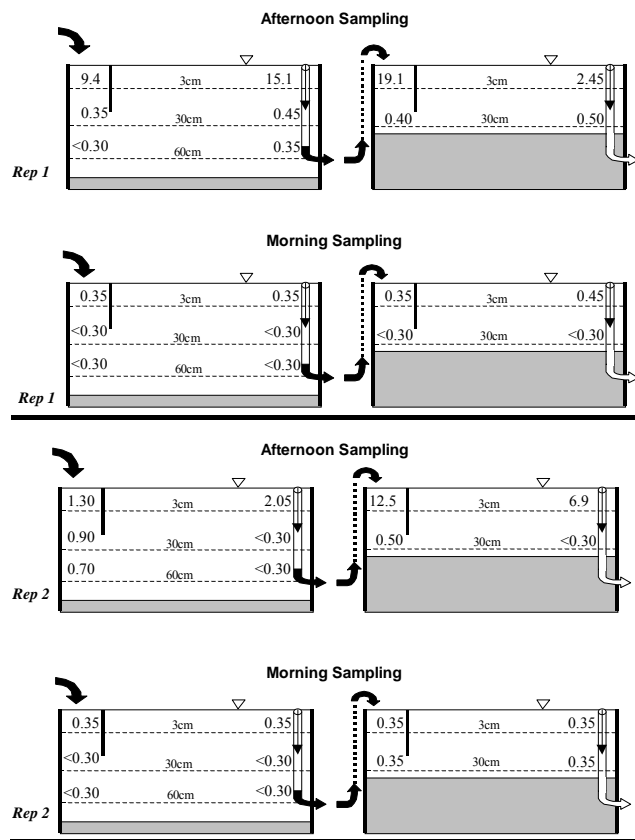


Figure 2.34. Dissolved oxygen (mg/L) profiles during the Spatial-Temporal evaluation on September 23-24, 1999 in the Sequential SAV mesocosms.

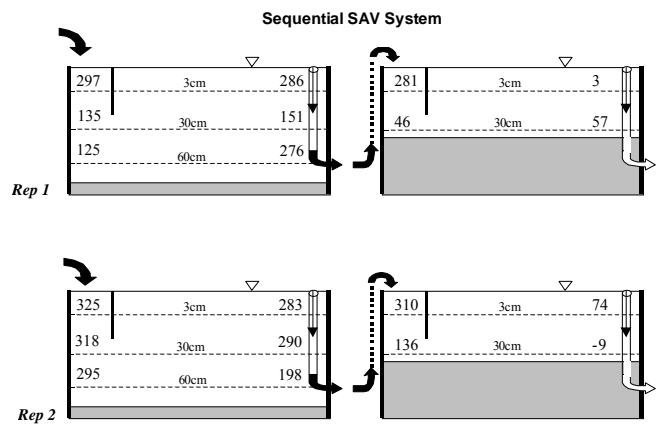
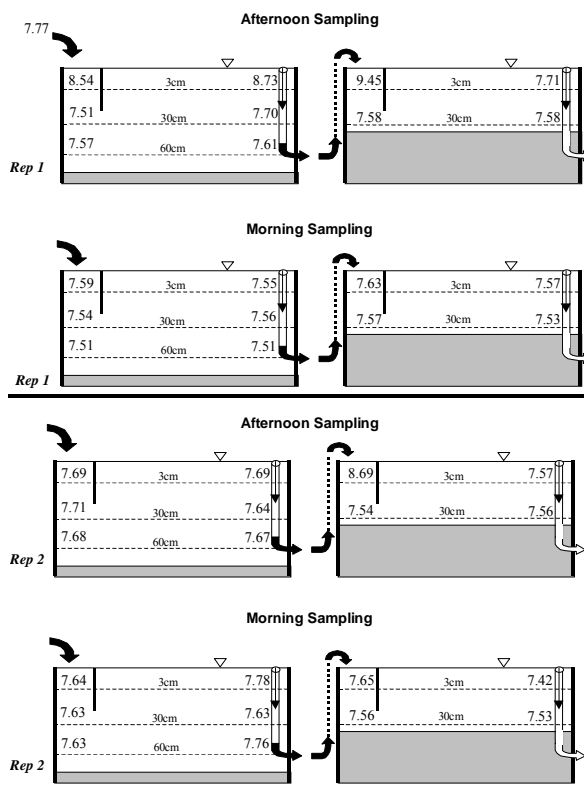


Figure 2.35. Mean values for daytime Eh (mV) profiles on November 10, 1999 in the Sequential SAV mesocosms.

Daytime dissolved Ca and alkalinity levels between the duplicate treatment trains diverged in a manner similar to pH values (cf. Figures 2.36 – 2.38). For the first replicate of the sequential treatment train, daytime surface pH values were considerably higher in three of the four stations than they were for the respective stations of the second replicate treatment train (Figure 2.36). Calcium concentrations were markedly reduced at those stations where the daytime pH values exceeded 8.5, as compared to the dissolved Ca levels at the other stations where pH values were more in the mid-7 range during both daytime and nighttime. As in the static water depth mesocosms, calcium precipitation as a carbonate, induced by a photosynthetic rise in the pH, is the likely explanation for this relationship.

Figure 2.36. Spatial-Temporal evaluation pH profiles during the on September 23-24, 1999 in the Sequential SAV mesocosms.



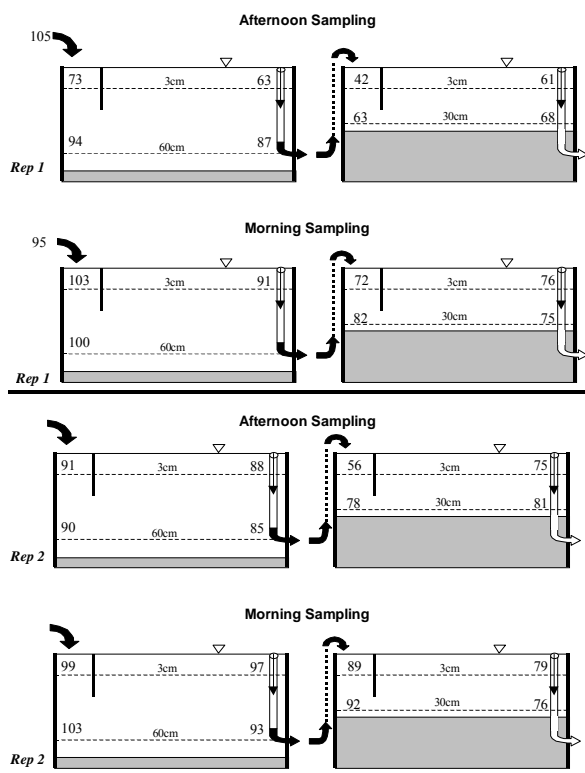
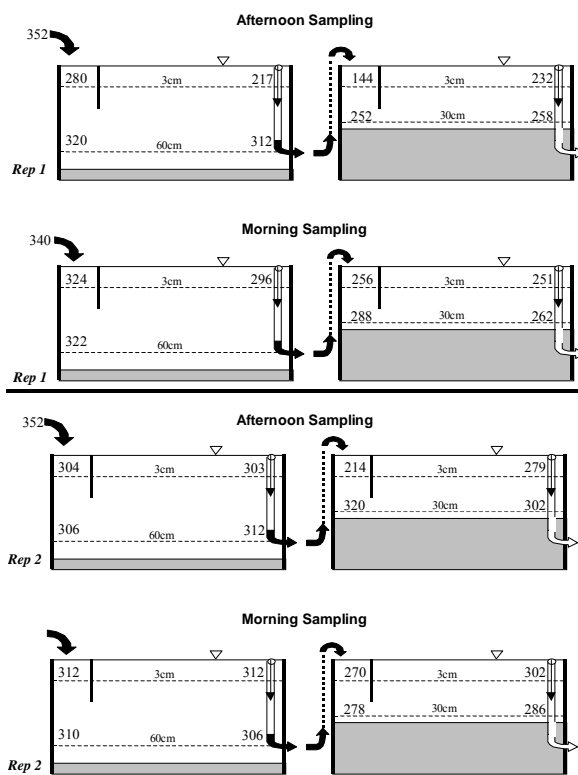


Figure 2.37. Dissolved calcium concentration (mg/L) profiles during the Spatial-Temporal evaluation on September 23-24, 1999 in the Sequential SAV mesocosms.

Figure 2.38. Alkalinity concentration (mg CaCO_3/L) profiles during the Spatial-Temporal evaluation on September 23-24, 1999 in the Sequential SAV mesocosms.



Daytime correlations among pH, calcium and SRP concentrations for surface waters in the Static Depth mesocosms were much stronger than those for the Sequential mesocosms. The r^2 values for daytime pH vs. Ca and Ca vs. SRP concentrations were 0.19 and 0.57, respectively, for the surface water stations of the Sequential mesocosms. This implies that P coprecipitation with calcium carbonate may not be as prominent of a removal mechanism for P as it was in the Static Depth mesocosms.

Prior to these measurements in the sequential mesocosms, the SAV standing crop had exhibited a marked decline. Visual observations of the dominant SAV species (*Chara*) indicated a stressed condition, where most of the macroalga was either necrotic or chlorotic. Sulfide odor was noticeable, and in some areas of the mesocosms filamentous blue-green algae (i.e., *Lyngbya* and *Oscillatoria*) formed contiguous surface and subsurface mats.

2.6.5 Conclusions

After six months of high P treatment performance, the initial *Chara* community in the SAV mesocosms began to die. The exact cause of this is unknown, but we believe it was most likely due to light limitation imposed by the robust *Chara* population, which lead to necrosis of the lower thalli of the macroalga and an additional oxygen demand.

The aggregated water quality data suggest that decomposition rates were high in the Sequential SAV mesocosms, caused by the mortality of the colonizing *Chara*. Rapid decomposition resulted in a community metabolism where respiration exceeded primary production, which in turn lead to the observed low pH values, redox potentials, and D.O. concentrations, and the high SRP and Ca levels. Sporadic surface planktom blooms and attached cyanobacteria colonies resulted.

2.7 Comparison of Phosphorus Removal Performance by Cattail- and SAV-Dominated Systems

Wetlands dominated by emergent macrophytes such as cattails may function differently than wetlands dominated by SAV. Submerged macrophytes can enhance both photosynthesis and nutrient uptake within the water column. Daytime pH levels increase with water column photosynthesis, which can result in a chemical immobilization of P in hard waters by

coprecipitation with calcium carbonate (see Coprecipitation Assessment). As part of this effort, we test the hypothesis that P removal is more efficient in a SAV community than in a cattail community when the inflow waters have high hardness concentrations.

During Phase I, we established two cattail- (*Typha*) dominated mesocosms (2.2m L x 0.79m W x 1.0m D, water depth 0.40m), to provide a comparison to the performance of the SAV mesocosms. The two cattail mesocosms exhibited different P removal efficiencies. One mesocosm was covered with less duckweed (*Lemna*), and contained less SAV (*Najas*) but contained more cattail than the other. These differences in the vegetation species and density were thought to be related to the observed differences in P removal. The variable composition of the plant community may affect light penetration into the water column, decomposition rates, and substrate quality for microbial processes, in addition to controlling the rate of P uptake by the plants themselves. One or more of these factors may explain mechanistically the differences in the P removal efficiencies observed between the two cattail mesocosms, as well as differences between cattails and SAV.

2.7.1 Phosphorus Removal Comparisons

Methodology

In order to make valid comparisons of the P removal performances by the two communities, we selected the shallow SAV mesocosms which had equivalent tank dimensions, water column depths (0.4 m), HLRs (10 cm/day), and HRTs (3.6 days). The SAV community was approximately 6 months older than the cattails; monitoring started in mid-July 1998 and end of December 1998 for the SAV and cattail mesocosms, respectively.

Inflow and outflow waters were monitored periodically from June 23, 1998 through August 14, 2001, for TP, SRP, PP, calcium, alkalinity, specific conductance, pH and temperature. From December 1, 1999 – June 8, 2001, weekly grab samples from both sets of mesocosms were composited for a two-week period before being analyzed for SRP, TSP, and TP. Analysis for alkalinity and calcium levels began January 25, 2001, and specific conductance began in February. Prior to December 1999 and after June 2001, weekly grab samples were analyzed independently. The number of replicate shallow depth SAV mesocosms was reduced from 3 to 1 on March 28, 2000, which was the date when two of the three mesocosms were subjected to

fluctuating water depths under Subtask 5ii. Thus only the SD-2 mesocosm, which served as a control under constant water depth (maintained at 0.4 m), was used in the comparison with the cattail mesocosms after March 28, 2000.

Results

Average concentrations and ranges of values for the cattail and SAV mesocosms suggest different P removal performance by the two plant communities (Table 2.15). The SAV and the two cattail mesocosms provided average outflow TP concentrations of 26, 42 and 62 µg/L, respectively, for the period December 29, 1998 to August 8, 2001. Total P concentration reductions indicated 35% and 56% removal for cattail mesocosms 1 and 2, respectively, and 73% removal by the SAV system (Figure 2.39). The variable performance between the cattail mesocosms depended on the relative abundances of the submerged community (SAV and green filamentous algae) and duckweed within the “cattail” mesocosms, as well as on the density of cattail vegetation itself.

Particulate P and SRP concentrations were lower in the SAV outflow than in the cattail outflow. Dissolved organic P (DOP) concentrations remained constant through the cattail-dominated system but decreased in the SAV mesocosm. In addition, the pH was higher and the alkalinity concentration reductions were greater in the SAV community than in the cattails, suggesting that more calcium carbonate precipitation was occurring within the SAV system.

Table 2.15. Comparison between one SAV- and two cattail-dominated mesocosms at the NATTS. Average values and range in the inflow and outflow concentrations of SRP, DOP, PP, TP, dissolved calcium, alkalinity, specific conductance, pH and temperature during the period of record from December 29, 1998 to August 8, 2001. The inflow values represent the average of samples collected from one of the cattail mesocosms and the SAV mesocosm. Means for TP followed by different letters are significantly different (P <0.05).

Station	pH	SRP (µg/L)	DOP (µg/L)	PP (µg/L)	TP (µg/L)	Diss. Ca (mg/L)	Alk (mg CaCO ₃ /L)	Temp. (° C)	Sp Cond (µmho/cm)
<i>Average</i>									
Inflow	7.89	53	15	29	96	72	206	27.1	943
Cattail Outflow									
Rep 1	7.83	15	17	31	62 ^a	69	202	24.8	935
Rep 2	7.91	9	10	23	42 ^b	70	204	24.5	941
SAV Outflow	9.01	3	10	13	26 ^c	47	135	26.7	824
<i>Range</i>									
Inflow	7.45-8.36	13- 172	0-51	0-148	33-248	37-112	84-329	13.7-36.1	454-1369
Cattail Outflow									
Rep 1	7.05-8.78	4-71	5-71	10-496	27-520	41-105	117-309	11.0-33.5	494-1335
Rep 2	6.95-9.68	1-40	1-18	4-364	14-399	41-110	116-320	10.4-34.5	492-1351
SAV Outflow	7.49-10.83	1-9	0-34	0-69	11-85	28-70	40-200	12.2-35.8	429-1110

*pH, temp values from 12/29/98-6/12/00, weekly grab samples/analysis

**dissolved Ca values from 1/31/00-7/6/00, biweekly composite analysis of weekly grab samples

*** TP, SRP, TSP values from 12/29/98-11/9/99 and 2/15/00-8/8/01; weekly grab samples/analysis from 12/29/98-12/7/99; biweekly composite analysis of weekly grab samples from 12/7/99-6/8/01; weekly grab samples/analysis from 6/8/01-8/8/01

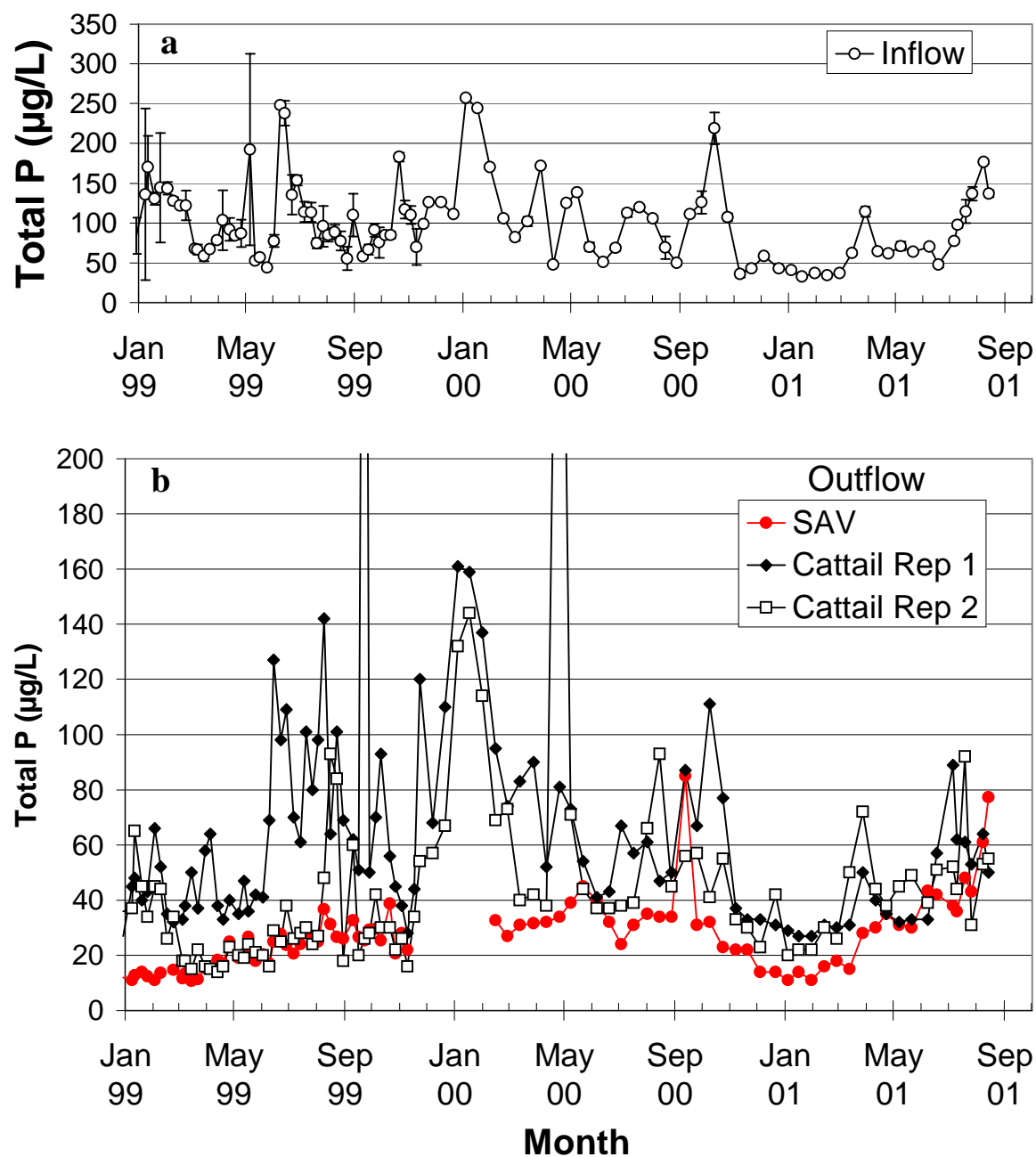


Figure 2.39. Total phosphorus concentrations in the inflow (a) and outflow (b) waters from mesocosms dominated by cattail and submerged aquatic vegetation (SAV). SAV outflow values from 12/29/98-11/9/99 represent the mean of triplicate mesocosms. Inflow values represent the mean \pm s.d. of one inflow measurement from two mesocosms from 12/29/98-11/9/99 and from 2/15/00-8/8/00. All other values are from unreplicated mesocosms.

2.7.2 Vegetation and Sediment Phosphorus Storage

A characterization of the vegetation was performed in late August and early September 2001, at the end of the monitoring period, in order to provide further insight into the relationships between species composition, biomass, and P removal performance.

Methodology

The vegetation in both cattail mesocosms was collected and separated into the following categories: live cattail, dead cattail, cattail roots, and SAV tissue (*Najas*). Vegetative biomass was divided into inflow and outflow regions. Live cattail shoots were cut to the sediment surface and separated into live (green) and dead shoots. Triplicate cores (15.9 cm²) were then retrieved from the inflow- and outflow-region sediments. The underlying native muck was segregated and discarded. Wet volumes and oven-dry weights (60°C to constant wt.) of accrued sediments were recorded for bulk density. *Najas*, along with the below-ground cattail biomass, were collected after sediment sampling was complete. Wet weights for the vegetation samples were recorded in the field. All vegetation and sediment samples were homogenized and analyzed for TP, TN, TC, TCa, TOC, and TIC.

Results

Based on P mass balances of the “input to” minus the “output from” the mesocosms, the P removal rates for the two replicate cattail mesocosms were 1.2 (rep 2) and 2.0 (rep 2) g/m²-yr. Only 31-35% of this mass P reduction through the cattail mesocosms was accounted for in the cattail and SAV compartments, and in the accrued sediments (Table 2.16). Cattail P concentrations for live tissues, dead leaves and root/rhizomes agree reasonably well with those measured previously in the Everglades (Toth 1988) (Table 2.17). While the below-ground cattail (roots+rhizome) comprised 39% of the total recovered biomass P in Rep 1, Toth (1988) measured ~30% of total biomass P as belonging to below-ground; rep 2 below-ground cattail biomass was 65% of the total biomass P stored (Figure 2.40). The disparity in the below-ground cattail P storage between the replicates is readily explainable by the higher above-ground standing crop of cattail in replicate mesocosm #2 (Figure 2.40). Though the 31-35% recovery of the removed P in the vegetation and sediments was low, a greater P storage was observed in

replicate 2, which also exhibited greater TP concentration reductions between inflow and outflow over the 2.7-year assessment period.

Table 2.16. Phosphorus removed from the water column over the 2.7-year assessment period, and P recovered in the *Najas* and cattail vegetation and sediments upon termination of the project on August 20, 2001.

	Cat 1	Cat 2	Average
Input-Output (water) mass removed (g P/m ²)	3.2	5.4	4.3
Vegetation Storage (g P/m ²)	1.1	1.6	1.3
Sediment Storage (g P/m ²)	0.04	0.04	0.04
Recovery (%)	35	31	33

Table 2.17. Phosphorus concentrations (mg/kg) in the live and dead cattail shoots, below-ground cattail (roots and rhizomes), and SAV tissues retrieved from within the cattail-dominated mesocosms on August 20, 2001.

	Live cattail shoots	Dead cattail shoots	Below-ground cattail	SAV
Rep 1	790	180	620	5300
Rep 2	710	190	630	3300
Toth 1988	580-1000	160-260	570-740	

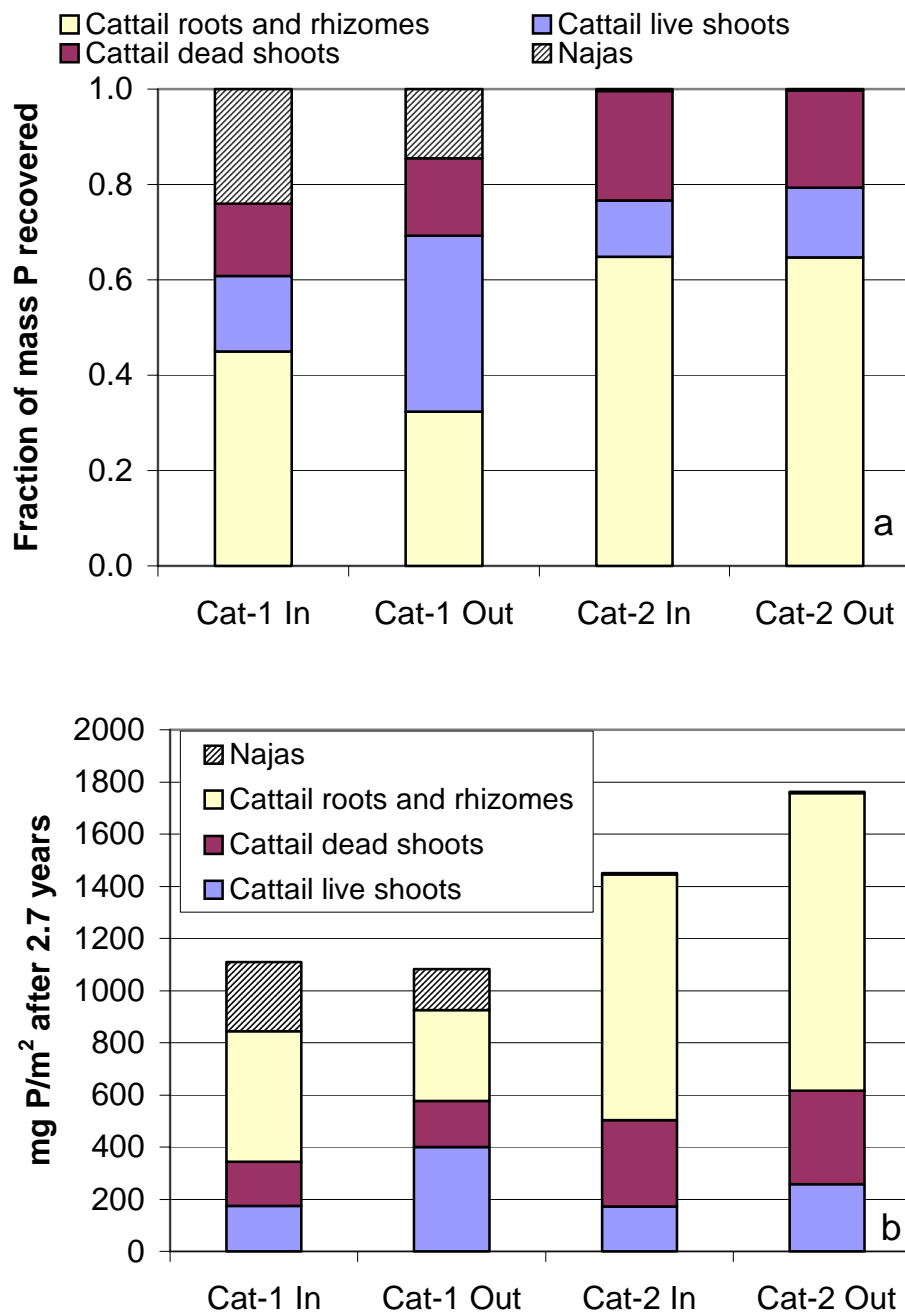


Figure 2.40. Relative partitioning (a) and total recovered biomass (b) of stored P within the *Najas* and cattail tissues from the inflow (In) and outflow (Out) regions of two cattail-dominated mesocosms operated from December 1998 through August 2001.

2.8 Shallow Low Velocity SAV/Periphyton/Limerock Systems

In 1998, we established long, narrow raceways at the South Advanced Treatment Technology Site (SATTs) to evaluate the treatment effectiveness of a shallow SAV/periphyton/LR system.

We operated these triplicate shallow SAV/periphyton raceways (44m L x 0.3m W x 0.15m D) at the SATTs from June 1998 through November 28, 2000. The raceways contained a limerock substrate (3 cm) beneath a 9 cm water column. Raceway outflow waters were fed to limerock barrels (similar to those described in the Long-Term Phosphorus Removal in Mesocosms evaluation) which had HRTs of 0.5 or 1 hr, depending on whether the raceways were operated at HLRs of 22 and 11 cm/day (HRT of 0.4 or 0.8 days, respectively).

Six liters of a periphyton slurry collected from WCA-2A was inoculated into the system after the commencement of flows in June 1998. Additionally, *Najas*, *Chara* and *Ceratophyllum* were each distributed along each replicate raceway at a stocking rate of 1.3 kg wet/m². Weekly sampling of total and soluble reactive phosphorus, pH and temperature began July 2, 1998, and continued until the end of the evaluation in November 2000. Biweekly (every two weeks) grab samples were collected from August 26, 1998 through November 3, 1999, and analyzed for TSP, calcium, alkalinity.

On February 4, 2000, we doubled the HLR to the raceways from 10 to 22 cm/day. At about the same time, the inflow (STA-1W outflow) total P concentrations also doubled (Figure 2.41), resulting in a four-fold increase in the total P loading to the raceways. In response to the higher loading, the total P concentrations in the outflow from the raceways and LR beds trended higher, exceeding the benchmark 10 µg/L that had been maintained since the beginning of data collection (Figure 2.41). During March, the raceways maintained the outflow total P concentrations at ~20 µg/L, levels first observed in February after the hydraulic loading was doubled. Outflow TP concentrations near (and occasionally above) the inflow concentrations occurred in April, even though the HLR was returned to 11 cm/day on April 11, 2000. Total P concentrations in the limerock outflow, which also trended higher in the February-April 2000, continued to provide additional P removal (except on two occasions in April).

The SRP concentration dropped from 5 $\mu\text{g/L}$ to below the method detection limit (2 $\mu\text{g/L}$) in the first quarter of the raceway, and remained low in the effluent (Table 2.18). Because of this decline in SRP, effluent total P consisted entirely of dissolved organic P (DOP) and PP fractions.

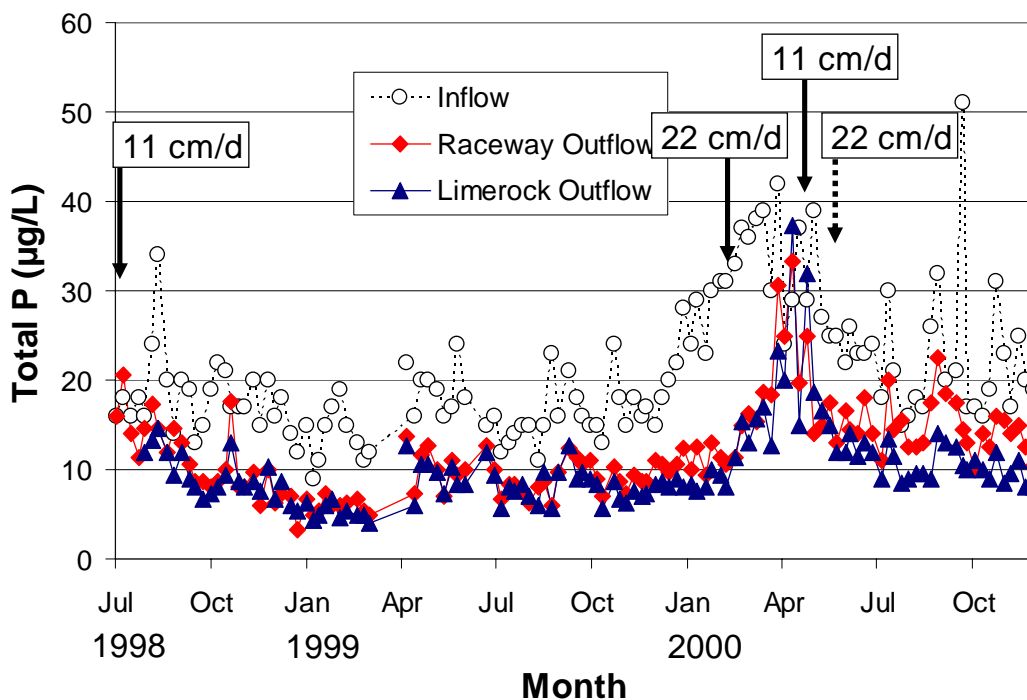


Figure 2.41. Total P concentrations in the inflow and outflows of triplicate shallow, low velocity, SAV/periphyton raceways and in the outflow of the subsequent limerock beds. Dates of flow manipulations are depicted on the figure. Values after the second 22 cm/day flow adjustment represent the means of duplicate raceways.

During May 2000, influent TP concentrations to the SAV/periphyton systems at the SATT site, which previously had exceeded 40 $\mu\text{g/L}$, began to decline. Concurrent with this decline in inflow TP levels, P removal performance of the shallow raceways began to improve (Figure 2.41). From May through July 2000, the raceway and limerock effluents averaged 15 and 13 $\mu\text{g/L}$, respectively.

During May-July 2000, *Chara* began to colonize more of the inflow region, and remained the dominant vegetation in that region of the raceways through the end of the assessment. This

represented a shift away from *Cladophora* sp. dominance; the middle and outflow regions were always comprised of cyanobacteria (e.g. *Scytonema*, *Schizothrix*).

Table 2.18. Soluble reactive phosphorus concentrations ($\mu\text{g/L}$) at four stations along the shallow, low velocity raceway gradient during the February–April 2000 quarter. Values represent the average of weekly grabs in the replicate raceways.

Date	Influent	1 st Quarter	Midpoint	Effluent
March 21	5	2	2	2
April 3	5	2	2	2
April 10	2	<2	<2	<2
April 17	3	2	2	2
April 24	3	2	2	2
Average	4	2	2	2

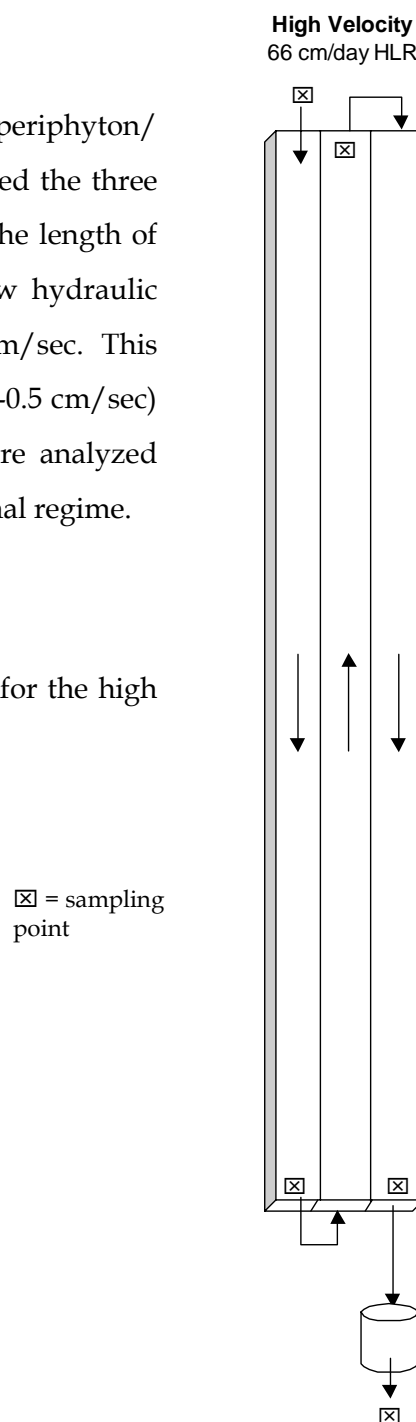
After continuous operation for 29 months, the overall mass removal rate for the raceway/LR system was $0.43 \text{ g P/m}^2/\text{yr}$. The raceways reduced average TP concentrations in the Post-STA waters from 21 to $12 \mu\text{g/L}$, and back-end limerock filters provided further removal to $10 \mu\text{g/L}$ over the entire period of record.

Effects of Flow Velocity on Phosphorus Removal by Shallow SAV/Periphyton Communities

Many investigators believe that flow velocity is an important variable in controlling the performance of SAV and periphyton systems. This parameter is difficult to test at the mesocosm scale, however, because any increase in flow (to increase velocity) also results in an increase in P loading. Also, to adequately address the effect of flow velocity on P removal using mesocosms, a long evaluation platform is required.

Upon completion of the “Shallow, Low Velocity SAV/periphyton/LR Systems” assessment on November 28, 2000, we joined the three 44 m long raceways together in series, thereby tripling the length of the flow path (Figure 2.42). We also tripled the inflow hydraulic loading rate to 66 cm/day, providing a velocity of 0.36 cm/sec. This flow rate is in the middle of the mean velocity range (0.2-0.5 cm/sec) proposed for the STAs. Inflow and outflow waters were analyzed weekly for TP for a six-month period under this operational regime.

Figure 2.42. Modified flow path and sampling locations for the high velocity SAV/periphyton raceway evaluation.



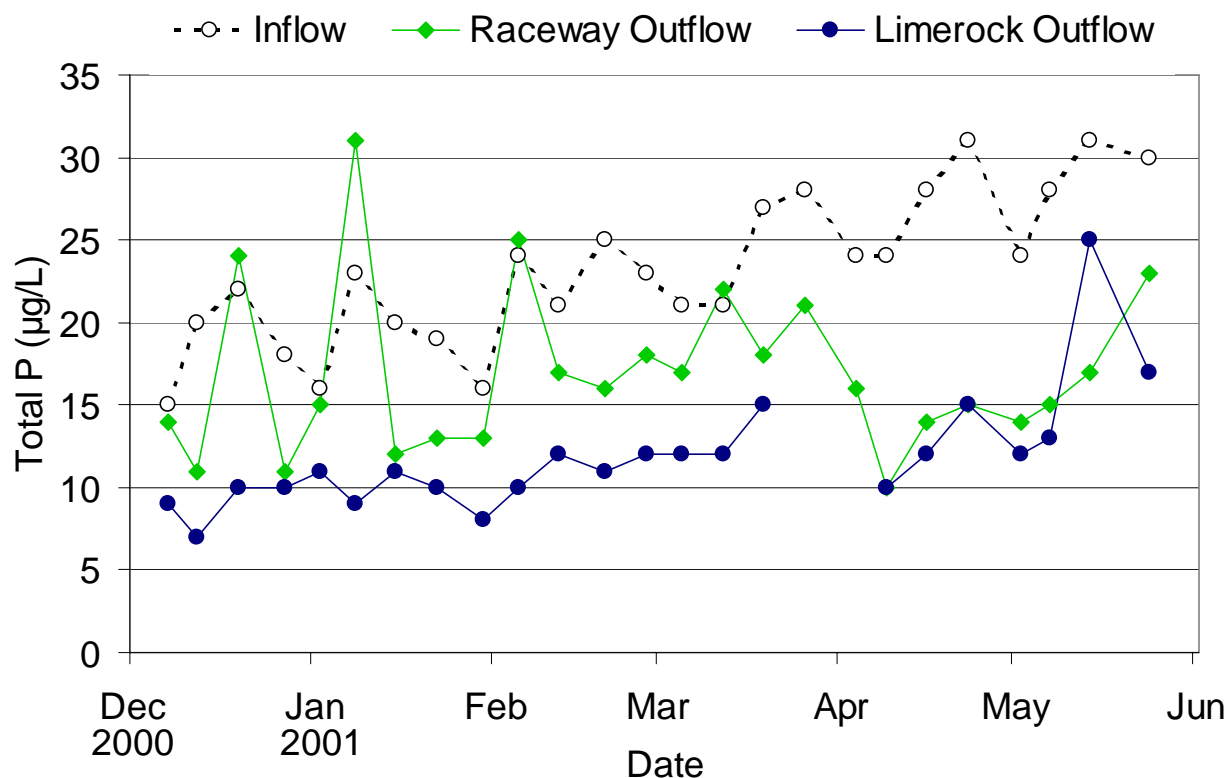


Figure 2.43. Total phosphorus concentrations in the inflow (Post-STA) waters and raceway and limerock outflow waters during the “high velocity” (0.27-0.36 cm/sec) operational period.

During the first weeks of high velocity operation, *Chara* established dominance along the inflow region of the raceway, while calcareous periphyton dominated most of the remaining 132m long raceway. Interspersed with the calcareous periphyton that dominated the raceway downstream of the inflow zone was a mixture of *Chara* and periphyton. This vegetation corresponded to sections of the raceway where the pre-existing inflow communities had developed under the previous parallel flow paths of the “Shallow, Low Velocity Raceway” evaluation.

Over the six-month evaluation, the high velocity shallow raceway reduced TP concentrations in Post-STA (STA-1W outflow) water from 23 to 17 µg/L, and the outflow limerock bed further reduced TP concentrations to 12 µg/L (Figure 2.43). In terms of outflow concentration, these P levels for the raceway and limerock bed are slightly higher than the long-term mean P concentration obtained when the flow velocities were much lower (0.06-0.12 cm/sec) in the

parallel configuration (Table 2.19). Thus, the higher flow velocities do not appear to have a pronounced effect on P removal by this shallow system.

Table 2.19. Total P concentrations in the inflows and outflows from shallow SAV/periphyton raceways and outflows from subsequent limerock beds during periods of high and low flow velocity. Removal efficiencies describe TP concentration reductions from inflow to limerock outflow.

	Replicate Raceways	Flow Velocity (cm/sec)	Inflow TP (µg/L)	Raceway Outflow (µg/L)	Limerock Outflow (µg/L)	Raceway/LR TP Removal (%)
July 2, 1998 - February 1, 2000	3	0.06	18	10	8	55
May 8, 2000 - November 28, 2000	2	0.12	23	15	11	52
December 7, 2000 - April 6, 2001	1	0.36	21	17	11	48
April 7, 2001 - May 24, 2001	1	0.27	28	15	15	46

2.9 Growth of SAV in Post-STA Waters on Muck, Limerock, and Sand Substrates

In this effort, SAV was cultured in mesocosms containing a 15 cm deep substrate of either muck, limerock or sand. The water depth was maintained at 0.4m throughout the evaluation. Duplicate treatment trains, each consisting of three polyurethane tanks (0.61m L x 1.22m W x 0.61m D) plumbed in series (Figure 2.44), received STA-1W outflow (Post-STA) waters at the SATTS from May 25, 1999 through November 20, 2001. The limerock (¼-½ inch diameter) and muck were obtained from the same sources as were used in the other mesocosm studies. The sand was commercial builder's sand.



Figure 2.44. Photo of three substrate treatments (sand, muck and limerock), each consisting of three mesocosms in series.

Chara, *Ceratophyllum*, and *Najas* were inoculated into each of the duplicate substrate mesocosms at a density of 1.3 kg (wet)/m² for each genus on June 18 and 21, 1999. Water sampling for TP at the inflow to the first mesocosm and the outflow of the third mesocosm for each treatment train was initiated in early July 1999, and water pH and temperatures were recorded in the field.

The hydraulic loading rate (HLR) was adjusted periodically throughout the period of record, in an effort to understand the interaction between HLR and different substrates (Figure 2.45). We initiated the assessment using a HLR of 30 cm/day. We reduced the HLR by 50% on three occasions (February 9, April 17, and May 23, 2000), eventually attaining a minimum HLR of 3.8 cm/day. On October 10, 2000 and again the following January 9, flows were doubled, to return the HLR to 15 cm/day. Afterward, and for the remainder of the assessment, the HLR was held at 15 cm/day.

Inflow water P concentrations were quite low throughout the assessment period (mean \pm s.d. = 23 \pm 2 μ g TP/L), with some variation over the 28-month monitoring period (Figure 2.45). This natural variation, along with flow rate changes, caused wide fluctuations in the inflow P loading to these systems (range, 0.2 – 3.4 g P/m²/yr).

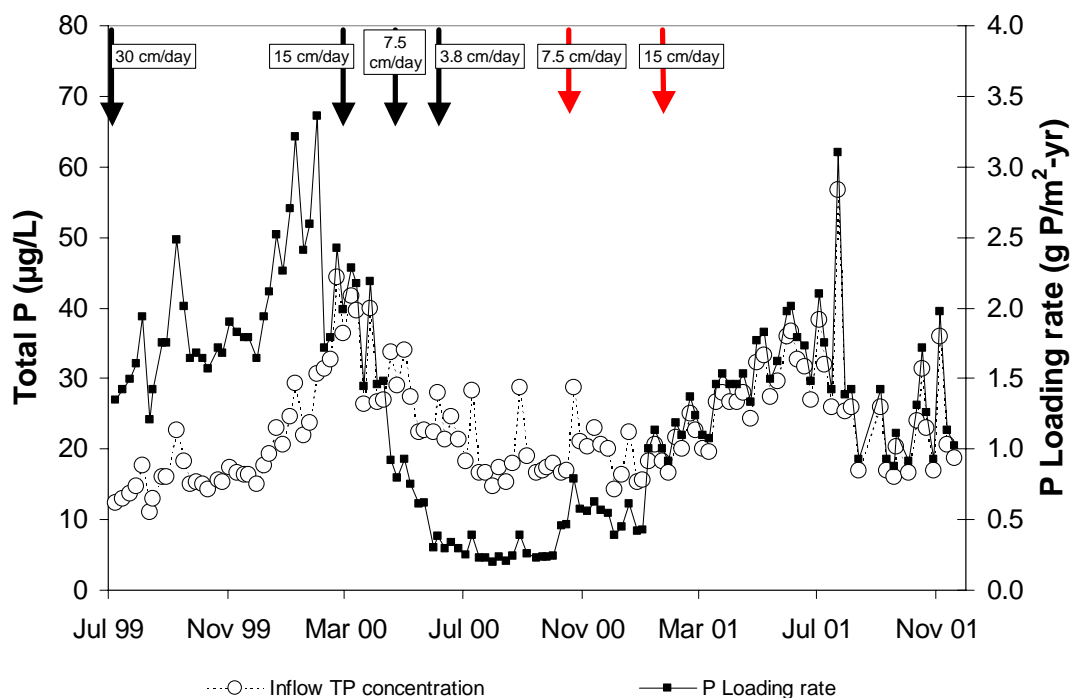


Figure 2.45. Inflow TP concentrations and P loadings to the substrate mesocosm evaluation. The black arrows denote dates when HLR was successively reduced 50%. The red arrows denote dates when HLR was doubled.

Although each treatment system reduced water column P concentrations from Post-STA outflow waters, the P removal performance was not equal among the three treatments (39, 35, and 22% for limerock, muck and sand, respectively). Replication between duplicate treatment trains (Figure 2.46) was adequate to statistically show significant differences ($p < 0.05$) in outflow TP concentrations between the limerock and sand substrate, and the muck and sand substrate mesocosms, but not for the limerock and muck-based treatments (Table 2.20).

The sand substrate appeared unfavorable for SAV-based treatment over the entire period of record. Although differences between treatments were small, the muck substrate appears to have provided lower outflow concentrations during periods of increasing inflow concentration and P loading (July 1999-February 2000 and February – July 2001 in Figure 2.45) (Figure 2.47), possibly due to more abundant nutrients available for biomass growth. The limerock substrate appears to have outperformed the muck substrate during a period of declining P loading rate (April 17, 2000 – January 9, 2001) when flows were lowered from 15 to 7.5 dm/day, and then to

3.8 cm/day (Figure 2.47 and Table 2.20). Chemical processes such as sorption onto limerock surfaces may have become more prominent in the limerock treatment while the decrease in P loading negatively affected the SAV-laden muck treatment by causing SAV senescence or sediment P release.

Table 2.20. Mean (\pm s.d.) total phosphorus concentrations in the inflow and outflows from SATT mesocosms established on muck, limerock and sand substrates during the entire period of record (July 1999 – November 2001) and during reduced hydraulic loading (April 17, 2000 – January 9, 2001).

	Inflow	Muck	Limerock	Sand
<i>Entire Period of Record</i> July 1999 – November 2001	23 \pm 2	15 \pm 1	14 \pm 2	18 \pm 3
<i>Period of Low Hydraulic Loading</i> (HLR = 3.75-7.5 cm/day) April 17, 2000 – January 9, 2001	21 \pm 1	15 \pm 3	13 \pm 1	20 \pm 5

Although the SAV biomass was sparse (and little periphyton was present) in the limerock substrate mesocosms, they performed as well as (and at times better than) the muck substrate mesocosms, which did support dense SAV populations. To help define P removal mechanisms among the substrate types, we collected and analyzed TP, SRP and TSP during an eight-week low HLR period in August and September 2000 (Table 2.21). Outflow PP concentrations were higher for the muck than the limerock treatments; dramatically higher particle export from the sand-based mesocosms also occurred during this period. In response to the lower P loading rates, SAV senescence and sloughing may have contributed particulate P in the muck substrate mesocosms. Alternatively, the lower HLR may have promoted phytoplankton growth in the water column of the muck treatments

Clearly, removal mechanisms other than SAV uptake probably are occurring within the “low biomass” limerock mesocosms. These mechanisms include microbial uptake (bacterial and nanoplankton), enzymatic P hydrolysis, adsorption, photolysis and particle P sedimentation.

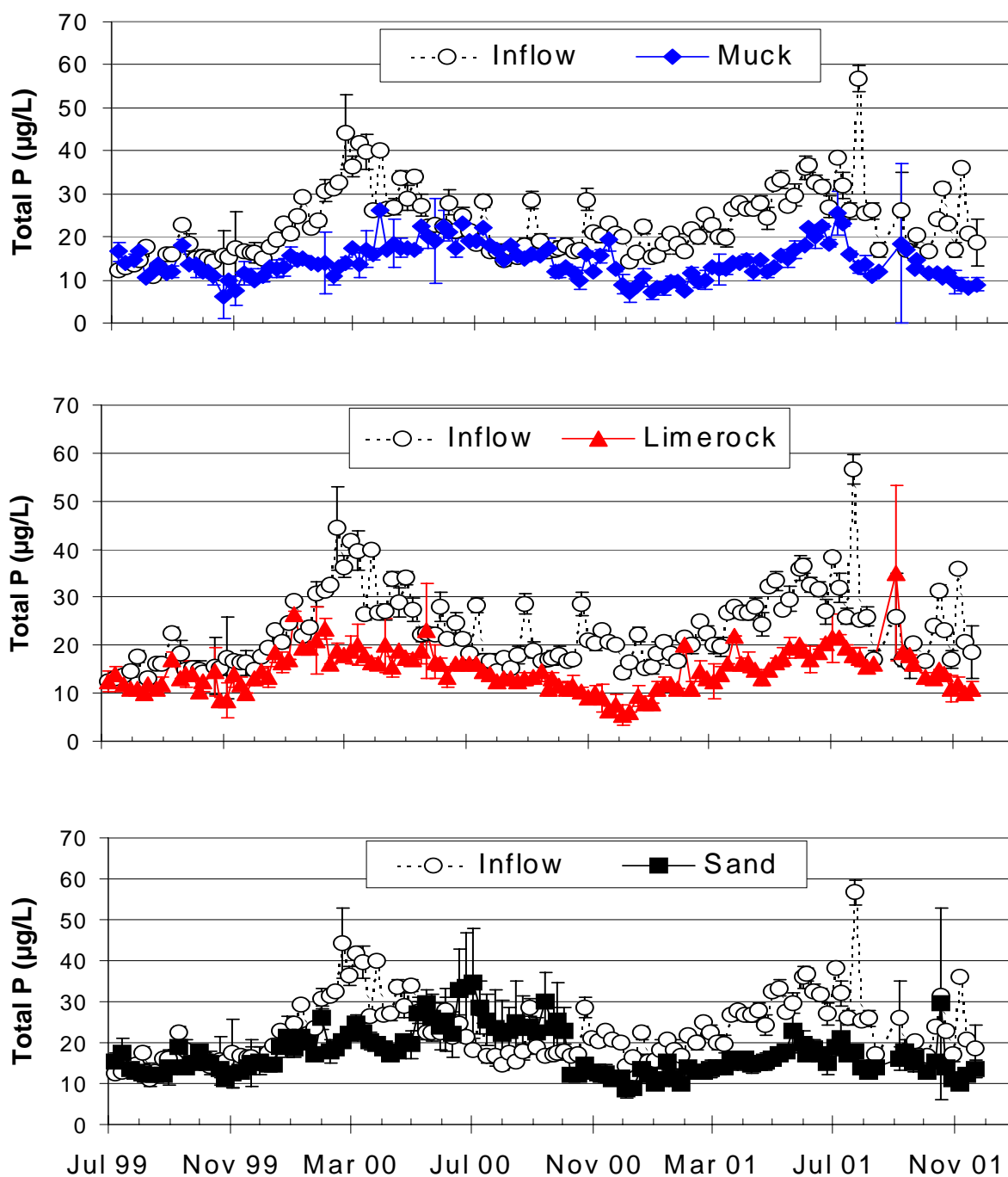


Figure 2.46. Mean TP concentrations in the inflow (shown on each panel) and outflow waters of the muck (top), limerock (middle), and sand (bottom) substrate mesocosms from July 1999 through November 2001. Error bars represent \pm s.d.

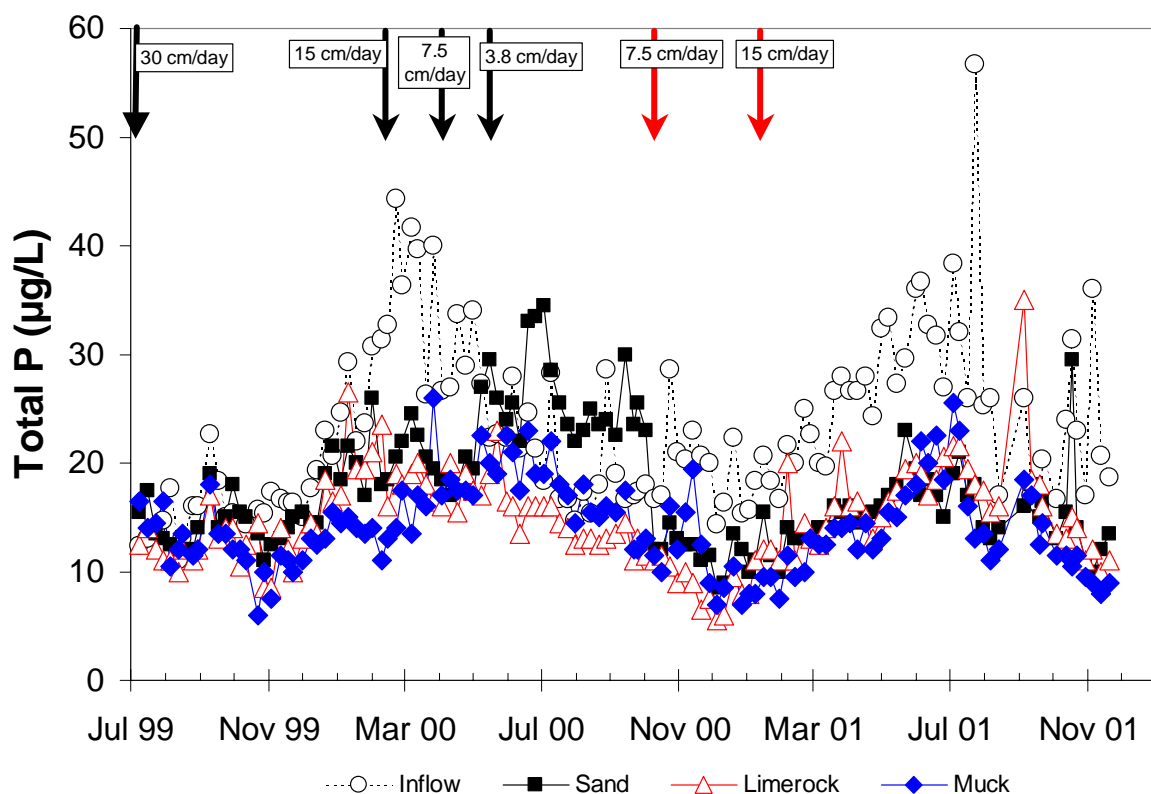


Figure 2.47. Total P concentrations in the inflow and outflow waters of the muck, limerock, and sand substrate mesocosms from July 1999 through November 2001. Black arrows denote 50% reductions of flows on February 9, April 17 and May 31, 2000. The red arrows denote doubling of flows on October 10, 2000 and January 9, 2001.

Table 2.21. Mean phosphorus concentrations (µg/L) in the inflow and outflows of duplicate substrate mesocosms during an eight-week period (August - September 2000) of low hydraulic loading (3.75 cm/day).

	Inflow	Limerock Outflow	Muck Outflow	Sand Outflow
Total P	19	13	15	25
SRP	4	1	2	2
DOP	9	5	6	7
PP	6	6	8	16

2.10 Effect of Filter Media and Operating Conditions on P Removal Performance

DBE's initial work with the SAV/LR concept at the North and South Advanced Treatment Technology Sites demonstrated that the LR bed is serving principally as a physical filter for particulate P. However, alternative media came to our attention which we considered worthy of evaluating alongside limerock. We therefore divided this subtask into two separate evaluations. The first focused on screening different media types and sizes for their P removal performances. The second evaluation aimed at examining different water depths, shading and tanks-in-series effects on P removal using LR as the sole substrate.

2.10.1 Media Type and Sizes

During this follow-on assessment, DBE and HSA personnel screened four other filter media in addition to limerock. Our final selections of four different filter media within various size ranges are shown in Table 2.22. One of the four media types (quartz sand or pebbles) served as a control (i.e., inert) medium. The other three media were selected for their potential P- removal capabilities. Pro-Sil™ Plus is a commercially available soil-liming material that is processed from Ca and Mg silicates. It is reported by the distributor to have a high P adsorption capacity. Iron-coated sand was collected from a construction site in central Florida. The last filter medium, limerock, was obtained from the West Palm Beach Aggregates quarry located adjacent to STA-1W.

Table 2.22. Media types and sizes used in the Filter Media Evaluation.

Sieve No.	Size Range	Filter Media Type			
		Quartz Sand or Pebbles	Limerock	Pro-Sil Plus™*	Fe-coated Sand
<No. 3 >No. 6	Coarse 3.35-6.86 mm	✓	✓	✓	
<No. 6 >No. 10	Medium 2.00-3.35 mm	✓	✓	✓	
<No. 20 >No. 60	Fine 0.25-0.85 mm	✓			✓

* A combination of Ca and Mg silicates.

In this evaluation, Post-STA (low soluble reactive and particulate P) waters were pumped to three supply tanks (4.66m long x 0.79m wide x 1.00m deep) containing SAV and then gravity-fed through PVC columns (20.3 cm ID), with 56 cm depth of packed medium, providing a hydraulic retention time of 91-131 min. Support for the filter medium within each column consisted of layers of glass wool and pea gravel (Figure 2.48). This prevented the loss of the fine-grained media in the column outflow.

Sampling of the column inflows and outflows was performed from August 18 to November 17, 2000 (13 weeks). Total, total soluble, and soluble reactive phosphorus concentrations were analyzed as twice-weekly grab samples, while specific conductance, calcium and alkalinity samples were composited each week.

Mean inflow and outflow concentrations of TP, SRP, DOP, PP, Ca and alkalinity are presented in Table 2.23. Outflow TP concentrations were slightly lower for the limerock and Pro-Sil Plus™ (13 - 14 µg/L) than the quartz sand treatments (14 - 17 µg/L). There were no differences between coarse and medium size filter media in TP removal (Figures 2.49 - 2.51). The TP concentrations in the twice-weekly grabs varied less toward the end of the sampling period across all three substrates within each size fraction (Figures 2.52 and 2.53).

Differences in particulate P removal depended more on the size of the filter medium than the type (Table 2.23). Removal of PP at 50% or better was achieved in the medium (2.0 - 3.4 mm) and fine (0.25-0.85mm) size sands except for the iron-coated sand. Removal of DOP was negligible across all size ranges and filter media types (Table 2.23). DOP was released in the iron-coated sand treatment.

Calcium and alkalinity concentrations were essentially unaffected by media type or size: the Pro-Sil Plus™ reduced calcium and alkalinity concentrations by only ~5%, whereas for other media types these constituents increased negligibly or remained unchanged (Table 2.23). The iron-coated sand columns released large quantities of SRP once flow was initiated (Figure 2.54). Although the release rate decreased over time, export continued through the last week of the assessment.

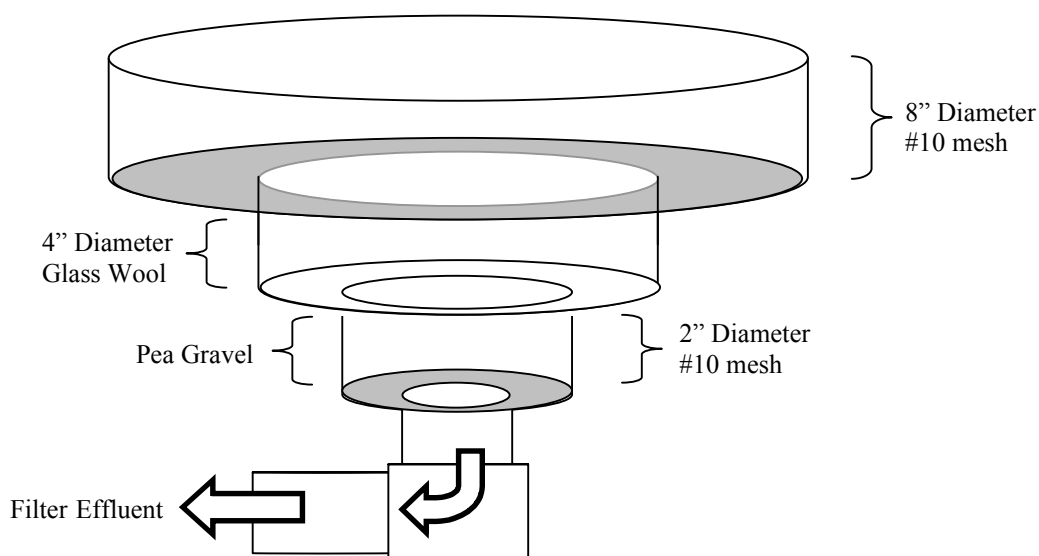


Figure 2.48. Schematic of the column outflow structure used in the Filter Media evaluation.

Table 2.23. Mean (± 1 s.d.) TP, SRP, PP, DOP, calcium and alkalinity concentrations in the inflow and outflows of filter media columns during the August 18-November 17, 2000 period of record.

	Inflow	Outflow							
		Quartz			Limerock		Pro-Sil Plus™		Iron-coated Sand
		Coarse	Med.	Fine	Coarse	Med.	Coarse	Med.	Fine
Total P ($\mu\text{g/L}$)	17 \pm 4	15 \pm 5	14 \pm 4	17 \pm 5	14 \pm 4	13 \pm 6	13 \pm 4	13 \pm 3	122 \pm 74
SRP ($\mu\text{g/L}$)	3 \pm 1	4 \pm 2	4 \pm 2	7 \pm 3	3 \pm 2	3 \pm 1	3 \pm 1	2 \pm 1	87 \pm 14
PP ($\mu\text{g/L}$)	6 \pm 2	4 \pm 1	3 \pm 2	2 \pm 2	4 \pm 1	3 \pm 2	4 \pm 2	3 \pm 1	19 \pm 23
DOP ($\mu\text{g/L}$)	8 \pm 2	7 \pm 1	7 \pm 1	8 \pm 2	7 \pm 1	7 \pm 1	7 \pm 1	7 \pm 2	17 \pm 5
Calcium (mg/L)	74 \pm 5	77 \pm 6	76 \pm 6	77 \pm 5	77 \pm 5	77 \pm 5	71 \pm 12	72 \pm 12	73 \pm 7
Alkalinity (mgCaCO ₃ /L)	253 \pm 12	261 \pm 14	261 \pm 12	260 \pm 17	260 \pm 14	263 \pm 12	248 \pm 46	246 \pm 50	263 \pm 16

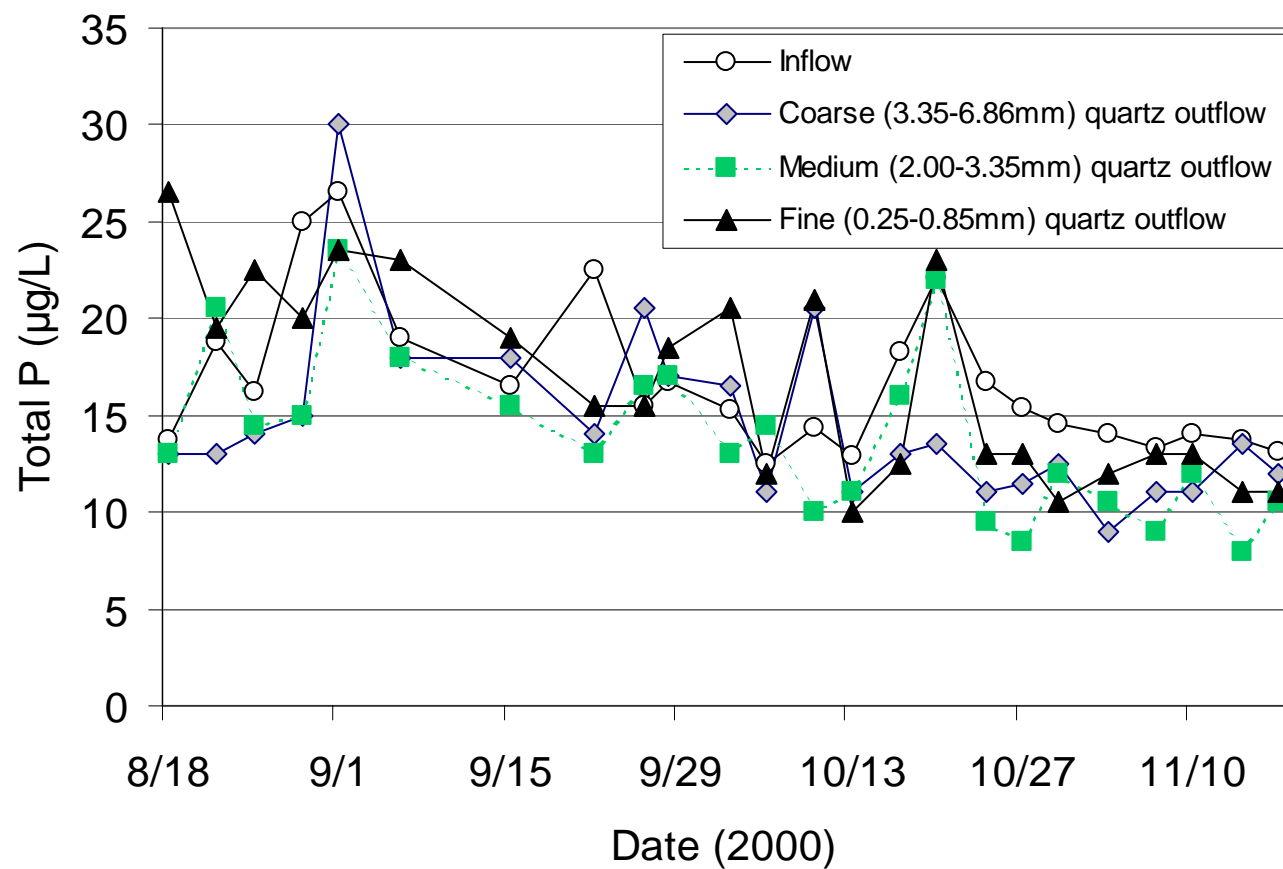


Figure 2.49. Mean total phosphorus concentrations in the inflow and outflow of duplicate filter columns with each pair containing one of three size fractions of quartz filter matrix. Post-STA water was fed to the columns during a three-month monitoring period.

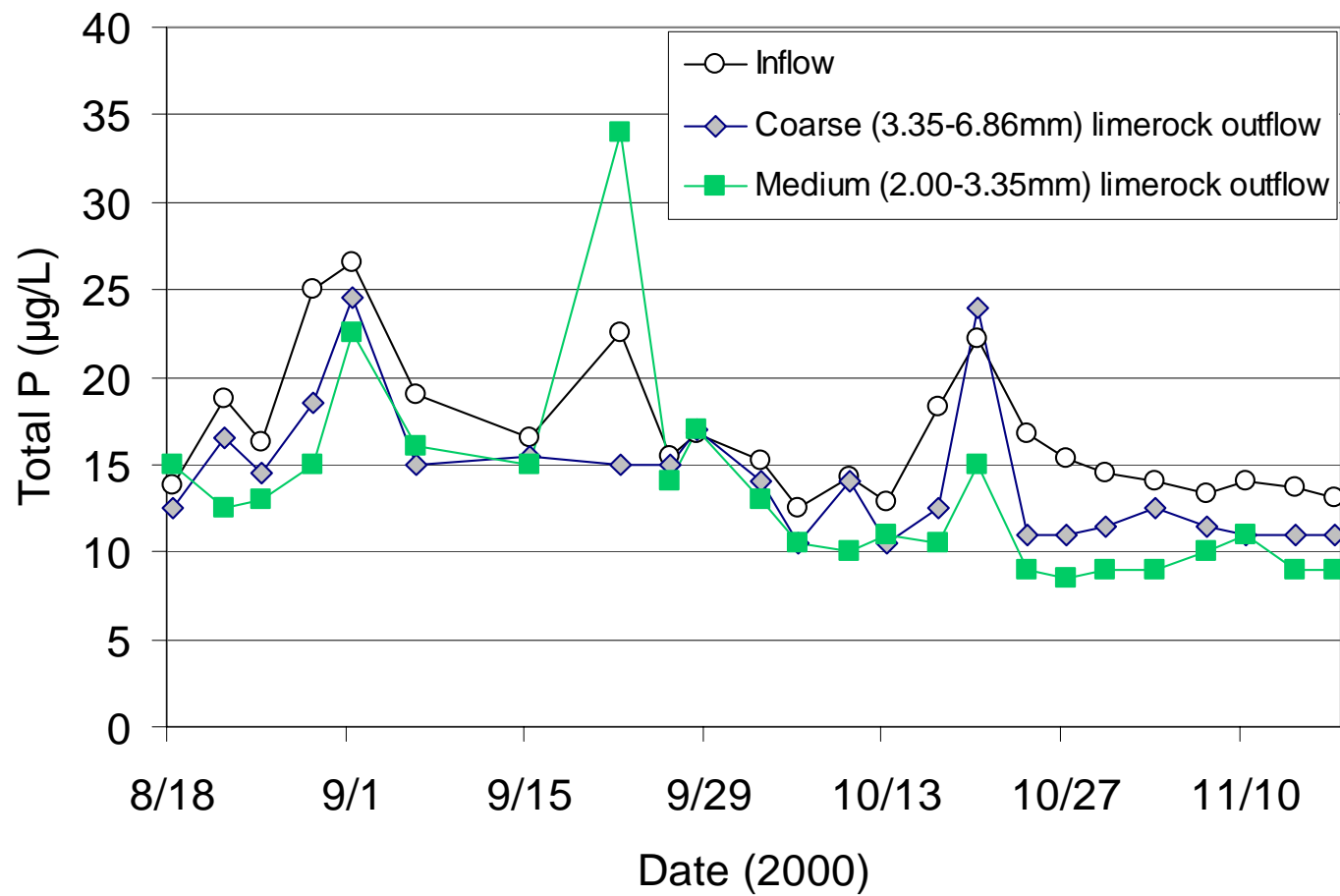


Figure 2.50. Mean total phosphorus concentration in the inflow and outflows of duplicate filter columns with each pair containing one of two size fractions of limerock. Post-STA water was fed to the columns during a three-month period.

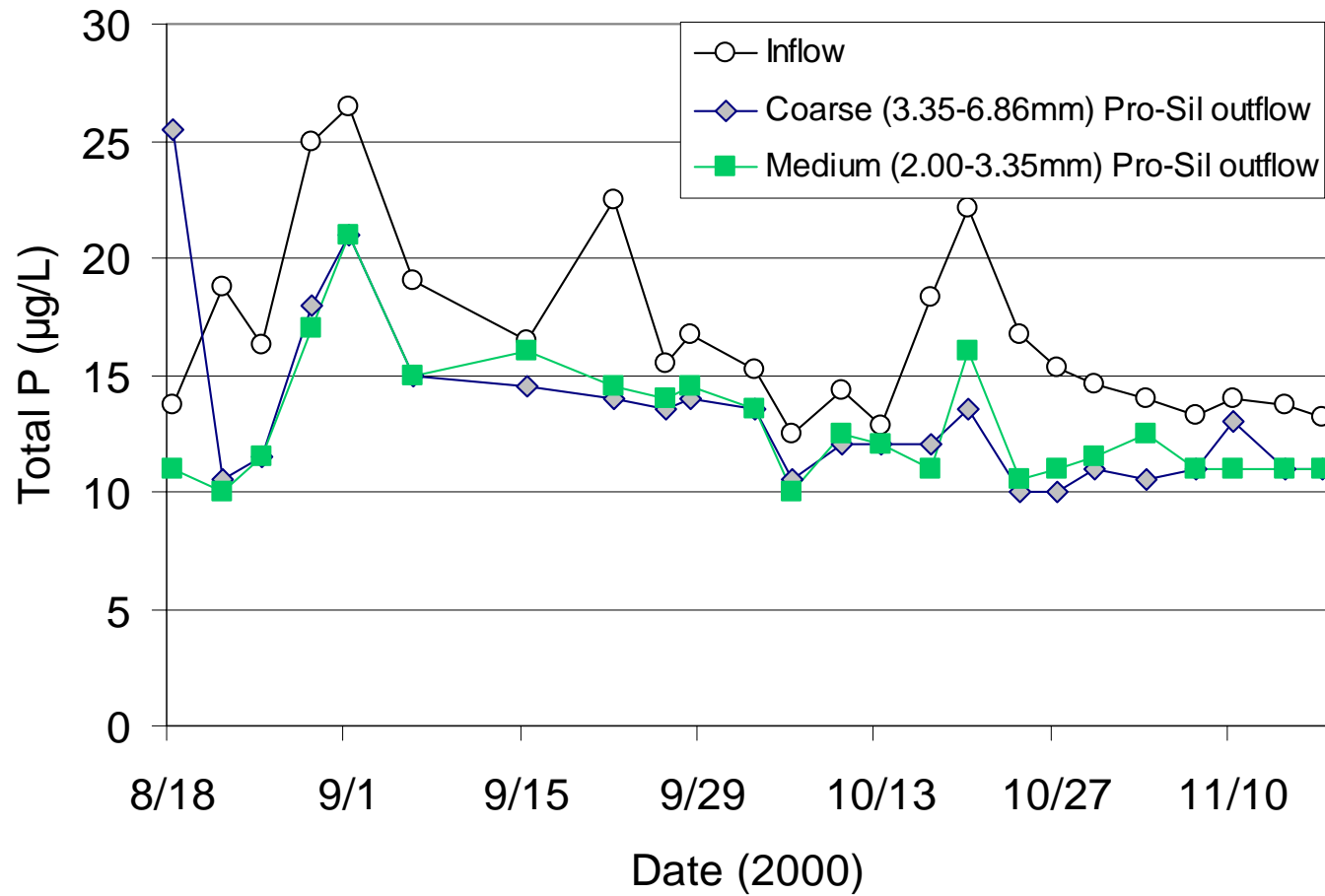


Figure 2.51. Mean total phosphorus concentration in the inflow and outflows of duplicate filter columns with each pair containing one of two size fractions of Pro-Sil™ (Ca-Mg silicate). Post-STA water was fed to the columns during a three-month period.

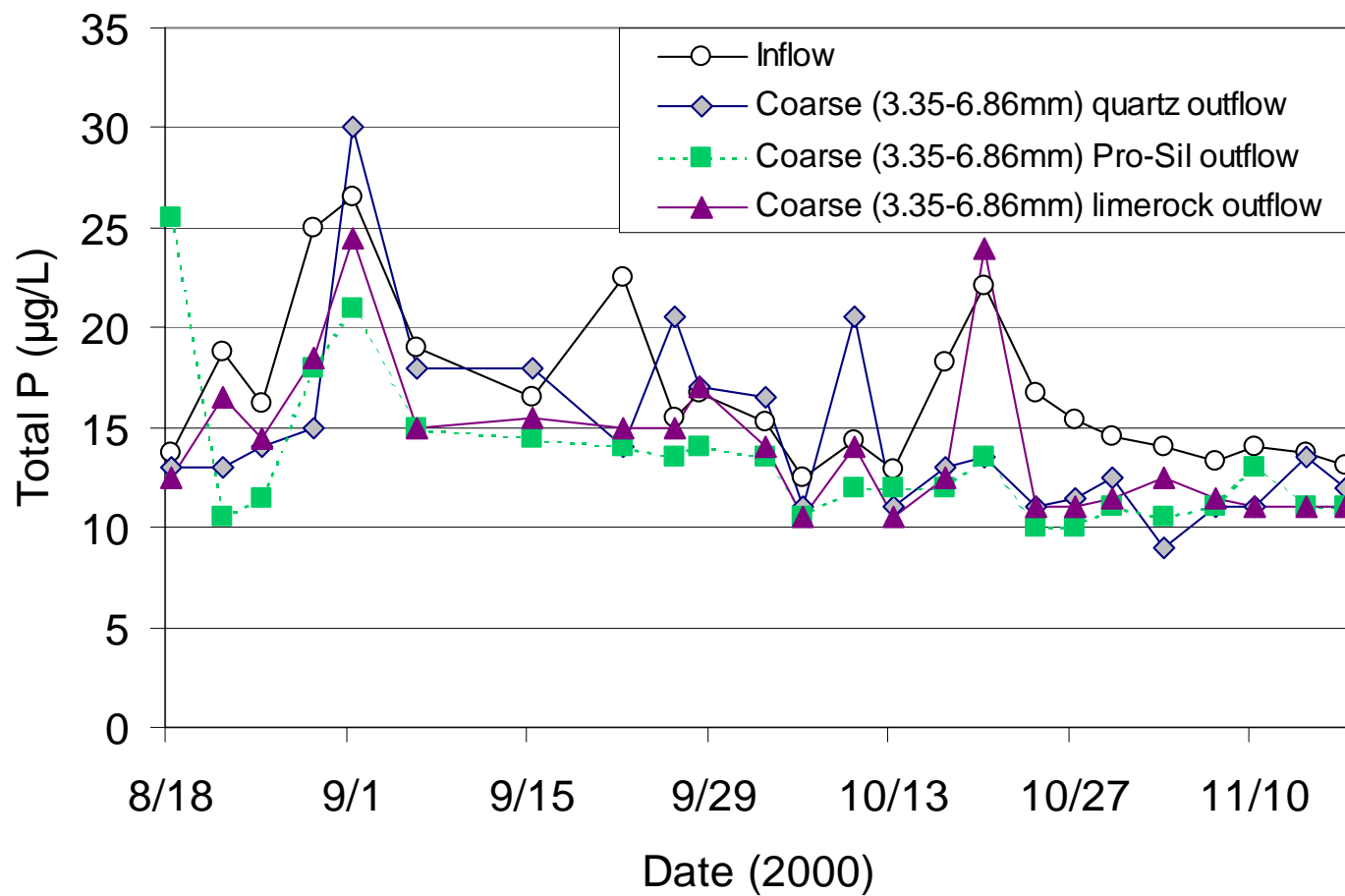


Figure 2.52. Mean total phosphorus concentrations in the inflow and outflows of duplicate filter columns with each pair containing a coarse grade of one of three substrate types. Post-STA water was fed to the columns during a three-month period.

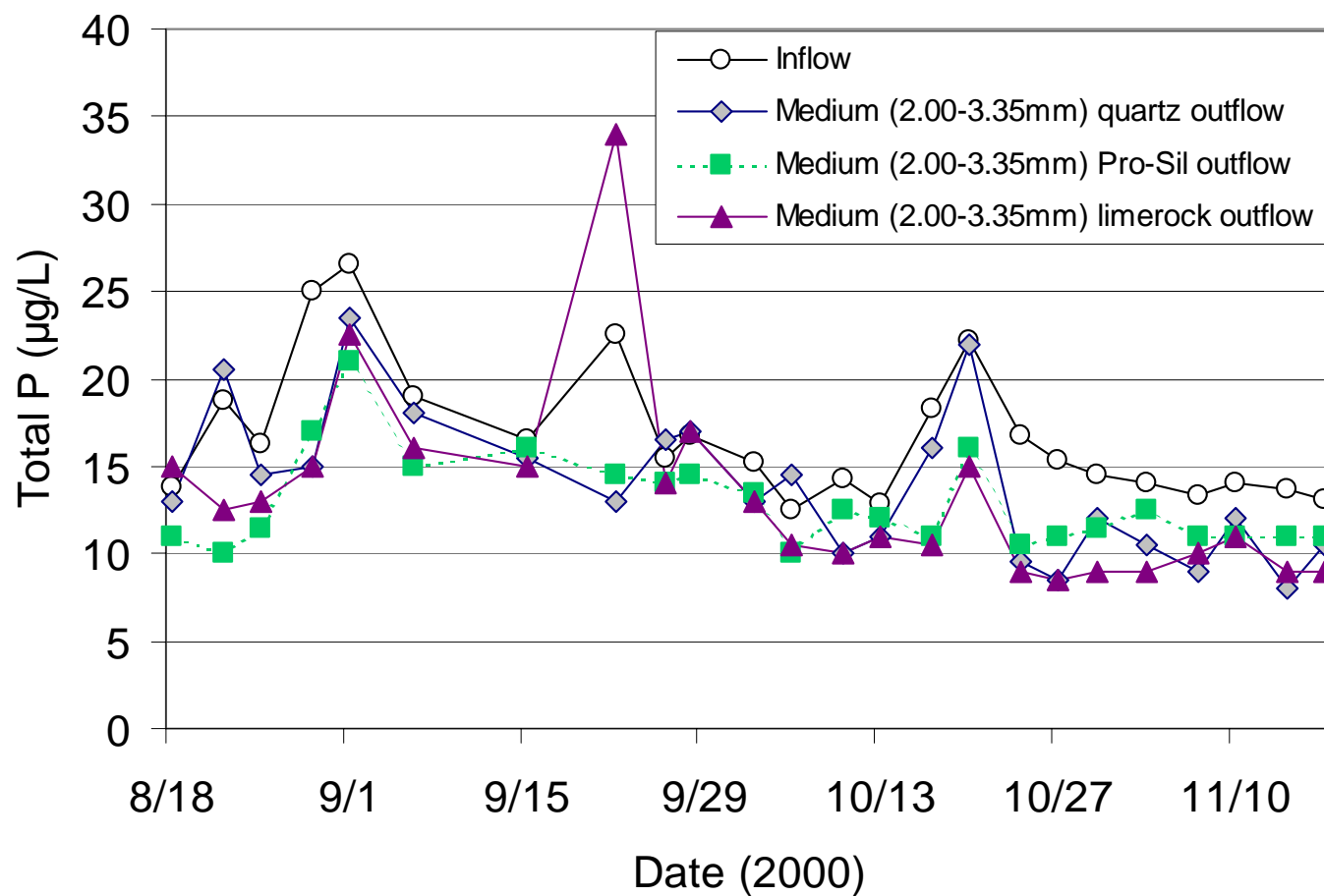


Figure 2.53. Mean total phosphorus concentrations in the inflow and outflows of duplicate filter columns with each pair containing a medium grade of one of three substrate types. Post-STA water was fed to the columns during a three-month period.

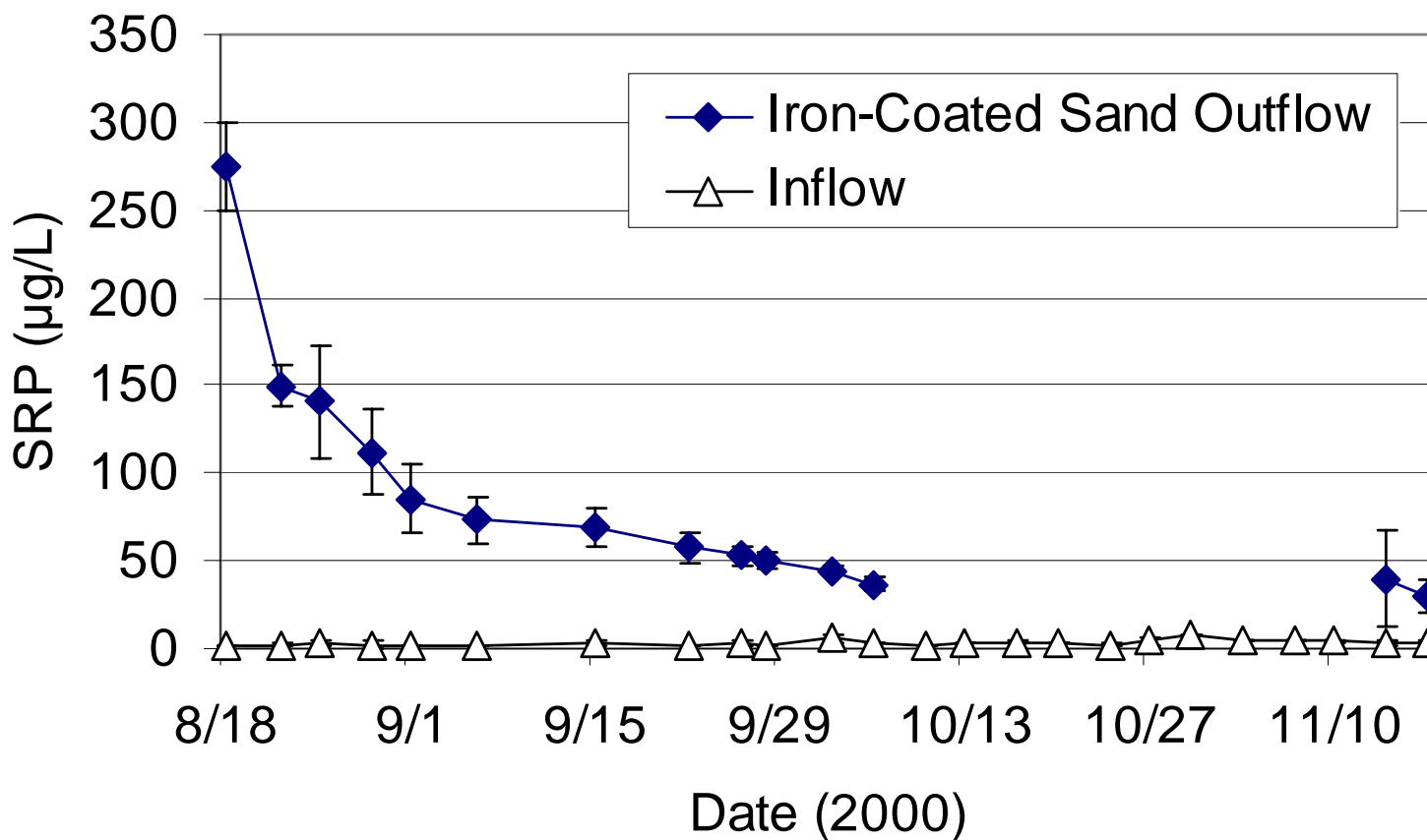


Figure 2.54. Mean (\pm s.d.) soluble reactive phosphorus concentrations in the inflow and outflow of duplicate iron-coated sand filter columns. Post-STA water was fed to the columns during a three-month monitoring period.

2.10.2 Water Depth and Treatment Unit Configuration

Two media types – Pro-Sil™ Plus and limerock – were selected for further investigation based on the results from our original filter media assessment, which concluded in November 2000. In that 13-week evaluation, inflow TP concentrations were reduced from 17 to 14 and 13 µg/L, in small filter columns (5.8 L, HRT = 91-131 min.) containing limerock and Pro-Sil™ media, respectively. In order to more thoroughly understand the P removal potential of these filter media, we began the second round of filter media assessments at the SATT site during March 2000. We wanted to evaluate the SRP, PP and DOP removal effectiveness of slightly larger filters, operated under steady-state hydraulic loadings.

Each of eight plastic barrels (208 L) were filled with 30 cm of either limerock or Pro-Sil™ Plus (2.0-3.4 mm diam.) and plumbed to receive Post-STA waters via gravity flow from a head tank. An external standpipe maintained a constant water depth at either 10 or 45 cm above the filter media. Outflow from the duplicate barrels containing limerock media at 45 cm water depth were fed in a downflow fashion into barrels containing 30 cm of limerock and 10 cm of overlying water.

Beginning in May, 22, 2001, Post-STA inflow and outflows from each of the treatment beds were analyzed weekly for TP, SRP, and pH during the 33-week monitoring period. There were no obvious differences in SRP or TP concentrations between the duplicate beds of Pro-Sil™ with either 10 or 45 cm of overlying water during the first month of operation. Unfortunately, pozzolonic activity associated with the Pro-Sil™ caused the material to solidify after one month, which rendered the bed impermeable. We therefore discarded the Pro-Sil™, and replaced the four barrels with LR and returned the water depths to the original values of 10 and 45 cm, but covered the barrels with several layers of shade cloth to occlude light (Figure 2.55).

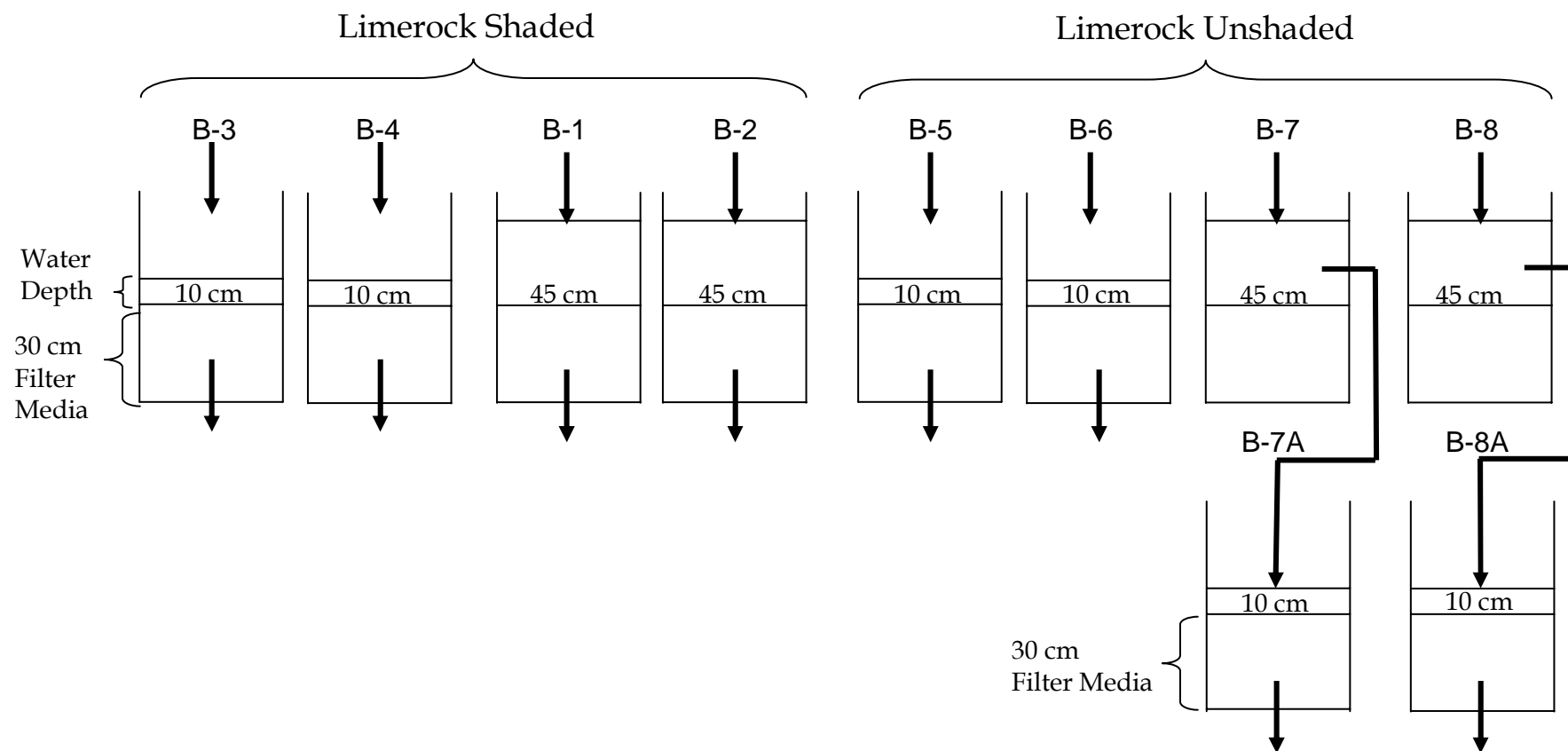


Figure 2.55. Schematic of second filter media evaluation at the SATT site after replacing the Pro-Sil™ with limerock on June 22, 2001.

Initially (post-July 1, 2001), the LR beds without light removed TP to the same extent that the LR beds exposed to sunlight, but this was not consistent during the 33-week monitoring period. At the end of October, three of the four shaded LR beds began to exhibit higher TP concentrations in the outflows relative to the inflow or sun-exposed LR bed outflow TP concentrations. For SRP, this phenomenon occurred earlier (end of August). For most sampling dates, SRP concentrations for outflows were always higher than the inflow concentration, regardless of treatment (water depth or sun vs. shade). The transformation of PP and DOP to SRP has been observed in other assessments where LR has been added to the back-end of an SAV treatment unit (Long-Term Monitoring; Test Cells), allowing us to state conclusively that LR beds not only trap PP, but also convert some of it to readily labile (and easily plant assimilated) SRP.

In contrast to the shaded LR beds, there was enhanced TP removal in the sun-exposed sequential LR beds, especially in one (B-7A) of the second tanks-in-series (Figure 2.56). Moreover, higher P removals and lower outflow TP concentrations were achieved as the assessment progressed (Figure 2.56). On October 30, 2001, B-7A contained a thick submersed green filamentous alga, whereas B-8A was absent of a high algal biomass community. We surmise that the improved TP removal performance for B-7A is likely attributable to the filamentous algal community, which may be enzymatically hydrolyzing DOP or assimilating SRP produced within the LR bed. SRP concentrations of the B-7A outflow were among the lowest of any treatment bed since October, which coincides with when the low TP concentrations were consistently observed for this treatment (Figure 2.57).

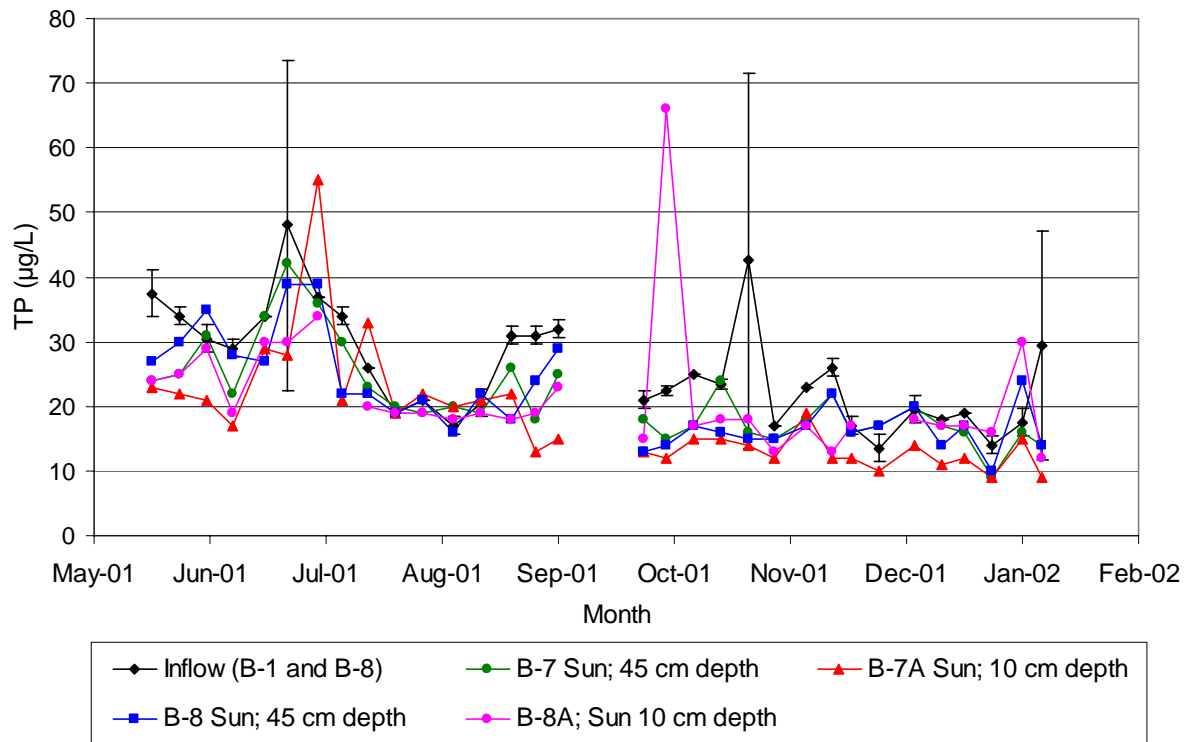


Figure 2.56. Mean total P concentrations in the inflow and outflows of duplicate limerock filter beds maintained at different water depths. The B-7A and B-8A filter beds represent sequential units that receive the outflow from B-7 and B-8 filter beds, respectively. The error bars for the inflow represent ± 1 s.d.

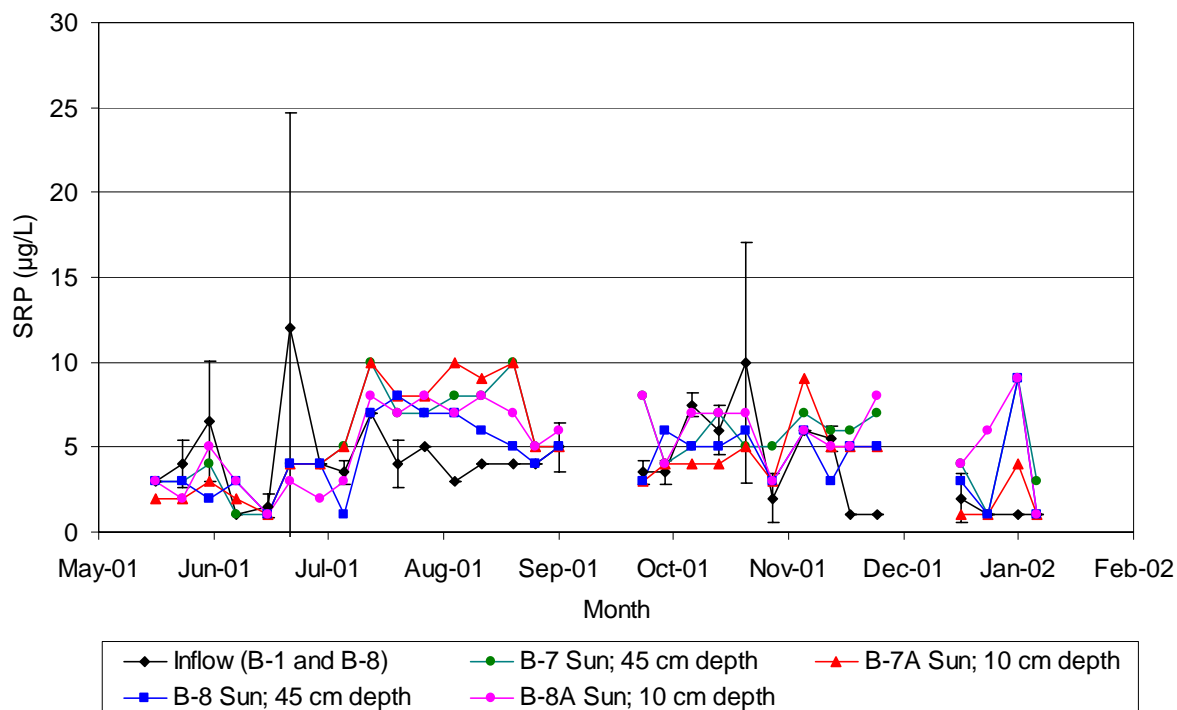


Figure 2.57. Mean soluble reactive phosphorus concentrations in the inflow and outflows of duplicate limerock filter beds maintained at different water depths. The B-7A and B-8A filter beds represent sequential units that receive the outflow from B-7 and B-8 filter beds, respectively. The error bars for the inflow represent ± 1 s.d.

2.11 Effects of Calcium/Alkalinity and Soluble Reactive Phosphorus Concentrations on Phosphorus Coprecipitation

Findings from our Phase I efforts using Post-BMP waters suggest that P removal in an SAV system is controlled in part by water column hardness and alkalinity (DBE 1999). In Phase II, we designed two assessments to demonstrate P coprecipitation in an SAV community (batch incubations) and to identify controlling factors of P removal by this mechanism (flow-through microcosms).

2.11.1 Assessment 1: Batch Incubations

The first assessment performed in April 2000, entailed subjecting previously conditioned P-“enriched” and P-“deficient” *Najas* to a constant SRP concentration at high and low levels of calcium and alkalinity over a two-day measurement period. The relative importance of P

uptake by SAV vs. coprecipitation of P in the water column was then evaluated. We hypothesized that the nutritional status of *Najas* tissues could be a dominant factor influencing SRP removal rate differences between treatments.

Methodology

We performed screening runs in March and April 2000 in order to obtain preliminary data on SRP uptake and release by *Najas*, precision among replicates, source water characterization and the appropriate light and temperature regimes under which to conduct the evaluation. Tap water from the City of West Palm Beach was selected as the source water for Assessment 1 because of its consistently low calcium (30 mg/L) and alkalinity (56 mg CaCO₃/L) relative to the 71 mg/L Ca and 227 mg CaCO₃ alkalinity measured in STA-1W agricultural drainage waters (ADW). We chose to add the desired alkalinity and Ca concentrations to the source water (tap water) rather than attempt to chemically remove them from the Post-BMP ADW. Opting for chemical removal would alter the water chemistry to such a degree that it would invalidate any comparison between low alkalinity/Ca (chemically “softened”) and the untreated high alkalinity/Ca waters.

We began the definitive assessment by treating W. Palm Beach tap water for chlorine and SRP removal. This was accomplished by placing water hyacinths (*Eichhornia crassipes*) in the tap water container for six days. Water hyacinths successfully removed both the chlorine and SRP present in the tap water. Using an average six-day exposure period, SRP concentrations were reduced from as high as 118 µg/L to a range of 5 to 20 µg/L; total chlorine residual, which was as high as 3.6 mg/L, was removed to undetectable (<0.1 mg/L) concentrations.

After the six-day contact with water hyacinths, the water was then pumped to a contact chamber where inorganic N, potassium, and micronutrient supplements were added (Table 2.24). After adding the nutrient amendments, the water volume (~ 20 gallons) was then split in half, and 10 gallons were delivered to each of the two aquaria. Prior to delivery of the replenished water, the *Najas* was removed from each aquarium, and the existing three-day old water was drained. To the aquarium containing the P-enriched *Najas*, we added P at a final concentration of ~ 200 µg/L to the newly added replenishment water. The P-deficient and P-

enriched *Najas* were then returned to their original aquaria, and allowed to incubate under charcoal sun screen shade cloth in the new growth medium for three days before the entire replenishment process was started anew.

Table 2.24. Final concentration of nutrients and micronutrients amended to W. Palm Beach tap water during the P-deficient and P-enriched conditioning period (35 days) and the final incubation (29.5 hr).

Compound	Nutrient	Final Concentration
KCl	K ⁺	10.8 mg/L *
NH ₄ Cl	NH ₄ ⁺	0.5 mg N/L
KNO ₃	NO ₃ ⁻	0.5 mg N/L
H ₃ BO ₃	B	10.8 µg/L
MnSO ₄ ·H ₂ O	Mn	10.8 µg/L
ZnSO ₄ ·7H ₂ O	Zn	5.2 µg/L
CuSO ₄ ·5H ₂ O	Cu	1.2 µg/L
(NH ₄) ₆ Mo ₇ O ₂₄ ·7H ₂ O	Mo	0.4 µg/L
FeCl ₃ ·6H ₂ O	Fe (in EDTA)	16 µg/L
Na ₂ EDTA	EDTA	94 µg/L
Cyanocobalamin	B-12	3 µg/L

* 9.4 mg/L from KCl and 1.4 mg/L from KNO₃

At the end of the 35-day conditioning period, the P-deficient *Najas* had nearly the same dry/wet weight ratio as the P-enriched *Najas* (0.063 and 0.067, respectively). However, we found nearly two-fold higher P concentrations in the P-enriched *Najas* (3770 mg/kg) than in the P-deficient *Najas* (1930 mg/kg). The initial dry/wet weight ratios and P concentrations in the *Najas* inoculum 35 days prior were 0.071 and 2160 mg/kg, respectively.

After the 35-day conditioning period, we assembled the following treatments and controls in triplicate by adding 125 µg SRP/L to 2L of tap water having the same concentrations of inorganic N, K, micronutrients as listed in Table 2.24:

1. P-enriched *Najas* in low Ca (21 mg/L) and alkalinity (52 mg CaCO₃/L) water
2. P-enriched *Najas* in high Ca (85 mg/L) and alkalinity (356 mg CaCO₃/L) water
3. P-deficient *Najas* in low Ca and alkalinity water
4. P-deficient *Najas* in high Ca and alkalinity water
5. Low Ca and alkalinity control water (no *Najas*)

6. High Ca and alkalinity control water (no *Najas*)

The tap water, which originally contained 21 mg Ca/L, was spiked with $\text{CaCl}_2 \cdot 2\text{H}_2\text{O}$ to obtain a final calcium concentration of 85 mg/L for the high Ca treatment. Likewise, sodium bicarbonate (NaHCO_3) was applied to the tap water to raise the alkalinity level from 52 to 356 mg CaCO_3 /L.

Based on our preliminary findings, we introduced 26.4 g fresh wt of either P-enriched or P-deficient *Najas* into each 3.785L incubation vessel containing two liters of growth medium (ratio of 76 mL of medium to 1 g fresh wt plant). *Najas* tissues were briefly rinsed with distilled water (410 mL) before inoculating the culture chambers and after withdrawal at the end of the incubation.

The incubation period began at 12:30 on May 25, 2000 and ended at 18:00 on May 26, 2000. We sampled SRP, total soluble P (TSP), dissolved Ca, total alkalinity, pH, and specific conductance at the beginning and end of the incubation period. In addition, we collected samples for SRP analysis and measured pH after 5.5, 17.5, and 26.5 hours from the onset of the incubation.

Incubation Results

The P-deficient *Najas* rapidly depleted the initial SRP concentration of 110 or 120 $\mu\text{g/L}$ within the first 5.5 hours of incubation in both the high and low Ca/alk treatments (Figure 2.58). The SRP concentrations in the controls (amended medium without *Najas*), on the other hand, remained near their spiked levels of 110 and 120 $\mu\text{g/L}$. This indicates that in P-deficient *Najas*, coprecipitation of Ca and P is irrelevant compared to the nutritional needs of the plant. Because of the high precision among the triplicates, the rate of aqueous SRP decrease was statistically different ($P < 0.05$; Mann-Whitney U Test) between the high Ca/alk and low Ca/alk treatments, even though the average slopes were nearly identical (Figure 2.58).

However, a different picture emerges when we examine the time course of SRP depletion for the P-enriched *Najas* exposed to high and low Ca/alk treatments (Figure 2.58). The added Ca and alkalinity constituents in the high Ca/alk treatment caused a two-fold faster decrease in the SRP concentrations within the first 5.5 hours of the incubation than in the low Ca/alk treatment

(8.6 $\mu\text{g/L}$ per hour vs. 4.0 $\mu\text{g/L}$ per hour). The slopes of these two treatments during this period are significantly different ($P < 0.05$) from each other, according to a Mann-Whitney U test. Interestingly, the slopes of the SRP removal for both treatments were nearly equal during the succeeding 12-hour nighttime period. This indicates that the supplemental removal by the P coprecipitating with the calcium carbonate ceased during the night, as expected. The pH values decreased to an early morning low of 7.57 (low Ca/alk) and 8.26 (high Ca/alk) (Figure 2.59), suggesting a reduced likelihood of CaCO_3 saturation.

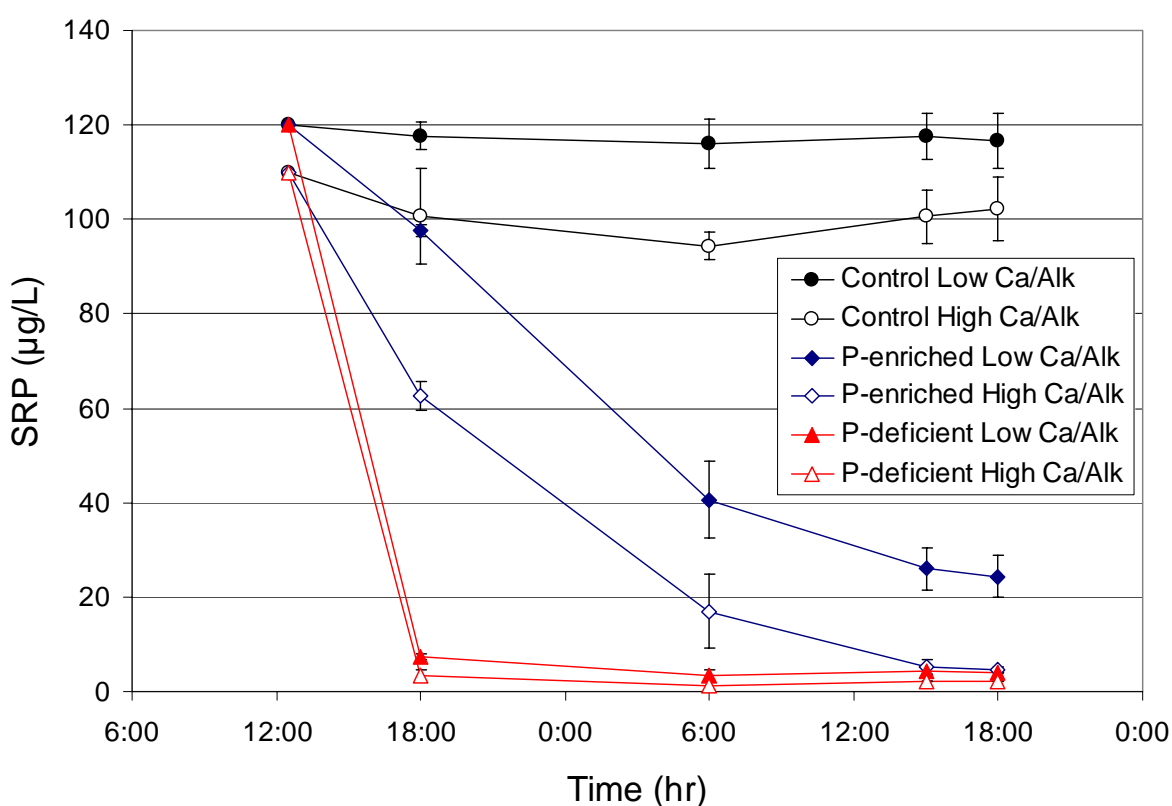


Figure 2.58. Time course (29.5 hr) for SRP inoculated at 120 $\mu\text{g P/L}$ initial concentration into high and low calcium/alkalinity water containing *Najas* previously cultured under P-enriched and P-deficient conditions for 35 days. Controls represent incubation without *Najas*. Each data point represents the mean \pm 1 s.d. of 3 replicate flasks. The date of assessment was May 25 – 26, 2000.

The reductions in the calcium and alkalinity concentrations were the same in both the P-deficient and P-enriched high Ca/alk treatments during the 29.5-hour incubation period (Table

2.25). This leads to two significant observations regarding calcium carbonate chemistry. First, a SRP concentration of 120 $\mu\text{g/L}$ does not appear to substantially inhibit the extent of calcium carbonate production. Previous studies (Vaithiyathan et al. 1997) have suggested that the presence of inorganic P in the water column can inhibit CaCO_3 precipitation, but this phenomenon was not observed in this evaluation. Second, although SRP was exclusively taken up by the P-deficient plant in the high Ca/alk treatment, the extent of calcium carbonate production was the same as for the P-enriched high Ca/alk treatment. This suggests that the precipitation of calcium carbonate is independent of the nutritional status of the SAV as long as sufficiently high pH levels are maintained during the day.

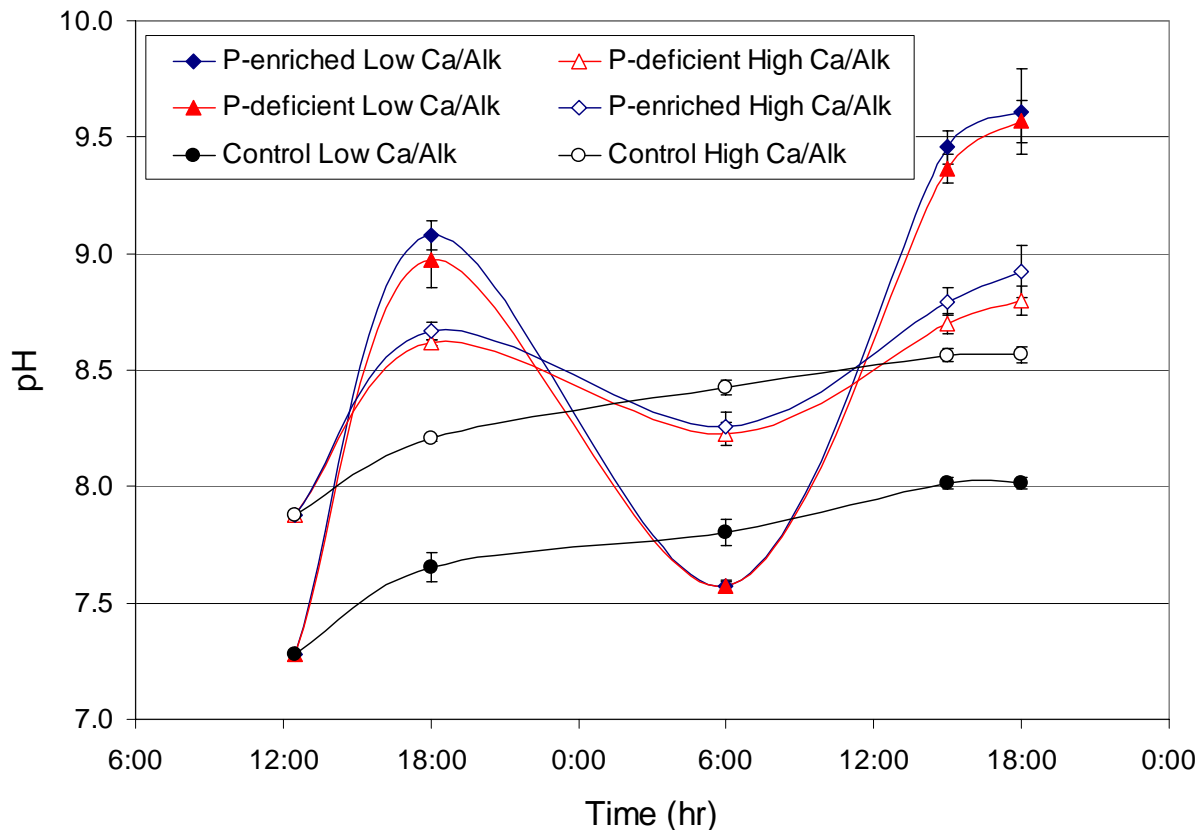
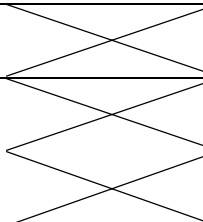
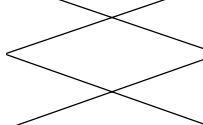


Figure 2.59. Time course (29.5 hr) for pH after SRP (120 $\mu\text{g P/L}$) was inoculated into high and low calcium/alkalinity water containing *Najas* previously cultured under P-enriched and P-deficient conditions for 35 days. Controls represent incubations without *Najas*. Each data point represents the mean \pm 1 s.d. of 3 replicate flasks. The date of assessment was May 25 – 26, 2000.

Further insights into the P and Ca chemistry can be found by examining the dry:wet weight (wt) ratios and P and Ca concentrations of the P-enriched and P-deficient *Najas* at the end of the incubation period. The final dry:wet wt ratios were significantly higher, and the tissue P concentrations significantly lower ($p < 0.05$), in the P-enriched high Ca/alk treatment compared to those in the P-enriched low Ca/alk treatment. This was also true for the dry:wet wt ratios in the P-deficient treatments, but not for the tissue P concentration. Significant differences ($p < 0.05$) were also found between the tissue Ca concentrations of the high and low Ca treatments in both the P-deficient and P-enriched plant incubations at the end of the 29.5 hr incubation (Table 2.25). From 67% (P-deficient) to 81% (P-enriched) of the aqueous Ca decreases in the high Ca waters were recovered in the incubated plant tissues. Combining the P and Ca data, it appears that most of the calcium carbonate precipitation is occurring on the surface of the *Najas* plant, which is adding to the dry weight of the plant as well as diluting the concentration of tissue P.

Table 2.25. Chemical characteristics of water column and plant tissues before and after a 29.5 hr incubation of *Najas* tissues in low- and high-calcium/alkalinity waters. Control values represent flasks without *Najas* inoculum. Plant tissues were pre-conditioned in waters with (P-enriched) or without (P-deficient) SRP amendments (See text for details). Final concentrations represent means \pm 1 s.d. of triplicate incubation flasks.

	Ca/Alk Treatment	Initial T = 0	Final T = 29.5 hr			
			P-enriched	P-deficient	Control	
Total Ca (mg/L)	Low Ca/Alk	21	21 ± 1	22 ± 1	23 ± 2	
	High Ca/Alk	85	33 ± 8	31 ± 2	85 ± 0	
Total Alkalinity (mg CaCO ₃ /L)	Low Ca/Alk	52	52 ± 0	52 ± 0	56 ± 0	
	High Ca/Alk	356	188 ± 21	182 ± 9	358 ± 2	
Tissue Ca (wt %)	Low Ca/Alk	1.6	1.4 ± 2	1.6 ± 2		
	High Ca/Alk	1.6	4.5 ± 8	3.8 ± 6		
Tissue P (mg/g)	Low Ca/Alk	3.20 P-deficient	6.24 ± 0.34	3.19 ± 0.29		
		6.64 P-enriched				
	High Ca/Alk	3.20 P-deficient	6.43 ± 0.23	3.60 ± 0.15		
		6.64 P-enriched				

2.11.2 Assessment 2: Flow-Through Microcosms

Our second assessment began in November 2000. Factors not explored in the short-term assessment, such as the effects of SRP concentrations on the rate and extent of P coprecipitation,

were pursued in this assessment, where a longer incubation period (5 months) using flow-through systems was utilized.

Methodology

Tap water from the City of West Palm Beach was again selected as the source of experimental water because of its consistently “low” calcium and alkalinity concentrations relative to the Post-BMP ADW. As in Assessment 1, dechlorination and SRP stripping were found to be necessary pre-treatment steps. This was accomplished by placing water hyacinths (*Eichhornia crassipes*) in the tap water reservoir for seven days. After pre-treatment with water hyacinths, the water was pumped in 151L batches to four 208-liter holding reservoirs (Figure 2.60).

In addition to the Ca, alkalinity, and SRP amendments, all the 208-L barrels received inorganic N, potassium, and micronutrient supplements (Table 2.24). After adding the nutrient amendments, the contents of each barrel was pumped to duplicate 75-liter microcosms (Figure 2.60). Each of the eight microcosms (duplicates x 4 treatments) was initially stocked with 800 g (fresh wt) of *Najas guadalupensis*. No sediment was added to the microcosms.

A flow rate of 12 mL/min (17.3 L/day) was provided to each of the microcosms, which contained 60.6 L (16 gal) of water. This produced a HRT of 3.5 days (HLR=9.6 cm/day).

During the first month of operation, inflow amendments for each treatment were re-adjusted to represent calcium and alkalinity concentrations more typical of levels measured in post-BMP waters. Beginning November 22, 2000, the phosphorus amendment was increased from 125 to 160 µg/L. The Ca/alk amendments were reduced from target concentrations of 100 to 80 mg Ca/L and from 375 to 325 mg CaCO₃/L on January 26, 2001. Subsequent to these modifications, the following Ca, alkalinity, and SRP amendments were added to each of the holding reservoirs for the remaining 3 months of the assessment.

1. Treatment #1 – Low calcium/alkalinity (unamended) and low SRP (stripped with water hyacinth beforehand)

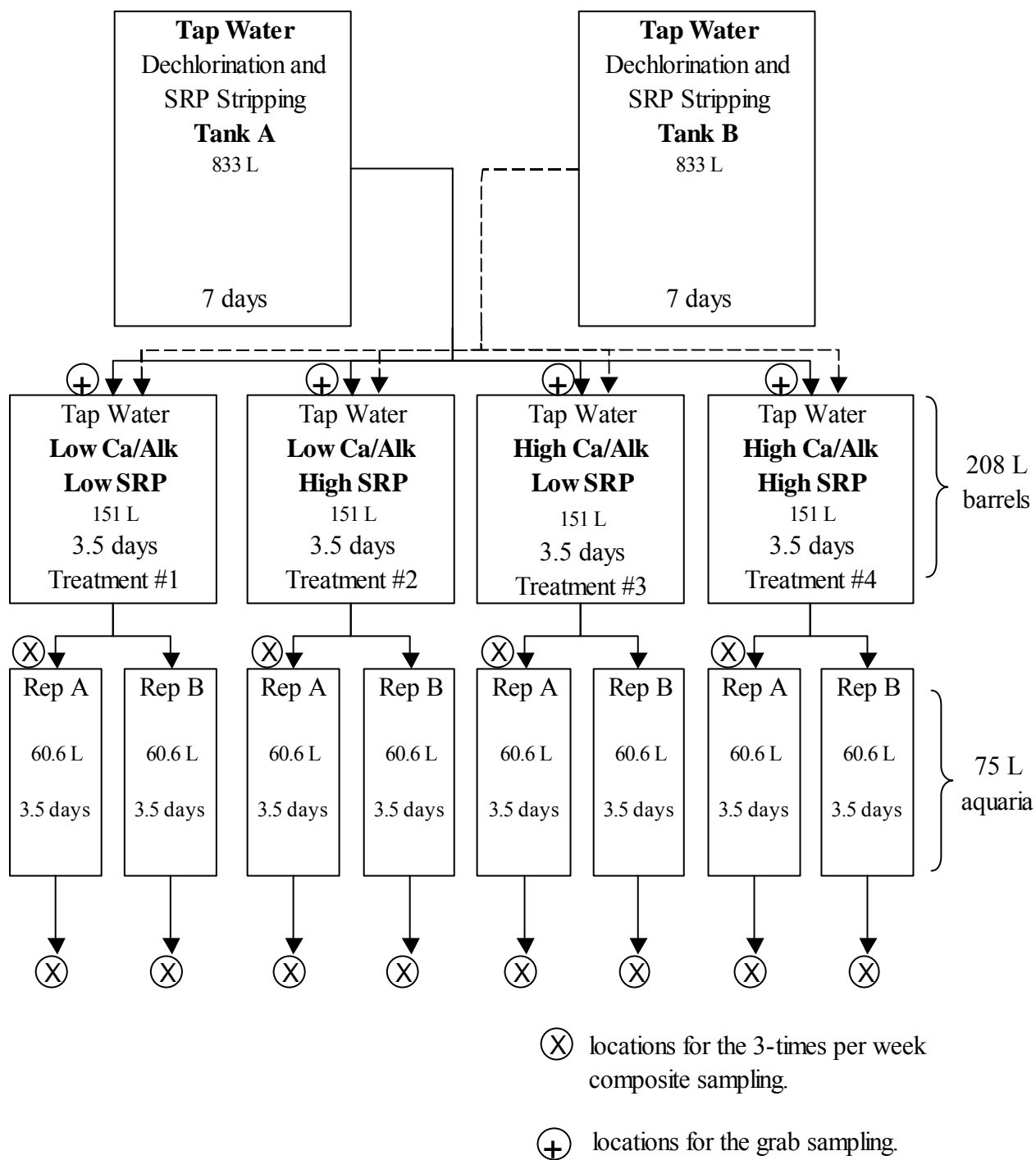


Figure 2.60. Flow chart detailing the evaluation design for the flow-through Coprecipitation Assessment 2.

2. Treatment #2 - High calcium/alkalinity (amended to a final concentration of 80 mg Ca/L and 325 mg CaCO_3 /L) and low SRP (stripped)
3. Treatment #3 - Low calcium/alkalinity (unamended) and high SRP (stripped, then amended with 160 μg SRP/L)
4. Treatment #4 - High calcium/alkalinity (amended to a final concentration of 80 mg Ca/L and 325 mg CaCO_3 /L) and high SRP (stripped, then amended with 160 μg SRP/L)

Although we recognize that these evaluation concentrations do not represent the extreme “low” and “high” values under all environments, these treatments will henceforth be referred to as Low Ca/alk, Low SRP (treatment #1); High Ca/alk, Low SRP (treatment #2); Low Ca/alk, High SRP (treatment #3); and High Ca/alk, High SRP (treatment #4).

Composite samples of three grabs per week were collected at each sampling location (Figure 2.60) for TP, SRP, TSP, Ca, alkalinity, and conductance measurements. In addition to the composite sampling, we also collected grab samples after each time a new batch of source water was amended and stored within the holding tanks (Figure 2.60). Water temperature and pH measurements were taken in the field for each sample.

At the conclusion of five months of operation and monitoring of the coprecipitation assessment, we quantified the mass of P present in the live SAV and sediment floc within each microcosm. Along with total wet and dry weight, elemental (P, Ca, C, N) analysis of each compartment was performed for the eight microcosms.

Phosphorus Removal and Related Water Chemistry Changes

During the five-month assessment, mean inflow TP and TSP concentrations were comparable between P-unamended treatments (#1 and #2 in Table 2.26) and between P-amended treatments (#3 and #4). Inflow calcium and alkalinity concentrations were also comparable between like treatments, as shown in Table 2.26.

Beginning on December 29, 2000, the outflow pH values in the High and Low SRP treatments receiving Ca and alkalinity amendments began to diverge (Figure 2.61). Although the outflow pH in both sets of treatments began to increase on that date, the higher pH values tended to be more associated with the High SRP treatment.

The most likely explanation for the higher pH values associated with the effluents of the SRP-amended treatments is the change in the nutritional status of the *Najas*. Initially, the P content of the *Najas* inoculated into all the treatments was 1306 mg/kg. After 8 weeks of exposure (November 6 - December 29, 2000) to SRP concentrations of 7 ± 5 µg/L, the *Najas* became P “deficient” in the P-unamended treatments. By contrast, *Najas* in the P-amended microcosms receiving SRP concentrations of 99 µg/L (High Ca/alk) and 125 µg/L (Low Ca/alk) became P “enriched”. The result of the different P treatments was that after 8 weeks of exposure, the *Najas* populations that received the higher SRP concentrations had higher rates of primary production than the populations grown in low SRP medium, regardless of whether they were growing in High or Low Ca/alkalinity water.

Table 2.26. Mean (± 1 s.d.) total P, TSP, SRP, dissolved Ca and alkalinity concentrations in the inflows and outflows from duplicate aquaria operated under four treatments during the five month evaluation (November 6, 2000 – April 15, 2001). Means for TP followed by the same letter are not significantly different ($p > 0.05$).

	Treatment #1 Low Ca/alk Low P	Treatment #2 High Ca/alk Low P	Treatment #3 Low Ca/alk High P	Treatment #4 High Ca/alk High P
TP (µg/L)				
Inflow	32	30	166	170
Outflow	17 ± 3^a	13 ± 2^b	68 ± 10^c	25 ± 2^d
TP Removal	15	17	98	145
TSP (µg/L)				
Inflow	22	22	157	161
Outflow	11 ± 2	7 ± 1	55 ± 9	17 ± 3
TSP Removal	11	15	102	144
SRP (µg/L)				
Inflow	12	10	136	116
Outflow	2 ± 0	2 ± 1	36 ± 9	5 ± 3
SRP Removal	9	8	100	111
Alkalinity (mg CaCO₃/L)				
Inflow	65	315	68	317
Outflow	69 ± 3	248 ± 10	71 ± 2	230 ± 7
Alkalinity Removal	-4	67	-3	87
Diss. Calcium (mg/L)				
Inflow	27	77	28	77
Outflow	28 ± 1	50 ± 3	29 ± 1	45 ± 3
Calcium Removal	-1	28	-2	31

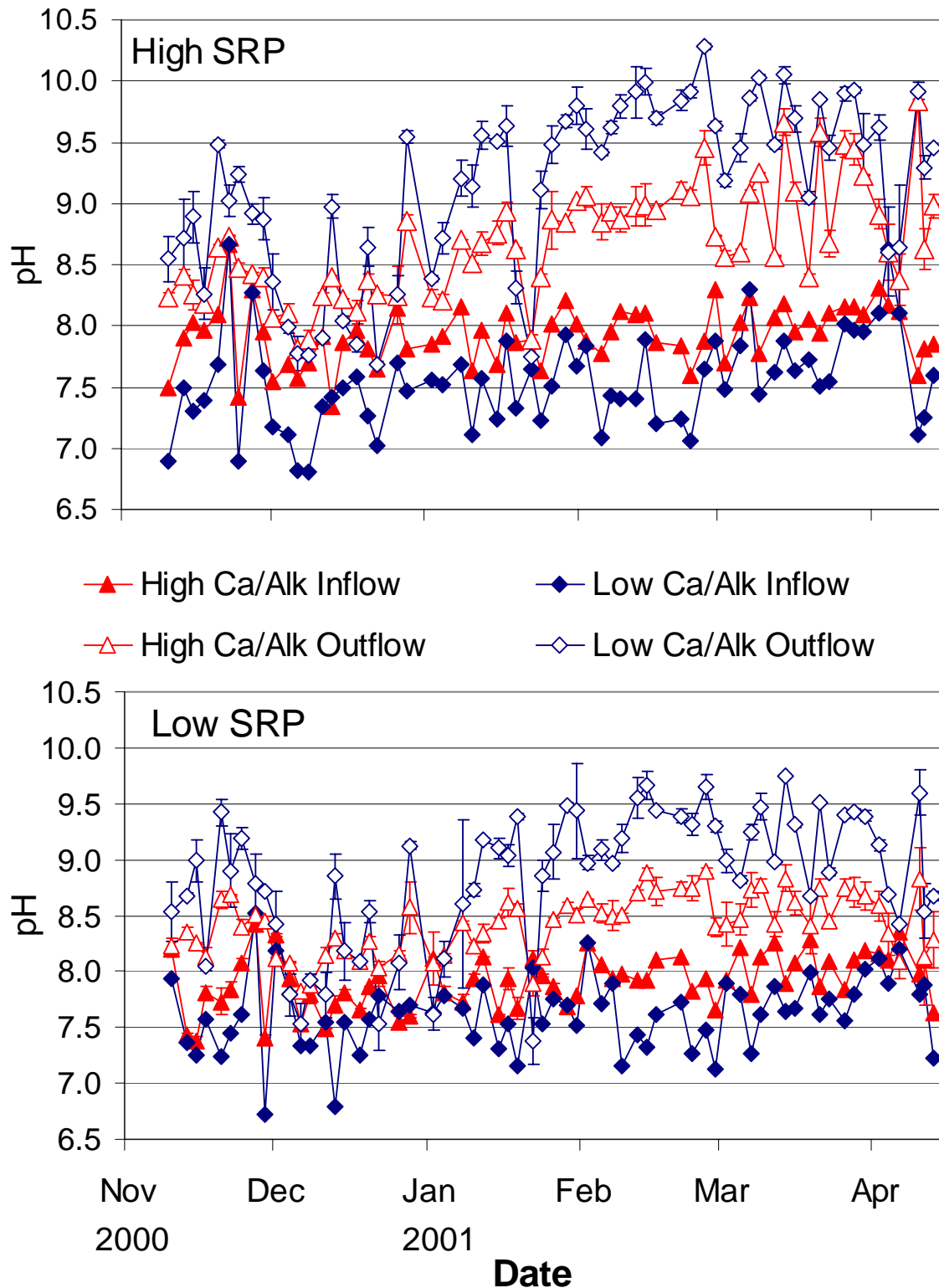


Figure 2.61. Mean inflow and outflow pH levels from microcosms which received tap water that was either unamended (Low) or amended (High) with concentrations of SRP and Ca/alkalinity for 160 days.

Table 2.27. CaCO₃ saturation indexes (SI) and pH values in the inflow and outflow waters from microcosms which received tap water unamended (Low) and amended (High) with SRP and Ca/alkalinity for 160 days. s.d. = ± standard deviations

	Inflow				Outflow			
	pH	s.d.	SI	s.d.	pH	s.d.	SI	s.d.
<u>Entire Period of Record, November 6, 2000 through April 15, 2001</u>								
Low Ca/alk, Low SRP	7.62	0.33	0.3	0.2	8.85	0.59	7.3	6.4
Low Ca/alk, High SRP	7.54	0.40	0.4	0.9	9.14	0.70	15.0	13.9
High Ca/alk, Low SRP	7.91	0.24	5.7	1.7	8.42	0.26	9.2	3.2
High Ca/alk, High SRP	7.93	0.24	6.0	1.9	8.67	0.45	13.2	5.6
<u>Before December 29, 2000</u>								
Low Ca/alk, Low SRP	7.55	0.39	0.2	0.1	8.46	0.54	2.6	1.8
Low Ca/alk, High SRP	7.40	0.45	0.2	0.1	8.53	0.56	3.6	2.7
High Ca/alk, Low SRP	7.80	0.29	5.2	1.6	8.26	0.22	7.4	2.1
High Ca/alk, High SRP	7.87	0.31	6.1	1.9	8.30	0.24	8.7	2.6
<u>After December 29, 2000</u>								
Low Ca/alk, Low SRP	7.66	0.28	0.3	0.2	9.06	0.51	9.9	6.5
Low Ca/alk, High SRP	7.62	0.35	0.6	1.1	9.46	0.52	21.5	13.4
High Ca/alk, Low SRP	7.97	0.19	5.9	1.7	8.51	0.24	10.3	3.3
High Ca/alk, High SRP	7.97	0.19	6.0	1.9	8.87	0.41	15.8	5.1

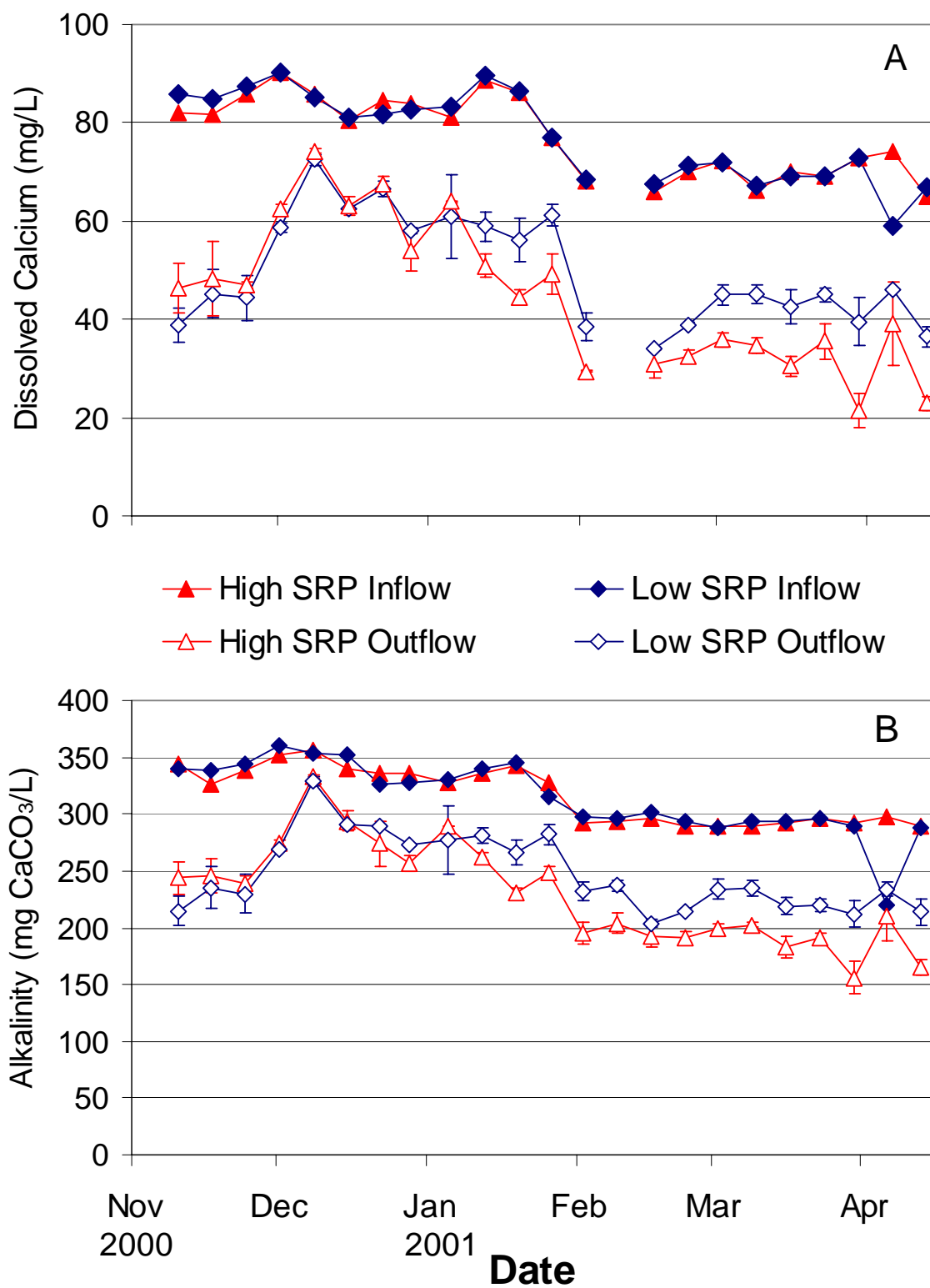


Figure 2.62. Mean inflow and outflow (A) dissolved calcium and (B) total alkalinity concentrations from microcosms which received tap water amended with Ca/alkalinity and either unamended (Low) or amended (High) with SRP for 160 days.

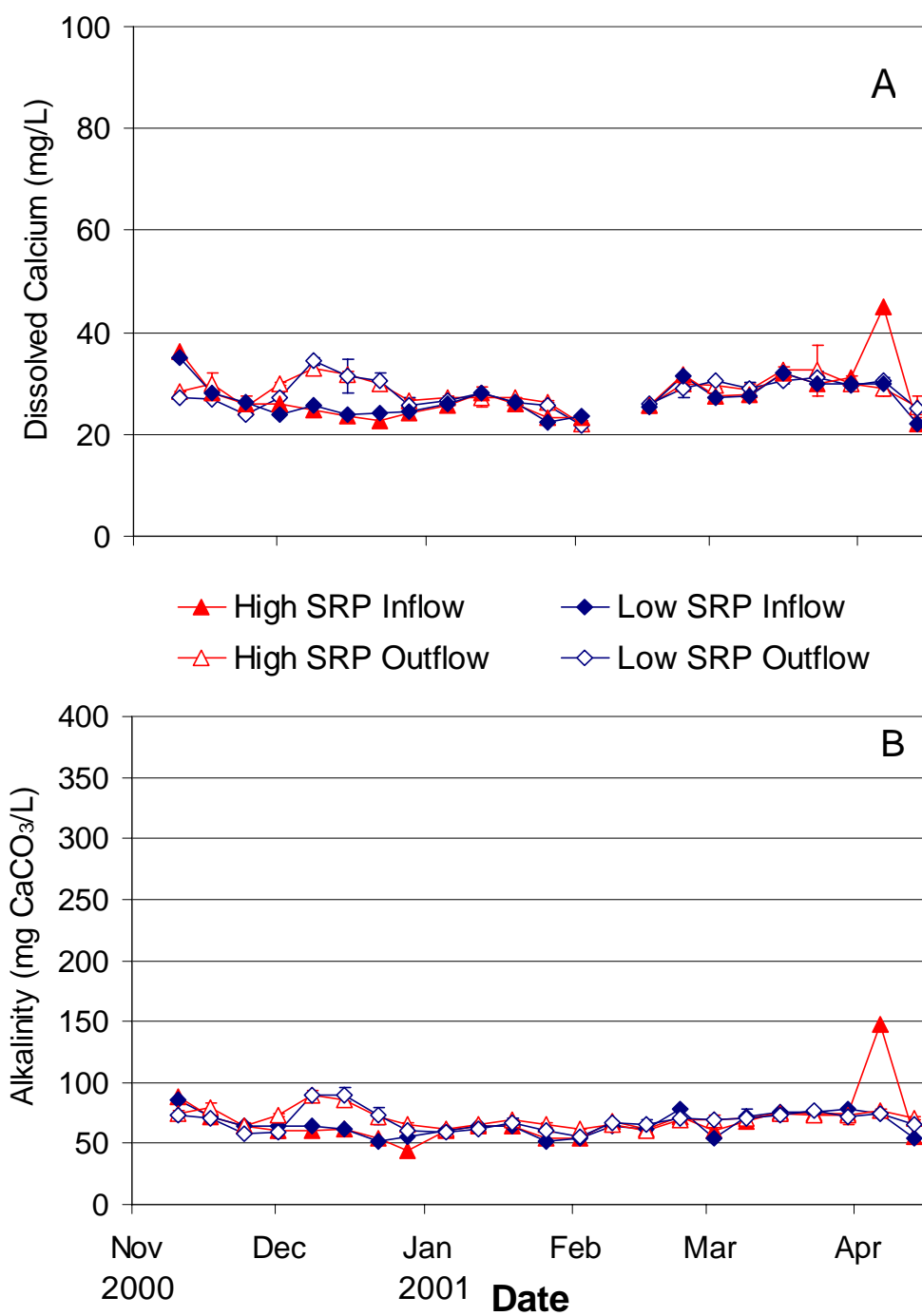


Figure 2.63. Mean inflow and outflow (A) dissolved calcium and (B) total alkalinity concentrations from microcosms which received tap water without Ca/alkalinity amendments, and either unamended (Low) or amended (High) with SRP for 160 days.

Along with increased pH levels observed in the High Ca/alk, High SRP microcosm outflows after December 29th, concentration reductions of Ca and alkalinity after that date were greater than those observed during the initial eight weeks of operation (Figure 2.62). Outflow waters were more supersaturated with respect to CaCO₃ after December 29 than before (Table 2.27), due primarily to higher observed pH levels. The same trends were less pronounced in the High Ca/alk, Low SRP treatments (Figure 2.63) due to poorer P nutrition of the *Najas*, and subsequently smaller pH elevations. Although a similar divergence in pH levels also occurred after December 29th in both sets (High and Low SRP) of the unamended Ca/alk treatments (Figure 2.61), reductions of water column calcium and alkalinity did not occur (Figure 2.63).

Among the high Ca/alk treatments, the inflow waters were supersaturated with respect to CaCO₃ in both the P-amended and unamended treatments (saturation index, SI = 6.0 and 5.7, respectively). The inflow waters to the treatments without Ca/alk additions were undersaturated (SI = 0.3-0.4), and although photosynthetically-driven pH elevations created supersaturated conditions in the outflow from those systems (Table 2.27), no net removal of Ca or alkalinity occurred over the five-month monitoring period (Table 2.26). In the Ca/alk-amended treatments, however, Ca and alkalinity (as CaCO₃) were removed in nearly a 1:1 molar ratio (Figure 2.64), indicating that precipitation of CaCO₃ was the primary Ca removal mechanism in those treatments.

Considering that both SRP and dissolved organic carbon (and thus dissolved organic P [DOP]) can both be coprecipitated with CaCO₃ (Seuss 1970; Murphy et al. 1983; Danen-Louwerse et al. 1995), we examined the TSP component of our water quality data for the relevance of the P coprecipitation process. Within the P-amended treatments, TSP concentration was reduced to a greater extent in the High Ca/alk treatment than in the Low Ca/alk treatment (Table 2.26, Figure 2.65). Since no net removal of Ca or alkalinity occurred in the low Ca/alk systems, these data suggest that coprecipitation in the P-amended mesocosms receiving High Ca/alk inflow waters accounted for ~25% of the P removal in the mineral-amended tapwater.

In the microcosms not amended with P, TSP concentration reductions were only slightly greater in the High than the Low Ca/alk treatment (15 $\mu\text{g/L}$ vs. 11 $\mu\text{g/L}$). Even though the absolute TSP concentration reductions were lower in the P-unamended microcosms than the P-amended systems, the differences in the TSP removals between the High and Low Ca/alk treatments were about the same on a percentage basis (25-30%) within each treatment group. The coprecipitation of P with CaCO_3 in high Ca/alk mineral-amended waters therefore appeared to increase P removal by 25-30% (Figure 2.65), regardless of the inflow TSP concentration.

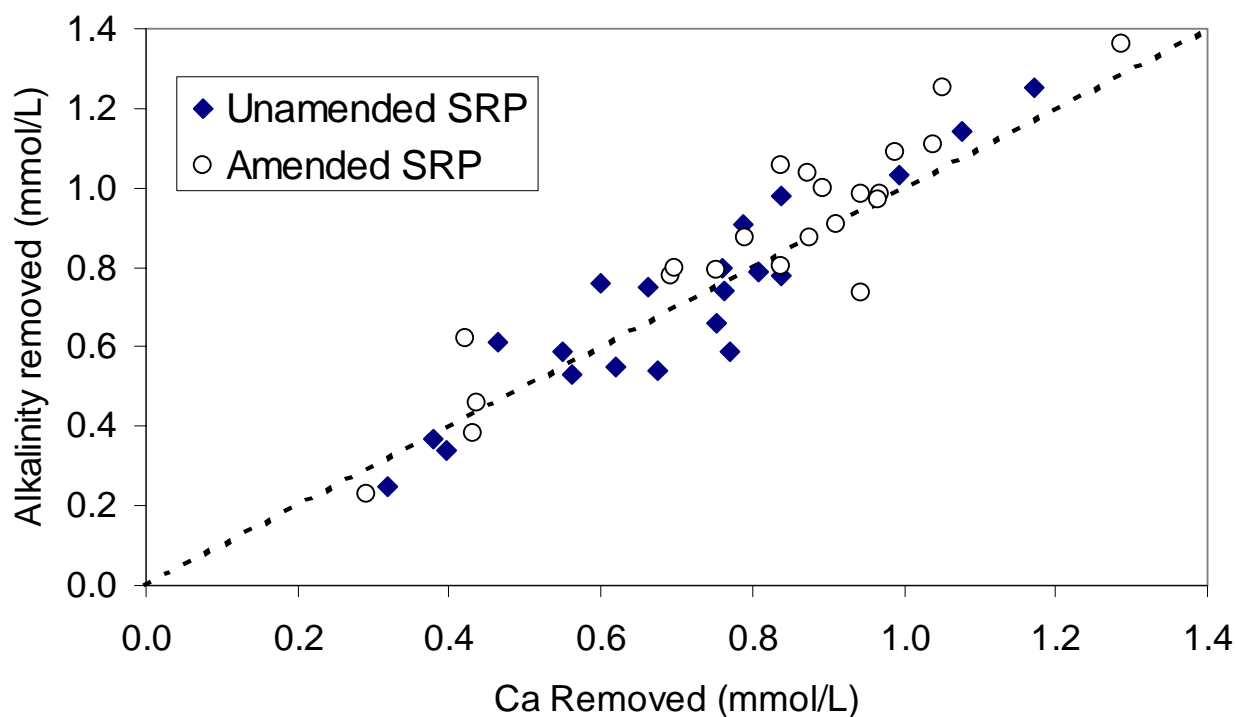


Figure 2.64. Calcium and alkalinity removals from amended (High) Ca/alk treatment waters with and without SRP amendments during the 160-day assessment. The dashed line represents removal of equal molar amounts of calcium and alkalinity as CaCO_3 .

Since the level of calcium and alkalinity has an effect on the removal of TSP in the SRP-amended treatments, then it may be expected that outflow TP concentration would also be significantly different. Indeed, we found this to be the case. Whereas, mean outflow TP concentrations were not significantly different ($p>0.05$) between the two treatments that were not amended with SRP, the mean outflow TP concentration ($25\text{ }\mu\text{g/L}$) from the high Ca/alk treatment that was amended with SRP was significantly lower ($p<0.05$) than the mean TP concentration ($68\text{ }\mu\text{g/L}$) leaving the SRP-amended low Ca/alk treatment mesocosms (Table 2.26). This indicates that the degree of water hardness affects the extent of P removal by *Najas* in an artificial medium with SRP concentrations ($160\text{ }\mu\text{g/L}$) comparable to the upper concentration levels found in Post-BMP waters. This is the same conclusion we reported for the results of the batch incubation in Assessment 1.

On two occasions during the five month investigation, the suite of parameters typically sampled during peak daylight hours were sampled just prior to dawn. These “snapshot” sampling events on December 28, 2000 and March 5, 2001 revealed nighttime outflow water quality (Table 2.28) similar to that observed during the day (Table 2.27), with the exception of lower pH levels at night.

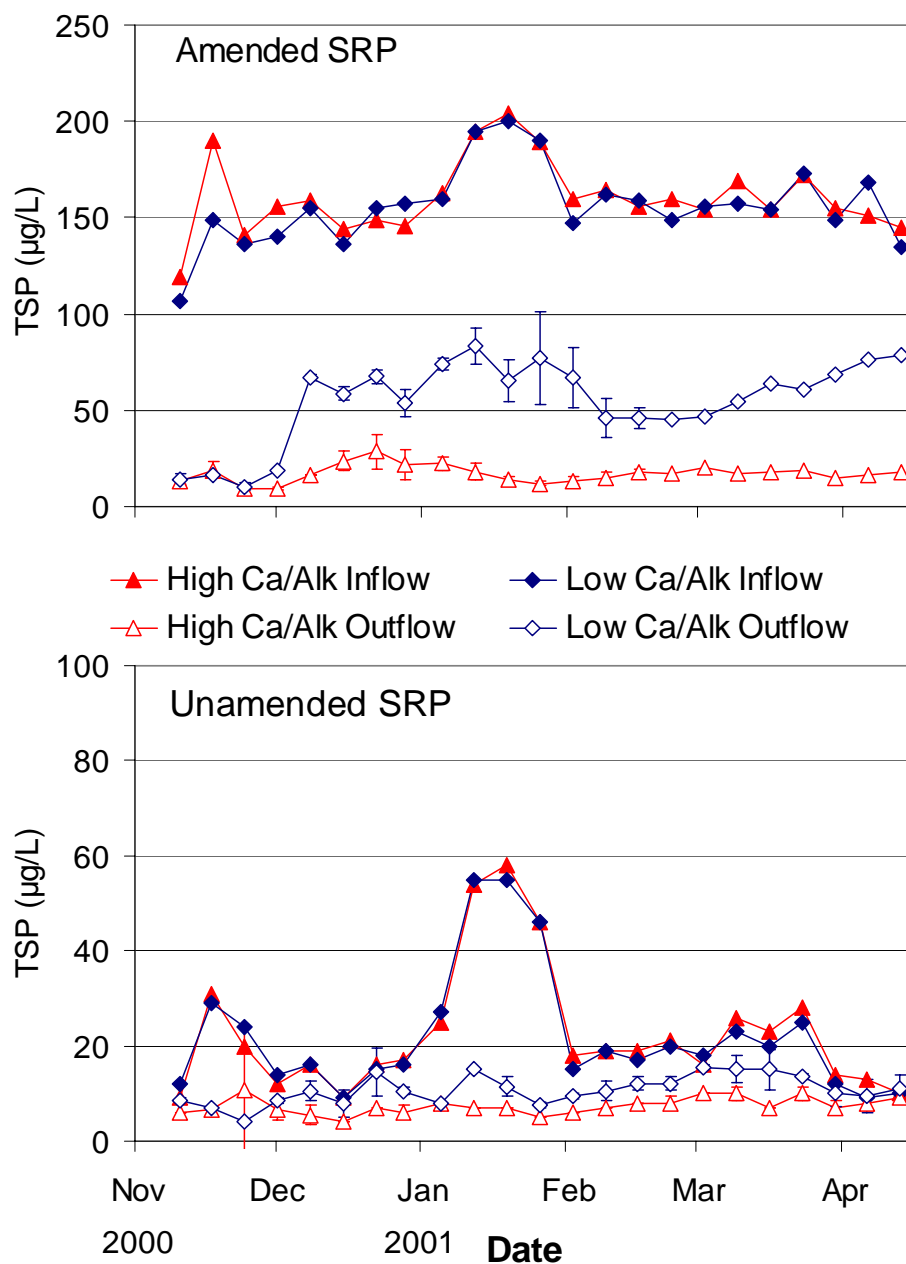


Figure 2.65. Mean total soluble P concentrations in the inflow and outflow waters from microcosms which received tap water unamended (Low) and amended (High) with SRP and Ca/alkalinity for 160 days.

Table 2.28. Concentration ranges for inflows and outflows from duplicate microcosms operated under conditions of unamended (Low) and amended (High) calcium, alkalinity, and SRP. Values represent two grab sampling events just prior to dawn on December 28, 2000 and March 5, 2001.

Parameter	Units	Low Calcium/Low Alkalinity				High Calcium/High Alkalinity			
		Inflow		Outflow		Inflow		Outflow	
		Range	Mean	Range	Mean	Range	Mean	Range	Mean
<i>Low SRP Microcosms</i>									
Total P	µg/L	20 - 24	22	13 - 24	18	22 - 25	24	10 - 16	13
SRP	µg/L	4 - 7	6	1 - 3	2	3 - 7	5	1	1
DOP	µg/L	9 - 12	10	6 - 13	10	9 - 18	14	4 - 11	8
PP	µg/L	4 - 8	6	3 - 8	6	4 - 6	5	3 - 6	4
Alkalinity	mg CaCO3 /L	60 - 64	62	60 - 76	68	284 - 328	306	242 - 290	266
Dissolved Ca	mg/L	25 - 27	26	26 - 32	29	69 - 81	75	49 - 65	57
PH	SU	7.28 - 7.34	7.31	7.68 - 8.19	7.94	7.69 - 7.98	7.84	7.72 - 8.16	7.94
Temperature	°C	16.7 - 19.3	18	17.4 - 18.3	18.8	17.6 - 18.6	18.1	17.2 - 19.1	18.2
Specific Conductivity	µS/cm	649-788	718	695 - 871	783	1436 - 2072	1754	1372 - 1530	1451
<i>High SRP Microcosms</i>									
Total P	µg/L	159 - 160	160	44 - 67	56	155 - 170	162	17 - 27	22
SRP	µg/L	132 - 144	138	16 - 40	28	111 - 121	116	4 - 12	8
DOP	µg/L	11 - 18	14	12 - 22	17	28 - 48	38	6 - 17	12
PP	µg/L	5 - 9	7	6 - 15	10	6 - 11	8	4 - 9	6
Alkalinity	mg CaCO3 /L	58 - 60	59	64 - 72	68	288 - 344	316	239 - 274	256
Dissolved Ca	mg/L	26 - 27	26	26 - 30	28	68 - 82	75	47 - 59	53
pH	SU	7.42 - 7.43	7.42	7.87 - 8.08	7.98	7.76 - 8.00	7.88	8.00 - 8.20	8.10
Temperature	°C	16.9 - 20.8	18.9	18.0 - 19.7	18.8	17.5 - 19.7	18.6	16.8 - 18.1	17.4
Specific Conductivity	µS/cm	638 - 793	716	673 - 895	784	1457 - 2072	1764	1417 - 1536	1476

Sediment Deposition

Sediment production was influenced more by calcium and alkalinity levels than by P levels in the inflow waters (Table 2.29). The High Ca/alk microcosms generated more bulk sediment overall.

Phosphorus and Calcium Storages

The final *Najas* standing crop biomass (526 – 785 g fresh weight) in each microcosm was lower than the initial inoculum of 800g fresh weight. Despite the decline in biomass, macrophyte P mass increased over the five-month assessment in the P-amended microcosms due to increased tissue P concentrations (Figure 2.66). *Najas* tissue P concentrations declined in the P-unamended microcosms, which along with the decreased biomass, resulted in a final biomass P mass lower than the inoculum. Periphyton, where present, comprised 3-7% of the total P stored in the microcosms (Figure 2.67).

The total dry mass (inorganic and organic fractions) of newly accrued sediments was higher in the High Ca/alk treatments (Table 2.29), where CaCO_3 comprised $64 \pm 1\%$ of the total mass. Calcium carbonate comprised only 34 ± 2 and $18 \pm 1\%$ of the sediments recovered from the Ca/alk-unamended treatments of Low and High SRP, respectively. The sediment differences between High and Low P treatments observed in the Ca/alk-unamended (Low Ca/alk) microcosms were due to a more productive P-amended (High SRP) system depositing more organic matter in the sediments while CaCO_3 accrual was minimal in both systems due to Low Ca/alk concentrations in the inflow waters (Table 2.29).

Total P concentrations in the High Ca/alk sediments were lower than in sediments receiving Low Ca/alk waters (Table 2.29). This was primarily due to increased CaCO_3 deposition in the High Ca/alk treatment systems, which reduced the relative proportion of P in those sediments. Nevertheless, on a mass and percentage basis, sediment floc-P constituted a greater fraction of the total P recovered in the High Ca/alk treatments than in the Low Ca/alk treatments of equivalent inflow P concentrations (Figures 2.66 and 2.67).

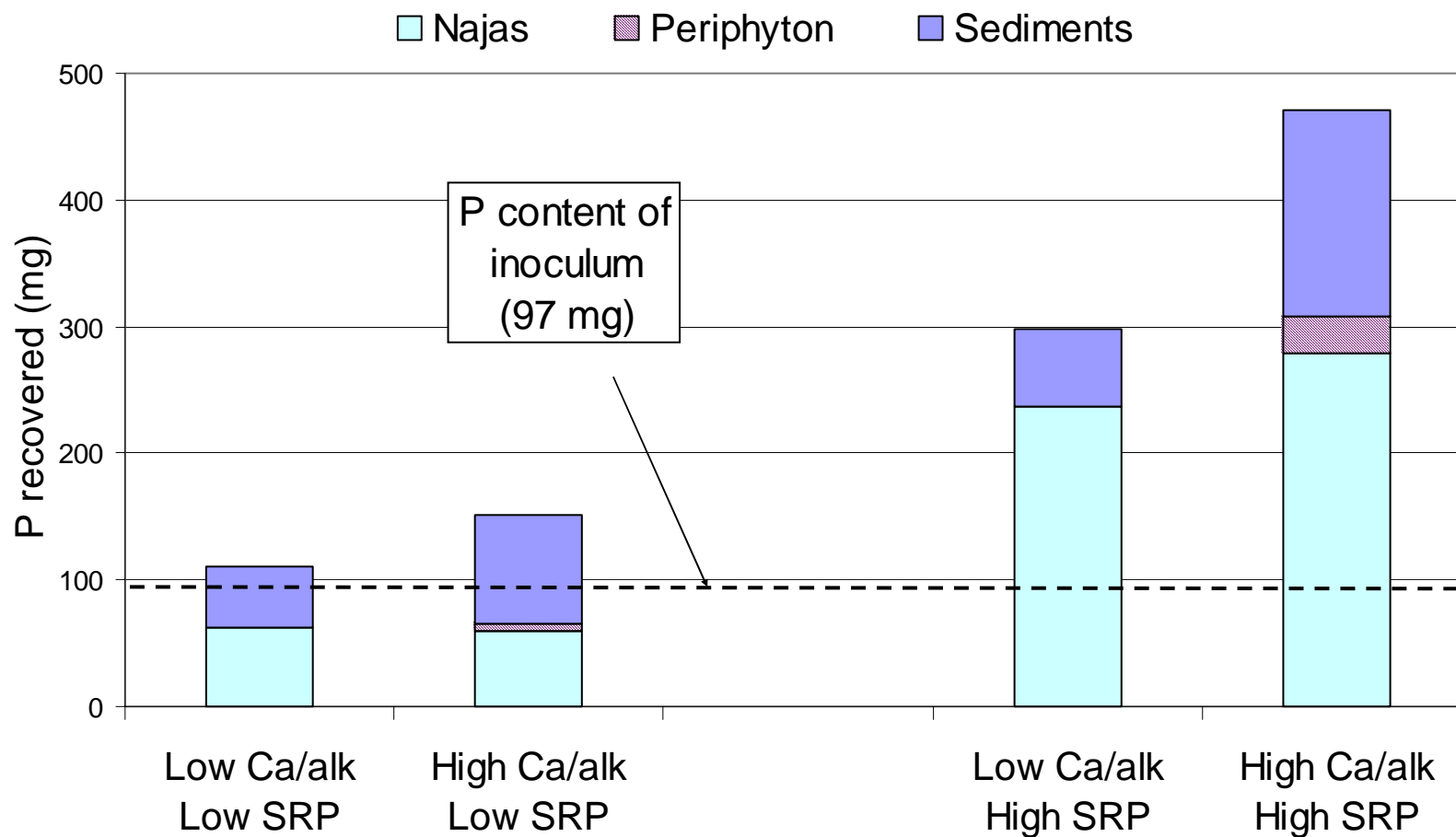


Figure 2.66. Phosphorus (by mass) stored in *Najas* and periphyton tissues and the sediments recovered from microcosms which received tap water unamended (Low) and amended (High) with SRP and Ca/alkalinity for 160 days. The dashed line represents the 97 mg P stored in *Najas* tissues inoculated into each microcosm at the beginning of the evaluation.

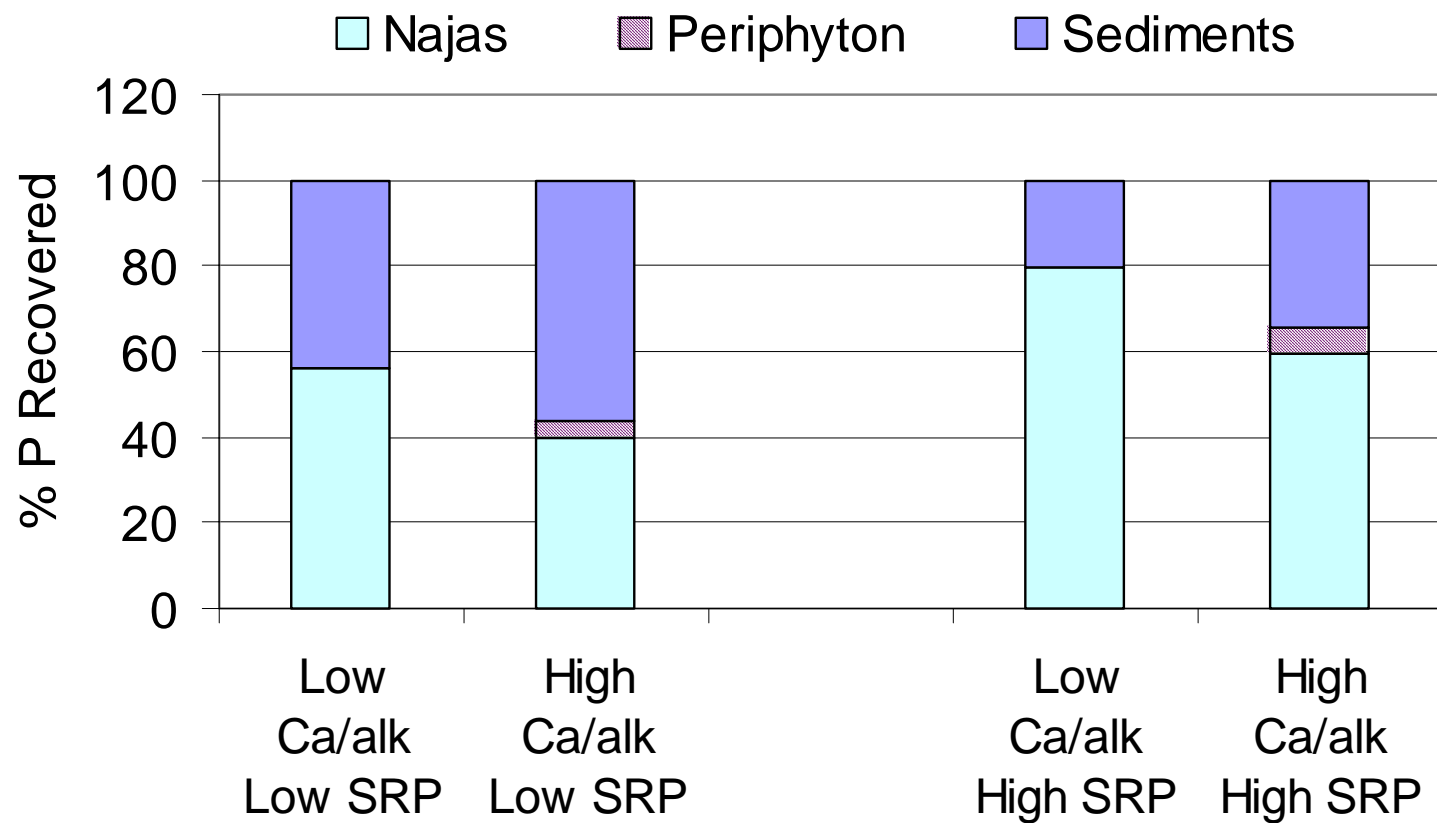


Figure 2.67. Distribution of phosphorus (% of P recovered) stored in *Najas* and periphyton tissues and the sediments recovered from microcosms which received tap water unamended (Low) and amended (High) with SRP and Ca/alkalinity for 160 days.

Table 2.29. Total deposited dry mass and total phosphorus, inorganic carbon, organic carbon and calcium concentrations of sediments collected from microcosms which received tap water unamended (Low) and amended (High) with SRP and Ca/alkalinity for 160 days.

	Total Dry Mass (g/m²)	TP (mg/kg)	TIC (% Wt.)	TOC (% Wt.)	TCa (% Wt.)
Low Ca/alk Low SRP	199	1380	5.3	19.4	13.5
High Ca/alk Low SRP	749	643	9.0	8.2	26.0
Low Ca/alk High SRP	176	1945	5.5	22.4	7.2
High Ca/alk High SRP	795	1155	9.4	7.8	25.5

2.11.3 Summary

These assessments provide direct evidence that coprecipitation of soluble P compounds and ions can occur within SAV beds, but it appears to account for less P removal than biological uptake by the SAV and/or bacterial communities. The rate and extent of P coprecipitation are predicated on the initial SRP (and TSP), alkalinity, and hardness concentrations of the water, and the nutritional status of the SAV. In natural systems, the removal of SRP may depend more on the physiological needs of the plant than on the extent and amount of calcium carbonate precipitation. Some of the calcium carbonate precipitate, regardless of whether it takes place within a P-enriched or P-deficient SAV community, appears to be formed and retained at the leaf surfaces of the plant. In addition to its importance as a water column P removal mechanism, CaCO₃ precipitation should be investigated for its influence on quantity and P-retention properties of newly formed sediments in SAV communities.

2.12 Particulate Phosphorus and Dissolved Organic Phosphorus Characterization and Stability

Findings from DBE's Phase I efforts demonstrated that the outflow TP from the moderate HLR SAV and LR filter mesocosms (11 – 22 cm/day) consists largely of PP (27 – 50%) and DOP (DBE 1999). The ability of a supplemental technology to achieve the 10 ppb TP target depends on its ability to reduce these fractions to extremely low levels. The capabilities of the supplemental technologies to “treat” these P species will vary, depending on their size fraction, stability, and transportability. It would be helpful in the design of STAs to understand whether particles

exported from a SAV or cattail unit process are the same particles in the inflow source water, or if they are generated internally in the wetland. Understanding the differences, if any exist, of particle type, size and zeta potential (the potential difference between the plane of shear and the bulk phase), will provide insight on the transport potential of those particles.

We performed laboratory characterizations of PP and dissolved DOP collected from STA-1W Cell 4, test cells and mesocosm waters. In one assessment, DOP and PP size fractions were isolated from Cell 4 inflow and outflow regions and analyzed for enzymatic SRP release, and SRP release under low pH redox conditions. In our second assessment, alkaline phosphatase activity in ecosystem compartments (sediment, detritus, surface water and biomass) was analyzed using bench-scale incubations. Finally, PP isolated from SAV and cattail communities inhabiting the inlets and outlets of the test cells and Cell 4 was characterized and compared to assess PP transport and degradation characteristics.

2.12.1 Particle Concentration Methodology

DBE employed a tangential-flow filtration technique to concentrate particles in waters at various stages of treatment (i.e. Post-BMP, Cell 4 effluent, test cell effluent). This technique allows the processing of large sample volumes while at the same time minimizing the artifacts from concentration polarization that are observed with typical stirred-cell filtration devices (Cooper et al. 1999).

On July 5, 2000, DBE and HSA personnel performed a practice run using the Consep Tangential Flow Filtration module and a Setec peristaltic pump. The sample water was a composite of Cell 4 inflow (volume-weighted equally from surface waters collected at culverts A, F, I). We selected polycarbonate filters (Osmonics) with pore sizes equal to the size fractions (0.40 and 0.05 μm) we believed would show the greatest differences in enzyme hydrolysis and SRP releases under low pH and redox conditions. A diagram of the sequential filtration procedure is shown in Figure 2.68. During the practice run, we familiarized ourselves with assembly and disassembly of the filter unit, operating conditions (i.e., pump speed and pressures across and through the membrane filter), and the times required to achieve a reasonable concentration factor (3 – 5X) for a given volume of raw water.

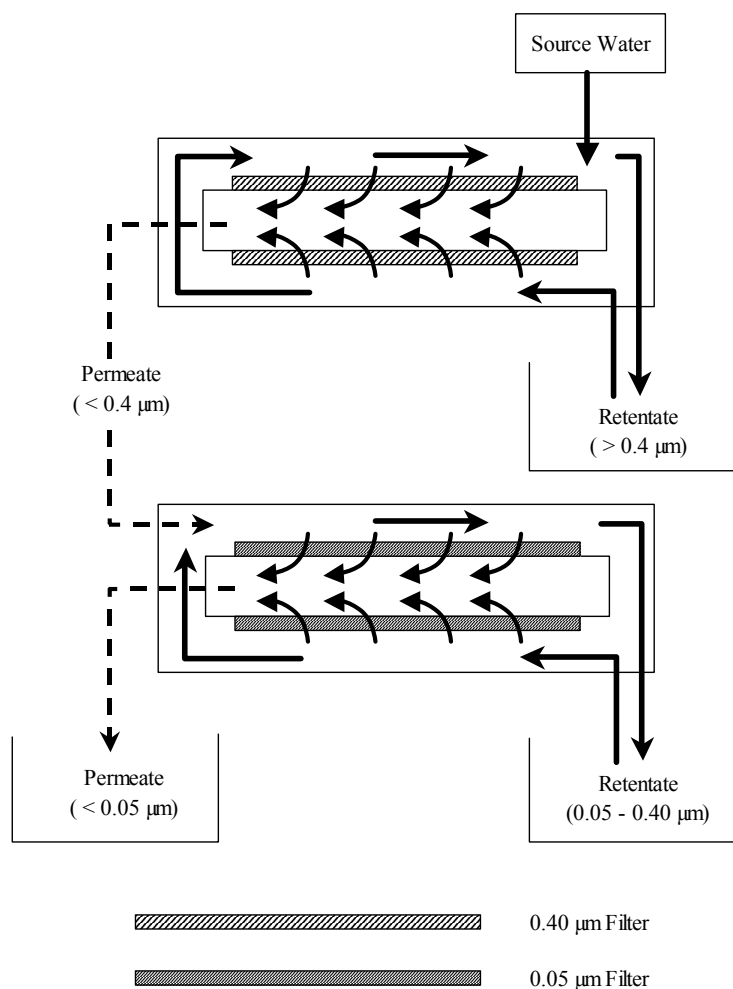


Figure 2.68. Sequential tangential-flow filtration procedure used in particle concentration of Cell 4 inflow water according to size ranges of 0.05 µm to 0.40 µm.

2.12.2 Particulate Phosphorus Characterization in the Inflows and Outflows of Test Cells and Cell 4.

Introduction

Under a subcontract to Dr. Willie Harris of the Soil and Water Science Department at the University of Florida, inflow and outflow particles from two of the test cells (NTC-1 and NTC-5) and Cell 4 were characterized. The objective was to compare the inflow and outflow particles according to their particle size, surface charge, and elemental and mineral composition. Changes in these properties upon passage through wetlands dominated by SAV and cattail communities indicate how wetlands process P-associated particulates. Separation of the particles into various size fractions was performed using tangential flow filtration (TFF).

Methods:

1. Sample collection, handling, and characterization

Water from the outflow and inflow of Cell 4 of STA-1W was sampled in 20-L plastic containers over the period 8/2/00 - 8/3/00. Twenty-L samples were also collected at the outflows of NTC-5 (cattail treatment) and NTC-1 (SAV treatment), and at the inflow of NTC-1. The 20-L samples were used to concentrate particulates using tangential flow filtration (TFF). Twenty-one additional samples were collected in plastic 4-L containers over the same time period for the purpose of replication at the Cell 4 inflow and outflow and at the Cell 2 outflow (which enters into Cell 4). Half (11) of the latter samples were inadvertently contaminated by traces of talc, which was later revealed by x-ray diffraction, and were not included in the evaluation. Another sampling using 4-L containers was conducted on 9/8/00. This latter sampling included 12 Cell 4 outflow samples, 6 Cell 4 inflow region samples, and 6 Cell 2 outflow samples. The source of the talc on the first sampling, a coarse screen used to remove floating debris, was eliminated on the second sampling. The same compositional trends were observed for both sampling periods, though higher concentrations of particulates and phosphorus were measured for the second sampling.

All sample containers were pre-washed with distilled de-ionized water. Containers for aliquots of samples to be used for TP, TSP, and SRP determinations were pre-washed with dilute HCl and rinsed with distilled de-ionized water. Stagnant areas near the shore or near culverts were avoided, as necessary, using a sampling extension tube and pump. Water was pulled through flexible tubing by the pump directly into containers. The tubing and containers were rinsed twice with the water at the sampling site prior to collecting each sample. Samples were maintained under cold (ice or refrigerator) and suppressed-light conditions prior to, during, and subsequent to the filtration processing as described below.

2. Particle concentration

Particles were concentrated into a slurry using TFF, which permits the processing of large volumes of water. Samples were filtered through two cassettes, each of which was fitted with two 0.40 μm polysulfonate filters, until volume reductions of approximately 15-fold (e.g., from

15 L to about 1 L) were achieved. The system was operated at the maximum cross flow velocity and minimum trans-membrane pressure, in order to minimize buildup of particles on the filters. Nevertheless, some material was observed on the filter, and particulate concentrations were not calculated from TFF concentrates. Instead, they were determined from dead-end filtration on replicated aliquots of the water samples.

Particles in the 4-L replication samples (35 total) were collected via "dead-end" filtration, using 0.45-micrometer filters. Retentate was removed from the filters and transferred to a glass slide while still moist, using a rubber policeman. The material was scraped from the glass slide onto weighing paper after it had air-dried, and then stored in vials at 4°C in the dark until analyzed.

3. Particle size and surface charge analyses

Particle size and surface charge characteristics, which relate to dispersibility and transport potential of particles, were conducted on each sample at the University of Florida Engineering Research Center (ERC).

Particle size was determined using light scattering technology (Weiss and Frock 1976). This is a well-established approach which exploits the relationship between particle size and the intensity, polarization, and angular distribution of light scattered from particles dispersed in a liquid medium (van de Hurst 1981). The instrument used was the Beckman Coulter LS 230 Enhanced Laser Diffraction Analyzer (Beckman Coulter, Inc, 1950 W. 8th Ave., Hialeah, FL). This instrument is reported to discriminate in the 0.04 - 2000 μm particle size range. (The original plan of work specified that particle size analysis would be conducted using electroacoustic analysis, but preliminary assessment of the sample indicated that light scattering would be more applicable given the dilute nature of the sample suspensions being analyzed.)

Surface charge of particles was determined by electrophoretic light scattering, which entails assessment of doppler shifting in relation to a reference beam (Thompson 1992). The instrument used is the Model "Zeta Plus" Zeta Potential Analyzer (Brookhaven Instrument Corporation, 750 Bluepoint Road, Holtsville, NY). This instrument is reported to be suitable for particles with the size range of 0.005 to 30 μm .

4. Micro-morphological and elemental analyses

Morphology of particles was assessed using a scanning electron microscope (SEM) located at the Major Analytical Instrument Cooperative (Materials Engineering Department). Secondary electron images were obtained at various magnifications. Care was taken for the replicated samples to collect at least one image at a standard magnification for each sample. In addition, elemental spectra were generated from individual particles and from masses of particles using energy-dispersive x-ray fluorescence analysis, which is an accessory capability of the SEM instrumentation. Elemental spectra of selected thermogravimetry (TG) residues were also obtained in order to confirm that silicon, calcium, and oxygen comprised the bulk of the residues. Elemental dot maps relating concentrations of P, Si, Ca, S, Cl and Fe to discrete particles within the field of view of the image were generated.

5. Mineralogical analysis

Mineralogical analyses were conducted at the Soil Mineralogy Laboratory (Soil and Water Science Department). Bulk mineralogy of the suspended material was determined by x-ray diffraction (Whittig and Allardice 1986) and thermal analysis (Karathanasis and Harris 1994). Mineralogy was determined on the residue after selective dissolution of carbonates and organic matter, and on magnetic separates collected using the High Gradient Magnetic Separation (HGMS) system. The intent was to evaluate the possibility that discrete calcium phosphate or iron phosphate phases are forming, as opposed to sorption of phosphate on calcium carbonate.

a. X-ray diffraction

Crystalline components in samples were analyzed by x-ray powder diffraction (Whittig and Allardice 1986). Samples were mounted as a powder on specially cut quartz crystals that minimize background x-ray scattering (noise). Samples were scanned from 2 to 40 degrees 2 θ (or higher if necessary) under Cu K α radiation, using a computer-controlled x-ray diffractometer equipped with stepping motor and graphite crystal monochromator. Minerals were identified from diffraction peaks using reference diffraction data of minerals compiled by the International Center for Diffraction Data (1601 Park, Lane, Swarthmore, PA 19081) (Bayliss et al. 1980).

b. Thermal analysis

Solids were analyzed by thermogravimetry (TG), which is a technique in which the mass of a substance is monitored as a function of temperature or time as the sample is subjected to a controlled temperature program (Earnest 1988). Mass loss or gain as the sample is heated can be used diagnostically to corroborate the presence of solid phases present in the sample, and in some cases (e.g., calcite) to quantify a phase based on the stoichiometry of the reaction (Karathanasis and Harris 1994). The TG analyses were conducted using a computer controlled thermal analysis system, which collects and stores data digitally and permits computer calculations of reaction weight losses. The percentage of organic matter was estimated to be the loss upon ignition. Calcium carbonate content was calculated based upon CO₂ evolution that began between 670-700 °C. 'Silica' content was calculated by subtracting the weight of CaO in the TG residue from the total residue weight.

6. Chemical analysis

Characterization on aliquots of each sample prior to and following TFF concentration included pH, electrical conductivity (EC), total solids, total P (TP), total soluble phosphorus (TSP), soluble reactive P (SRP), total C (TC), and inorganic C (IC). Phosphorus analyses for the TFF samples were performed by DB Environmental (DBE); P analyses for the replicated samples were performed both by DBE and UF in August, and exclusively by UF in September. There were three replicates per location in the sampling scheme. Determinations of pH and EC were made using standard laboratory meters. Descriptions of other chemical methods are given below.

a. Total solids

Methods used to determine total and suspended solids deviated from U.S. E.P.A. (1979) method 160.1-160.2 because solids in water samples were significantly lower than the practical range of determination for these methods. Total solids determinations were performed in triplicate. Five-ml aliquots of homogenized water samples were pipeted into desiccated pre-weighed aluminum weighing dishes. Samples were dried at 40 °C and placed in a desiccator for approximately 48 hours. The weighing dishes were then re-weighed, and total solids were

quantified via subtraction. For suspended solids determinations, 450 ml aliquots of homogenized water samples were filtered through pre-washed 0.40 μm filters. Material retained by the filter was then washed with three 15-ml aliquots of distilled de-ionized water. Filters were dried at 40 °C and placed in a desiccator for approximately 48 hours. Filters were then re-hydrated with distilled de-ionized water. Material was removed and allowed to dry under laboratory conditions. Removal of material from filters was performed on two consecutive days, and the relative humidity as measured by a 'relative humidity meter' was stable over this period.

b. TP and TSP

Aliquots of water samples used for TSP determinations were filtered using 0.45 μm PES syringe filters within 6 hours of sample collection. Both TP and TSP samples were preserved with H_2SO_4 and iced on 8/2-8/3. Samples were refrigerated until digested. Samples were digested in an autoclave on 8/9 and quantified colorimetrically according to U.S. E.P.A. (1979) Method 365.2. PP was calculated by subtraction ($\text{TP} - \text{TSP} = \text{PP}$). QA/QC protocols followed included the digestion of replicate samples and matrix spikes as well as an external organic P standard.

c. SRP

Aliquots of water samples used for SRP determinations were filtered and immediately iced. Samples were kept at approximately 4 °C prior to determination. SRP was quantified on 8/7 according to EPA (1979) Method 365.2.

d. TC and IC

TC and IC of the TFF filtrate and retentate, and the filtrate and raw water of the replicated samples, were determined on 8/11 and 8/19 using a total carbon analyzer. Samples used for C determinations were refrigerated and kept dark prior to analysis. TC and IC analyses were based upon the pyrolysis of C compounds and the analysis of liberated CO_2 by infrared spectrophotometry. QA/QC protocols followed included the analysis of replicate samples and matrix spikes. TOC was calculated by subtraction ($\text{TC} - \text{IC} = \text{TOC}$).

Results and Discussion

1. North Test Cells

Calcite was present in the inflow water to NTC-1 (dominated by SAV) and the outflow waters from NTC-1 and the cattail dominated NTC-5 (Figure 2.69). Kaolinite was present in the NTC-1 outflow particulates, which may have been caused by a resuspension of the bottom muck layers by a population of small alligators. The absence of prominent peaks suggest that most of this material is noncrystalline. Elemental spectra (EDX) indicate higher S in the particles in NTC-5 outflow compared to either the inflow or outflow of NTC-1. NTC-1 outflow has higher aluminum than any other sample, which is consistent with the presence of kaolinite detected by XRD. Results of thermal gravimetric (TG) analysis show that organic matter is the most abundant particulate matter in all the samples (see Figure 2.70 for an example of a TG weight loss curve for particles collected from Cell 4).

2. Cell 4

The dominant suspended particulate components in STA-1W Cell 4 water samples were organic matter, silica, and calcium carbonate (Figure 2.70). Although calcite was present in all samples, it was most abundant in Cell 4 outflow particulates (Figure 2.69). Algae (including diatoms) appear to comprise a substantial portion of the sample, based on optical and SEM observations (Figure 2.71). Most of the silica was probably derived from diatoms (Figure 2.72). This assessment did not involve a quantitative assessment of algae, or the relative contributions among algae, bacteria, fungi, and detritus to the organic matter pool. SEM analyses (Figure 2.72) support a direct association between suspended solids and particulate P, and between particulate organic matter and particulate P (Figure 2.73), but an association between CaCO_3 and particulate P did not exist (Figure 2.74).

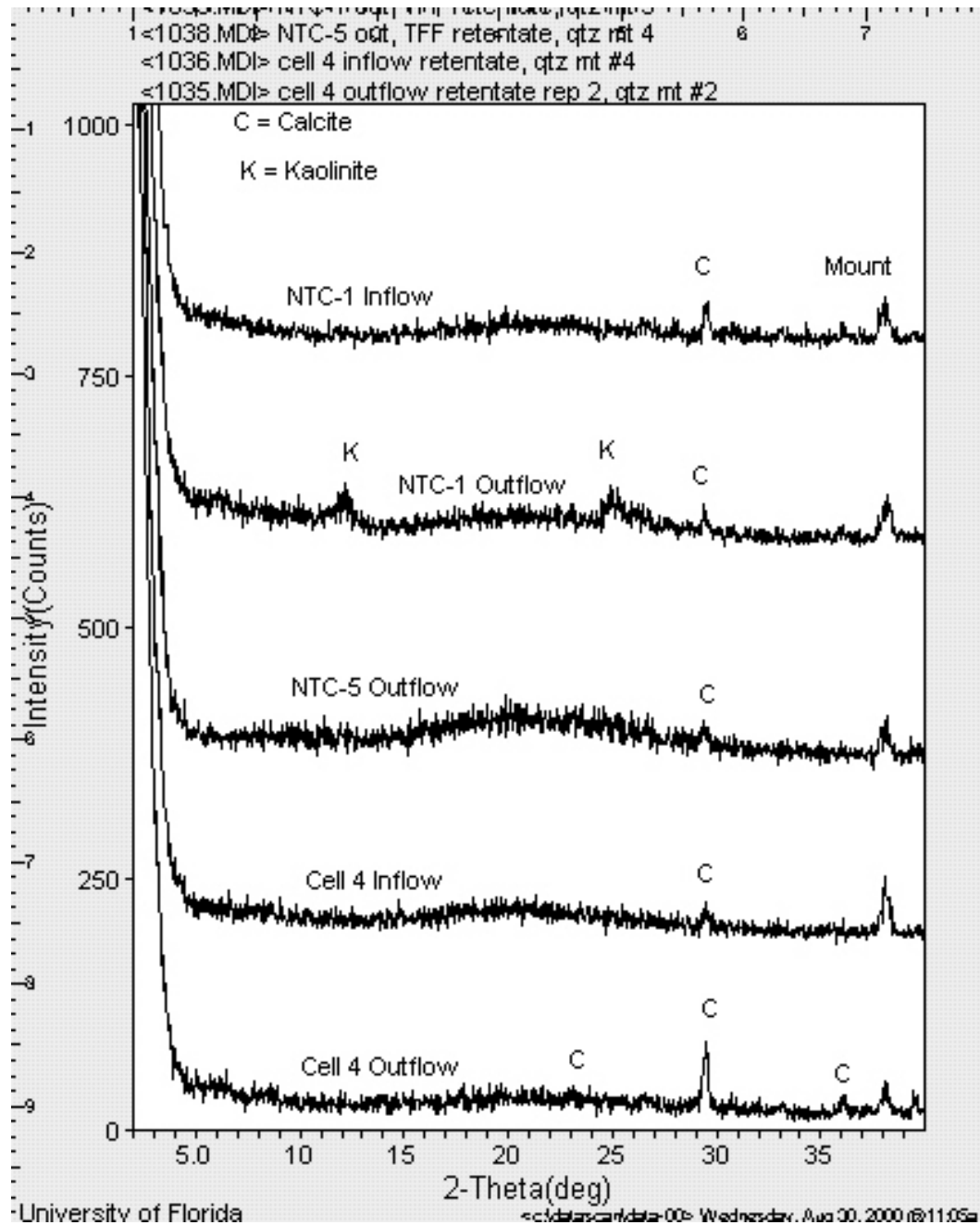


Figure 2.69. X-ray diffraction (XRD) patterns of TFF-concentrated particulates from Cell 4 and test cells.

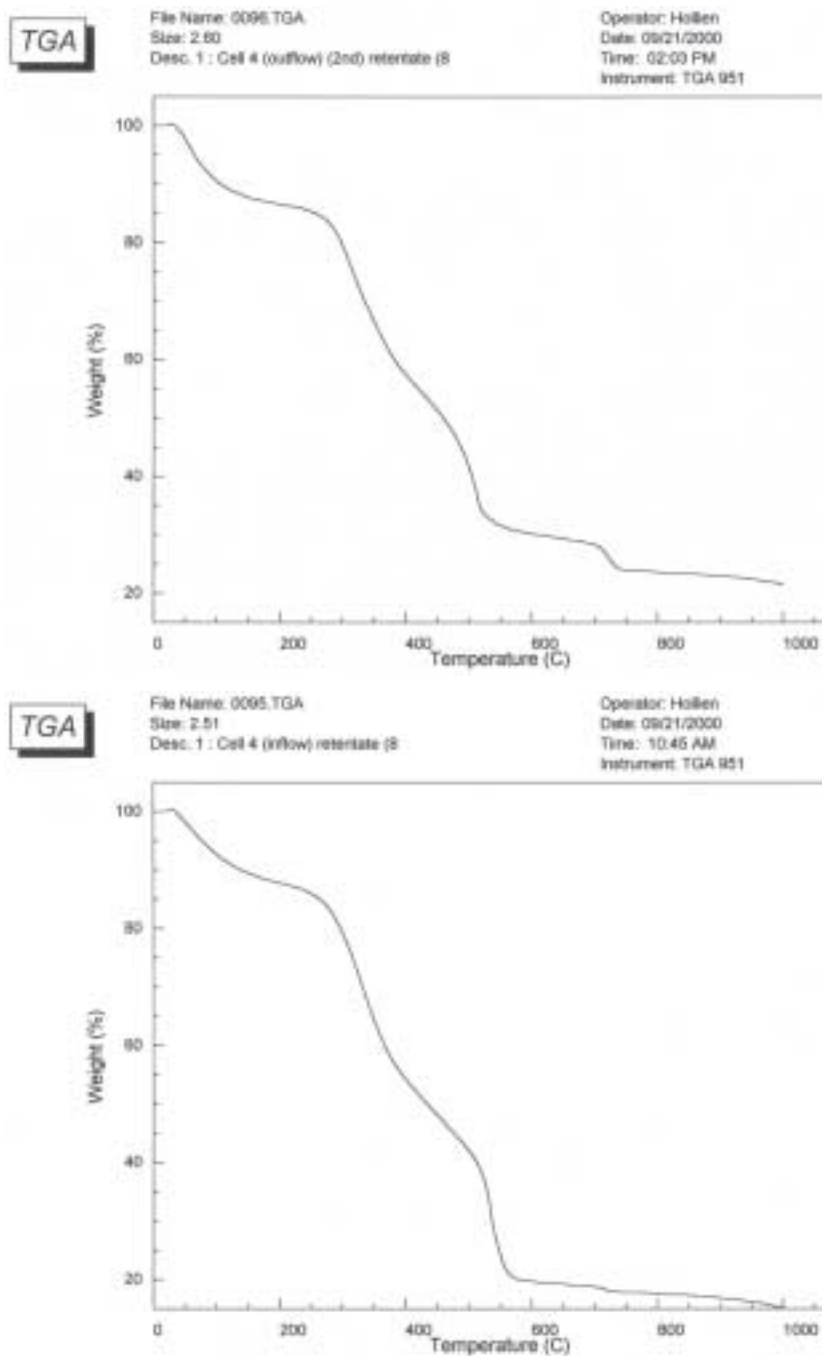


Figure 2.70. Thermal gravimetric weight loss curves for particulates collected from Cell 4 outflow (top) and inflow region (bottom), shown as examples. Weight loss in the range of about 325 to 550° C is attributed to organic matter combustion (CO₂ “loss on ignition”), and in the range of about 700-750° C, to conversion of calcite (CaCO₃) to CaO (CO₂ loss).

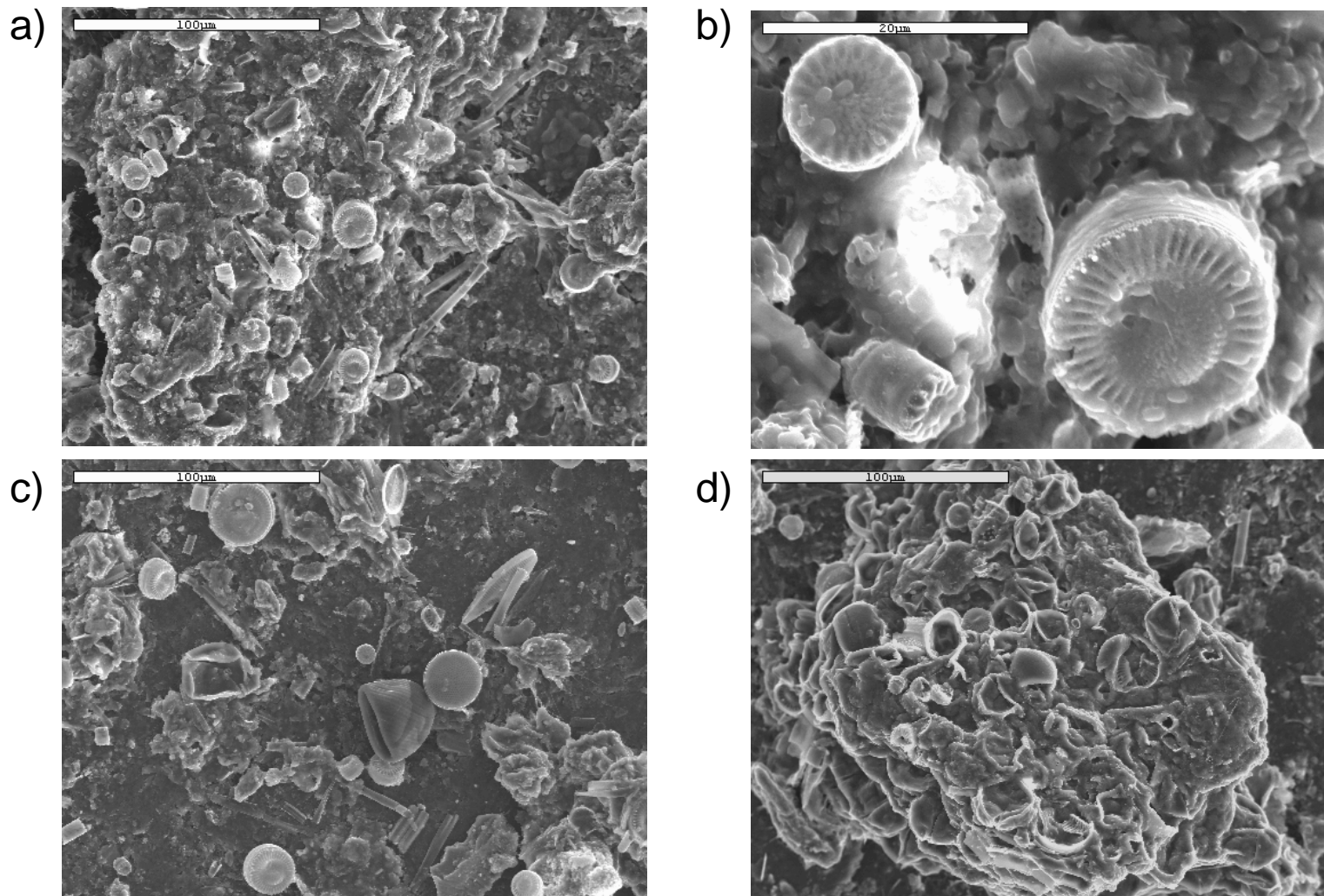


Figure 2.71. Algal abundance illustrated in four-image composite of SEM micrographs (clockwise from upper left) a) centric diatoms present in suspended solids from Cell 2 outflow in the September sample magnified 500x; b) diatoms from "a)" magnified 2700x; c) C-based algal 'cells' from Cell 2 outflow in the August sample; d) C- based cells and both centric and pinnate diatoms present in Cell 4 inflow region during September.

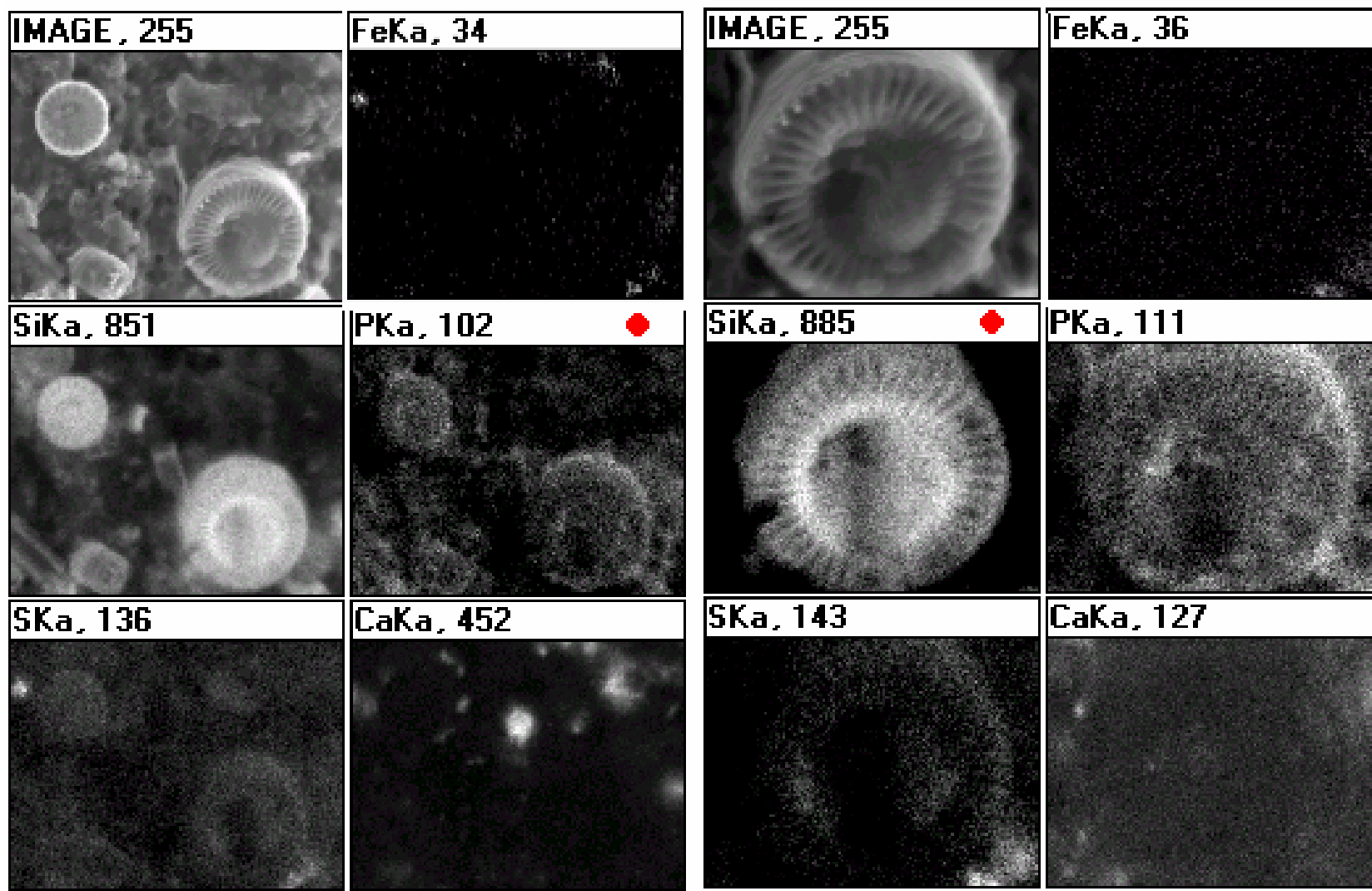


Figure 2.72. Two six-image composites of SEM micrographs. a) Left composite: At upper left is the same secondary electron image shown in Figure 24b. Other images are elemental dot maps of Fe, Si, P, S, and Ca, showing an association of Si and P with diatoms. b) Right composite: At upper left is a higher magnification image of the largest diatom shown in the right composite. This composite illustrates that whereas both Si and P are both associated with the diatom, they don't show strong spatial association with each other within the diatom.

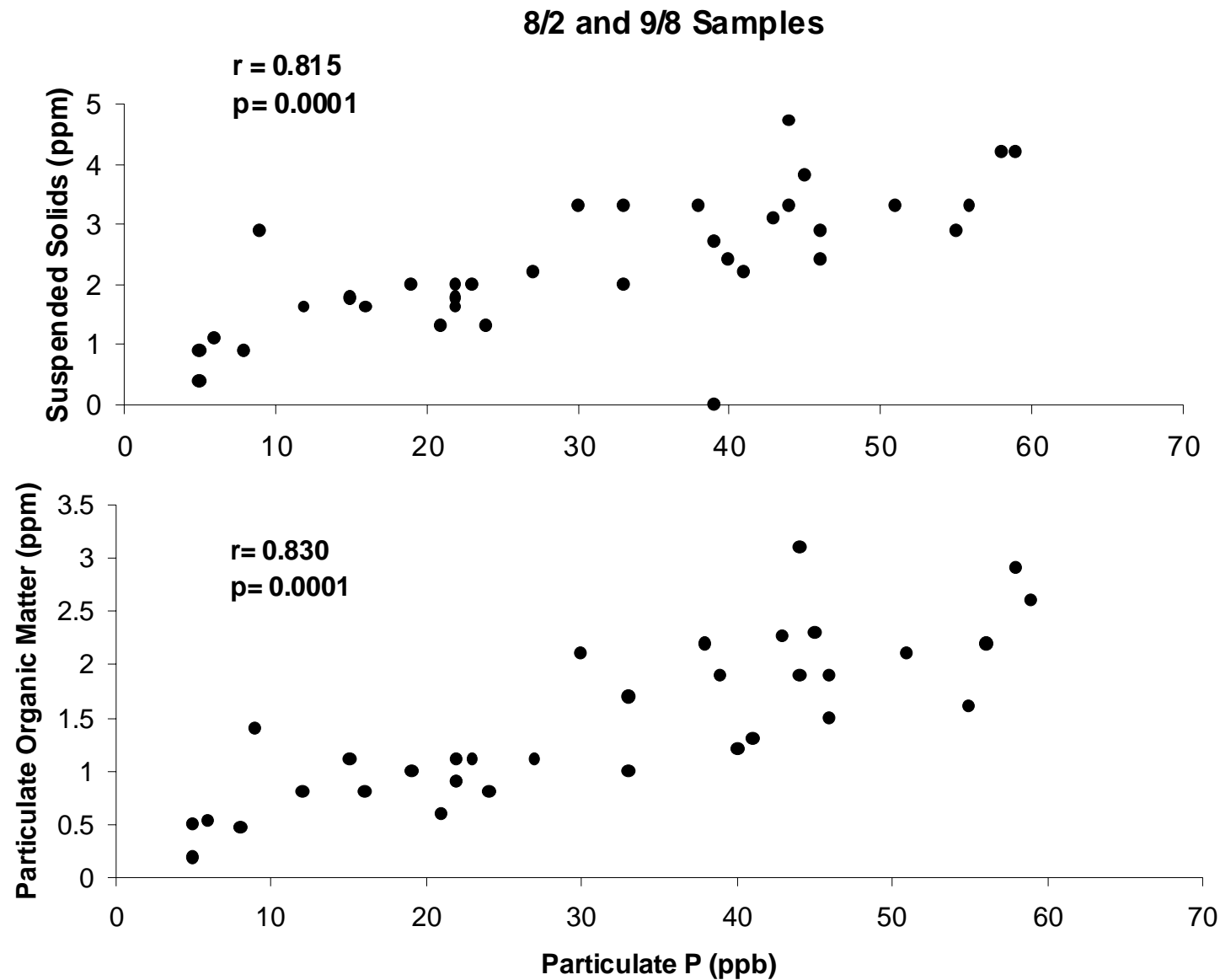


Figure 2.73. Scatter plots of particulate P with particulate organic matter and suspended solids for Cell 4 inflow and outflow waters.

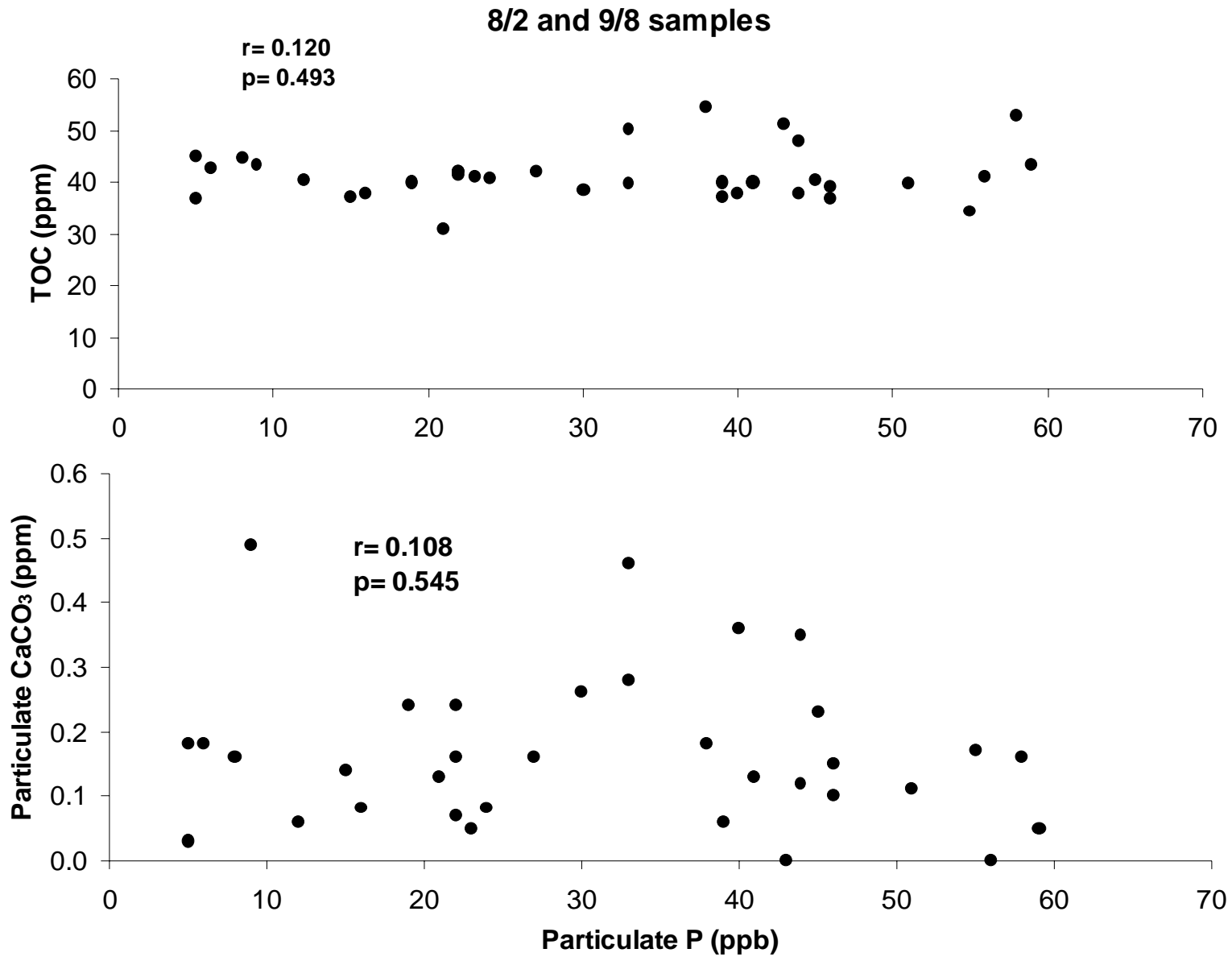


Figure 2.74. Scatter plots of particulate P with particulate CaCO_3 and particulate organic matter for Cell 4 inflow and outflow waters.

2.12.3 Alterations in pH/Redox Potential and Phosphatase Enzyme Concentrations on the Mobilization of Phosphorus in Different Size Classes of Particles of Cell 4 Surface Waters

The evaluation of the potential hydrolysis and mineralization of organic P in Cell 4 may provide useful information for optimizing the removal of P and determination of the ecological significance of the released water to the Everglades. Therefore, this assessment was conducted to determine the potential (1) alkaline phosphatase (APase)- and phosphodiesterase (PDEase)-induced hydrolysis of organic P, and (2) mineralization of P under different redox and pH conditions in the inflow and the outflow waters of Cell 4.

Materials And Methods

Sample Collection

A sequential tangential-flow filtration procedure was used on the initial unfiltered inflow and outflow waters from the Cell 4 of the STA-1 West to obtain >0.4, 0.4 - 0.05, and <0.05 μm sized particulate suspensions (Figure 2.68). Size ranges were selected based on ecological relevance and practical considerations. The concentration factors for both 0.4 and 0.05 μm filter retentates of the inflow waters were 6.0 times each. For the outflow waters, the concentration factors were 6.2 and 7.3 for the 0.4 and 0.05 μm filter retentates, respectively. The phosphorus concentrations and pH values for each size fraction as well as the unfiltered water samples are given in Table 2.30.

Table 2.30. Phosphorus concentrations and pH of unfiltered and particle size-fractionated inflow and outflow waters of Cell 4.

Sample source	Sample ID	pH	Total P ($\mu\text{g/L}$)	Soluble reactive P ($\mu\text{g/L}$)	Organic P* ($\mu\text{g/L}$)
<i>Inflow</i>					
	Unfiltered water	8.1	83	7	76
	0.4 μm retentate	8.1	302	17	286
	0.05 μm retentate	8.2	54	6	48
	0.05 μm permeate	8.2	71	2	69
<i>Outflow</i>					
	Unfiltered water	8.1	25	<2	25
	0.4 μm retentate	8.2	104	5	99
	0.05 μm retentate	8.2	31	5	31
	0.05 μm permeate	8.2	6	<2	6

*: Determined by subtracting soluble reactive P from total P.

Enzyme Incubation

Alkaline phosphatase and PDEase, obtained from Sigma-Aldrich Co., USA, were evaluated for their capacity to hydrolyze organic P in the fractionated outflow and inflow waters. The APase (Type VII-T) was prepared from bovine intestinal mucosa suspended in 3.0 M NaCl containing 1 mM MgCl_2 and 0.1 mM ZnCl_2 and 30 mM triethanolamine at pH 7.6. It had 2,000-4,000 units activity per mg enzyme protein and 1 unit hydrolyzed 1.0 μmole of p-nitrophenyl phosphate per min at pH 9.8 at 37°C. The PDEase was prepared from *Crotalus adamanteus* venom, and is a lyophilized powder containing approximately 35% tris buffer salts with 0.2-0.4 unit activity per mg solid at pH 8.8 at 37°C; one unit hydrolyzed 1.0 μmole of bis(p-nitrophenyl) phosphate per min at pH 8.8 at 37°C.

Unless otherwise stated, all the buffer solutions were prepared from tris-HCl. All the enzymes were prepared in pH 8.0 buffer an hour before the assessment was carried out. The PDEase solution contained 0.5 unit enzyme activity mL^{-1} . Similarly, APase containing 5 units enzyme activity mL^{-1} was prepared in pH 7.5, 8.0 and 9.0 buffers. Because of the high SRP measured in the PDEase, it was dialyzed against pH 8.0 buffer to remove background SRP for 10 h at 4°C, prior to assaying the Cell 4 waters (Pant et al. 1994).

To inhibit microbial activities during the incubation, 50 μL of 5.2% sodium azide (NaN_3) solution was added to the 10 mL triplicate samples (unfiltered inflow and outflow waters, 0.4 μm retentate, and retentate and permeate of the 0.05 μm filter) to yield a final concentration of 4 mmol L^{-1} . Thereafter, 1 mL of enzyme solutions (APase and PDEase) in the pH 8.0 buffer were added to each vial separately, and incubated for 6 h at 25°C. The activity of each enzyme required during the incubations was pre-determined by measuring the organic P concentration in the samples, and then adding the sufficient amount of enzymes. For the controls, 10 mL samples were spiked with 50 μL NaN_3 and 1 mL buffer (pH 8.0), and incubated for 6 h at 25°C. To determine the chemical hydrolysis of organic P by buffer (pH 8.0) and the NaN_3 separately and in combination, 10 mL samples were spiked with 50 μL NaN_3 and 1 mL deionized water, and with 1.05 mL deionized water only, and incubated for 6 h at 25°C.

For the Cell 4 outflow water only, the samples (unfiltered water, 0.4 μm filter retentate, and retentate and permeate of 0.05 μm filter) were also incubated at pH 7.5 and 9.0 to determine if organic P hydrolysis by APase at different pH values affected the bioavailability. Control evaluations were also performed at the same pH values.

The amount of enzyme-hydrolyzed organic P during the 6-hour incubation was calculated by subtracting SRP measured in the sample incubated without enzymes from the sample incubated with enzymes. This represented the potentially hydrolyzable amount of organic P in the samples.

Incubations for Mineralization at Different Redox and pH

Four hundred ml of each size fraction (unfiltered water, 0.4 μm filter retentate, and retentate and permeate of 0.05 μm filter) of inflow and outflow surface waters were placed in duplicate reactors and incubated in the dark with frequent stirring on a magnetic stirrer for 30 days at 25 \pm 2°C. The pH and Eh treatments of the incubated water samples are provided in Table 2.31. An aliquot of 25 ml water was sampled to measure SRP and pH levels in the waters at 0 and 8 h, and 1, 2, 4, 10, 20 and 30 days intervals. A similar set of samples (control) was also incubated as described above, but no attempt was made to adjust pH so that mineralization of P at ambient pH of the water (\sim 8.5) could be determined. However, air was bubbled frequently through the

controls to maintain aerobic conditions, and the changes in pH as well as in SRP concentration were measured.

Table 2.31. The pH and Eh values of Cell 4 unfiltered and size- fractioned inflow and outflow waters incubated under different environmental conditions.

Sample source	Incubation condition	pH	Eh
<i>Inflow water</i>	Air only	8.3±0.2	231±31
	Air + CO ₂	7.4±0.1	225±26
	CO ₂ + N ₂	7.4±0.1	-33±125
	N ₂ only	9.2±0.2	-62±100
<i>Outflow water</i>	Air only	8.7±0.4	246±20
	Air + CO ₂	7.5±0.3	267±16
	CO ₂ + N ₂	7.6±0.4	-27±143
	N ₂ only	9.1±0.4	-25±174

A similar set of evaluations was also conducted under anoxic conditions by bubbling N₂ + 0.3% CO₂ intermittently, and the pH of the suspension was maintained near neutrality (~7.5). An aliquot (25 mL) of water was sampled for pH and SRP determinations at 0 and 8 h, and 1, 2, 4, 10, 20 and 30 d intervals. As a control, N₂ only was bubbled instead of N₂ + 0.3% CO₂, and the pH of the suspension was maintained at ~9.

For both the pH and redox treatments, and the controls, the potential mineralization rate of organic P was calculated by plotting the SRP release in the water vs. time. The measured SRP in the water represented the increase in the concentrations over the period of incubations. The cumulative SRP released over the 30-day incubation period divided by total organic P present in the sample provided the potentially mineralizable fraction of the organic P under the incubation conditions.

Phosphorus Analysis

Soluble reactive P in all the samples was determined using an automated ascorbic acid method (Method, 365.1, USEPA 1979). Total P in the water samples and the sediment extracts were also determined by the above method after persulfate digestion (Method, 365.1 USEPA, 1979). The difference between TP and SRP, occasionally referred to as unreactive P, is considered as

organic P in this evaluation. Unless otherwise stated, all the assessments were performed in triplicates, and the data analyzed by two-way ANOVA using SAS (SAS Institute Inc. 1996). The mean comparisons were done by Least Significant Difference (LSD) at $p < 0.05$ level.

Results And Discussion

Enzymatic Hydrolysis

After dialysis, the background SRP concentration of the commercially prepared PDEase was reduced to less than 1 $\mu\text{g/L}$ from its initial 129 $\mu\text{g/L}$. Based on the control incubations, chemical hydrolysis of organic P in the inflow and outflow waters was not attributable to effects from the buffer or sodium azide (NaN_3) that were used in the incubation of size-fractionated surface waters with the enzymes.

Alkaline phosphatase did not hydrolyze more than 10% of the total organic P in the unfiltered inflow water, while PDEase hydrolyzed 71% of the total organic P (Figure 2.75). A maximum hydrolysis by PDEase of only 27% of the organic P in the 0.4 μm retentate may suggest that relatively stable (i.e., unhydrolyzable) organic P compounds and particles are mainly associated with particulates $>0.4\mu\text{m}$ diameter. APase did not hydrolyze organic P in the 0.05 μm retentate and permeate of inflow water, whereas PDEase hydrolyzed the P completely. This may indicate the lack of monoesterase-hydrolyzable P and the domination of diesterase-hydrolyzable P in the retentate and permeate from the 0.05 μm filter. Since Cell 4 is a polishing cell (receiving partially treated agricultural drainage waters), the low APase induced hydrolysis of the organic P in the inflow indicates that more labile P compounds may have been hydrolyzed in the treatment cell (Cell 2) upstream of Cell 4, leaving only relatively stable P compounds entering Cell 4. The amount (76 $\mu\text{g L}^{-1}$) and the potential hydrolysis (71% by PDEase) of organic P in the unfiltered water from the inflow to Cell 4 indicate that the polishing cell could play a crucial role in removing P from the drainage water prior to its release to the Everglades.

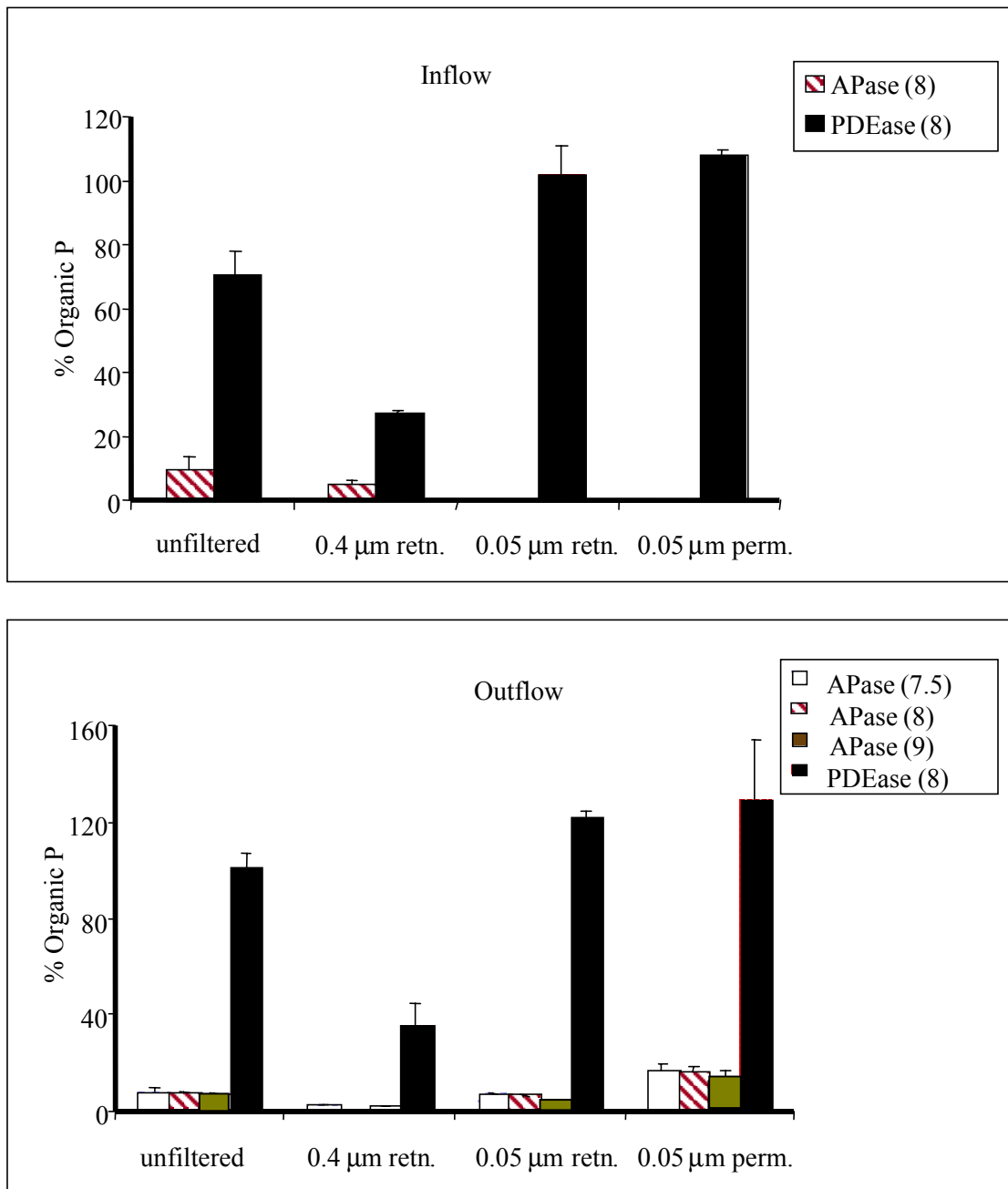


Figure 2.75. Enzymatic hydrolysis of organic P in waters of Cell 4 of STA-1W. The numbers in parentheses indicate the pH of the enzyme incubations. retn. = retentate, and perm. = permeate.

Overall, organic P hydrolysis in the unfiltered outflow water by APase was about 8% of the total organic P (Figure 2.75). Although we did not further investigate the inability of APase to hydrolyze organic P in the unfiltered water of both inflow and outflow, we believe the most likely reason is the lack of monoester P, which is the substrate for APase. The effect of pH (7.5, 8.0 and 9.0) was not apparent in the hydrolysis of organic P by APase, probably due to the overall low availability of a suitable substrate

The complete hydrolysis of organic P in unfiltered, 0.05 μm retentate, and 0.05 μm permeate of outflow water by PDEase mimics the results for the inflow water (Figure 2.75), indicating the organic P in both waters were dominated by diesterase-hydrolyzable compounds. As in the inflow water, only 35% of the organic P found in the 0.4 μm outflow retentate was hydrolyzed by PDEase. Considering the extent of the hydrolysis of organic P in unfiltered and <0.4 μm permeate outflow water, the substantial reductions in the P hydrolysis by PDEase that occurred in 0.4 μm retentate from both the inflow and outflow appear to be related to particle size. Particles greater than 0.4 μm in Cell 4 inflow and outflow waters include detritus and algae (Harris and Farve 2001), which in themselves are not directly accessible to the enzymes. Moreover, an increase in the concentrations of inhibitory species including SRP (Table 2.30) could suppress the enzyme activities (Rai et al. 1998; Kang and Freeman 1999).

This assessment indicates that although 68% of the organic P had been removed within Cell 4 (from 76 to 25 $\mu\text{g TP L}^{-1}$), the majority of which was probably from settling and decomposition of particulate P, the remaining 33% (25 $\mu\text{g/L}$) is potentially hydrolyzable. The complete hydrolysis of both the retentate and permeate of the 0.05 μm filter of the inflow and outflow surface waters by PDEase may suggest the domination of highly soluble diesterase-hydrolyzable P components. However, the 25 $\mu\text{g L}^{-1}$ of organic P in the unfiltered outflow water, which was entirely susceptible to PDEase, suggests a lack of the appropriate enzymes in high enough concentrations in Cell 4 to totally hydrolyze the DOP.

Mineralization at Different Redox and pH

Under anaerobic high pH (~9.2) conditions, overall organic P mineralization was low ($\leq 10\%$ of total organic P) in all fractions of the inflow waters, though the mineralization was substantial in the incubated outflow waters (Figure 2.76). The elevated pH (~9) could have led to an increase in precipitation of Ca-P (Stevenson 1986) in the outflow water, and a decrease in microbial activities (Kuehn et al. 2000). Under aerobic ambient pH (8.3) conditions, the P mineralization was low ($\leq 9\%$ of the total organic P) in the unfiltered inflow and outflow waters, 0.05 μm retentate, and 0.05 μm permeate of the inflow, but was 39% of the total organic P in 0.4 μm retentate. This suggests that P associated with particulates $>0.4 \mu\text{m}$ is relatively unstable compared to the smaller size fractions, including the permeate of the 0.05 μm filter (dissolved P). The likely reason is the nature of the particles in this size fraction, which for Cell 4 consist mainly of detritus and algae (Harris and Farve 2001), that are susceptible to microbial decomposition (Stevenson 1986; Correll 1998).

A higher cumulative P mineralization was expected at pH 7.4 under aerobic than anaerobic incubations because of the expected higher microbial activity under aerobic conditions (Pettersen 1980; Newman and Reddy 1993). However, no significant differences were found between aerobic and anaerobic incubations at pH 7.4 in either type of source water (Figure 2.76). Both conditions (air + CO_2 , and N_2 + CO_2) yielded a similar pH (~7.5) as well as percentage of P mineralization. This may indicate that pH and/or anaerobic respiration were more important than aerobic respiration in affecting the P mineralization in these water samples, which is supported by the data collected for the higher pH and anaerobic treatments.

An overall higher percent of organic P mineralization occurred in 0.4 μm retentate than the other size fractions for both in inflow and outflow waters (Figure 2.76). This suggests that P associated with particulates $>0.4 \mu\text{m}$ is not as stable as the P associated with smaller size fractions, in contrast to the findings of enzymatic hydrolysis assessments. The discrepancy between the mineralization and enzymatic hydrolysis of P associated with particulate $>0.4 \mu\text{m}$ may have been due to the supply of the energy sources to bacterial communities. According to carbon (C) limitation theory (Currie and Kalff, 1984a, b, c), the supply of C apparently controls the bacterial mineralization of organic P, especially in C limited systems. Since C is likely to be

more abundant in particulate than dissolved fractions, the consequent preferential utilization of particulates by bacteria induces P mineralization.

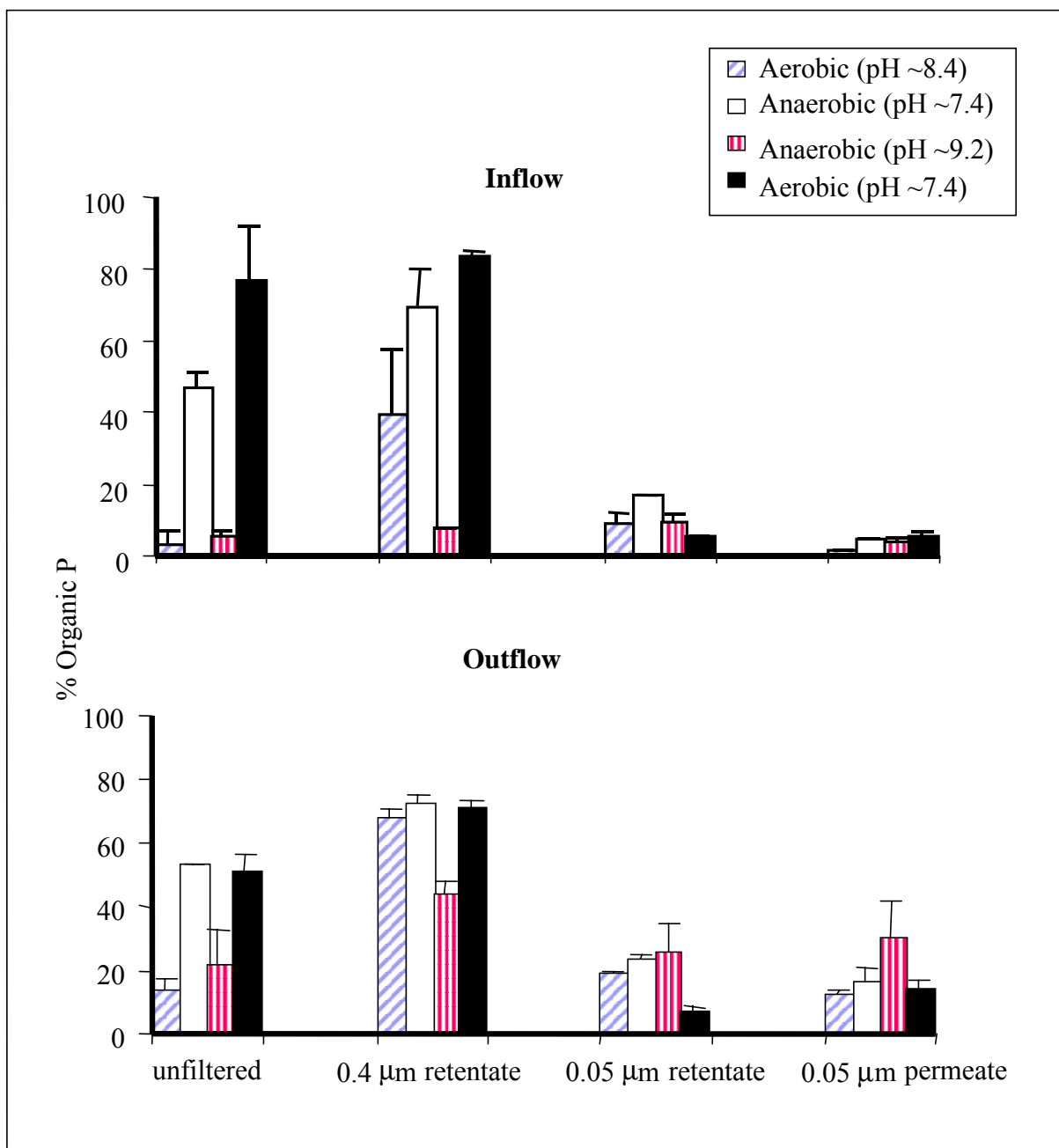


Figure 2.76. Cumulative P mineralization in waters of Cell 4 of STA-1 West under different redox and pH conditions during 30 days of incubation.

For the unfiltered inflow and outflow waters and their 0.4 μm retentates, the cumulative organic P mineralization under aerobic or anaerobic conditions maintained at pH around neutral (~ 7.4) was significantly higher compared to the mineralization under aerobic or anaerobic conditions that were maintained at higher pH conditions (ambient, ~ 8.4 and anaerobic, ~ 9.2) (Figure 2.76). No significant differences in the cumulative P mineralization were observed in 0.05 μm permeates of the inflow and outflow waters under any treatment conditions, probably because of the very low average mineralization rates ($< 0.4 \mu\text{g L}^{-1} \text{ day}^{-1}$).

In general, the 24-hour (potential) P mineralization rates were significantly greater than the 30-day (average) P mineralization rates both in the inflow and outflow waters (Table 2.32), indicating readily degradable P compounds were a more significant factor in the shorter incubation period. Considering the average hydraulic retention time of 4 days for Cell 4, then the *in situ* mineralization rates would lie somewhere between those reported for the 24-hour and 30-day incubations. Of course, these laboratory derived rates do not include the dissolved or particulate P that are being supplied by external inputs (dry deposition; inflow water) or recycled from the plants and sediment within Cell 4.

Conclusions

This assessment highlighted the importance of particle size classes in accounting for hydrolysis and mineralization of organic P in Cell 4. Larger particles ($> 0.4 \mu\text{m}$) were more amenable to bacterial mineralization than they were to enzymatic hydrolysis, while smaller particles ($< 0.4 \mu\text{m}$), colloids, and soluble constituents, which dominated at the outflow, were susceptible to enzyme hydrolysis, particularly by PDEase.

We found that the potential hydrolysis of the organic P in the inflow and outflow waters of Cell 4 is high, provided that the right amounts of particular enzymes are present. Although other enzymes such as phytase and adenosine triphosphatase (ATPase) have yet to be tested, we found that PDEase was more effective than APase in reducing the DOP in both inflow and outflow waters. As much as 70-100% of the inflow and outflow DOP could theoretically be

hydrolyzed if enough PDEase was present, and if internal P recycling near the back-end of the cell was negligible.

Table 2.32. Phosphorus mineralization rates in inflow and outflow waters of the SAV-dominated Cell 4 in STA-1 West under different incubation times and conditions. No mineralization rates are reported for the 0.05 μm permeate since the measured SRP concentrations were too low ($<6 \mu\text{g L}^{-1}$). Values followed by the same letter in a column for each sample are not significantly different.

Sample ID	Incubations conditions	P mineralization rates ($\mu\text{g P L}^{-1} \text{ day}^{-1}$)			
		24-hour incubation		30-day incubation	
		Inflow	Outflow	Inflow	Outflow
Unfiltered water	(Control) Air only	4.4b	3.3a	<0.1	<0.1
	Air + CO_2	10.9a	5.8a	1.8a	0.3a
	N_2 + CO_2	2.8b	4.5a	1.2a	0.4a
	(Control) N_2 only	4.4b	2.7a	0.1b	0.1b
0.4 μm retentate	(Control) Air only	31.9a	3.5a	2.7b	1.9b
	Air + CO_2	31.6a	0.5b	7.4a	2.3a
	N_2 + CO_2	11.6b	4.2a	6.5a	2.3a
	(Control) N_2 only	31.6a	6.4a	0.1b	1.1b
0.05 μm retentate	(Control) Air only	3.9a	0.6a	0.1a	0.2a
	Air + CO_2	1.1b	1.0a	0.3a	0.3a
	N_2 + CO_2	0.9b	1.2a	0.3a	0.2a
	(Control) N_2 only	3.4a	2.0a	0.1a	0.2a

2.12.4 Alkaline Phosphatase Activity in Ecosystem Compartments (Waters, Plants, and Sediments) of STA-1W

Introduction

The previous section described the results of adding two enzymes (APase and PDEase) to the surface waters of Cell 4, which were concentrated according to particle size. In this section, we assayed unconcentrated raw surface waters, sediments, and plant communities for activity of unamended APase by adding a labile fluorogenic substrate. Our purpose was to screen various ecosystem compartments in STA-1W for the presence of APase activity.

Methods

Fluorescence Measurements

Table 2.33 provides a summary of the various platforms that were sampled for alkaline phosphatase activity (APA) among surface waters and solid substrates. The alkaline phosphatase (phosphomonoesterase) activities of five ecosystem compartments (water, SAV, cattail, periphyton, and sediment) were measured fluorometrically using 100 μM of 4-methylumbelliferyl phosphate (MUFP) as the initial substrate. The fluorogenic hydrolysis product of MUFP, 4-methylumbelliferone (MUF), was measured on a Turner Model 10-AU fluorometer with excitation and emission filters of 300-400 and 410-600 nm, respectively, and a >300 nm soft glass reference filter. The excitation and emission filters were both fitted with 1:75 attenuator plates. The light source was a near-UV lamp. The standard curve was linear to 5 μM and the detection limit was 0.01 $\mu\text{g/L}$.

The fluorometer was calibrated with 4-methylumbelliferone (MUF) in 0.1 M Tris buffer (pH=8.3) using solutions prepared daily (in deionized water) ranging from 1 to 5 μM . For all incubations, the fluorescence at $t=0$ was subtracted from the subsequent readings to remove autofluorescence emitted from the dissolved organic matter within the incubation water and any initial MUF contaminating the MUFP assay enzyme. A 10 mM stock solution of MUFP in autoclaved deionized water was stored at -4°C .

Chemical Analysis of Substrates

Table 2.33 provides a summary of the various platforms that were sampled for APA among surface waters and solid substrates. SRP, TP, TSP, pH and color were analyzed on all waters collected from each sampled location. In addition to the aqueous samples, total phosphorous, nitrogen, carbon, inorganic and organic carbon, dry weight, and ash-free dry weight were analyzed on all solid samples (SAV, periphyton, cattail, and sediment).

Table 2.33. Sampling locations of the surface waters, sediments, periphyton, *Chara*, and cattail used for assaying alkaline phosphatase activity.

Substrate	NTC-15		STC-1		STC-4		Cell 4		Shallow-Raceways	
	In	Out	In	Out	In	Out	In	Out	In	Out
Surface Water	√	√					√	√		
Sediment			√	√			√	√		
<i>Scytonema</i>										√
<i>Chara</i>					√	√			√	

Waters Inflow and outflow water samples were collected from NTC-15 and Cell 4 on October 25, 2001. Samples were transported to the laboratory on ice in an insulated chest, and then kept refrigerated (2°C) until analysis which was within 20 hrs of collection.

Before being analyzed, samples were brought to room temperature. Then 0.5 ml of 100 µM MUFP and 0.5 ml of 0.1 M autoclaved Tris buffer (pH=8.3) were added to 4.0 ml of unfiltered sample water. Samples were then incubated at 25°C in the dark in 10 x 120 mm glass test tubes, and agitated every 15 min. Fluorescence was measured immediately upon addition of the MUFP and Tris buffer and after 30 and 60 min. Analysis was conducted in triplicate, and included color blanks (4.0 ml of site water and 1.0 ml of 0.1 M Tris buffer) and MUFP controls (4 ml deionized water, 0.5 ml of MUFP, and 0.5 ml of 0.1 M Tris buffer). Alkaline phosphatase activity (APA) was described as the MUFP hydrolyzed in nM/min. The buffered pH, measured on the incubation waters after analysis, was 8.23±0.01.

SAV, Cattail, and Periphyton *Chara* was collected on November 4, 2001 from the inflow and periphyton (*Scytonema*) from the outflow regions of the shallow (9 cm deep) raceways at the SATTS. *Chara* was also collected from the inflow and outflow of STC-4 on November 15, 2001. Although the *Chara* plants were collected in their entirety, some fragmentation of the plants occurred during transport, especially in the *Chara* sampled from STC-4 inflow. *Typha* was also harvested, with their roots and rhizomes intact, from STC-1 inflow and outflow on November 15. The *Typha* plant collected from the inflow region was 12 mm in diameter (measured just

below the water line) and 1.13 m tall. The outflow region plant was 1.42 m tall and ellipsoid in diameter with the long axis measuring 31 mm and the short axis measuring 17 mm. *Chara* (for the two dates sampled), periphyton, and *Typha* samples were transported at ambient temperature and analyzed within 21 and 8, 7.5, and 25 hrs, respectively. From each sampling location, site waters were also collected and transported to the laboratory on ice.

The plants were lightly rinsed in site water before incubation. *Chara* (1.5 g wet weight) and 5.0 g wet weight of the periphyton collected from the shallow raceway were combined with 22.5 ml of site water and 2.5 ml of 100 μ M MUFP in 0.1 M Tris. The incubation water used for the periphyton was from the shallow raceway inflow instead of the outflow region from where the periphyton had been collected. Other than this exception, all plants were incubated with waters collected from their respective harvest sites. To the *Chara* collected from STC-4, 40.5 ml of site water and 4.5 ml of 100 μ M MUFP in 0.1 M Tris buffer were added to 5.0 g wet weight of *Chara*. For the *Typha*, 1.5 g of the outer epidermis was thinly sliced just below the water line using a razor to which 40.5 ml site water and 4.5 ml of 100 μ M MUFP in 0.1 M Tris were added.

All plant samples were carefully swirled before each subsampling of the incubation water. Fluorescence was measured after 0, 5, 15, and 30 minutes for the triplicate vessels containing *Chara* and periphyton collected from the shallow raceway. Fluorescence was measured initially and after 15 and 30 min in duplicate samples of *Typha* and *Chara* collected from STC-1 and STC-4, respectively. In addition, autofluorescence was determined by substituting 0.1 M Tris buffer for the 100 μ M of MUFP. Incubations were conducted under ambient light in the lab at 25°C in 30 or 50 ml glass beakers. The pH of the waters after the incubation period was 8.06 ± 0.08 and 8.15 ± 0.08 for the periphyton and both the *Chara* and *Typha*, respectively. Dry and ash-free dry weights were measured for each plant species to determine the rate of enzyme activity (APA) as the nmol of MUFP hydrolyzed /min/g dry wt or ash-free dry wt.

Sediments Sediments from SAV and cattail dominated wetlands were sampled from the inflow and outflow of Cell 4 and STC-1 on November 7, 2001. Samples were transported on ice in an insulated chest and analyzed within 27 hrs of collection.

Three cubic cm of sediment were weighed out in quadruplicate, including a fluorescence background control. For the three replicates, 21 ml of 100 μ M MUFP in 0.1 M Tris buffer were added to each vessel. Instead of adding the MUFP to the samples, 21 ml of 0.1 M Tris was added for the background control. Each vessel was swirled prior to subsampling the incubation water, which occurred after incubation times of $t=0$, 20, and 50 min; the incubation time also included centrifuging for 5 min at 7,000 rpm. The supernatant was poured into borosilicate tubes and the fluorescence measured. The pH of the sediment incubation waters were 8.36 ± 0.08 following analysis. The dry and ash-free-dry weights for each replicate were determined and the rates of enzyme activity calculated as nmol MUFP hydrolyzed/min/g dry wt or ash-free-dry wt.

Results

Water Chemistry

SRP, TP, TSP, Color, and pH of the waters for each sampling location are provided in Table 2.34. Inflow waters were typically higher for all parameters analyzed with the exceptions of pH and color. SRP, TSP, and TP concentrations of Cell 4 inflow waters (at 80, 103, 138 μ g/L) were higher than the outflows (4, 13, 21 μ g/L). Inflow waters to NTC-15 also exhibited higher P concentrations than outflow waters.

Table 2.34. SRP, TP, TSP and color concentrations, and pH of the surface waters in NTC-15 and Cell 4 sampled on October 25.

Parameter	Units	Cell 4		NTC-15	
		In	Out	In	Out
SRP	μ g/L	80	4	27	<2
TP	μ g/L	138	21	53	35
TSP	μ g/L	103	13	40	18
Color	CPU	338	288	321	309
pH	units	8.02	7.96	8.06	8.79

Tissue and Sediment Composition

The highest tissue total phosphorus concentration was measured in the *Chara* sampled from the inflow of the shallow raceways (1620 mg/kg) and the outflow of STC-4 (1550 mg/kg) (Table 2.35). In addition, the highest total nitrogen concentrations were also found in the *Chara* sampled from these two locations, at 2.15 and 2.23 % dry wt, respectively. The inflow *Chara*

sampled from STC-4 contained less tissue phosphorus than the outflow plants. For the *Typha* sampled from STC-1, however, the inflow phosphorus concentration was higher than the outflow. The lowest periphyton TP concentrations were found in the periphyton collected from the outflow of the shallow raceways (166 mg/kg). The lowest TN content was found in the cattail from the inflow of STC-1. The inflow and outflow *Typha* of STC-1 had the highest concentrations of total carbon (TC) and organic carbon (TOC). The other locations were within the same range of concentration of TC and TOC. The highest tissue total inorganic carbon was found in *Scytonema* and *Chara* collected from the shallow raceways. The highest organic matter content (ash-free dry weight) was measured in the cattail (92.8%) sampled from STC-1, while the periphyton sampled from the shallow raceways had the lowest organic matter content (38.7%).

For the SAV-dominated sediment from Cell 4, the total phosphorous concentration of the inflow (1440 mg/kg) was greater than the outflow (528 mg/kg) (Table 2.35). The inflow of the cattail-dominated sediment sampled from STC-1, however, contained less phosphorous than the outflow. The total nitrogen, carbon and organic carbon concentrations and ash-free dry weight also followed the same pattern with the inflow being higher than the outflow for SAV-dominated sediment from Cell 4, and the outflow being higher than the inflow for the cattail-dominated sediment from STC-1. For total inorganic carbon, however, the reverse was true.

Background Corrections

Autofluorescence from the dissolved organic carbon in the incubation waters was measured by adding Tris buffer to each sample instead of MUFP. In most cases, samples had similar autofluorescence, except for the SAV and cattail-dominated sediments, and little variation was observed between replicates (Table 2.36). In addition, we conducted another set of background checks during each incubation where MUFP was added to deionized water instead of a sample to determine possible MUF contamination of the MUFP assay enzyme. As in the autofluorescence incubations, there was little variation in fluorescence, either within replicates or between substrates (Table 2.36). The fluorescent measurements did, however, clearly indicate some hydrolysis of the MUFP enzyme had occurred during or after its manufacture.

Table 2.35. Total phosphorus, nitrogen, carbon, organic and inorganic carbon concentrations, and ash-free dry wt, from inflow and outflow locations where SAV, cattail, periphyton, and sediment were sampled for APA.

Location	Substrate	TP (mg/kg)	TN (% wt)	TC (% wt)	TOC (% wt)	TIC (% wt)	Ash-free Dry Wt (%)
Shallow-Raceway Out	Periphyton (<i>Scytonema</i>)	166	0.944	20.08	11.56	8.52	38.1±0.6
Shallow-Raceway In	<i>Chara</i>	1620	2.15	25.08	17.64	7.44	75.2±1.4
STC-4 In	<i>Chara</i>	1180	1.72	25.38	18.81	6.57	51.5±2.4
STC-4 Out	<i>Chara</i>	1550	2.23	29.81	26.85	2.96	72.4±1.5
STC-1 In	Cattail	442	0.561	42.21	40.30	1.91	92.8
STC-1 Out	Cattail	398	0.745	38.68	37.28	1.10	88.1
Cell 4 In	SAV Dominated Sediment	1440	1.95	29.34	24.00	5.34	62.3±1.4
Cell 4 Out	SAV Dominated Sediment	528	1.43	26.27	19.31	6.96	48.3±3.1
STC-1 In	Cattail Dominated Sediment	602	1.12	17.98	13.41	4.57	32.1±4.0
STC-1 Out	Cattail Dominated Sediment	697	1.29	19.86	18.06	1.81	43.0

Table 2.36. Fluorescent background checks for sample water autofluorescence and MUF contamination of the MUF assay enzyme. Each mean and standard deviation is based on triplicates.

Substrate	Sample Location	Incubation Water Autofluorescence Mean ± 1 SD as nM		MUF Contamination of Assay Enzyme Mean ± 1 SD as nM
		Inflow	Outflow	
water	NTC-15	0.330±0.019	0.265±0.017	0.180±0.001
water	Cell 4	0.309±0.001	0.307±0.002	
periphyton	raceway	0.319±0.002		0.168±0.001
<i>Chara</i>	raceway	0.315±0.009		0.168±0.001
cattail	STC-1	0.294±0.001	0.247±0.002	0.200±0.001
<i>Chara</i>	STC-4	0.300±0.008	0.306±0.004	0.200±0.001
SAV Dominated Sediment	Cell 4	0.101±0.014	0.096±0.002	0.199±0.001
Cattail Dominated Sediment	STC-1	0.110±0.008	0.124±0.009	

Surface Waters

The APA for the inflow and outflow waters of NTC-15 and Cell 4, reported as nM/min and calculated using the 30 min incubation time, are presented in Table 2.37. The APA was greater in the outflow waters, particularly in NTC-15. The difference between the APA measured in the inflow and outflow waters of NTC-15 was considerably greater than for the same station locations in Cell 4, which is likely due to higher concentrations of alkaline phosphatase produced by the bacterial and algal communities inhabiting the outflow region of NTC-15.

Table 2.37. Alkaline phosphatase activity for waters collected from NTC-15 and Cell 4 on October 25, 2001.

	APA (nM/min)	
	Inflow	Outflow
NTC-15	1.04	22.8
Cell 4	0.522	0.900

Periphyton

Since no periphyton existed at the inflow of the shallow, low velocity raceway receiving post-STA waters, APA was measured only using outflow-region periphyton. As noted previously, inflow water was used during the incubation. Two incubation times, 5 and 30 min, are represented in the final calculations since the rate of MUFPP hydrolysis was not linear. Consequently, the highest APA was observed after the 5 min incubation and declined after the 30 min incubation (Table 2.38). The nonlinear response notwithstanding, there was considerable APA associated with the outflow-region periphyton.

Table 2.38. Alkaline phosphatase activity of the periphyton (*Scytonema* spp.) collected from the outflow of the shallow raceways on November 4, 2001.

Incubation Time (min)	APA Outflow	
	(nmol/min/g dry wt)	(nmol/min/g AFDW)
5	11.2	112
30	6.36	63.7

Cattails and SAV

The highest alkaline phosphatase activity of all the solid substrates, 79.5 nmol/min/g dry wt, was measured in the outer layers of epidermis of the *Typha* sampled from STC-1 outflow (Table 2.39). In addition, tissues from the culm of *Typha* growing in the inflow region of STC-1 also exhibited high APA.

The high APA associated with the culm epidermis of *Typha* may be the result of an artifact of excising the tissue from the stem. Cutting probably released labile intracellular organic compounds, which may have added phosphatase enzymes or stimulated bacterial growth during the incubation. *Chara* sampled from the inflow waters of the shallow, low velocity raceway also had a high APA, 14.2 nmol/min/g dry wt (Table 2.39). The lowest APA was measured in the *Chara* sampled from the outflow waters at STC-4 on both a g dry wt and an AFDW basis (Table 2.39). There were minor differences in APA between the inflow and outflow of the *Chara* inhabiting STC-4.

Table 2.39. Alkaline phosphatase activity of the *Chara* collected from the shallow raceways on November 4, and *Typha* and *Chara* collected from STC-1 and STC-4 on November 15, 2001.

	Sample Location	Incubation Time (min)	APA			
			(nmol/min/g dry wt)		(nmol/min/g AFDW)	
			Inflow	Outflow	Inflow	Outflow
<i>Chara</i>	raceways	30	14.2		105	
<i>Chara</i>	STC-4	30	1.64	1.62	17.9	28.1
Cattail	STC-1	30	30.7	79.5	491	401

Sediments

Differences in alkaline phosphatase activity occurred between the inflow and outflow of the SAV-dominated sediment sampled from Cell 4 after 20 and 50 min incubation times (Table 2.40). Again this indicates a lack of linearity in the hydrolysis rate during the assay. Nevertheless, the outflow sediments had a greater APA than the inflow water and sediments (Table 2.40).

There were pronounced differences between the inflow and outflow of the cattail-dominated sediments sampled from STC-1: the outflow of the cattail-dominated sediment exhibited an APA of 28.6 nmol/min/g dry wt after 50 min compared to only 2.88 nmol/min/g dry wt for the sediment collected at the inflow (Table 2.40). A less obvious difference in APA was observed between the inflow and outflow calculated on an ash-free dry wt basis after incubation for 20 min (Table 2.40).

Table 2.40. Alkaline phosphatase activity of SAV- and cattail-dominated sediments.

	Sample Location	Incubation Time (min)	APA			
			(nmol/min/g dry wt)		(nmol/min/g AFDW)	
			Inflow	Outflow	Inflow	Outflow
SAV Dominated	Cell 4	20	5.97	9.57	11.5	66.0
		50	9.34	12.5	45.0	215
Cattail Dominated	STC-1	20	4.11	20.5	28.5	33.1
		50	2.88	28.6	49.9	115

APA Comparison Among Ecosystem Compartments

Based on a 30 min incubation, the APA was higher in the *Chara* collected from the inflow of the shallow raceways (14.2 nmol/min/g dry wt) than the periphyton (6.36 nmol/min/g dry wt) collected from the outflow. The cattail-dominated sediment collected from the inflow of STC-1 after 20 min incubation had a lower APA (4.11 nmol/min/g dry wt) than the *Typha* tissue collected from the outflow analyzed after a 30 min incubation (30.7 nmol/min/g dry wt). Furthermore, APA of the *Typha* tissues from the STC-1 outflow was also greater than from the cattail-dominated sediment, at 79.5 and 20.5 nmol/min/g dry wt, respectively (Table 2.39 and Table 2.40).

For the four surface waters (NTC-15 and Cell 4 inflow and outflow) and the four sediments assayed for APA, an inverse correlation ($r = -0.51$ and -0.73 , respectively) was found between APA and the initial SRP concentration. Although the correlations were not significant at the 0.05 level, the inverse relationship is consistent with alkaline phosphomonoesterase being a repressible enzyme. That is, it is synthesized when the concentration of orthophosphate, the

repressor, becomes very low. This should not be confused with orthophosphate inhibition of the enzymatic reaction performed by alkaline phosphatases (Pettersson 1980), even though the effect is the same as repressing enzyme production. On the other hand, there was a weak positive correlation ($r = 0.43$) between APA and initial SRP concentration for the plants (*Chara*, periphyton, and cattail) that were assayed, which indicates that SRP concentration may affect the physiological state of the plant during incubation, especially for *Chara* and periphyton. The nutritional status of the plant may influence the production of the extracellular phosphomonoesterase by *Chara* and periphyton. The high APA for cattail is probably unrelated to the SRP concentration in the medium during the assay, but more a function of the release of phosphomonoesterase from within the cells due to tissue excision.

The levels of APA (based on a single grab sample), especially in the outflow regions of the mesocosms, test cells, and Cell 4, indicate P deficiency among the bacteria and algal communities. As such, enzymatic hydrolysis of DOP compounds may be significant in SAV wetlands treating Post-BMP waters. For example, we observed DOP concentration reductions in Cell 4 from 27 $\mu\text{g/L}$ to 10 $\mu\text{g/L}$ during the 24-day STSOC verification period. Low levels of hydrolysis occurred when alkaline phosphatase (APase) was added to Cell 4 waters over a pH range of 7.5 to 9.0 (Figure 2.76), yet we found high activity when a labile phosphate ester-containing compound (MUFP) was added to the waters, sediments, and algae of Post-BMP and Post-STA wetland environments. This strongly suggests that select DOP compounds in wetland waters may require a suite of enzymes, or a sequence of steps (e.g. UV and enzymes), for hydrolysis.

Section 3: Test Cell Evaluations

The test cell evaluations detailed below comprise Task 6 of DBE's Experimental Design Plan (DBE, 2000c). Additional details regarding methodologies can be found in that document. The test cells represent an SAV assessment platform that is intermediate in scale (0.22-0.25 ha) compared to the mesocosms (1.7-3.7 m²) and Cell 4 (147 ha). Two SAV-dominated test cells (NTC-1 and NTC-15) at the north bank of 15 test cells received "Post-BMP" waters from Cell 1 and the two SAV-dominated test cells (STC-4 and STC-9) at the south bank of 15 test cells received "Post-STA" water from Cell 3 of STA-1W. Initially all 4 test cells were inhabited by cattail, and were subsequently converted to SAV by the District in 1998. *Chara* dominated all four cells initially, but *Hydrilla* became co-dominant in the two south test cells by 2000. Baseline monitoring of the SAV-dominated test cells began on September 1, 1999. Due to the LR berms being installed at NTC-15 and STC-9, and aquatic plant (*Hydrilla*) control in STC-4 and STC-9 in April and May 2000, monitoring of NTC-15 was suspended from April 5, 2000 until June 23, 2000, and monitoring of the south test cells was suspended from March 14, 2000, until August 4, 2000. Monitoring of all test cells was subsequently performed until September 14, 2001.

For this section, we have divided our discussion into seven topics: Plant Management, Hydrologic Assessment, Tracer Studies, LR Berm Installation and Permeability, Sediment Characteristics and Accretion, Nitrogen and Suspended Solids Removal, and P Removal Performance. Additional information on test cell performance is provided in the draft final STSOC report (DBE 2002).

3.1 Plant Management

Because of *Hydrilla* and emergent plant infestations at the south test cells (STC-4 and STC-9), we found it necessary to apply herbicides, manipulate water levels, and re-stock with native SAV. During the month of June 2000, water levels in STC-4 and STC-9 were drawn down in an effort to eliminate *Hydrilla*, so that other macrophytes, including *Najas*, could be established. A topical herbicide (Rodeo®) was sprayed on emergent plants including *Typha* sp. (cattails), *Panicum repens* (torpedo grass) and *Echinochloa* sp. (barnyard grass). Afterward, the water level in each of the south test cells was lowered to expose the muck substrate, and another herbicide,

Endotholl®, was applied to discourage regrowth of *Hydrilla* tubers. After two weeks, the water level was raised to 0.4 m in both test cells. After another two-week equilibration period, *Najas* was harvested from the northeast corner of Cell 4, and stocked into STC-4 and STC-9 at approximately 0.9 kg wet/m². *Ceratophyllum* (~1 metric ton) was added to the influent region of NTC-1 on July 11. This aquatic plant management strategy was successful in decreasing the biomass of *Hydrilla*.

3.2 Hydrologic Assessments

The goal of our test cell hydrologic assessments was to develop an optimum protocol for collecting and analyzing water budget data. A sound water budget is critical for the conduct of both tracer studies and P mass balances, and for this we required accurate test cell stages and inflow and outflow rates. In this section, we describe hydrologic measurements performed prior to, and during our first hydraulic tracer assessment (October-November, 1999). For water budget assessments, stage and inflow rates were used to calculate nominal hydraulic retention times (HRT), and test cell outflows were used to flow-weight concentration measurements in mass balance calculations.

Prior to October 10, 1999, the four SAV test cells (NTC-1, NTC-15, STC-4, STC-9) were maintained by the District at an approximate depth of 1.1 m and approximate loading rate of 2.6 cm/d (using a 0.75" inflow orifice). On October 10, 1999, we performed three activities in NTC-1 and NTC-15 that altered test cell hydrology and hydraulics:

- Stage was lowered in NTC-1 and NTC-15 to approximate depths of 0.9m and 0.5m, respectively.
- Loading rate was increased in both cells from 3 cm/d to approximately 11 cm/d (1.5" orifice on inlet pipe).
- Hydraulic distribution manifolds were installed on both test cell influent lines in an attempt to improve hydraulic efficiency, and hence treatment performance, compared to point-source inflows (Persson et al., 1999).

Figure 3.1 shows a photograph of the installed hydraulic distribution manifolds during dye injection. The PVC manifold was plumbed directly onto the test cell inflow pipe using off-the-

shelf fittings and adapters. The manifolds were equipped with 10 adjustable discharge ports (9 for NTC-1, which is 10% narrower than other test cells) to evenly distribute flow across the head of the test cells. The same modifications were performed to STC-4 and STC-9, the two south SAV-based test cells, on October 17, 1999.



Figure 3.1. Photo of NTC-1 distribution manifold, shown during injection of Rhodamine WT dye for the hydraulic tracer assessment.

3.2.1 Test Cell Stage

Test cell stage was measured by the District with two Stephen's stage recorders per test cell located at headwater (influent) and tailwater (effluent) positions. The digitized Stephen's gauge data have a 0.01' resolution ($\pm 1/16''$). We estimated test cell stage by averaging headwater and tailwater stage data. Figure 3.2 shows a time history of NTC-1 and NTC-15 stage for a period of three weeks before tracer injection through assessment completion. The plotted data are daily mean stage values averaged from Stephen's data recorded at 15-minute intervals. In response to the October 10 weir adjustments, test cell stage decreased rapidly over the following

4-5 days and remained dynamic for several days after that. Dye injection was on October 26, 1999 and by that time test cell stage was stable. There was a single significant rainfall event during the assessment, which occurred on November 1st. With the exception of the response to this event, stage remained relatively constant throughout assessment duration.

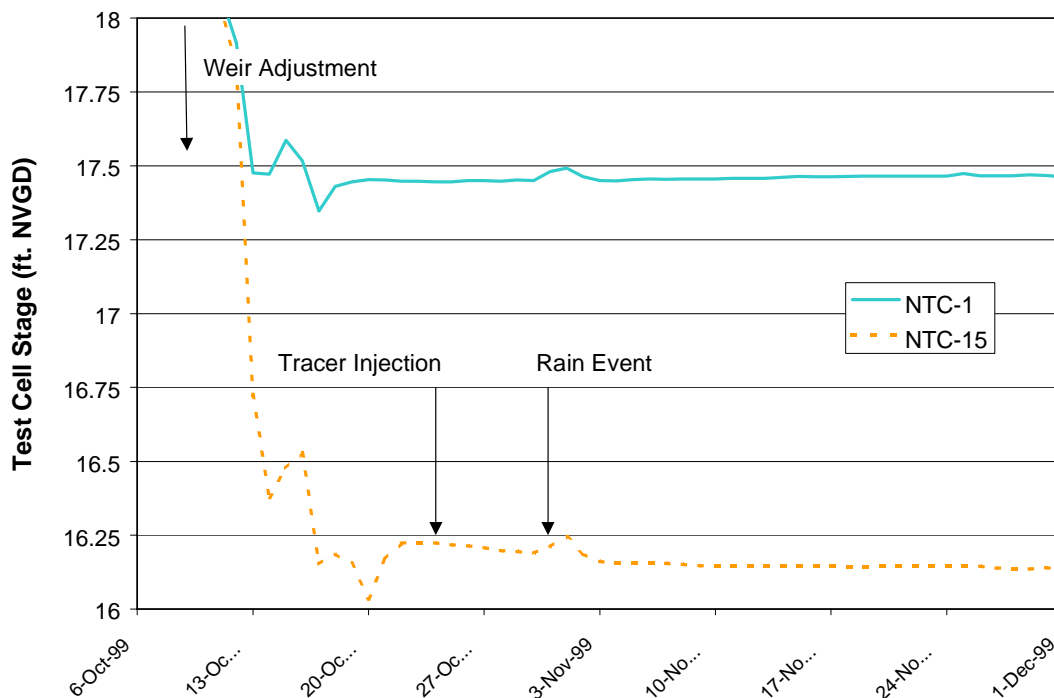


Figure 3.2. Stage histories of north test cells prior to and during the dye tracer assessment.

3.2.2 Test Cell Inflow

We performed in-field calibration of test cell inflows through the newly installed distribution manifolds. Since test cell inflow is dependent on stage in the water storage cell, flow from each manifold was measured three times at intervals corresponding to high, mid, and low stage in the storage cell, and hence high, mid, and low flow conditions. Flows were measured from each of the manifold orifices by capturing a timed 10-second volume in a 4-L graduated cylinder. Each measurement was repeated twice. Test cell inflow was taken as the sum of orifice flows.

Table 3.1 summarizes our inflow calibrations. At a steady storage tank stage, repeatability of the summed inflow measurement was within 5%. The average test cell inflow was taken as the average of high, mid, and low flow measurements. Compared to the average flow, high flow was about 7% higher, and low flow about 7% lower. Note that the average NTC-1 inflow was between 10-20% lower than flows measured in the other three test cells. After the tracer assessment was complete, we discovered that the ball valve on the NTC-1 inflow line was not completely open. Once the valve was opened fully, NTC-1 flow was measured at 303 m³/day, which is comparable to the other three test cells. As the inflow ball valves are not well-marked, this was a relatively easy mistake to make and points to the importance of individually calibrating test cell inflows on future assessments. Because our calibrated inflows were between 13-24% higher than District reported flows, we continued to check the accuracy of our inflows by performing manifold flow measurements biweekly during the test cell monitoring period.

Table 3.1. Summary of calibration measurements for test cell inflows.

Head Tank Stage (ft)		NTC-1 (m ³ /d)	NTC-15 m ³ /d)	STC-4 (m ³ /d)	STC-9 (m ³ /d)
High (23.7')	Rep 1	281	359	313	323
	Rep 2	281	356	313	327
Mid (23.2')	Rep 1	261	334	306	331
	Rep 2	276	332	305	327
Low (22.6')	Rep 1	253	308	285	307
	Rep 2	252	306	285	308
DBE Average		267	333	301	320
Avg. District Reported		267	273	260	258

3.2.3 Test Cell Outflow

We calculated test cell outflows based on water balance relations using calibrated inflow measurements and District-measured test cell stage. Throughout most of the tracer assessment duration, test cell hydrology was typified with near-constant stage (storage volume), constant inflow, no seepage, and no rain. Under these conditions, test cell outflows were equal to the

calibrated inflows. The transient response of test cell outflow to a November 1 rain event was estimated by examining District-supplied 15-minute resolution stage data for the period of October 31 through November 2. The rain event was sudden and heavy, dropping approximately 1.75" in less than 6-hours; after the event, it took approximately 24 hours for test cell stage to recover to nominal values. Supplemental outflow from the rainfall event was estimated from the rate of change in the decreasing stage history after the rain event.

For estimating test cell outflow rates, the water balance approach yields greater accuracy for tracer assessment mass balances than applying the V-notch weir equation:

$$Q_w = C_w H_w^{2.5}$$

where Q_w = flow, in cfs

C_w = weir coefficient, value = 2.5

H_w = head on weir, in ft.

The difficulty in applying the V-notch weir equation to test cell outflow lies in determining an accurate estimate of head on the V-notch weir. Head on the V-notch weir is calculated by subtracting stage from the absolute position of the bottom of the V-notch weir. As equipped by the District, the closest measurement of stage to the V-notch weir is the tailwater Stephen's gauges, which are approximately 25 meters away. As described earlier in this section, the Stephen's gauges have a +/- 1/16" resolution. The absolute position of the V-notch was determined using a field calibration technique previously standardized for all test cells. Through replicate attempts, we found a +/- 1/8" error in repeatability of the field calibration technique. Hence, compounding uncertainties in weir position and stage measurement yield an uncertainty in the head on the V-notch weir gate position of approximately +/- 0.19".

Table 3.2 summarizes errors introduced into outflow estimation based on this range of uncertainty in head on the weir. A 0.19" uncertainty in head estimate can result in a 18% error in flow estimate. By comparison, we estimate that outflow rates calculated with water balance techniques are accurate within 5%.

Table 3.2. Errors in test cell outflow calculations due to head estimation uncertainty

Accuracy of H_w	Calculated Flow (cfs)*	% Deviation from Actual Flow
+3/16"	.144	11.3%
+1/8"	.138	8.7%
0	.127	0
-1/8"	.117	-7.9%
-3/16"	.111	-11.4%

* Based on 11 cm/d loading = 0.127 cfs

3.2.4 Summary of Hydrologic Parameters for Tracer Assessment

Table 3.3 summarizes stage, depth, estimated storage volume, measured inflow rates, and calculated HRT for the test cells during the tracer assessment. Inflow rates are from in-field calibrations using the methods described above. Nominal test cell depth was calculated by subtracting average test cell stage from the sediment surface at 14.5'. Storage volume was calculated based on trapezoidal cross-sectional profiles as detailed in the test cell blueprints. Nominal hydraulic retention time (HRT) was calculated by dividing storage volume by nominal inflow. Nominal HLR is calculated by dividing test cell inflow by surface area, which was measured in the field.

Table 3.3. Summary of hydrologic parameters during the first test cell tracer assessment.

Test Cell	Inflow (m ³ /d)	Depth (m)	Storage Volume (m ³)	Nominal HRT (days)	Nominal HLR (cm/d)
NTC-1	267	0.91	2033	7.6	10
NTC-15	333	0.49	1185	3.6	13
STC-4	301	0.51	1230	4.1	12
STC-9	320	0.79	2000	6.3	11

3.3 Tracer Studies

We performed two tracer studies in this task to further our understanding of the hydraulic characteristics (e.g., flow path, detention behavior, nominal vs. actual retention times, dispersion)

of test cells dominated by SAV. These data facilitated our interpretation of the P removal efficiencies of various wetland configurations (e.g., as a function of water depth, HLR, HRT, SAV density) and also helped provide insight into P removal processes (e.g., chemical precipitation and adsorption, biological uptake), which are likely strongly influenced by hydraulic characteristics.

3.3.1 Laboratory Analysis of Dye Tracer

Rhodamine-WT concentrations were measured on a Turner Designs Model 10-AU-005-CE fluorometer with excitation and emission filters of 550 and > 570 nm, respectively (Wilson et al. 1986). The emission filter consisted of an orange sharp-cut filter. A reference filter (>535 nm) reduced baseline drift and instrument noise by filtering out scattered light. The light source was a clear quartz lamp. The standard curve was linear to 80 mg/L and the method detection limit was 0.1 µg/L. Since Rhodamine-WT fluorescence is sensitive to temperature, both standards and samples were analyzed at room temperature. Background fluorescence (from dissolved organic matter) was subtracted from each of the sample fluorescence readings. Prior to analysis, all water samples were stored in amber-colored bottles.

3.3.2 Computations for Determining Hydraulic Parameters

Calculations for determining selected hydraulic parameters for the test cells, based on the tracer data, were performed as follows.

The nominal HRT, τ , is the ratio of the volume of water in the treatment wetland (V) divided by the volumetric flow rate of water (Q):

$$\tau = V/Q \quad (1)$$

The tracer residence time, τ_a , is defined as the average time that a tracer particle spends in Cell 4, and is the first moment of the residence time distribution (RTD) function. The RTD represents the time various fractions of water spend in the test cells. It is the contact time distribution for the system (Kadlec 1994). The RTD defines the key parameters that characterize the actual detention time. Levenspiel (1989) uses the RTD in the analysis of reactor behavior.

The mean residence time, τ_a , was calculated by dividing Eq. 4 of the tracer flow distribution, by Eq. 3, both of which are based on mean outflow rates and tracer concentrations (Kadlec 1994):

$$\tau_a = M_1/M_0 \quad (2)$$

$$M_0 = \int_0^{t_f} Q_e(t) C(t) dt \quad (3)$$

$$M_1 = \int_0^{t_f} t Q_e(t) C(t) dt \quad (4)$$

where $C(t)$ = exit tracer concentration (mg/m³); Q_e = flow rate (m³/day); t = time (days); and t_f = total time span of the outflow pulse (days).

To find the RTD, the concentration response curve (experimental $C(t)$ vs. t curve) is converted to an E_t curve by changing the concentration scale so that the area under the response curve is unity (Levenspiel 1989). This is accomplished by multiplying the concentration readings by the volumetric flow rate divided by the mass (M) of injected tracer:

$$E_t = C(Q_e/M) \quad (5)$$

where E_t = RTD function in reciprocal time units.

The RTD function is normalized when it is expressed in terms of the dimensionless time scale by multiplying the Y-axis (i.e., the E_t function) units by τ (the nominal HRT):

$$E_\Theta = \tau E_t \quad (6)$$

where E_Θ = dimensionless RTD function,

and dividing the time units of the X-axis by τ :

$$\Theta = t/\tau \quad (7)$$

where Θ = dimensionless time scale and represents the number of mean HRTs.

This changes the X and Y axes so that the area under the curve is still equal to one, but the Y and X axes are normalized to τ (Levenspiel 1972). The purpose of creating the normalized distribution function, E_Θ , is to be able to compare the flow performance among wetlands of different sizes and containing different plant communities and densities.

Whereas τ_a represents the centroid of the distribution and is the first moment of the RTD, the variance (σ^2) is the square of the spread of the distribution, or a measure of the dispersive processes, and is expressed in units of (time)²:

$$\sigma^2 = \frac{\int_0^{t_f} t^2 Q_e(t) C(t) dt}{\int_0^{t_f} Q_e(t) C(t) dt} - \tau_a^2 \quad (8)$$

The variance, which is the second moment of the RTD, is particularly useful for matching experimental curves to one of a family of theoretical curves (Levenspiel 1972).

The variance can be rendered unitless by dividing by the square of the tracer detention time:

$$\sigma_\Theta^2 = \frac{\sigma^2}{\tau_a^2} \quad (9)$$

where σ_Θ^2 is the dimensionless variance of the tracer pulse.

Two common one-parameter models used to characterize non-ideal flows are the tank-in-series (TIS) and dispersion models (Levenspiel 1972). The TIS model views flow through a series of equal-size ideal stirred tanks, and the one parameter in this model is the number of tanks (N) in the chain. The number of constantly stirred tanks in the series that best matches the tracer response curve is given by N, which is determined by:

$$N = \frac{1}{\sigma_\Theta^2} \quad (10)$$

To construct an idealized dimensionless tracer response curve for N = 1, 2, etc.:

$$E_\Theta = \frac{N}{(N-1)!} \left(N \frac{t}{\tau_a} \right)^{N-1} e^{-N \frac{t}{\tau_a}} \quad (11)$$

The second model is a dispersed plug flow, or dispersion model, which draws on an analogy between mixing in actual flow and a diffusional process. Here the dispersion process is superimposed on a plug flow model, and mixing is presumed to follow a diffusion equation

(Kadlec and Knight 1996). For boundary conditions that are closed-closed, the following relation for the dimensionless variance has been found (Fogler 1992):

$$\sigma_{\theta}^2 = \frac{2}{Pe} - \frac{2}{Pe^2} (1 - e^{-Pe}) \quad (12)$$

where Pe is the Peclet number, dimensionless.

Eq (12) can be converted to the wetland dispersion number (D , dimensionless) by utilizing:

$$D = \frac{D}{uL} = \frac{1}{Pe} \quad (13)$$

where L = distance from inlet to outlet, m

u = superficial velocity, m/day

D = dispersion constant, m²/day

Combining Eqs. (12) and (13) yields:

$$\sigma_{\theta}^2 = 2D - 2D^2 (1 - e^{-\frac{1}{D}}) \quad (14)$$

3.3.3 Methodology of the First Tracer Assessment

The first tracer assessment on October 26 - November 30, 1999 was designed to examine vertical (depth-related) short-circuiting on key hydraulic efficiency parameters (e.g., HRT and dispersion). All four of the SAV-dominated test cells (two north test cells: NTC-1 and NTC-15; two south test cells: STC-4 and STC-9) were utilized. To achieve the desired depths in the first dye assessment, water surface levels in all four test cells were lowered on October 10, 1999 from the operational depth of approximately 1.1 m that had been maintained for five months prior. The water column depths of two of the test cells (NTC-15 and STC-4) were set at 0.5 m each; the remaining two test cells (NTC-1 and STC-9) were deeper (0.91 m and 0.79 m respectively). The hydraulic loading rates (HLR) in all four test cells were increased from the historic 3 cm/day loading and maintained within a narrow range of 10-13 cm/day throughout the assessment. At the time of the tracer assessment, the dominant SAV was *Chara* in the two north test cells (NTC-1 and NTC-15) and *Hydrilla* in the two south test cells (STC-4 and STC-9).

Tracer Injection Mass

On October 26, 1999, we introduced 75.9, 44.0, 44.0, and 88.0 g, respectively, of Rhodamine-WT dye into the influent manifolds of NTC-1, NTC-15, STC-4, and STC-9. The tracer was applied in 3.8-L volumes over a one-minute time span to each test cell (Figure 3.1).

Sampling Frequency

Samples were collected from the effluent weir location at 0, 3, 6, 9, 18, and 24 hours after injection, and then 4 times daily for the next 5.5 days, twice daily for the following three days, once daily for another 8 days, and finally every-other-day for the final week.

3.3.4 Methodology of Second Tracer Assessment

Only the two north test cells (NTC-1 and NTC-15) were used for the second tracer assessment (December 16, 1999 to February 1, 2000). In this evaluation, we assessed the effect of HLR-driven short-circuiting on hydraulic efficiency. Flow to the 0.9 m deep NTC-1 was quadrupled on December 9, 1999, to simulate a pulse load of runoff. On the same date the depth of NTC-15 was increased from 0.5 to 0.84 m, to assess the effects of a rapid stage increase on hydraulic performance.

Tracer Injection Mass

The amounts of Rhodamine-WT dye added to the influent manifolds of NTC-1 and NTC-15 on December 16, 1999, were 113.6 and 103.3 g, respectively. The tracer was applied in 3.8-L volumes over a one-minute time span to each test cell.

Sampling Frequency

Samples were collected from the NTC-15 effluent weir location at the following frequencies: 6 times per day (every 4 hours) for the first 4 days; 3 times per day (every 8 hours) for the next two days; twice daily for the next 5 days; daily for the next 10 days; and finally twice a week for the next 3.5 weeks. The same sampling schedule was followed for NTC-1 through the 14th day. Daily samples were then collected for only 3 days (instead of 10 days) at NTC-1, with the final sample taken 4 days after the last daily sample.

3.3.5 Results of the Two Dye Studies

Tracer Response Curves

The concentration response curves for the test cells exhibited non-ideal flow distributions, where neither plug flow reactor (PFR) nor constantly stirred tank reactor (CSTR) flow patterns occurred (Figure 3.3 - Figure 3.5). For all test cells that received a HLR of 10 - 13 cm/day, the tracer appeared at the effluent regions sooner than expected, based on the nominal HRTs. We observed lags ranging from 0.5 to 2.5 days before the maximum tracer concentration reached the effluent region of the cells (Figure 3.3 - Figure 3.5). After the lag periods, the ascending limb of the tracer curve in 3 of the test cells peaked close to the maximum concentrations (36 - 44 µg/L) expected for CSTR behavior (Figure 3.3a and Figure 3.4a and b).

The effects of a quadrupling of the HLR in NTC-1 during the second tracer assessment resulted in a profile for well-mixed hydraulics (Figure 3.6). Unfortunately, the increased flows caused some of the biota to be exported from the test cell, which subsequently was trapped on the discharge weir screen. The blockage reduced the discharge flow early during the assessment, thereby compromising the outflow data to such an extent that calculations for determining tracer recovery, mean HRT (τ_a) and variance (σ^2) could not be performed.

Tracer Mass Balances

The Rhodamine-WT mass balances were calculated by comparing the injected tracer mass to the tracer mass detected at the effluent. The total mass of tracer exiting the SAV test cells is given by Eq. 3. A comparison of the recovered tracer mass and the amount injected to each test cell demonstrates a good recovery for Rhodamine-WT, with higher recoveries associated with the South Test Cells (Table 3.4).

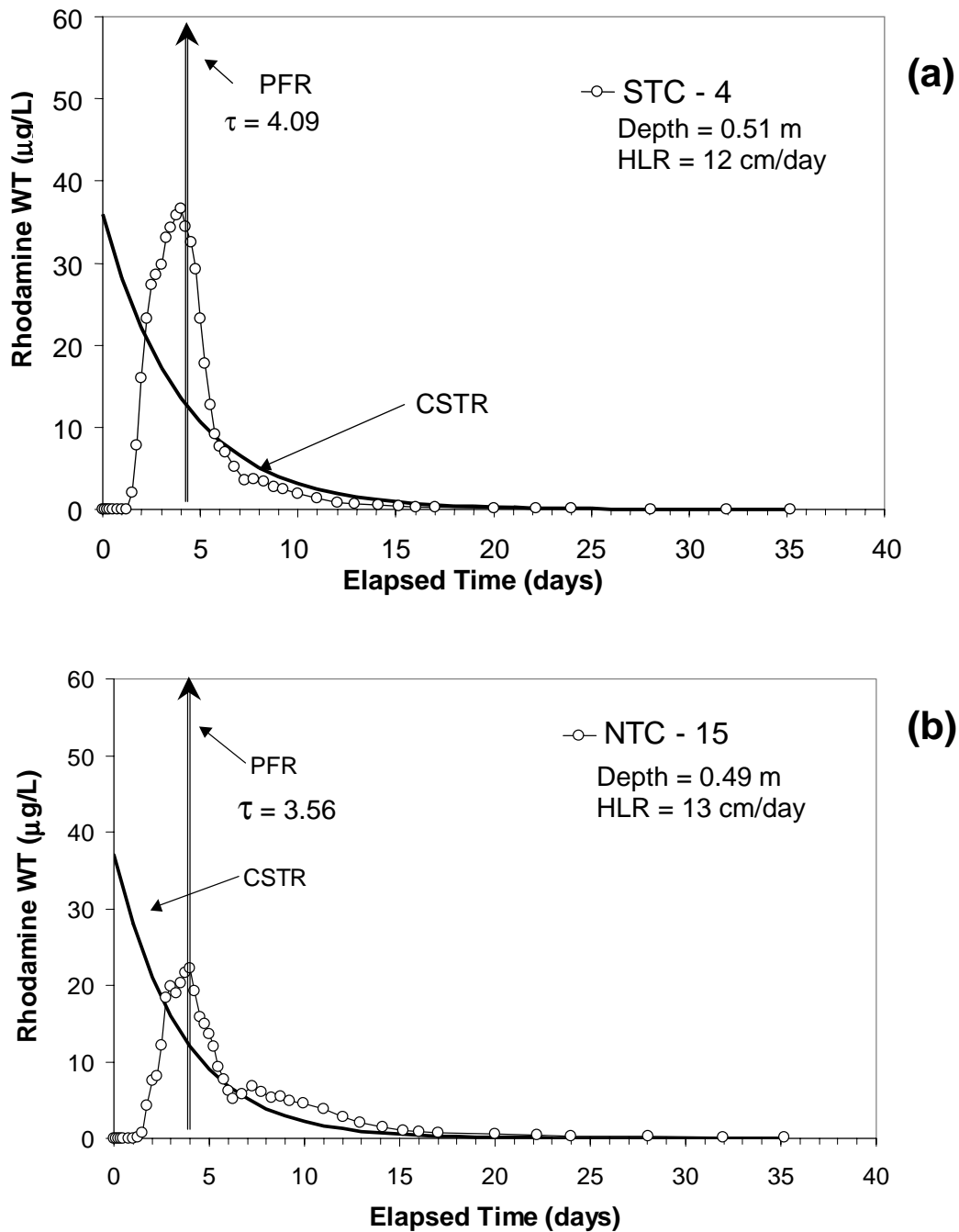


Figure 3.3. Tracer response curves for the fluorescent dye Rhodamine-WT applied to the shallow test cells during the first tracer assessment. Graph (a) reflects the South Test Cell (STC-4) and graph (b) reflects the North Test Cell (NTC-15). Responses to ideal well-mixed (CSTR) and plug flow (PFR) conditions are represented by the exponential decay and vertical (coinciding with the nominal HRT, τ) lines.

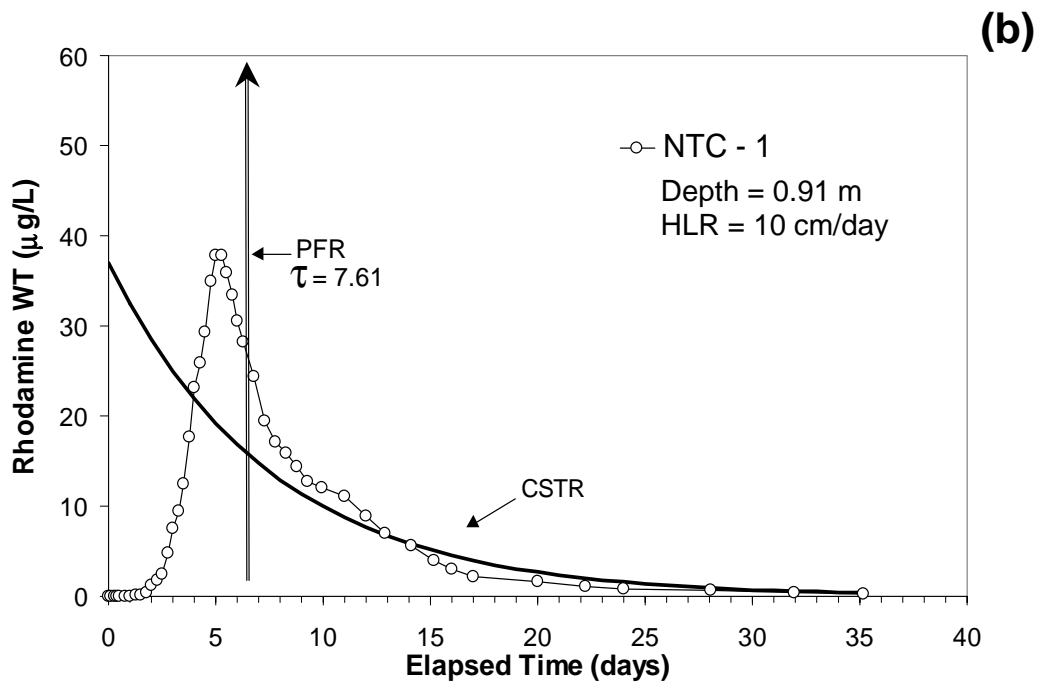
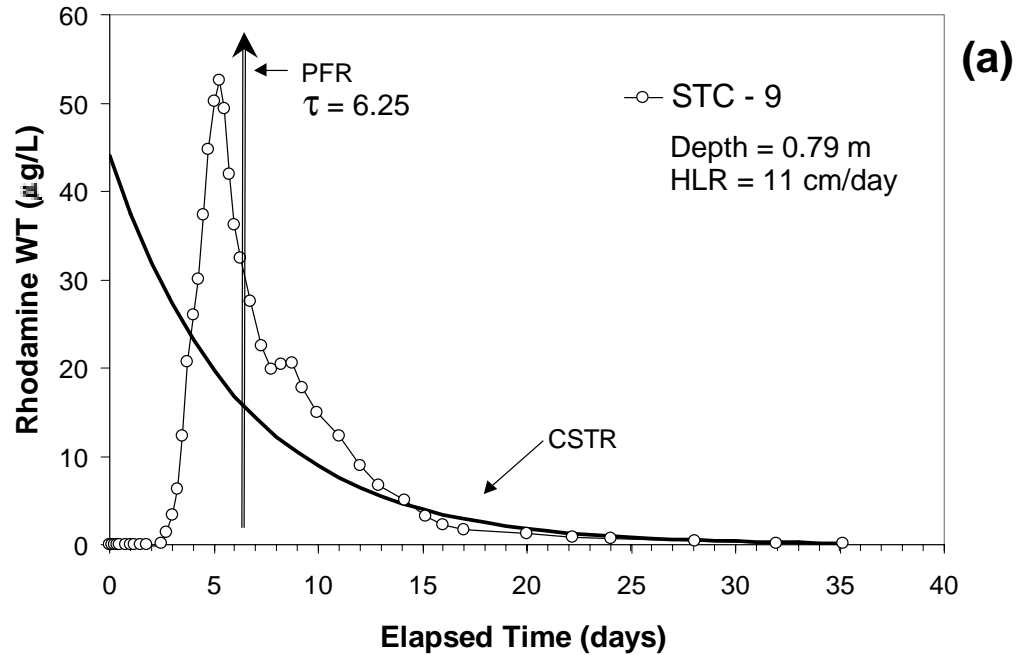


Figure 3.4. Tracer response curves for the fluorescent dye Rhodamine-WT applied to the deeper test cells during the first tracer assessment. Graph (a) reflects the South Test Cell (STC-9) and graph (b) reflects the North Test Cell (NTC-1). Responses to ideal well-mixed (CSTR) and plug flow (PFR) conditions are represented by the exponential decay and vertical (coinciding with the nominal HRT, τ) lines.

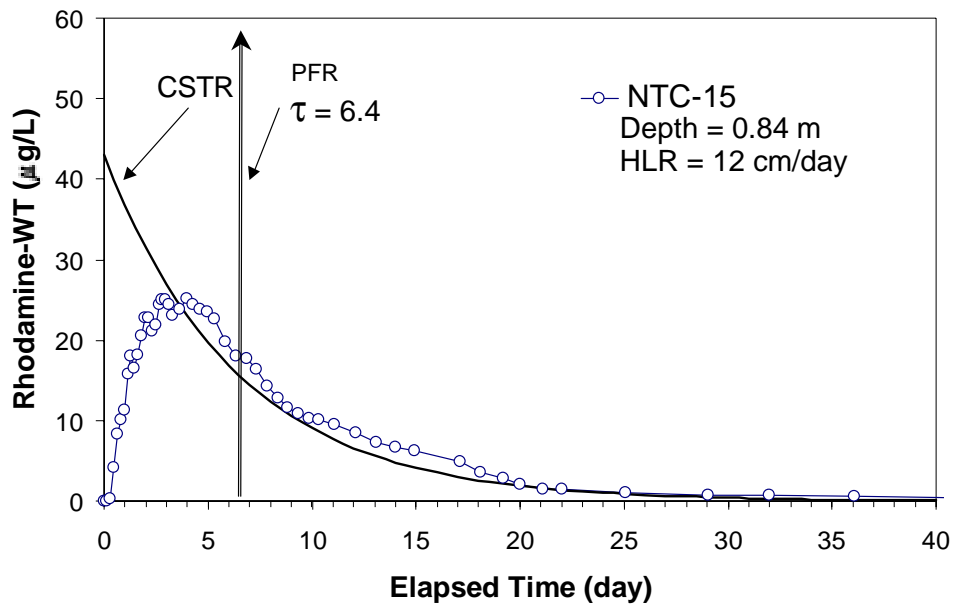


Figure 3.5. Tracer response curve for the fluorescent dye Rhodamine-WT applied to a deep test cell (NTC-15) during the second tracer assessment. Responses to ideal well-mixed (CSTR) and plug flow (PFR) conditions are represented by the exponential decay and vertical (coinciding with the nominal HRT, τ) lines.

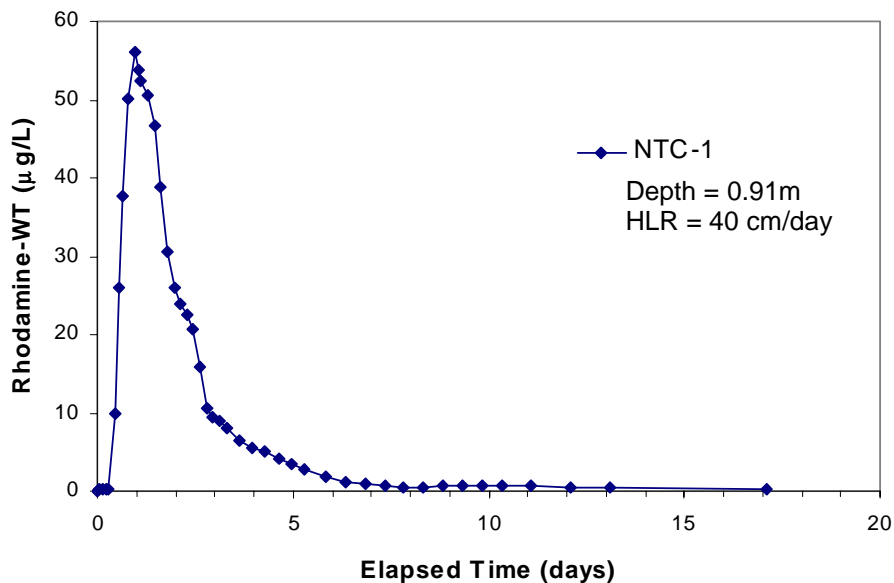


Figure 3.6. Tracer response curve for the fluorescent dye Rhodamine-WT applied to NTC-1 during the second tracer assessment.

Table 3.4. Comparison of recovered dye mass with the dye amounts injected to test cells operated at two different water depths during two separate dye investigations.

Dye						
Assessment	Test Cell	Depth	HLR	Mass	Mass	%
Investigation	Designation	(m)	(cm/day)	Injected (g)	Recovered (g)	Recovery
No. 1	NTC-1	0.91	10	75.9	59.4	78
No. 1	NTC-15	0.49	13	44.0	35.3	80
No. 1	STC-4	0.51	12	44.0	39.5	90
No. 1	STC-9	0.79	11	88.0	77.7	88
No. 2	NTC-15	0.84	12	103.3	81.8	79

Tracer Detention Time

Our data show that the tracer detention time (τ_a) was slightly longer than the nominal detention time (τ) in all the test cells (Table 3.5). This suggests there may have been some inaccuracies associated with the flow, mass, or volume (particularly depth) measurements. Given the careful measurements of injection mass and flow, we suspect that cell volume (inconsistent bottom substrate elevations) or vegetation effects likely account for the disparity between the measured and nominal HRTs.

Table 3.5. Comparison of nominal (τ) and measured (τ_a) hydraulic retention times for four test cells during two separate dye tracer investigations.

Dye						
Assessment	Test Cell	Depth	HLR	τ	τ_a	
Investigation	Designation	(m)	(cm/day)	(days)	(days)	τ_a/τ
No. 1	NTC-1	0.91	10	7.6	8.6	1.13
No. 1	NTC-15	0.49	13	3.6	6.9	1.92
No. 1	STC-4	0.51	12	4.1	4.7	1.15
No. 1	STC-9	0.79	11	6.25	8.0	1.29
No. 2	NTC-15	0.84	12	6.4	8.9	1.39

Hydraulic Efficiency

Figure 3.7 shows a comparison of the dimensionless RTD functions (E_θ) from the four test cells during the first and second dye studies. Table 6 shows a comparison of calculated hydraulic parameters from the dye studies.

The tanks-in-series (TIS) model is a commonly used technique for comparing the hydraulic efficiency of different wetlands. It compares the dimensionless RTD function (E_θ) of a wetland with the theoretical RTD functions of increasing tanks-in-series (TIS) according to Eq. 10. Special cases of the TIS are the single CSTR ($N=1$) and the PFR ($N=\infty$). In other words, the higher N that a wetland represents, the closer it resembles a PFR and less of a CSTR. Hydraulic characteristics of a PFR are more conducive to more efficient treatment of P since the average time that inflow water is retained in the wetland more closely approaches the HRT; or alternatively, a lesser proportion of the inflow water leaves the wetland early.

The calculated TIS values for the test cells lie between 1.35 and 3.3 (Table 3.6). Kadlec and Knight (1996) report a typical range of $2 < N < 8$ for treatment wetlands; three of the five TIS values for SAV dominated test cells fall within this range.

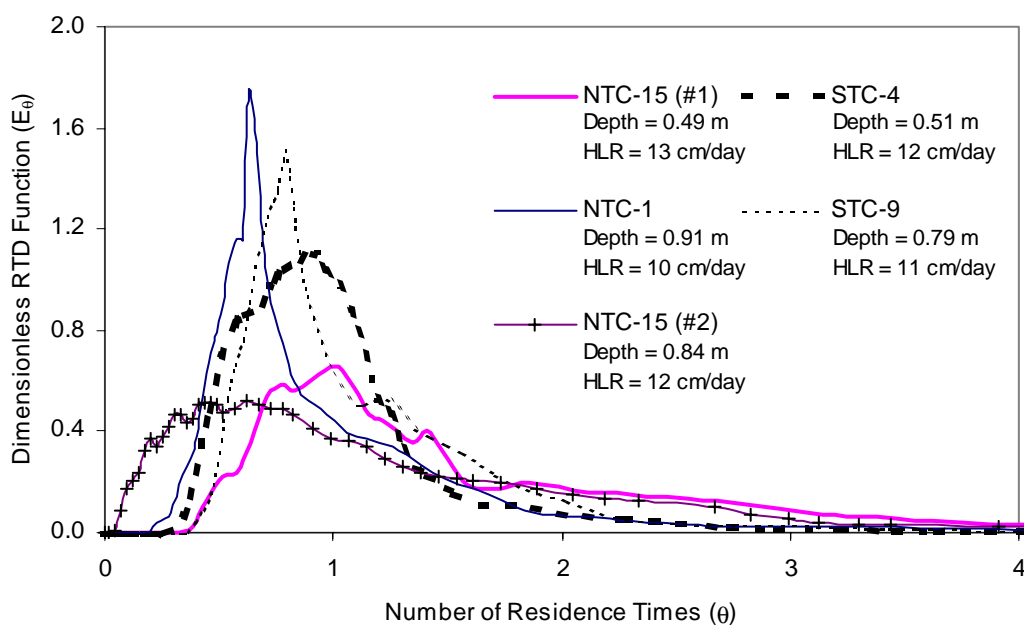


Figure 3.7. Dimensionless residence time distribution (RTD) functions for five test cells during the first and second tracer investigations. The two shallower (0.5 m) test cells (NTC-15 #1 and STC-4) had nominal hydraulic retention times of 3.6 - 4.1 days; the three deeper (0.8 - 0.9 m) test cells (NTC-1, NTC-15 #2, and STC-9) had nominal HRTs of 6.3 - 7.6 days.

A second parameter used to compare hydraulic performance between wetlands is the wetland dispersion number, D , which is a parameter in a dispersed plug flow model. The dispersion number is calculated as the dispersion coefficient divided by the product of the superficial velocity and length of the wetland ($D/[uL]$ in Eq. 13) and describes the ratio of the rate of tracer transport by diffusion or dispersion to convection (bulk flow). Alternately, the Peclet number, Pe , which is the inverse of the dispersion number (Eq. 10), represents the ratio of convection (bulk flow) to transport by diffusion or dispersion processes.

Kadlec (1999) states that values of D range from 0.2 to 0.4 in wetlands (predominantly emergent macrophyte wetlands), which places them in the "large amount of dispersion" category. The D values obtained for the four SAV-dominated test cells in the first dye assessment are mostly within that range (Table 3.6). Although there was some overlap in D between the shallow and deep test cells, the deep test cells were more hydraulically efficient than the shallow test cells.

Table 3.6. Comparison of key hydraulic parameters among four test cells during the first and second dye studies.

Wetland Cell Designation	Water Depth (m)	Nominal HRT τ , days	Measured HRT τ_a , days	Variance σ^2 , day ²	Dimensionless Variance σ_e^2	Tanks-in-Series N	Wetland Dispersion Number D	Peclet Number Pe
NTC-15	0.49	3.6	6.9	28.4	0.60	1.7	0.56	1.79
STC-4	0.51	4.1	4.7	8.4	0.40	2.6	0.27	3.70
NTC-1	0.91	7.6	8.6	29.1	0.39	2.5	0.26	3.85
STC-9	0.79	6.3	8.0	19.3	0.30	3.3	0.18	5.55
NTC-15*	0.84	6.4	8.9	58.5	0.74	1.35	1.00	1.00

* second dye assessment

The range of values for dispersion and Peclet numbers (Table 3.6) indicates that transport within the four SAV dominated test cells was controlled mainly by bulk flow ($D < 1$, $Pe > 1$) during the first dye assessment, but that transport processes in NTC-15 during the second dye assessment were equally proportioned between bulk flow and dispersion. Considering that hydraulic efficiency in treatment wetlands is thought to be enhanced by plug flow rather than dispersive or diffusive flow processes, then some of the test cells (i.e. STC-9) performed better than others (i.e. NTC-15 in the first and second dye studies) from a hydraulic perspective.

The results from the first dye assessment, where duplicate sets of shallow (0.5 m) and deep (0.8 and 0.9 m) SAV-dominated cells were tested, showed near equality in the σ_θ^2 , N , D , and Pe for one deep and one shallow treatment (NTC-1 and STC-4 in Table 3.6). However, there was at least a two-fold difference in these hydraulic parameters between the other pair of deep and shallow test cells, with the deeper cell (STC-9) expressing more plug flow behavior than the shallower (NTC-15). This finding is contradictory to what we would have expected, based on the test cell antecedent conditions (maintained at 1.1 m deep for 5 previous months) and modifications to the test cells prior to this evaluation (lowering depth to values indicated in Table 6 within two weeks prior to evaluation). Assuming that the test cells had equal volumetric SAV densities prior to stage changes, the shallow test cells would have had a more dense SAV community (on a volumetric basis) than the deeper cells, since the same biomass was occupying less volume of water. Nepf et al (1997) and Kadlec et al. (1993) both suggest a tendency towards decreased dispersion with increased vegetation density, however our findings (Table 6) for SAV systems suggest the opposite.

Figure 3.8 shows a comparison between the dimensionless RTD for NTC-15 after a decrease in stage (first dye assessment) and after an increase in stage (second dye assessment). We attribute the early breakthrough in the second dye assessment to vertical short-circuiting over top of the SAV community before the SAV expanded to occupy the entire water volume. Clearly, the effect of water stage change on hydraulic performance (Figure 3.8) is much more pronounced in SAV wetlands than in emergent macrophyte wetlands.

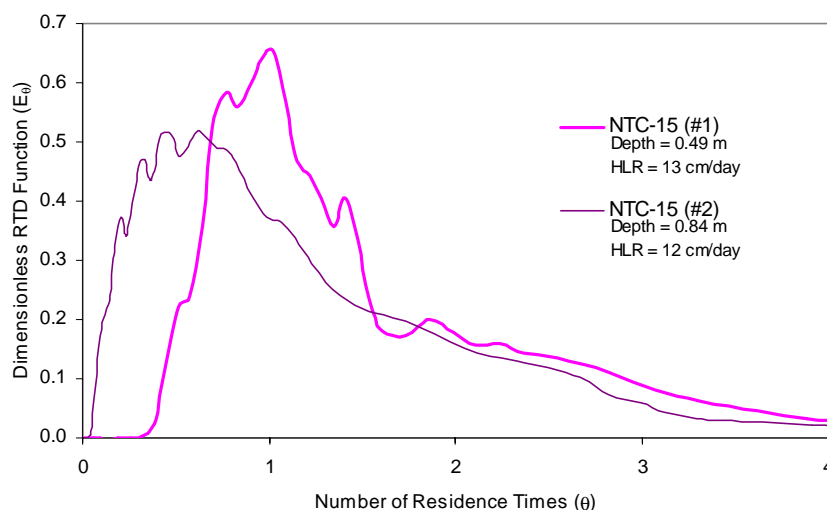


Figure 3.8. Dimensionless residence time distribution (RTD) functions for test cell NTC-15 at depths of 0.49 m (NTC-15 #1, $\tau=3.6$ days) and 0.84 m (NTC-15 #2, $\tau=6.4$ days) during the first and second tracer studies.

3.4 Limerock Berm Installation and Permeability

3.4.1 Installation of Limerock Berms

In our Phase 1 project, we demonstrated that filtration of SAV mesocosm effluent through limerock columns was beneficial in removing some fraction of the dissolved organic and particulate phosphorus, which may ultimately transform to SRP (DBEL 1999). Any SRP released in this manner will be removed by the SAV located between the berm and the outflow weir. To investigate this premise at a larger scale, we installed limerock berms in two of our test cells, NTC-15 and STC-9, in April 2000.

The berms are located approximately 88% down the length of the test cells from the inflow. Each berm was constructed directly on top of the existing test cell peat substrate. The foundation of each berm was comprised of two layers of structural geotechnical fabrics, sandwiching 6 inches of limerock base fill material. The foundation served two purposes: to provide a 'snowshoe' effect by distributing the weight of the berm evenly over the peat substrate and to protect the test cell liner during installation and removal. Each berm foundation is approximately 16 feet wide.

The washed limerock comprising the berms is No. 4 Ballast Stone (approximately 1 inch diameter). Each berm is approximately 4 feet tall and 4 feet wide at the top, with sides that taper from the 4 feet top width to the 16 feet foundation width. Each fully installed berm contains approximately 130 yd³ of limerock.

Assuming an average water depth of 1.3' (40 cm), the mean length of travel in the direction of flow through the berm (berm width) is approximately 14'. For reference, if the test cell HLR was 10 cm/day (HRT = 4 days), the mean residence time in the berm would be about 5 hours, which is comparable to residence times in limerock column studies from our Phase 1 work (DBEL 1999).

3.4.2 Limerock Berm Head Loss Assessment

Following berm construction, we conducted head loss measurements in NTC-15 on June 16 and STC-9 on June 19, 2000. Head loss was again measured in NTC-15 on October 3 and 4, 2001, at

the end of the assessment. This was performed by increasing the influent aperture to allow maximum flow through the cell, and measuring the water stage with surveying equipment on either side of the berm. The berms caused no measurable difference ($\pm 1/100$ foot) in stage either just after berm construction, or after seventeen months of operation.

3.5 Sediment Characteristics and Accretion

Sediments were cored (core barrel inside diameter of 10 cm) at four locations along the longitudinal centerline from each of the four test cells upon completion of the monitoring period, on September 20 and 21, 2001. The first (A), second (B), third (C), and fourth (D) cores retrieved from each test cell represented areas that were 20, 50, 80, and 90% distant from the inflow manifold. For the two cells with limerock berms (NTC-15 and STC-9), this meant that one of the cores was taken immediately before the berm on the upstream side, while the other was collected immediately after the berm on the downstream side.

The accrued sediment was separated from the underlying muck soil in the field. After measuring the depth of the accrued layer, the sediment bulk density, total P and total Ca were characterized in the lab.

Bulk density, total P and total Ca concentrations varied considerably among the four stations within each test cell (Table 3.7). While the bulk densities were highest at the station cored nearest to the inflow manifold in each cell, total P concentration was frequently the lowest. For all four test cells, but especially in STC-4 and STC-9, sediment P concentrations were considerably higher near the outflow than they were for some or all of the interior (i.e., upstream) stations (Table 3.7). We attribute this heterogeneity in sediment P composition at the south test cells to a low P loading rates (0.53-0.58 g P/m²-yr) and a low inflow SRP concentration (mean=6 µg/L; range=1-30 µg/L). Although P loading rates (3.0-4.1 g P/m²-yr) and inflow SRP concentrations (mean=26 µg/L; range=2-106 µg/L) were higher for the north test cells than the south test cells, the uncertainty of the P loading rates prior to September 1999 and the low number of cores (4) taken within each cell, also contributed to the heterogeneous findings. Based on survey work performed by DBE staff, the bottom sediment contours are very uneven in both the north test cells; areas within the center of NTC-1 separated by a distance of

15 m had water depths that frequently varied by 0.4 m. This also contributed to the variability in the sediment accrual rate (Table 3.7).

Table 3.7. Bulk density, total P and total Ca concentrations, P storage, and accrual rate for sediments along a longitudinal gradient in each SAV-dominated test cell. Sediment samples were collected September 20 – 21, 2001.

Station	Horizontal Distance from Inflow	Bulk Density (g/cm ³)	Accrual Rate* (cm/yr)	Total Ca (%)	Total P	
					Conc. (mg/kg)	Storage (g/m ²)
NTC-1A	20%	0.148	3.3	17	607	9.2
NTC-1B	50%	0.103	4.6	18	534	7.7
NTC-1C	80%	0.114	2.9	11	306	3.1
NTC-1D	90%	0.103	3.4	20	503	5.4
NTC-1 Mean		0.117	3.6	16	488	6.4
NTC-15A	20%	0.137	1.3	14	358	2.1
NTC-15B	50%	0.081	3.8	23	594	5.5
NTC-15C	80%	0.079	2.2	25	553	2.9
NTC-15D	90%	0.084	2.2	22	595	3.7
NTC-15 Mean		0.095	2.4	21	527	3.5
STC-4A	20%	0.242	1.3	17	234	1.9
STC-4B	50%	0.095	1.4	26	561	1.9
STC-4C	80%	0.104	1.1	20	530	1.6
STC-4D	90%	0.070	0.5	16	758	0.7
STC-4 Mean		0.128	1.1	20	521	1.5
STC-9A	20%	0.169	1.1	21	458	2.2
STC-9B	50%	0.094	1.8	22	412	1.8
STC-9C	80%	0.142	1.1	12	346	1.3
STC-9D	90%	0.086	1.6	19	766	2.8
STC-9 Mean		0.123	1.4	18	496	2.0

* September 1, 1998 to September 20, 2001 for north test cells and March 1, 1999 to September 20, 2001 for south test cells.

Due to wide variability among the test cell sediment cores, we were unable to discern a longitudinal sediment P concentration gradient (which is contrary to what we have seen for other platforms (i.e., Cell 4 and mesocosms)). We also found similar mean sediment total P concentration values among the four test cells (Table 3.7). Considering that the P loading was over five times higher in the north than the south test cells, differences in the P sediment

deposition should have been observed after 37 months (north test cells) and 31 months (south test cells) of operation. Although there was a general pattern of decreasing P storage with distance from the inflow manifold, the pattern was by no means consistent within several of the test cells (Table 3.7). Again, the spatial heterogeneity of the bottom contours coupled with the low number of sediment cores retrieved from each cell, probably led to these incongruous findings.

By contrast, the average P mass stored in the sediment did show an expected ranking between the north (post-BMP) and south (post-STA) test cells. Both NTC-1 and NTC-15 sediment P storages, although differing by almost 100% (6.4 vs. 3.5 g P/m²), were still considerably higher than the P accumulation in the sediments of the south test cells (STC-4: 1.5 g P/m² and STC-9: 2.0 g P/m²).

To assist our efforts in quantifying the accretion of sediments in the test cells, feldspar horizon markers were installed on August 23, 2000 in each of the four SAV test cells (NTC-1, NTC-15, STC-4 and STC-9). We selected four stations within each test cell for placement of the feldspar marker locations - two were placed one-quarter distant from the inlet manifold (20 m) and about one-third distant from each side bank, and two were located three-quarters distant from the inlet manifold (60 m), and again one-third from each side bank.

At each of the four designated horizon marker locations within each test cell, we poured approximately 1.25 gallons of dry feldspar (potash of soda G-200) into a 43-cm diameter open-ended metal enclosure. This produced an initial horizon thickness of 3.3 cm. To allow enough time for the deposition of the feldspar, the metal enclosures were left in place for 24 hours after the initial pour. The location of each horizon marker was designated by four upright equally-spaced PVC poles arranged along the circumference of the feldspar layer.

The area inside each of the horizon markers was cored (4 cores per marker location) on September 20 – 21, 2001. The inside diameter of the cores was 4.4 cm. The cores were frozen and the sediment later extruded from the core barrel while still frozen. The depth of accrued sediment relative to the surface of the feldspar layer at the left edge, center and right edge of

each sediment core was measured. The mean of the left and right edge measurements were averaged with the center depth to arrive at an overall mean depth value for the accrued sediment layer.

Based on 13 months of deposition, the feldspar horizon markers indicated sediment accrual rates that were higher (Table 3.8) than sedimentation rates obtained from other platforms (mesocosms and Cell 4). The latter measurements relied on the readily identifiable nonconformity between the underlying native muck and the accrued wetland organic marl as the marker. In most of the cores retrieved from the feldspar marker pads, the feldspar horizon rested just above the more consolidated muck layer. We offer the following explanations as to why there was higher than expected sediment accrual rates using the feldspar horizon marker technique.

1. Since the SAV was removed from the area prior to applying the feldspar powder, removal of some of the substrate attached to the roots or holdfasts may have occurred.
2. The period of SAV colonization prior to laying down the feldspar layer may have been characterized by low plant growth (and little detritus production). Low HLRs (< 6 cm/day) were provided for most of the period from September 1999 until the date of feldspar application (August 23, 2000) for NTC-15, STC-4, and STC-9. Thereafter, loading rates were increased to 12-24 cm/day in the north test cells (south test cells continued to receive 5-6 cm/day).
3. Test cells NTC-15, STC-4, and STC-9 were dried out for several months in 2000 for aquatic plant management purposes and LR berm installation (NTC-15 and STC-9 only), which may have partially oxidized and consolidated the SAV-derived sediment layer.
4. The feldspar marker may have slowly sunk into the loosely aggregated sediments over time, until it rested on top of the heavier and more consolidated native muck horizon.

Table 3.8. Accrual rates (cm/yr) of sediments according to feldspar horizon markers in four SAV-dominated test cells from August 23, 2000 to September 20-21, 2001. Each of the four feldspar marker locations sites (Front North, Front South, Back North, Back South) within a test cell represents the mean of four cores.

Site	Accrual Rate	Site	Accrual Rate
NTC-1 Front North	10.2	STC-4 Front North	2.7
NTC-1 Front South	9.6	STC-4 Front South	3.7
NTC-1 Front Mean	9.9	STC-4 Front Mean	3.2
NTC-1 Back North	5.6	STC-4 Back North	2.1
NTC-1 Back South	7.8	STC-4 Back South	2.9
NTC-1 Back Mean	6.7	STC-4 Back Mean	2.5
<i>NTC-1 Mean</i>	<i>8.3</i>	<i>STC-4 Mean</i>	<i>2.8</i>
NTC-15 Front North	8.3	STC-9 Front North	2.4
NTC-15 Front South	8.8	STC-9 Front South	0.2
NTC-15 Front Mean	8.6	STC-9 Front Mean	1.3
NTC-15 Back North	9.0	STC-9 Back North	3.3
NTC-15 Back South	2.9	STC-9 Back South	2.2
NTC-15 Back Mean	6.0	STC-9 Back Mean	2.8
<i>NTC-15 Mean</i>	<i>7.3</i>	<i>STC-9 Mean</i>	<i>2.0</i>
<i>NTC Mean</i>	<i>7.8</i>	<i>STC Mean</i>	<i>2.4</i>

3.6 Nitrogen and Suspended Solids Removal

From October 4, 2000 to April 16, 2001, and then again beginning on July 18, 2001, monthly grab-sampled test cell inflow and outflow waters were analyzed for total suspended solids (TSS), total Kjeldahl nitrogen (TKN), nitrite + nitrate (NO_x), and ammonium (NH_4). For the north test cells, the largest nitrogen concentration reductions on a percentage basis were for $\text{NH}_4\text{-N}$ (Table 3.9). Removal was higher in NTC-1 than NTC-15 for all the major nitrogen species. Even though we observed higher nitrite + nitrate concentrations in the inflow of the south test cells than in the north test cells, outflow concentrations at the south site were still below the detection limit. Total Kjeldahl N removal was inconsistent across the four test cells. Apparently organic nitrogen, the largest contributor to the TKN, is not readily removed in the

SAV communities. The presence of a LR berm may have contributed some ammonium to the water column since the outflow concentrations of NH₄-N were higher in test cells with berms than in the comparable cells without berms.

Total suspended solids (TSS) concentrations in the outflow increased in three of the four test cells compared to the inflow concentrations. Nevertheless, the outflow concentrations were still low (≤ 3.1 mg/L) and within acceptable water quality guidelines.

Table 3.9. Mean monthly total Kjeldahl nitrogen (TKN), nitrite + nitrate nitrogen (NO_x-N), and ammonium nitrogen (NH₄-N) concentrations in the inflow and outflow of four test cells (NTC-1, NTC-15, STC-4, STC-9) dominated by submersed aquatic vegetation from October 14, 2000 to April 16, 2001 and on July 18, 2001. All values are in units of mg/L.

	NTC-1		NTC-15		STC-4		STC-9	
	Inflow	Outflow	Inflow	Outflow	Inflow	Outflow	Inflow	Outflow
TKN	2.23	2.73	2.65	2.55	2.54	2.68	3.72	2.27
NH ₄ -N	0.317	0.054	0.312	0.127	0.134	0.061	0.151	0.152
NO _x -N	0.049	0.022*	0.048	0.022*	0.12	0.022*	0.116	0.022*
TSS	1.0	1.7	1.1	0.8	0.7	3.1	0.5	2.6

* denotes concentrations below the detection limit.

3.6.1 Phosphorus Removal Performance

Operational Changes

North Test Cells

During the period of operation, NTC-1 and NTC-15 were subjected to a gradually increasing flow regime (Table 3.10). From July 2000 – March 2001, NTC-15 inflows averaged 140 m³/day (5.1 cm/day). From March – May 2001, inflows averaged 320 m³/day (11.7 cm/day), and from June – Sept. 2001, mean inflows were 588 m³/day (21.5 cm/day). The HLR for NTC-1 was higher than NTC-15, increasing from 12.1 cm/day during September 2000 to June 2001 to 22.5 cm/day from June to September 2001.

As a result of a test cell water depth survey conducted by DBE personnel, the water depths were adjusted by manipulating the weirs on April 6, 2001 to more desirable target depths (Table 3.10). These verified depths, along with the increase in HLRs in the two north test cells on June 1st, altered the HRT within each of the cells (Table 3.10).

Table 3.10. The history of water depths, hydraulic loading rates (HLR), and hydraulic retention times (HRT) in the test cells from August 4, 2000 until termination of the assessment (September, 2001). Water depths and HLRs were changed frequently in the prior operational period (pre-August 2000).

Test Cell	Depth (m)		HLR (cm/day)		HRT (days)	
	8/4/00	4/6/01	8/4/00	6/1/01	8/4/00	6/1/01
	to 4/5/01	to 9/14/01	to 6/1/01	to 9/14/01	to 6/1/01	to 9/14/01
NTC-1	0.74	0.60	12.1	22.5	6.1	2.7
NTC-15	0.96	0.60	7.3**	20.5	12.9**	3.5
STC-4	0.22	0.30	5.5	5.7	4.5	5.3
STC-9	0.45	0.45*	6.0	6.1	7.5	7.5

* Water depth was decreased to 0.30 m on April 6, 2001 and increased from 0.30 to 0.45 m on May 1, 2001.

** Represents the time-weighted average of 5.6 cm/day from August 4, 2000 to March 7, 2001 and 11.2 cm/day from March 8 to June 1, 2001.

South Test Cells

Flows and water depths in the two south test cells were subject to less variation than for the north test cells (Table 3.10). As a result of the DBE depth survey in STC-4, the water level in that cell was increased from 0.22 to 0.30 m in April 2001. With the exception of a three-week period in May where the water depth was 0.3 m, the test cell water depth was maintained between 0.45 and 0.55 m in STC-9.

Phosphorus Removal Performance

We analyzed P water quality performance data by splitting the data set into two periods, representing “before” and “after” the installation of the LR berms in NTC-15 and STC-9 during April and May 2000. For the period prior to the placement of the LR berm (September 1, 1999 to April 4, 2000), the average total P concentration was higher in the outflow of NTC-1 by 6 µg/L than in the outflow of NTC-15 (Table 3.11). Differences in the outflow TP concentrations probably reflect the considerable changes in the HLR to the cells during this period. For example, the HLR was increased from 10-13 cm/day to 40 cm/day in NTC-1 for 20 days, and then was reduced to 2-3 cm/day for the following 6 months. The HLR for NTC-15 was never set higher than the initial 10-13 cm/day, and was maintained at the lower rate of 2-3 cm/day for only 53 days. Thus NTC-1 was subjected to the extremes in HLR more frequently and for longer

periods than was NTC-15, which may have affected the TP removal performance of the wetland.

Table 3.11. Soluble reactive P (SRP), dissolved organic P (DOP), particulate P (PP), and total P (TP) removals in the north test cells before (September 1, 1999 to April 4, 2000) and after (June 23, 2000 to September 14, 2001) the installation of the LR berm at NTC-15. Values are means \pm 1 standard deviation.

	SRP ($\mu\text{g/L}$)		DOP ($\mu\text{g/L}$)		PP ($\mu\text{g/L}$)		TP ($\mu\text{g/L}$)	
	Pre-LR Period	Post-LR Period	Pre-LR Period	Post-LR Period	Pre-LR Period	Post-LR Period	Pre-LR Period	Post-LR Period
NTC-1 Inflow	-	25 \pm 23	-	15 \pm 19	-	33 \pm 15	71 \pm 27	73 \pm 37
NTC-1 Outflow	-	3 \pm 7	-	10 \pm 5	-	12 \pm 5	27 \pm 14	24 \pm 15
Removal ($\mu\text{g/L}$)	-	22	-	5	-	21	44	49
Removal (%)	-	88%	-	33%	-	64%	62%	67%
NTC-15 Inflow	-	28 \pm 24	-	16 \pm 12	-	31 \pm 14	73 \pm 27	74 \pm 38
NTC-15 Outflow	-	2 \pm 1	-	8 \pm 3	-	10 \pm 5	21 \pm 7	20 \pm 6
Removal ($\mu\text{g/L}$)	-	26	-	8	-	21	52	54
Removal (%)	-	93%	-	50%	-	68%	71%	73%

We observed marked performance differences between NTC-1 and NTC-15 from June 2001 to the end of the evaluation in mid-September 2001 (Figure 3.9). After placement of the LR berm in NTC-15 and resumption of P monitoring in that test cell on June 23, 2000 (which included SRP and TSP), the mean TP outflow concentration from NTC-15 was lower than that of NTC-1 by 4 $\mu\text{g/L}$ (Table 3.11). Reductions in both DOP and PP concentrations within NTC-1 and NTC-15 contributed to the overall reduction in TP concentration in the test cells (Table 3.11). Since the HLR (and thus the P loading) to NTC-1 was more than double that to NTC-15 (12.1 vs. 5.1 cm/day) for 5 of the 15 months of the post-LR berm installation period, the mass removals achieved in the two test cells (3.25 $\text{g P/m}^2\text{-yr}$ for NTC-1 and 2.20 $\text{g P/m}^2\text{-yr}$ for NTC-15) cannot be compared based only on the presence or absence of the LR berm. However, a slightly higher percentage of the loaded P was removed in NTC-15 (75%) than in NTC-1 (73%) during a 3.5-month period (6/02/01-9/14/01) when HLRs to both test cells were comparable (20.5 and 22.4 cm/day) (Table 3.12). It is thus possible that the presence of a LR berm may have enhanced P removal, even at these high HLRs.

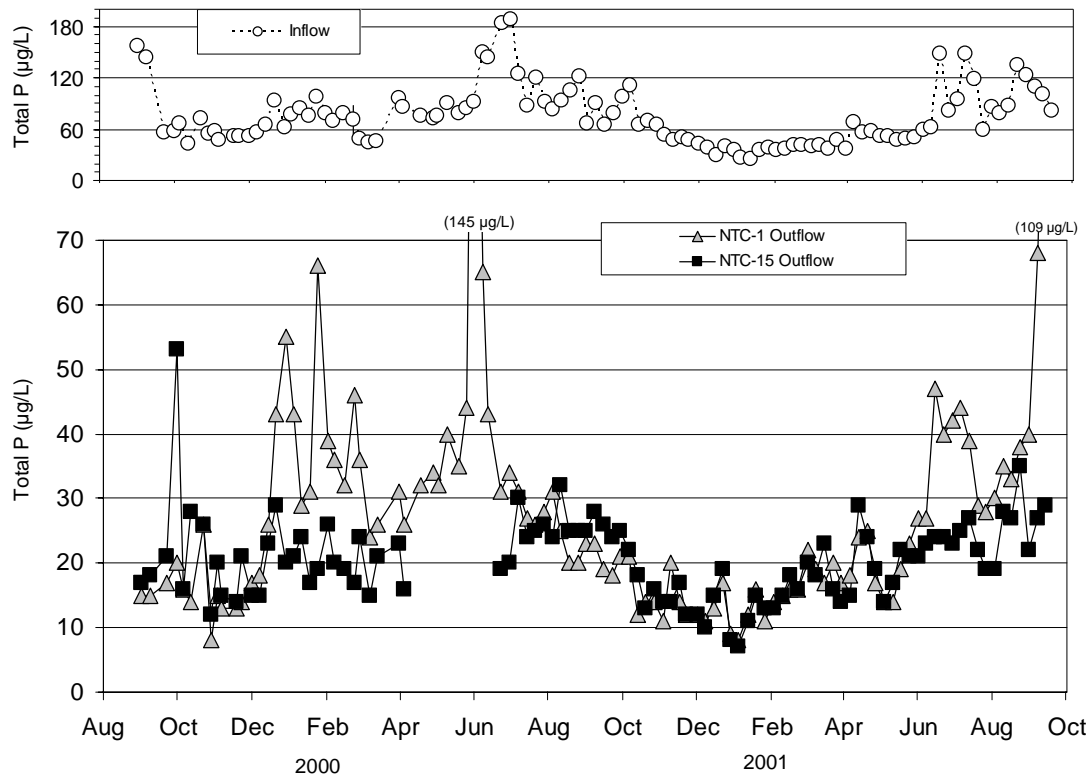


Figure 3.9. Total phosphorus concentrations in the inflows and outflows of two north test cells (NTC-1 and NTC-15) dominated by SAV before (September 1, 1999 to April 4, 2000) and after (June 23, 2000 to September 14, 2001) the installation of the NTC-15 limerock berm. The inflow total phosphorus represents the mean of two samples collected at each of the two test cells.

Table 3.12. Hydraulic loading rate (HLR) and phosphorus mass loading and removal rates for the north and south test cells after installation of limerock berms in NTC-15 and STC-9. Data from the north test cells are divided into the entire period of record after limerock berm installation (6/23/00 to 9/14/01) and a shorter period (6/02/01 to 9/14/01) for when hydraulic loading rates were high (22.4 and 20.5 cm/day).

Test Cell	Period of Record	Loading Rate		P Removal	
		HLR (cm/day)	P (g/m ² -yr)	P (g/m ² -yr)	%
NTC-1	6/23/00-9/14/01	14.5*	4.11	3.25	79
NTC-1	6/02/01-9/14/01	22.4	8.28	6.07	73
NTC-15	6/23/00-9/14/01	10.1*	3.01	2.20	73
NTC-15	6/02/01-9/14/01	20.5	7.54	5.68	75
STC-4	8/04/00-9/14/01	5.6	0.53	0.08	15
STC-9	8/04/00-9/14/01	6.1	0.58	0.20	34

* Time-weighted mean

During the evaluation period, we collected samples for TP analysis from in front of the limerock berm (“pre-berm” samples), as well as from the test cell outflows. This enabled us to quantify the performance of the LR berm and associated downstream “polishing wetland”. For STC-9, the berm and the “polishing wetland” immediately provided some P removal, although it was sporadic over time. Although the relative contributions of the LR berm and “polishing wetland” in the incremental removal of P are unknown, we believe most of the enhanced P removal originates from processes associated with the LR berm. For example, TP removal by the LR berm at NTC-15 was delayed, with initial export of TP, followed by increasing removal over time (Figure 3.10). This is consistent with our LR data from mesocosms treating Post-BMP water, which indicated that a several month conditioning period is required before particulate P removal will occur within a LR bed. We believe that some of the organic particles trapped within LR beds undergo mineralization to SRP, which can then be readily assimilated by the downstream SAV community.

The enhanced P removal afforded by a LR berm notwithstanding, the efficient P removal performance in the test cell without the LR berm (NTC-1) under a HLR of 22.5 cm/day demonstrates the effective P removal of SAV-dominated wetlands under high loadings. A key factor in this performance is the thorough depletion of inflow SRP: the SAV community in both test cells removed essentially all of the SRP from the Post-BMP waters, reducing levels of this constituent from 25 and 28 to 2-3 µg/L. Over 60% of the particulate P also was removed within the two north test cells (Table 3.11).

The outflow TP concentration of STC-9 was higher by 6 µg/L than that of STC-4 during the September 1, 1999 to March 13, 2000 period before installation of the LR berm in STC-9 (Table 3.13). Since total P concentrations in the outflow of STC-9 were higher than the inflow concentrations, P was being exported from the test cell prior to the installation of the LR berm. Most of the export occurred during the beginning of the monitoring period (Figure 3.11), and may have been due to high P leaching from the native muck that was deposited into the cell during construction. Since a cattail community inhabited the cell prior to being converted into a

SAV-dominated system, release from decomposing cattail tissues or cattail-derived organic detritus may also have contributed to a flush of P at the beginning of the monitoring period.

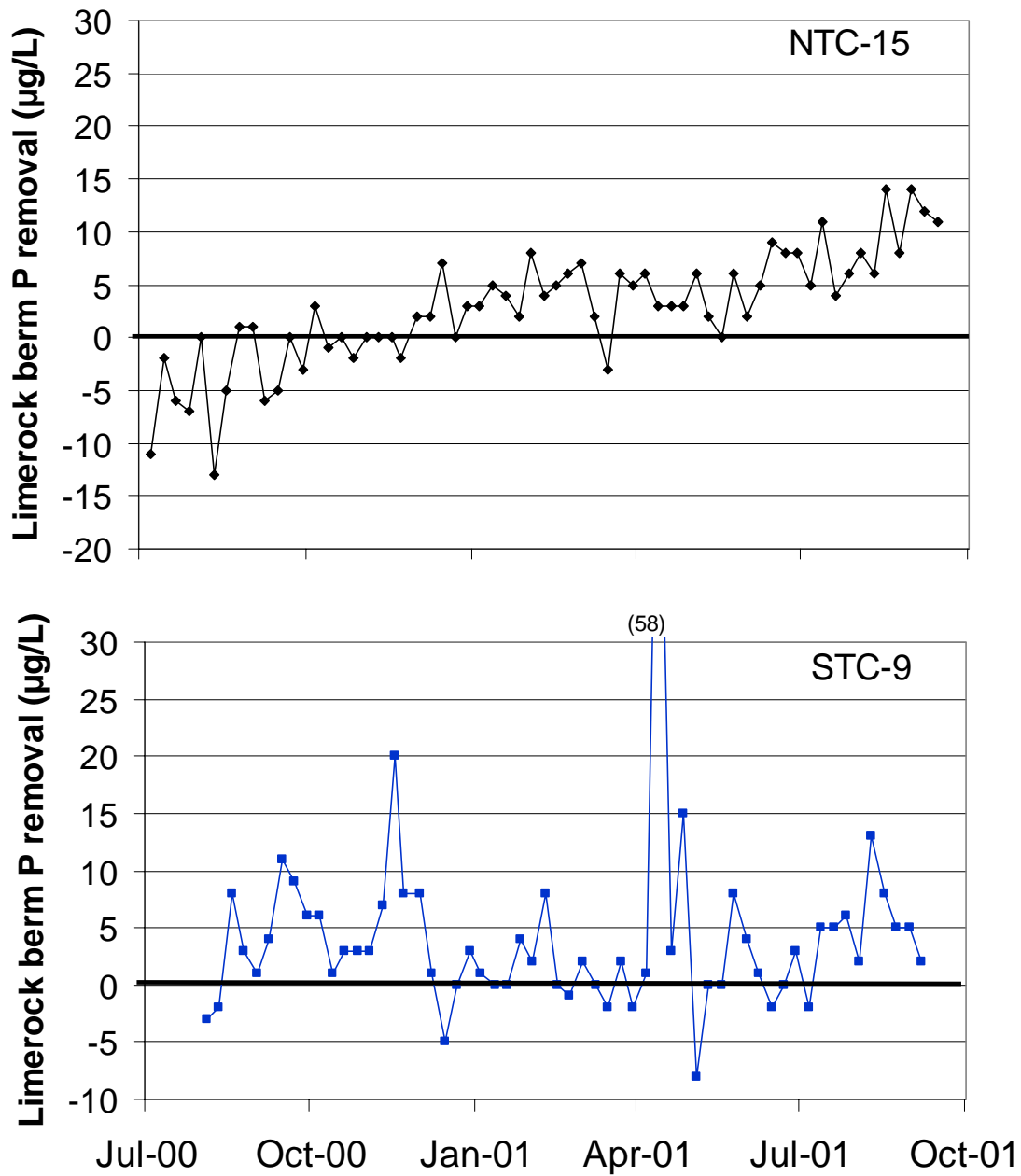


Figure 3.10. Total P removal provided by limerock berms (and downstream “polishing” wetlands) in NTC-15 and STC-9.

Table 3.13. Soluble reactive P (SRP), dissolved organic P (DOP), particulate P (PP), and total P (TP) removals in the south test cells before (September 1, 1999 to March 13, 2000) and after (August 4, 2000 to September 14, 2001) the installation of the LR berm at STC-9. Values are means \pm 1 standard deviation.

	SRP ($\mu\text{g/L}$)		DOP ($\mu\text{g/L}$)		PP ($\mu\text{g/L}$)		TP ($\mu\text{g/L}$)	
	Pre-LR Period	Post-LR Period	Pre-LR Period	Post-LR Period	Pre-LR Period	Post-LR Period	Pre-LR Period	Post-LR Period
STC-4 Inflow	-	5 \pm 3	-	10 \pm 3	-	11 \pm 8	18 \pm 4	26 \pm 9
STC-4 Outflow	-	2 \pm 1	-	9 \pm 2	-	11 \pm 4	16 \pm 4	22 \pm 4
Removal ($\mu\text{g/L}$)	-	3	-	1	-	0	2	4
Removal (%)	-	60%	-	10%	-	0%	11%	15%
STC-9 Inflow	-	6 \pm 4	-	10 \pm 3	-	10 \pm 8	18 \pm 4	26 \pm 9
STC-9 Outflow	-	2 \pm 1	-	8 \pm 3	-	7 \pm 4	22 \pm 8	17 \pm 4
Removal ($\mu\text{g/L}$)	-	4	-	2	-	3	-4	9
Removal (%)	-	67%	-	20%	-	30%	-22%	35%

After LR berm installation at STC-9 and the resumption of monitoring on August 4, 2000, the outflow concentration at STC-9 was on average 5 $\mu\text{g/L}$ lower than that of STC-4 (Table 3.13). Dissolved organic P and PP made up most of the TP differential in the outflow concentrations between the two south test cells (Table 3.13); SRP in the inflow waters (5-6 $\mu\text{g/L}$) was stripped to background levels (2 $\mu\text{g/L}$) with passage through both wetlands. Temporally, the greatest divergence in the outflow TP concentrations of the two south test cells occurred during the last 3 months of the assessment, although there was a consistent difference in the outflow concentrations apparent soon after the resumption of data collection (Figure 3.11). Even though P loading was similar for each test cell (Table 3.12), mass P removal was higher for STC-9 than for STC-4 (0.20 g P/m²-yr vs. 0.08 g P/m²-yr) during the post LR-berm installation period (August 4, 2000 to September 14, 2001). The difference in the P removal efficiencies between the STC-4 (15%) and STC-9 (34%) is likely due to the LR berm in STC-9. The likelihood of the LR berm having a significant positive effect on the P removal in Post-STA waters is further supported by the reversal of the net export of P in STC-9 before LR berm placement to a condition of net P removal afterwards (Table 3.12).

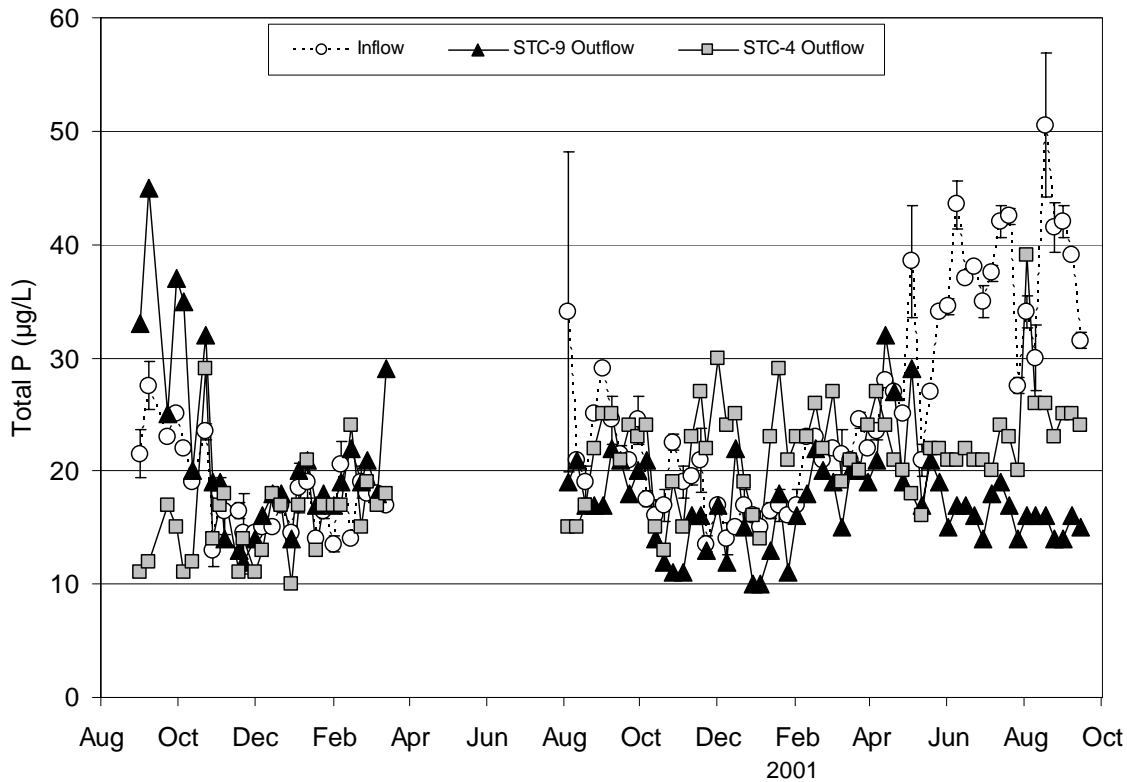


Figure 3.11. Total phosphorus concentrations in the inflows and outflows of two south test cells (STC-4 and STC-9) dominated by SAV before (September 1, 1999 to March 13, 2000) and after (August 4, 2000 to September 14, 2001) the installation of a limerock berm at STC-9. The inflow total phosphorus represents the mean (± 1 s.d.) of two samples taken at each of the two test cells.

Dissolved calcium and total alkalinity concentrations and specific conductance decreased from inflow to outflow stations in all the test cells during the post-LR berm installation period. The south test cells exhibited a greater reduction in constituents than did the north test cells (Table 3.14), probably because of their higher pH values (Table 3.14), shallower depths, and lower HLRs (Table 3.10).

Table 3.14. Dissolved calcium and total alkalinity concentrations, specific conductance, and pH in the north and south test cells after the installation of the LR berms at NTC-15 (June 23, 2000 to September 14, 2001) and at STC-9 (August 4, 2000 to September 14, 2001). Values are means \pm 1 standard deviation.

	Calcium (mg/L)	Alkalinity (mg CaCO ₃ /L)	Conductance (μ S/cm)	pH
NTC-1 Inflow	83 \pm 7	295 \pm 24	1209 \pm 117	7.48 \pm 0.21
NTC-1 Outflow	59 \pm 14	235 \pm 44	1095 \pm 137	7.88 \pm 0.43
Removal	24	60	114	Δ =0.40
NTC-15 Inflow	82 \pm 10	296 \pm 24	1212 \pm 114	7.42 \pm 0.20
NTC-15 Outflow	56 \pm 15	231 \pm 35	1087 \pm 135	7.73 \pm 0.23
Removal	26	65	125	Δ =0.31
STC-1 Inflow	71 \pm 10	274 \pm 20	1175 \pm 123	7.65 \pm 0.24
STC-1 Outflow	31 \pm 12	182 \pm 51	1006 \pm 171	8.71 \pm 0.46
Removal	40	92	169	Δ =1.06
STC-9 Inflow	71 \pm 10	273 \pm 20	1177 \pm 131	7.62 \pm 0.25
STC-9 Outflow	38 \pm 9	200 \pm 43	1033 \pm 170	8.37 \pm 0.33
Removal	33	73	144	Δ =0.75

Conclusions

The 0.2 ha-size test cells demonstrated that SAV-dominated wetlands are very efficient in removing P in post-BMP waters (73-79%), even at high hydraulic (20-22 cm/day) and P (7.5-8.3 g P/m²-yr) loading rates. Soluble reactive P was the most readily sequestered P species at the north and south test cells. Regardless of the inflow SRP concentrations and HLRs, essentially all SRP was removed within all four of the test cells. The installation of LR berms appears to have enhanced the total P removal efficiency more at the south test cell than the north test cell, but this may have been a function of a longer “conditioning time” required for the LR berm at the north test cell. At the south site, the SAV test cell containing a LR berm provided twice the mass P removal of the SAV test cell without a berm.

Section 4: STA-1W Cell 4 Studies and Model Development

STA-1W Cell 4 is likely the most intensively-studied SAV treatment wetland in the world. Cell 4 was initially flooded in September 1993, and flow-through operations were initiated on August 18, 1994. Instrument installation and data reporting began in February 1995. Because of its size (147 ha), operational period (8 yrs), and historical database (8 yrs of hydraulic flows and water quality), we believe it is the best platform for addressing issues of SAV sustainability, P removal performance and costs. During this Phase II project period, we intensively sampled Cell 4 inflows, outflows and internal water quality constituents. We also collected and analyzed Cell 4 sediments, performed sediment-water column flux measurements, sediment organic/inorganic P fractionations, sediment P stability/release assessments, and assessed Cell 4 vegetation characteristics. This effort comprised all of the assessments described under Tasks 7, 8 and 9 in our Experimental Design Plan (DBE, 2000c). We initiate this section with a discussion of Cell 4 Performance during 1998 and 1999, the years of lowest outflow TP concentrations.

4.1 1998 – 1999 Cell 4 Outflow TP Removal Performance

For its entire period of record (2/1/95 – 9/30/02), mean TP inflow and outflow concentrations for Cell 4 have averaged 52 and 22 µg/L, respectively (Figure 4.1). Mass P removal by Cell 4 during this period averaged 1.65 g P/m²-yr, with a mean TP removal rate of 62%. Figure 4.2 shows a time history of inflow and outflow TP concentrations for 1998 – 1999, the period of lowest outflow TP concentrations. The plotted concentrations are from the District's weekly composite TP data collected at the G254 and G256 culverts. Inflow concentrations for the two-year period averaged 46 µg/L and outflow concentrations averaged 14 µg/L. Outflow concentrations were relatively stable during this period, with some evidence of a trend towards rising effluent concentrations beginning December 1999. The Cell 4 effluent TP concentration on December 27, 1999 was 28 µg/L.

Figure 4.2 also highlights composite samples that measured less than or equal to 10 µg/L TP. In 1998, there were three occurrences (out of 47 reported samples) of ≤ 10 µg/L, whereas in 1999

there were 13 occurrences (out of 51 reported samples). Figure 4.3 summarizes 1999 performance with a frequency distribution of TP measurements grouped in 5 µg/L increments. In 1999, 26% of Cell 4 outflow TP measurements were ≤ 10 µg/L, while 78% of measurements were ≤ 15 µg/L.

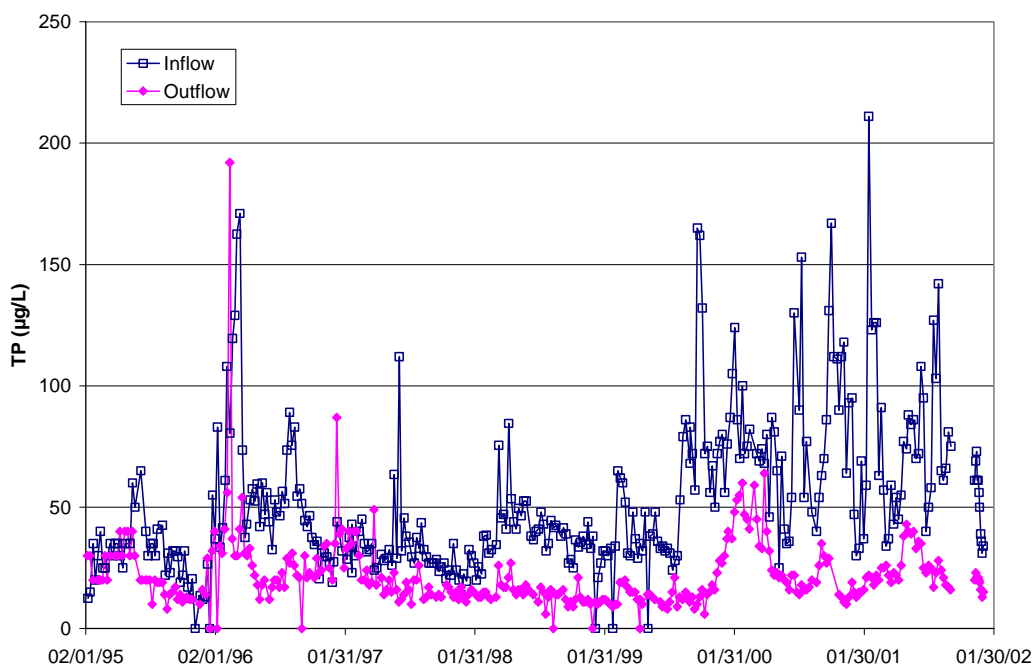


Figure 4.1. Inflow and outflow TP concentrations for STA-1W Cell 4.

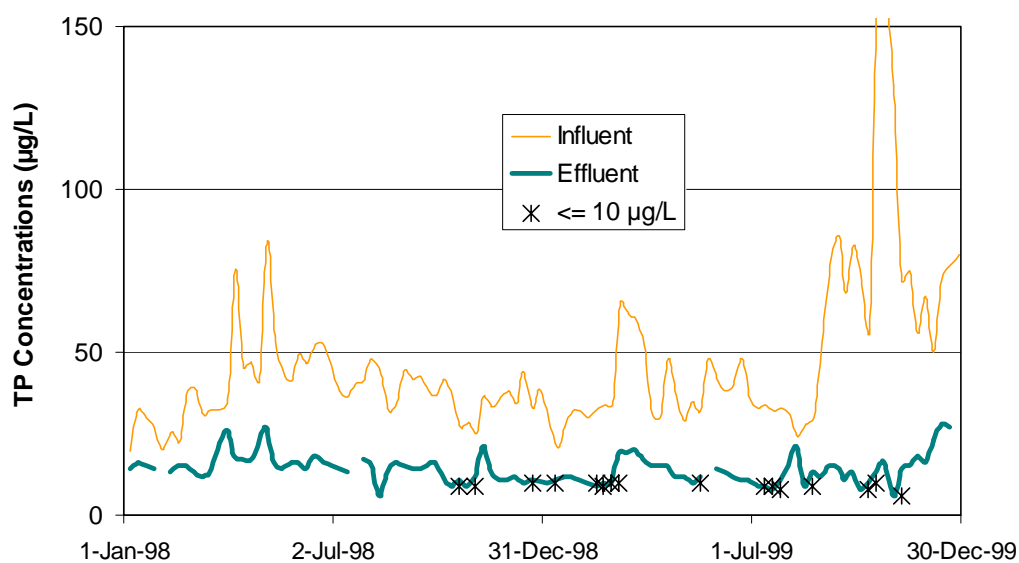


Figure 4.2. Influent and effluent TP concentrations for 1998 – 1999.

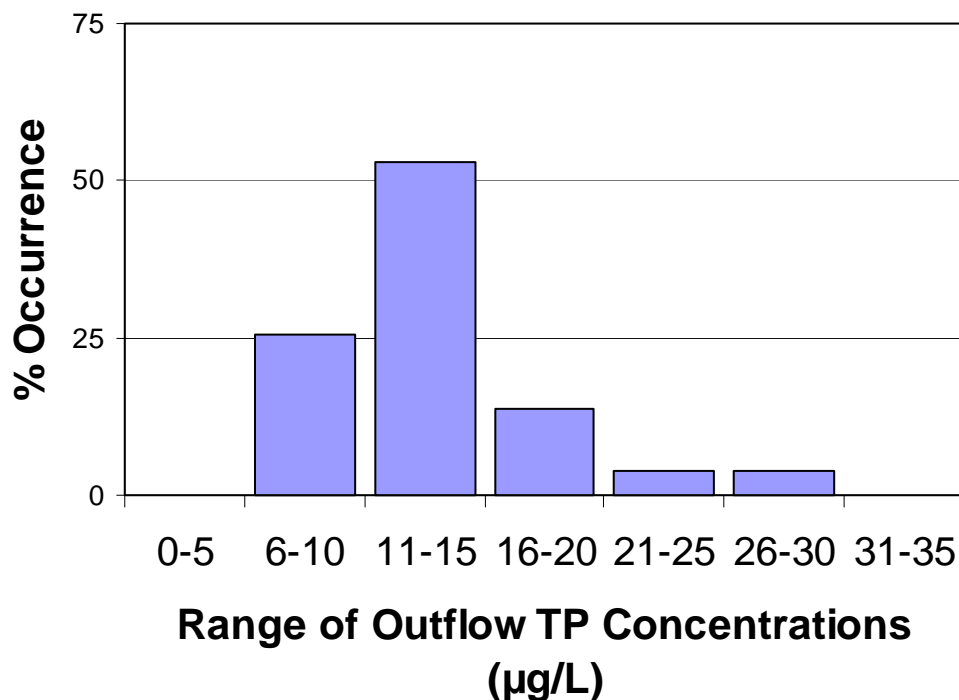


Figure 4.3. Frequency distribution of outflow TP concentrations for 1999, based on 51 weekly composites.

The hydraulic loading rate (HLR) during 1998-1999 ranged between 0.2 and 33 cm/day (Figure 4.4), and averaged 12 cm/day. Beginning September 1999, there was a sustained increase in HLR to an average value of 16 cm/day, approximately 33% higher than the average of the previous 20 months.

Mass loading was calculated by multiplying the daily HLR by the appropriate weekly composite inflow TP concentration. The measured value of TP concentrations from composite samples were assumed to apply to the day collected as well as to the six previous days (composite samples were comprised of 3x daily grabs collected for 7 days). Annualized mass loading averaged 1.5 g/m²/yr for the 20 month period of January 1998 through August 1999, and 4.9 g/m²/yr beginning September 1999. Mass loading to Cell 4 more than tripled in the last months of 1999 (Figure 4.5), primarily because inflow concentrations more than doubled in the last four months of 1999 compared with months previous (Figure 4.2).

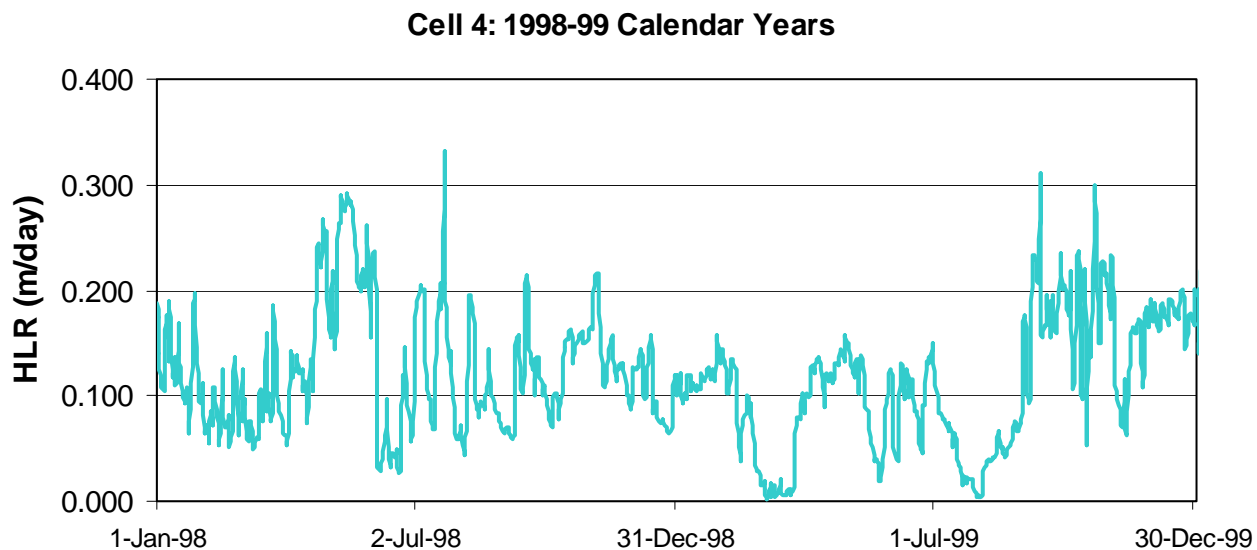


Figure 4.4. Cell 4 hydraulic loading rate (HLR) for 1998 – 1999.

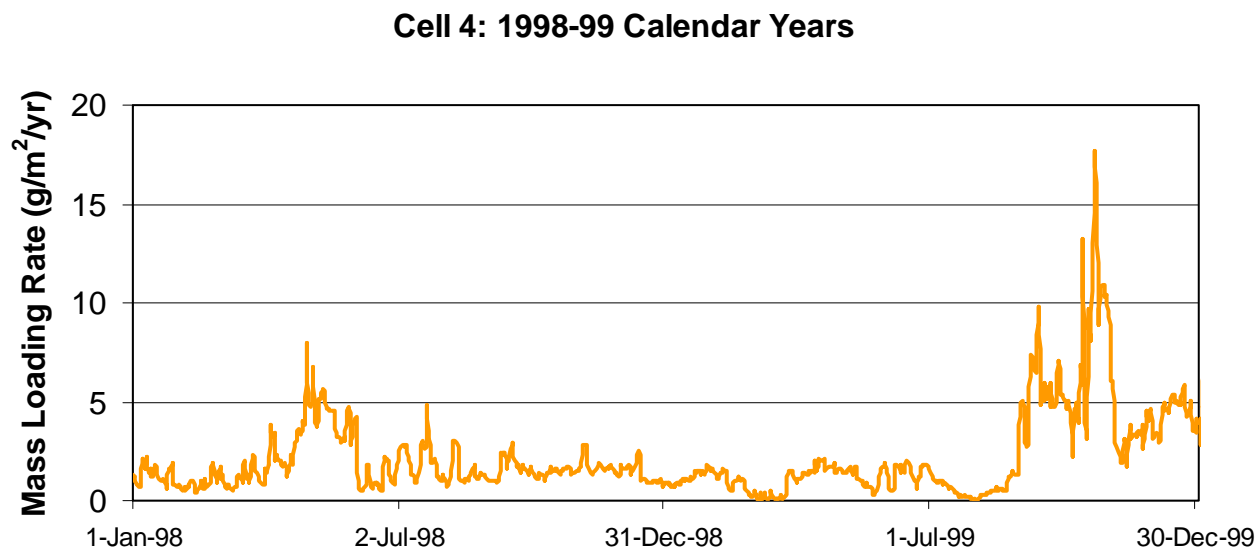


Figure 4.5. Cell 4 annualized TP mass loading rate for 1998 – 1999.

We believe that the December 1999 rise in outflow concentrations (Figure 4.2) was a direct result of the near step-function increase to Cell 4 mass loading that began in September 1999 (Figure 4.5). It is important to note the apparent three-month lag period between increased mass loading (September) and a noticeable response in outflow TP concentrations (December). In fact, during this three month period, there were two occurrences of weekly TP measurements that were $\leq 10 \mu\text{g/L}$. This apparent lag between inflow loading and outflow discharge could be indicative of a short-term storage capacity within SAV systems and a capacity to 'buffer' surges in TP loading, up to a limit.

4.2 Operational and Water Quality Regression Relationships

We performed regression analyses on the 1998 - 1999 Cell 4 data to determine the relative significance of operational parameters on outflow TP concentration and on the TP settling rate (k). The operational parameters that we analyzed were HLR, mass loading, water depth, and nominal velocity (based on an average Cell 4 width of approximately 700 m). To reduce the influence of hydraulic retention time on input/output regression analyses, we used weekly average values for all parameters. Weekly average values of HLR, mass loading, depth, velocity, and settling rate were calculated for the same days as composite TP samples were collected (in the District's data set) using the previous week's flow and depth data. Therefore, the regression analyses for 1998-1999 were based on 98 data points (47 from 1998, 51 from 1999) that represented weekly average values of the plotted parameters.

Figure 4.6 and Figure 4.7 show typical regression plots for mass loading versus TP concentration and TP settling rate (k), respectively. Table 4.1 summarizes correlation coefficients (r^2) for the eight regression analyses performed. Note that the K vs. HLR and K vs. mass loading regressions should be interpreted with caution, as there is a potential for auto-correlation in both of these calculations (common variables are used to calculate both parameters in these regressions). As could be expected, direct correlations between operational parameters and outflow TP concentration were weak, while correlations with settling rate were much stronger. In both cases, the most significant factor (highest r^2) influencing TP removal was the TP mass loading rate. HLR was also an important factor. Positive correlations were evident between settling rate and both velocity and depth, but they were substantially weaker

than compared to TP mass loading (which, as discussed above, could be artificially inflated due to auto-correlation).

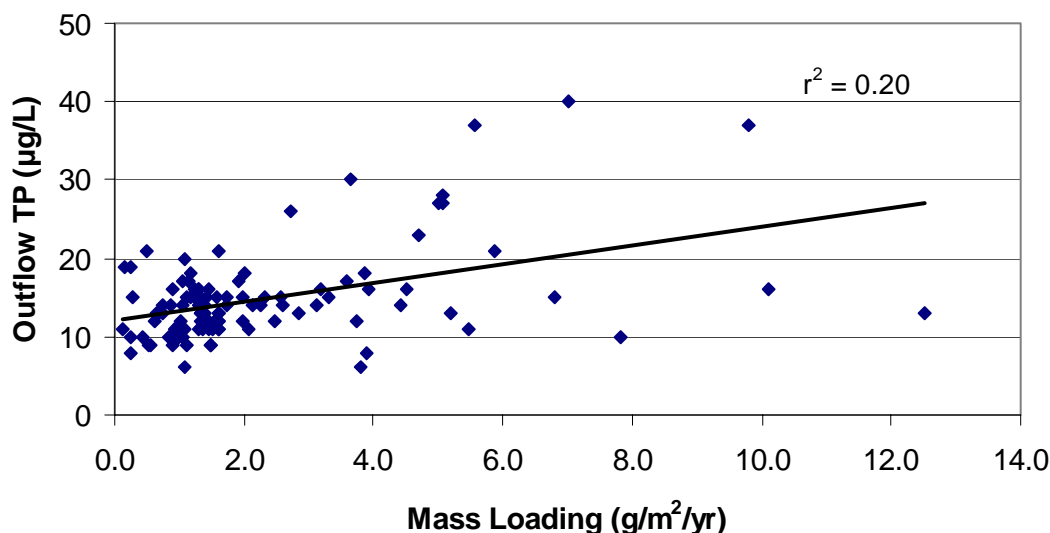


Figure 4.6. Regression analysis of weekly average (composite) outflow TP concentration with weekly average TP mass loading from 1998 - 1999 data.

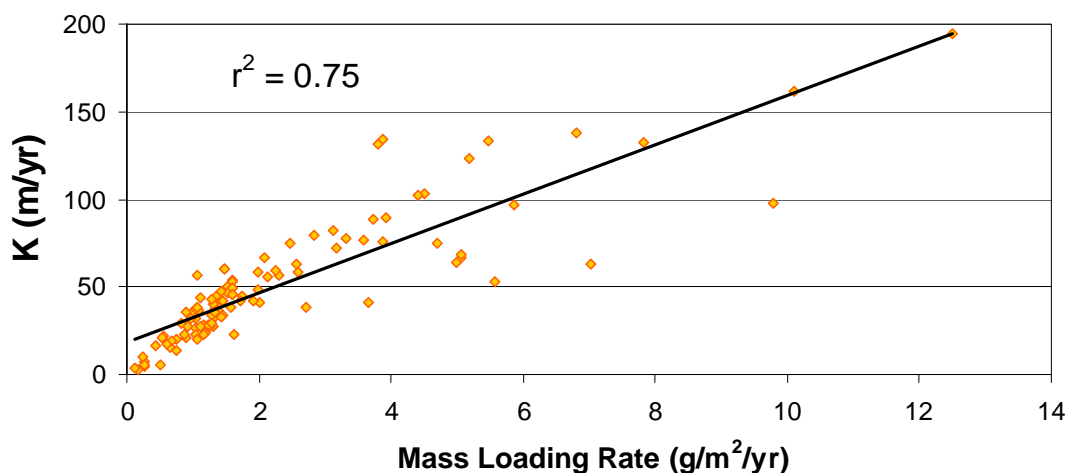


Figure 4.7. Regression analysis of weekly average TP settling rate (k) with weekly average TP mass loading from 1998 - 1999 data. Note that equations for calculating K and mass loading both contain terms for inflow concentration and hydraulic loading rate. Therefore, auto-correlation is partly responsible for the high correlation.

Table 4.1. Summary of Cell 4 regression analyses based on 1998 – 1999 Data. Note that K vs. HLR and K vs. mass loading regressions should be interpreted with caution, as there is a degree of auto-correlation in these calculations.

Operational Parameter	Coefficient of Determination (r ²)	
	Outflow TP Concentration	TP Settling Rate (k)
Water Velocity	0.12	0.41
Water Depth	0.001	0.58
HLR	0.14	0.61
TP Mass Loading	0.20	0.75

4.3 Relationship Between SAV Performance and Flow Velocity

Treatment performance in SAV systems might increase as a function of flow velocity through the system; this has been termed the ‘velocity effect’. The implication is that results at the mesocosm scale, which typically operate with much slower velocities than STA-scale systems, may not be indicative of STA-scale performance. To investigate this premise, we performed a comparative analysis of a 4-month period in the Cell 4 data record (September 1999 - December 1999) to a DBE mesocosm that has operated for over 20 months under similar average hydraulic and nutrient loading conditions as the Cell 4 period. Table 4.2 summarizes this comparison. Nominal flow velocity is approximately two orders of magnitude less in the mesocosm compared to Cell 4, while other operational parameters (HLR, mass loading) are quite similar. Similarities in both outflow concentrations and settling rates (k) between scales suggest that the velocity effect may not be significant for these SAV species.

Table 4.2. Summary of Cell 4 and Mesocosm ‘Velocity Effect’ Comparison.

	Cell 4: 9/99 – 1/00 (5 month average)	Mesocosm* (20 month average)
HLR (cm/day)	18	22
HRT (days)	3.6	3.5
Mass Load (g/m ² /yr)	5.6	8.2
Mean Velocity (cm/s)	0.54	0.0015
TP-in (µg/L)	85	102
TP-out (µg/L)	19	29
K (m/yr)	98	101

* moderately loaded (22 cm/day) mesocosm from hydraulic loading evaluation at the NATTS.

4.4 Post-1999 Cell 4 Modifications and Operations

During the period that Cell 4 was operated as part of the ENRP, the wetland was subjected to relatively consistent hydraulic loadings. Since fall 2000, however, it has received highly variable loadings, with an extended period of stagnation, followed by dramatic flow peaks (Figure 4.8). Cell 4 also was subjected to extensive structural modifications in 2001, which included deployment of LR “plugs”, deepening of the transverse C-7 canal, construction of a secondary outflow structure (G-309), and dredging of the sill buildup adjacent to the north levee. To gain a better understanding of the P dynamics within Cell 4, we performed an extensive sampling of water column P in the wetland on several occasions during our Phase II effort.

4.4.1 Effects of Limerock “Plugs” on Internal Phosphorus Profiles

During our Cell 4 tracer assessment performed in December 1999, we conducted “internal” water column sampling for TP at numerous stations within the wetland. Flows and TP concentrations before, during, and after that sampling period were relatively constant (average inflow of 2.53×10^5 m³/day with an average TP concentration of 96 µg/L). In that assessment, we were able to demonstrate a relationship between P removal efficiency and the internal flow dynamics.

Since the tracer assessment demonstrated that short-circuited areas coincided with areas of reduced P removal efficiency, we presented several alternative structural changes within the footprint of Cell 4 to enhance P removal (DBEL 2000a). One of these recommendations, the construction of LR “plugs” perpendicular to the east and west levees where most of the short-circuiting occurred, was implemented by the District. Subsequent to the deployment of the LR “plugs”, and prior to the commencement of modifications to the transverse C-7 canal, we performed a second internal sampling within Cell 4. The major goal of this internal P survey was to evaluate the effects of the LR “plugs” on P removal and distribution, and to measure the P concentrations within what appeared to be newly established short-circuiting channels.

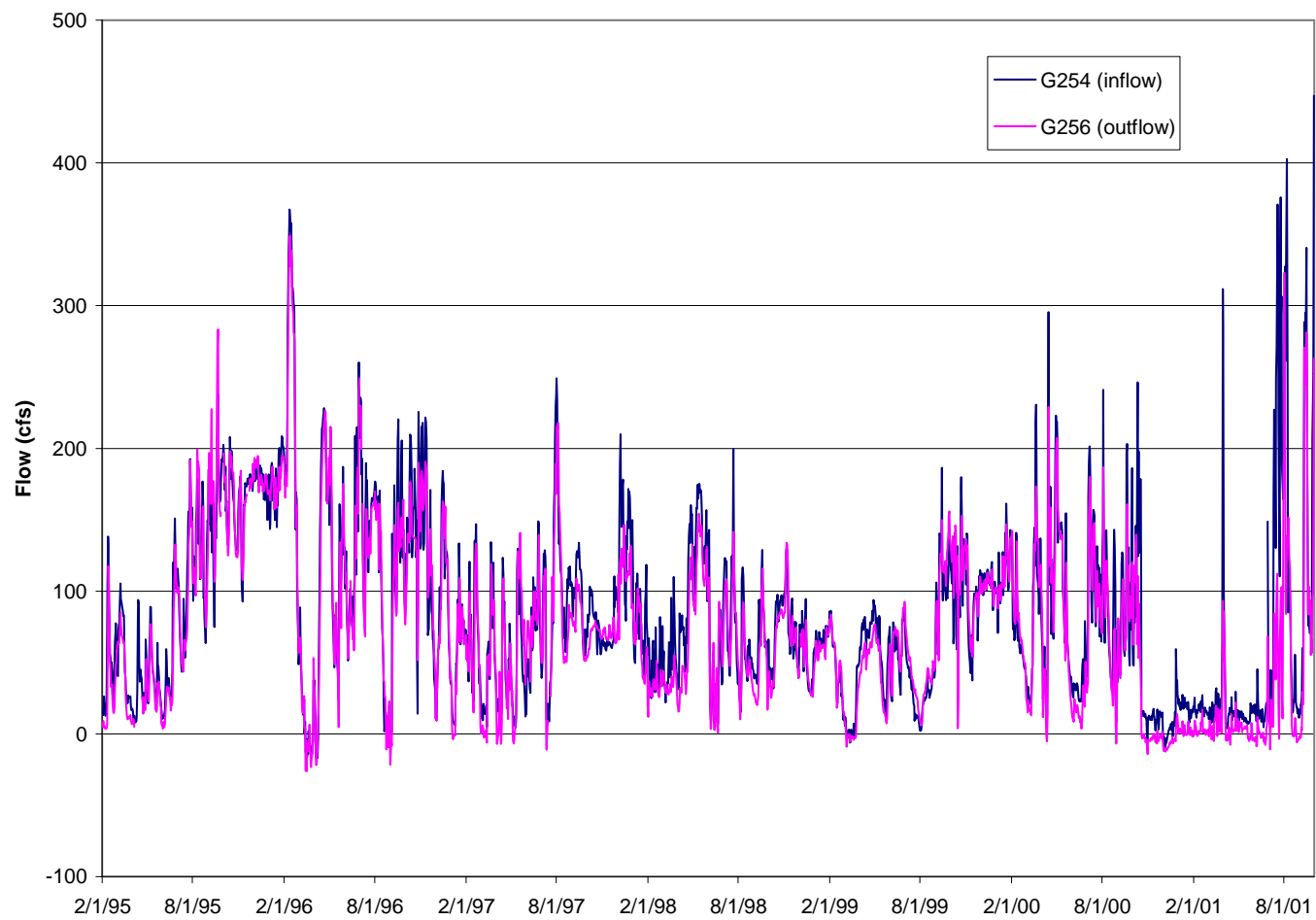


Figure 4.8. Historical flow record for the Cell 4 inflow levee culverts (G254) and the southernmost outflow culverts (G256).

On August 9, 2000, we sampled surface water at 44 internal stations along 7 east-west transects and 1 north-south transect in Cell 4 (Figure 4.9). Temperature and pH were recorded in the field, and water samples were collected for SRP and TP analyses. Twenty-six of the 44 internal sampling stations coincided with the station locations of the previously sampled TP during the tracer assessment (DBEL 2000b). The 18 additional stations were selected to correspond to spatial gaps in the sampling grid that were recognized after our tracer assessment. For example, we added an additional transect at the northern-most boundary of the cell (Figure 4.9), which should better reflect the influent water quality. We also included stations along a north-south short-circuit that recently developed in a relic farm canal along the western boundary. Besides the internal sampling, we also composited inflows (August 8-10) and outflow (August 8-15, except for August 13) samples on a daily basis.

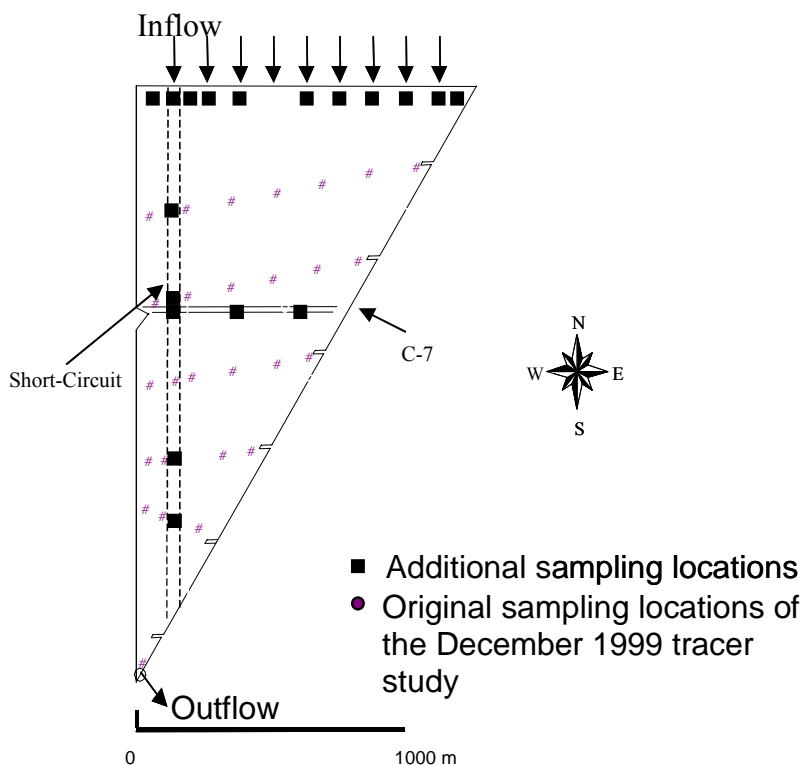


Figure 4.9. Internal sampling locations (44 total) in Cell 4 at which water quality (TP, SRP, pH, temperature) was evaluated on August 9, 2000.

Phosphorus concentrations varied considerably within the cell (Figure 4.10). As expected, TP and SRP concentrations were higher in the inflow region than in the rest of the cell. Areas of higher concentrations for both TP and SRP were found along the eastern and western levees of the cell, associated with short-circuited zones.

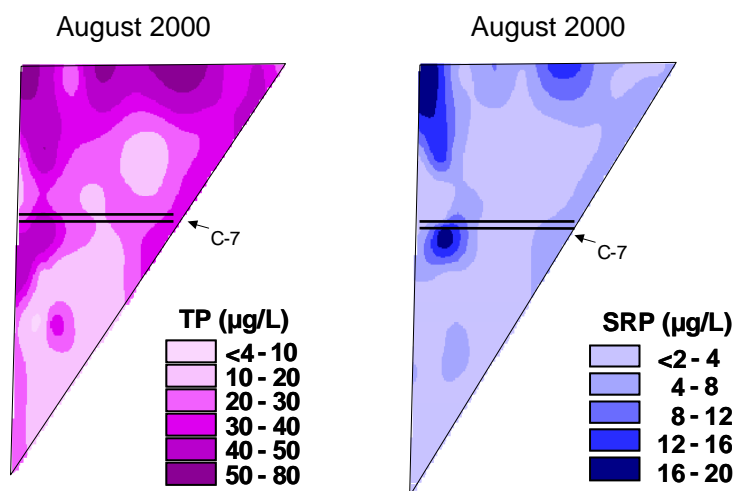


Figure 4.10. Total and soluble reactive phosphorus concentration gradients interpolated from 44 stations internal to Cell 4 on August 9, 2000.

The short-circuiting was observed along the eastern side of the cell, but was confined to the northern half (Figure 4.11) of the wetland. We believe the flow along the eastern levee was diverted westward along the C-7 canal, where it resumed a southern course along the western levee.

Although the limerock plugs were partially successful in deflecting the flow away from the western levee, they may have promoted a new short-circuit flow path just to the east of the west levee. This is suggested by the TP spatial concentration gradients in the western regions of Cell 4 before and after installation of the limerock plugs (Figure 4.11). Hence, during the second internal sampling of Cell 4, the flow was still unevenly distributed as new preferential flow paths were established along relic farm canals following curtailment of the old ones by the structural modifications.

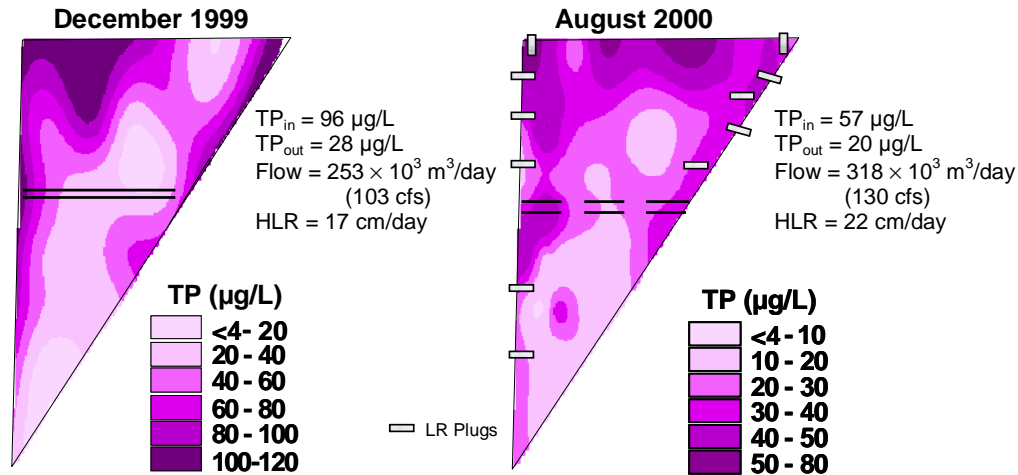
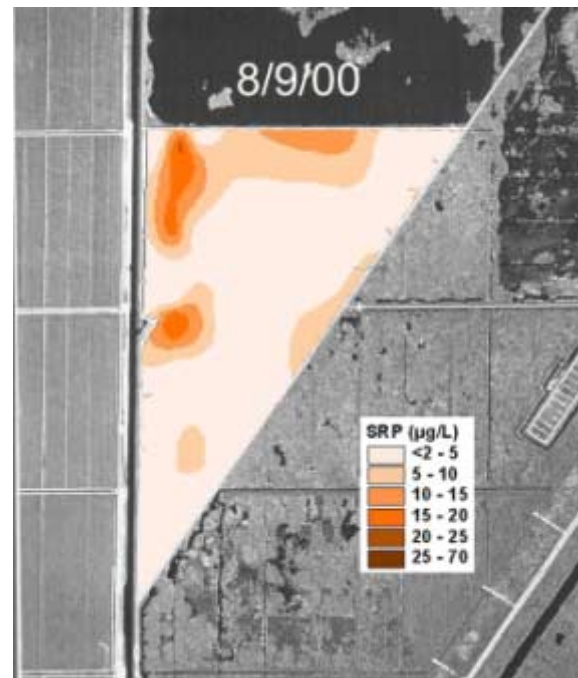
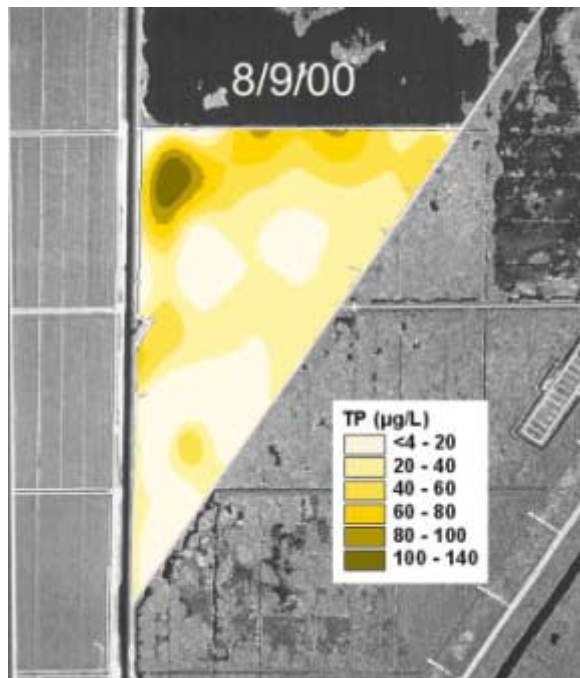


Figure 4.11. Spatial gradients in total P concentrations within Cell 4 before (sampled December 17, 1999) and after (sampled August 9, 2000) the addition of limerock “plugs”.

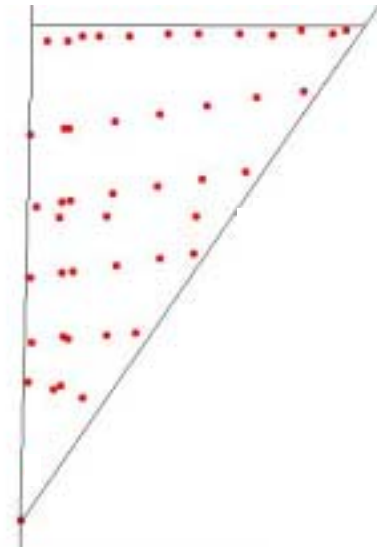
4.4.2 Temporal and Spatial Phosphorus Profiles

On seven occasions from August 9, 2000 to November 9, 2001, we performed internal water quality sampling in Cell 4 along seven east-west transects (44 stations on August 9 and approximately 26 stations for the others). All stations except the southern-most one immediately upstream of the outflow weirs were located within SAV beds; this exception was located within a cattail stand. At each station we measured both TP and SRP. With data obtained from those internal stations, we used the GIS mapping program Arcview to generate 2-D spatial concentration gradients for Cell 4.

The internal sampling events revealed large spatial and temporal variations in water column SRP and TP within Cell 4 (Figures 4.12 – 4.18). Concentrations of SRP were as high as 150 µg/L near the inflow culverts on November 9, 2001 (Figure 4.18), but were < 5 µg/L for almost the entire cell on August 9, 2000, April 12, July 26 and October 1, 2001 sampling dates (Figures 4.12; 4.15 – 4.17). The zones of higher SRP concentrations (along the western and northern levees) also coincided with elevated TP concentrations. The prominent and recurring longitudinal area of high P concentrations near the west levee corresponded to a path of short-circuiting that was ‘scoured’ since our first tracer assessment in late 1999. Interpretation of the temporal variability in Cell 4 water column P levels is facilitated by the hydraulic loading rate data for each of the sampling days, which we discuss below.

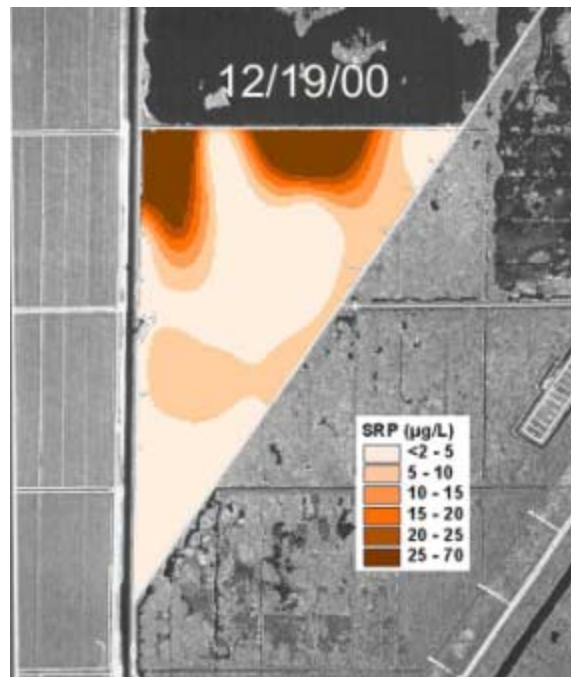
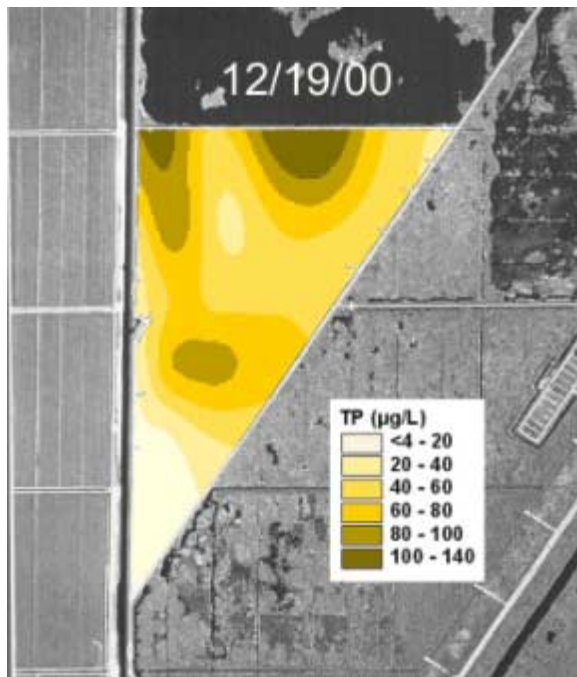


Sample Locations

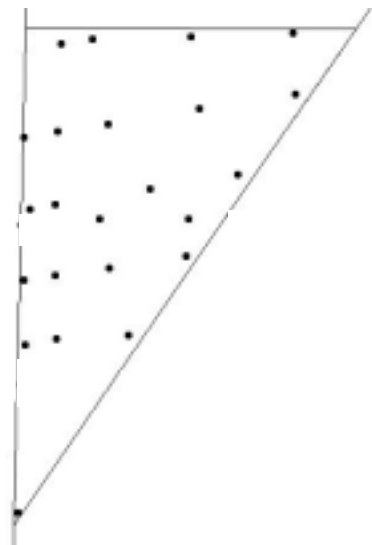


Internal Sampling Date:	8/9/2000						
	8/3/2000	8/4/2000	8/5/2000	8/6/2000	8/7/2000	8/8/2000	8/9/2000
Depth (ft)	2.88	3.04	2.79	2.46	2.26	2.37	2.57
G254 Flow (cfs)	241.1	117.7	68.5	64.0	90.2	142.1	142.6
G256 Flow (cfs)	186.8	143.6	103.2	95.0	82.0	95.4	120.9
	8/8/2000	8/9/2000	8/10/2000	8/11/2000	8/12/2000	8/14/2000	8/15/2000
TP in (µg/L)	63	53	54				
TP out (µg/L)	19	17	28	19	19	19	17
SRP in (µg/L)	17	10	12				
SRP out (µg/L)	2	4	4	4	3	3	3

Figure 4.12. Soluble reactive and total P concentration isopleths from internal sampling of Cell 4 on August 9, 2000.

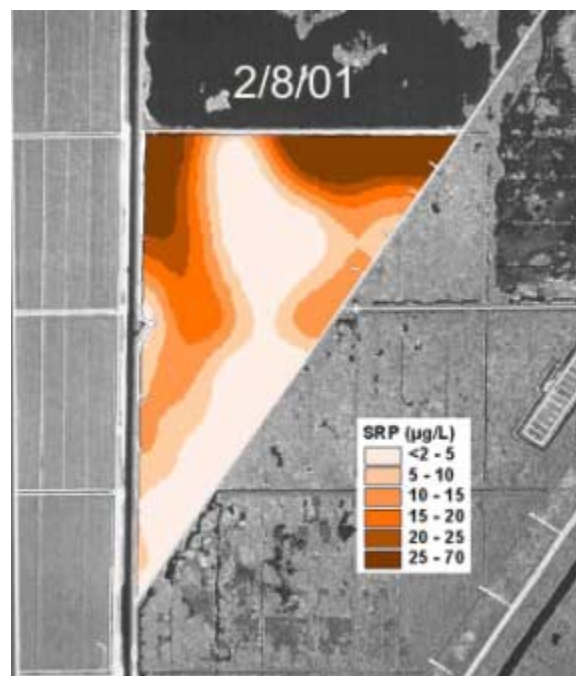
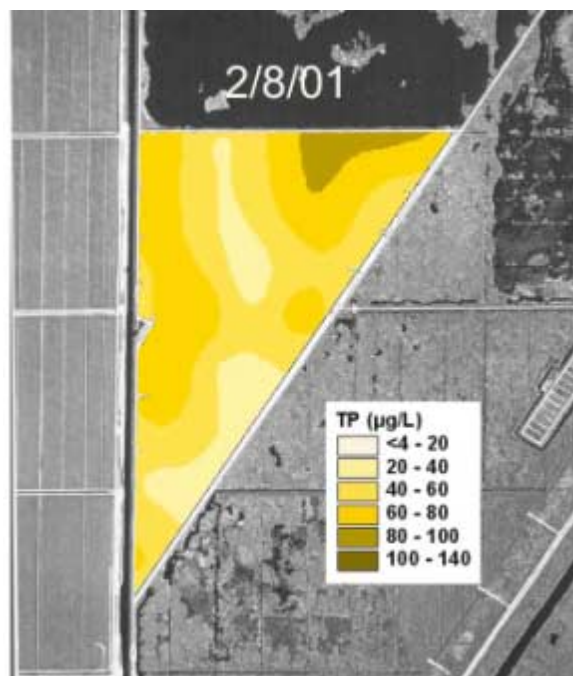


Sample Locations

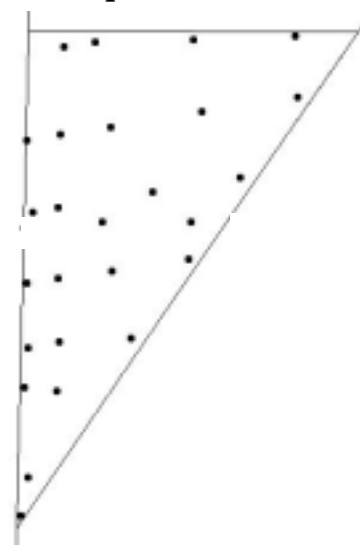


Internal Samping Date:	12/19/2000						
	12/13/2000	12/14/2000	12/15/2000	12/16/2000	12/17/2000	12/18/2000	12/19/2000
Depth (ft)	2.07	2.05	2.02	2.00	1.97	1.97	1.95
G254 Flow (cfs)	2.5	3.6	4.7	3.0	7.4	3.2	2.7
G256 Flow (cfs)	-8.4	-7.3	-6.2	-6.9	-5.1	-5.0	-5.1
	12/15-12/21						
TP in (µg/L)	109						
TP out (µg/L)	45						
SRP in (µg/L)	59						
SRP out (µg/L)	18						

Figure 4.13. Soluble reactive and total P concentration isopleths from internal sampling of Cell 4 on December 19, 2000.

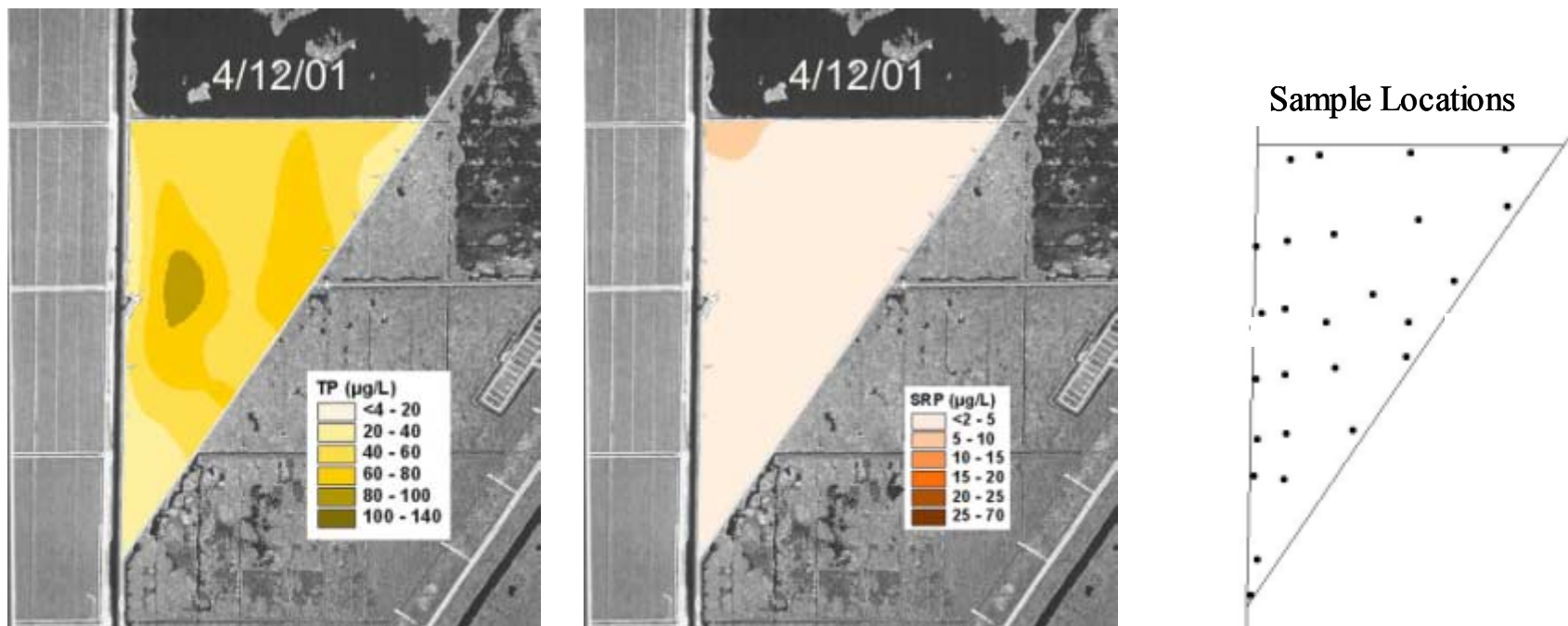


Sample Locations



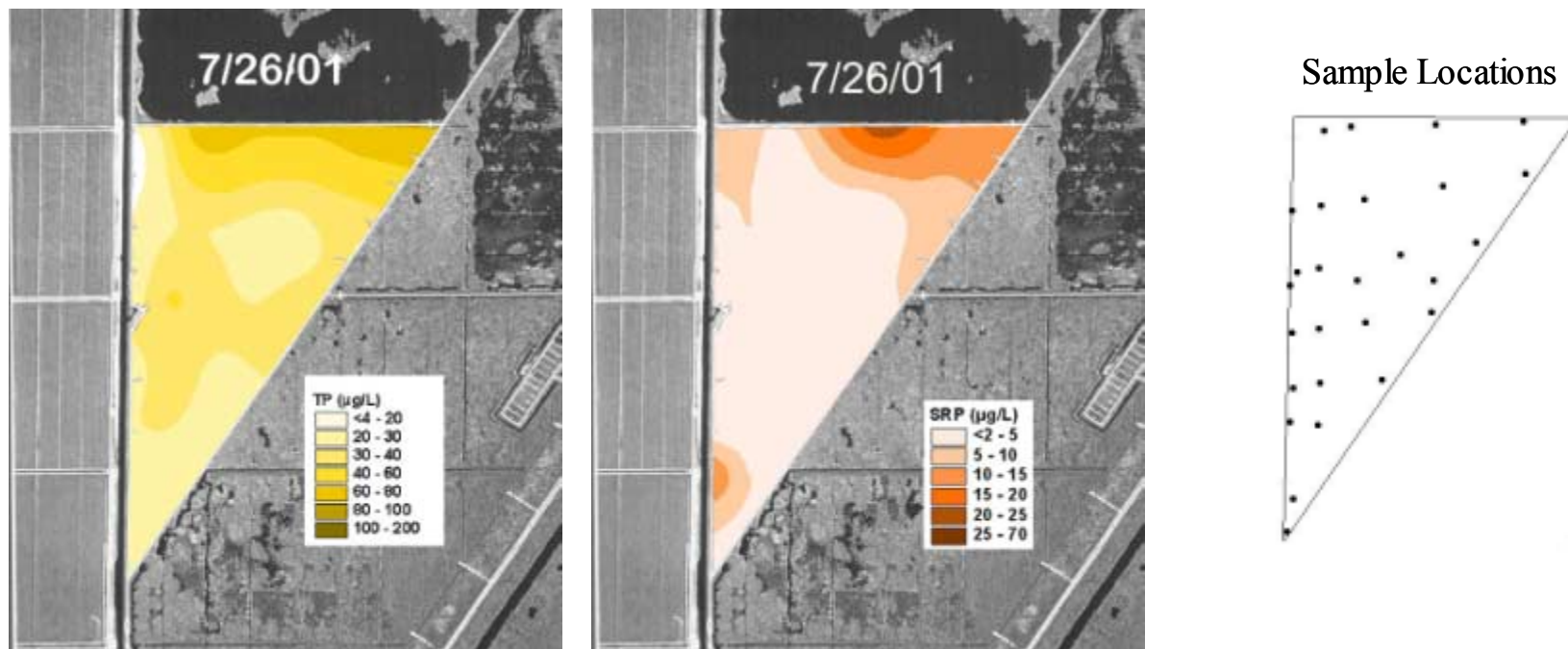
Internal Sampling Date:	2/8/2001						
	2/2/2001	2/3/2001	2/4/2001	2/5/2001	2/6/2001	2/7/2001	2/8/2001
Depth (ft)	2.17	2.18	2.16	2.16	2.14	2.14	2.13
G254 Flow (cfs)	25.4	18.1	15.4	14.5	11.3	16.5	14.5
G256 Flow (cfs)	6.6	9.4	2.6	5.6	-0.1	1.8	-1.6
	2/6/2001	2/7/2001	2/8/2001	2/9/2001	2/10/2001		
TP in (µg/L)	97	100	90				
TP out (µg/L)	27	27	36	33	33		
SRP in (µg/L)	73	78	57				
SRP out (µg/L)	3	4	3	7	4		

Figure 4.14. Soluble reactive and total P concentration isopleths from internal sampling of Cell 4 on February 8, 2001.



Internal Sampling Date:	4/12/2001						
	4/6/2001	4/7/2001	4/8/2001	4/9/2001	4/10/2001	4/11/2001	4/12/2001
Depth (ft)	1.84	1.80	1.77	1.73	1.68	1.64	1.64
G254 Flow (cfs)	7.2	4.3	7.4	5.9	3.8	11.6	14.1
G256 Flow (cfs)	-1.0	-4.8	0.0	-1.6	-4.6	-1.4	4.5
	4/10/2001	4/11/2001	4/12/2001	4/13/2001			
TP in (µg/L)	68	57	55	57			
TP out (µg/L)			29	26			
SRP in (µg/L)	10	8	5	7			
SRP out (µg/L)			2	2			

Figure 4.15. Soluble reactive and total P concentration isopleths from internal sampling of Cell 4 on April 12, 2001.

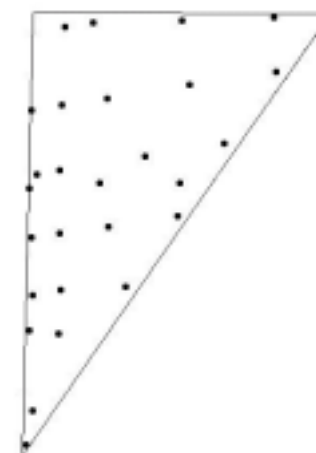


Internal Sampling Date:	7/26/2001						
	7/20/2001	7/21/2001	7/22/2001	7/23/2001	7/24/2001	7/25/2001	7/26/2001
Depth (ft)	1.62	1.33	1.32	1.89	2.35	2.72	3.20
G254 Flow (cfs)	317.2	216.8	154.2	110.4	315.1	375.8	293.1
G256 Flow (cfs)	53.8	18.8	-3.5	53.3	72.4	93.6	99.6
	7/23/2001	7/24/2001	7/25/2001	7/26/2001	7/27/2001		
TP in (µg/L)	35	34	35	43	49		
TP out (µg/L)		28	25	27	31		
SRP in (µg/L)	3	7	7	10	12		
SRP out (µg/L)		5	2	2	2		

Figure 4.16. Soluble reactive and total P concentration isopleths from internal sampling of Cell 4 on July 26, 2001.

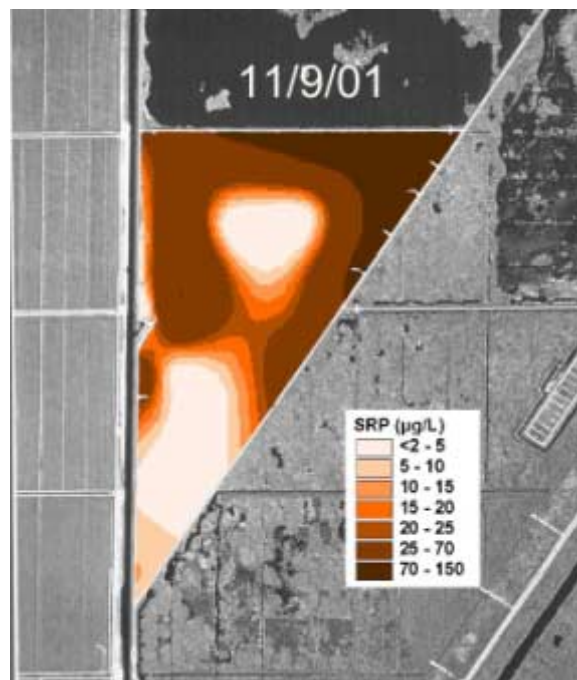
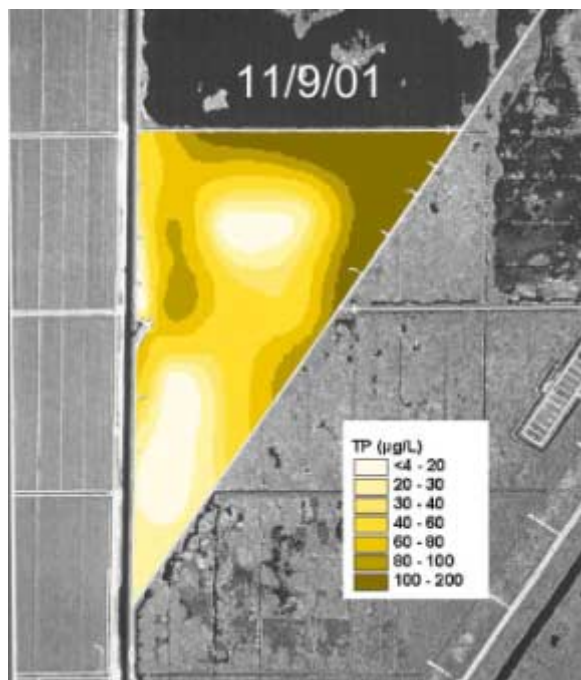


Sample Locations

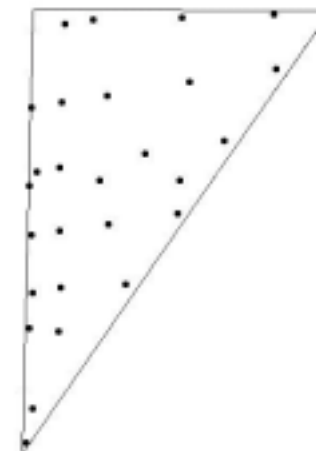


Internal Sampling Date:	10/1/2001						
	9/25/2001	9/26/2001	9/27/2001	9/28/2001	9/29/2001	9/30/2001	10/1/2001
Depth (ft)	2.28	2.48	2.59	3.22	3.81	3.85	3.95
G254 Flow (cfs)	81.6	79.0	207.6	237.8	252.1	447.0	425.2
G256 Flow (cfs)	66.2	56.7	95.3	99.2	140.4	263.0	269.6
			9/27/2001	9/28/2001			10/1/2001
TP in (µg/L)			73	79			62
TP out (µg/L)				20			22
SRP in (µg/L)			8	16			
SRP out (µg/L)				1			3

Figure 4.17. Soluble reactive and total P concentration isopleths from internal sampling of Cell 4 on October 1, 2001.



Sample Locations



Internal Sampling Date:	11/9/2001						
	11/3/2001	11/4/2001	11/5/2001	11/6/2001	11/7/2001	11/8/2001	11/9/2001
Depth (ft)	1.76	1.66	1.84	2.28	2.79	3.14	3.24
G254 Flow (cfs)	123.1	142.7	176.5	108.7	115.1	89.5	36.3
G256 Flow (cfs)	88.9	74.6	61.4	75.0	76.9	22.0	2.1
				11/06/01	11/07/01	11/08/01	11/09/01
TP in (µg/L)				110	115	131	134
TP out (µg/L)				28	24	28	38
SRP in (µg/L)				86	91	96	106
SRP out (µg/L)				12	11	7	7

Figure 4.18. Soluble reactive and total P concentration isopleths from internal sampling of Cell 4 on November 9, 2001.

4.4.3 Cell 4 Performance in Response to Fluctuations in Flow, Depth and TP Loadings

To scrutinize what effects flow, water column depth, and P loading have on P removal performance in Cell 4, we focused on two sampling periods. The first, on October 1, 2001, represented high hydraulic and P loadings. The second, on November 9, 2001, was characterized by a gradual decline in the inflows to very low rates, but with increasing surface water depths.

Results of the two internal sampling efforts in fall 2001 are depicted in Figures 4.17 and 4.18. The October 1, 2001 event is noteworthy because it represents a high flow event that also caused a rapid increase in wetland water depth (Figure 4.17). At the time of internal sampling, the top of the SAV beds throughout the wetland were covered by at least 15 cm of clear water. The reductions in P concentrations observed with distance from the inflow suggests that there may be adequate mixing between this “overtopping” flow of water and the underlying vegetation.

Additionally, although the secondary Cell 4 outflow (structure G-309) was opened during this flow pulse, the wetland outflow through G-256 still was quite high, equivalent to a HLR of 47 cm/day. Under these conditions, Cell 4 reduced the inflow TP concentrations of 62 µg/L to 22 µg/L. Figure 4.19 provides a perspective of flows, depths and Cell 4 inflow and outflow concentrations during both the October 1 and November 9, 2001 sampling events.

The November 9, 2001 internal Cell 4 sampling event depicts the spatial profiles of TP and SRP within the wetland coincident with a rapid decline in flow, but with an increase in the water depth (Figure 4.18). Inflow TP concentrations, and in particular, SRP concentrations, were extraordinarily high on this date, and on the preceding days during the high flow period. Despite these high inflow P concentrations, Cell 4 provided a reasonable level of treatment, reducing the four-day mean inflow TP levels of 123 µg/L to a mean outflow of 30 µg/L.

The data from these two sampling events suggest that if the hydrology of the cell is such that there is a “free water” zone above the SAV, efficient P removal can be achieved regardless of the hydraulic loading, especially if SRP represents a significant portion of the TP. We believe that under such hydraulic circumstances, mixing is enhanced while the proportion of the flow routed through the short-circuits is reduced.

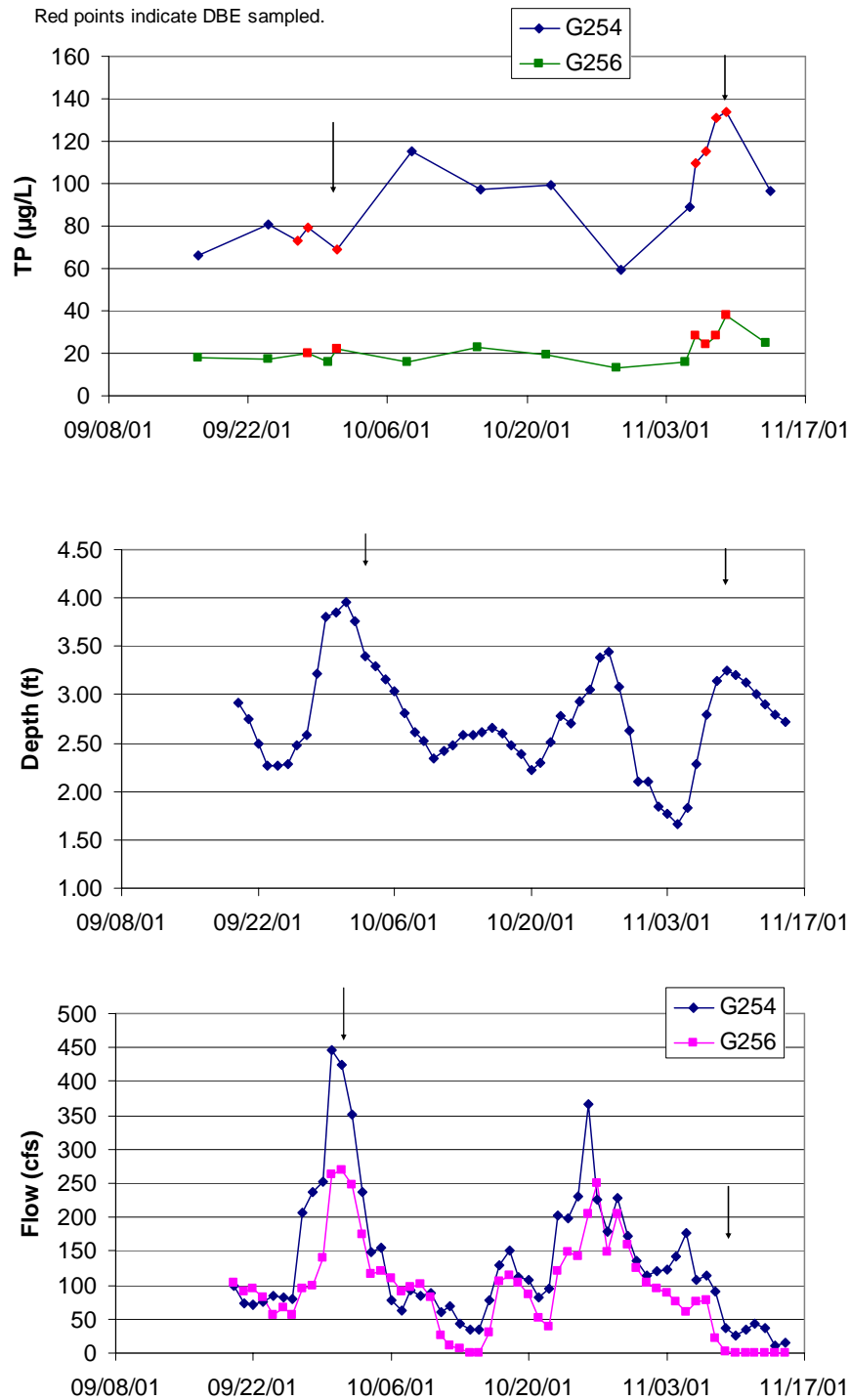


Figure 4.19. Cell 4 flow, water depths and inflow/outflow TP concentrations during fall 2001. The arrows denote days when Cell 4 was sampled. On the TP graph, note that data points after October 1, 2001 (with the exception of the data in red) did not pass QA/QC checks (sample holding times were exceeded).

4.4.4 Constraints on Cell 4 Outflow Phosphorus Concentrations

Our analyses of Cell 4 data suggest that at a constant hydraulic loading, inflow TP concentration (and thus P loading) is a critical factor in defining the outflow TP concentration. Thus, phosphorus removal performance by the upstream wetland, Cell 2, is an important determinant of the P loadings to Cell 4. During certain times, such as during the verification period of STSOC, Cell 2 was exporting, rather than removing P (Figure 4.20). Average TP concentrations increased during passage through Cell 2 from 40 to 52 $\mu\text{g/L}$, but were then reduced by Cell 4 to 19 $\mu\text{g/L}$. We observed a similar trend during October and November 2001: the large upstream Cell 2 wetland was consistently exporting P during the period that Cell 4 was challenged with extreme flow pulses and high inflow P concentrations.

From this “system-wide” analysis, it is apparent that Cell 4 TP removal efficiency is directly linked to the performance of Cell 2. Therefore, improvements in the P removal capacity in Cell 2, such as controlling scouring by cattail islands, promoting SAV communities and reducing hydraulic short circuits, should enhance the ability of Cell 4 to achieve low outflow P concentrations.

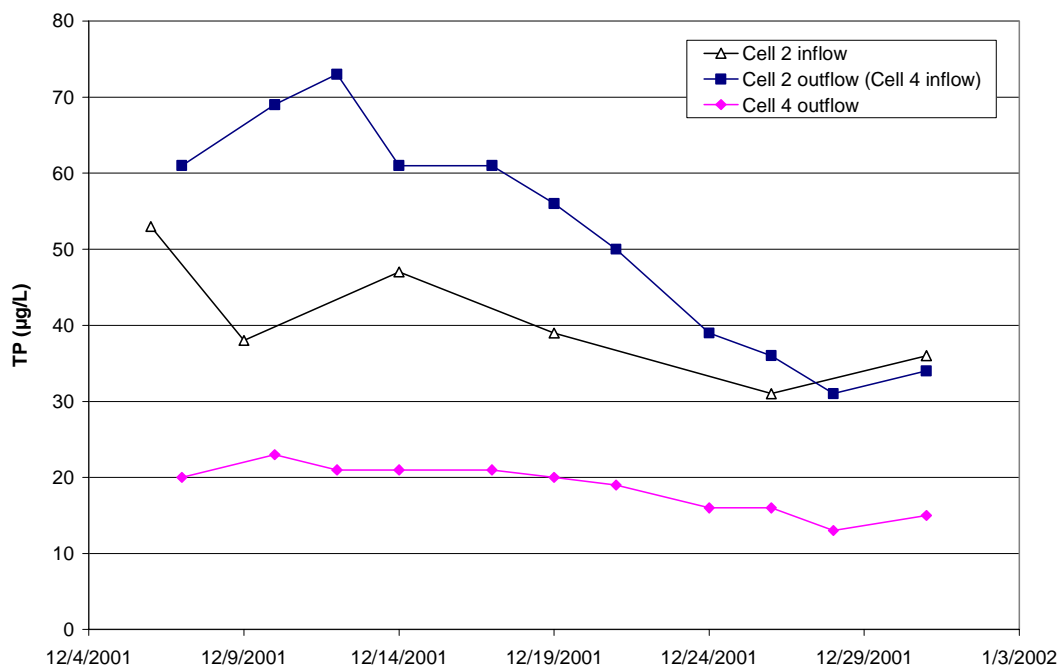


Figure 4.20. Inflow and outflow TP concentrations for Cells 2 and 4 during the Cell 4 STSOC ‘verification’ period.

4.5 Spatial Characterization of Sediments and SAV

Sediment cores from Cell 4 were collected at a subset of 16 sites along four of the seven internal transects sampled during the internal water quality monitoring we performed from August 9, 2000 to November 9, 2001. The sediment layer deposited in the wetland since the beginning of flooding in 1993 was easily discerned by its lighter color and less consolidated nature compared to the native underlying muck of the former agricultural fields. After locating the boundary between the two soil types, we measured the depth of the accreted wetland sediment before separating it from the underlying muck soil. Accrued wetland sediments and native muck soils (subset) were each analyzed for bulk density and P, N, and Ca contents.

We also harvested submerged vegetation from 0.24 m² sampling plots at the time of sediment collection (April 24 – 25, 2001). Eleven stations along 4 transects coinciding with the sediment sampling stations, were selected for SAV harvesting. After measuring the standing crop wet biomass of SAV at each station, a sample of the dominant macrophyte was collected for dry matter, N, P and Ca analyses.

We divided the cell into inflow and outflow ‘halves’ for comparing the P, N and Ca concentrations and storages. For the inflow half section of Cell 4, *Najas guadalupensis* and *Ceratophyllum demersum* dominated, whereas *C. demersum* was absent in the outflow half of the cell. Total P and TN concentrations in *C. demersum* tissue were higher than in *N. guadalupensis* tissue, but the reverse was true for tissue Ca content (Table 4.3). In the more P-limited outflow section of Cell 4, TP concentration of the *N. guadalupensis* was 14% lower than for the *N. guadalupensis* inhabiting the inflow half. Based on the limited number of sample sites, the SAV standing crop (including the subdominants) was higher in the outflow half of the cell than the inflow half.

The phosphorus gradient noted for the SAV tissues was also observed in the accrued wetland sediment. Namely, sediment TP concentrations were 33% higher in the inflow half than the outflow half of the wetland (Table 4.5). Sediment TN concentrations also were 25% higher in the inflow half of the wetland. Sediment calcium concentrations were high over the entire cell. In contrast, negligible differences existed for the P, N, and Ca contents of the underlying native

muck between inflow and outflow portions of the wetland (Table 4.5). The rate of accretion of the wetland sediment in the inflow half was more than twice that of the back half, indicating higher community production and possibly import of particulates from the upstream Cell 2.

Table 4.3. Standing stock of SAV and tissue P, N, and Ca contents in the dominant submerged species at 11 locations in Cell 4 on April 25, 2001. Values represent the means \pm 1 s.d.

	Dominant Species	Sample No.	Biomass (g dry/m ²)	Dry:Wet Wt	TP (mg/kg)	TN (%)	TCa (%)
Inflow Half	<i>Najas</i>	3	161 \pm 106	0.0807 \pm 0.044	1946 \pm 724	1.8 \pm 0.2	17.2 \pm 1.7
	<i>guadalupensis</i>						
	<i>Ceratophyllum demersum</i>	3	165 \pm 180	0.0812 \pm 0.0151	2190 \pm 473	2.1 \pm 0.4	7.7 \pm 3.0
	Combined	6	217 \pm 147*	-	2003 \pm 510	1.9 \pm 0.4	12.3 \pm 5.3
Outflow Half	<i>Najas guadalupensis</i>	5	262 \pm 294	0.0811 \pm 0.0173	1675 \pm 621	1.9 \pm 0.2	16.0 \pm 1.0

* Total SAV biomass including subdominant species

Table 4.4. Accrual depth, bulk density and P, N, and Ca concentrations in the native muck and accrued wetland sediments from Cell 4. Values represent the means \pm 1 s.d.

	Sediment Type	Sample Date	Sample No.	Accrual Rate (cm/yr)	Bulk Density (g/cm ³)	TP (mg/kg)	TN (%)	TCa (%)
Inflow Half	Wetland	6/14/2000	3	1.7	0.082 \pm 0.038	1301 \pm 411	1.6	19.8*
	Wetland	4/24/2001	7	1.3	0.112 \pm 0.008	922 \pm 109	2.2	15.2 \pm 7.4
	Combined	-	10	1.5 \pm 0.6	0.103 \pm 0.024	1035 \pm 281	2.0 \pm 0.6	16.6
	Muck	4/24/2001	3	-	0.168 \pm 0.035	498 \pm 189	1.7 \pm 0.4	10.2 \pm 7.5
Outflow Half	Wetland	7/19/2000	3	0.5	0.155 \pm 0.018	631 \pm 69	0.91	23.0*
	Wetland	4/24/2001	3	0.6	0.132 \pm 0.024	927 \pm 237	2.4	14.4 \pm 5.5
	Combined	-	6	0.6 \pm 0.1	0.144 \pm 0.033	779 \pm 225	1.6 \pm 0.8	18.7
	Muck	4/24/2001	2	-	0.178 \pm 0.075	544 \pm 214	1.5 \pm 0.2	14.4 \pm 10

* Analysis performed on composite sample

Based on the relative P storages in the accrued wetland sediment and the SAV, we found 2.5 times more P stored in the sediments of the inflow half of the cell than the outflow (Table 4.4). For SAV biomass, there was only a 25% higher P storage in the inflow than outflow half.

Sediment N storage mimicked the P storage in that there was 2.5 times more N stored in the sediments of the inflow than the outflow half of the wetland.

Table 4.5. The P, N, and Ca sediment and SAV wetland storages in the inflow and outflow halves of Cell 4.

	Sampling Date	Sample No.	Sediment (g/m ²)			SAV (g/m ²)
			P	N	Ca	P
Inflow Half	6/14/2000	3	11.2 ±3.5	143 ±44	1994 *	-
	4/24/2001	7	11.2 ±4.9	278 ±179	1700 ±700	0.46 ±0.36
	Combined	10	11.2 ±4.3	237 ±161	1788	-
Outflow Half	7/19/2000	3	3.5 ±0.38	52 ±21	1312*	-
	4/24/2001	3	5.4 ±1.9	137 ±39	900 ±600	0.37 ±0.27
	Combined	6	4.5 ±1.6	95 ±54	1106	-

* Analysis performed on a composite sample

4.6 Sediment P Stability and Characterization

We initiated work on this task in June 2000, using sediments collected from the inflow region of Cell 4. We continued this effort using sediments collected from the southern region (near the outfall) of Cell 4 during July 2000.

4.6.1 Methodology

Sediment Collection

Three stations adjacent to the northern levee and three stations along an east-west transect in the southern region of Cell 4 were cored (10.1 cm ID aluminum corer) on June 14th and July 18th in 2000. The calcium-enriched sediment (average 7-15 cm deep in the north and 3 cm deep in the south) accrued after flooding was separated from the underlying agricultural muck soil. One core from each station was kept separate for the fractionation analyses of the accrued sediment, while the accrued calcareous sediment in the remaining 7 (north site) or 10 to 12 (south site) cores from each station were composited and homogenized to provide substrate for the stability/release assessments. Additional extractions for P fractionation were also performed on each composited sample. To prevent oxidation of the sediments during storage, nitrogen gas was injected into the headspace of the composite container and into the zip-lock bags holding the sediments for P fractionation.

Inorganic Phosphorus Fractionation

Sequential P fractionations were conducted on the six sediment samples (three from the north and three from the south). The inorganic-P fractionation scheme followed a methodology suitable for calcareous sediments (Hieltjes and Lijklema 1980). Briefly, 5 grams of wet sediment were exposed to the following extractants (40 mL) on a sequential basis: 1M NH₄Cl (pH adjusted to 7.0) for two 2 hr extraction periods; 0.1N NaOH for 17 hr; and 0.5 N HCl for 24 hr. Analysis for SRP (filtered with Whatman™ 0.45 µm) within each extraction, and TP (filtered through Whatman™ 41) on only the 0.1N NaOH extraction, yield the fractions of P in the porewater, loosely sorbed, and CaCO₃-associated (NH₄Cl), iron and aluminum bound-P (NaOH-SRP), biogenic-P (NaOH-TP minus NaOH-SRP), and the Ca mineral-P (HCl).

Sediment Stability

Sediments from the Cell 4 inflow and outflow regions were subjected to a range of environmental conditions to assess stability of the associated P. The following eight treatments including controls were each replicated in triplicate:

1. 3% CO₂ in air to induce a low pH
2. 0.3% CO₂ in air to induce a moderately low pH
3. 0% CO₂ in air (CO₂-free) to induce a high pH
4. 0.03% CO₂ in N₂ to lower the redox potential
5. Air-only + Ca spikes (50 mg/L) to provide hard water
6. Air-only + SRP spike (125 µg/L) to simulate increased ambient P concentrations
7. Air-only to serve as a control for the pH and redox altered sediment, and the Ca/alk and SRP spiked sediment
8. Air-only upon reflooding of desiccated (48 hr drying time) sediment

Incubations usually began the day following field collection of the composited sediment, but no longer than 5 days in some cases. The composited sediment samples were refrigerated under a blanket of nitrogen during the 1 to 5 days following field collection and prior to the incubations. Each 500-mL incubation flask received 100 mL of wet sediment plus 400 mL of Cell 4 outflow water, which had been collected the same day (June 14 or July 18) as the sediment coring. The

gases were sparged through distilled water prior to being gently bubbled (8-10 mL/min) into the water column of each incubation vessel. Frequent redox and pH measurements within each vessel permitted adjustment of the gas flows for maintaining targeted redox and pH values.

Incubations were performed in the dark, within a water bath held at room temperature. The minimum and maximum temperatures during the entire incubation period (12.6 days) were 19 and 23°C, respectively.

Water samples were collected at the beginning and end of the incubation period from each incubation vessel for the following analyses: SRP, TSP, alkalinity, calcium, specific conductance, pH, redox potential, and iron. Additionally, sampling for SRP, pH, and redox potential was conducted on a more frequent basis, occurring after 0.3, 0.7, 1.5, 3.0, and 6.0 days in addition to the initial and ending times. Sediment bulk density was measured prior to incubations.

4.6.2 Results and Discussion

Effects of pH

Prior to being exposed to different pH treatments, the initial ($t = 0$) pH ranges were 7.58 to 7.79 for the inflow sediment and 8.06 to 8.13 for the outflow sediment. The effect of pH on the release of SRP from inflow sediment was negligible among the three higher pH treatments (0.3, 0.03, and 0.0% CO₂ provided average pH values of 7.76, 8.42, and 8.88, respectively) for the first 36 hours (Figure 4.21). After an elapsed time of 72 hours, the SRP release began to show a pH effect in the 0.3% CO₂ treatment (mean pH of 7.76). In contrast, the lowest pH treatment (3% CO₂ with mean pH = 7.01) yielded an immediate and significantly higher release rate than the three higher pH treatments (Figure 4.21).

All the pH treatments exhibited a common release pattern in that SRP release was highest during the first 16 hours, and then gradually decreased beyond that time (Figure 4.21). For the high pH treatment (0.0% CO₂), the SRP release became negligible during most of the incubation period, while in the remaining treatments the release continued until the end of the incubation period, albeit at a reduced rate. These lower release rates during the latter 90% of the incubation period compared to the first 36 hours can be explained by one or more of the following phenomena:

- 1) The SRP released initially into the water column reached an equilibrium with the remaining P in the sediment, whereby the law of mass action prevented a further net release of SRP.
- 2) The available pool of sediment P simply became exhausted first at the higher pH treatments, and then later on in the lower pH treatments.
- 3) The initial high SRP release rates are associated with a more labile sediment P pool which is exhausted quickly, whereas the longer, lower rate of SRP release is attributable to a separate less labile, and perhaps larger sediment P pool.

Which of the above explanations is responsible cannot be defined without further evaluations, although the data from the P fractionations indicates that there were still adequate reserves of labile P pools (e.g., $\text{NH}_4\text{Cl-P}$) in the post-incubated (12.6 days) sediment (Figure 4.22). What the data do unequivocally demonstrate is that both the rates and extent of SRP release from the organic marl is affected by the pH of the ambient water in an inverse and linear manner (Figure 4.24). After a 302-hour exposure period, 120 $\mu\text{g SRP/L}$ can be released for every decrease in pH of one unit.

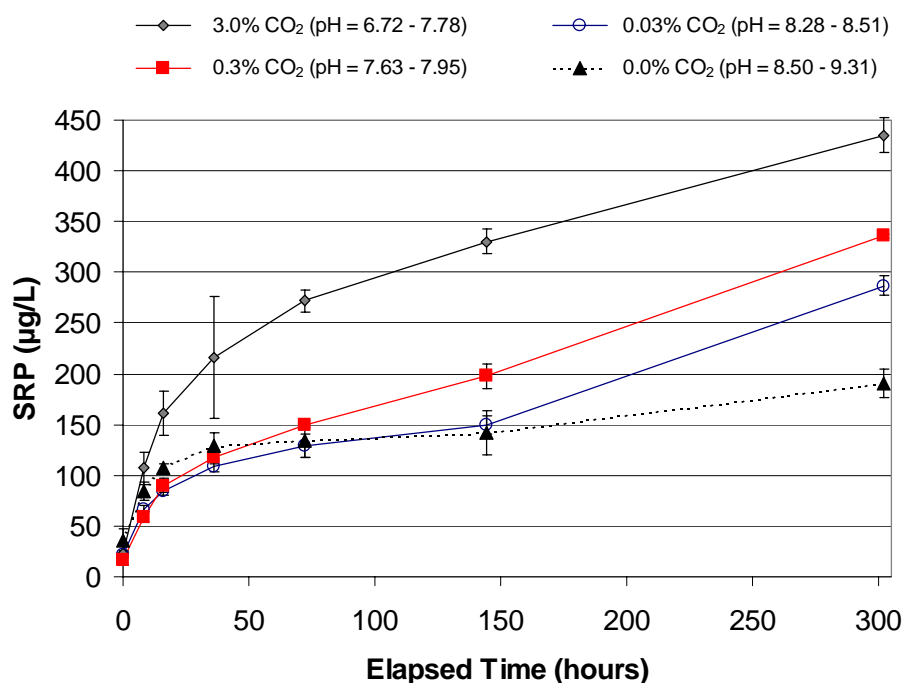


Figure 4.21. Time course for SRP release from Cell 4 inflow region sediments exposed to varying pH values. Each data point represents the mean \pm 1 s.d. of 3 replicates.

Cell 4 Inflow Sediment

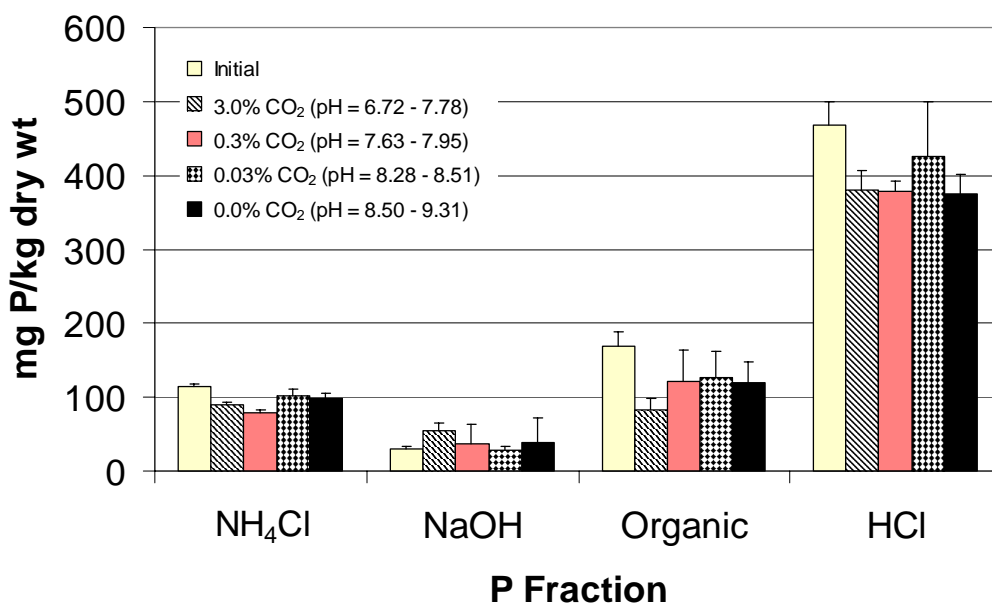


Figure 4.22. Inorganic P fractionation of Cell 4 inflow region sediments before (Initial) and after incubations at varying levels of pH for 12.6 days. The bars above the histogram columns represent + 1 standard deviation.

Based on the inorganic P fractionations of pre- and post-incubated sediment (Figure 4.22), there are three possible sources of P that contributed to the release under low pH exposure. The differences between the initial and post-incubated $\text{NH}_4\text{Cl-P}$, HCl-P , and organic-P fractions indicate that all three of these pools could have contributed P since they all lost P during the incubation period (Figure 4.22). Most of the decrease in sediment P occurred in the HCl-P and organic-P pools, indicating that relative to the more labile $\text{NH}_4\text{Cl-P}$ and NaOH-P , the less labile organic-P and HCl-P pools are the major sources of the released P. Considering the high calcareous nature of the sediment and the known effect that pH has on CaCO_3 solubility (Stumm and Morgan 1981), it is likely that the inverse relationship between pH and SRP release observed in the data set (Figure 4.23) is due to the desorption from, and dissolution of, CaCO_3 .

For each of the four pH treatments, SRP releases from the outflow sediments were negligible (Figure 4.23), and considerably lower than the releases found for the inflow sediment under the same treatments (Figures 4.21 and 4.23). Apparently the sediment P pools that were susceptible to lower pH at the inflow did not exist to any great extent at the outflow.

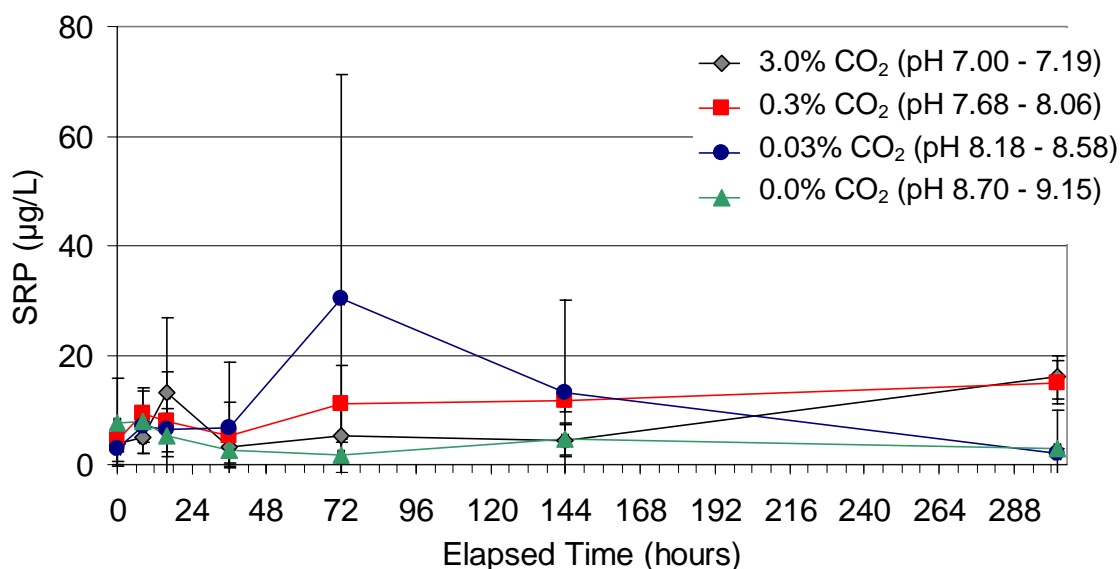


Figure 4.23. Time course for SRP release from Cell 4 outflow region sediments exposed to varying pH values. Each data point represents the mean \pm 1 s.d. of three replicates.

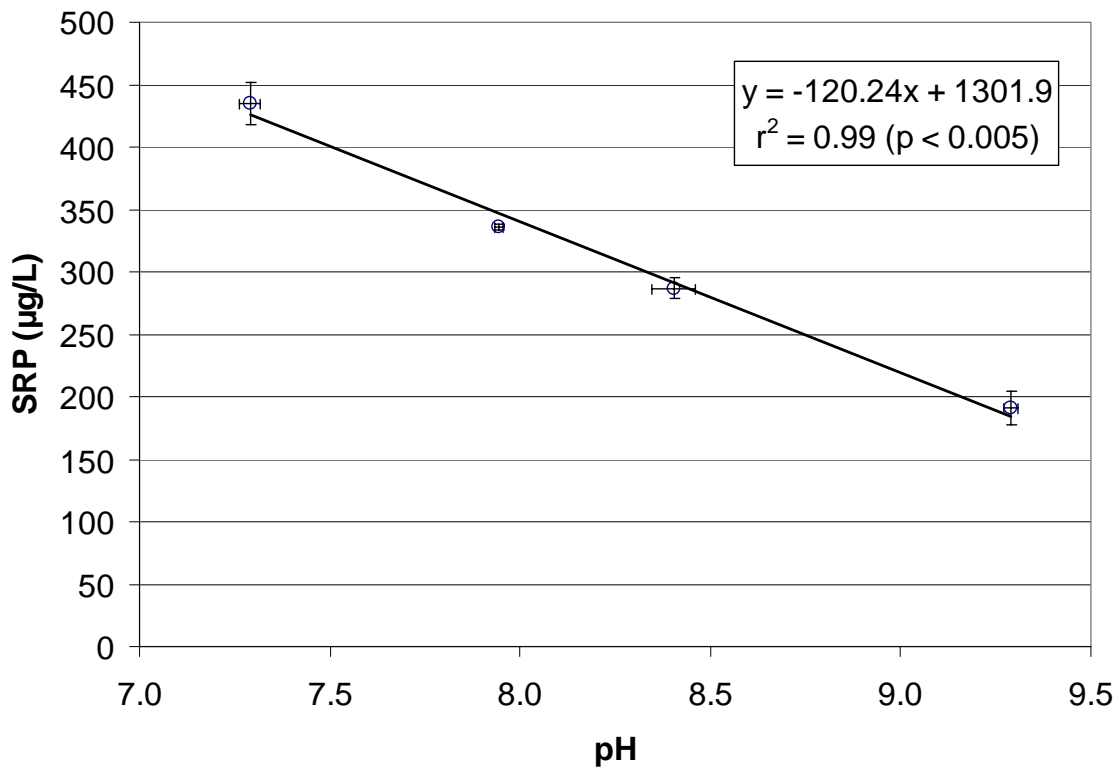


Figure 4.24. The effect of pH on the release of SRP from sediments composited from three locations in the inflow region of Cell 4. The incubation period was 302 hours (12.6 days). Each data point represents the mean \pm 1 s.d. of 3 replicates

Effect of Anoxia

Anoxic conditions (average $E_{h7} = +114$ mV) produced an immediate and extended response in SRP release from the inflow region sediments compared to the oxic control (average $E_{h7} = +495$ mV) (Figure 4.25). This indicates that there were significant quantities of Fe-associated P in the marl, or that bacteria containing surplus P released it during anoxia (Gächter and Meyer 1993).

Theoretically, a decline in the NaOH-P fraction should have occurred for the anoxic treatment if the P release originated in the iron pool. Since this was not the case (Figure 4.26), another mechanism other than Fe reduction may have been operating, such as bacterial release (Gächter and Meyer 1993). Indeed, the organic-P pool did show a slight decrease between the initial and the end of the incubation period (Figure 4.26), but it was not statistically significant.

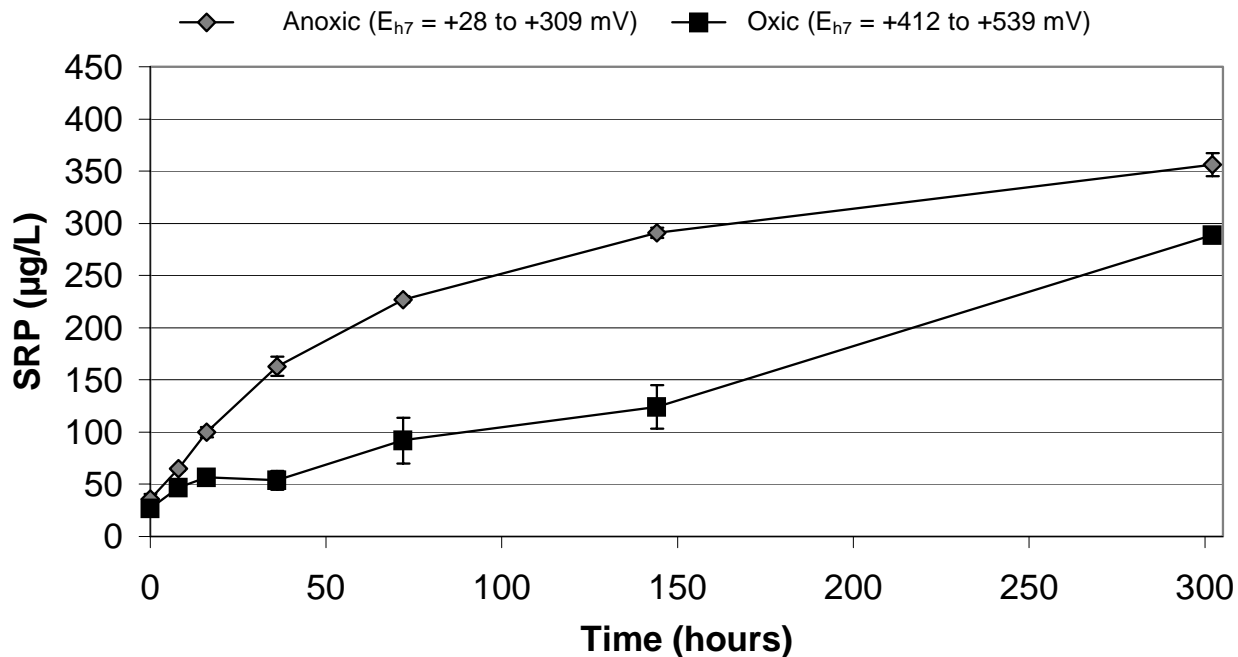


Figure 4.25. Time course for SRP release from Cell 4 inflow region sediments exposed to oxic and anoxic conditions. Each data point represents the mean \pm 1 s.d. of 3 replicates.

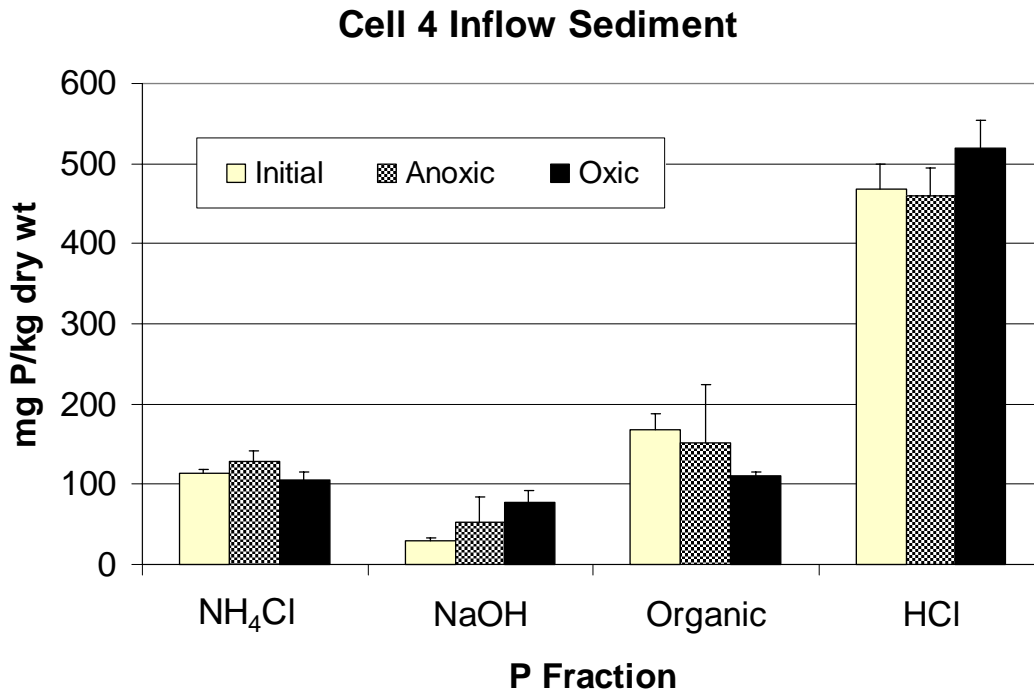


Figure 4.26. Inorganic phosphorus concentrations of Cell 4 inflow region sediments composited before (Initial) and after incubations under anoxic and oxic conditions for 12.6 days. The bars above the histogram columns represent + 1 standard deviation.

As was found for the inflow sediment, anoxic conditions resulted in an immediate release of SRP from the outflow sediment (Figure 4.27). The release was short-lived, occurring only within the first 6 hours of incubation. On the other hand, the sediment exposed to air released negligible SRP for the first 36 hours, before SRP concentrations increased to near the anoxic treated levels. However, the increase was ephemeral in the outflow sediment as the SRP concentration decreased to near the detection limit ($2\text{ }\mu\text{g/L}$) by the end of the incubation (Figure 4.27). Whether the “first flush” effect at the onset of anoxia was associated with iron reduction or microbial release requires further evaluation.

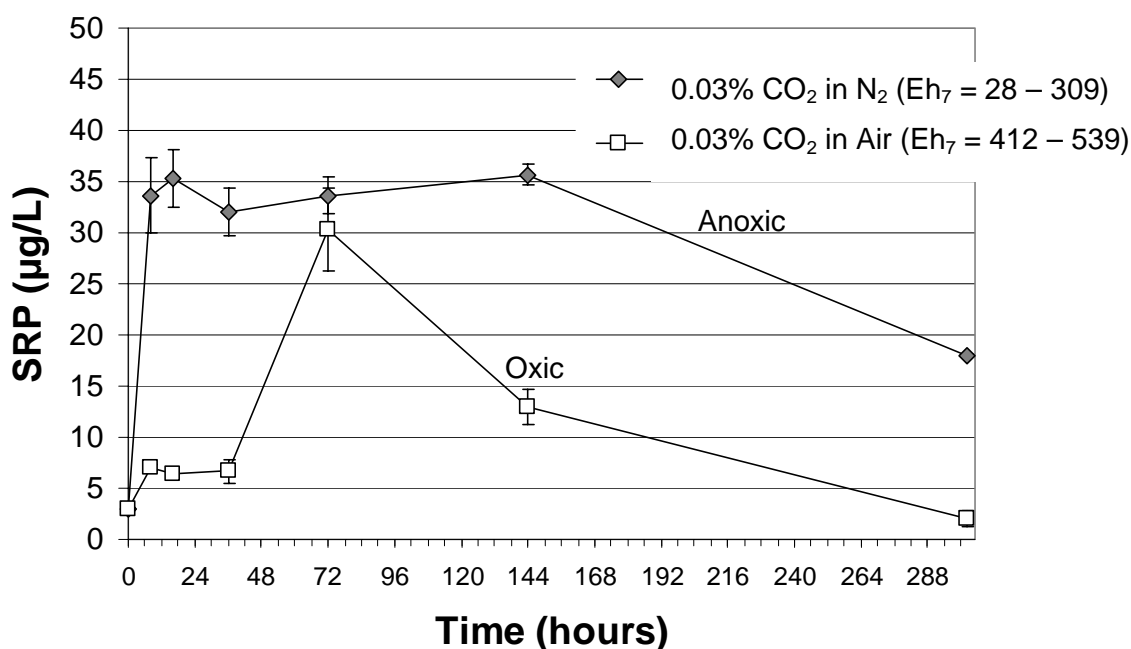


Figure 4.27. Time course for SRP release from Cell 4 outflow region sediments exposed to oxic and anoxic conditions. Each data point represents the mean ± 1 s.d. of three replicates.

Desiccation Followed by Reflooding

To assess effects of drydown and reflooding on sediment P release, we dried both Cell 4 inflow and outflow sediments in sunlight to achieve a partial desiccation. Following the partial desiccation outdoors, a subset of duplicate flasks for each sediment type was sacrificed by completely drying the sediment in an oven at $70 - 80^\circ\text{C}$ so that the extent of the outdoor desiccation would be known.

Table 4.6 provides dry:wet weight ratios before (initial) and after (final) desiccation, as well as the duration of desiccation. Because of the greater percentage of water in the inflow sediments compared to those of the outflow region, moisture loss was higher and the final dry:wet weight was lower for the former sediment type.

Table 4.6. Duration of desiccation, and before (initial) and after (final) dry:wet weight ratios and moisture loss, for the inflow and outflow sediments of Cell 4.

	Duration of Desiccation (hr)	Initial Dry:Wet	Final Dry:Wet	Moisture Loss
Inflow Rep A	99	0.073	0.158	2.2 x
Inflow Rep B	99	0.073	0.150	2.1 x
Outflow Rep A	72	0.160	0.234	1.5 x
Outflow Rep B	72	0.160	0.184	1.2 x

Desiccation followed by reflooding resulted in significant release of SRP from both the inflow and outflow sediments (Figure 4.28 a,b). In terms of the total quantity of SRP released from the two sediment types, the inflow sediment, with its higher sediment P pools, released almost three times more SRP than the outflow sediment. When compared to the control sediment that was not desiccated, the amount of SRP initially released in both the Cell 4 inflow and outflow sediments was the same. The release of SRP from the control inflow sediment under the imposed oxic conditions was probably attributable to desorption and organic matter decomposition; both P pools supporting these processes are likely to be considerably higher in the inflow than outflow sediments.

These results are similar to those of Twinch (1987), who reported a decrease in the phosphate-buffering capacity and an increase in the phosphate equilibrium concentration when sediments were air-dried. This suggests that the mechanism of the SRP release for both sediment types may be desorption, although the oxidation of organic matter and bacterial lysis may have also contributed P (Qiu and McComb 1994).

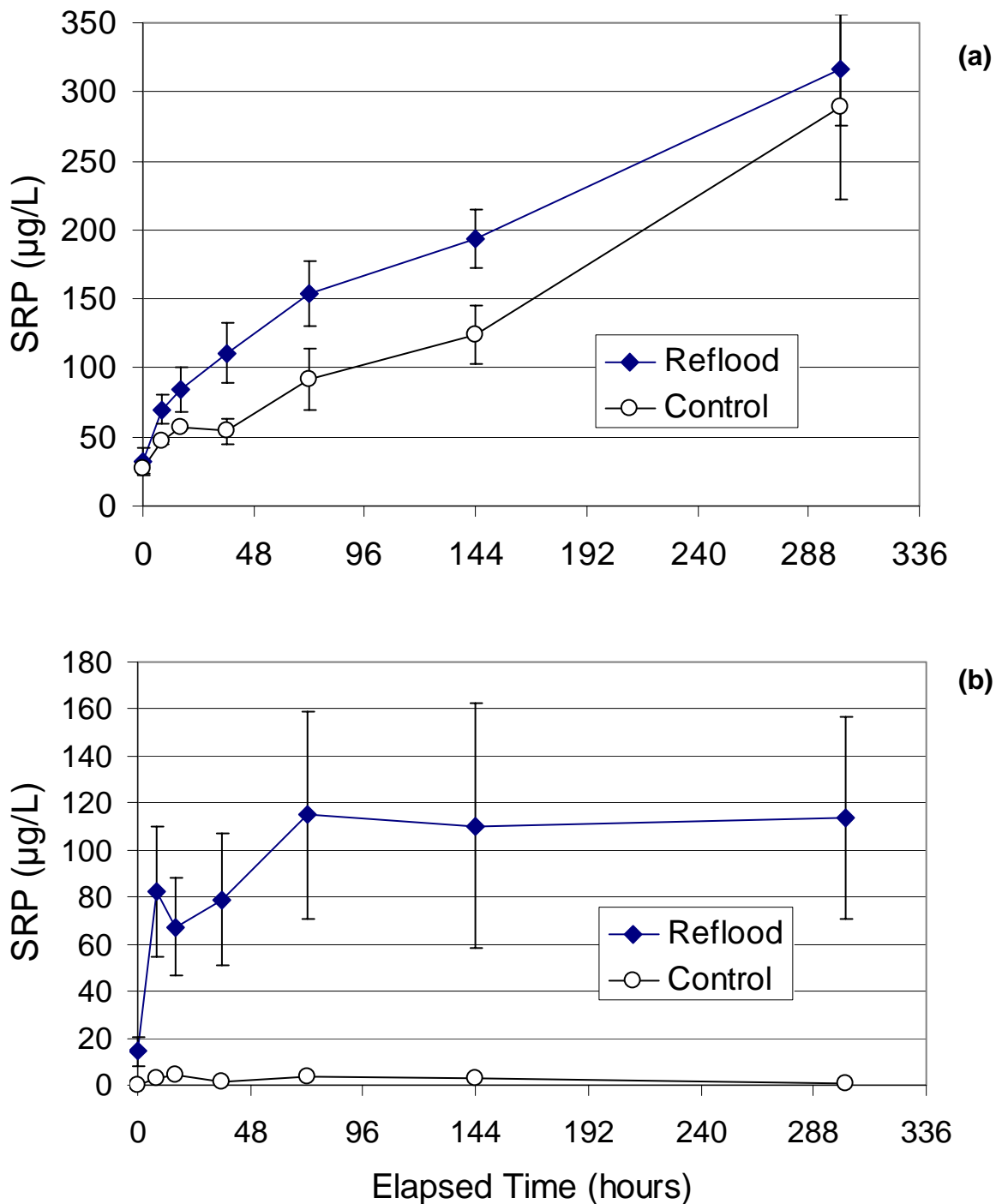


Figure 4.28. The release of soluble reactive P (SRP) from the desiccation of Cell 4 inflow (a) and outflow (b) sediments over 99 and 72 hours, respectively, upon reflooding with Cell 4 outflow water. The control represents a “no desiccation” treatment. Each data point represents the mean \pm s.d. of triplicate incubation vessels.

High Ca and Alkalinity Concentrations

Since the outflow water from Cell 4, which was used in the incubations of both inflow and outflow sediment types, had low concentrations of Ca and alkalinity, we added both components to the outflow water to evaluate the effects of increased calcium/alkalinity levels on P release (Table 4.7). Three triplicate flasks of each sediment type were incubated under oxic conditions.

Table 4.7. Dissolved calcium and alkalinity concentrations and specific conductance values in Cell 4 inflow and outflow waters before and after Ca/alkalinity amendments.

Sediment Type	Diss. Calcium (mg/L)	Alkalinity (mg CaCO ₃ /L)	Sp. Cond. (µmho/cm)
Initial Inflow	38	140	893
Amended Inflow	71	260	1069
Initial Outflow	44	168	758
Amended Outflow	70	248	1279

The higher Ca and alkalinity concentrations (76 – 85 mg Ca/L and 244 – 259 mg CaCO₃/L) in the overlying water during the incubations of the inflow sediment inhibited the release of SRP relative to the control (36 – 52 mg Ca/L and 150 – 185 mg CaCO₃/L) (Figure 4.29a). The pH values for the treated and control sediments were similar throughout the incubation period (mean treatment pH = 8.54 and mean control pH = 8.42). This indicates that higher hardness water *per se* (i.e. independent of pH) can reduce the release rate of SRP from sediments that have a significant pool of labile P. The formation of calcium phosphate compounds, CaCO₃-P coprecipitation, or P sorption onto freshly precipitated CaCO₃ surfaces are the likely P retention mechanisms. Release of SRP from the control sediment was probably due to desorption and decomposition of organic matter under the oxic conditions.

By contrast, we observed only minor differences between the release rates from outflow sediments containing high Ca and alkalinity concentrations in the overlying water and those same sediments exposed to more moderate levels of Ca and alkalinity (Figure 4.29b). In both the treated and control sediments, the mean SRP concentrations never exceeded 9 µg/L.

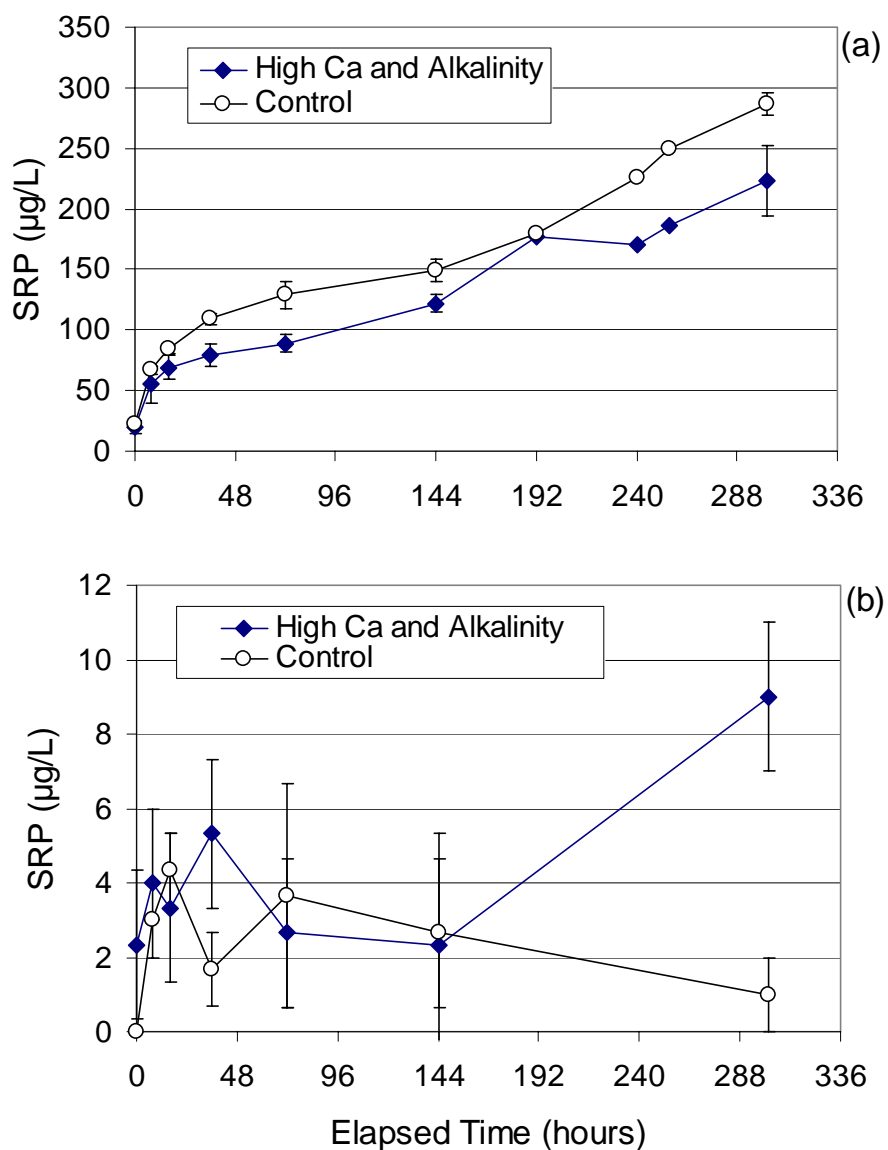


Figure 4.29. The release of soluble reactive P (SRP) from Cell 4 inflow (a) and outflow (b) sediments with Ca- and alkalinity-amended (70 – 71 mg Ca/L and 248 – 260 mg CaCO_3 /L) Cell 4 outflow water. The control treatment received no calcium or alkalinity amendments. Each data point represents the mean \pm s.d. from triplicate incubation vessels.

Soluble Reactive Phosphorus Amendments

The Cell 4 outflow water, which was used in the incubations for both the inflow and outflow sediments, had a SRP concentration of 2 µg/L or lower. To ascertain the potential release rate of SRP from sediments exposed to higher SRP water, we spiked the incubation waters to yield final SRP concentrations of 128 and 120 µg/L for the inflow and outflow sediment studies, respectively.

The SRP spike of 128 µg/L caused the initial SRP concentrations in the overlying waters of the treated and untreated (control) inflow sediments to differ by 116 µg/L (Figure 4.30a). However, the difference in SRP concentrations between the SRP-spiked and un-spiked (control) waters narrowed throughout the incubation period; after 302 hours water column differences in SRP concentrations were indistinguishable. It therefore appears that increased SRP concentration within the overlying water temporarily hinders the release of sediment P into the water column (Figure 4.30a). The general increasing trend in the SRP concentrations for both the treated and control inflow sediments indicates adequate labile P pools in the sediment exist, which can be mobilized under the oxic conditions imposed in the laboratory. The nearly identical SRP concentrations for the control and SRP-spiked sediments at the end of the incubation period (Figure 4.30a) demonstrate the sediment has a high SRP buffering capacity.

The incubation with Cell 4 outflow sediments provided a markedly different result. In this case, the spiked SRP concentration (120 µg/L) declined asymptotically to within 12 µg/L of the un-spiked (control) sediment after 72 hours (Figure 4.30b). Thereafter, the SRP concentrations remained relatively constant for both the control and evaluation waters. It appears that the P equilibria among the outflow sediment's exchangeable P pools and the water column favored SRP transfer from the water column into the sediment. In other words, the exchangeable sites associated with the outflow sediment are not fully occupied by P; most of those sites are available for SRP immobilization.

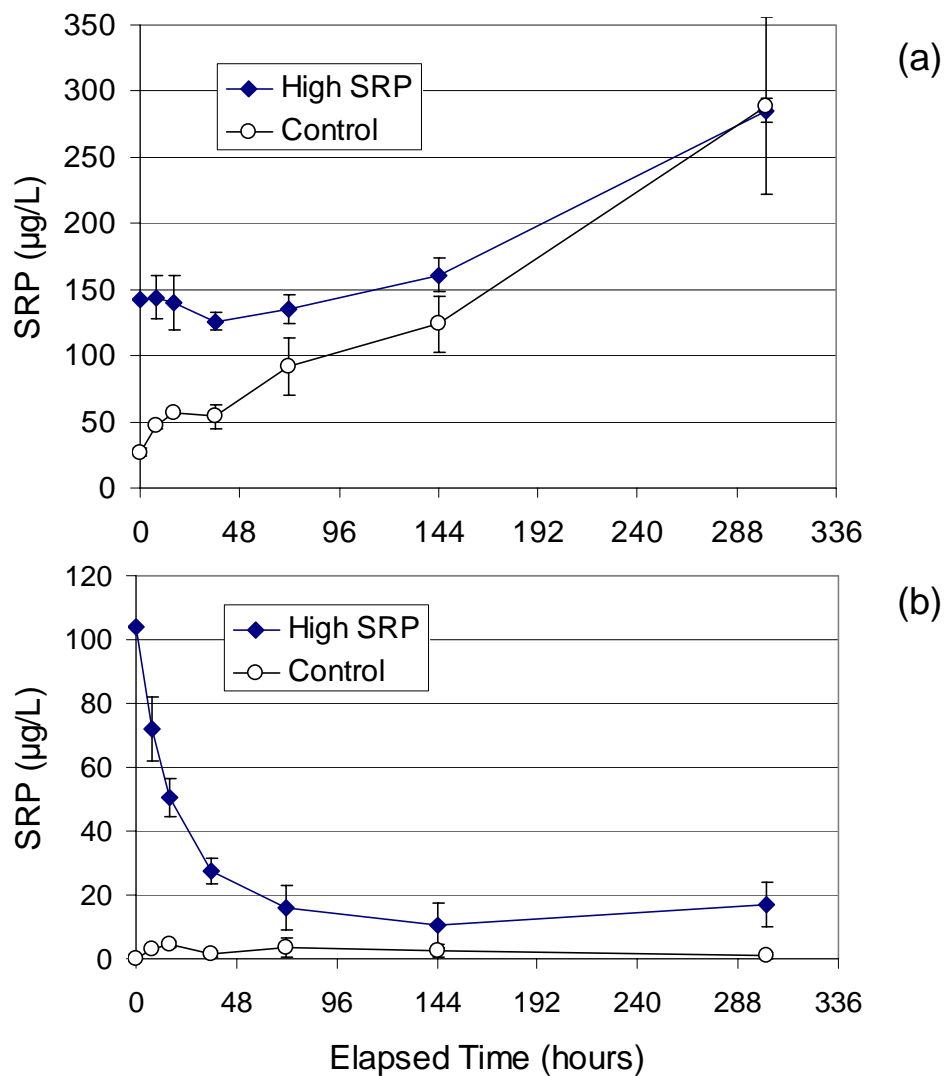


Figure 4.30. Soluble reactive P (SRP) concentrations for the SRP-amended and unamended overlying Cell 4 outflow water in contact with Cell 4 inflow (a) and outflow (b) sediments. The control treatment received no SRP amendments. Each data point represents the mean \pm s.d. from triplicate incubation vessels.

Comparison of P Fractionations Between Inflow and Outflow Sediments

The P fractionation data help to explain the SRP release data for both sediment types and relative to the inflow sediment P pools (Figure 4.31). The outflow sediments contained lower concentrations of P in each of the extracted fractions. This difference was particularly true for the labile pools (NH_4Cl -SRP, NaOH -SRP, and NaOH -org P), which undoubtedly reflects the higher loading rates of the more labile P species in the inflow region. For both sediment types, the non-labile fractions (HCl -SRP and Residue-TP) made up the majority of the sediment TP, leaving only 18 and 7 % comprising the inflow and outflow labile pools, respectively.

For all treatments (pH, redox, desiccation/reflooding, Ca/alk amendments, SRP spikes), the mass of SRP released from the inflow sediment was significantly higher than that released from outflow sediment. The obvious explanation, which is supported by our P fractionations, is that P is quickly removed within the Cell 4 wetland, leaving very little P to be incorporated into biomass (and ultimately, as labile P in the sediments) in the outflow region.

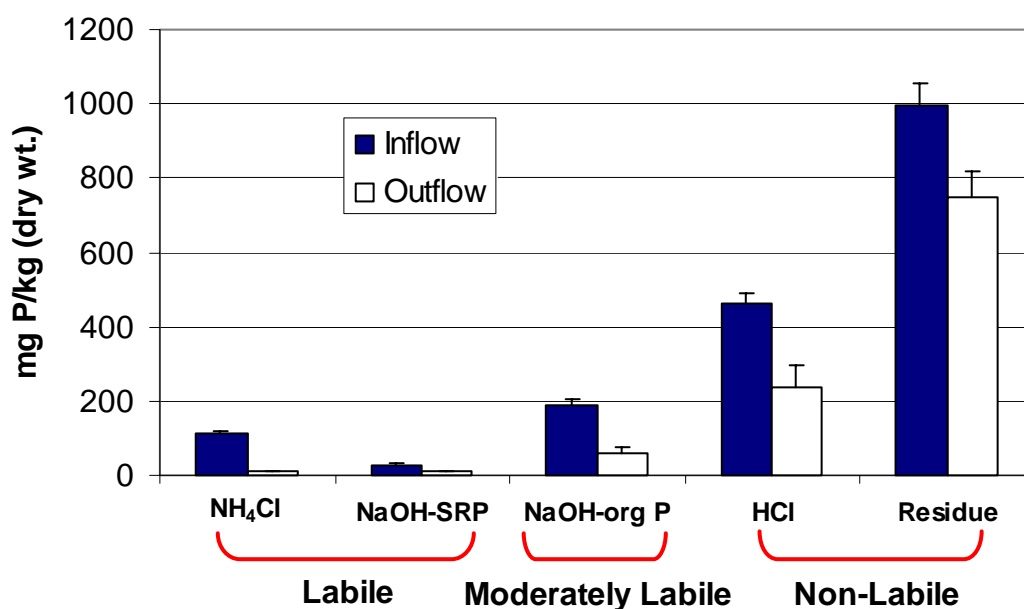


Figure 4.31. Inorganic P fractionation of composited Cell 4 inflow and outflow region sediments. Error bars indicate +1 standard deviation.

4.6.3 Conclusions

Although these data indicate that lower pH and redox conditions affect Cell 4 sediment SRP release, particularly in the inflow region, the ecological implications may not be as clear. An important consideration is the length of time that a low pH or anoxic event would likely occur in the field. Our assessment lasted 12.6 days. Low pH or redox conditions typically may be of shorter duration in the field. For example, while inflow waters to our NATTS mesocosms did on occasion reach a pH of 7.0 during the day, the daytime pH of the outflow from those mesocosms was never less than 7.6. We never observed a pH value less than 7.4 in our more limited nighttime database for the mesocosms. Similarly, the temporal and spatial profiling of SAV mesocosms during Phases I and II usually revealed redox values above +250 mV, particularly in the surface waters.

It also is important to note that all of the sediment SRP release evaluations were performed in the absence of SAV. It is very possible that a given "flush" of sediment SRP initiated by low pH or redox conditions would immediately be taken up by the SAV community, particularly if the plants were P-limited. The SRP data collected throughout our Phase I and II projects have indicated that SRP does not travel very far down the flow path of a SAV bed before it is reduced to below detection limits. Thus the presence of the SAV community may actually "buffer" the wetland from episodic sediment releases and discharges of SRP into downstream waters.

4.7 Sediment Diffusion Fluxes at the Inflow and Outflow Regions of Cell 4

One source of internal loading of P in a wetland is diffusional flux from enriched P sediments to the overlying water, which contains lower P concentrations. In this section, we seek to document and contrast the soluble P fluxes from the sediments in the inflow and outflow of Cell 4. In addition to soluble P, we also measured flux rates for calcium, alkalinity and iron, and recorded the gradient profiles for pH and redox.

4.7.1 Methods

Micro-profiles of pH, redox, SRP, TSP, dissolved Fe, dissolved Ca, and alkalinity were constructed in the inflow and outflow regions of Cell 4 using sediment-porewater equilibrators

(Hesslein, 1976). The equilibrators consisted of a 38 cm long X 10 cm wide X 2.0 cm thick Lexan base, and a 0.5 cm thick acrylic cover 7 cm long X 0.8 cm wide with cells spaced at 1 cm intervals. A 0.2 μm hydrophilic polyether sulfone membrane (Gelman Supor-200) approximately 11.4 cm X 38.1 cm was fitted between the base plate and the cover. A nylon mesh was placed over the membrane for protection. The cells were filled with N_2 -purged deionized water, then submerged in a cooler filled with N_2 -purged deionized water before deployment the following day. The equilibrators were inserted into the sediment and allowed to equilibrate 19 days for Cell 4 inflow (October 25 to November 13, 2001) and 18 days for Cell 4 outflow (November 26 to December 14, 2001). The sediment-water interface was marked beforehand on the equilibrators using duct tape. Duplicate equilibrators were inserted into the sediment at each of the three stations along a horizontal transect for both the inflow (Station 1: 26°38.041'N, 80°25.990'W, Station 2: 26°38.039'N, 80°26.173'W, and Station 3: 26°38.048'N, 80°26.318'W) and outflow regions (Station 1: 26°37.230'N, 80°26.552'W, Station 2: 26°37.250'N, 80°26.625'W and Station 3: 26°37.267'N, 80°26.693'W) of Cell 4.

After the equilibration period, samples were extracted from two adjacent cells using a syringe and composited providing a 2-cm depth resolution. Cell 4 inflow samples were taken from equilibrator cells from 4 cm above the sediment-water interface to 14 cm below. Outflow samples were withdrawn from 8 cm above the sediment-water interface to 14 cm below. Samples for pH, redox, SRP, TSP, alkalinity, dissolved Ca and Fe analyses were typically processed within 30 minutes and no longer than 70 minutes from the time of equilibrator retrieval in the field. Subsamples for pH, redox, and SRP were collected first from each sampled equilibrator cell. Besides pH and redox, alkalinity was also analyzed immediately in the field for Cell 4 outflow; however, alkalinity was analyzed in the lab within 48 hr after sampling for Cell 4 inflow. SRP and TSP were analyzed within 48 hr after collection.

Flux rates were calculated from the sediment to the overlying water based on Fick's First Law:

$$F_i = - \Phi D_i \theta^{-2} dc_i / dz$$

where F_i is the flux of the dissolved species i ; Φ is porosity of the sediment at the sampling location; D_i is the diffusion coefficient of the species (i) in particulate-free water; θ is the tortuosity factor; c_i is the concentration of the i^{th} species; and z is the sedimentary depth (cm) measured positively downward. The best estimate of the concentration gradient (dc_i/dz) between the sediment-porewater interface within the 4 cm below to 4 cm above interval was determined by least-squares.

We estimated porosities from sediment cores retrieved from each region (inflow and outflow) from wet and dry weight (60°C) measurements of known sediment volumes. The free-solution molecular diffusion coefficient (D_o) was corrected to temperature-induced viscosity changes according to the Stokes-Einstein relationship (Li and Gregory 1974) by measuring mean water temperature at the time of peeper retrieval at the inflow region (22°C) and during peeper deployment (18 days) at the outflow region (23°C). Because SRP represents polyprotic species, each of which has a different diffusion mobility (Li and Gregory 1974), the diffusion coefficient, D_o , represents a composite diffusion coefficient to account for the relative importance of each species (i.e. H_2PO_4^- and HPO_4^{2-}).

There was no way for us to measure tortuosity (θ) directly, but it has been shown to be related to porosity (Ullman and Aller 1982; Sweerts et al. 1991). We have employed the following regression equation reported by Sweerts et al. (1991) for freshwater sediments in determining θ^2 from porosity (Φ):

$$\theta^2 = - 0.47 \Phi + 1.91 \quad r = - 0.43$$

4.7.2 Results and Discussion

Comparison Among Stations

In the inflow region of Cell 4, SAV (*Ceratophyllum*) was present at Stations 1 and 3, but was absent at Station 2. Concentrations of SRP, TSP, and DOP increased with sediment depth for all three inflow region stations, with the highest concentrations recorded at Station 1 (Figures 4.32, 4.33, and 4.34). Similar concentration gradients were measured for SRP and TSP at Stations 1

and 3, which were steeper than the concentration gradient in the porewaters collected at Station 2. SRP porewater concentrations were also lower at Station 2 than Stations 1 and 3, which may, in part, be due to the absence of SAV at Station 2. Water may be moving more freely at this station than at the other two stations which were inhabited by dense stands of SAV. Dense SAV canopies may create a “barrier” to mixing, resulting in pockets of isolated water that, coupled with light limitation, promote an environment near the sediment-water interface that cause a build-up of SRP. The low Ca and alkalinity concentrations (Figures 4.35 and 4.36), and higher pH readings (Figure 4.37), at Station 2 relative to the other two stations inhabited by SAV indicate that respiration may be higher under the SAV canopies at Stations 1 and 3. This, coupled with a likelihood that SRP uptake by the SAV in the inflow region is slow because of tissue P concentrations being P-saturated, may explain the differences in the SRP and TSP concentration profiles between stations that were inhabited by SAV and the one that was not.

Dense beds of *Najas* were present at all three stations located in the outflow region of Cell 4. SRP and TSP concentrations were similar for all three stations above the sediment-water interface; however, below the interface, concentrations increased more rapidly in Stations 1 and 3 (Figures 4.38 and 4.39). DOP concentrations were similar for all three stations (Figure 4.40). A steep transition at the sediment-water interface was observed in Stations 1 and 2 for E_h (Figure 4.41), which increased confidence that the sediment-water interface had been accurately marked in the field. Station 3 exhibited the most distinct transition between the sediment-water interface for dissolved Ca, and alkalinity (Figures 4.42, and 4.43). Since the dissolved Ca and alkalinity were similar at Stations 1 and 2 throughout the depth profile, very small concentration gradients existed at the sediment-water interface (Figures 4.42 and 4.43).

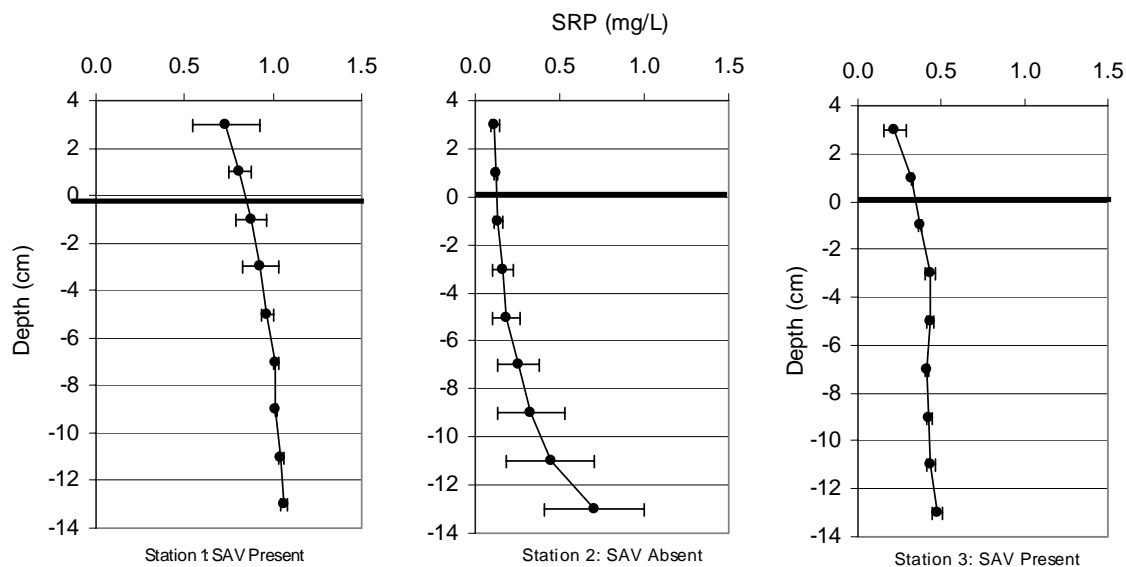


Figure 4.32. Average porewater soluble reactive P concentrations in the **inflow** region of Cell 4 on November, 13, 2001. The dark horizontal line corresponds to the sediment-water interface. The error bars represent the range of duplicate porewater equilibrators at each station.

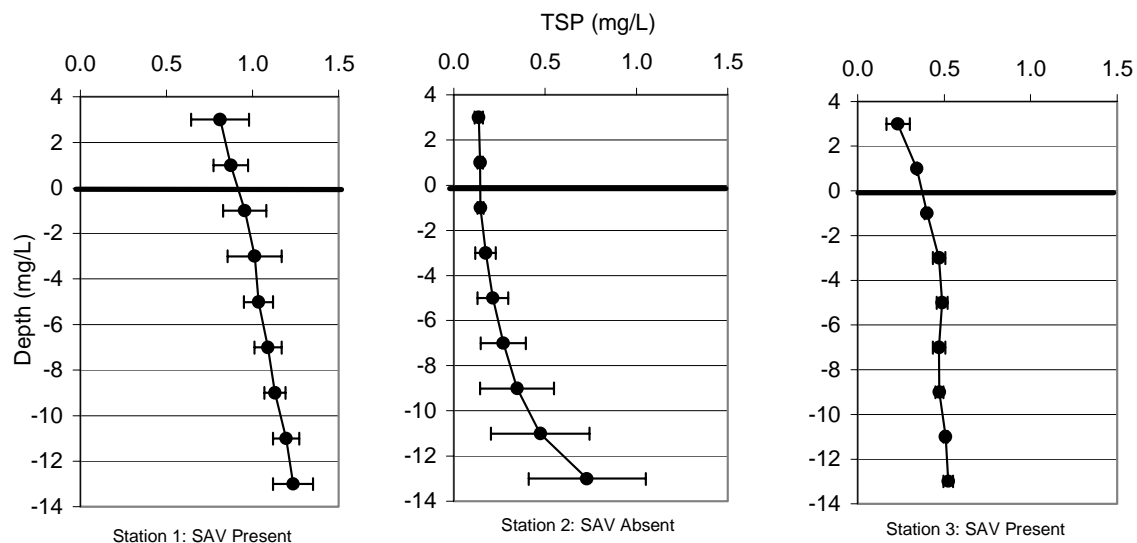


Figure 4.33. Average porewater total soluble P concentrations in the **inflow** region of Cell 4 on November, 13, 2001. The dark horizontal line corresponds to the sediment-water interface. The error bars represent the range of duplicate porewater equilibrators at each station.

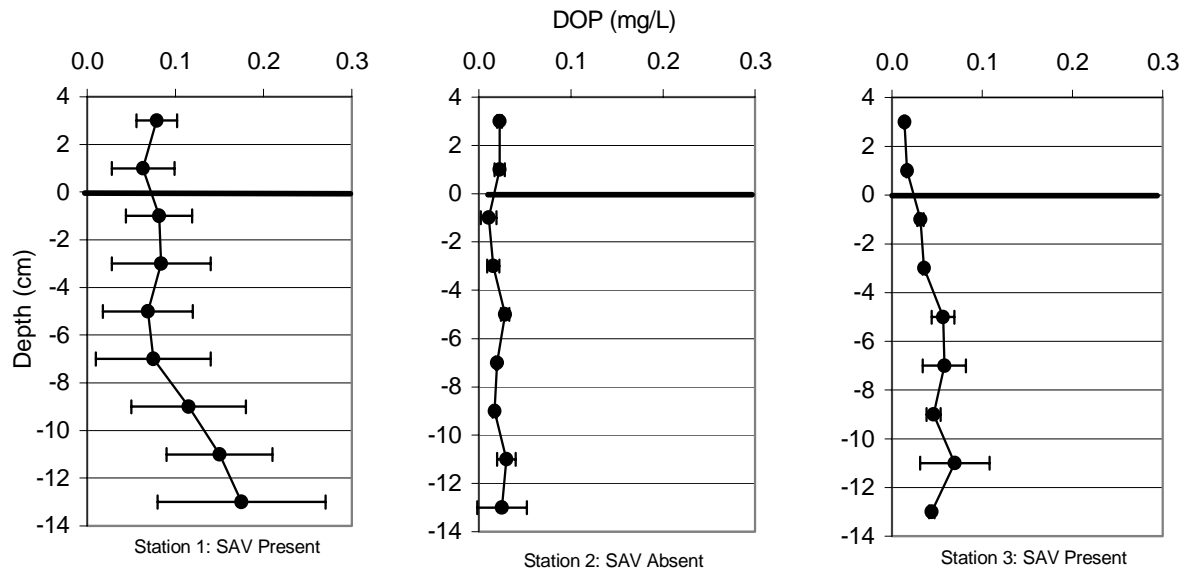


Figure 4.34. Average porewater dissolved organic P concentrations in the **inflow** region of Cell 4 on November 13, 2001. The dark horizontal line corresponds to the sediment-water interface. The error bars represent the range of duplicate porewater equilibrators at each station.

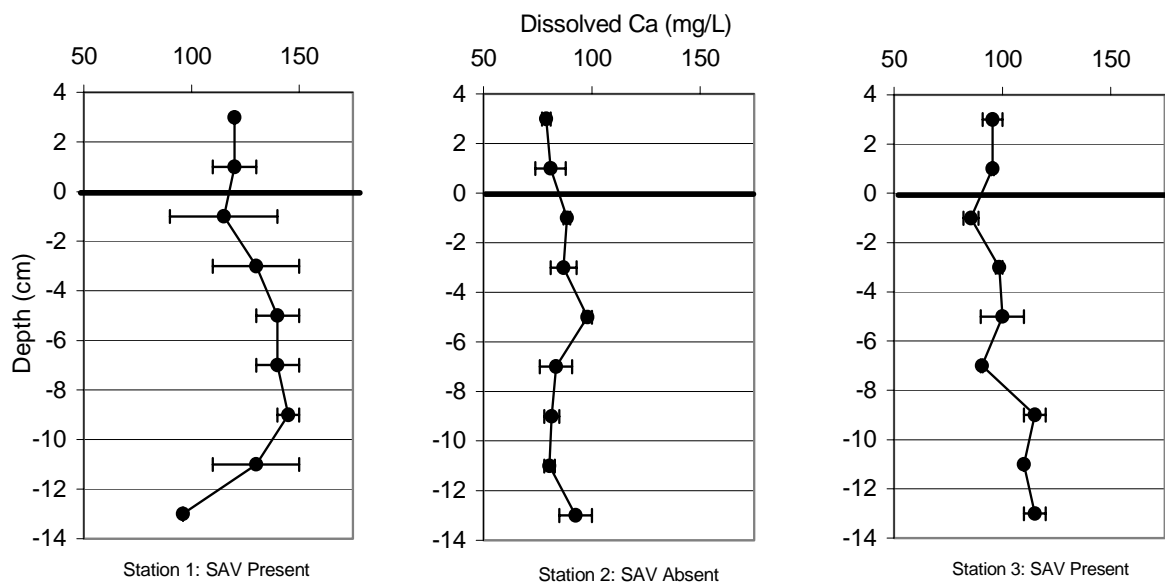


Figure 4.35. Average porewater dissolved calcium concentrations in the **inflow** region of Cell 4 on November 13, 2001. The dark horizontal line corresponds to the sediment-water interface. The error bars represent the range of duplicate porewater equilibrators at each station.

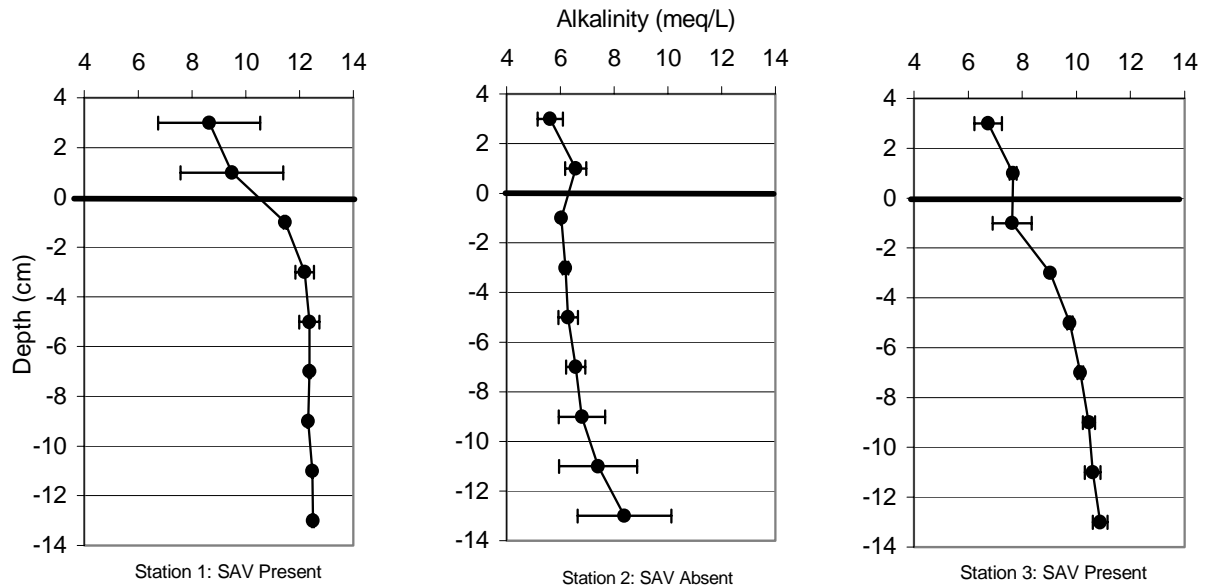


Figure 4.36. Average porewater alkalinity concentrations in the **inflow** region of Cell 4 on November 13, 2001. The dark horizontal line corresponds to the sediment-water interface. The error bars represent the range of duplicate porewater equilibrators at each station.

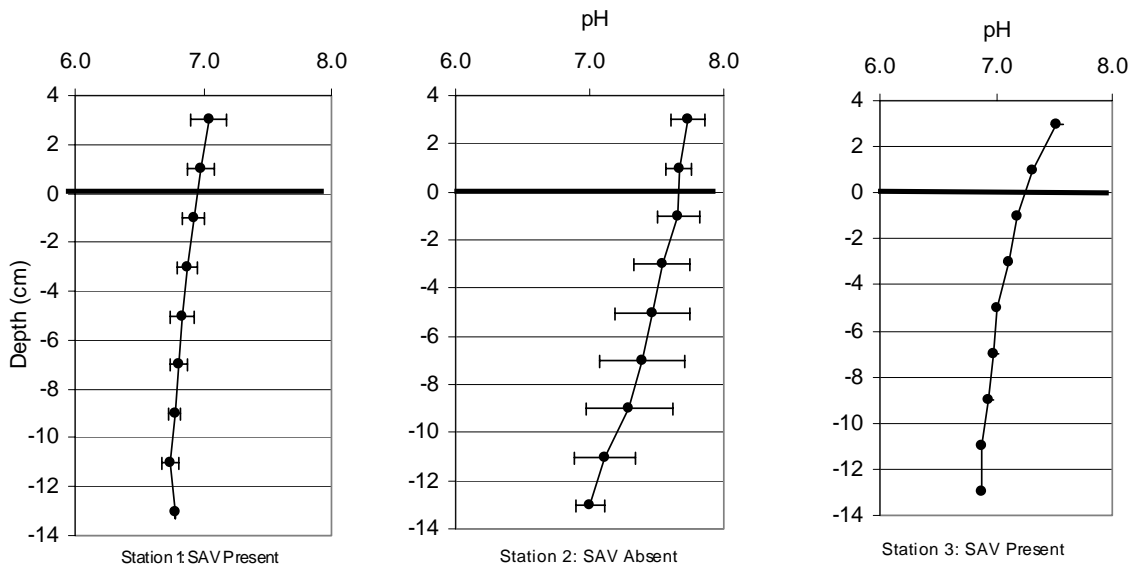


Figure 4.37. Average porewater pH values in the **inflow** region of Cell 4 on November, 13, 2001. The dark horizontal line corresponds to the sediment-water interface. The error bars represent the range of duplicate porewater equilibrators at each station.

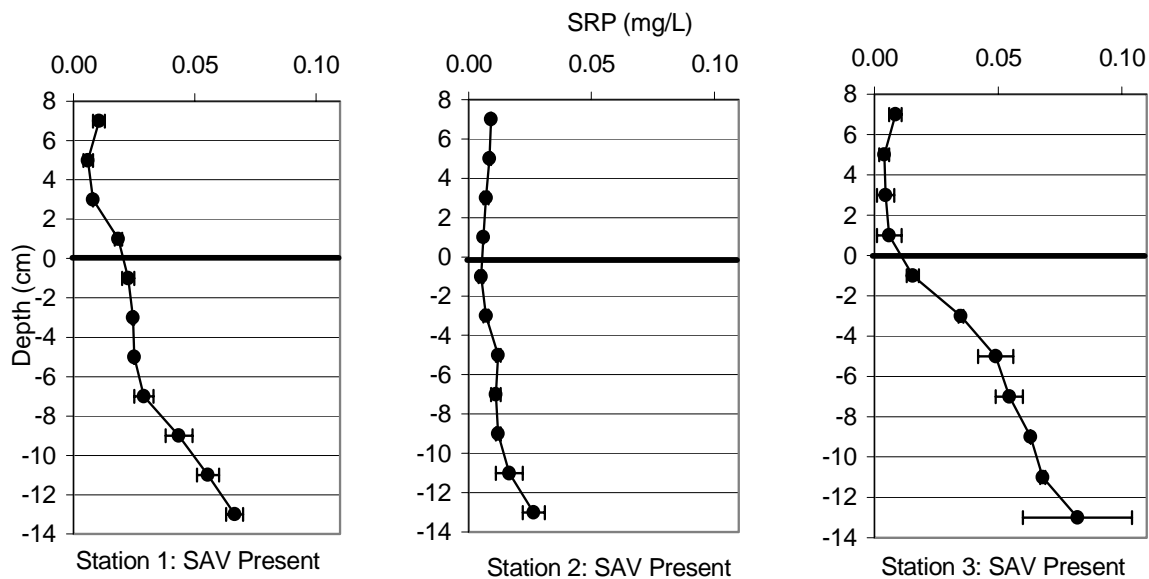


Figure 4.38. Average porewater soluble reactive P concentrations in the **outflow** region of Cell 4 on December 14, 2001. The dark horizontal line corresponds to the sediment-water interface. The error bars represent the range of duplicate porewater equilibrators at each station.

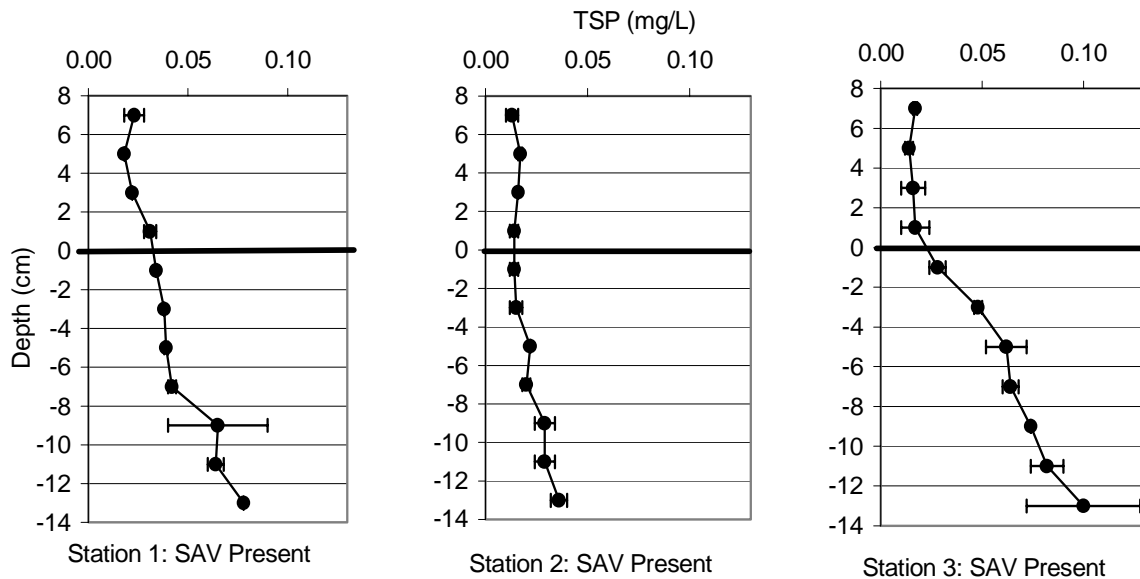


Figure 4.39. Average porewater total soluble P concentrations in the **outflow** region of Cell 4 on December 14, 2001. The dark horizontal line corresponds to the sediment-water interface. The error bars represent the range of duplicate porewater equilibrators at each station.

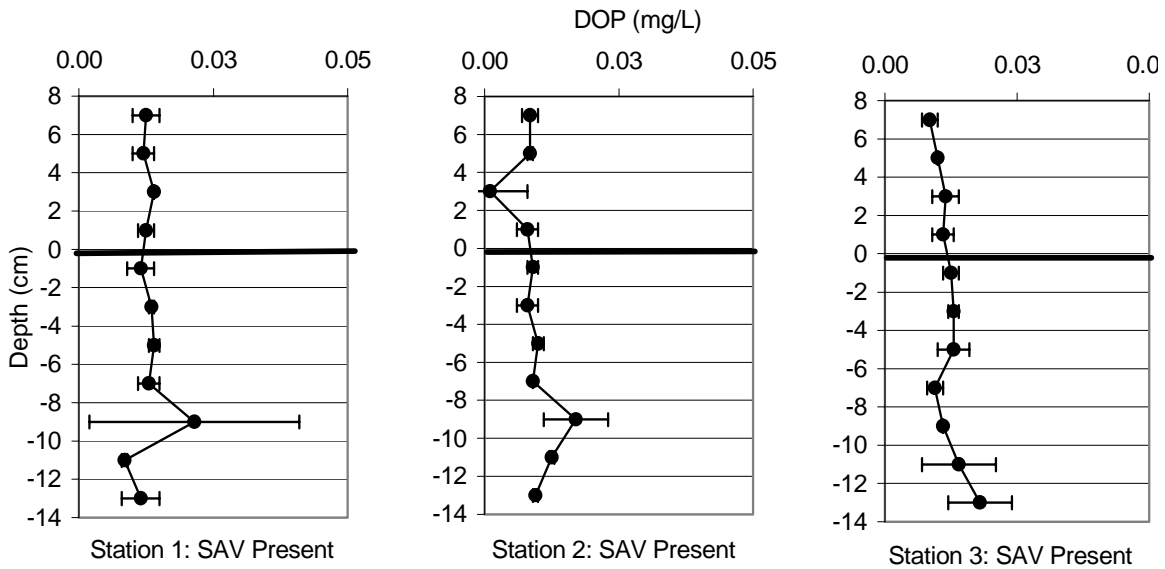


Figure 4.40. Average porewater dissolved organic P concentrations in the **outflow** region of Cell 4 on December 14, 2001. The dark horizontal line corresponds to the sediment-water interface. The error bars represent the range of duplicate porewater equilibrators at each station.

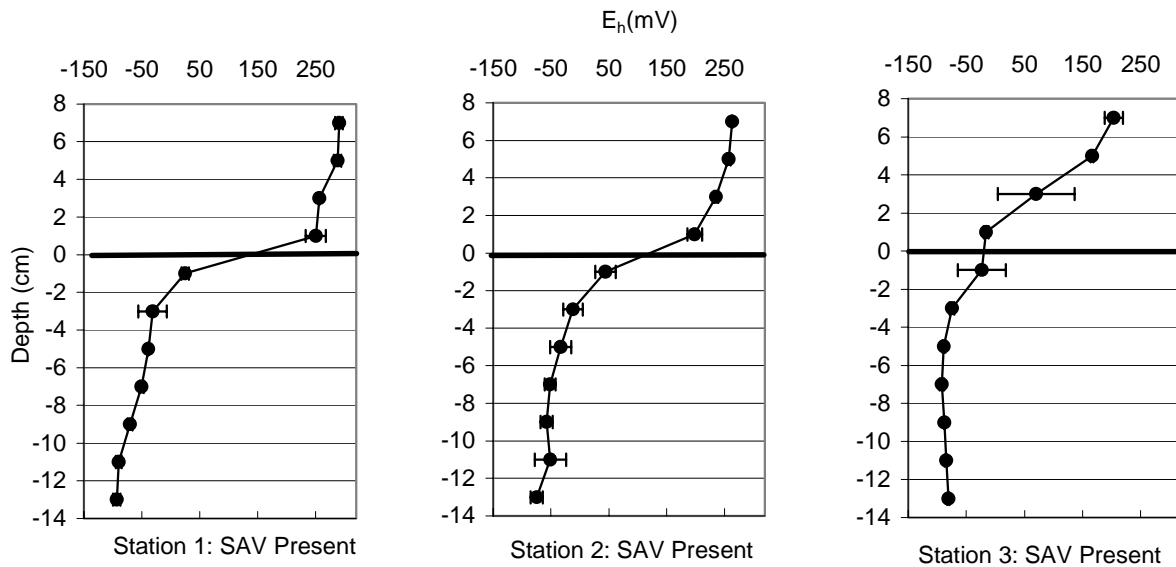


Figure 4.41. Average porewater E_h measurements in the **outflow** region of Cell 4 on December 14, 2001. The dark horizontal line corresponds to the sediment-water interface. The error bars represent the range of duplicate porewater equilibrators at each station.

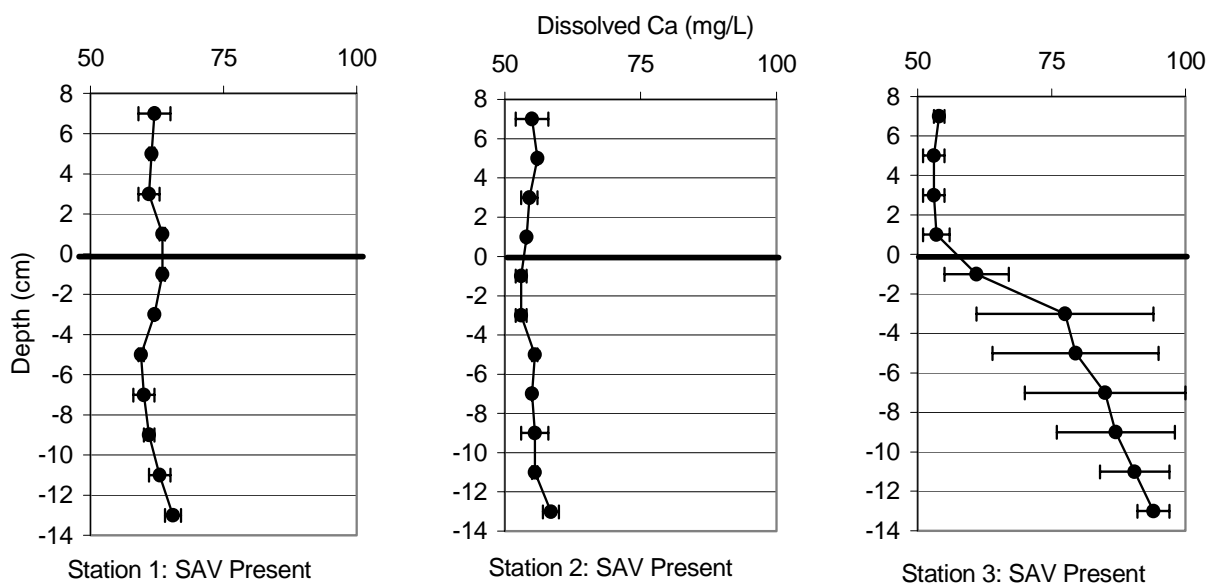


Figure 4.42. Average porewater dissolved calcium concentrations in the **outflow** region of Cell 4 on December 14, 2001. The dark horizontal line corresponds to the sediment-water interface. The error bars represent the range of duplicate porewater equilibrators at each station.

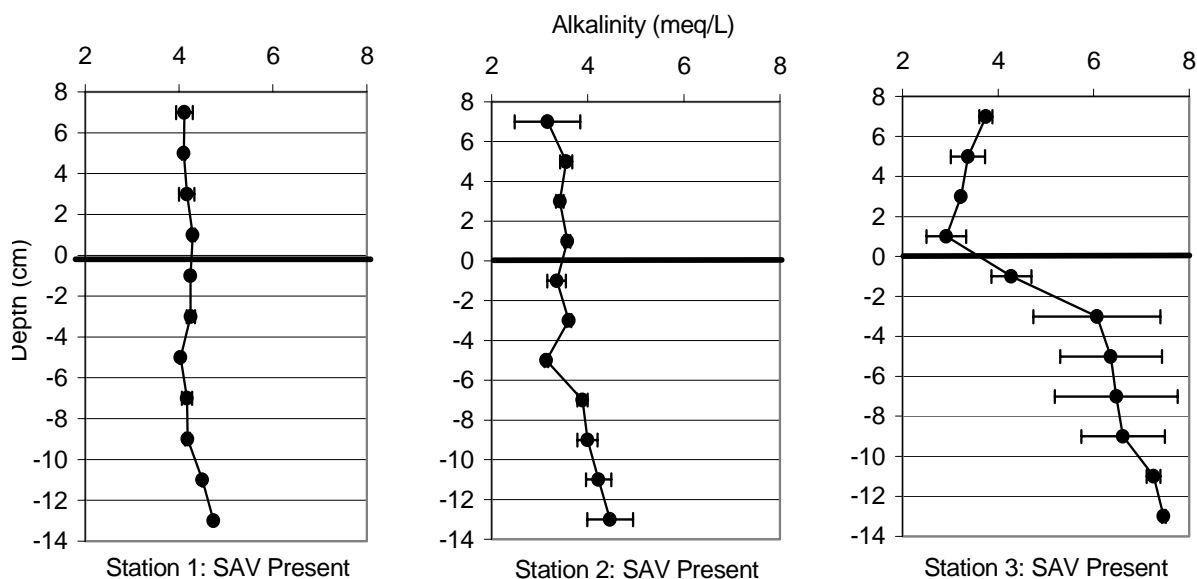


Figure 4.43. Average porewater alkalinity concentrations in the **outflow** region of Cell 4 on December 14, 2001. The dark horizontal line corresponds to the sediment-water interface. The error bars represent the range of duplicate porewater equilibrators at each station.

Comparison of Inflow and Outflow Regions of Cell 4

The averages of all three inflow stations for SRP (0.535 mg/L), TSP (0.588 mg/L), dissolved Ca (104 mg/L), and alkalinity (9.1 meq/L) concentrations were considerably higher than for the outflow stations (0.025 mg/L, 0.036 mg/L, 63 mg/L, and 4.39 meq/L, respectively). Reducing conditions above- and below the sediment interface at the inflow region were indicated by the low E_h measurements (-64 ± 20 mV), and the lack of a distinct concentration gradient between the sediment and water column (Figure 4.44).

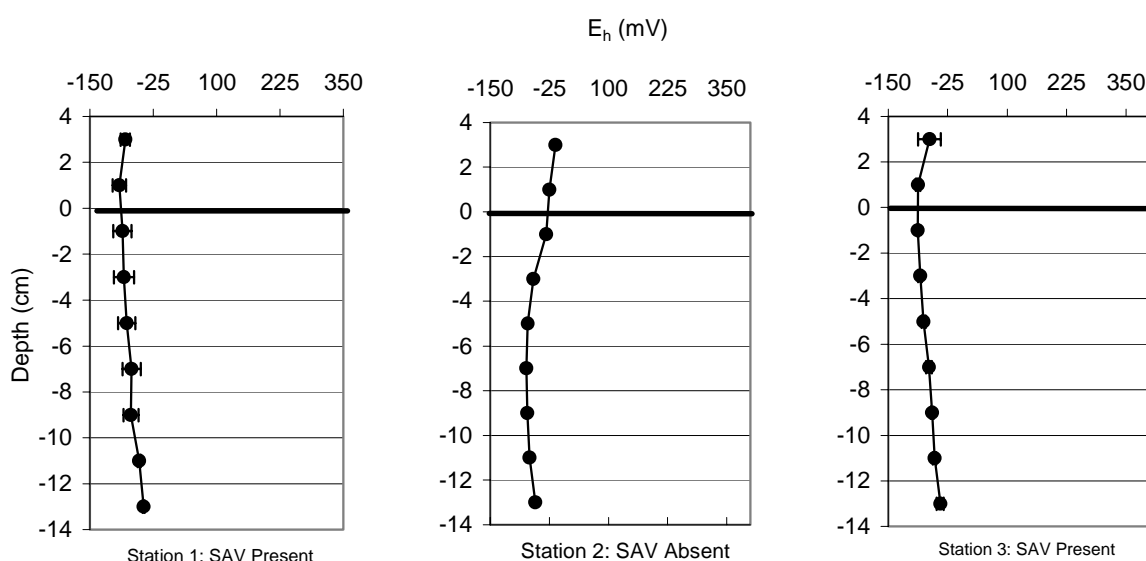


Figure 4.44. Average porewater E_h measurements in the **inflow** region of Cell 4 on November 13, 2001. The dark horizontal line corresponds to the sediment-water interface. The error bars represent the range of duplicate porewater equilibrators at each station.

Two factors may be contributing to the reducing conditions found in the inflow region: (1) higher organic loading, and (2) lack of hydraulic flushing. Because of the higher organic loading and primary productivity in the inflow region, microbial respiration is likely contributing to the lower pH measurements in that region (7.13) in comparison to the outflow (7.33) (Figures 4.37 and 4.45).

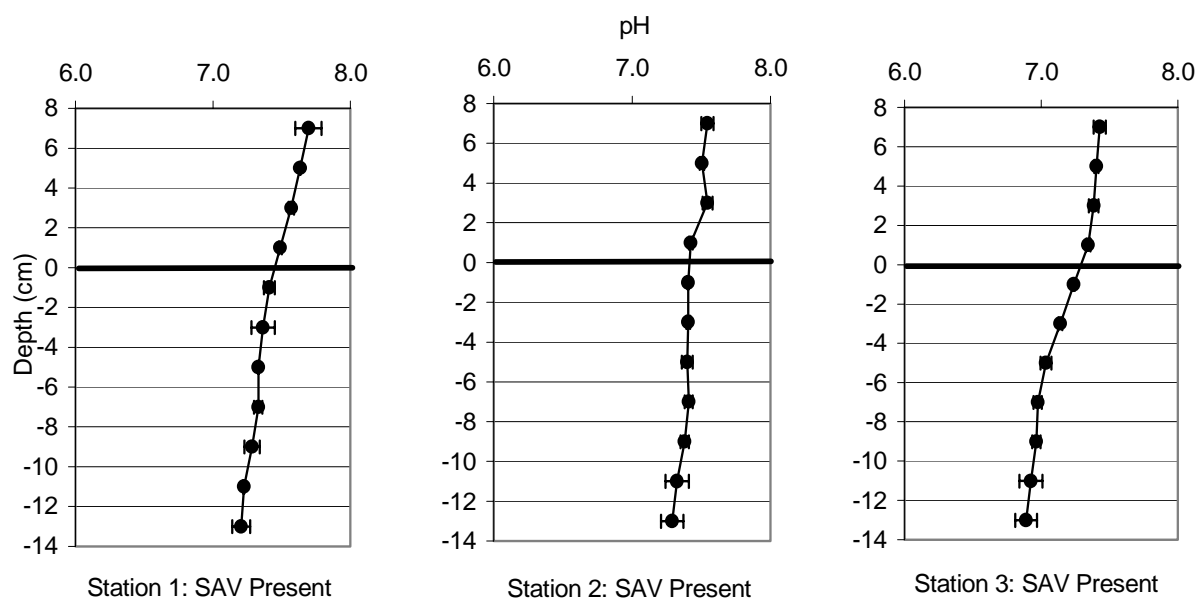


Figure 4.45. Average porewater pH values in the outflow region of Cell 4 on December 14, 2001. The dark horizontal line corresponds to the sediment-water interface. The error bars represent the range of duplicate porewater equilibrators at each station.

In addition, isolated patches of SAV that are not in line with the flow paths of the water entering into Cell 4 from Cell 2 may not be hydraulically flushed. Such conditions could easily lead to oxygen depletion within these stagnant areas. Although the deepest cells of the porewater equilibrators were likely contacting native muck soil in the outflow region, we could not discern any obvious discontinuities in the porewater profile with respect to any of the measured analytes. This means that enough time had elapsed since Cell 4 was flooded (8 yrs) for the establishment of steady-state diffusion gradients between the native muck soil and the calcareous accreted sediments.

Flux Rates

Diffusion typically occurred from the sediments to the water column. The flux rates for SRP were identical between Stations 1 and 3 for the inflow, which was 4 times higher than at Station 2 where no SAV was present (Table 4.8). Since the porewater SRP concentrations were high, we had anticipated a greater flux rate for the inflow region; however, SRP concentrations in the water column just above the sediments were also high, and therefore, precluded the

establishment of a sharp gradient. Station 2 had the highest flux rates for dissolved Ca in the inflow region (6.2 mg Ca/m²/day), 2 times greater than Station 1. Station 3 exhibited a negligible dissolved Ca flux into the sediment from the water column (Table 4.8).

The average flux rate of 0.007 mg/m²/day of SRP in the outflow region was 14 times lower than that of the inflow region (0.10 mg SRP/m²/day) (Table 4.9). All 3 stations in the outflow had similar flux rates for SRP. Dissolved Ca flux rates for the outflow region (4.9 mg Ca/m²/day) were higher than the inflow region (3.0 mg Ca/m²/day). Outflow Station 3 had the highest flux rate for dissolved Ca (15 mg Ca/m²/day), while a negative flux, or transport from the overlying water to the sediment, was measured at Station 2 (Table 4.9).

Table 4.8. SRP and dissolved Ca diffusion flux rates (mg/m²/day) for the inflow region of Cell 4. The values are the averages (and ranges) of the duplicate porewater equilibrators at each station.

		Station 1	Station 2	Station 3	Average
SRP	Mean	0.13	0.03	0.13	0.10
	Range	(-0.05 & 0.30)	(0.004 & 0.05)	(0.072 & 0.19)	
Ca	Mean	3.3	6.2	-0.49	3.0
	Range	(-11.5 & 18.2)	(4.9 & 7.4)	(-3.3 & 2.3)	

Table 4.9. SRP and dissolved Ca diffusion flux rates (mg/m²/day) for the outflow region of Cell 4. The values are the averages (and ranges) of the duplicate porewater equilibrators at each station.

		Station 1	Station 2	Station 3	Average
SRP	Mean	0.01	-0.01	0.02	0.007
	Range	(0.01 & 0.01)	(0.00 & -0.02)	(0.02 & 0.02)	
Ca	Mean	0.56	-1.0	15	4.9
	Range	(-3.8 & 1.5)	(-2.6 & 0.56)	(6.4 & 24)	

4.8 Stable Isotope Sampling and Preparation

4.8.1 Introduction

Organic carbon processing within SAV-dominated test cells and Cell 4 was investigated by comparing the stable isotopic composition of particulate and dissolved organic matter of inflow and outflow waters. We hypothesized that if significant organic matter processing (i.e., carbon turnover) was occurring within the wetland, then the isotopic composition of the carbon compounds and particulates entering the wetland from the EAA would be different from the isotopic composition leaving the wetland. Before routinely sampling North Test Cells and Cells 2 and 4 for stable isotope analysis, we first embarked on the development of a methodology for concentrating the dissolved carbon in the filtrates. We explored the efficacy of evaporating water samples at varying temperatures (40-100°C) as an inexpensive means of concentrating filtrates.

4.8.2 Methods Development

Dissolved Residue (Filtrate)

For the NTC-1 inflow and outflow samples, which were collected on January 26, 2001, 1-2 L of water were filtered through pre-combusted (500°C for 2 hours) Whatman™ 0.45 µm pore size (47 mm diameter) glass fiber filters. A pre-rinse with about 50 ml of distilled water (which was discarded) preceded the sample filtration. After filtering the particulates, the filtrates were frozen until February 26, at which time they were thawed, subdivided into three aliquots of 600-mL, and placed into 1-L Pyrex beakers. On the following day, each aliquot was placed into a drying oven at one of three temperatures: 60, 80 or 100°C, and allowed to evaporate to dryness. A 30 mg/L peptone standard was also dried at each of the three temperatures. After 3 days, the 600-ml water sample was completely evaporated under each of the 60, 80 and 100°C drying temperatures. Whereas the dried residue of the sample waters was easily scraped from the sides and bottom of each beaker, the residue from the dissolved 30 mg/L peptone could not be scraped and isolated because of the firm adherence of the thin coat of peptone to the glass surfaces.

Although the results of this initial test were encouraging for both particulate and dissolved residues, in that it appeared that temperature did not affect the carbon isotope ratio (Table 4.10),

the exclusion of a peptone standard (because of failure to recover the dried 30 mg/L peptone standard) meant that we could not state with confidence that temperature effects were unimportant in determining the carbon isotope ratio. We therefore initiated a second temperature-effect assessment by increasing the concentration of the peptone standard from 30 to 300 mg/L, and then exposing the higher concentration to temperatures of 40, 60 and 80°C. We found that it was easier to recover the dried peptone residue at this higher concentration,

Table 4.10. Effects of different evaporation temperatures on the recoveries of N, C, $\delta^{15}\text{N}$, $\delta^{13}\text{C}$ in peptone and dissolved organic matter from surface waters collected in the inflow and outflow of NTC-1 on January 26, 2001.

Sample	Temp (°C)	% N	% C	$\delta^{15}\text{N}$ (‰)	$\delta^{13}\text{C}$ (‰)	Ave. $\delta^{13}\text{C}$ (‰)
Peptone-A	Undiss	8.26	39.1	0.76	-24.7	-24.8
Peptone-B	Undiss	8.43	38.7	0.59	-24.9	
Peptone-A	40	7.04	32.4	1.78	-24.4	-24.3
Peptone-B	40	7.37	34.1	1.85	-24.2	
Peptone-A	60	6.77	32.4	3.35	-24.3	-24.5
Peptone-B	60	6.96	34.8	2.99	-24.7	
Peptone-A	80	5.81	30.8	1.75	-24.2	-24.4
Peptone-B	80	5.62	30.6	1.62	-24.7	
NTC-1 In-A	60	0.21	5.0	3.92	-20.4	-20.5
NTC-1 In-B	60	0.21	4.9	3.79	-20.6	
NTC-1 In-A	80	0.22	4.9	3.65	-21.3	-21.5
NTC-1 In-B	80	0.23	5.0	3.58	-21.7	
NTC-1 In-A	100	0.19	4.6	4.05	-20.4	-20.7
NTC-1 In-B	100	0.20	4.7	3.63	-21.0	
NTC-1 Out-A	60	0.17	3.2	3.94	-24.6	-24.7
NTC-1 Out-B	60	0.21	3.9	3.98	-24.7	
NTC-1 Out-A	80	0.20	4.1	3.90	-22.9	-22.9
NTC-1 Out-B	80	0.23	4.7	3.54	-22.8	
NTC-1 Out-A	100	0.20	4.1	3.50	-23.0	-23.0
NTC-1 Out-B	100	0.20	4.0	3.61	-22.9	

especially at 40°C. The results of the isotope and elemental concentration analyses were encouraging (Table 4.10). Despite losses in the N and C concentrations that increased with temperature, the $\delta^{13}\text{C}$ was unaffected. This means that although temperature affects the carbon and nitrogen contents of the peptone, the C-13 and C-12 components of the dissolved organic matter are equally affected, resulting in the ratio remaining unaltered.

Particulate Residue

After collection of the solid residue, several drops of 1 N HCl were added to each filter and fumed overnight. Filters were then washed with deionized water, and dried at 40-60°C overnight before being shipped to the University of Alaska-Fairbanks for stable isotope analysis (Table 4.11).

Table 4.11. Stable isotopes ($\delta^{15}\text{N}$ and $\delta^{13}\text{C}$) in particulate organic matter filtered from surface waters collected in the inflow and outflow of NTC-1 on January 26, 2001.

Sample	$\delta^{15}\text{N}$ (‰)	$\delta^{13}\text{C}$ (‰)	Ave. $\delta^{13}\text{C}$ (‰)
NTC-1 In-A	-2.07	-33.9	-34.4
NTC-1 In-B	0.56	-35.0	
NTC-1 Out-A	3.15	-29.8	-30.4
NTC-1 Out-B	-2.43	-31.0	

4.8.3 Standard Preparation Procedure for the Dissolved Residue (Filtrate)

As a result of these preliminary trials, the following procedure was followed when concentrating the filtrates from sampled stations within the north test cells and STA-1W. The filtrate was concentrated immediately, except on one occasion when it was refrigerated 24 hours prior to concentration. The concentration process consisted of evaporating each sample filtrate to dryness at an average temperature of 45°C (range of 38 to 50°C). It took 10-20 days to evaporate a 1L sample to dryness at these temperatures. After reaching dryness, the dried

filtrate residue was scraped from the sides and bottom of the beaker. After an overnight fumigation with 1 N HCl, the residue was rinsed with distilled water and re-dried before being shipped to the University of Alaska for isotope analysis. An internal sample (peptone Hy-Soy J enzymatic hydrolysate, Sigma Lot # 46H0862) was also dried from solution and recovered in the same manner as the sample water residue. All samples, blanks, and internal standards for both particulate and dissolved residues were processed in duplicate.

4.8.4 Results

Surface water samples were retrieved from the inflow and outflow of Cells 2 and 4 at 2-14 week intervals from August 10, 2001 to March 8, 2002, and from the inflow and outflow of NTC-15 and the outflow of NTC-5 collected at 2-12 week intervals from July 26, 2001 to January 27, 2002. Samples were processed in the lab for analysis of stable isotope ratios ($\delta^{13}\text{C}$) on filtered and unfiltered fractions. The results are shown in Tables 4.12 to 4.15.

Table 4.12. Mean \pm s.d. (n=2) $\delta^{13}\text{C}$ (‰) for dissolved and particulate fractions of surface water samples collected from NTC-15 inflow and outflow, and NTC-5 outflow, from July 26, 2001 to January 27, 2002.

Date	<u>Dissolved</u>			<u>Particulate</u>		
	In	Out	NTC-5 Out	In	Out	NTC-5 Out
7/26/01	-10.78 \pm 0.90	-12.41 \pm 0.48	-11.16 \pm 0.63	-27.78 \pm 0.32	-31.37 \pm 0.76	-28.87 \pm 0.13
10/9/01	-13.24 \pm 0.35	-14.56 \pm 0.50	-13.71 \pm 0.79	-36.45 \pm 0.49	-30.72 \pm 0.37	-31.93 \pm 2.67
10/18/01	-13.55 \pm 0.30	-16.39 \pm 0.47	-14.13 \pm 0.42	-36.65 \pm 0.21	-28.36 \pm 0.18	-30.24 \pm 0.30
12/11/01	-14.64 \pm 0.90	-14.28 \pm 0.72	-14.67 \pm 0.14	-31.77 \pm 0.23	-26.29 \pm 0.38	-30.68 \pm 0.11
1/4/02	-14.37 \pm 1.02	-14.11 \pm 0.28	-14.09 \pm 0.42	-29.78 \pm 0.26	-23.71 \pm 1.16	-27.38 \pm 2.13
1/27/02	-13.80 \pm 0.52	-13.94 \pm 1.30	-13.64 \pm 0.40	-26.45 \pm 1.20	-26.23 \pm 0.45	-30.82 \pm 0.35

Table 4.13. Mean \pm s.d. (n=2) $\delta^{15}\text{N}$ (‰) for dissolved and particulate fractions of surface water samples collected from NTC-15 inflow and outflow, and NTC-5 outflow, from July 26, 2001 to January 27, 2002.

Date	<u>Dissolved</u>			<u>Particulate</u>		
	<u>NTC-15</u> In	<u>NTC-15</u> Out	<u>NTC-5</u> Out	<u>NTC-15</u> In	<u>NTC-15</u> Out	<u>NTC-5</u> Out
7/26/01	8.34 \pm 0.02	3.67 \pm 0.21	2.60 \pm 0.49	9.71 \pm 0.10	5.60 \pm 0.57	0.97 \pm 0.05
10/9/01	2.89 \pm 0.26	2.97 \pm 0.14	2.63 \pm 0.11	9.87 \pm 0.40	6.58 \pm 1.91	1.00 \pm 0.08
10/18/01	2.83 \pm 0.26	3.03 \pm 0.10	2.44 \pm 0.07	7.27 \pm 0.37	6.94 \pm 1.21	1.00 \pm 0.11
12/11/01	2.42 \pm 0.38	2.22 \pm 0.26	1.62 \pm 0.31	4.48 \pm 1.62	3.89 \pm 0.01	1.52 \pm 0.01
1/4/02	1.93 \pm 0.24	2.41 \pm 0.16	1.73 \pm 0.23	12.13 \pm 6.14	7.57 \pm 1.74	6.82 \pm 6.24
1/27/02	2.38 \pm 0.42	2.33 \pm 0.50	2.36 \pm 0.20	21.73 \pm 23.80	5.03 \pm 5.28	-0.33 \pm 0.17

Table 4.14. Mean \pm s.d. (n=2) $\delta^{13}\text{C}$ (‰) for dissolved and particulate fractions of surface water samples collected from the inflow and outflow of Cell 2 and Cell 4 from August 10, 2001 to March 8, 2002. All inflow and outflow culverts at a particular levee were composited on each sampling date.

Date	<u>Dissolved</u>			<u>Particulate</u>		
	<u>Cell 2</u> In	<u>Cell 2</u> Out *	<u>Cell 4</u> Out	<u>Cell 2</u> In	<u>Cell 2</u> Out *	<u>Cell 4</u> Out
8/10/01	-11.79 \pm 1.61	-10.17 \pm 1.01	-8.81 \pm 0.23	-27.29 \pm 0.13	-33.65 \pm 0.45	-26.56 \pm 0.17
9/24/01	-8.45 \pm 1.67	-7.45 \pm 1.97	-11.53 \pm 1.05	-27.52 \pm 0.24	-35.95 \pm 4.43	-28.98 \pm 0.16
11/7/01	-13.74 \pm 0.57	-13.42 \pm 0.23	-13.86 \pm 0.40	-26.63 \pm 0.39	-29.80 \pm 0.04	-27.83 \pm 0.01
2/20/02	-11.06 \pm 0.36	-11.73 \pm 0.62	-11.44 \pm 1.66	-26.08 \pm 0.13	-33.52 \pm 5.52	-27.09 \pm 0.37
3/8/02	-11.44 \pm 0.43	-13.36 \pm 1.01	-13.20 \pm 0.43	-28.05 \pm 0.15	-29.79 \pm 0.32	-26.77 \pm 0.00

* Cell 2 outflow= Cell 4 inflow

Table 4.15. Mean \pm s.d. (n=2) $\delta^{15}\text{N}$ (‰) for dissolved and particulate fractions of surface water samples collected from the inflow and outflow of Cell 2 and Cell 4 from August 10, 2001 to March 8, 2002. All inflow and outflow culverts at a particular levee were composited on each sampling date.

Date	<u>Dissolved</u>			<u>Particulate</u>		
	<u>Cell 2</u>		<u>Cell 4</u>	<u>Cell 2</u>		<u>Cell 4</u>
	In	Out *	Out	In	Out *	Out
8/10/01	6.93 \pm 0.49	5.72 \pm 0.22	4.61 \pm 0.60	4.42 \pm 0.15	11.90 \pm 0.01	8.13 \pm 0.32
9/24/01	2.28 \pm 0.25	-0.83 \pm 1.48	-0.20 \pm 0.66	6.33 \pm 0.13	8.94 \pm 1.26	5.97 \pm 0.83
11/7/01	3.58 \pm 0.09	4.59 \pm 0.13	3.91 \pm 0.10	4.86 \pm 1.17	9.52 \pm 0.62	6.12 \pm 0.81
2/20/02	2.42 \pm 0.23	3.48 \pm 0.32	4.19 \pm 0.42	6.35 \pm 0.52	9.15 \pm 2.56	3.63 \pm 1.32
3/8/02	4.60 \pm 0.45	2.79 \pm 0.12	2.67 \pm 0.27	8.80 \pm 0.38	8.19 \pm 0.19	6.56 \pm 0.33

* Cell 2 outflow= Cell 4 inflow

4.9 Cell 4 Hydraulic Tracer Assessment

4.9.1 Introduction

Field observations suggest that relic borrow canals within Cell 4 (particularly along the east and west levees) may result in hydrologic short-circuiting. Not only are these canals deeper than the adjacent wetland, but they also contain less SAV than open water sites. District scientists and other investigators have been concerned that the hydraulic short-circuiting may compromise the efficiency of P removal within the cell. The first tracer assessment (DBE 2000a), initiated December 16, 1999, was designed to document the short-circuiting and its effect on P removal efficiency, in addition to quantifying the typical hydraulic parameters of interest (i.e., hydraulic retention time (HRT) and dispersion). Once the short-circuit pathways were identified, a follow-up Feasibility Assessment (DBE 2000b) investigated the potential for optimizing Cell 4 hydraulic and total P removal performance by structurally altering the wetland.

This section describes the second of two tracer studies that we performed within Cell 4. This second dye tracer assessment was performed after completion of construction activities and modifications to Cell 4 (in part to reduce short-circuiting) in 2000. These activities included placing

limerock plugs at intervals along the north-south length of perimeter borrow canals, deepening the inflow region mixing zone at the north end of the cell, dredging the east-west cross-canal (C-7) and adjacent spoil berm buildup, and constructing a new gate (G-309) at the western end of C-7 (Figure 4.46). The aim of the second tracer assessment was to document changes in the flow patterns, HRT, dispersion characteristics, and P removal efficiency that may have resulted from these structural modifications.

4.9.2 Cell 4 Hydrologic and Hydraulic Conditions

We examined the relative flow distribution between the nine inflow culverts for the week prior to the assessment to determine whether tracer additions to the culvert flows should be flow-weighted. Hydrologic parameters of stage and inflow rates were used to determine nominal hydraulic retention times (HRTs) during the assessment, and Cell 4 outflows were used to flow-weight concentration measurements in mass balance calculations.

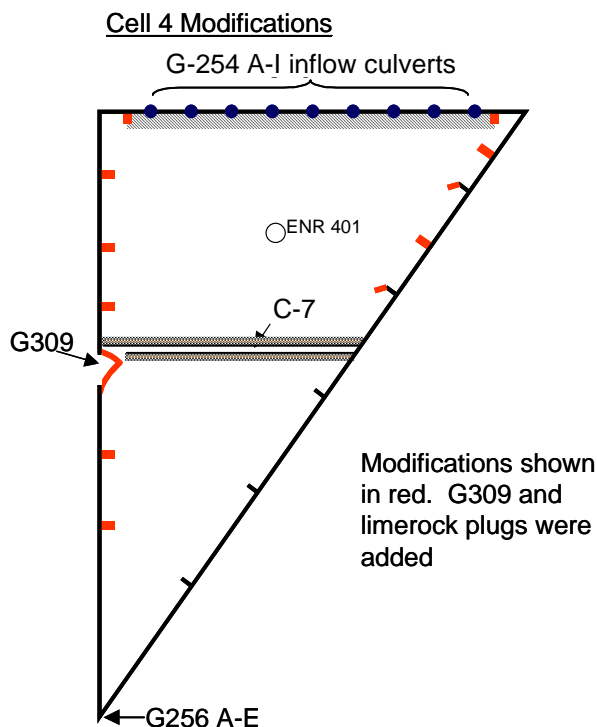


Figure 4.46. Cell 4 modifications (shown in red) which included construction of G-309, deepening the cell adjacent to the northern berm and canal 7, and the addition of limerock plugs.

4.9.3 Flow Measurement Instrumentation

There are nine inlet culvert structures spaced evenly along the northern levee (G254 A-I) and five outflow culverts grouped together at the southern corner of Cell 4 (G256 A-E) (Figure 4.46). Each culvert is instrumented with an ultra-sonic velocity meter (UVM) to measure flow rate. The District records and stores UVM data at 15-minute intervals. Stage is measured within Cell 4 at four locations. There are two stage recorders located along the northern levee (G254 A/B and G254 D/E), one stage recorder located internally at the ENR401 station, and a stage recorder located in the deep zone in front of the G256 culverts (Figure 4.46). Stage is recorded by the District at 15-minute intervals.

4.9.4 Water Balance During Tracer Assessment Period

District flow data during the 27-day tracer monitoring period indicates that average Cell 4 culvert outflows were equal to culvert inflows. ET losses and rainfall (1 cm of rainfall occurred during the 27-day monitoring period) were negligible compared to inflows, and approximately equal to each other.

4.9.5 Cell 4 Inflows

Culvert Flow Distributions Before Tracer Injection

Figure 4.47 shows a time history of culvert inflows for one week prior to tracer injection, developed from District data measured at 15-minute intervals. Note that no data were recorded for culverts G254 A and C because of malfunctioning UVMs. However, based on the average of available culvert flow data, the flow distribution between culverts was within +/- 20%. Based on this analysis, we applied uniform volumes of tracer to each culvert with no flow-weighting.

Inflow History Throughout Tracer Assessment

Figure 4.48 shows the history of net G254 culvert flow for the tracer assessment duration. Net flow is the summed flow of the nine culvert stations. For culverts A and C with missing or negative data, net flow was calculated by averaging the remaining 7 culvert data and using this average for each of the two culverts.

The heavy line in Figure 4.48 shows a 24-hour rolling average (12 hours before, 12 after) of G254 inflows. Average G254 flow throughout the tracer assessment duration was 90.5 cubic feet per

second (cfs); this corresponds to a Cell 4 hydraulic loading rate of 15.1 cm/day. The average tracer assessment flow and hydraulic loading were near the historic averages, which were 94 cfs and 15.7 cm/day, respectively, between January 1995 and April 1999. Throughout the tracer assessment, the rolling average of inflow varied within +/- 50% of the average flow. Except for the first two days, flow was relatively steady during the 27-day assessment.

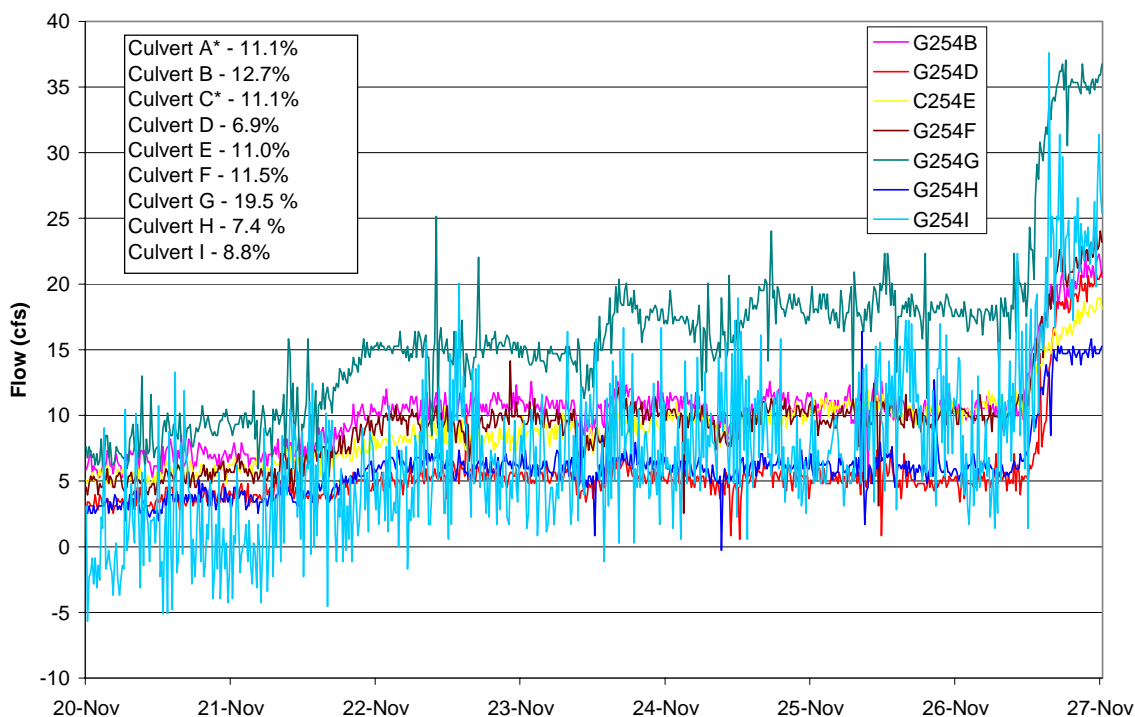


Figure 4.47. Volumetric flow rate through the nine inlet culverts to Cell 4 for a one week period prior to tracer injection. Flows for culverts A and C represent the average of the remaining seven culverts. These flows have not been corrected for the UVM calibration factor of 0.841.

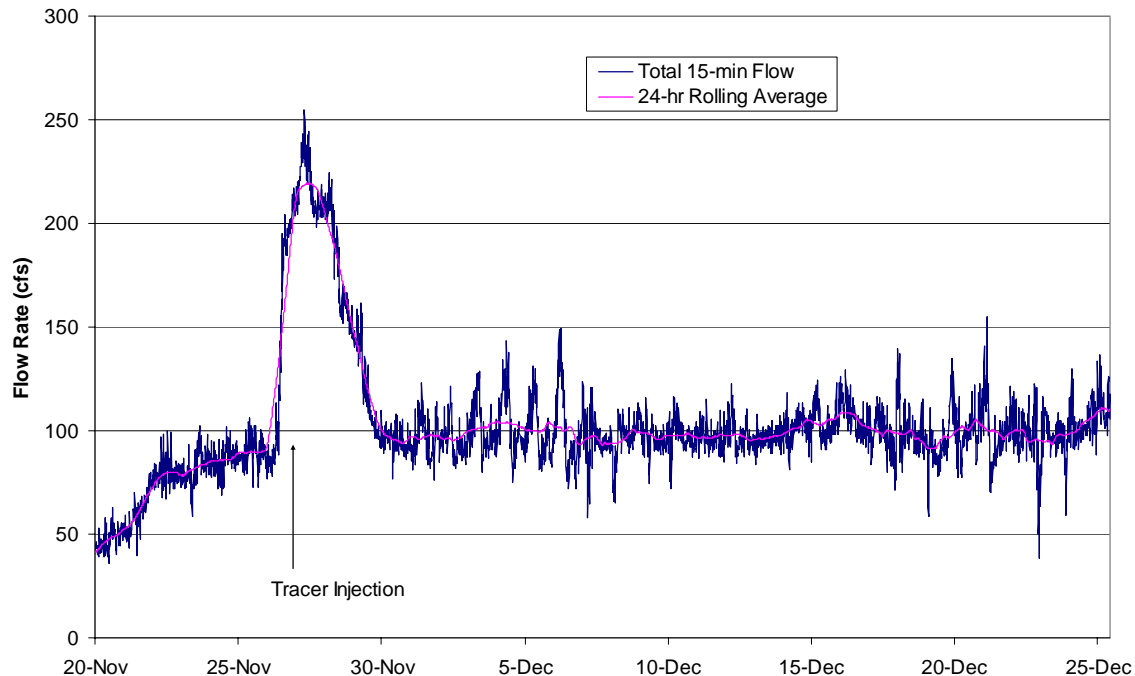


Figure 4.48. Net volumetric flow rate through the nine inlet culverts prior to and during the tracer monitoring period (November 27 to December 23, 2001). These flows have not been corrected for the UVM calibration factor of 0.841.

4.9.6 Cell 4 Outflows

The heavy line in Figure 4.49 depicts a 24-hour rolling arithmetic mean (12 hours before, 12 after) for Cell 4 outflows. The average G256 flow during the tracer assessment was 91 cfs, which was equivalent to the measured inflow.

4.9.7 Cell 4 Stage

Figure 4.50 shows the history of Cell 4 stage during the tracer assessment, using data averaged from 4 stage recording stations within the cell. The mean Cell 4 stage throughout the tracer assessment was 12.08 ft. Assuming an average Cell 4 ground elevation of 9.66', this corresponds to an average Cell 4 water depth of 0.74 m throughout the tracer assessment.

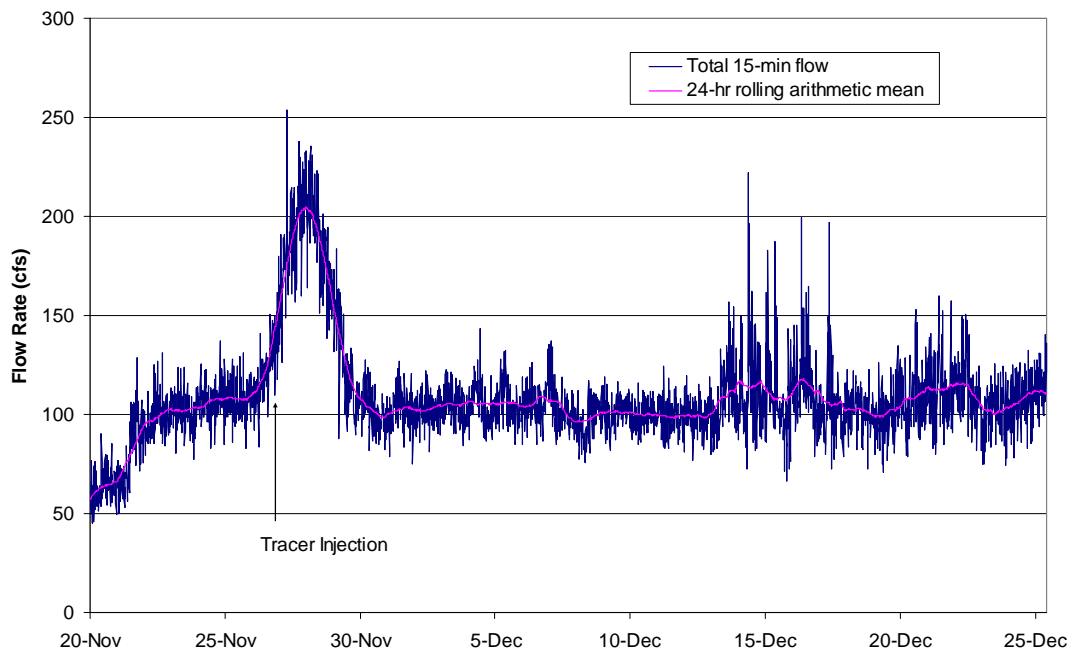


Figure 4.49. Net volumetric rate through the G-256 outflow structure prior to and during the tracer monitoring period (November 27 to December 23, 2001). These flows have not been corrected for the UVM calibration factor of 0.841.

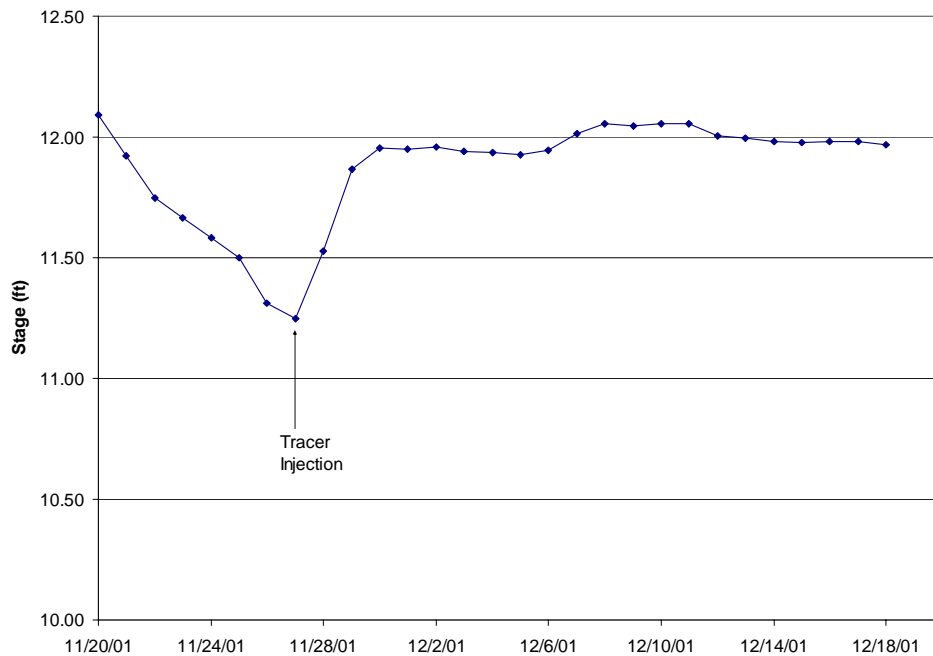


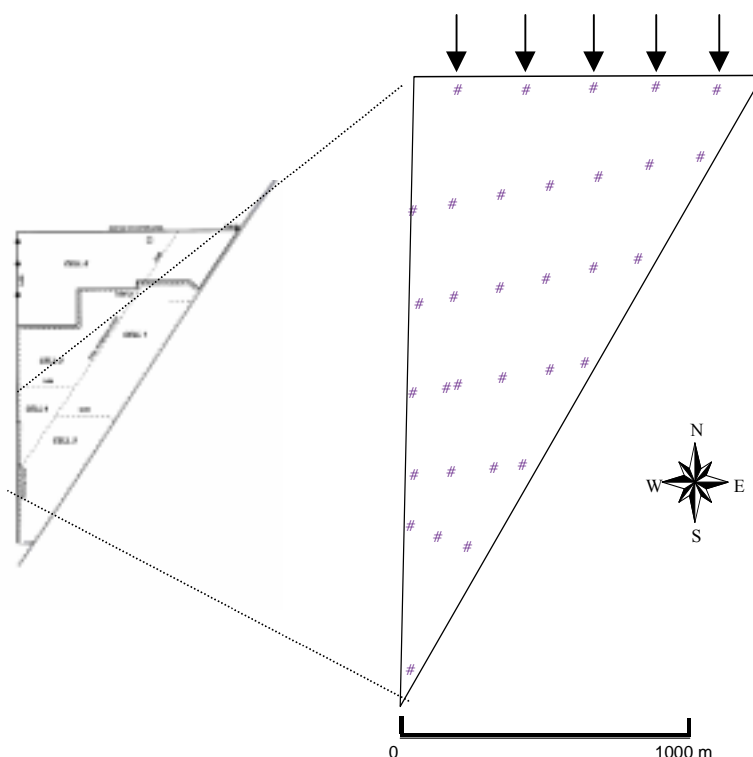
Figure 4.50. Stage fluctuations in Cell 4 during the tracer assessment period.

4.9.8 Tracer Assessment Methodology

Internal Sampling Locations

We modified the sampling grid that was established in the first tracer assessment because of the evolution of new short-circuit pathways following the structural modifications discussed above. We also added four stations near the discharge culverts into Cell 4 and one in the cattail region near the outflow to better describe the spatial variability of the tracer and P concentrations. In order to keep the number of internal sampling stations (25-26) approximately the same between the two tracer studies, we deleted some of the stations within the 5-transect sampling grid that had been established during the first tracer assessment. The sampling grid for the second tracer assessment is depicted in Figure 4.51. Each of the internal sampling stations was marked by a stake. Precise coordinates of these stations were later obtained by use of differential GPS.

Figure 4.51. Locations of the internal tracer and phosphorus sampling stations within Cell 4. The small projections along the east levee are pads constructed by FP&L for their power lines. The transverse canal near the middle of the cell is a relict channel which routes some of the short-circuited flow.



Tracer Injection

We added 231 kg (54 gallons) of 21.3% Rhodamine-WT (48.6 kg active ingredient) into Cell 4 on November 27, 2001. The dye delivery system consisted of nine 55 gallon drums equipped with outflow valves in the bottom. The concentrated dye was subdivided into nine equal parts (i.e., 6 gallons), and each 6 gallon aliquot was poured into one of the nine 55 gallon drums, and mixed with site water to a volume of 53.5 gallons (1:9 dilution). The valves for all nine of the dispensing drums were then opened at the same time, allowing the contents of the drums to enter the flow paths of the nine major inflow culverts simultaneously. The delivery time ranged from 45 to 55 minutes for each of the 9 drums.

Sampling Frequency

We sampled the dye tracer intensively at the Cell 4 outfall particularly during the first few days of the assessment (Table 4.16). In addition, we included internal wetland surface water stations in our sampling program in order to gain an understanding of the extent and exact locations of dead zones and short-circuiting areas. We sampled the 25 internal stations at elapsed times of 6, 25, and 48 hours after dye injection. On two occasions (25 and 48 hours), we also collected samples for analysis of total P concentrations coincident with the dye sampling at the internal stations.

Table 4.16. Number of samples collected at the Cell 4 outfall each day after injecting Rhodamine-WT into the wetland.

Day	1	2	3	4	5	6	7	8	9	10	11	12	13	14
Sample Numbers	4	6	6	5	4	4	4	3	3	3	3	3	3	3
Day	15	16	17	18	19	20	21	22	23	24	25	26	27	
Sample Numbers	3	3	3	2	2	1	2	2	1	1	1	1	1	

Laboratory Analysis of Dye Tracer

Rhodamine-WT concentrations were measured on a Turner Designs Model 10-AU-005-CE fluorometer with excitation and emission filters of 550 and > 570 nm, respectively (Wilson et al.

1986). The emission filter consisted of an orange sharp-cut filter. A reference filter (>535 nm) reduced baseline drift and instrument noise by filtering out scattered light. The light source was a clear quartz lamp. The standard curve was linear to 80 mg/L and the method detection limit was 0.1 µg/L. Since Rhodamine-WT fluorescence is sensitive to temperature, both standards and samples were analyzed at room temperature (24-27 °C). Background fluorescence (from dissolved organic matter) was subtracted from each of the sample fluorescence readings. Prior to analysis, all water samples were stored in amber-colored bottles.

Computations for Determining Hydraulic Parameters

Calculations for determining selected hydraulic parameters for Cell 4, based on the tracer data, were performed as follows.

The nominal HRT, τ , is the volume of water in the treatment wetland (V) divided by the volumetric inflow rate of water (Q):

$$\tau = V/Q \quad (1)$$

The tracer residence time, τ_a , is defined as the average time that a tracer particle spends in Cell 4, and is the first moment of the residence time distribution (RTD) function. The RTD represents the time various fractions of water spend in Cell 4. It is the contact time distribution for the system and defines the key parameters that characterize the actual detention time (Kadlec 1994). Levenspiel (1989) uses the RTD in the analysis of reactor behavior.

The mean residence time, τ_a , was calculated by dividing Eq. 4 of the tracer flow distribution, by Eq. 3, both of which are based on mean outflow rates and tracer concentrations (Kadlec 1994):

$$\tau_a = M_1/M_0 \quad (2)$$

$$M_0 = \int_0^{t_f} Q_e(t) C(t) dt \quad (3)$$

$$M_1 = \int_0^{t_f} t Q_e(t) C(t) dt \quad (4)$$

where C(t)=exit tracer concentration (mg/m³); Q_e = flow rate (m³/day); t = elapsed time (days); and t_f = total time span of the outflow pulse (days).

To find the RTD, the concentration response curve (experimental $C(t)$ vs. t curve) is converted to an E_t curve by changing the concentration scale so that the area under the response curve is unity (Levenspiel 1989). This is accomplished by multiplying the concentration readings by the volumetric flow rate divided by the mass (M) of injected tracer:

$$E_t = C(Q_v/M) \quad (5)$$

where E_t = RTD function in reciprocal time units.

The RTD function is normalized when it is expressed in terms of the dimensionless time scale by multiplying the Y-axis (i.e., the E_t function) units by τ (the nominal HRT):

$$E_\theta = \tau E_t \quad (6)$$

where E_θ = dimensionless RTD function,

and dividing the time units of the X-axis by τ :

$$\Theta = t/\tau \quad (7)$$

where Θ = dimensionless time scale and represents the number of mean HRTs.

This changes the X and Y axes so that the area under the curve is still equal to one, but the Y and X axes are normalized to τ (Levenspiel 1972). The purpose of creating the normalized distribution function, E_θ , is to be able to compare the flow performance among wetlands of different sizes and containing different plant communities and densities.

Whereas τ_a represents the centroid of the distribution and is the first moment of the RTD, the variance (σ^2) is the square of the spread of the distribution, or a measure of the dispersive processes, and is expressed in units of (time)²:

$$\sigma^2 = \frac{\int_0^{t_f} t^2 Q_e(t) C(t) dt}{\int_0^{t_f} Q_e(t) C(t) dt} - \tau_a^2 \quad (8)$$

The variance, which is the second moment of the RTD, is particularly useful for matching experimental curves to one of a family of theoretical curves (Levenspiel 1972).

The variance can be rendered unitless by dividing by the square of the tracer detention time:

$$\sigma_\theta^2 = \frac{\sigma^2}{\tau_a^2}$$

(9)

where σ_{Θ}^2 is the dimensionless variance of the tracer pulse.

Two common one-parameter models used to characterize non-ideal flows are the tank-in-series (TIS) and dispersion models (Levenspiel 1972). The TIS model views flow through a series of equal-size ideal stirred tanks, and the one parameter in this model is the number of tanks (N) in the chain. The number of constantly stirred tanks in the series that best matches the tracer response curve is given by N, which is determined by:

$$\sigma_{\Theta}^2 = \frac{1}{N} \quad (10)$$

To construct an idealized dimensionless tracer response curve for N = 1, 2, etc.:

$$E_{\Theta} = \frac{N}{(N-1)!} \left(N \frac{t}{\tau_a}\right)^{N-1} e^{-N \frac{t}{\tau_a}} \quad (11)$$

The second model is a dispersed plug flow, or dispersion model, which draws on an analogy between mixing in actual flow and a diffusional process. Here the dispersion process is superimposed on a plug flow model, and mixing is presumed to follow a diffusion equation (Kadlec and Knight 1996). For boundary conditions that are closed-closed, the following relation for the dimensionless variance has been found (Fogler 1992):

$$\sigma_{\Theta}^2 = \frac{2}{Pe} - \frac{2}{Pe^2} (1 - e^{-Pe}) \quad (12)$$

where Pe is the Peclet number, dimensionless.

Eq (12) can be converted to the wetland dispersion number (D , dimensionless) by utilizing:

$$D = \frac{D}{uL} = \frac{1}{Pe} \quad (13)$$

where L = distance from inlet to outlet, m

u = superficial velocity, m/day

D = dispersion constant, m²/day

Combining Eqs. (12) and (13) yields:

$$\sigma_{\theta}^2 = 2D - 2D^2(1 - e^{-\frac{1}{D}}) \quad (14)$$

4.9.9 Results

Tracer Response Curve for Cell 4

The tracer concentration response curve for Cell 4 illustrates a non-ideal flow distribution, where neither plug flow reactor (PFR) nor constantly stirred tank reactor (CSTR) flow patterns exist. The tracer concentration curve more closely mimicked a well-mixed reactor, however, than a plug flow reactor (Figure 4.52). During the first day, the dye appeared at the outflow region of Cell 4 within 5-9 hours after tracer addition because of short-circuiting and the higher flow rate (184 cfs). After the lag period, the ascending limb of the tracer curve peaked short of the maximum concentration (44.6 µg/L) expected for CSTR behavior (Figure 4.52). The resemblance of the tracer response to a well-mixed system is also indicated by the shape of descending limb, which was coincident with that of the idealized CSTR during the post-nominal HRT period.

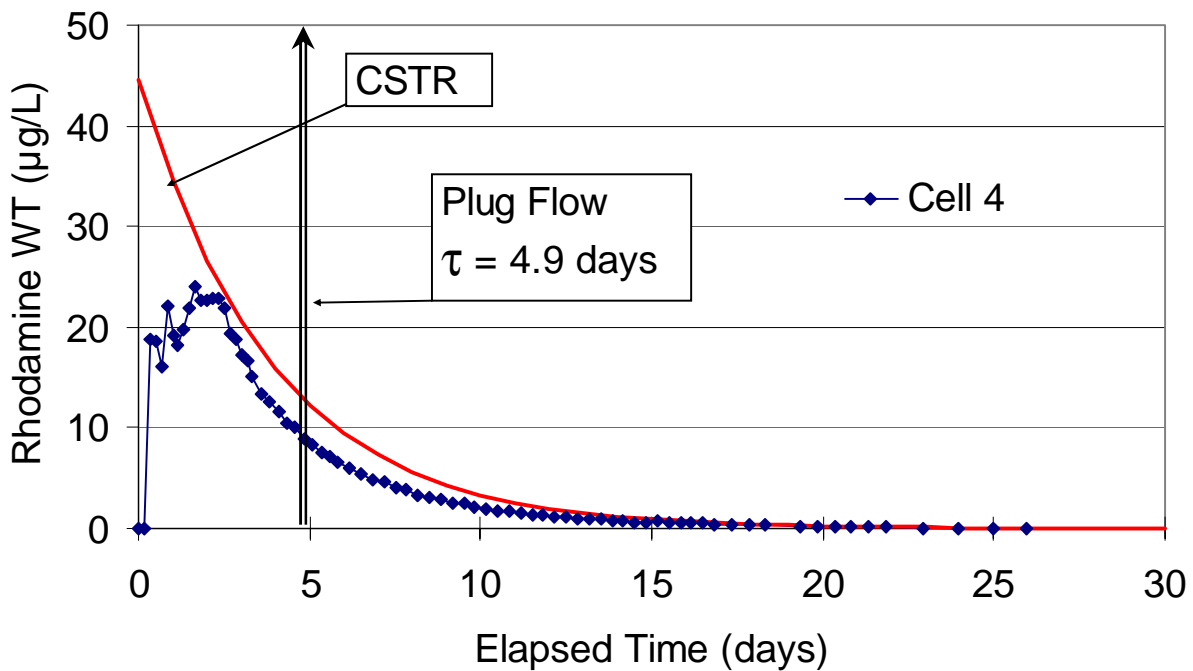


Figure 4.52. Tracer response curve of Rhodamine-WT dye applied to Cell 4 on November 27, 2001. Responses to ideal well-mixed (CSTR) and plug flow (PFR) conditions are represented by the exponential decay and vertical (coinciding with the nominal HRT, τ) lines.

Tracer Mass Balance

The Rhodamine-WT mass balance was calculated by comparing the added mass to the tracer mass recovered at the effluent. The total mass of tracer exiting Cell 4 is described in Eq. 3. A comparison of the recovered tracer mass and the amount added to Cell 4 demonstrates a 52% Rhodamine-WT recovery for the assessment.

Tracer Detention Time

The average Cell 4 depth (0.74 m) can be divided by average loading (15.1 cm/day) to yield a nominal 4.9-day HRT.

Our data show that the tracer detention time ($\tau_a=3.9$ days) is shorter than the nominal HRT ($\tau=4.9$ days). This shortened HRT indicates the presence of severe short-circuits within the cell, especially during the high flows (184, 159, and 108 cfs) that occurred in the first three days of the assessment.

Two-Dimensional Time Series Plots of Tracer Concentrations

The two-dimensional time series plots for the dye concentrations were produced in Arcview GIS (Version 3.1). We used the Spline/Tension interpolator in the Arcview program to fit a minimum-curvature surface through the input concentrations.

The appearance of the dye at the Cell 4 outflow soon after tracer injection suggests that this wetland exhibits a prominent short-circuit. The internal samples proved useful in identifying the locations of both short-circuits and dead zones.

Pronounced short circuits along the eastern and western levees are readily observed in the 6-hour elapsed time sequence (Figure 4.53). However, dye concentrations along the western levee, coinciding with the new short-circuit path formed after the first tracer assessment in December 1999, were nearly dissipated 25 hours after injection. In the 19 hours between the first and second isopleth maps shown in Figure 4.53, the concentrated dye mass in the northeast corner of the cell had moved south the middle of the cell, and may have merged with the dye cloud from the western levee that was transported to the east along the C-7 canal. Most of the tracer had exited the wetland 48 hours after injection (Figure 4.53). The short-circuiting apparent in Figure 4.53

provides a level of detail that aids in the following discussion of the wetland hydraulic parameters (e.g., measured HRT, tanks-in-series number, wetland dispersion number).

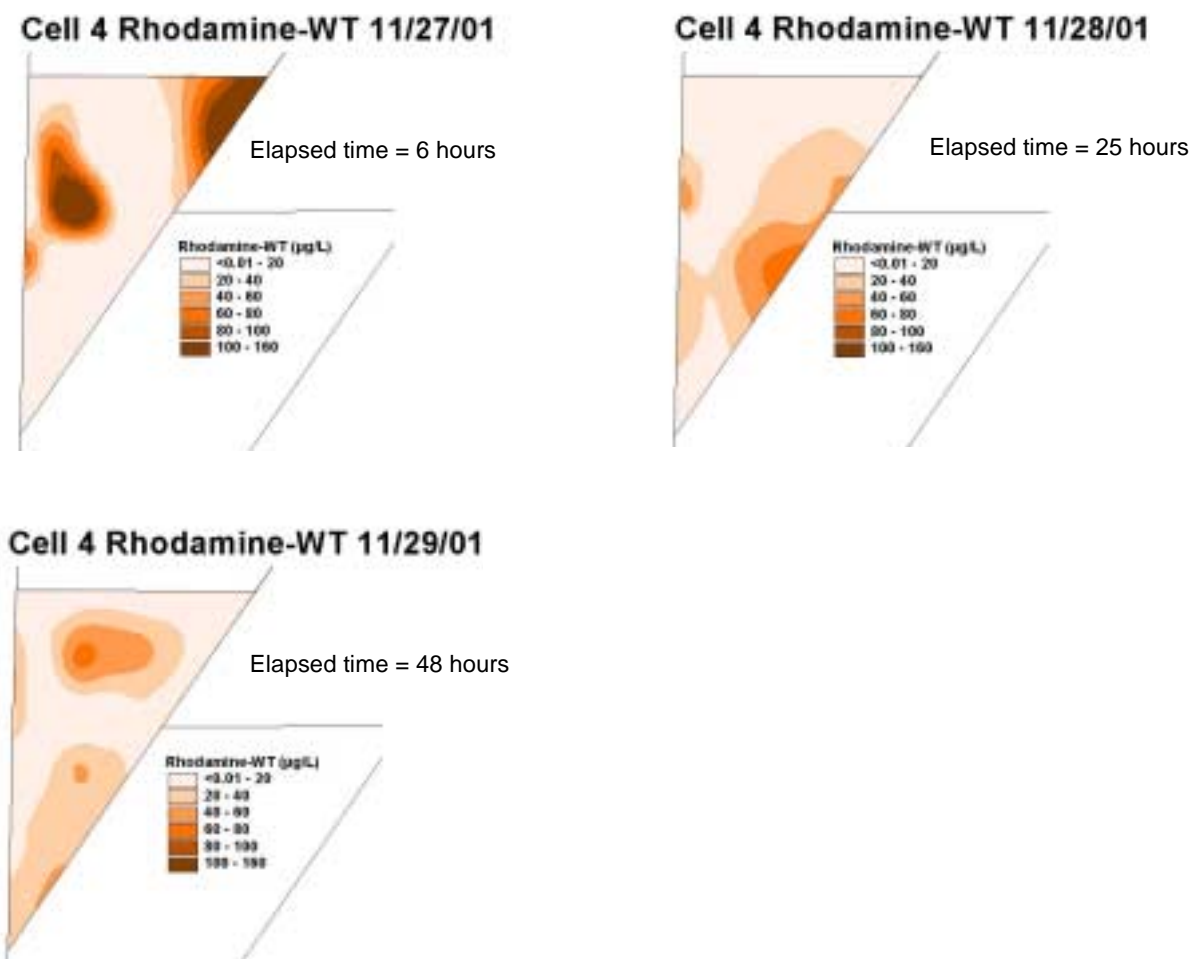


Figure 4.53. Time series showing the progression of the Rhodamine-WT dye through Cell 4.

Hydraulic Efficiency of Cell 4

We compared the hydraulic characteristics of the two tracer studies in Cell 4 on the basis of the normalized residence time distribution (RTD) function (E_0), expressed in dimensionless units, and the hydraulic parameters (HRT, variance, TIS and wetland dispersion numbers). The comparison of the hydraulic characteristics between the two tracer studies can be considered most valid if similar hydrologic conditions existed during the two tracer monitoring periods. As shown in Table

4.17, the HLR and HRT were nearly the same during the two tracer studies, and the water depth was equivalent during both.

Table 4.17. Key hydrologic variables present during the two Cell 4 tracer studies.

Date	Depth (m)	HLR (cm/day)	Nominal HRT (τ , days)
December 16, 1999 to January 15, 2000	0.74	17	4.4
November 27 to December 23, 2001	0.74	15	4.9

Figure 4.54 compares the dimensionless RTD functions for the two tracer studies, which clearly shows that considerably more tracer mass exited earlier from Cell 4 during the second tracer assessment than in the first. Thus hydraulic efficiency was significantly reduced during the latter assessment.

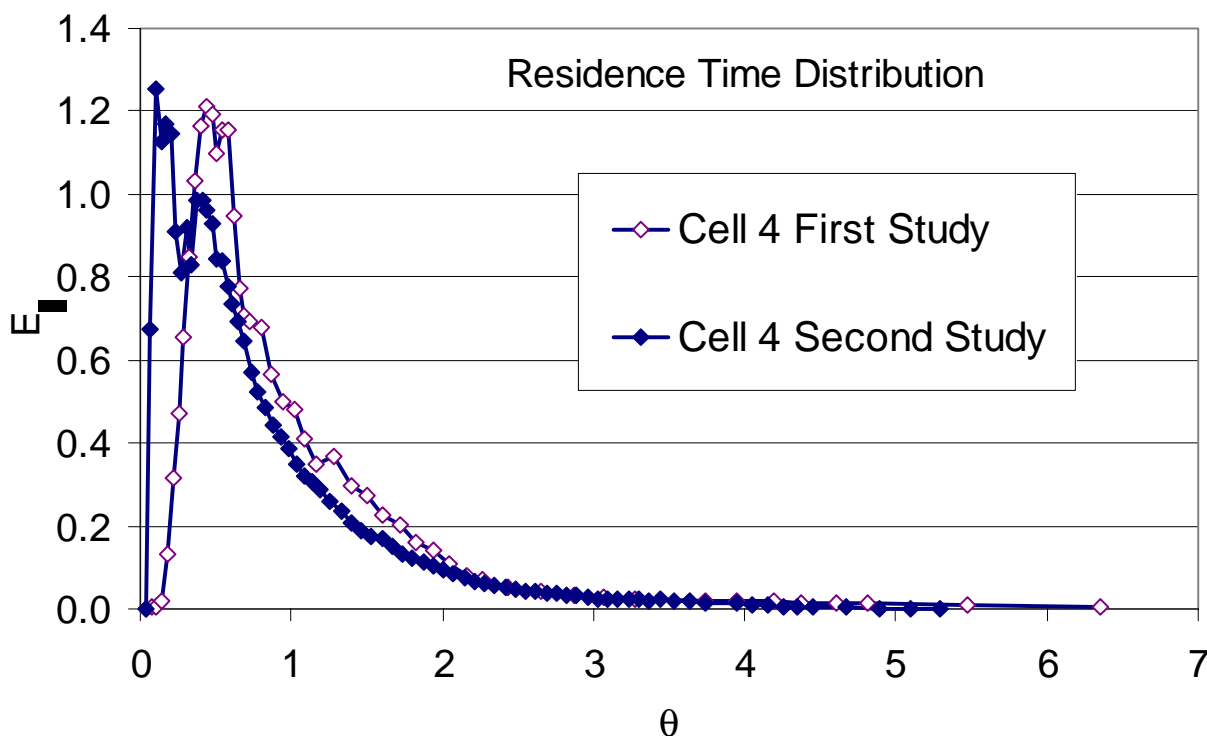


Figure 4.54. Dimensionless residence time distribution (RTD) functions for Cell 4 during the first (December 16, 1999 – January 15, 2000) and second (November 27 – December 23, 2001) tracer studies.

The more impaired hydraulic efficiency during the second tracer assessment is readily seen by comparing the key hydraulic parameters (Table 4.3). Our calculation resulted in a tanks-in-series number of $N = 1.1$, which is an extremely low value for a wetland. Most surface flow wetlands have reported TIS values of $2 < N < 8$ (Kadlec and Knight 1996). The higher N that a wetland exhibits, the closer it resembles a PFR and less a CSTR. Hydraulic characteristics of a PFR are more conducive to more efficient treatment of P since the average time that inflow water is retained in the wetland more closely approaches the HRT; or alternatively, a lesser proportion of the inflow water leaves the wetland early.

Table 4.18. Comparison of key hydraulic parameters for the two tracer studies in Cell 4.

Date	Nominal HRT τ , days	Measured HRT τ_a , days	Variance σ^2 , day ²	Dimensionless Variance σ_θ^2	Tanks-in- Series N	Wetland Dispersion Number D	Peclet Number Pe
12/16/99 to 1/15/00	4.4	4.7	17.2	0.78	1.3	1.25	0.80
11/27/01 to 12/23/01	4.9	3.9	13.4	0.89	1.1	2.75	0.36

Besides the TIS model, the other commonly deployed one-parameter model for evaluating flows through wetlands is the dispersion number, D , which is equal to the dispersion coefficient divided by the product of the superficial velocity and length of the wetland ($D/[uL]$ in Eq. 13). Kadlec (1999) states that values of D range from 0.2 to 0.4 in wetlands (predominantly emergent macrophyte wetlands), which places them in the "large amount of dispersion" category. The D values obtained for both of the Cell 4 tracer studies are for outside that range (Table 4.18).

The inverse of D , the Peclet number (Pe), describes the ratio of the rate of tracer transport by convection (bulk flow) to the rate of transport by diffusion or dispersion (uL/D). The comparison of the Pe values for Cell 4 in Table 4.18 indicates that Cell 4 transport is dominated by diffusion and dispersion ($Pe < 1$), instead of bulk flow ($Pe > 1$). Considering that hydraulic efficiency in treatment wetlands is thought to be enhanced by plug flow rather than dispersive or diffusive flow processes, then Cell 4 has not performed well, either before or after structural alterations, from a hydraulic perspective.

The Phosphorus Removal Efficiency of Cell 4

It is well known that treatment wetlands exhibit spatial variations in vegetation density that affect treatment efficiency (DBEL 1999; Kadlec 1999). When sparse vegetation dominates within a flow path, the removal efficiency is lower because of higher velocities and more dispersion compared to the slower flow paths through dense biomass. Some of the “dead zones” (areas within the wetland that are hydraulically isolated) may be associated with dense SAV biomass.

The rapidly changing spatial profiles for dye concentrations in Cell 4 were a result of the batch-addition, or the transient nature of the dye pulse (Figure 4.53). By contrast, Cell 4 was essentially at a “steady-state” with respect to TP levels during the assessment, as indicated by the comparable spatial TP profiles at 25 and 48 hours (Figure 4.55) and the consistent inflow and outflow TP concentrations (Table 4.19). The zones of high water column TP levels in the northern half of the cell correspond to the locations of the prominent short-circuits (Figures 4.53 and 4.55).

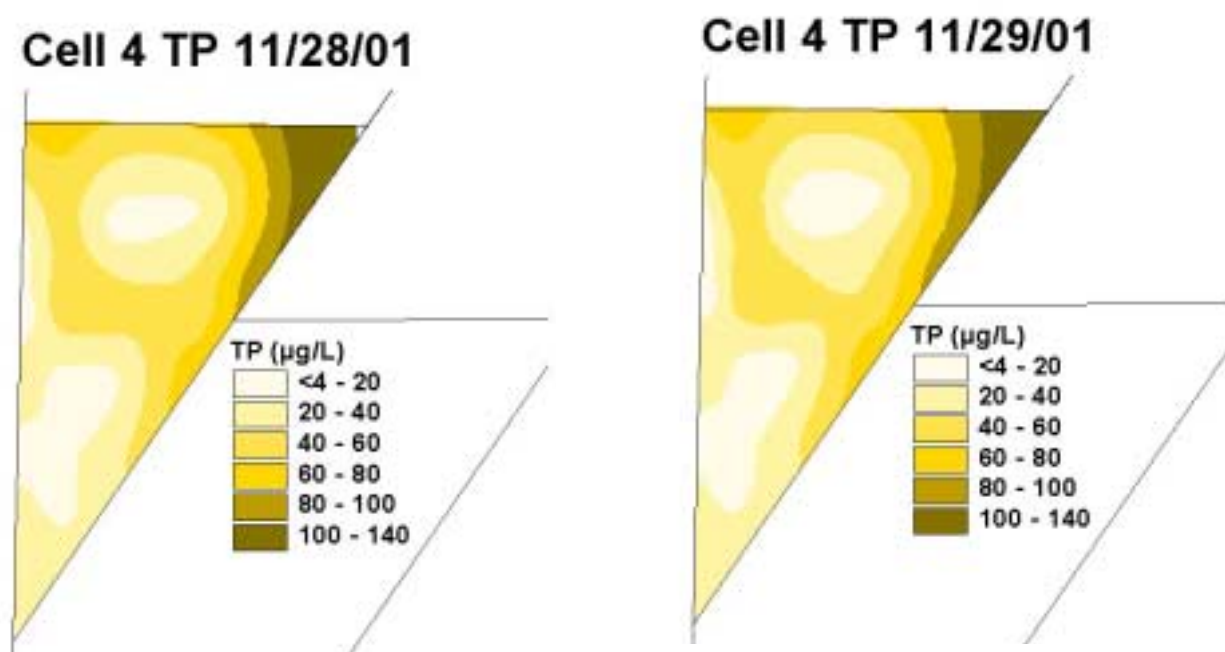


Figure 4.55. Spatial distribution of total phosphorus concentrations (µg/L) within Cell 4 at 25 and 48 hours following tracer injection.

Table 4.19. Total P concentrations in the inflows and outflows of Cell 4 during the second dye tracer assessment. Rhodamine-WT was injected on November 27, 2001.

	Elapsed Time (days)	Inflow* (µg/L)	Outflow** (µg/L)
November 20, 2001	-7	107	24
December 26, 2001	29	38	15
December 31, 2001	34	40	18

* Average of grab samples collected from culverts A through I at G-254.

** Composite of grab samples from culverts A,B,C,D, and E at G-256

4.10 Literature Review: Modeling Phosphorus Removal in Wetlands

4.10.1 Background

As part of our SAV assessment, we conducted a literature review to investigate past efforts of modeling phosphorus removal in aquatic systems. The purpose of this review was to identify the types of models that have been developed in the past and to assess the utility of various modeling features for our process model development.

We reviewed nine different approaches that have been used for modeling P removal in aquatic systems. Water quality models are commonly categorized as either empirical or mechanistic. Empirical models are based on statistical summaries of input-output relationships. Mechanistic models are based on the modeler's interpretation of the fate and transport of water quality parameters with one or more mathematical equations (Reckhow 1994). Mechanistic models, which can also be described as 'process' models, aim for a 'correct' yet simplified interpretation (theory) of reality. In contrast, empirical models aim for accurate parameter estimation with less emphasis on process description (Reckhow 1994). In Figure 2.56, the nine models that we reviewed are placed along a continuum from empirical to highly articulated mechanistic models. Figure 4.56 can also represent a continuum of increasing model resolution and complexity. We found this continuum concept to be a helpful way to organize and relate models to one another.

4.10.2 Empirical Models for P Removal in Wetlands

Kadlec and Knight (1996) calibrated a P mass balance model to predict long-term average TP removal based on the collective behavior of 20 individual wetland systems (a cross-sectional database). The model assumes that wetland hydraulics are described by plug flow behavior with no mixing. The model also assumes that phosphorus removal occurs in direct proportion to the in-column TP concentration; this is commonly referred to as a 1st order removal model. The coefficient of proportionality between removal and in-column concentration is termed the TP settling rate, k , and was estimated, in this case, using a wetland's long-term average input and output TP concentrations.

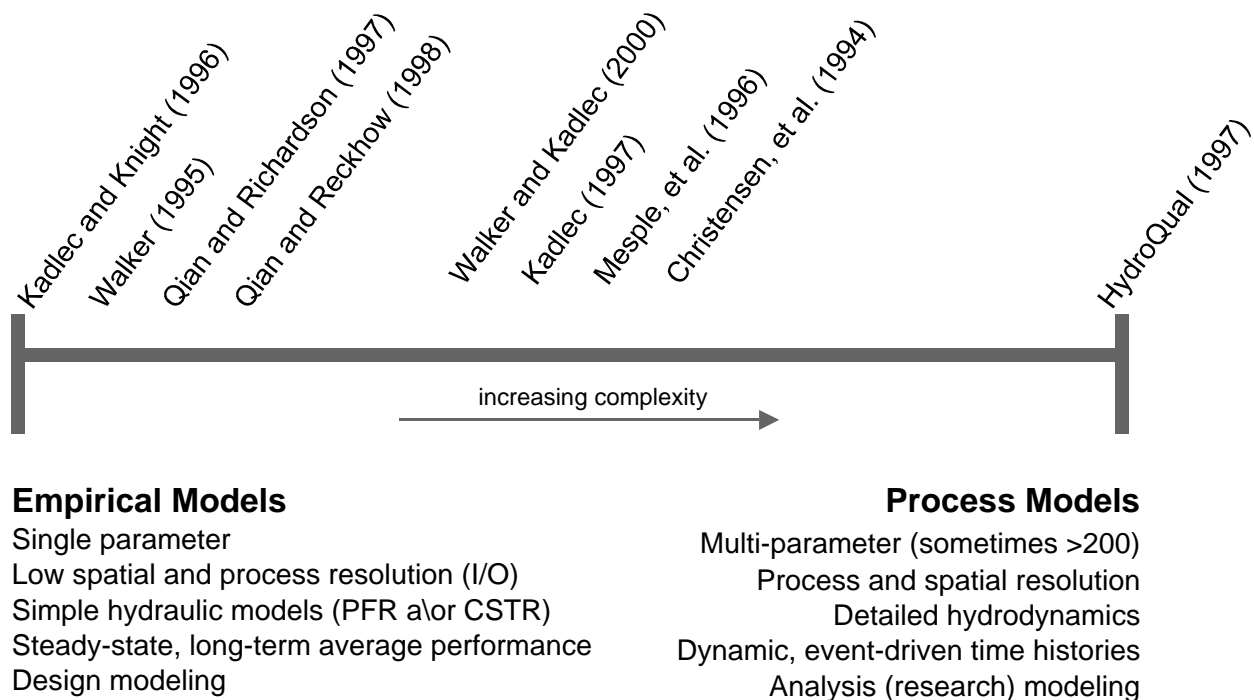


Figure 4.56. Literature review of nine different approaches to modeling P removal in aquatic systems.

As is typical of other empirical models, this model structure does not attempt to represent specific physical processes, only their net consequences. Kadlec and Knight's (1996) recommended design value for emergent wetlands, $k = 12.1 \text{ m/yr}$, resulted from averaging

individual k 's calculated from 20 wetlands located throughout the United States. This relatively simple model establishes a mathematical relationship between inflow concentration, outflow concentration, settling rate, flow rate, and surface area and can be readily solved for the parameter of interest. A common criticism of models based on the collective behavior of many wetlands is that they are too general to apply to a single particular wetland design, since the represented collective behavior may not be pertinent to particular site-specific conditions (Qian and Reckhow 1998).

Walker (1995) also developed an empirical model for TP removal based on assumptions of plug flow hydraulics and first order TP removal. The model consists of a coupled water and mass balance representing long-term steady-state conditions in the wetland. Rather than calibrate to input/output data from a cross-sectional database as did Kadlec and Knight (1996), Walker calibrated to the spatial gradient of water-column and peat accretion data within a single wetland, Water Conservation Area-2A (WCA-2A). Using a least squares estimation technique, Walker (1995) demonstrated that the 26-year-average rate of peat accretion was proportional to average water column concentration, with a proportionality constant of $k = 10.2$ m/yr. The simplicity of the model and strength of Walker's statistical analysis (demonstrating that the 90 percent confidence interval for parameter estimation lies between 8.9 and 11.6 m/yr), led to adoption of this model as the design basis for long-term performance in SFWMD Stormwater Treatment Areas (STAs). In design mode, the model was used to size STA surface areas given average expected influent flows and TP loads and a target outflow concentration of 50 ppb (Walker 1995).

A common criticism of a design tool based on analysis of a single system is that the information could be too site-specific to be meaningfully applied elsewhere (Qian and Richardson 1997). However, Walker's model was applied only to wetland designs that shared similar climate (sub-tropical Florida), similar intended plant community (emergent macrophytes), similar influent water quality (TP enriched), and similar sediment conditions (peat) to the source wetland, so the approach may be justifiable in this case.

Qian (1997) also criticized Walker's approach on the basis that it failed to take into account the effect of uncertainty in data and model variables, that the sheet flow assumption may have been grossly violated, and the data set was arbitrarily truncated. Qian (1997) employed estimation techniques that he argued were more appropriate to these circumstances and arrived at a more conservative settling rate of approximately $k = 6 \text{ m/yr}$. Walker (1997) countered Qian's criticism by pointing out the visibly superior fit to the WCA-2 data using his parameter estimation technique and by justifying his modeling assumptions.

Scientists at the Duke University Wetland Center (Qian and Richardson 1997; Qian and Reckhow 1998) also developed empirical design models based on the WCA-2 data, but used a different model structure than the first order-models of Walker (1995) and Kadlec and Knight (1996). The Duke models are based on a piece-wise linear relationship between TP loading rate and in-column TP concentration that was derived from review of the North American Data Base (NADB). The piece-wise relationship indicated that at loading rates below the breakpoint, phosphorus concentrations are much less sensitive to loading rates than at above the breakpoint. The two Duke teams employed slightly different Bayesian regression techniques, in each case allowing them to refine the collective trends evident in the cross-sectional data set (NADB) with site-specific data from WCA-2. They advocated that this approach (pooling cross-sectional and specific data sets) arrived at a more robust model. The resulting breakpoint from these analyses occurred at a TP loading rate of approximately $1 \text{ g m}^{-2} \text{ yr}^{-1}$ (Qian and Richardson 1997), which they suggested as the maximum "low-risk" mass load to a treatment wetland. A key feature of the Bayesian approach is that it describes prediction uncertainties as the probability of exceeding a given effluent standard, thus allowing users to directly manage the tradeoff between reliability and land area requirements.

Both Duke models predicted more conservatively than did Walker's model. For example, Qian and Reckhow (1998) estimated the total STA land area requirement is approximately three times greater than Walker's estimate (1995). Similarly, Qian and Richardson (1997) estimated Walker's STA design would exceed discharge criteria 75% of the time. During the first four years of operation, the three treatment cells in STA-1W dominated by emergent macrophytes demonstrated an average TP settling rate of $k = 11 \text{ m/yr}$ with a range of $k = 6\text{-}17 \text{ m/yr}$ (Walker,

1999). Performance during the last two of those four years was quite poor in two of the treatment cells (Cells 1 and 3), averaging $k = 3$ m/yr. Based on these values, we feel there is insufficient data at this point to judge the relative merits of the empirical models discussed above when they are used in design mode.

4.10.3 Mechanistic Models for P Removal in Wetlands

Kadlec and Walker (2000) are in the process of developing a quasi-process model for phosphorus removal in wetlands. The model is called the Dynamic Model for Stormwater Treatment Areas (DMSTA) and is designed specifically for analysis of the District's STAs. We refer to it as a 'quasi-process' model because of its highly aggregated representation of generalized wetland processes (Figure 4.57). Other process-models in this literature review specify considerably more detail than DMSTA, but this model elaborates significantly beyond the empirical models discussed above. DMSTA was specifically developed as a generalized analysis tool for broad application to emergent vegetation, SAV, and periphyton wetlands.

DMSTA simulates long-term dynamic behavior of phosphorus removal using daily flow and TP concentration input series. The model maintains a daily water balance and can model non-ideal hydraulics using a tanks-in-series (TIS) approach. The model maintains a daily phosphorus mass balance with fluxes (J_{gross} , J_{return} , J_{burial} in Figure 4.57) between three aggregated storage compartments: water column TP storage (SRP, DOP, PP), short-term labile P storage (biomass,

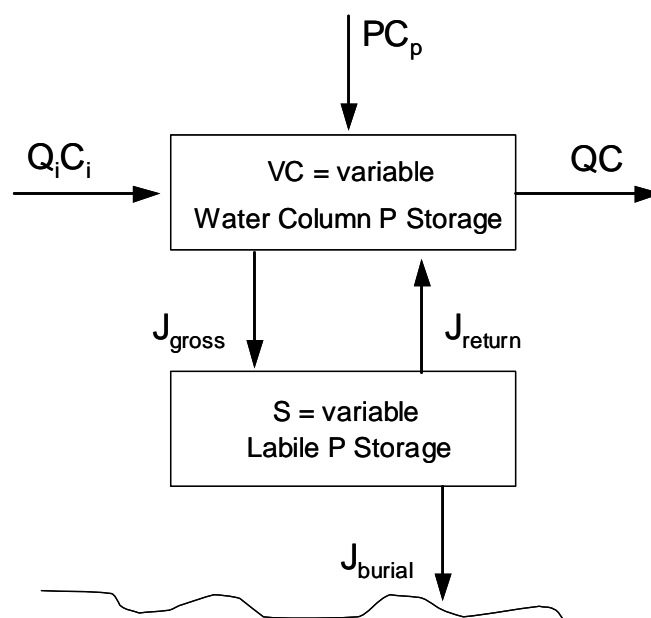


Figure 4.57. General model structure for DMSTA (Kadlec and Walker 2000) and biomachine models (Kadlec 1997).

new mineral and organic sediment), and long-term inactive P storage (buried sediment). TP enters the Cell 4 water column in concert with rain and influent flows and also via the recycle pathway from “labile P storage”. TP leaves the water column in concert with effluent flows and with first-order removal to the labile P storage compartment. A fraction of the modeled “active TP storage” is recycled to the water column, accounting for wetland processes such as desiccation, decomposition, dissolution, desorption. The recycle flux is, in essence, a dynamic background (C^*) flux. An additional fraction of “active TP storage” is buried to long-term inactive storage; this is the only pathway by which TP is permanently removed from the system. The model predicts a time history of effluent TP concentrations with a daily time step. Each TIS in the DMSTA model can be assigned its own coefficients, thus allowing the model to simulate sequential biological communities.

In its draft version, DMSTA had three calibration coefficients: the first-order removal constant for TP from the water-column to short-term storage, the fraction of short-term storage that is recycled to the water-column, and the turnover time of the short-term P storage. There is an ongoing effort to optimize model performance by improving the mathematical relationships defining fluxes between storages (Kadlec 2000); this may increase the number of calibration coefficients.

Kadlec (1997) developed a model with similar structure to DMSTA (Figure 4.57) but with increased process description. Kadlec’s model is called the “Autobiotic Wetland Phosphorus Model” or “biomachine” model. It is based on TP cycling associated with growth, death, and decomposition of biomass. As opposed to the draft DMSTA (Kadlec and Walker 2000), which used a first-order P removal based on water column concentration, the biomachine model ties P removal to the size and turnover rate of the lumped biomass storage. In the biomachine model, the growth and depletion of the labile P storage is described by a logistic growth function (Malthus’ Law) with a Monod limiting factor based on the P water concentration. The biomachine model requires calibration of five parameters: maximum total biomass (g/m^2), biomass growth half saturation constant ($\text{g P}/\text{m}^3$), biomass turnover rate (yr^{-1}), TP tissue content in biomass ($\text{g P}/\text{g}$), and fraction of senescent biomass (and buried TP) returned to water column. The model predicts a time history of average spatial distributions of TP concentration

and biomass within a wetland with a one-year time step (Kadlec 1997). The biomachine model has been successfully calibrated to a 600 ha northern peatland (Kadlec 1997) and to the 26-year WCA-2 data set (Kadlec and Walker 1999).

Mesple et al. (1996) produced one of the only models that we encountered that included both biological and chemical P removal processes. The French researchers developed a mechanistic model for high-rate algal ponds to provide “a rational basis for pond management policies” (Mesple et al. 1996). In their model, biological uptake was modeled as a function of algal growth, death and grazing, where growth rate was a function of temperature, solar radiation, and phosphorus concentration. Their evaluations indicated that P precipitation occurred with Ca species when pH elevated due to in-column photosynthesis. In the model, the daily amount of chemically precipitated P was determined using a relationship based solely on weekly measured pH data (i.e. pH was a model input). They justified not including a dependence upon Ca concentration in P precipitation calculations since Ca concentration was relatively constant from week-to-week. This model offered a more detailed representation of water-column processes than the biomachine model, which accounted for only biotic activity (Kadlec 1997). However, the model for the high-rate algal pond did not include any sediment processes, mainly because biomass in a high-rate pond is exported before settling as TSS (they propose that export of particulates, not accrual, is the ultimate removal in a high rate pond).

Christensen et al. (1994) produced a mechanistic P removal model that had a moderate amount of water-column and sediment process detail. Their model used six state variables to account for phosphorus storage within the wetland and had approximately 12 calibration coefficients in the equations that defined flow relationships between storages. The six state variables in the model were water volume, dissolved P, particulate P, algal biomass, macrophyte biomass and sediment P. The main goal of the model was to simulate cause-and-effect relationships between system forcing functions (stormwater inflow, pumped inflow, TP concentrations) and ecosystem processes and structure. The time units in the model were weeks, so it was more sensitive to flow and load events than Kadlec’s biomachine model (1997), which ran on an annual basis, but less sensitive than the model proposed by Kadlec and Walker (2000), which used a daily time step. The model did not take spatial movements of water or nutrients into

account, but it did provide an integrated process description of P removal and recycling based on the authors' knowledge of this particular wetland (Christiansen et al. 1994). This type of aggregated process model closely follows the systems ecology modeling principles advocated by Odum (1994). Christiansen et al. (1994) cautioned that without an independent data set, it is impossible to validate the model. But despite this shortcoming, they suggest that process models of this type are valuable to field assessment programs because they can help focus research questions and indicate which parameters should receive the most attention (Christensen et al. 1994).

HydroQual (1997) has developed a multi-dimensional hydrodynamic and water quality model to assist SFWMD water quality managers with the design and operation of STAs. The hydrodynamic component calculates time-variant, two-dimensional water surface elevations and flow patterns. The water quality component computes time-variant, two-dimensional distributions of dissolved and particulate nutrients. The water quality model consists of four submodels: a periphyton routine, a water chemistry routine, a sediment nutrient flux routine, and an emergent vegetation routine. The modeling equations incorporate over 45 state variables and over 200 calibration coefficients. A sample of some of the state variables tracked by HydroQual's model includes refractory particulate organic phosphorus, labile dissolved organic nitrogen, solid-phase calcite, sawgrass root carbon, and cattail fallen-dead phosphorus. A sample of some of the model's calibration coefficients include light attenuation factor on saturated periphyton growth rate, reaction velocity for denitrification in the aerobic layer, sawgrass basal respiration rate, first order decay coefficient for accumulated benthic stress, and fraction of root phosphorus lost during root mortality. Spatial resolution, which is a key feature of the model, is provided by dividing a wetland into a grid matrix and solving hydrodynamic and water quality subroutines within each grid cell. For example, the calibration to WCA-2 data utilized a 24x36 matrix (864 cells). Fitz and Sklar (1999) also applied a two-dimensional hydrodynamic and water quality model to WCA-2, using a somewhat different, but equally complex model structure.

4.11 Description of the Process Model for SAV (PMSAV)

The DBE dynamic simulation model for SAV systems is called the Process Model for Submerged Aquatic Vegetation, or PMSAV. The goal for PMSAV development was a compact symbolic and mathematical representation of essential hydraulic and phosphorus removal processes in SAV systems. The model enables a predictive capability for the performance of future SAV systems that will in all likelihood operate with different conditions (pulsed inflows, higher influent concentrations, and improved internal hydraulics) than those observed in SAV datasets during the past years.

Some significant features of PMSAV include the following:

- Representation of two P removal pathways: a biologically mediated pathway and a sedimentation pathway. The biologically mediated pathway aggregates plant uptake and coprecipitation processes. The sedimentation pathway models settling of the particulate TP fraction.
- Aggregated representation of sediment burial and recycle processes.
- Inclusion of biomass and sediment storage relationships from DBE mesocosm and test cell data.
- A hydraulic model specifically aimed at modeling the well-documented detrimental effects of hydraulic short-circuiting in Cell 4. This feature enables estimation of “intrinsic” rate constants from the Cell 4 data that would otherwise be tainted if the short-circuit were not explicitly modeled. The “intrinsic” constants are the most appropriate constants to use for future STA design efforts.

4.11.1 Model Description and Equations

PMSAV is comprised of three modeling components: hydrologic, hydraulic and P-cycling components. The hydrologic component simulates the overall daily water balance in the modeled wetland. The hydraulic component simulates the internal movement of water through the treatment cell using a modified tanks-in-series (TIS) approach. The P-cycling component simulates significant phosphorus processes in SAV wetlands including biologically mediated removal, sedimentation, sediment recycle, and long-term P burial.

Hydrologic Water Balance

Figure 4.58 shows a diagram illustrating the wetland water balance. Table 4.20 summarizes the source or equation used for each flow and for water storage (depth) in the hydrologic model. The table also shows average values of these parameters from the calibrated model. These values will be discussed further along with simulation results in a subsequent section. Table 4.21 summarizes the description and values for all constants in the water budget formulation. The procedure for calibrating the water balance model will also be discussed in a subsequent section.

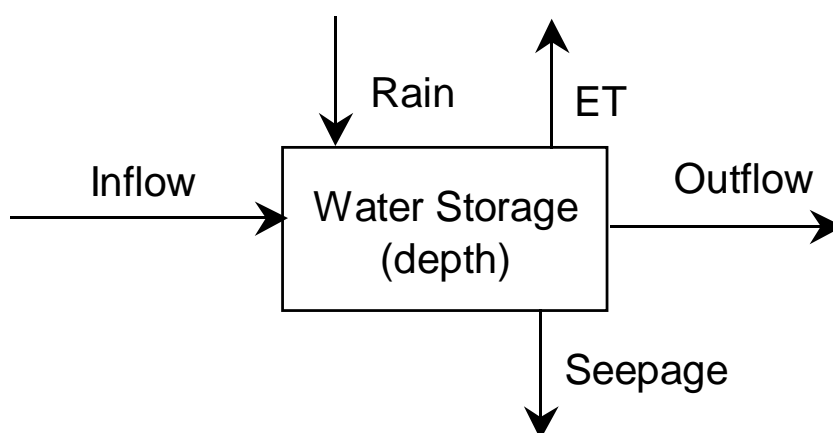


Figure 4.58. The wetland water balance

District-provided daily inflow, rain, and evapotranspiration time series are used as input datasets. Seepage is calculated with a Darcy flow equation that assumes the receiving body (which could be either groundwater or the canal along the western levee) is 0.5-m below the bottom of Cell 4. Daily outflow is calculated using a form of the depth-dependent flow equations suggested by Kadlec and Knight (1996). It should be noted that the form of seepage and outflow equations are borrowed from DMSTA.

Table 4.20 Summary of equations in the PMSAV water balance.

	Variable	Symbol	Source or Equation	Avg. Cell 4 Value *
Storage	depth	d	$\frac{d(d)}{dt} = q_{in} + ppt - et - s - q_{out}$	0.70 m
Flows	Inflow	q_i	Input time series from G254 data (equivalent to daily HLR)	0.124 m/d
	Rain	ppt	Input time series	0.004 m/d
	ET	et	Input time series	0.004 m/d
	Seepage	s	$= K_{seep} (d - d_s)$	0.002 m/d
	Outflow	q_o	$= K_o d^a w/A$ (if $d < d_m$ then $q_o = 0$)	0.121 m/d

* during January 1998 through October 2000 calibration period

Table 4.21 Summary of constants in the PMSAV water balance.

	Constant	Description	Units	Value
Assigned	A	Wetland surface area	m ²	1.46E6
	w	Average wetland width	m	700
	d_m	Wetland depth below which there is no outflow	m	0.4
	d_s	Assumed stage differential for Darcy seepage flow estimation	m	-0.5
Calibrated	K_{seep}	Coefficient for magnitude of seepage flows	1/d	0.002
	K_o	Coefficient for magnitude of wetland outflows	-	0.75
	a	Exponent for depth dependent hydraulic resistance in outflows	-	3.5

Hydraulic Processes

“Normal” Model

The normal hydraulic model used for post-BMP calibrations and for PMSAV in STSOC design mode is the standard tanks-in-series (TIS) formulation. In the TIS formulation, wetland hydraulic efficiency is modeled as a series of completely-stirred-tank-reactors (CSTRs) (Kadlec and Knight, 1996).

Hydraulic model for Cell 4 (post-STA) calibrations

DBE's dye tracer studies have identified the significance of short-circuit pathways on P removal in Cell 4. Consequently, the hydraulics component of PMSAV has been formulated with specific features to mathematically model these important processes for post-STA calibration. The Cell 4 hydraulics model enables a more accurate calibration of rate coefficients for TP removal based on the Cell 4 data set.

Figure 4.59 shows a schematic diagram of our model for Cell 4 hydraulic processes. Flow is modeled in the wetland with two parallel pathways: vegetated treatment and non-vegetated short-circuit pathways. The treatment zones are modeled as a three tanks-in-series (TIS) system. The short-circuit zones are modeled as 9 TIS pathway in parallel with the treatment zones. It is assumed that no P removal occurs in the short-circuit zones. There are three points in the hydraulic model at which complete mixing occurs between the two pathways.

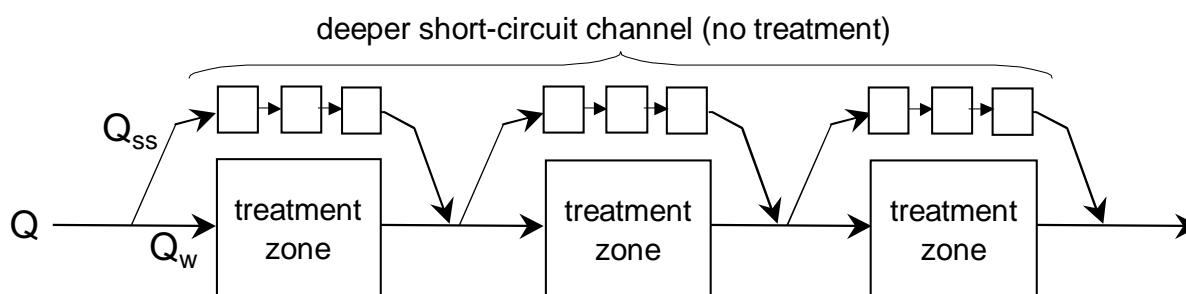


Figure 4.59. In addition to the standard TIS formulation, PMSAV has a hydraulics model specifically aimed at modeling Cell 4 hydraulic processes. The Cell 4 hydraulics model accounts for parallel treatment and short-circuiting pathways, with intermittent mixing between the two.

The short-circuit pathway in the model are primarily intended to emulate the prominent zigzag-shaped short-circuit through Cell 4 that was documented in the December 1999 DBE dye tracer assessment. It is not specifically intended to model the myriad of other smaller short-circuit pathways that seem inherent in most wetland hydraulic behavior, but probably captures some of this behavior anyway. The depth in the Cell 4 short-circuit pathway has been measured at over a meter deeper than average Cell 4 depths, and is accordingly prescribed a

deeper depth in the model. The higher number of series connected short-circuit tanks compared to vegetated tanks implies a greater degree of plug-flow through those zones. Mixing between vegetated and short-circuit pathways is an essential aspect of Cell 4's internal hydraulics as evidenced in the C-7 canal, which is a zone of complete mixing between the general north-south flow through vegetated zones and the zigzag flow of the documented short-circuit.

This model geometry assumes that Cell 4 would behave like a 3 TIS system if the prominent short-circuit were non-existent. In the first Cell 4 tracer assessment, DBE measured the hydraulic efficiency of Cell 4 as similar to a TIS=1.3 system (DBE, 2002). Therefore, the Cell 4 hydraulic model hypothesizes that the difference between Cell 4 acting as a 3 TIS system and as a 1.3 TIS system is caused by the fraction of total flow routed through the short-circuit pathway. Kadlec and Knight (1996) have suggested that TIS=3 is a good representative value for "typical" surface flow wetlands. Additionally, we validated the TIS=3 assumption during model calibration, where we also tested this model (with short-circuiting) using wetland TIS values of 2 and 4, both of which yielded reduced calibration effectiveness.

Mathematically, there are two parameters required to define the behavior of the hydraulic model shown in Figure 4.59: the fraction of wetland area occupied by the short-circuit and the fraction of flow diverted through the short-circuited pathway. The fractional area is an input constant, but the fractional flow is calculated based on depth-dependent relationships.

The equations that describe flow through vegetated and open-channel regions suggest that the flow proportioning between Cell 4's treatment and short-circuit zones may be dynamic and depth dependent. It is likely that flow through Cell 4's short-circuit behaves as an open-channel and could therefore be described with Manning's equation as:

$$Q_{ss} = \frac{1}{n} r^{2/3} S^{1/2} (A f_{area})$$

where Q_{ss} = flowrate through the short-circuit area (m³/d)

r = hydraulic radius of short-circuit channel

$$= \frac{((d + d_{ss}) w f_{area})}{(2 (d + d_{ss}) + w f_{area})}$$

n = manning's number

S = bed slope (constant)

f_{area} = fractional area occupied by the short-circuit

d_{ss} = additional depth in short-circuit channel below ground level of treatment region

Hydraulic resistance through densely vegetated wetland zones is not constant (as in open channel flow), but tends to decrease with increasing water levels (Reed, et al 1998, Kadlec and Knight 1996). Accordingly, Kadlec and Knight (1996) have proposed the following general form for estimating flow through densely vegetated areas:

$$Q_w = b_1 d^a S (A (1 - f_{area}))$$

where Q_w = flow rate through wetland areas (m^3/d)

b_1 = scalar constant (typically in the range of 1-5 e7)

a = exponent for depth dependent flow (see Table 4-2)

Combining these two equations and simplifying, the fractional flow through short-circuited areas (f_{flow}) can be represented as follows:

$$\begin{aligned} f_{flow} &= \frac{Q_{ss}}{Q_{ss} + Q_w} \\ &= \frac{r^{2/3}}{r^{2/3} + \frac{c d^a}{(f_{area}^{-1} - 1)}} \end{aligned}$$

where $c = n b_1 S^{1/2}$ and variables defined above.

The preceding equation suggests the potential for depth-dependent proportioning of flow between treatment and short-circuiting zones in Cell 4. The relationship suggests that the fractional flow through the wetland increases with increasing water levels in Cell 4 (the

shallower the water, the more the effects of short-circuiting). When linked with the P removal model, this relationship results in improved P removal at higher stages due to less short-circuited flows (more treated flows). Table 4.22 summarizes the calibration coefficients represented in this equation. The parameter f_{flow} in Table 4.22 was a calculated parameter and not a calibration coefficient, but is shown here for reference.

Table 4.22. Summary of coefficients and parameters for Cell 4 hydraulic model.

Constant	Description	Units	Value
f_{area}	Fraction of total wetland area occupied by the short-circuit channel	-	0.08
d_{ss}	Additional depth in short-circuit channel below ground level of treatment region	m	1.2
c	Combined constant that determines short-circuit flow distribution.	-	50
f_{flow}	Fraction of total wetland flow passing through the short-circuit channel	-	0.44*

* Average value of a dynamic time history

P Cycling Processes

Figure 4.60 shows a diagram of P removal processes modeled in PMSAV. These processes are modeled in each of the 'treatment zones' shown in Figure 4.59.

Table 4.23 shows the equations and sources of data for the storages and flows in the P-removal model. Table 4.24 summarizes the eight constants that require calibration in this model. As with previous tables presented in this section, the numeric values presented in these tables will be discussed further in subsequent sections.

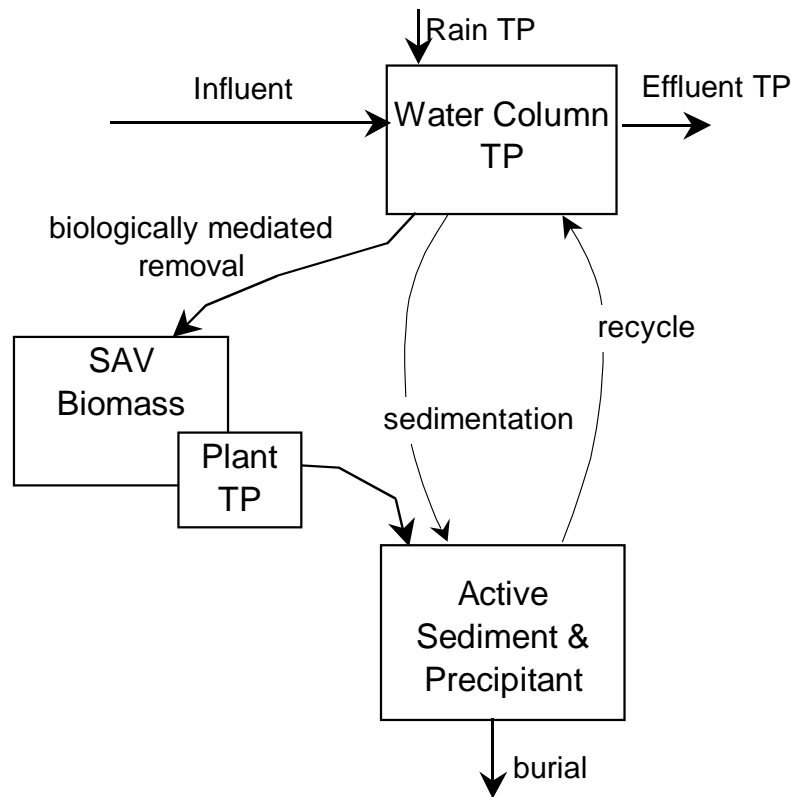


Figure 4.60. Process diagram for P-removal as modeled in PMSAV's treatment zone.

There are three active storages of phosphorus modeled in PMSAV: water column, biomass tissue, and active sediment storages. The phosphorus stored by burial is also a storage, but it is an inactive long-term deposit. SAV biomass is modeled separately from plant-P, as PMSAV simulates variable P removal as a function of water column concentration (luxury uptake), implying variable plant P concentrations (g-P/g-SAV).

Influent, effluent, rain-based, and seepage flows of phosphorus are calculated using daily water flow rates from the water balance model. Simulated biomass growth uses a modified Monod formulation including a linear growth rate (proportional to biomass standing crop) modified by nutrient (P) limitation. Simulated P-limitation uses a standard half-saturation constant formulation. Biomass burial (senescence) is proportional to the square of the standing crop.

Biologically mediated removal is a lumped pathway accounting for both P uptake and coprecipitation processes. Plant P storage assumes an instantaneous removal rate proportional

to the product of water column P concentration. The instantaneous uptake rate (the parenthetical term in the 'biomass uptake' equation in Table 4.23) is a piecewise linear equation. At very low ambient P concentrations, P is limiting and uptake occurs to maintain minimum tissue P content. At higher ambient P concentrations, P is not limiting and luxury uptake occurs. It is assumed in the model that phosphorus is lost from biomass tissue based on the daily rate of burial and daily average tissue-P concentration.

The sedimentation pathway includes settling of particulate phosphorus, which accounted for between 15-25% of TP removal in Cell 4. This pathway is modeled as a first-order process proportional to the water column TP concentration. This term can be set to zero when modeling systems with negligible particulate P inflows.

P recycled from the active sediment storage is assumed to be linearly proportional to the amount stored. The long-term burial rate from this storage is also assumed linear relative to the storage quantity

Table 4.23. Summary of equations in the PMSAV P-removal model.

	Variable	Symbol	Source or Equation	Units	Average Values	
					Post-BMP	Post-STA
Storages	Water column P	P $[P]$	$\frac{d(P)}{dt} = P_{in} + P_{ppt} - P_{out} - U - C + R$ $[P] = P/d$	µg/l	28	21
	Active sediment	Y	$\frac{d(Y)}{dt} = L + C - R - B$	g/m ²	1.05	0.70
	SAV biomass	SAV	$\frac{d(SAV)}{dt} = G - S$	g/m ²	783	685
	Plant associated P	T_p	$\frac{d(T_p)}{dt} = U - L$	mg-P/kg	2119	1709
Flows	Influent P concentration	$[P_{in}]$	Input time series from weekly composite TP samples	µg/l	80	59
	P in influent	P_{in}	$= q_i \cdot [P_{in}]$	g-P/m ² /yr	3.79	1.97
	P in effluent	P_{out}	$= q_o \cdot [P]$	g-P/m ² /yr	1.20	0.67
	P with rain	P_{ppt}	$= ppt \cdot [P_{ppt}]$	g-P/m ² /yr	0.02	0.02
	P with seepage	P_{seep}	$= s \cdot [P]$	g-P/m ² /yr	0.00	0.02
	Biomass growth	G	$= K_g \cdot SAV \cdot \frac{[P]}{[P] + [K_{P-1/2}]}$	$\frac{g-SAV}{m^2/yr}$	2281	1727
	Biomass burial (death and decay)	S	$= K_s \cdot SAV^2$	$\frac{g-SAV}{m^2/yr}$	2199	1696
	Biomass uptake	U	$= (K_u \cdot [P]) \cdot G$ where $(K_u \cdot [P]) \geq 700 \text{ mg-P/kg}$	g-P/m ² /yr	5.73	3.04
	P sedimentation	C	$= K_c \cdot [P]$	g-P/m ² /yr	0.57	0.39
	Biomass P burial	L	$= \frac{T_p}{SAV} \cdot S$	g-P/m ² /yr	4.99	3.17
	Sediment P recycle	R	$= g \cdot (1 - b) \cdot Y$	g-P/m ² /yr	3.68	1.88
	Sediment P burial	B	$= g \cdot b \cdot Y$	g-P/m ² /yr	1.58	1.48

Table 4.24. Summary of calibration constants for PMSAV.

	Constant	Description	Units	Post-BMP Value	Post-STA Value
Calibrated	K_g	Intrinsic growth rate	1/yr	5.6	5.6
	$K_{P-1/2}$	Half saturation constant for P as limiting nutrient in biomass growth	µg/l	25	25
	K_s	Biomass burial coefficient	m ² /g-SAV/yr	0.0035	0.0035
	K_u	Luxury uptake coefficient	m ³ /g-SAV	0.08	0.08
	K_c	Sedimentation coefficient	m/yr	20	20
	g	Sediment turnover rate	1/yr	5	5
	b	Sediment burial fraction	-	0.30	0.42

PMSAV Limitations

As with all models, simulation results should be used and interpreted only in light of a good understanding of the model's strengths and weaknesses. There are several limitations in the formulation of PMSAV and we think it is important to state them outright.

In terms of P removal processes, the model has two significant limitations. First, we have chosen to model only total phosphorus, rather than a potentially more accurate approach of addressing P speciation. We have much data suggesting the relative ease with which SRP is removed in SAV systems, compared to the more recalcitrant DOP and PP forms. Secondly, while sediment recycle and burial are modeled, internal sediment processes per se are not. We have data suggesting that P recycling from sediment is more specifically related to relative fractions of organic and calcium-bound materials that are present. While including these processes in PMSAV (both speciation and sediment) would have made for a more accurate representation of our process understanding, it would have also more than doubled model complexity. These processes can be addressed in future PMSAV endeavors beyond this Phase 2 project. It is also important to understand the limitations of the datasets that were used for calibration. The District's input/ output time series of Cell 4 P concentrations are the principle data used for calibration. This dataset is supplemented with DBE measurements of biomass, tissue-P, and sediment that were made (at infrequent intervals) in Cell 4 and numerous other

systems within the last few years. We have no time series data on internal process flows, nor is it reasonable to expect that we will have this information in the near future. This makes the calibration task somewhat analogous to mapping the internal traffic flows in a large city when the only available data is the daily flux of entering and leaving vehicles, along with a few spot measurements of internal flows made in several other smaller cities. In the case of PMSAV, we will never say that we have true 'confidence' in the predicted magnitudes of internal flows, but what we can say is that they seem 'sensible' to us based on our studies and experience.

Additionally, the model does not account for large-scale stochastic natural and human-caused events that have occurred during calibration periods that could have substantially influenced TP removal on short and long-term scales. These events include seasonal coot invasions (we noted significant SAV herbivory in Cell 4 during winter months of 2001), construction activities, and tropical storm events.

The calibration approach, and simulation results from PMSAV are provided in our recent STSOC final report (DBE, 2002).

Section 5: STA-1W Cell 5 Investigation

STA-1W Cell 5 was flooded in late spring 1999, but for several months continued to exhibit high water column levels of both phosphorus and color. The previously disturbed (farmed) organic soils are thought to be the source of the high water column constituent concentrations. As part of our work scope (Task 10), we investigated the colonization rate of SAV into Cell 5, inoculation techniques for SAV that might be suitable for large-scale wetland applications, and the use of a chemical amendment (lime) to reduce water column TP and color concentrations.

5.1 Lime-Addition Assessments

Previous small-scale jar tests demonstrated that lime can lower color and TP levels of Cell 5 waters. However, it is unknown how effective general broadcasting of lime into the large wetland cell will be, since there would be little mixing energy compared to that provided in jar tests, and because the organic soils may continue to act as a source of P and TOC.

5.1.1 Methods

To test the effectiveness of lime additions, we deployed *in situ* chambers (46 cm diameter transparent fiberglass cylinders) to isolate small portions of the Cell 5 sediments and water column. Six columns were deployed, with duplicate columns for each of these treatments: Control, Low Lime Dose, and High Lime Dose. We selected 66 mg/L and 198 mg/L as $\text{Ca}(\text{OH})_2$ for the low and high dosages, respectively. On November 9, 1999 the lime was added to the water surface as a slurry in four of the six columns, with no mixing provided. We discovered contamination (a large, dead fish) in one of the columns on the first sampling date, so only one control column was monitored during the evaluation. In addition to that Column Control, surface water outside the columns (i.e., an Ambient Control) was analyzed to discern if any “enclosure” effects had occurred. Following lime addition, the water column was sampled at 0 and 4 hr, and 1, 3, 7, 14, 21, 28 and 42 days, for temperature, pH, SRP, TP, total Ca, alkalinity, and color (apparent and true).

5.1.2 Results

After 24 hours, the SRP concentrations in the two sets of controls (water outside the enclosures [Ambient Control] and water inside the enclosure [Column Control]) diverged, as did the total P concentrations (Figure 5.1). The two types of controls were within close agreement with respect to true and apparent color, total calcium, and total alkalinity throughout most of the evaluation period (Figure 5.1).

Compared to the Column Control, both lime dosages provided lower concentrations of SRP and total P in Cell 5 surface water for the first three days (Figure 5.2). Both TP and SRP concentrations in the Low and High dosed columns converged with the concentration in the Column Control on the seventh day. For both lime dosages, SRP concentrations decreased from an average of 141 to 4 µg/L within the first 4 hours. By the third day, SRP concentrations had increased to 13 µg/L in both sets of dosed columns, which was still considerably lower than the 89 µg/L concentration in the Column Control. Total P concentrations, on the other hand, decreased to approximately half the Column Control values within the first three days (Figure 5.2). The differences between dosing treatments (66 vs. 198 mg Ca(OH)₂) in P removal were minimal.

Apparent color (unfiltered) concentrations were initially elevated in the pair of Low Dosage columns because of the increased turbidity from calcium carbonate precipitation, but the effect was short-lived (Figure 5.2). After the first day, the changes in apparent color concentrations within the Column Control and the lime-amended columns tracked each other closely for 28 days.

True color is a better measure for characterizing the removal of dissolved organic matter (DOM) than is apparent color since turbidity interference is removed by filtering the sample. Most removal of the DOM occurred immediately at the onset of the High Dosage lime amendment where the color concentration was nearly reduced by half within the first day (Figure 5.2). Over the 28-day measurement period, more of the DOM was removed in the Higher Dosed columns than the Lower Dosed columns.

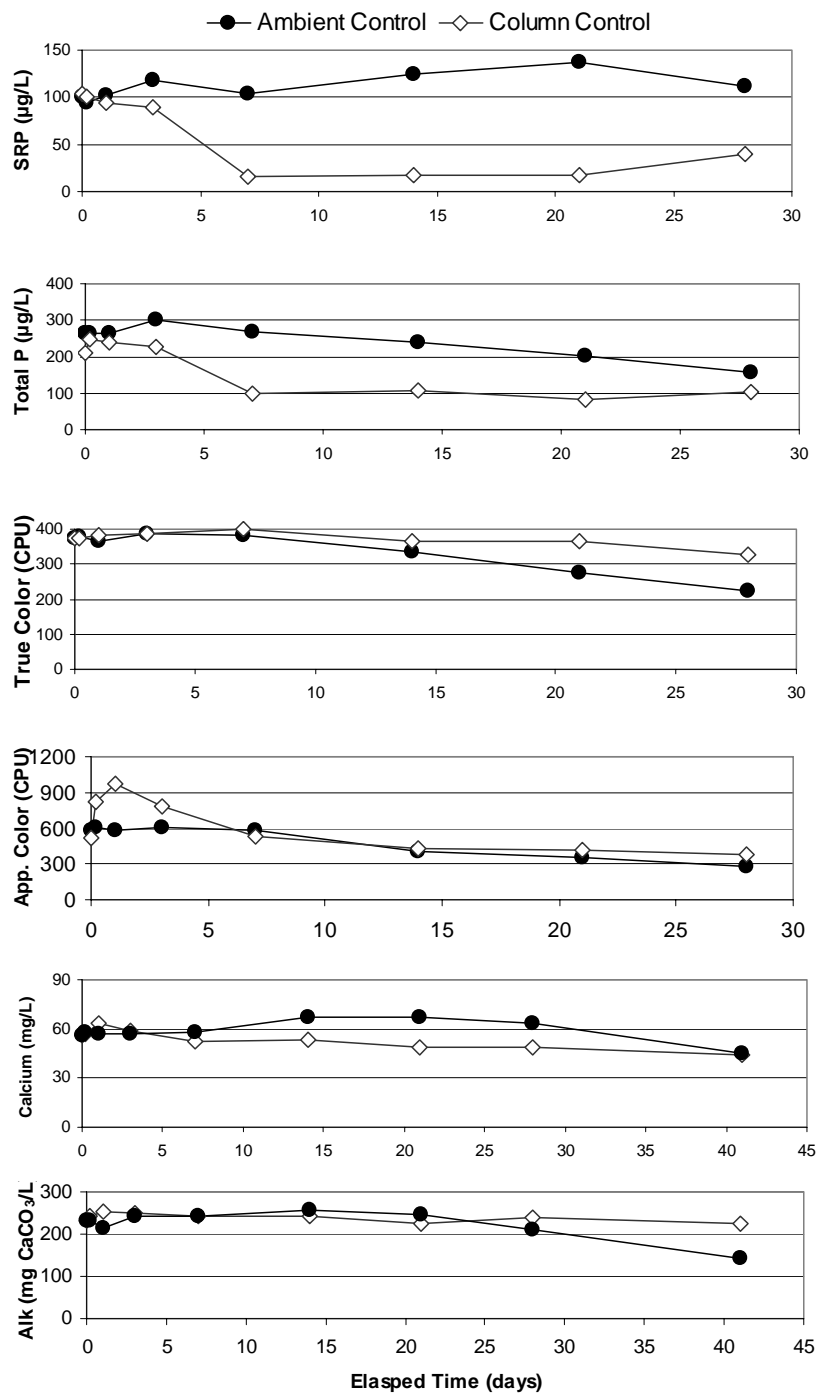


Figure 5.1. Concentrations of SRP, total P, true and apparent color, alkalinity and calcium for Cell 5 water outside (Ambient Control) and inside (Column Control) *in situ* columns during November 9 – December 7, 1999.

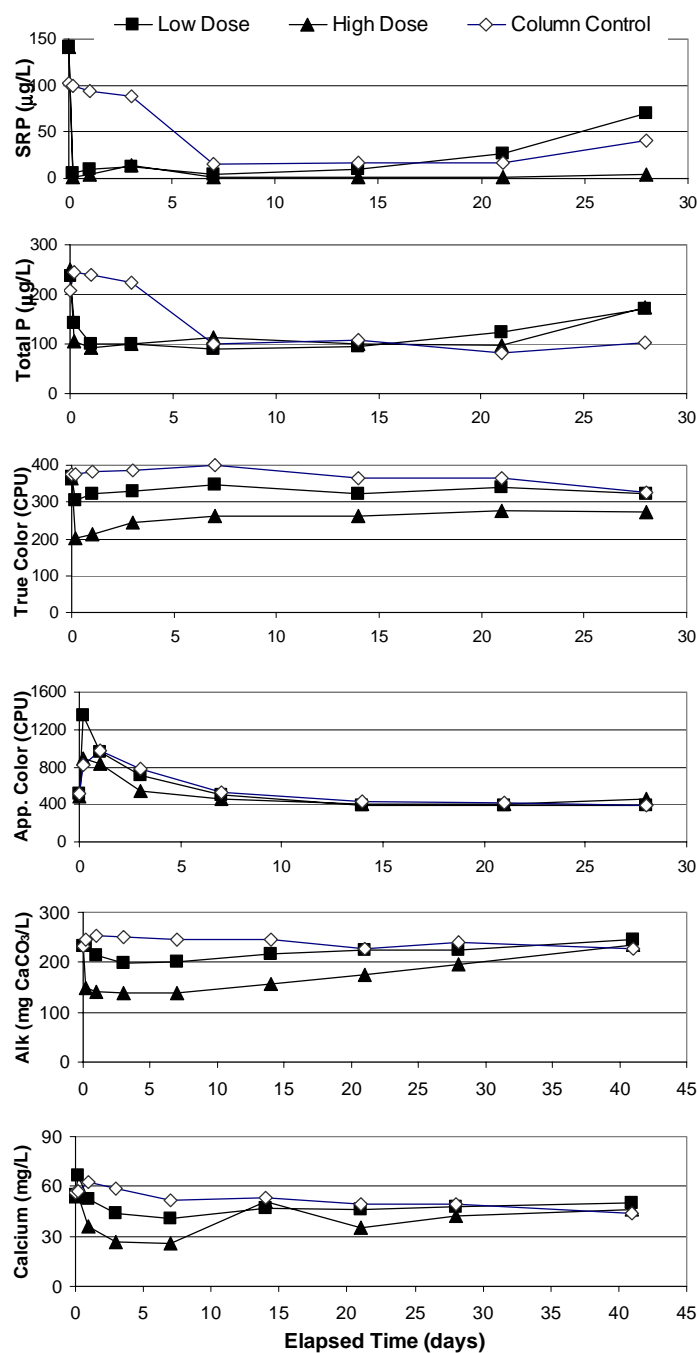


Figure 5.2. Concentrations of SRP, total P, true and apparent color, alkalinity and calcium for Cell 5 water contained within *in situ* columns receiving Low Dose (66 mg/L; duplicate columns) and High Dose (198 mg/L; duplicate columns) lime additions (as $\text{Ca}(\text{OH})_2$). The Column Control was not dosed.

Relative to the Column Control, total calcium and alkalinity concentrations declined inside the enclosures that received the lime (Figure 5.2); lower concentrations were observed up to 14 days for calcium and 28 days for alkalinity. Since the decreases in calcium and alkalinity concentrations during the first two weeks were due to the precipitation of calcium carbonate, the higher removals in the High Dosage columns were expected (Figure 5.2).

The longevity of the SRP removal appears at first to last 28 days in the High Dose columns and 21 days in the Low Dosed columns (Figure 5.2). However, the single untreated Column Control also removed SRP nearly as efficiently beginning on the seventh day, indicating "enclosure" effects may have influenced the SRP removal from that day forward. Besides the difficulty of determining the extent of "enclosure" effects during prolonged incubation periods (weeks), there is also the issue of larger, field-scale effects that are not represented within an enclosure. For example, water and sediment turbulence was dampened considerably within the enclosures compared to the external wetland waters and sediments. If lime was applied to all of Cell 5, wind-generated turbulence could either prolong (by resuspending the calcite floc layer) or shorten (by dispersing and diluting the sediment floc layer) the period of effective P removal.

5.2 SAV Inoculation Assessments in Cell 5

The most cost-effective approach for rapidly establishing submerged macrophytes in a large-scale SAV-dominated wetland is currently unknown. The western portion of STA-1W Cell 5 was flooded quickly during late spring 1999, at the time creating large areas of open water with few emergent macrophytes. At that time, it was not known whether these open areas would be rapidly colonized with SAV via natural recruitment, or if SAV inoculation ultimately would be required. The simplest means of SAV inoculation would be to obtain plant material from a nearby donor wetland (e.g., Cell 4), and disperse small aliquots throughout the cell from an airboat. However, the 930 ha western portion of Cell 5 has a large, open fetch, so widely distributed plant fragments could all be swept to one side of the wetland if a strong wind were to blow soon after plant stocking.

5.2.1 Methods

Beginning in December 1999, we initiated two evaluations to evaluate potential inoculation protocols for SAV in Cell 5. Both techniques involved “weighting” small aliquots of plants prior to stocking. In the first, we placed small, known quantities of the macrophytes *Ceratophyllum*, *Najas* and *Chara* into open mesh bags. Both small mesh (fiberglass screen) and large mesh (polypropylene “citrus” bags) were evaluated. The bags and enclosed plants were weighted with a small brick, and incubated just below the water surface, as well as at the sediment-water interface. Incubations at both locations were performed to determine whether the poor light transmittance in the water column (caused by high organic color levels) was inhibiting SAV growth. For the second technique, a narrow ceramic “ring” was placed over a small “handful” of plants, thereby providing a weight to hold that “cluster” of plants on the bottom. For both assessments, plants were retrieved and wet weight biomass measured at two and four weeks after stocking.

5.2.2 Results

Neither inoculation technique proved successful, primarily because portions of the stocked plants became stressed and died. Even though the plants were loosely stocked in the incubation bags, the plants actually in contact with the bag material either grew poorly or died. The plants directly in contact with the ceramic ring were similarly stressed. Some plants, in particular the *Ceratophyllum* that was not directly in contact with the bag or ring, grew well. Overall, *Ceratophyllum* and *Najas* exhibited positive growth in some of the bags, whereas all of the stocked *Chara* died. For *Ceratophyllum* and *Najas*, the large mesh bags were more effective than the small mesh bags in promoting SAV growth, and the plants incubated near the surface grew better than those incubated adjacent to the bottom. Data collected from the internal Cell 5 survey (see below) suggest that water column characteristics, rather than incubation techniques, may have been responsible for the mortality of the *Chara*.

5.3 Internal Cell 5 SAV Survey

5.3.1 Methods

In order to assess the colonization rate of SAV species into Cell 5, we performed quarterly assessments of SAV occurrence in the wetland. Early in February 2000, using Global Positioning System (GPS) coordinates, we established a grid of 120 equidistant sampling stations in the

western portion of STA-1W Cell 5. We marked each station in the field by driving a labeled PVC pole into the muck substrate. On February 10, 2000, we performed the first assessment of SAV occurrence. This work was performed from an airboat. Because of the highly colored waters, vegetation on the bottom was not visible, so we used a garden rake to collect submerged vegetation. We developed a “standard” collection technique, in which the rake was “dragged” along the bottom at two locations adjacent to each sampling site. Collected SAV species were identified, ranked qualitatively in terms of abundance, and returned to the water.

Note that our sampling efforts resulted in a simple assessment of plant species found immediately adjacent to each sampling location, and therefore do not represent vegetation occurring “between” stations. The area of the western portion of Cell 5 is ~ 930 ha, so each of our 120 sampling points is an 'approximation' of a ~8 ha parcel. However, to provide an extrapolation of potential vegetation colonization between sampling points, we used an ArcView program to create a spatial depiction of the likely colonization pattern throughout the wetland. These spatial visualizations for sampling dates in February 2000, May 2000, August 2000, November 2000, February 2001 and July 2001 are provided in Figures 5.3 to 5.5.

5.3.2 Results

During February 2000, *Ceratophyllum* was found to be the dominant SAV species in Cell 5, occurring in 64 of 120 stations. *Najas* was found in 17 stations, and *Chara* in none. In general, the biomass of SAV at most locations was quite low (only a few plant fragments), reflecting only very recent colonization. The northwest region of the wetland was open water, essentially devoid of macrophyte biomass. Secchi depths during this survey ranged from 0.05 to 0.45m, and averaged 0.25m.

Two main factors influence the distribution of SAV species in a newly flooded wetland. The first is the availability of SAV propagules, and the second is the suitability of environmental conditions, such as physical and chemical characteristics of the substrate and water column, for SAV growth. During the first year after startup, Cell 5 exhibited high concentrations of both total P and color in the water column. Based on both our inoculation evaluations and the SAV distribution in the cell, these conditions appear detrimental to *Chara*, but favorable for *Ceratophyllum*, and to a lesser extent, *Najas*.

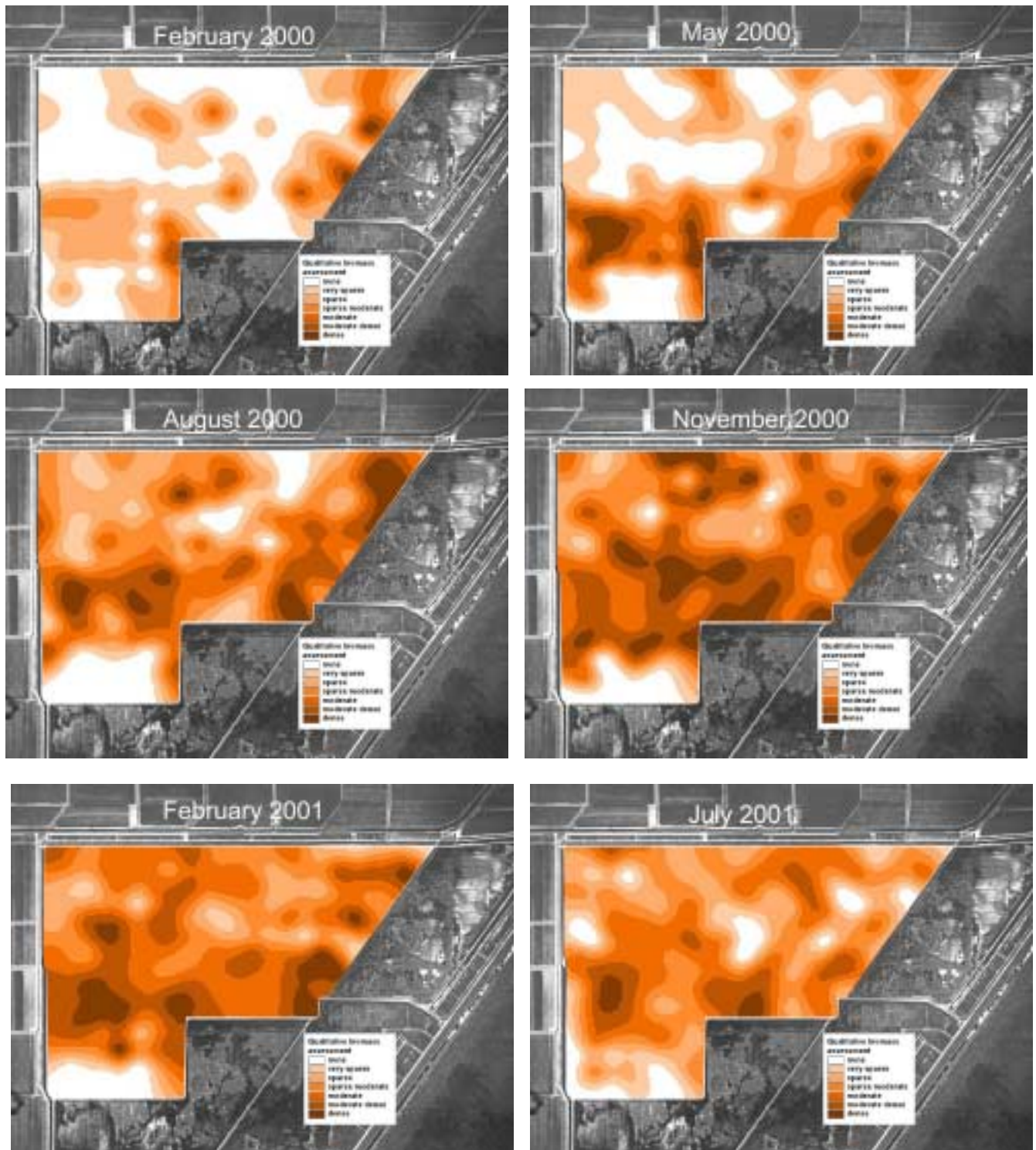


Figure 5.3. Cell 5 SAV colonization: Presence and distribution of *Ceratophyllum* during six 120 station qualitative surveys.

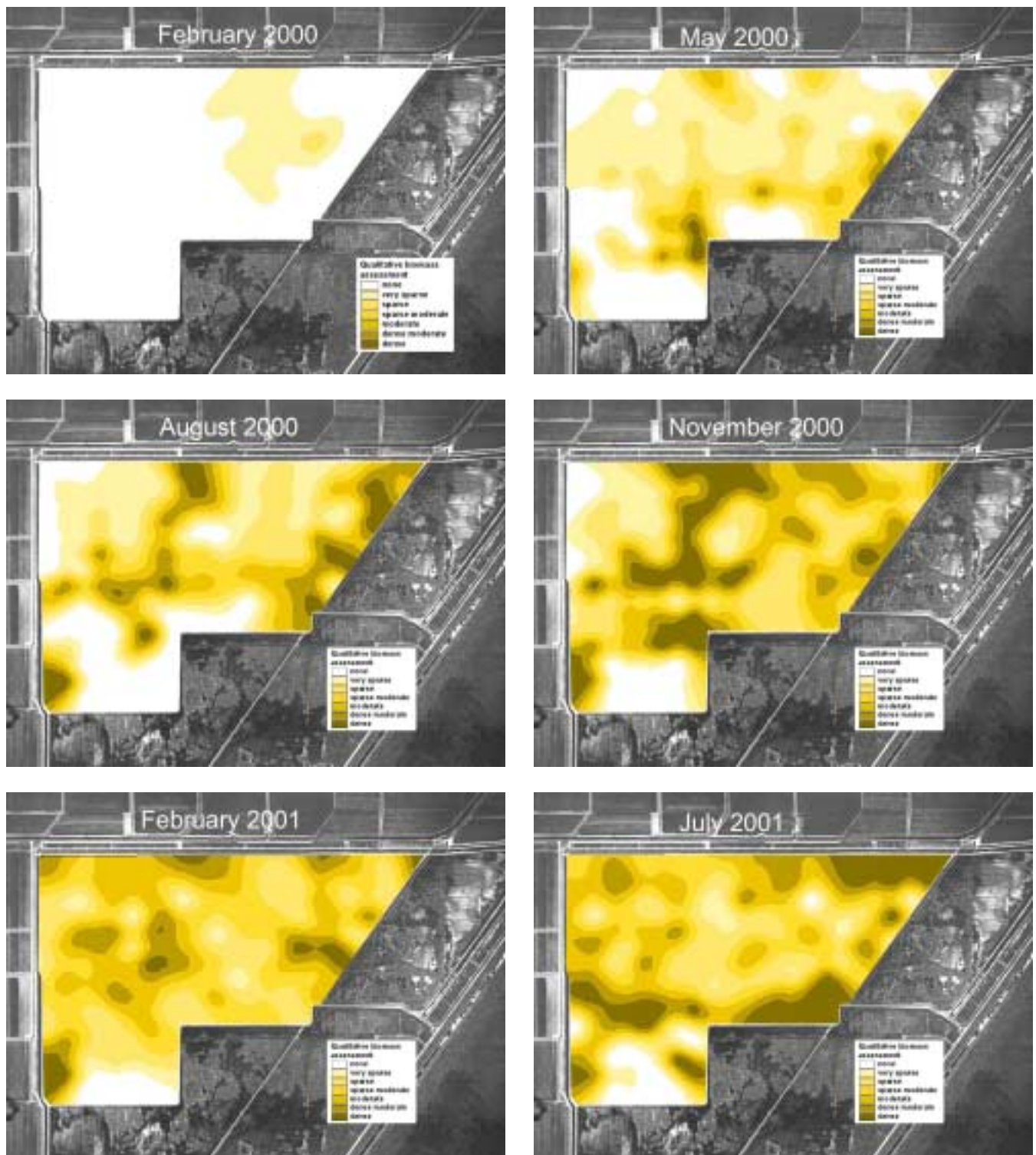


Figure 5.4. Cell 5 SAV colonization: Presence and distribution of *Najas* during six 120 station qualitative surveys.

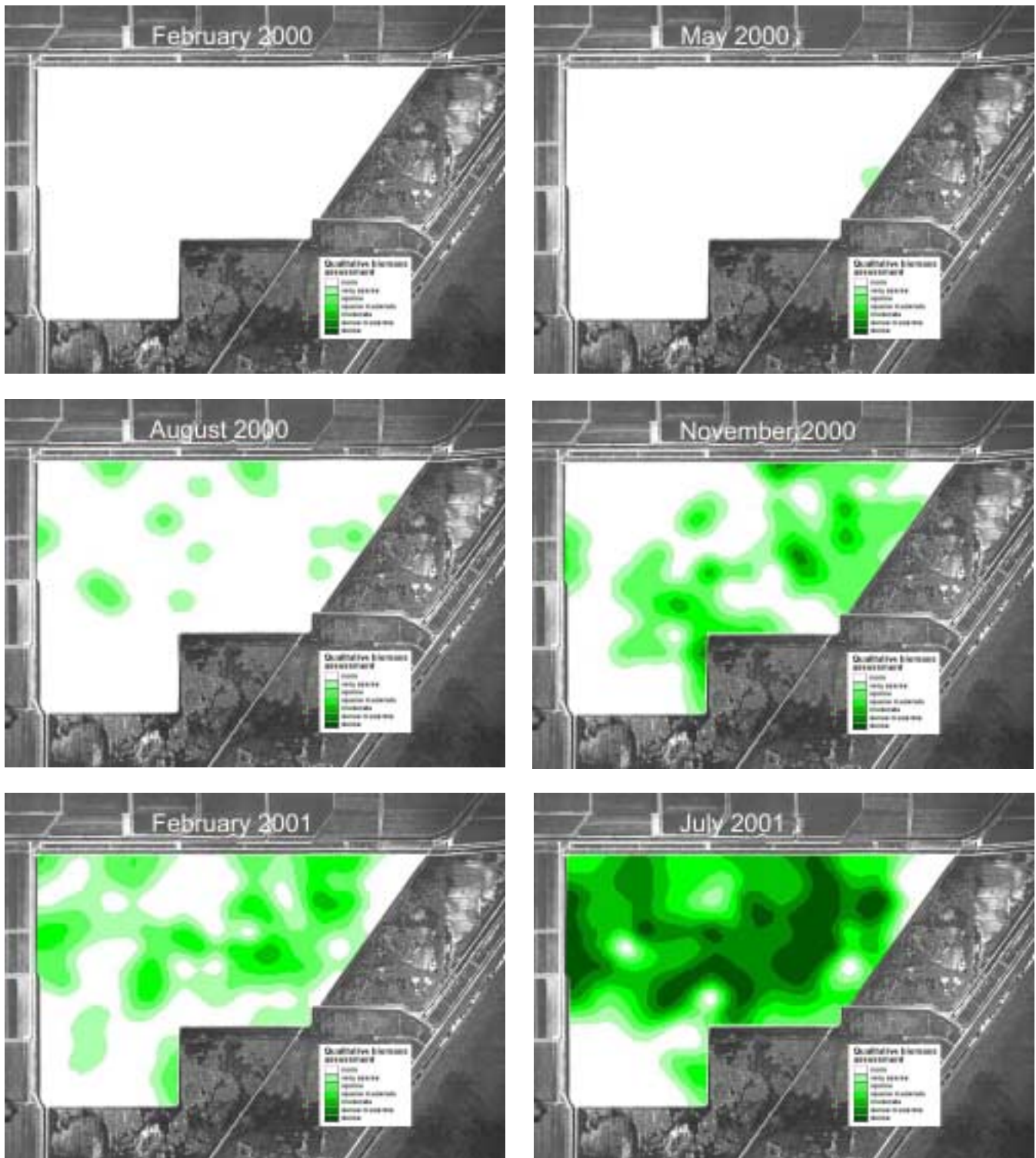


Figure 5.5. Cell 5 SAV colonization: Presence and distribution of *Hydrilla* during six 120 station qualitative surveys.

By August 2000, 16 months after flooding of Cell 5, both *Ceratophyllum* and *Najas* were well distributed throughout the wetland (Figures 5.3 and 5.4). *Hydrilla*, which was present in small patches on this date, expanded quickly throughout the wetland from November 2000 through July 2001 (Figure 5.5). *Hydrilla* appears to form a dense canopy at the water surface, with very little biomass beneath this surface layer. We suspect that *Hydrilla's* canopy structure may be detrimental to P removal performance in two respects: first, substantial short-circuiting of flow can occur beneath this dense surface mat; and second, the dense surface mat may promote anoxic conditions in the lower water column and at the sediment-water interface.

In addition to the qualitative SAV survey of Cell 5, on four dates we performed a quantitative biomass assessment at 25 stations throughout the wetland. *Ceratophyllum* was present at the highest mean standing crop biomass, at 58 g dry wt./m², followed by *Najas* (45 g dry wt/m²) and *Hydrilla* (6.3 g dry wt/m²). Unlike the standing crops of *Ceratophyllum* and *Najas*, which appeared relatively stable from August 2000 through May 2001, the standing crop biomass of *Hydrilla* steadily increased during the monitoring period (Figure 5.6).

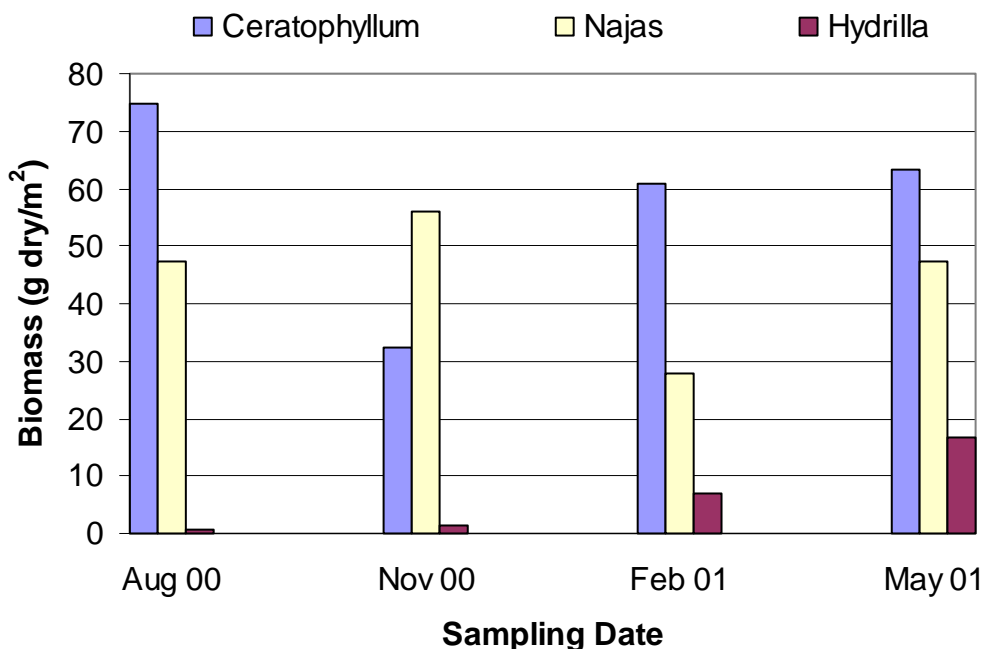


Figure 5.6. Standing crop biomass of SAV species colonizing STA-1W Cell 5 over a nine month period. Values represent average biomass from 25 stations. Initial flooding of the wetland occurred in spring 1999.

Section 6: References

Barko, J.W., D.G. Hardin and M.S. Matthews. 1982. Growth and morphology of submersed freshwater macrophytes in relation to light and temperature. *Can. J. Bot.* 60:877-887.

Bayliss, P., D.K. Smith, M.E. Morse, and L.G. Berry. 1980. Mineral powder diffraction file data book. International Center for Diffraction Data, Swarthmore, PA.

Browder, J.A., P.J. Gleason, D.R. Swift. 1994. Periphyton in the Everglades: spatial variations, environmental correlations, and ecological implications. In: S. Davis and J. Ogden, editors, *Everglades: The Ecosystem and Its Restoration*. St. Lucie Press, Delray Beach, FL. P 379-418.

Brown and Caldwell. 1992. Evaluation Methods and Procedures, Evaluation of Alternative Treatment Technologies, Everglades Protection Project. Contract C-3051. Report prepared for South Florida Water Management District West Palm Beach, FL.

Brown and Caldwell, 1993a. Phase I Evaluation of Alternative Treatment Technologies, Everglades Protection Project. Contract C-3051, Amendment 2. Report prepared for South Florida Water Management District West Palm Beach, FL.

Brown and Caldwell, 1993b. Phase II Evaluation of Alternative Treatment Technologies, Everglades Protection Project. Contract C-3051, Amendment 4. Report prepared for South Florida Water Management District West Palm Beach, FL.

Brown and Caldwell, 1993c. Analysis and Development of Chemical Treatment Processes, Everglades Protection Project. Contract C-3051, Amendment 6. Report prepared for South Florida Water Management District West Palm Beach, FL.

Chimney, M. J. and M. Z. Moustafa. 1999. Effectiveness and optimization of stormwater treatment areas for phosphorus removal. Everglades Interim Report. South Florida Water Management District, West Palm Beach, FL.

Christensen, N., W.J. Mitsch, and S.E. Jorgensen, 1994. A first generation ecosystem model of the Des Plaines River experimental wetlands. *Ecological Engineering* 3: 495-521.

Cooper, W.T., Y.P. Hsieh, W.M. Landing, L. Proctor, V.J.M. Salters, and Y. Wang. 1999. The Speciation and Sources of Dissolved Phosphorus in the Everglades. Final Report submitted to the South Florida Water Management District, West Palm Beach, FL.

Correl, D.L. 1998. The role of phosphorus in the eutrophication of receiving waters: A review. *J. Environ. Qual.* 27: 261-266.

Currie, D.J., and J. Kalff. 1984a. A comparison of the abilities of freshwater algae and bacteria to acquire and retain phosphorus. *Limnol. Oceanogr.* 29: 298-310.

Currie, D.J., and J. Kalff. 1984b. The relative importance of bacterioplankton and phytoplankton in phosphorus uptake in freshwater. *Limnol. Oceanogr.* 29: 311-321.

Currie, D.J., and J. Kalff. 1984c. Can bacteria outcompete phytoplankton for phosphorus? A chemostat test. *Microb. Ecol.* 10: 205-216.

Danen-Louwerse, H.J., J.Lijklema, and M. Coenraats. 1995. Coprecipitation of phosphate with calcium carbonate in Lake Veluwe. *Water Res.* 29: 1781 - 1785.

DeBusk, T.A., M.A. Langston, P.S. Burgoon and K.R. Reddy. 1990. A performance comparison of vegetated submerged beds and floating macrophytes for domestic wastewater treatment. In: P.F. Cooper and B.C. Findlater (eds.), *Constructed Wetlands in Water Pollution Control*. Pergamon Press, Oxford, England.

DeBusk, T.A., and F.E. Dierberg. 1999. Techniques for optimizing phosphorus removal in treatment wetlands. In: K.R. Reddy, G.A. O'Connor, and C.L. Schelske, editors, *Phosphorus Biogeochemistry in Subtropical Ecosystems*. Lewis Publishers, Boca Raton, FL P. 467-488.

DBE. 1999. A Demonstration of Submerged Aquatic Vegetation/Limerock Treatment System Technology for Removing Phosphorus from Everglades Agricultural Area Waters. Final Report submitted to the South Florida Water Management District and the Florida Department of Environmental Protection, West Palm Beach, FL.

DBE. 2000a. A Demonstration of Submerged Aquatic Vegetation/Limerock Treatment System Technology for Removing Phosphorus from Everglades Agricultural Area Waters: Follow-on Study. Cell 4 Feasibility Study submitted to South Florida Water Management District and the Florida Department of Environmental Protection. West Palm Beach, FL.

DBE 2000b. A Demonstration of Submerged Aquatic Vegetation/Limerock Treatment System Technology for Removing Phosphorus from Everglades Agricultural Area Waters: Follow-on Study. Cell 4 Tracer Study submitted to South Florida Water Management District and the Florida Department of Environmental Protection. West Palm Beach, FL.

DBE 2000c. A Demonstration of Submerged Aquatic Vegetation/Limerock Treatment System Technology for Removing Phosphorus from Everglades Agricultural Area Waters: Follow-on Study. Experimental Design Plan submitted to South Florida Water Management District and the Florida Department of Environmental Protection. West Palm Beach, FL.

DBE. 2002. Conceptual Designs and Planning Level Cost Estimates for a Full-Scale Submerged Aquatic Macrophyte/Limerock System: Draft Supplemental Technology Standard of Comparison Analysis for Submerged Aquatic Macrophyte/Limerock Technology. Final Report, prepared by DB Environmental, Inc. for the South Florida Water Management District.

Earnest, C.M. 1988. Compositional analysis by thermogravimetry. ASTM, Philadelphia, PA.

Fitz, H.C. and F.H. Sklar, 1999. Ecosystem analysis of phosphorus impacts and altered hydrology in the Everglades: a landscape modeling approach. In *Phosphorus Biogeochemistry in Subtropical Ecosystems*. Edited by K.R. Reddy, G.A. O'Conner and C.L. Schelske. Lewis Publishers, Boca Raton, FL.

Fogler, H.S. 1992. Elements of Chemical Reaction Engineering (2nd Ed.). Prentice-Hall, Inc., Englewood Cliffs, N.J.

Gächter, R. and J.S. Meyer. 1993. The role of microorganisms in mobilization and fixation of phosphorus in sediments. *Hydrobiol.* 253: 103-121.

Harris, W.G., and M. Farve. 2001. Assessment of colloidal phosphorus in Everglades agricultural runoff and treatment wetland effluents. Final Report to the South Florida Water Management District and DEB Environmental Inc, West Palm Beach, Florida.

Hesslein, R. H. 1976. An in situ sampler for close pore water studies. *Limnol. Oceanogr.* 21: 912-914.

Hieltjes, A.H.M., and L. Lijklema. 1980. Fractionation of inorganic phosphate in calcareous sediments. *J. Environ. Qual.* 9: 405-407.

Hesslein, R. H. 1976. An in situ sampler for close interval pore water studies. *Limnol. Oceanogr.* 21: 912-914.

HydroQual, Inc., 1997. SFWMD Wetlands Model: Calibration of the Coupled Periphyton/Vegetation Model to WCA-2. Prepared for South Florida Water Management District, West Palm Beach, FL.

Ivanhoff, D.B., K.R. Reddy, and S. Robinson. 1998 Chemical Fractionation of organic phosphorus in selected histosols. *Soil Science* 163: 36-45.

Kadlec, R.H. 1990. Overland flow in wetlands: Vegetation resistance. *J. Hydraulic Eng., ASCE*, 116:691-706.

Kadlec, R.H., G.R. Best, J.A. Browder, T.A. DeBusk, J.R. Grace, R. Johnson, M.D. Maffei, W.J. Mitsch, K.R. Reddy, C.J. Richardson, G.H. Snyder and A.K. Ward. 1991. The Everglades Nutrient Removal Project Technical Advisory Panel Report. Prepared for the South Florida Water Management District, West Palm Beach, FL.

Kadlec, R.H., W. Bastiaens, and D.T. Urban, 1993. Hydrological design of free water surface wetlands. In: G.A. Moshiri (ed.) *Constructed Wetlands for Water Quality Improvement*. Lewis Publishers, Boca Raton.

Kadlec, R.H. and R.L. Knight. 1996. *Treatment Wetlands*. 893 pp. Lewis Publishers, Boca Raton, FL.

Kadlec, R.H. 1994. Detention and mixing in free water wetlands. *Ecol. Engineering* 3:345-380.

Kadlec, R.H. and R.L. Knight, 1996. *Treatment Wetlands*. Lewis Publishers, Boca Raton, FL.

Kadlec, R.H., 1997. An autotrophic wetland phosphorus model. *Ecological Engineering* 8(2): 145-172.

Kadlec, R.H. and W.W. Walker, 1999. Management models to evaluate phosphorous impacts on wetlands. In *Phosphorus Biogeochemistry in Subtropical Ecosystems*. Edited by K.R. Reddy, G.A. O'Connor and C.L. Schelske. Lewis Publishers, Boca Raton, FL.

Kadlec R.H. 1999. The inadequacy of first-order treatment wetland models. *Ecol. Eng.* (in press).

Kadlec, R.H., 2000. The Autobiotic Wetland Phosphorus Model Related to DMSTA. memo communication.

Kadlec, R.H. and W.W. Walker, 2000. Dynamic Model for Stormwater Treatment Areas (DMSTA). Presented at DMSTA Modeling Subgroup Meeting held at South Florida Water Management District on August 3, 2000, West Palm Beach, FL.

Kang, H.J., and C. Freeman. 1999. Phosphatases and arylsulphatase activities in wetland soils: annual variation and controlling factors. *Soil Biol. Biochem.* 31: 449-454.

Karathanasis, A.A., and W.G. Harris. 1994. Quantitative thermal analysis of soil minerals. p. 360-411. In J. Ammonette and L.W. Zelazny (ed.) *Quantitative methods in soil mineralogy*. Soil Sci. Soc. Am. Miscellaneous Publication. Soil Sci. Soc. Am. Madison, WI.

Koch, M. S. and K.R. Reddy. 1992. Distribution of soil and plant nutrients along a trophic gradient in the Florida Everglades. *Soil Sci. Soc. Am. J.* 56:1492-1499.

Kuehn, K.A., M.J. Lemke, K. Suberkropp, and R.G. Wetzel. 2000. Microbial biomass and production associated with decaying leaf litter of the emergent macrophyte *Juncus effusus*. *Limnol. Oceanogr.* 45:862-870.

Levenspiel, O. 1972. *Chemical Reaction Engineering* (2nd Ed.). John Wiley & Sons, Inc. New York.

Levenspiel, O. 1989. *The Chemical Reactor Omnibook*. Oregon State University Book Stores, Corvallis, Oregon 97339.

Li, Y. and Gregory, S. 1974. Diffusion of ions in sea water and in deep-sea sediments. *Geochimica et Cosmochimica Acta*. 38: 703-714.

Mesple, F., C. Casellas, M. Trouseillier, J. Bontoux, 1996. Modeling orthophosphate evolution in a high rate pond. *Ecological Modeling* 89: 13-21.

Moutin, T., Gal, J.Y., Halouani, H., Picot, B., J. Bontoux. 1992. Decrease of phosphate concentration in a high rate pond by precipitation of calcium phosphate: theoretical and experimental results. *Water Research* 26(11): 1445-1450.

Murphy, T.P., K.J. Hall, and I. Yesaki. 1983. Coprecipitation of phosphate with calcite in a naturally eutrophic lake. *Limnol.Oceanogr.* 28: 59 - 69.

Newman, S. and K.R. Reddy. 1993. APase activity in the sediment-water column of a hypereutrophic lake. *J. Environ. Qual.* 22:832-838.

- Nepf, H.M., C.G. Mugnier, and R.A. Zavistoski. 1997. The effects of vegetation on longitudinal dispersion. *Estuarine, Coastal and Shelf Science*. 44: 675-684.
- Nurdogan, Y. and W.J. Oswald. 1995. Enhanced nutrient removal in high-rate ponds. *Water Science and Technology* 31(12): 33-43.
- Odum, H.T., 1994. *Ecological and General Systems*. University Press of Colorado, Niwot, CO.
- Otsuki, A. and R.G. Wetzel. 1972. Coprecipitation of phosphate with carbonates in a marl lake. *Limnol. Oceanogr.* 17: 763-767.
- Pant, H.K., A.C. Edwards and D. Vaughan. 1994. Extraction, molecular fractionation and enzyme degradation of organically associated phosphorus in soil solutions. *Biol. Fertil. Soils* 17:196-200.
- PEER Consultants/Brown and Caldwell. 1996. Desktop Evaluation of Alternative Technologies. Contract C-E008-A3. Report prepared for South Florida Water Management District, West Palm Beach, FL.
- Pettersson, K. 1980. Alkaline phosphatase activities and algal surplus phosphorus as phosphorus deficiency indicators in Lake Erken. *Arch. Hydrobiol.* 89: 54-87.
- Picot, B., Halouani, H., Casellas, C., Moersidik, S., and J. Bontoux. 1991. Nutrient removal by high rate pond system in Mediterranean climate (France). *Water Science and Technology* 23: 1535-1541.
- Qian, S.S., 1997. An illustration of model structure identification. *Journal of American Water Resources Association* 33(4): 811-824.
- Qian S.S. and K.H. Reckhow, 1998. Modeling phosphorus trapping in wetlands using a nonparametric Bayesian regression. *Water Resources Research* 34(7): 1745-1754.
- Qian, S.S. and C.J. Richardson, 1997. Estimating the long-term phosphorus accretion rate in the Everglades: a Bayesian approach with risk assessment. *Water Resources Bulletin* 33(7): 1681-1688.
- Qiu, S. and A.J. McComb. 1994. Effects of oxygen concentration on phosphorus release from reflooded air-dried wetland sediments. *Aust. J. Mar. Freshwater Res.* 45: 1319 – 1328.
- Persson, J., N.L.G. Somes, and T.H.F. Wong. 1999. Hydraulic efficiency of constructed wetlands and ponds. *Water Sci. Tech.* 40:291-300.
- Rai, L.C., Y. Husaini and N. Mallick. 1998. pH-altered interaction of aluminum and fluoride on nutrient uptake, photosynthesis and other variables of *Chlorella vulgaris*. *Aquatic Toxicol.* 42:67-84.
- Reckhow, Kenneth H., 1994. Water quality simulation modeling and uncertainty analysis for risk assessment and decision making. *Ecological Modeling* 72: 1-20.
- Reddy, K.R. and W. F. DeBusk. 1985. Nutrient removal potential of selected aquatic macrophytes. *J. Environ. Qual.*, 14:459-462.

Reddy, K.R., R.D. DeLaune, W.F. DeBusk, and M.S. Koch. 1993. Long-term nutrient accumulation rates in the Everglades. *Soil Sci. Soc Am. J.* 57:1147-55.

Salisbury, F.B., and C.W. Ross, 1978. *Plant Physiology*, 2nd ed. Wadsworth Publishing Co., Belmont, Ca.

SAS Institute Inc. 1996. *The SAS system for windows*, version 6.12, Cary, NC, USA.

Stevenson, F.J. 1986. *Cycle of Soils*. John Wiley and Sons Inc., N.Y., NY.

Seuss, E. 1970. Interaction of 5 organic compounds with calcium carbonate. 1. Association phenomena and geochemical implications. *Geochim. Cosmochim. Acta* **34**: 157 - 168.

South Florida Water Management District. 2000. *Everglades Consolidated Report*. South Florida Water Management District, Boca Raton, FL.

Steinman, A.D., R.H. Meeker, A.J. Rodusky, W.P. Davis, and S.J. Hwang, 1997. Ecological properties of charophytes in a large subtropical lake. *J.N. Am. Benthol. Soc* 16:781-793.

Stumm, W. and J.J. Morgan. 1981. *Aquatic Chemistry*. 2nd ed. John Wiley & Sons, NY.

Sweerts, J. R. A.; Kelly, C.A.; Rudd, J. W. M.; Hesslein, R.; Capenberg, T. E. 1991. Similarity of whole-sediment molecular diffusion coefficients in freshwater sediments of low and high porosity. *Limnol. Oceanogr.* 32(2): 335-342.

Tanner, C. C. 1996. Plants for constructed wetland treatment systems – A comparison of the growth and nutrient uptake of eight emergent species. *Ecol. Eng.*, 7: 59-83.

Thompson R.G. 1992. Practical zeta potential determination using electrophoretic light scattering. *Amer.Lab.* 8: 48-53.

Toth, L. A. 1988. Effects of Hydrologic regimes on lifetime production and nutrient dynamics of cattail. *SFWMD Tech Publ.* 88-6. West Palm FL.

Twinch, A.J. 1987. Phosphate exchange characteristics of wet and dried sediment samples from a hypertrophic reservoir: implications for the measurements of sediment phosphorus status. *Water Res.* 21:1225-1230.

Ullman, W. J.; Aller, R. C. 1982. Diffusion coefficients in nearshore marine sediments. *Limnol. Oceanogr.* 27(3): 552-556.

United States Environmental Protection Agency (EPA). 1979. *Methods for the Chemical Analysis of Water and Wastes*. EPA-600/4-79-020. Washington, D.C.

Vaithyanathan, P., T. Minto, and C. J. Richardson 1997, Calcium Carbonate Precipitation in the Everglades Sloughs: Influence of Water Column Phosphorus Concentration. Chapter 6 in *Effects of Phosphorus and Hydroperiod Alterations on Ecosystem Structure and Function in the Everglades*. 1996-97 Biennial Report submitted the Everglades Agricultural Area Environmental

Protection District. Duke Wetland Center Publication 97-05, Duke University, Durham, NC 27708-0333.

van de Hurst, H.C. 1981. Light scattering by small particles. Dover Publications, NY.

Walker, W.W., 1995. Design basis for Everglades stormwater treatment areas. Water Resources Bulletin 31(4): 671-685.

Walker, W.W., 1997. Discussion of "An illustration of model structure identification" by Song S. Qian, Journal of the American Water Resources Association 33(5): 1125-1126.

Walker, W.W. 1999a. Everglades Nutrient Removal Project Cell 4 Water Quality Data Analysis and Modeling. (A handout to SAV/LR Research Meeting held at SFWMD, West Palm Beach, FL, March 18, 1999).

Walker, W.W., 1999b. Contributions to Workshop on STA/Polishing Cell Design. Held at South Florida Water Management District, March 18, 1999.

Wilson, Jr., J.F., E.D. Cobb, and F.A. Kilpatrick. 1986. Fluorometric Procedures for Dye Tracing. U.S. Geological Survey Techniques of Water-Resources Investigations, Book 3, Chapt. A12, 34 p.

Whittig, L.D. and W.R. Allardice. 1986. X-Ray diffraction techniques. P. 331-362 In A. Klute (ed.) Methods of soil analysis, Part 1. American Society of Agronomy. Madison, WI.

Weiss, E.L., and N.H. Frock. 1976. Rapid analysis of particle size distribution using laser light scattering. Powder Technol. 14:287-293